Generation of All-pole 2-D Digital Filters from the Combination of All-pass Filters

Ajay Bhatt

A Thesis

in

The Department

of

Electrical and Computer Engineering

Presented in Partial Fulfillment of the Requirements
for the Degree of Master of Applied Science (Electrical Engineering) at
Concordia University,
Montreal, Quebec, Canada

July 2007

Your file Votre référence
ISBN: 978-0-494-34581-8
Our file Notre référence
ISBN: 978-0-494-34581-8

ABSTRACT

Generation of All-pole 2-D Digital Filters from the Combination of All-pass Filters

Ajay Bhatt

Two-dimensional digital filters are applied in signal processing and pro-imaging process, as well as communication systems where the frequency domain characteristics of digital filters are required to be adjustable. The main objective of this thesis is to propose a new technique for designing all-pole 2-D digital filters with variable magnitude characteristics. In this thesis, 2-D digital filters starting from the identical analog 1-D second-order Butterworth lowpass filter are generated through the combination of all-pass filters in Category A and Category B. A new type of all-pole 2-D analog lowpass filter is designed through the combination of all-pass filters. The transfer functions of these filters are verified for stability. The 2-D analog lowpass filter has been transformed to the digital domain by applying generalized bilinear transformation. The design of the 2-D digital lowpass filter gives rise to 2-D digital highpass, bandpass and bandstop filters in Category A and Category B. The 2-D digital highpass and bandstop filters have been designed from the 2-D lowpass filter using appropriate generalized bilinear transformation in both the categories. The 2-D digital bandpass filter has been obtained by a combination of the 2-D digital lowpass and highpass filters in both the categories.

The effect of the coefficients of the generalized bilinear transformation on the 2-D digital filter's transfer function is studied in detail for Category A and Category B. In the end, an application of the proposed 2-D lowpass filter in Category A and Category B is illustrated in image processing. The designed 2-D low-pass filter has been used to reduce the effect of additive white Gaussian noise on digital images in both the categories.

ACKNOWLEDGEMENTS

I would like to express my deepest gratitude to my thesis supervisor, Dr. Venkat Ramachandran for his invaluable guidance and encouragement in the accomplishment of this research work. It was Dr. Ramachandran's invaluable thoughts at the macro level which helped me to mould on a technical plane. It was Dr. Ramachandran's vision and ideas that provided the foundation for this thesis. He has been extremely helpful, understanding and extra-ordinarily patient in the critical review of my thesis. I feel deeply privileged to work under the supervision of Dr. Venkat Ramachandran.

I am heartily grateful to my parents, grandparents and my family members for their encouragement and support which have always been the key factor behind my every success in life. I would like to thank them for their love and sacrifices. I would also like to express my gratitude to my uncles, aunts and cousins who supported me with their love and understanding.

Finally, I would like to express my sincere and heartily thanks to my friends for their many contributions during the various stages of this work.

Ajay Bhatt, July 2007

Contents

List of Figures

List of Tables

List of Symbols and Abbreviations

1-D	:	One Dimension.
2-D	:	Two-Dimension.
2AP	:	Two multivariable All-Pass
$a_1,\ a_2$	:	Gain effecting coefficients of generalized bilinear transformation.
ADC	:	Analog to Digital Converter.
AMMI	:	Anti-Multivariable Mirror Image.
$b_1,\ b_2$	:	Polarity effecting coefficients of generalized bilinear transformation.
BIBO	:	Bounded Input Bounded Output.
DAC	:	Digital to Analog Converter
DFT	:	Discrete Fourier Transform.
$D(s_1, s_2)$	:	Denominator of a transfer function in the analog domain.
$D(z_1, z_2)$	:	Denominator of a transfer function in the digital domain.
DSP	:	Digital Signal Processing.
FIR	:	Finite Impulse Response.
GBT	:	Generalized Bilinear Transformation.
$H(s_1, s_2)$	:	Numerator of a transfer function in the analog domain.
$H(z_1, z_2)$	:	Numerator of a transfer function in the digital domain.
IDFT	:	Inverse Discrete Fourier Transform.

IIR	:	Infinite Impulse Response
K	:	Number of Variables
$k_1,\ k_2$	:	Bandwidth effecting coefficients of generalized bilinear transformation.
m_1	:	Even part of the denominator polynomial.
m_2	:	Even part of the numerator polynomial.
M, N	:	Number of columns and rows of digital image.
MMI	:	Multivariable Mirror Image.
MSE	:	Mean Square Error.
n_1	:	Odd part of the denominator polynomial.
n_2	:	Odd part of the numerator polynomial.
N	:	Order of the Filter.
PDF	:	Probability Density Function.
PSNR	:	Peak Signal to Noise Ratio.
$s_1,\ s_2$	:	Laplace domain parameters in two dimensions.
SHP	:	Strictly Hurwitz Polynomial.
VSHP	:	Very Strict Hurwitz Polynomial.
$z_1,\ z_2$	:	Z-domain parameter in two dimensions.
$*$	:	Convolution.
Σ	:	Summation.
μ	:	Mean of average value of the noise function.
σ	:	Standard deviation of the noise function.
$\omega_1,\ \omega_2$	:	Frequencies in radians in the analog domain parameter in first and second dimensions.

Chapter 1

Introduction

1.1 General

Signals arise in almost every field of science and engineering like acoustics, biomedical engineering, communications, control systems, radar, physics, seismology and telemetry, etc., to mention a few. Two general classes of signals can be classified, namely continuous-time and discrete-time signals. A continuous-time signal is defined at each and every instant of time. A discrete-time signal, on the other hand, is defined at discrete instants of time. A discrete-time signal, like continuous-time signal, can be represented by a unique function of frequency referred to as the frequency spectrum of the signal.

Filtering is a process by which the frequency spectrum of a signal can be modified, reshaped or manipulated according to some desired specifications. It may entail amplifying or attenuating a range of frequency components, rejecting or isolating some specific components, etc. The uses of filtering are manifold such as eliminating signal contamination such as noise, to remove signal distortion brought about by an imperfect transmission channel, to separate two or more distinct signals which were purposely mixed in order to maximize channel utilization, to resolve signals into frequency components, to demodulate signals, to convert discrete-time signals into continuous-time signals, and to band limit

Figure 1.1: Block Diagram of a filter

signals [1].

Filters are classified as analog and digital filters. Analog filters are used to processes analog signals, signals which are functions of continuous-time variable. Digital filters, on the other hand, process digitized continuous waveform.

1.2 Analog and Digital Filters

As stated earlier, in signal processing, the function of a filter is to remove unwanted parts of the signal, such as random noise, or to extract useful parts of the signal, such a the components lying within frequency range. The Figure 1.1 illustrates the basic idea.

1.2.1 Analog Filter

An analog filter uses analog electronic circuits made up from components such as resistors, capacitors and OpAmps to produce the required filtering effect. Such filter circuits are widely used in such applications as noise reduction, video signal enhancement, graphic equalisers in hi-fi systems, and also in many other areas. There are well-established standard techniques for designing an analog filter circuit for a given requirements. At all stages, the signal being filtered is an electrical voltage or current which is the direct analogue of the physical quantity involved.

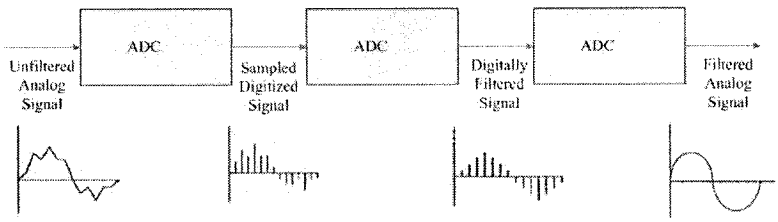

Figure 1.2: Block Diagram of Digital Filter

1.2.2 Digital Filter

Digital Filters are fundamental tools in Digital Signal Processing (DSP) applications mentioned above, and in general in data acquisition and processing applications. There are many problems in science and engineering whose solution involves use of multidimensional (K-D) digital filters. It is observed that due advantages and requirements of (K-D) digital filtering, its design is coming up as an important aspect in implementation and designing of various stable digital systems.

A digital filter is a device or program that performs a prescribed manipulation or algorithm on an input of numbers resulting in the desired output sequence of numbers. The numbers are limited to a finite precision. A digital filter uses a digital processor to perform numerical calculations on sampled values of the signal. The processor may be general-purpose computer such as PC, or a specialized DSP (Digital Signal Processor) chip.

The analog input signal must first be sampled and digitized using an ADC (analog to digital converter). The resulting binary numbers, representing successive sampled values of the input signal, are transferred to the processor, which carries out numerical calculations on them. These calculations typically involve multiplying the input values by constants and adding the products together. The results of these calculations, which now represent sampled values of the filtered signal, are fed through a DAC (Digital to Analog Converter) to convert the signal back to analog form. The signal is represented by a sequence of numbers, rather than a voltage or current [2]. Figure 1.2 shows the basic steps of such a system.

The following list gives some of the main advantages of digital filters:

1. Component tolerance are uncritical.

2. Component drift and spurious environmental signals have no influence on the system performance.

3. Accuracy is high.

4. Physical size is small.

5. Reliability is high.

An important additional advantage of digital filters is the case with which filter parameters can be changed in order to change the filter characteristics. This feature allows one to design programmable filters which can perform a multiplicity of filtering tasks. Also one can design new types of filters such as adaptive filters.

The computational efficiency of K-D signal processing algorithms plays an important role in implementation and design of digital systems. Remarkable advances in digital integrated circuits technology during the last few years have made the digital signal processing approach economically practical, flexible and reliable in many diverse fields. The design and implementation of K-D digital filters require considerable research effort over many years, in both K-D FIR and K-D IIR filters, due to increasing requirements in various applications.

1.3 Characterization of Digital Filters

Analog filters are characterized in terms of differential equations. Digital filters, on the other hand, are characterized in terms of difference equations. Two types of digital filters can be identified, non recursive and recursive filters.

Non recursive Filters

The response of a non recursive filter at instant nT is of form

$$y(nT) = f\{\cdots, x(nT-T), x(nT), x(nT+T), \cdots\} \tag{1.1}$$

If we assume linearity and time invariance, $y(nT)$ can be expressed as

$$y(nT) = \sum_{i=-\infty}^{\infty} a_i x(nT-T) \tag{1.2}$$

where a_i represents constants. Now by assuming causality and then using causality criterion it can be shown that $a_{-1} = a_{-2} = \cdots = 0$ and so

$$y(nT) = \sum_{i=0}^{\infty} a_i x(nT-T) \tag{1.3}$$

If in addition, $x(nT) = 0$ for $n < 0$ and $a_i = 0$ for $i > N$,

$$y(nT) = \sum_{i=0}^{\infty} a_i x(nT-T) + \sum_{i=n+1}^{\infty} a_i x(nT-T) \tag{1.4}$$

$$= \sum_{i=0}^{N} a_i x(nT-T) + \sum_{i=N+1}^{n} a_i x(nT-T) = \sum_{i=0}^{n} a_i x(nT-T) \tag{1.5}$$

Therefore, a linear, time-invariant, causal, non recursive filter can be expressed by an Nth-order linear difference equation where N is the order of the filter.

Recursive Filters

The response of a recursive filter is a function of elements in the excitation as well as the response sequence. In the case of a linear, time-invariant, causal filter

$$y(nT) = \sum_{i=0}^{N} a_i x(nT-T) - \sum_{i=0}^{M} b_i x(nT-T) \tag{1.6}$$

if the instant nT is taken to be the present, the response is a function of the present and past N values of the excitation as well as the past M values of the response. Note that the eqn. (1.6) simplifies to eqn. (1.5) if $b_i = 0$, and essentially the non recursive filter is a special

case of the recursive one [2, 3, 4].

1.4 Design of Digital Filter from analog filters

The design of filters involves the following stages:

(a) The specification of the desired properties of the systems,

(b) The approximation of the specifications using a causal discrete-time system, and

(c) The realization of the system.

In a practical setting, the desired filter is generally implemented with digital computation and used to filter a signal that is derived from a continuous-time signal by means of periodic sampling followed by analog-to-digital conversion.

1.4.1 Design of Digital IIR filters from analog filters

The traditional approach to the design of the discrete-time IIR filters involves the transformation of a continuous-time filter into a discrete-time filter meeting prescribed specifications, This is a reasonable approach for several reasons:

(1) The art of continuous-time IIR filter design is highly advanced, useful results can be achieved, and it is advantageous to use the design procedures already developed for continuous-time filters.

(2) Many useful continuous-time IIR design methods have relatively simple closed form design formulas. Therefore, discrete-time IIR filter design methods based on such standard continuous-time design formulas are rather simple to carry out.

(3) The standard approximation methods that work well for continuous-time IIR filters do not lead to simple closed-form design formulas when these methods are applied directly to the discrete-time IIR case [5, 6].

In designing a discrete-time filter by transforming a prototype continuous-time filter, the specifications for the continuous-time filter are obtained by a transformation of the specifications for the desired discrete-time filter. The system function $H_c(s)$ or impulse response $h_c(t)$ of the continuous-time filter is obtained through one of the approximations of the continuous-time filter. The system function $H(z)$ or impulse response $h[n]$ for the discrete-time filter is obtained by applying to $H_c(s)$ or $h_c(t)$ a transformation of the type discussed in this section. In such transformations, we generally require that the essential properties of the continuous-time frequency response be preserved in the frequency response of the resulting discrete-time filter. Specifically, this implies that the imaginary axis of the s-plane is mapped onto the unit circle of the z-plane. A second condition is that a stable continuous-time filter should be transformed to a stable discrete-time filter. There are two methods of digital filter design. The first method is Impulse Invariance method and second method is Bilinear Transformation [1, 3, 7].

1.4.1.1 Filter Design by Impulse Invariance

In the Impulse Invariance design procedure for transforming continuous-time filters into discrete-time filters, the impulse response of the discrete-time filter is chosen proportional to equally spaced samples of the impulse response of the continuous-time filter.

$$h[n] = T_d h_c(nT_d) \tag{1.7}$$

where T_d represents a sampling interval, $h_c(nT_d)$ is the impulse response of the continuous time filter.

In the impulse invariance design procedure, the relationship between continuous-time and discrete-time frequency is linear. Consequently, except aliasing, the shape of the frequency response is preserved. Thus the impulse invariance techniques is appropriate only for band limited filters.

1.4.1.2 Filter Design by Bilinear Transformation

The problem of aliasing is avoided by using the Generalized Bilinear Transformation (GBT) [8] instead of impulse invariance method. Bilinear Transformation is an algebraic transformation between the variables s and that maps the entire $j\Omega - axis$ in the $s - plane$ to the unit circle in the $z - plane$. Since $-\infty \leq \Omega \leq \infty$ maps onto $-\pi \leq \Omega \leq \pi$, the transformation between the continuous-time and discrete-time frequency variables must be non-linear. Therefore, the use of this techniques is restricted to situations in which the corresponding warping of the frequency is acceptable.

With $H_c(s)$ denoting the continuous-time system function and $H(z)$ the discrete-time system function, the generalized bilinear transformation [8] corresponds to replacing s by

$$s = k_i \frac{z_i - a_i}{z_i + b_i}, \quad i = 1, 2 \tag{1.8}$$

where k_i, a_i and b_i are coefficient of the generalized bilinear transformation. By replacing one for the coefficients for 1-D, we get $s = \frac{z-1}{z+1}$, i.e.,

$$H(z) = H_c\left[\frac{z-1}{z+1}\right] \tag{1.9}$$

1.4.2 Design of Digital FIR filters

Non recursive filters are also called Finite Impulse Response (FIR) filters, which have their transfer function resulting from a finite input sequence. The output of non recursive filter at any point can be computed as a linear combination of a finite number of input samples. The main properties for non recursive filter are its inherent stability and linear phase feature. There are many methods, such as Windows method, frequency transformation, and linear programming and these are generally used in a non recursive filters design [1, 9].

1.5 Different Types of Filters

A frequency-selective filter is one that passes signals whose frequencies are in certain ranges or bands, called the *passbands*, and blocks or attenuates signals whose frequencies are in other ranges, called the *stopbands*. The nature of the amplitude function $|H(j\omega)|$ or the loss function $\alpha(\omega)$ may be used to classify the various types of filters according to the location of their passbands and stopbands. An ideal filter is one which has a linear phase response in its passbands, zero loss in its passband, and infinite loss $|H(j\omega)| = 0$ in its stopband.

The different types of frequency-selective filters mostly encountered are defined as follows:

(1) Low-pass Filter : A low-pass filter is one with a single passband between zero and a cutoff frequency ω_c, with all frequencies higher than ω_c constituting the stopband. The bandwidth is defined as $B = \omega_c$.

(2) High-pass Filter: A high-pass filter is one with stopband $0 < \omega < \omega_c$, and passband $\omega > \omega_c$ where ω_c is the cutoff frequency.

(3). Band-pass Filter: A band-pass filter is one with a passband between two cutoff frequencies ω_c and $\omega_U > \omega_L$ and two stopbands, $0 < \omega < \omega_L$ and $\omega > \omega_L$. The Bandwidth is defined as $B = \omega_U - \omega_L$.

(4) Band-Reject Filter: A band-reject filter is one with a stopband of $\omega_L < \omega < \omega_U$ and two possible passbands, $0 < \omega < \omega_L$and $\omega > \omega_U$.

(5) All-pass Filter: An all-pass filter is one which passes all frequencies equally well. That is, $|H(j\omega)|$ is constant for all frequencies, with the phase $\phi(\omega)$ generally a function of frequency [3].

1.6 All-Pass Filter

The digital all-pass filter is a computationally efficient signal processing building block which is quite useful in many signal processing applications. In many signal processing applications, the designer must determine the transfer function of a digital filter subject to constraints on the frequency selectivity and/or phase response which are dictated by the application at hand. Once a suitable transfer function is found, the designer must select a filter structure from the numerous choices available. Ultimately, finite precision arithmetic is used on any digital filter computation, and traditionally the round off noise and coefficient sensitivity characteristics have formed the basis of selecting one filter structure in favor of another. [10].

1.6.1 Definitions and Properties

Definition

The frequency response $A(e^{j\omega})$ of an all-pass filter exhibits unit magnitude at all frequencies, i.e., for all ω.

$$\left|A(e^{j\omega})\right|^2 = 1 \tag{1.10}$$

The transfer function of such a filter has all poles and zeros occurring in conjugate reciprocal pairs, and takes the form

$$A(z) = e^{j\theta} \prod_{k=1}^{M} \frac{\gamma_k^* - z^{-1}}{1 - \gamma_k z^{-1}} \tag{1.11}$$

For stability reasons, we assume $|\gamma_k| < 1$ for all k to place all the poles inside the unit circle. Now, if $A(z)$ is constrained to be a real function, we must have $\theta = 0$ or $\theta = \pi$, and any complex poles at $z = \gamma_k$ must be accompanied by a complex conjugate pole at $z = \gamma_k^*$.

In this case $A(z)$ can be expressed in the form

$$A(z) = \frac{z^{-M} D(z^{-1})}{D(z)} \tag{1.12}$$

In effect, the numerator polynomial is obtained from the denominator polynomial by reversing the order of the co-efficients. For example,

$$A(z) = \frac{a_2 + a_1 z^{-1} + z^{-2}}{1 + a_1 z^{-1} + a_2 z^{-2}} \tag{1.13}$$

is a second order all-pass function of the form of eqn. (1.13) above, since the numerator coefficients appear in the reverse order of those in the denominator, In this case, the numerator and denominator polynomials are said to form a mirror-image pair.

If we lift the restrictions that $A(z)$ be a real function, then $A(z)$ takes the more general form

$$A(z) = \frac{z^{-M} D^*(1/z^{-1})}{D(z)} \tag{1.14}$$

The numerator and denominator polynomials now form a Hermitian mirror image pair. For example,

$$A(z) = \frac{\alpha_2^* + \alpha_1^* z^{-1} + \alpha_0^* z^{-2}}{\alpha_0 + \alpha_1 z^{-1} + \alpha_2 z^{-2}} == e^{j\theta} \frac{(\alpha_2/\alpha_0)^* + (\alpha_1/\alpha_0)^* z^{-1} + z^{-2}}{1 + (\alpha_1/\alpha_0) z^{-1} + (\alpha_2/\alpha_0) z^{-2}} \tag{1.15}$$

where $\theta = arg(\alpha_0^*/\alpha_0)$, is recognized as a complex all-pass function due to the Hermitian mirror-image relation between the numerator and denominator polynomials [10].

Properties

From the definition of an all-pass function in eqn. (1.10), setting $A(z) = Y(z)/U(z)$ reveals, for all ω,

$$\left|Y(e^{j\omega})\right|^2 = \left|U(e^{j\omega})\right|^2 \tag{1.16}$$

Upon integrating both sides from $\omega = -\pi$ to π and applying Parseval's relation [11], we obtain

$$\sum_{n=-\infty}^{\infty} |y(n)|^2 = \sum_{n=-\infty}^{\infty} |u(n)|^2 \tag{1.17}$$

It is convenient to interpret the two sides of eqn. (1.17) as the output energy and input energy of the digital filter, respectively [3, 11]. Thus an all-pass filter is loseless, since the output energy equals the input energy for all finite energy inputs. If the all-pass filter is stable as well, it is termed Lossless Bounded Real (LBR) [12], or more generally Lossless Bounded Complex [13] if the coefficients are not all real.

Another useful property follows for eqn. (1.10) with the aid of the maximum modulus theorem. In particular, since a stable all-pass function has all its poles inside the unit circle, all its zeros outside, and exhibits unit magnitude along the unit circle, one can deduce

$$|A(z)| = \begin{cases} < 1 & for \quad |z| > 1 \\ = 1 & for \quad |z| = 1 \\ > 1 & for \quad |z| < 1 \end{cases} \tag{1.18}$$

This relation is useful in verifying stability in lattice realization of all-pass filters.

The last property of interest is the change in phase for real all-pass filter over the frequency range $\omega \varepsilon [0, \pi]$. We start with the group delay function $\tau(\omega)$ of an all-pass filter, which is usually defined as

$$\tau(\omega) = -\frac{d}{d\omega}\left[argA(e^{j\omega})\right] \tag{1.19}$$

Note that the phase function must be taken as continuous or "unwrapped" [3] if $\tau(\omega)$ is to be well-behaved. Since an all-pass function is devoid of zeros on the unit circle

according to eqn. (1.10), the phase function $argA(e^{j\omega})$ can always be unwrapped with no ambiguities. Now, the phase response of a stable all-pass function is a monotonically decreasing function of ω, so that $\tau(\omega)$ is everywhere positive. An $Mth-order$ real all-pass function, in fact, satisfies the property

$$\int_0^\infty \tau(\omega)d\omega = M\pi \tag{1.20}$$

The interpretation of eqn. (1.20) is that the change in phase of the all-pass function as ω goes from 0 to π is $-M\pi$ radians [10].

1.6.2 Combinations of all-pass filters

One of the methods of designing 1-D (single-variable) complementary filters both in analog and discrete domains is to properly combine the outputs of two all-pass filters. The all pass filter are combined either in series or parallel. Different types of filter structures are stated in [10]. The necessary and sufficient conditions for the physical realizability of this category of filters, which will be designated here as 2AP filters, have been studied and obtained in [15]. The implementation of such types of filters is possible using the structures obtained in [16] for which all-pass characteristics are maintained even when the multiplier coefficients are varied.

The generation of transfer functions obtained by the sum or difference of two multivariable (designated as k-D, k is the number of variables) all-pass functions are studied [14]. The realizability conditions of the corresponding filters are obtained, both in the analog and discrete domains. It is shown that these conditions are independent of the number of variables and also the order of each variable. Design methods for 2-D 2AP filters are given. These methods can be extended to any number of variables $(k - D)$. The implementation of the 2-D 2AP filters is possible using the 2-D all-pass filter realizations given in [17, 18].

1.6.2.1 Discrete Polydomain

Considering two all-pass filters connected in parallel. The output of the two all-pass filters could be added or subtracted resulting in different outputs. Let the transfer function of the first all-pass filter be $H_{Ad}(Z)$ and that of the second all-pass filter be $H_{Bd}(Z)$. The function $H_{Ad}(Z)$ is considered first. It can be written as

$$H_{Ad}(Z) = \left\{ \prod_{i=1}^{k} z_i^{p_i} \right\} \frac{D_{Ad}(Z^{-1})}{D_{Ad}(Z)} \tag{1.21}$$

where p_i is the order of the variable z_i.

It is assumed that $D_{Ad}(Z)$ satisfies the required condition for stability [19, 20]. It has been shown that [20, 21] such a polynomial can always be decomposed as the sum of the multivariable mirror-image polynomial (MMI) $F_{A1}(Z)$, and the anti-mirror-image polynomial (AMMI) $F_{A2}(Z)$ which are given by:

$$F_{A1}(Z) = \frac{1}{2}\left[D_{Ad}(Z) + \left(\prod_{i=1}^{k} z_i^{p_i} \right) D_{Ad}(Z^{-1}) \right] \tag{1.22}$$

$$F_{A2}(Z) = \frac{1}{2}\left[D_{Ad}(Z) - \left(\prod_{i=1}^{k} z_i^{p_i} \right) D_{Ad}(Z^{-1}) \right] \tag{1.23}$$

Obviously, $H_{Ad}(Z)$ can be written as

$$H_{Ad}(Z) = \frac{F_{A1}(Z) - F_{A2}(Z)}{F_{A1}(Z) + F_{A2}(Z)} \tag{1.24}$$

Similarly, the transfer function $H_{Bd}(Z)$ can be written as

$$H_{Bd}(Z) = \left(\prod_{l=1}^{k} z_l^{p_l} \right) \frac{D_{Bd}(Z^{-1})}{D_{Bd}(Z)} = \frac{F_{B1}(Z) - F_{B2}(Z)}{F_{B1}(Z) + F_{B2}(Z)} \tag{1.25}$$

where p_l is the order of z_l, and $F_{B1}(Z)$, $F_{B2}(Z)$ are, respectively, the multivariable mirror-image, and anti-mirror-image polynomials of $D_{Ad}(Z)$ given by:

$$F_{B1}(Z) = \frac{1}{2}\left[D_{Bd}(Z) + \left(\prod_{l=1}^{k} z_l^{p_l}\right) D_{Bd}(Z^{-1})\right] \tag{1.26}$$

$$F_{B2}(Z) = \frac{1}{2}\left[D_{Bd}(Z) - \left(\prod_{l=1}^{k} z_l^{p_l}\right) D_{Bd}(Z^{-1})\right] \tag{1.27}$$

Theorem 1 discusses the conditions under which a transfer function can be realized as a sum of the transfer functions of two all-pass filters.

Theorem 1. The necessary and sufficient conditions that the transfer function $H_1(Z)$ given by:

$$H_1(Z) = \frac{1}{2}\left[H_{Ad}(Z) + H_{Bd}(Z)\right] = \frac{N_{d1}(Z)}{D_d(Z)} = \frac{F_{A1}(Z)\cdot F_{B1}(Z) - F_{A2}(Z)\cdot F_{B2}(Z)}{D_{d1}(Z)\cdot D_{d2}(Z)} \tag{1.28}$$

should satisfy in order that it can be realized as the sum of two all-pass filters $H_{Ad}(Z)$ and $H_{Bd}(Z)$ are:

1. The denominator polynomial $D_d(Z)$ shall be product-separable as $D_{d1}(Z)\cdot D_{d2}(Z)$, *and*

2. The numerator polynomial $N_{d1}(Z)$ shall be the numerator of the even part of $\left(\frac{1}{2}\cdot\frac{D_{d1}(Z)}{D_{d2}(Z)}\right)$ or $\left(\frac{1}{2}\cdot\frac{D_{d2}(Z)}{D_{d1}(Z)}\right)$ and is given by:

$$N_{d1}(Z) = F_{A1}(Z)\cdot F_{B1}(Z) - F_{A2}(Z)\cdot F_{B2}(Z) \tag{1.29}$$

Proof.

Necessity: Condition (1) is obvious. For condition (2) eqn. (1.28) is obtained as follows:

Consider the even part of $\frac{D_{d1}(Z)}{D_{d2}(Z)}$ which is:

$$E\left\{\frac{D_{d1}(Z)}{D_{d2}(Z)}\right\} = \frac{F_{A1}(Z) + F_{A2}(Z)}{F_{B1}(Z) + F_{B2}(Z)} + \frac{F_{A1}(Z) - F_{A2}(Z)}{F_{B1}(Z) - F_{B2}(Z)} \tag{1.30}$$

The numerator is given by:

$$N_{d1}(Z) = 2\left[F_{A1}(Z) \cdot F_{B1}(Z) - F_{A2}(Z) \cdot F_{B2}(Z)\right] \tag{1.31}$$

and hence condition (2) is verified. It is noted that $N_{d1}(Z)$ is a multivariable mirror-image (MMI) polynomial. The same numerator results, if the even part of $\frac{D_{d2}(Z)}{D_{d1}(Z)}$ is considered.

Sufficiency:

We shall start from the transfer function

$$H_1(Z) = \frac{F_{A1}(Z) \cdot F_{B1}(Z) - F_{A2}(Z) \cdot F_{B2}(Z)}{D_{d1}(Z) \cdot D_{d2}(Z)} \tag{1.32}$$

By adding and subtracting $(F_{A1} \cdot F_{B1} - F_{A2} \cdot F_{B2})$ to the numerator, it is readily shown that

$$H_1(Z) = \left[\frac{F_{A1}(Z) - F_{A2}(Z)}{F_{A1}(Z) + F_{A2}(Z)} + \frac{F_{B1}(Z) - F_{B2}(Z)}{F_{B1}(Z) + F_{B2}(Z)}\right] \tag{1.33}$$

which is realizable as sum of two all-pass filters having transfer functions $H_{Ad}(Z)$ and $H_{Bd}(Z)$.

The Theorem 1 is thus proved. Theorem 2 discusses the conditions under which a transfer function can be realized as the difference of the transfer functions of two all-pass filters

Theorem 2. The necessary and sufficient conditions that

$$H_2(Z) = \frac{1}{2}\left[H_{Ad}(Z) - H_{Bd}(Z)\right] = \frac{N_{d2}(Z)}{D_d(Z)} = \frac{F_{A1}(Z) \cdot F_{B2}(Z) - F_{A2}(Z) \cdot F_{B1}(Z)}{D_{d1}(Z) \cdot D_{d2}(Z)} \tag{1.34}$$

should satisfy so that it can be realized as the difference of two all-pass filters $H_{Ad}(Z)$ and $H_{Bd}(Z)$ are:

1. The denominator polynomial $D_d(Z)$ shall be product-separable as $D_{d1}(Z) \cdot D_{d2}(Z)$, *and*

2. The numerator polynomial $N_{d2}(Z)$ shall be the numerator of the odd part of $\left(\frac{1}{2} \cdot \frac{D_{d1}(Z)}{D_{d2}(Z)}\right)$ or $\left(\frac{1}{2} \cdot \frac{D_{d2}(Z)}{D_{d1}(Z)}\right)$ and is given by:

$$N_{d2}(Z) = F_{A1}(Z) \cdot F_{B2}(Z) - F_{A2}(Z) \cdot F_{B1}(Z) \tag{1.35}$$

The proof of this theorem is similar to that of Theorem 1 and hence is omitted for the sake of brevity. The polynomial $N_{d2}(Z)$ is clearly a multivariable anti-mirror-image polynomial.

Note : It is worthwhile mentioning that if we consider the function $P(Z)$ defined as:

$$P(Z) = \frac{F_{A1}(Z) + F_{A2}(Z)}{F_{B1}(Z) + F_{B2}(Z)} = E(Z) + O(Z) \tag{1.36}$$

which has even and odd parts $E(Z)$ and $O(Z)$, respectively, given by:

$$E(Z) = \frac{F_{A1}(Z) \cdot F_{B1}(Z) - F_{A2}(Z) \cdot F_{B2}(Z)}{[F_{B1}(Z) + F_{B2}(Z)] \cdot [F_{B1}(Z) - F_{B2}(Z)]} \tag{1.37}$$

$$O(Z) = \frac{F_{A2}(Z) \cdot F_{B1}(Z) - F_{A1}(Z) \cdot F_{B2}(Z)}{[F_{B1}(Z) + F_{B2}(Z)] \cdot [F_{B1}(Z) - F_{B2}(Z)]} \tag{1.38}$$

then, eqn. (1.29) and (1.35) are respectively the numerators of $E(Z)$ and $O(Z)$. This means that the polynomials $N_{d1}(Z)$ and $N_{d2}(Z)$ can be generated by at least another function $P(Z)$. However, such functions might not be realizable as $k - D$ 2AP filters, because the conditions given by Theorems 1 and 2 must be satisfied. Certain relationships exist between $H_1(Z)$ and $H_2(Z)$ which are given by the following theorem.

Theorem 3. It can be shown that:

$$H_1(Z) \cdot H_1(Z^{-1}) + H_2(Z) \cdot H_2(Z^{-1}) = 1 \tag{1.39}$$

which leads to the relationship:

$$N_{d1}(Z) \cdot N_{d1}(Z^{-1}) + N_{d2}(Z) \cdot N_{d2}(Z^{-1}) = D_d(Z) \cdot D_d(Z^{-1}) \tag{1.40}$$

These relationship are proved by straightforward algebraic simplification and hence the proofs are omitted for the sake of brevity. It is noted that the relationships given by eqn. (1.39) and (1.40) are derived for 1-D in [15] and hence, these equations can be constructed as the k-variable generalizations of the earlier results obtained in [15]. However, it has to be pointed that the results of Theorems 1 and 2 are valid for $k-$variables including the case when $k = 1$.

1.6.2.2 Analog Polydomain

In the previous section we have established the required conditions to be satisfied by the transfer functions which are obtained by adding or subtracting two all-pass functions in the discrete polydomain. Similar results can be obtained in the analog polydomain also and these are discussed below.

Let the transfer function of the first all-pass filter be $T_{Aa}(S)$ and that of the second all-pass filter be $T_{Ba}(S)$. The function $T_{Aa}(S)$ is considered first. It can be expressed as:

$$T_{Aa}(S) = \frac{D_{Aa}(-S)}{D_{Aa}(S)} = \frac{M_{Aa}(S) - N_{Aa}(S)}{M_{Aa}(S) + N_{Aa}(S)} \tag{1.41}$$

where $M_{Aa}(S)$ is the even part of

$$D_{Aa}(S) = \frac{1}{2}\left[D_{Aa}(S) + D_{Aa}(-S)\right] \tag{1.42}$$

and $N_{Aa}(S)$ is the odd part of

$$D_{Aa}(S) = \frac{1}{2}\left[D_{Aa}(S) - D(-S)\right] \tag{1.43}$$

Similarly, the transfer function $T_{Ba}(S)$ can be written as

$$T_{Ba}(S) = \frac{D_{Ba}(-S)}{D_{Ba}(S)} = \frac{M_{Ba}(S) - N_{Ba}(S)}{M_{Ba}(S) + N_{Ba}(S)} \tag{1.44}$$

where $M_{Ba}(S)$ is the even part of

$$D_{Ba}(S) = \frac{1}{2}\left[D_{Ba}(S) + D_{Ba}(-S)\right] \tag{1.45}$$

and $N_{Ba}(S)$ is the odd part of

$$D_{Ba}(S) = \frac{1}{2}\left[D_{Ba}(S) - D_{Ba}(-S)\right] \tag{1.46}$$

It is tacitly assumed that the required stability conditions are satisfied by $D_{Aa}(S)$ and $D_{Ba}(S)$ [19].

Theorem 4. The necessary and sufficient conditions that

$$T_1(S) = \frac{1}{2}\left[T_{Aa}(S) + T_{Ba}(S)\right] = \frac{N_{a1}(S)}{D_a(S)} = \frac{M_{Aa}(S)\cdot M_{Ba}(S) - N_{Aa}(S)\cdot N_{Ba}(S)}{D_{Aa}(S)\cdot D_{Ba}(S)} \tag{1.47}$$

should satisfy in order that it can be realized as the sum of two all-pass filters $T_{Aa}(S)$ and $T_{Ba}(S)$ are:

1. The denominator polynomial $D_a(S)$ shall be product-separable as $D_{Aa}(S)\cdot D_{Ba}(S)$ *and*

2. The numerator polynomial $N_{a1}(S)$ shall be the numerator of the even part of $\left(\frac{1}{2}\cdot\frac{D_{Aa}(S)}{D_{Ba}(S)}\right)$ or $\left(\frac{1}{2}\cdot\frac{D_{Ba}(S)}{D_{Aa}(S)}\right)$ and is given by:

$$N_{a1}(S) = M_{Aa}(S)\cdot M_{Ba}(S) - N_{Aa}(S)\cdot N_{Ba}(S) \tag{1.48}$$

The proof is similar to that of Theorem 1 and hence is omitted for the sake of brevity. It is noted that $N_{a1}(S)$ is an even polynomial in the $k-$variables S.

Theorem 5. The necessary and sufficient conditions that

$$T_2(S) = \frac{1}{2}\left[T_{Aa}(S) - T_{Ba}(S)\right] = \frac{N_{a2}(S)}{D_a(S)} = \frac{M_{Aa}(S)\cdot N_{Ba}(S) - M_{Ba}(S)\cdot N_{Aa}(S)}{D_{Aa}(S)\cdot D_{Ba}(S)} \tag{1.49}$$

should satisfy so that the same can be realized as the difference of two all-pass filters $T_{Aa}(S)$ and $T_{Ba}(S)$ are:

1. The denominator polynomial $D_a(S)$ shall be product-separable as $D_{Aa}(S)\cdot D_{Ba}(S)$ *and*

2. The numerator polynomial $N_{a2}(S)$ shall be the numerator of the odd part of $\left(\frac{1}{2}\cdot\frac{D_{Aa}(S)}{D_{Ba}(S)}\right)$ or $\left(\frac{1}{2}\cdot\frac{D_{Ba}(S)}{D_{Aa}(S)}\right)$ and is given by:

$$N_{a2}(S) = M_{Aa}(S)\cdot M_{Ba}(S) - M_{Ba}(S)\cdot N_{Aa}(S) \tag{1.50}$$

The proof of this theorem is similar to that of Theorem 2 and hence is omitted for the sake of brevity. It is noted that $N_{a2}(S)$ is an odd polynomial in the k--variables S. Certain relationships exit between $T_{Aa}(S)$ and $T_{Ba}(S)$, which are given by the following theorem.

Theorem 6. It can be shown that

$$T_{Aa}(S)\cdot T_{Aa}(-S) + T_{Ba}(S)\cdot T_{Ba}(-S) = 1 \tag{1.51}$$

which leads to the relationship

$$N_{a1}(S)\cdot N_{a1}(-S) + N_{b1}(S)\cdot N_{b1}(-S) = D_a(S)\cdot D_a(-S) \tag{1.52}$$

It can be observed that there is one-to-one correspondence between the theorems derived in the discrete polydomain and those which refer to the analog polydomain. More specifically, Theorems 4-6 are the analog counterparts of Theorems 1-3. This stems from the correspondence between the even and the odd parts of $S-$domain polynomials and the MMI and AMMI polynomials [20, 21]. These results can be utilized to design certain types

of filters.

In the design of such filters, the first condition that has to be satisfied is that the denominator polynomial shall be product-separable. In 1-D (analog and discrete), this condition does not pose any problem, since such polynomial can always be factored. However, when the number of variables k exceeds unity, a given polynomial may or may not be factorable, testing for the factorability is also quite cumbersome.

In addition, it should be noted that in 1-D analog systems, it is always possible to associate a strictly Hurwitz polynomial to either the numerator of the real part or the imaginary part of a given positive real function and obtain another strictly Hurwitz polynomial $D_{a1}(s_1)$ or $D_{a2}(s_2)$. The same is true in the case of 1-D discrete systems also [22]. However in the case of multivariable analog systems ($k > 1$), it is known that it is not possible to generate a positive real function starting from its real or imaginary part, unless the denominator Hurwitz polynomial satisfies certain additional conditions which are dependent on the numerator [23].

1.7 Two Dimensional Digital Filters and its Importance

The topic of Multidimensional systems (MDS) analysis and design has attracted considerable attention during recent years and is still receiving increased attention by theorists and practitioners. Specifically, interest has been directed by researchers into the area of two-dimensional (2-D) digital systems due to several reasons: high efficiency due to high-speed computations; permitting better image processing and analysis; great application flexibility and adaptivity; decreasing cost of software or hardware implementations due to the large expansion and evolution of computers, microcomputers, microprocessors, and high integration digital circuits. In general, two-dimensional digital filters are designed by combining two one-dimensional digital filters. Similar to one-dimensional digital filters, two

dimensional digital filters can be classified into two main groups. The first group comprises a finite sequence transfer function and so the filters in this group are called Finite Impulse (FIR) filters. The second group comprises an infinite sequence transfer function and so the filters in this group are called Infinite Impulse Response (IIR) filters [6, 9, 24].

Recent studies in two dimensional (2-D) signal processing activities for example, image processing, has stimulated active research in the area of 2-D circuits and systems, both recursive and non recursive. There are various problems that call for digital filtering of sampled two-dimensional data to process and analyze various digital systems. For example, 2-D variable recursive digital filters are applied in signal processing, image processing, video processing processes, as well as communication systems where the frequency-domain characteristics of digital filters are required to be adjusted, and also in the geophysical industry uses 2-D filtering for processing seismic records, gravity and magnetic data, enhancement of photographic data such as weather photos, air photos and medical X-rays, etc. The uses of digital filters range from simple noise reduction to the complex spectral processing and analysis used in speech processing and recognition, audio, and communications.

The applications vary from filter banks in image processing via fan filtering in seismology to modeling of physical systems such as fluid flow. Due to the rapidly increasing interest in High-Definition TV, Multimedia, etc., the processing of still and motion, monochrome and color pictures has become a great importance. 2-D linear phase FIR filters have been used particularly in scanning rate converters, PAL decoders and digital video codecs based on the Discrete Cosine Transform(DCT), sub-band and pyramidal coding schemes.

It is observed that recursive filters based on the all-pass filter offers strong competition to FIR filters because they require less computation per sample. Although the structures are recursive, stability is assured given certain conditions and furthermore, unlike other recursive filters, approximately linear phase can be achieved easily [25, 26, 27].

There are many works concentrating on the use of 2-D filters in image and video signal

processing problems. The first application area is image enhancement. 2-D highpass filters can be used to increase local contrast and sharpen an image and 2-D low pass filters can improve noisy images. The second application area of 2-D filter is image coding. Because of the need to transmit pictures using existing speech transmission channels, for example in video conferencing, many new techniques for coding the image have been developed. One of these techniques is sub-band coding in which the image is split into a number of frequency bands and, as a result, the sampling rate can be reduced (decimation). After transmission and storage, these sub-bands are recombined (interpolation) to reconstruct the image and these require 2-D digital filtering. There are many applications in the video field for $(K-D)$ filters. Some of these were discussed in early BBC and IBA technical papers. Principally they are used in pre-filtering and post-filtering of high definition signals so as to reduce the data rate for digital transmission. 2-D filters used for pattern recognition operations permit the extraction of significant information and configuration from the images for final interpretation and utilization. hence, 2-D filters have various application associated with image enhancement pattern recognition and restoration [19, 28].

1.8 Stability of 2-D Filters

In one-dimensional (1-D) systems (both analog and discrete), one can use suitably chosen transfer functions having no common factors between the numerator and denominator in order to design a filter having required specifications. Let

$$H_a = \frac{N_a(s)}{D_a(s)} \tag{1.53}$$

be a transfer function in the analog domain with $N_a(s)$ and $D_a(s)$ being relatively prime. For the transfer function $H_a(s)$ to be stable, $D_a(s)$ should be strictly a Hurwitz polynomial (SHP). A SHP contains its zeros strictly in the left-half of the s-plane. Similarly, if

$$H_d(z) = \frac{N_d(z)}{D_d(z)} \tag{1.54}$$

be a transfer function in discrete domain with $N_d(z)$ and $D_d(z)$ being relatively prime, then $D_d(z)$ should be a Schur polynomial in order that $H_d(z)$ shall be stable. A Schur polynomial contains its zeros strictly within the unit circle [29].

In the case of 2-D analog systems, it is possible that both the even and odd parts of a polynomial may become simultaneously zeros at specified sets of points, but not in their neighborhood. If this occurs in the denominator of the transfer function, it is called non-essential singularity of the first kind. In addition, in 2-D transfer functions, both the numerator and denominator polynomials can become zero simultaneously at a given set of points. When this happens, it is known as non-essential singularity of the second kind. Mathematically, for a 2-D analog transfer function

$$H_a(s_1, s_2) = \frac{N_a(s_1, s_2)}{D_a(s_1, s_2)} \tag{1.55}$$

the above two cases may be expressed as [29].

(a) $D_a(s_1, s_2) = 0$ and $N_a(s_1, s_2) \neq 0$ constitute non-essential singularity of the first kind at (s_1, s_2).

(b) $D_a(s_1, s_2) = 0$ and $N_a(s_1, s_2) = 0$ constitute non-essential singularity of the second kind at (s_1, s_2).

A similar situation exists in the case of 2-D discrete systems also. One of the well-known methods of designing digital filters is to start from a given analog filter transfer function and then apply the generalized bilinear transformation $s_i \longrightarrow k_i \frac{z_i + a_i}{z_i + b_i}$, $i = 1, 2$, in order to obtain the corresponding digital transfer function [8].

The occurrence of the non-essential singularities of the first kind always results in an unstable filter and hence cannot be used in the design of stable filters. The occurrence of the non-essential singularity of the second kind in a transfer function may or may not cause

instability. It is not possible to determine the stability by inspection [30, 31].

One important issue concerning the above types of filters is the stability of the filter. It is known that FIR filters are inherently stable. IIR filters may or may not be stable depending upon the transfer function.

The most commonly used stability criterion is based on the bounded-input and output (BIBO) criterion [32]. This criterion states that a filter is stable if its response to a bounded input is also bounded. Mathematically, for causal linear shift-invariant systems, this corresponds to the condition that

$$\sum_{n_1=0}^{\infty}\sum_{n_2=0}^{\infty}|h(n_1,n_2)|<\infty \tag{1.56}$$

where $h(n_1, n_2)$ is the impulse response of the filter.

The above eqn. (1.56) points out an important observation that the stability criterion is always verified if the number of terms of the impulse response is finite, which is the case with FIR filters. However, the above condition does not prove feasible to the test of stability for IIR filters. In the 1-D case, it is possible to relate the BIBO stability condition to the positions of the z-transfer function poles which have to be within the unit circle and it is possible to test the stability by determining the zeros of the denominator polynomial. Similarly, in the 2-D case, a theorem establishing the relationship between the stability of the filter and the zeros of the denominator polynomial, can be formulated. This theorem states that [8], for 2-D IIR causal quarter-plane filters, if $B(z_1, z_2)$ is a polynomial in z_1 and z_2, the expansion of $\frac{1}{B(z_1,z_2)}$ in the negative powers of z_1 and z_2 converges absolutely if and only if

$$B(z_1,z_2)\neq 0 \; for \; |z_1|\geq 1,\; |z_2|\geq 1 \tag{1.57}$$

The above theorem has the same form as in the 1-D case, i.e., it relates the stability of the filter to the singularities of the z-form. However, in the 2-D case such a formulation

for stability condition does not produce an efficient method for stability test, as in 1-D, due to the lack of appropriate factorization theorem of algebra. Therefore, it is necessary in principle, to use an infinite number of steps to test the stability. Also, even if it is possible to find methods to test conditions equivalent to eqn. (1.57) in a finite number of steps [33], computationally it is not easy to incorporate them in a design method and there is a problem of stabilizing the filters which may become unstable.

A widely used approach involves the design of two-variable stable analog transfer function and use bilinear transformation to obtain the corresponding digital transfer function. For example, first design a two-variable passive (hence guaranteed stable) analog filter via a computer-aided optimization technique and then obtain a 2-D IIR transfer function by applying a double bilinear transformation on the transfer function of the analog filter [34, 35].

The 2-D filter stability testing problem can also be avoided by designing a separable 2-D IIR filter approximating the frequency response characteristic. For separable filter, the 2-D transfer function $H(z_1, z_2)$ can be expressed as a product of two 1-D transfer functions, i.e., $H(z_1, z_2) = H(z_1) \cdot H(z_2)$. In this case, the testing of stability reduces to that of checking the stability of the 1-D filters, which is considerably simpler. Moreover, a separable filter is also more economical to implement. For example, [36] describes a computer- aided method of designing separable filters.

From the point of view of stability tests, there can be two different approaches that can be considered, in designing an IIR filter. One method is to carry out the stability test in every stage of the filter design so that the eventual filter is stable. In the second method, stability is not considered as a part of the design and an magnitude-squared transfer function is first designed. Then a stable filter is obtained, by choosing the poles in the stability region. Such an approach is convenient, because squared magnitude functions can be in a simple form and it is easy to find the poles of the filter.

In the view of the above difficulties in 2-D design, it will be highly convenient, if we start with Very Strict Hurwitz Polynomials (VSHP) in the denominator of a 2-D transfer

function, because such polynomial do not contain non-essential singularities of the second kind. This ensures stability of the designed filter. We will briefly review some of its properties in the next section.

1.9 Overview of Very Strict Hurwitz Polynomial and its Properties

1.9.1 Definition of Very Strict Hurwitz Polynomial

The class of polynomials which do not contain non-essential singularities of the second kind (discussed in Sec. 1.8) is called Very Strict Hurwitz Polynomials (VSHP) [29]. A VSHP is defied as follows:

"$D_a(s_1, s_2)$ is VSHP, if $\frac{1}{D_a(s_1,s_2)}$, does not possess any singularities in the region

"$\{(s_1, s_2) \mid Re(s_1) \geq 0,\ Re(s_2) \geq 0,\ |s_1| \leq \infty,\ and\ |s_2| \leq \infty\}$".

In the view of this definition, a VSHP has to be necessary a Strictly Hurwitz Polynomial (SHP) [29]. After ensuring that a given two-variable polynomial is a SHP, then one can proceed further to ascertain the absence of singularities at points of infinity. The points of infinity are studied by considering the reciprocal of the variable. In view of the two variables considered, the following possibilities exist:

(a) $s_1 \rightarrow \infty,\ s_2 =$ finite,

(b) $s_1 =$ finite, $s_2 \rightarrow \infty$,

(c) $s_1 \rightarrow \infty$ and $s_2 \rightarrow \infty$.

That is, in (a) and (b), only one of the variables goes to infinity, while the other remains finite, whereas in (c), both the variables go to infinity simultaneously. Another alternate definitions for VSHP is proposed by in [37].

1.9.2 Some Properties of VSHP

In this section, we shall discuss some of the properties of VSHP. Our discussion for the properties of VSHP are based on the following definition of 2-D analog transfer function [38]

$$H_a(s_1, s_2) = \frac{N_a(s_1, s_2)}{D_a(s_1, s_2)} \tag{1.58}$$

where

$$N_a(s_1, s_2) = \sum_{i=0}^{m} \sum_{j=0}^{n} B_{ij} s_1^i s_2^j \tag{1.59}$$

$$D_a(s_1, s_2) = \sum_{i=0}^{k} \sum_{j=0}^{l} B_{ij} s_1^i s_2^j \tag{1.60}$$

Property 1:

The transfer function $H_a(s_1, s_2)$ (defined in [38]) does not possess any singularity in the closed right-half of the (s_1, s_2) - biplane, if and only if $D_a(s_1, s_2)$ is a VSHP.

In the above, the closed right-half biplane is

$$\{(s_1, s_2) \mid Re(s_1) \geq 0,\ Re(s_2) \geq 0, |s_1| \leq \infty \ and \ |s_2| \leq \infty\} \tag{1.61}$$

This property is obtained from the definition of VSHP.

Property 2:

$D(s_1, s_2) = [D_1(s_1, s_2)] \cdot [D_2(s_1, s_2)]$ shall be a VSHP, if and only if $[D_1(s_1, s_2)]$ and $[D_2(s_1, s_2)]$ are individually VSHPs.

This property demonstrates clearly that a product of two VSHPs results in a VSHP. Also, if a VSHP is product-separable, the individual factors shall be VSHPs.

Property 3:

If $D_a(s_1, s_2)$ is a VSHP, $\frac{\partial D_a(s_1, s_2)}{\partial s_1}$ and $\frac{\partial D_a(s_1, s_2)}{\partial s_2}$ are also VSHP.

Property 4:

The polynomial $E_i(s_2),\ i = 0, 1, 2.....,p$ and $F_j(s_1),\ j = 0, 1, 2....., q$ defined in [39] are SHPs (Strictly Hurwitz Polynomial) in s_1 and s_2, respectively.

Property 5:

Each of the functions $\frac{E_i(s_2)}{E_{i-1}(s_2)}, i = 1, 2, ..., p$ is a minimum reactive positive real function in s_2 (where a positive real function $E(s)$ is called minimum reactive (susceptive), if it has no poles or zeros on the imaginary axis of s). Similarly, each of the functions $\frac{F_j(s_1)}{F_{j-1}(s_1)}, j = 1, 2, ..., q$ is a minimum reactive positive real function in s_1.

1.10 Generation of VSHP

When VSHP is used in the denominator of a 2-D analog transfer function, it is guaranteed that the resulting 2-D digital bilinear transfer function obtained through the application of the well-known bilinear transformation is stable [31, 40]. Therefore, VSHP is highly useful in the 2-D digital filter design. We can first generate a two-variable Very Strictly Hurwitz Polynomial (VSHP) using its various properties and assign the generated VSHP to the denominator of the the 2-D analog transfer function, then obtain the digital transfer function through double bilinear transformations. Here, we review some methods, which are used to generate VSHP.

1.10.1 Using Terminated n-port Gyrator Networks

For a n-port gyrator network, its ports are terminated by capacitances. In much a case, the overall admittance matrix will be

$$A = \begin{bmatrix} \mu_1 & g_{12} & g_{13} & \cdots & g_{1n} \\ -g_{12} & \mu_2 & g_{23} & \cdots & g_{2n} \\ -g_{13} & -g_{23} & \mu_3 & \cdots & g_{3n} \\ \vdots & \vdots & \vdots & \ddots & \vdots \\ -g_{1n} & -g_{2n} & -g_{3n} & \cdots & \mu_n \end{bmatrix} \tag{1.62}$$

The determinant of the matrix A can be expressed as

$$D_n = \sum_{1\leq i\leq n} \mu_i |A_i| + \sum_{1\leq i_1<i_2<i_3<n} \mu_{i_1}\mu_{i_2}\mu_{i_3} |A_{i_1 i_2 i_3}| + \ldots + \mu_1\mu_2\mu_3 \ldots \mu_n \quad (n \; is \; odd) \tag{1.63}$$

or

$$D_n = |A_n| + \sum_{1\leq i_1<i_2<n} \mu_{i_1}\mu_{i_2} |A_{i_1 i_2}| + \sum_{1\leq i_1<i_2<i_3<i_4<n} \mu_{i_1}\mu_{i_2}\mu_{i_3}\mu_{i_4} |A_{i_1 i_2 i_3 i_4}| + \ldots + \mu_1\mu_2\mu_3 \ldots \mu_n \quad (n \; is \; even) \tag{1.64}$$

where $|A_{i_1 i_2}|$ is the determinant of the sub-matrix of A obtained by deleting both i_1^{th} and i_2^{th} rows and columns, the same holds for $|A_{i_1 i_2 i_3}|$, $|A_{i_2 i_3 i_4}|$, etc.

By making some of the $\mu_i's$ equal to $s_1$and some of $\mu_i's$ equal to s_2, under certain conditions, eqn. (1.63) and (1.64) will yield two-variable VSHPs [41].

1.10.2 Using the properties of positive semi-definite matrices

In this case, we first define three $n \times n$ square matrices A, μ and G as

$$A = \begin{bmatrix} a_{11} & a_{12} & \cdots & a_{1n} \\ a_{21} & a_{22} & \cdots & a_{2n} \\ \vdots & \vdots & \ddots & \vdots \\ a_{1n} & a_{2n} & \cdots & a_{nn} \end{bmatrix} \tag{1.65}$$

$$\mu = \begin{bmatrix} \mu_1 & \cdots & \cdots & \cdots & 0 \\ \vdots & \mu_2 & & & \\ \vdots & & \mu_3 & & \\ \vdots & & & \ddots & \\ 0 & \cdots & \cdots & \cdots & \mu_n \end{bmatrix} \tag{1.66}$$

$$G = \begin{bmatrix} 0 & g_{12} & g_{13} & \cdots & g_{1n} \\ -g_{12} & 0 & g_{23} & \cdots & g_{2n} \\ -g_{13} & -g_{23} & 0 & \cdots & g_{3n} \\ \vdots & \vdots & \vdots & \ddots & \vdots \\ -g_{1n} & -g_{2n} & -g_{3n} & \cdots & 0 \end{bmatrix} \tag{1.67}$$

where A is a general symmetrical $n \times n$ square matrix, μ is an $n \times n$ diagonal matrix and G is an $n \times n$ skew-symmetric matrix. These matrices A, μ and G are physically realizable.

Now, we define a matrix C as:

$$C = A\mu A^T + G \tag{1.68}$$

The determinant of matrix C is given by

$$M = det(C) \tag{1.69}$$

The polynomial M_n

$$M_n = M + \sum_{j=1}^{n} k_j \frac{\partial M}{\partial \mu_i} \tag{1.70}$$

is a two-variable VSHP when some of the $\mu_i's$ are properly made equal to s_1 and some of the $\mu_i's$ are equal to s_2 and it is made sure the requirements of VSHP are met [42].

1.10.3 Using the properties of the derivative of even or odd parts of Hurwitz polynomial

From eqn.(1.65) and (1.72), one can obtain an n^{th} order polynomial M_n as

$$M_n = det\,[\mu I + A] \tag{1.71}$$

From, the diagonal expansion of the determinant of matrix, M_n can be written as eqn. (1.63) and (1.64). We can observe that M_n is the odd (even) part of a n-variable Hurwitz polynomial when n is odd (even), so $\frac{\partial M_n/\partial \mu_i}{M_n}$ is a reactance function. Therefore,

$$M_n = M + \sum_{j=1}^{n} k_j \frac{\partial M}{\partial \mu_i} \tag{1.72}$$

is a n-variable Hurwitz polynomial.

Assigning some of $\mu_i's$ to s_1 and some to s_2, and ensuring the condition of two-variable VSHP, a two-variable VSHP could be generated for eqn. (1.72) [43, 44].

1.11 Objective of the Thesis

The main objective of the thesis is to propose a new technique in the design of the all-pole 2-D digital filters having variable magnitude characteristics. Ramachandran [14] et al. derived the necessary and sufficient conditions for the derivation of $k - D$ filter transfer functions via a combination of two all-pass transfer functions. However, using the method described in [14], only the development of all-pole 2-D band-pass and band-elimination filters will be feasible. It is not possible to derive the all-pole 2-D low pass and high pass filters using [14]. In this thesis, we have proposed a new technique to design such stable all-pole 2-D analog and digital lowpass and highpass filters using a combination of the all-pass filters. We have further extended this technique to derive the transfer functions for the all-pole 2-D analog and digital band-pass and band-stop filters.

The objectives of this thesis can be summarized as:

- Design of a all-pole 2-D digital lowpass and highpass filters having variable magnitude characteristics using the combination of all-pass filters.
- This technique has been further extended to design all-pole 2-D bandpass and bandstop filters having variable magnitude characteristics.
- Application of the designed all-pole 2-D digital lowpass filter in image processing.

1.12 Organization of the Thesis

The organization of the thesis is as follows. In Chapter 2, we will generate 2-D digital lowpass filter in Category A and the all-pole 2-D digital lowpass filter in Category B from the combination of all-pass filters. First, the second order Butterworth lowpass transfer function is taken and connected in all-pass filter manner. The analog transfer function of 2-D lowpass filter in both the categories are obtained. Then generalized bilinear transformation (GBT) is applied to the analog function to get its digital function. Also, in this chapter, the stability of the 2-D lowpass filters in both the categories will be defined and proved by verifying the denominator of the transfer function polynomial to be a very strict Hurwitz polynomial (VSHP). The conditions for each of the coefficients of the generalized bilinear transformation is defined for the 2-D digital lowpass filter in Category A and the all-pole 2-D lowpass filter in Category B. The effect of each coefficient of the generalized bilinear transformation resulting in the 2-D lowpass digital filter's magnitude response in both the categories is studied in detail.

In Chapter 3 and Chapter 4, we will generate the 2-D digital highpass filter and 2-D bandpass filter, respectively,in Category A and Category B, by using the 2-D digital lowpass filter in Category A and the all-pole 2-D digital highpass filter in Category B, proposed in Chapter 2. The conditions for each of the coefficients of the generalized bilinear transformation are defined for the 2-D digital highpass and bandstop filters, similar to 2-D digital lowpass filter in both the categories. The effect of each coefficient of the generalized

bilinear transformations resulting in 2-D highpass and bandpass digital filter's magnitude response in both the categories is studied in detail.

In Chapter 5, we will generate the 2-D digital bandstop filter from the 2-D analog lowpass filter in Category A and the all-pole 2-D digital bandstop filter from the the all-pole 2-D analog 2-D lowpass filter in Category B, proposed in Chapter 2. The 2-D analog lowpass filter is transformed to thee 2-D analog bandstop filter using lowpass to bandstop transformation technique in both the categories. The 2-D digital bandstop filter will then be generated by applying the generalized bilinear transformation to the 2-D analog bandstop filter in both the categories. Similar to Chapter 3, 4 and 5, the conditions for each of the coefficients of the generalized bilinear transformation is defined for the 2-D digital bandstop filter in both the categories. The effect of each coefficient of the generalized bilinear transformations resulting in the 2-D bandstop digital filter's magnitude response in both the categories is studied in detail.

In Chapter 6, we will discuss the application of the 2-D digital filters in image processing. The application will include recovering standard images degraded by the additive white Gaussian noise by using 2-D digital lowpass filtering in Category A and the all-pole 2-D lowpass filtering in Category B.

Chapter 7 gives the summary of the thesis, conclusion and the directions for the future investigations.

Chapter 2

All-pole 2-D Lowpass Filters Using All-Pass Filters

2.1 Introduction

In various applications we already have an existing network or we have to implement a multidimensional stable filter that does not have its 1-D equivalents. In multidimensional domain, filter design analysis becomes a tedious process. Often, design of such filters is based on various conditions and assumptions, which make the design of these filters practically feasible. Hence if we consider a transfer function obtained from combination of two all-pass filters, its generation as a stable 2-D filter requires certain conditions to be satisfied. But in 2-D network, specifying necessary and sufficient conditions for the coefficients of the filter is often a tedious task. Our emphasis in this chapter will be to find the possible ways to specify those conditions in a simple manner which allow the desired response to be achieved in 2-D digital filters.

In this chapter, we will design 2-D lowpass filters in analog and digital domain by considering the transfer function obtained by the combination of all-pass filters in Category A and Category B. The different methods for obtaining the network function from its real

or imaginary part are discussed. In this we will obtain 2-D analog lowpass filters from the generation of the transfer function obtained by the sum or difference of the single variable all-pass function in both the categories.

Section 2.2 gives a brief introduction to the 2-D lowpass Butterworth filter. Section 2.3 briefly describes the different methods to calculate the network function given its real part. In Section 2.4, we obtain the entire network function taking the given Butterworth function as the real part of the function. In Section 2.5, we will obtain the analog 2-D lowpass filters from the combination of the 2-D all-pass filters and ensure its stability by verifying it to be a VSHP. The derived analog lowpass filters is classified into two categories: Category A in which denominator polynomial is n^{th} order Butterworth polynomial and the numerator polynomial is $(n-1)^{th}$ order Butterworth polynomial, and Category B in which denominator polynomial is n^{th} order Butterworth polynomial and the numerator polynomial is the corresponding $(n-1)^{th}$ order real part of the n^{th} order Butterworth polynomial. By applying the generalized bilinear transformation, the analog lowpass filters can be transformed to its digital form. In Section 2.6 we will discuss and study the effects of the coefficients of the generalized bilinear transformation of the 2-D digital lowpass filters in Category A and the all-pole 2-D digital lowpass filters in Category B on the amplitude-frequency response. Finally, Section 2.7 gives the summary, discussions and comparison of the results contained in this chapter.

2.2 Butterworth Low-Pass Filter

The ideal low-pass amplitude is shown in Figure 2.1, in which ω_c is the normalized cutoff frequency. The amplitude function $|H(j\omega)|$ is an even function since it is the square root of the sum of the squares of the real and imaginary parts of $|H(j\omega)|$, which are respectively, even and odd functions. Therefore $|H(j\omega)|$ is a function of ω^2. A realizable $|H(j\omega)|^2$

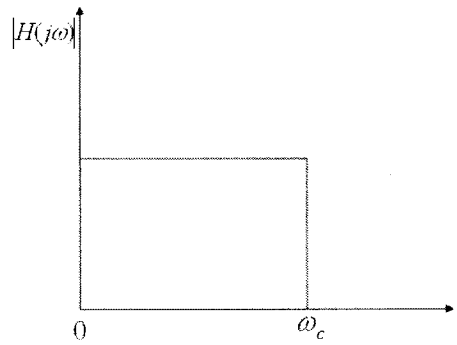

Figure 2.1: An ideal low-pass magnitude response

which approximates the ideal case of Figure 2.1 is given by

$$|H(j\omega)|^2 = \frac{A}{1 + f(\omega^2)} \tag{2.1}$$

where

$$f(\omega^2) \gg 1, \;\; \omega > \omega_c, 0 \leq f(\omega^2) \ll 1, \;\; 0 \ll \omega \ll \omega_c \tag{2.2}$$

This is evidently true since in the passband $0 \ll \omega \ll 1$, we have $|H(j\omega)|^2 \approx 1$, and in the stopband, $\omega > 1$, we have $|H(j\omega)|^2 \approx 0$, when $f(\omega^2)$ is given by eqn. (2.2).

One function suitable for use in eqn. (2.1) and (2.2) is given by

$$f(\omega^2) = \omega^{2n} \;\; ; \;\; n = 1, 2, 3, ... \tag{2.3}$$

It was first suggested by Butterworth. In this case

$$|H(\omega)| = \frac{1}{\sqrt{1 + \omega^{2n}}} \;\; ; \;\; n = 1, 2, 3..... \tag{2.4}$$

which is defined as the amplitude response of the $nth-order\ Butterworth\ filter$. This is a monotonically decreasing function and this it attains its maximum value, $|H(j\omega|_{max} = 1$, at $\omega = 0$. The approximation in eqn. (2.4) is better for higher values of n, since for $n_1 \gg n_2$, we have $\omega^{2n_1} \gg \omega^{2n_2}$ for $\omega > 1$. It is particularly good for near $\omega = 0$, by

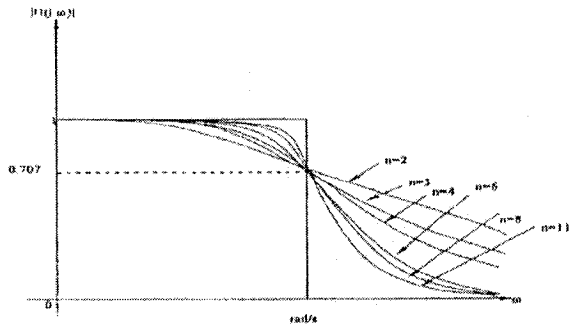

Figure 2.2: Butterworth Amplitude Response

expanding eqn. (2.4) using the binomial theorem, this results in

$$|H(j\omega)| = 1 - \frac{1}{2}\omega^{2n} + \frac{3}{8}\omega^{4n} - \frac{5}{16}\omega^{6n} + \frac{35}{128}\omega^{8n} - \cdots \tag{2.5}$$

which is valid for ω near 0. The first $(2n-1)$ derivatives of $|H(j\omega)|$ in eqn. (2.5) will contain a factor ω, and this will be zero at $\omega = 0$. Therefore for n large, the function $|H(j\omega)|$ near $\omega = 0$ is exceedingly flat, or it is *maximally flat*. For $\omega \gg 1$, the Butterworth amplitude function may be approximated by

$$|H(j\omega)| \approx \frac{1}{\omega^n} \tag{2.6}$$

with the loss in dB given by $\alpha_{dB}(\omega) \approx 20\log_{10}\omega^n = 20n\log_{10}\omega$.

Thus if the loss is plotted versus ω in decades, then for large ω, the loss $\alpha_{dB}(\omega)$ has a slope of $20n$dB/decade. The loss thus increases rapidly for large n, which indicates a good approximation to the ideal case [9].

Plots of $|H(j\omega)|$ and $\alpha_{dB}(\omega)$ are shown in the Figure 2.2 and Figure 2.3, for various values of n. Evidently the approximation to the ideal amplitude improves as n increases.

The transfer function of Butterworth filter whose amplitude is given in eqn. (2.4) is obtained by replacing ω^2 by $-s^2$ in $|H(j\omega)|^2$

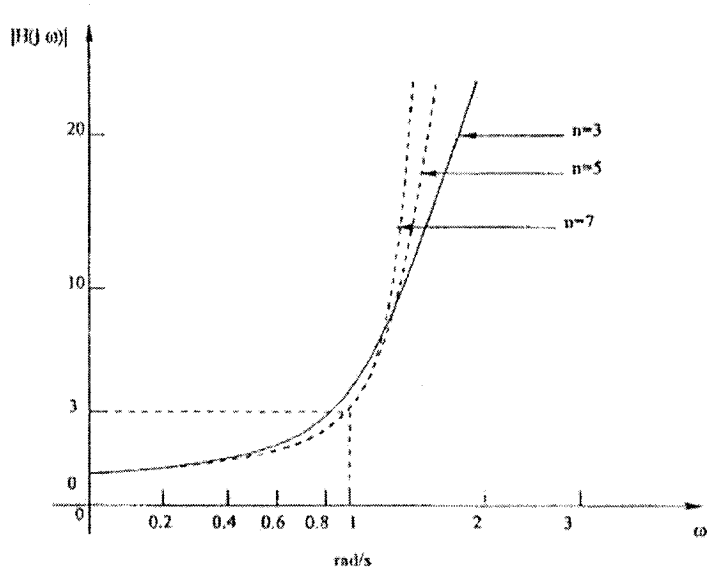

Figure 2.3: Butterworth Loss Curve

$$H(s)H(-s) = \frac{1}{1+(-s^2)^n} \tag{2.7}$$

so that

$$H(s) = \frac{1}{Q(s)} \tag{2.8}$$

where $Q(s)$ is the Hurwitz polynomial satisfying

$$Q(s)Q(-s) = 1 + (s^2)^n \tag{2.9}$$

As an example, if $n = 2$, the case of the second order Butterworth filter becomes

$$Q(s)Q(-s) = 1 + s^4 \tag{2.10}$$

which may be written as

$$Q(s)Q(-s) = (s^2 + \sqrt{2}s + 1)(s^2 - \sqrt{2}s + 1) \tag{2.11}$$

The first factor in the right member is the Hurwitz factor and is therefore $Q(s)$. Thus the transfer function of the second-order Butterworth low-pass filter

$$H(s) = \frac{K}{(s^2 + \sqrt{2}s + 1)} \tag{2.12}$$

where the constant K should be of any real numbers [2, 4].

2.3 Calculation of a Network Function from a Prescribed Real Part

In this section, it will be shown that given one part of a network function (e.g., the real part), the entire network function can be obtained. There are several approaches whereby a solution can be obtained in this case, namely Gewertz's method, Bode's method, and Mitra's method. Before discussing any of these methods, the following manipulation is considered [45].

The desired $H(s)$ is

$$H(s) = \frac{n(s)}{d(s)} = \frac{Evn(s) + Odn(s)}{Evd(s) + Odd(s)} = \frac{A(s) + sB(s)}{C(s) + sD(s)} \tag{2.13}$$

Hence,

$$H(s) = \frac{A(s) + sB(s)}{C(s) + sD(s)} \frac{C(s) - sD(s)}{C(s) - sD(s)} \tag{2.14}$$

$$= \frac{A(s)C(s) - s^2B(s)D(s)}{[C(s)]^2 - s^2[D(s)]^2} + \frac{sB(s)C(s) - sD(s)A(s)}{[C(s)]^2 - s^2[D(s)]^2} \tag{2.15}$$

where

$$EvH(s) = \frac{P(s)}{Q(s)} = \frac{A(s)C(s) - s^2B(s)D(s)}{[C(s)]^2 - s^2[D(s)]^2}$$

and

$$OdH(s) = \frac{R(s)}{Q(s)} = \frac{sB(s)C(s) - sD(s)A(s)}{[C(s)]^2 - s^2[D(s)]^2}$$

Therefore,

$$H(s) = \frac{P(s)}{Q(s)} + \frac{R(s)}{Q(s)} \tag{2.16}$$

Thus,

$$ReH(j\omega) = EvH(s)|_{s=j\omega} = \left.\frac{P(s)}{Q(s)}\right|_{s=j\omega} = \frac{A(j\omega)C(j\omega) + \omega^2 B(j\omega)D(j\omega)}{[C(j\omega)]^2 + \omega^2[D(j\omega)]^2} \tag{2.17}$$

Now substituting of $j\omega = s$ in the denominator of eqn. (2.17), yields

$$\begin{aligned} \left.[C(j\omega)]^2 + \omega^2[D(j\omega)]^2\right|_{j\omega=s} &= [C(s)]^2 - s^2[D(s)]^2 \\ &= [C(s) + sD(s)][C(s) - sD(s)] \\ &= [C(s) + sD(s)][C(-s) - sD(-s)] \end{aligned} \tag{2.18}$$

The eqn. (2.18) follows from the fact that $C(s)$ and $D(s)$ are even functions.

Now let the polynomial $C(s) + sD(s)$ in eqn. (2.18) be factored and assume that one such factor is $s + \alpha$, where α is in general a complex number. Then the polynomial $[C(-s) - sD(-s)]$ in eqn. (2.18) contains the factor $(-s + \alpha)$. Note that if $s = -\alpha$ is a pole in the left half plane (LPH), the pole $s = \alpha$ must lie in the right half plane (RHP), as in Figure 2.4. Because the poles of the network function $H(s)$ lie in the LPH, the procedure for obtaining denominator $d(s)$ of $H(s)$ (when $ReH(j\omega)$ is known) is clear. It consists of the following steps:

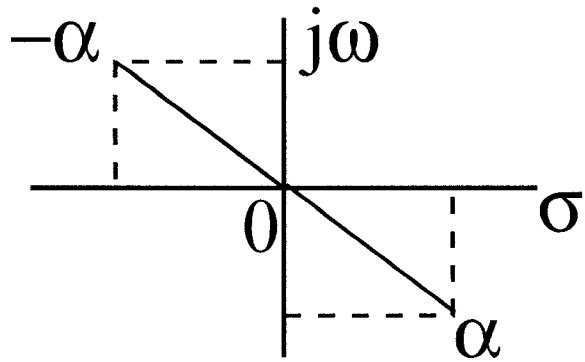

Figure 2.4: Location of the poles $-\alpha$ and α of $[C(s)]^2 - s^2[D(s)]^2$

Step 1a. Substitute s for $j\omega$ in the denominator polynomial of $ReH(j\omega)$, or alternatively, because this polynomial is even,

Step 1b. Substitute $-s^2$ for ω^2 in the denominator polynomial of $ReH(j\omega)$.

Step 2. Factor the polynomial.

Step 3. Collect all factors of the form $(s+a)$, (a^2+bs+c), where a, b and c are real and non-negative. The product of these factors yields $d(s)$.

Note that the zeros of $Q(s)$ on the $j\omega$ axis must be double, hence these zeros can be split between $d(s)$ and $d(-s)$. Thus, the preliminary manipulation yields the denominator $d(s) = [C(s) + sD(s)]$ of $H(s)$. It remains now to determine $n(s)$ and this the desired network function $H(s)$. This is done by one of the three methods mentioned at the outset, viz. Gewertz's, Bode's, or Mitra's [45].

2.3.1 Gewertz's Method.

This is an algebraic method and requires simultaneously solution of linear equations. The desired $H(s)$ is

$$H(s) = \frac{n(s)}{d(s)} = \frac{a_0 + a_1 s + \cdots + a_m s^m}{b_0 + b_1 s + \cdots + b_n s^n} \tag{2.19}$$

The $a's$ are the unknowns to be found, $d(s)$ (and hence, the $b's$) were determined by the

preliminary manipulation as explained above. Now by eqn. (2.17)

$$ReH(j\omega) = \frac{(a_0 - a_2\omega^2 + \cdots)(b_0 - b_2\omega^2 + \cdots)}{[C(j\omega)]^2 + \omega^2 [D(j\omega)]^2} + \frac{\omega^2(a_1 - a_3\omega^2 + \cdots)(b_1 - b_3\omega^2 + \cdots)}{[C(j\omega)]^2 + \omega^2 [D(j\omega)]^2} \tag{2.20}$$

But $ReH(j\omega)$ is given. Assume that it has the general form

$$ReH(j\omega) = \frac{P(j\omega)}{Q(j\omega)} = \frac{A_0 + A_2\omega^2 + \cdots + A_{2l}\omega^{2l}}{B_0 + B_2\omega^2 + \cdots + B_{2n}\omega^{2n}} \tag{2.21}$$

Equating the numerator coefficients of like powers of ω in eqn. (2.20) and (2.21) leads to

$$\begin{aligned} A_0 &= a_0 b_0 \\ A_2 &= a_0 b_2 - a_2 b_0 + a_1 b_1 \\ A_4 &= a_0 b_4 + a_2 b_2 + a_4 b_0 - a_1 b_3 - a_3 b_1 \end{aligned} \tag{2.22}$$

Solution of the simultaneous eqn. (2.22) yields the $a's$ and hence the desired $H(s)$.

2.3.2 Bode's Method:

This method utilizes the partial fraction expansion and it exhibits $H(s)$ in the partial fraction form. From equation

$$EvH(s) = \frac{1}{2}[H(s) + H(-s)]$$

we get

$$2EvH(s) = H(s) + H(-s) \tag{2.23}$$

Hence, if $2EvH(s)$ is expanded using partial fraction, the part corresponding to $H(s)$ has all the poles in the left half plane (LPH). Similarly $H(-s)$ is the part with all its poles in the right half plane (RHP). A constant term in $2EvH(s)$ is divided equally between $H(s)$ and $H(-s)$ [45].

2.3.3 Mitra's Method

This method has the great advantage of simplicity. In many cases Mitra's method gives $H(s)$ by inspection. In general, Mitra's method reduces to a modified Gewertz or Bode method. In this method one first determines $d(s) = C(s) + sD(s)$ and forms

$$\frac{P(s)}{C(s)sD(s)} = \frac{A(s)C(s) - s^2B(s)D(s)}{C(s)sD(s)} \tag{2.24}$$

where $P(s)$ is the numerator of $EvH(s)$ and hence can be found from the numerator of $ReH(j\omega)$ by substitution of $-s^2$ for ω^2. Thus eqn. (2.24) becomes

$$\frac{P(s)}{C(s)sD(s)} = \frac{A(s)}{sD(s)} - \frac{sB(s)}{C(s)} \tag{2.25}$$

By separating eqn. (2.25), it yields the even function $A(s)$ and the odd function $sB(s)$. Hence, the numerator $n(s) = A(s) + sB(s)$ can be formed [45].

2.4 Obtaining the function from its real part.

There are three methods for obtaining the function given its real or imaginary parts as explained in Section 2.3. Here we use Mitra's method to obtain a function given its real or imaginary part as this method has the advantage of greater simplicity as compared to the other two methods [45]. Taking a function of the form

$$F(s) = \frac{m_2 + n_2}{m_1 + n_1} \tag{2.26}$$

where m_1 is the even part of the denominator polynomial, n_1 is the odd part of the denominator polynomial, m_2 is the even part of the numerator polynomial and n_2 is the odd part of the numerator polynomial of the n^{th} order. The real part of the $F(s)$is given by

$$ReF(s) = \frac{m_1 m_2 - n_1 n_2}{m_1^2 - n_1^2} \tag{2.27}$$

Using Mitra's method,

$$ReF(s) = \frac{m_1 m_2 - n_1 n_2}{m_1 n_1} = \frac{k}{m_1 n_1} = \frac{m_2}{n_1} - \frac{n_2}{m_1} \tag{2.28}$$

where

$$m_1 m_2 - n_1 n_2 = k \tag{2.29}$$

where k is a positive constant. This is the required numerator of the real part.

Expanding eqn. (2.28) into partial fractions, we get m_2 and n_2.

Here we are taking $m_1 + n_1$ as the n^{th} Butterworth Polynomials and we are finding $m_2 + n_2$ of the $(n-1)^{th}$ order.

2.4.1 First Order Butterworth Polynomial

The first order Butterworth polynomial is given by

$$H(s) = m_1 + n_1 = s + 1 \tag{2.30}$$

where $m_1 = 1$ and $n_1 = s$

Using Mitra's method eqn. (2.28) and (2.29) i.e.,

$$ReF(s) = \frac{m_1 m_2 - n_1 n_2}{m_1 n_1} = \frac{k}{m_1 n_1} = \frac{m_2}{n_1} - \frac{n_2}{m_1} \tag{2.31}$$

Therefore, from eqn. (2.31)

$$\frac{k}{s} = \frac{m_2}{s} - \frac{n_2}{1} \tag{2.32}$$

Comparing eqn. (2.31) and (2.32), we get,

$m_2 = k$ and $n_2 = 0$ and so $m_2 + n_2 = k$

Therefore, taking first order Butterworth Polynomial $m_1 + n_1 = s + 1$ as a denominator function, we get $m_2 + n_2 = k$ as a numerator function.

2.4.2 Second Order Butterworth Polynomial

Taking the second order Butterworth polynomial,

$$H(s) = m_1 + n_1 = s^2 + 1.414s + 1 \tag{2.33}$$

where $m_1 = s^2 + 1$ and $n_1 = 1.414s$.

Using Mitra's method eqn. (2.28) and (2.29) i.e.,

$$ReF(s) = \frac{m_1 m_2 - n_1 n_2}{m_1 n_1} = \frac{k}{m_1 n_1} = \frac{m_2}{n_1} - \frac{n_2}{m_1} \tag{2.34}$$

where $m_1 m_2 - n_1 n_2 = k$ a positive constant.

Substituting the values of m_1 and $n_1$in eqn. (2.34) we get,

$$\frac{m_1 m_2 - n_1 n_2}{m_1 n_1} = \frac{k}{m_1 n_1} = \frac{k}{(s^2 + 1)(1.414s)} = \frac{k}{1.414s(s + j)(s - j)} \tag{2.35}$$

Using partial fraction expansion we get,

$$\frac{m_1m_2 - n_1n_2}{m_1n_1} = \frac{k}{m_1n_1} = \frac{k}{(s^2+1)(1.414s)} = \frac{k}{1.414s} - \left(\frac{0.7072ks}{s^2+1}\right) \tag{2.36}$$

Comparing eqn. (2.34) and (2.36), we get,

$$m_2 = k \; and \; n_2 = 0.7072ks$$

Therefore, taking the second order Butterworth polynomial $m_1 + n_1 = s^2 + 1.414s + 1$ as a denominator function, we get $m_2 + n_2 = 0.7072ks + k$ as a numerator function.

2.4.3 Third Order Butterworth Polynomial

Taking the third order Butterworth polynomial,

$$H(s) = m_1 + n_1 = s^3 + 2s^2 + 2s + 1 \tag{2.37}$$

where $m_1 = s^2 + 1$ and $n_1 = s^3 + 2s$

Using Mitra's method eqn. (2.28) and (2.29) i.e.,

$$ReF(s) = \frac{m_1m_2 - n_1n_2}{m_1n_1} = \frac{k}{m_1n_1} = \frac{m_2}{n_1} - \frac{n_2}{m_1} \tag{2.38}$$

where $m_1m_2 - n_1n_2 = k$ a positive constant.

Substituting the values of $m_1$and $n_1$in eqn. (2.37) we get,

$$\frac{k}{(2s^2+1)(s^3+2s)} = \frac{k}{s(s^2+2)(2s^2+1)} \tag{2.39}$$

$$= \frac{k}{s(s+j\sqrt{2})(s-j\sqrt{2})(2s^2+1)} \tag{2.40}$$

Using partial fraction expansion of eqn. (2.40) we get,

$$\frac{k}{s(s+j\sqrt{2})(s-j\sqrt{2})(2s^2+1)} = \frac{\frac{2s^2}{3}+k}{s^3+2s} - \frac{\frac{4ks}{3}}{2s^2+1} \tag{2.41}$$

Comparing eqn. (2.37) and (2.41), we get,

$$m_2 = \frac{2ks^2}{3} + k = 0.6666ks^2 + k \; and \; n_2 = \frac{4ks}{3} = 1.3333ks$$

Therefore, taking the third order Butterworth polynomial $m_1 + n_1 = s^3 + 2s^2 + 2s + 1$ as a denominator function, we get $m_2 + n_2 = 0.6666ks^2 + 1.3333ks + k$ as a numerator function.

N= Order of Filter	Denominator Function $m_1 + n_1$ is a Butterworth Polynomial	Numerator Function $m_2 + n_2$
1	$s+1$	k
2	$s^2 + 1.414s + 1$	$0.7072sk + k$
3	$s^3 + 2s^2 + 2s + 1$	$0.6666ks^2 + 1.3333ks + k$
4	$(s^2 + 0.765s + 1)(s^2 + 1.848s + 1) =$ $s^4 + 1.848s^3 + 2.765s^2 + 4.026s + 1$	$1.14ks^3 + 2.11ks^2 + 1.21ks + k$
5	$(s+1)(s^2 + 0.618s + 1)(s^2 + 1.618s + 1) =$ $s^5 + 3.23s^4 + 5.2359s^3 + 5.2359s^2 + 3.236s + 1$	$0.6598ks^4 + 2.0943ks^3 +$ $3.1502ks^2 + 2.588ks + 1$
6	$(s^2 + 0.518s + 1)(s^2 + 1.414s + 1)$ $(s^2 + 1.932s + 1) = s^6 + 3.864s^5 + 7.465s^4 +$ $9.143s^3 + 7.4651s^2 + 3.8464s + 1$	$0.6436ks^5 + 2.4876ks^4 +$ $4.5694ks^3 + +4.9753ks^2 +$ $3.2194ks + k$

Table 2.1: Numerator of the corresponding denominator for Butterworth Polynomial

Similarly, using different order of Butterworth polynomials taken as the denominator of a network function, we can find the numerator function of the entire network, which is shown in the Table 2.1 up to sixth order. Here we have assume the value of $k = 1$ without any loss of generality.

2.5 Transfer Function of 2-D Lowpass Filters using All-pass Filters

In this section, a new technique has been introduced to design 2-D low pass filters in the digital domain by considering the transfer function obtained by the combination of all-pass filters. The all-pass filters combination is presented in the block diagram shown in Figure 2.5

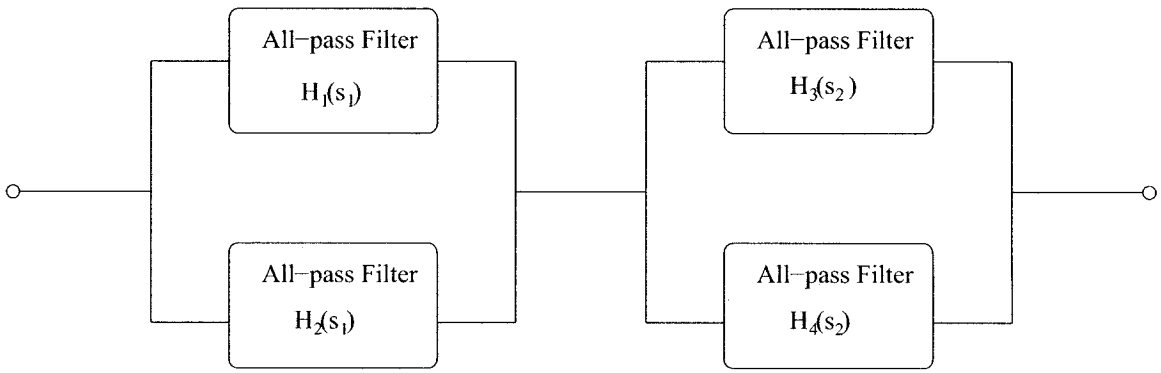

Figure 2.5: Block Diagram of the all-pass filter combination

A new transfer function can be obtained in the analog and digital domain by the combination of the all pass filters as shown in Figure 2.5. One can start from the analog domain and then apply the required bilinear transformation [8].

$$s_i \rightarrow k_i \frac{z_i - a_i}{z_i + b_i} \tag{2.42}$$

where $i = 1, 2$ for 2-D filters, to obtain the required digital transfer function. For resulting 2-D filters to be stable, it is required that $k_i > 0$, and $|a_i| < 1$ and in particular $b_i = 1$ for a low pass filter. If the filter in the analog domain is stable, then by applying generalized bilinear transformation and satisfying stability criteria, the digital filter will also be stable.

There are two possible cases to obtain the transfer function of a 2-D lowpass filters when $H_1(s)$ and $H_3(s)$ are the n^{th} order Butterworth polynomials connected in all-pass filters manner.

Category A: When the $(n-1)^{th}$ order filters, $H_2(s)$ and $H_4(s)$ are the corresponding Butterworth polynomial connected in all pass filters manner.

Category B: When the $(n-1)^{th}$ order filters, $H_2(s)$ and $H_4(s)$ are the corresponding real part of the n^{th} order Butterworth polynomial connected in all-pass filters manner.

2.5.1 Transfer Function of the 2-D Lowpass Filters using All-pass Filters in Category A

In this section we will derive the transfer function of 2-D low pass filters using the Category A mentioned above. In this case we consider the n^{th} order Butterworth polynomial and the corresponding $(n-1)^{th}$ order also as Butterworth polynomial.

Here we are considering second order Butterworth polynomial connected in an all pass way. Here $H_1(s_1)$ is of n^{th} order, i.e. second order Butterworth polynomial, and $H_2(s_1)$ is of $(n-1)^{th}$ order, i.e. first order Butterworth polynomial in one dimension, and both the transfer functions are connected in an all pass manner.

$$H_1(s_1) = \frac{s_1^2 - 1.414s_1 + 1}{s_1^2 + 1.414s_1 + 1} \tag{2.43}$$

$$H_2(s_1) = \frac{-s_1 + 1}{s_1 + 1} \tag{2.44}$$

Similarly $H_3(s_2)$ is of n^{th}order, i.e. second order Butterworth polynomial, and $H_4(s_2)$ is of $(n-1)^{th}$ order, i.e. first order Butterworth polynomial in second dimension, and both the transfer functions are connected in an all pass manner.

$$H_3(s_2) = \frac{s_2^2 - 1.414s_2 + 1}{s_2^2 + 1.414s_2 + 1} \tag{2.45}$$

$$H_4(s_2) = \frac{-s_2 + 1}{s_2 + 1} \tag{2.46}$$

Adding $H_1(s_1)$ and $H_2(s_1)$ we get,

$$H_{12}(s_1) = H_1(s_1) + H_2(s_1) \tag{2.47}$$

$$= \frac{s_1^2 - 1.414s_1 + 1}{s_1^2 + 1.414s_1 + 1} + \frac{-s_1 + 1}{s_1 + 1} \tag{2.48}$$

Therefore,

$$H_{12}(s_1) = \frac{2 - 0.828s_1^2}{s_1^3 + 2.414s_1^2 + 2.414s_1 + 1} \tag{2.49}$$

Similarly adding $H_3(s_2)$ and $H_4(s_2)$ we get,

$$H_{34}(s_2) = H_3(s_2) + H_4(s_2) \tag{2.50}$$

$$= \frac{s_2^2 - 1.414s_2 + 1}{s_2^2 + 1.414s_2 + 1} + \frac{-s_2 + 1}{s_2 + 1} \tag{2.51}$$

Therefore,

$$H_{34}(s_2) = \frac{2 - 0.828s_2^2}{s_2^3 + 2.414s_2^2 + 2.414s_2 + 1} \tag{2.52}$$

Multiplying eqn. (2.49) and (2.52), we get,

$$H(s_1, s_2) = H_{12}(s_1).H_{34}(s_2) \tag{2.53}$$

$$= \left(\frac{2 - 0.828s_1^2}{s_1^3 + 2.414s_1^2 + 2.414s_1 + 1}\right) \cdot \left(\frac{2 - 0.828s_2^2}{s_2^3 + 2.414s_2^2 + 2.414s_2 + 1}\right) \tag{2.54}$$

Therefore the analog transfer function is given by

$$H(s_1, s_2) = \frac{N(s_1, s_2)}{D(s_1, s_2)} \tag{2.55}$$

where

$$N(s_1, s_2) = 4 - 1.656s_1^2 - 1.656s_2^2 + 0.685584s_1^2 \tag{2.56}$$

and

$$D(s_1, s_2) = \begin{bmatrix} s_1^3(s_2^3 + 2.414s_2^2 + 2.414s_2 + 1)+ \\ s_1^2(2.414s_2^3 + 5.827396s_2^2 + 5.827396s_2 + 2.414)+ \\ s_1(2.414s_2^3 + 5.827396s_2^2 + 5.827396s_2 + 2.414)+ \\ 1(s_2^3 + 2.414s_2^2 + 2.414s_2 + 1) \end{bmatrix} \tag{2.57}$$

Therefore the resultant analog transfer function is given by

$$H(s_1, s_2) = \frac{4 - 1.656s_1^2 - 1.656s_2^2 + 0.685584s_1^2 s_2^2}{\begin{bmatrix} s_1^3(s_2^3 + 2.414s_2^2 + 2.414s_2 + 1)+ \\ s_1^2(2.414s_2^3 + 5.827396s_2^2 + 5.827396s_2 + 2.414)+ \\ s_1(2.414s_2^3 + 5.827396s_2^2 + 5.827396s_2 + 2.414)+ \\ 1(s_2^3 + 2.414s_2^2 + 2.414s_2 + 1) \end{bmatrix}} \tag{2.58}$$

The stability of the filter is defined by the denominator of the transfer function, we have to make the filter's transfer function free from singularities of the first and second kind (see Section 1.8). Therefore, we should prove the denominator polynomial to be a VSHP [29]. If we simplify the denominator polynomial, i.e. eqn. (2.57), it can be readily verified that the denominator polynomial is a Strictly Hurwitz Polynomial (SHP) [29]. Further, based on the test methodology to check for VSHP[29], we get,

$$D(s_1, s_2) = D\left(\frac{1}{s_1}, s_2\right) = D\left(s_1, \frac{1}{s_2}\right) = D\left(\frac{1}{s_1}, \frac{1}{s_2}\right) \neq \frac{0}{0} \tag{2.59}$$

where $s_1 = 0$ and $s_2 = 0$.

Since the non-essential singularities of the first and the second kind are ruled out, we can conclude that the denominator polynomial, $D(s_1, s_2)$is a VSHP. If we go into the discrete (z) domain by applying analog to digital transformation, the generalized bilinear transformation, the transfer function so obtained will also be stable.

For the 2-D filter transfer function in the analog domain given in eqn. (2.58), applying the generalized bilinear transformation [8], i.e., $s_1 = k_1\left(\frac{z_1 - a_1}{z_1 + b_1}\right)$ and $s_2 = k_2\left(\frac{z_2 - a_2}{z_2 + b_2}\right)$, where $k_1 > 0$, $k_2 > 0$, $|a_1| < 1$, $|a_2| < 1$ and $b_1 = b_2 = 1$ in particular to obtain a low pass filter transfer function, the 2-D digital transfer function using second order Butterworth polynomial is given by,

$$H(z_1, z_2) = \frac{P(z_1, z_2)}{Q(z_1, z_2)} \tag{2.60}$$

where

$$P(z_1, z_2) = \begin{bmatrix} 4(z_1+1)^3(z_2+1)^3 - 1.656k_1^2(z_1+1)(z_1-a_1)^2(z_2+1)^3 \\ -1.656k_2^2(z_2+1)(z_2-a_2)^2(z_1+1)+ \\ 0.6855k_1^2k_2^2(z_1+1)(z_2+1)(z_1-a_1)^2(z_2-a_2)^2 \end{bmatrix} \tag{2.61}$$

and

$$Q(z_1, z_2) = k_1^3(z_1 - a_1)^3 \begin{bmatrix} k_2^3(z_2-a_2)^3+ \\ 2.414k_2^2(z_2+1)(z_2-a_2)^2+ \\ 2.414k_2(z_2+1)^2(z_2-a_2)+ \\ (z_2+1)^3 \end{bmatrix}$$

$$
\begin{aligned}
&+ \quad k_1^2(z_1-a_1)^2(z_1+1)\begin{bmatrix} 2.414k_2^3(z_2-a_2)^3+ \\ 5.8274k_2^2(z_2+1)(z_2-a_2)^2+ \\ 5.8274k_2(z_2+1)^2(z_2-a_2)+ \\ 2.414(z_2+1)^3 \end{bmatrix} \\
&+ \quad k_1(z_1-a_1)(z_1+1)^2\begin{bmatrix} 2.414k_2^3(z_2-a_2)^3+ \\ 5.8274k_2^2(z_2+1)(z_2-a_2)^2+ \\ 5.8274k_2(z_2+1)^2(z_2-a_2)+ \\ 2.414(z_2+1)^3 \end{bmatrix} \\
&+ \quad (z_1+1)^3\begin{bmatrix} k_2^3(z_2-a_2)^3+ \\ 2.414k_2^2(z_2+1)(z_2-a_2)^2+ \\ 2.414k_2(z_2+1)^2(z_2-a_2)+ \\ (z_2+1)^3 \end{bmatrix}
\end{aligned} \tag{2.62}
$$

The transfer function of 2-D lowpass filter in analog domain is given by eqn. (2.58) and the transfer function of 2-D lowpass filter in digital domain is given by eqn. (2.60). As seen from the eqn. (2.58) and (2.60), we are getting stable transfer functions of 2-D lowpass filters in analog and digital domain. But we are not able to obtain the transfer functions in analog and digital domain for the all-pole 2-D lowpass filters.

We can also design all-pole analog and digital lowpass filters which can be obtained by using the Category B mentioned above. The transfer functions of the all-pole 2-D lowpass filters in analog and digital domain is derived in the next section.

2.5.2 Transfer Function of the All-pole 2-D Lowpass Filters using All-pass Filters in Category B

In this section we will derive the transfer function of the all-pole 2-D low pass filters in analog and digital domain using the Category B mentioned above. In this case we will consider the n^{th} order Butterworth polynomial and the corresponding $(n-1)^{th}$ order from its real

part derived in the previous Section 2.4. The Butterworth polynomial and its corresponding real part is shown in Table 2.1.

The transfer function of the all-pole 2-D lowpass filter is designed in analog and digital domain. One can start from the n^{th} order Butterworth polynomial and taking $(n-1)^{th}$ order as its corresponding real part connected in all-pass way as shown in the block diagram Figure 2.5.

Here we are considering second order Butterworth polynomial connected in all pass way. $H_1(s_1)$ is of n^{th} order, i.e. second order Butterworth polynomial, and $H_2(s_1)$ is of $(n-1)^{th}$ order, i.e. first order real part of the Butterworth polynomial in one dimension, and both the transfer function are connected in an all pass manner.

$$H_1(s_1) = \frac{s_1^2 - 1.414s_1 + 1}{s_1^2 + 1.414s_1 + 1} \tag{2.63}$$

$$H_2(s_1) = \frac{-0.707s_1 + 1}{0.707s_1 + 1} \tag{2.64}$$

Here we have assumed the value of $k = 1$ without any loss of generality.

Similarly $H_3(s_2)$ is of n^{th} order, i.e. second order Butterworth polynomial, and $H_4(s_2)$ is of $(n-1)^{th}$ order, i.e. first order real part of the Butterworth polynomial in second dimension, and both the transfer function are connected in an all pass manner

$$H_3(s_2) = \frac{s_2^2 - 1.414s_2 + 1}{s_2^2 + 1.414s_2 + 1} \tag{2.65}$$

$$H_4(s_2) = \frac{-0.707s_2 + 1}{0.707s_2 + 1} \tag{2.66}$$

Here we have assumed the value of $k = 1$ without any loss of generality.

Adding eqn. (2.63) and (2.64) and taking $k = 1$, i.e,

$$H_{12}(s_1) = H_1(s_1) + H_2(s_1) \tag{2.67}$$

$$= \frac{s_1^2 - 1.414s_1 + 1}{s_1^2 + 1.414s_1 + 1} + \frac{-0.707s_1 + 1}{0.707s_1 + 1} \tag{2.68}$$

Therefore we get,

$$H_{12}(s_1) = \frac{2}{0.707s_1^3 + 2s_1^2 + 2.12s_1 + 1} \tag{2.69}$$

Similarly, adding eqn. (2.65) and (2.66) and taking $k = 1$, i.e.,

$$H_{34}(s_2) = H_3(s_2) + H_4(s_2) \tag{2.70}$$

$$= \frac{s_2^2 - 1.414s_2 + 1}{s_2^2 + 1.414s_2 + 1} + \frac{-0.707s_2 + 1}{0.707s_2 + 1} \tag{2.71}$$

Therefore we get,

$$H_{34}(s_2) = \frac{2}{0.707s_2^3 + 2s_2^2 + 2.12s_2 + 1} \tag{2.72}$$

Multiplying eqn. (2.69) and (2.72),

$$H(s_1, s_2) = H_{12}(s_1).H_{34}(s_2) \tag{2.73}$$

$$= \left(\frac{2}{0.707s_1^3 + 2s_1^2 + 2.12s_1 + 1}\right) \cdot \left(\frac{2}{0.707s_2^3 + 2s_2^2 + 2.12s_2 + 1}\right) \tag{2.74}$$

Therefore the analog transfer function is given by

$$H(s_1, s_2) = \frac{N(s_1, s_2)}{D(s_1, s_2)} \tag{2.75}$$

where

$$N(s_1, s_2) = 4 \tag{2.76}$$

$$D(s_1, s_2) = \begin{bmatrix} s_1^3(0.5s_2^3 + 1.414s_2^2 + 1.5s_2 + 0.707) + \\ s_1^2(1.414s_2^3 + 4s_2^2 + 4.24s_2 + 2) + \\ s_1(1.5s_2^3 + 4.24s_2^2 + 4.5s_2 + 2.12) + \\ 1(0.707s_2^3 + 2s_2^2 + 2.12s_2 + 1) \end{bmatrix} \tag{2.77}$$

The stability of the filter is defined by the denominator of the transfer function and thus, we have to make the filter's transfer function free from singularities of the first and second kind (see Section 1.8). Therefore, we should prove the denominator polynomial to be a VSHP. [29]. If we simplify the denominator polynomial i.e. eqn. (2.77), it can be readily verified that the denominator polynomial is a strictly Hurwitz polynomial (SHP) [29]. Further, based on the test methodology to check for VSHP [29], we get,

$$D(s_1, s_2) = D\left(\frac{1}{s_1}, s_2\right) = D\left(s_1, \frac{1}{s_2}\right) = D\left(\frac{1}{s_1}, \frac{1}{s_2}\right) \neq \frac{0}{0} \tag{2.78}$$

where $s_1 = 0$ and $s_2 = 0$.

Since the non-essential singularities of the first and the second kind are ruled out, we can conclude that the denominator polynomial, $D(s_1, s_2)$ is a VSHP. If we go into the discrete (z) domain by applying analog to digital transformation, the generalized bilinear transformation, the transfer function so obtained will be stable.

The all-pole 2-D filter transfer function of lowpass filter in the analog domain is

$$H(s_1, s_2) = \frac{4}{\left[\begin{array}{c} s_1^3(0.5s_2^3 + 1.414s_2^2 + 1.5s_2 + 0.707)+ \\ s_1^2(1.414s_2^3 + 4s_2^2 + 4.24s_2 + 2)+ \\ s_1(1.5s_2^3 + 4.24s_2^2 + 4.5s_2 + 2.12)+ \\ 1(0.707s_2^3 + 2s_2^2 + 2.12s_2 + 1) \end{array}\right]} \tag{2.79}$$

Applying the generalized bilinear transformation [8], i.e., $s_1 = k_1\left(\frac{z_1 - a_1}{z_1 + b_1}\right)$ and $s_2 = k_2\left(\frac{z_2 - a_2}{z_2 + b_2}\right)$, where $k_1 > 0$, $k_2 > 0$, $|a_1| < 1$, $|a_2| < 1$ and $b_1 = b_2 = 1$ in particular to obtain a low pass filter transfer function, to eqn. (2.79), the all-pole 2-D digital transfer function of lowpass filter using second order Butterworth polynomial is given by

$$H(z_1, z_2) = \frac{P(z_1, z_2)}{Q(z_1, z_2)} \tag{2.80}$$

where

$$P(z_1, z_2) = 4(z_1 + b_1)^3(z_2 + b_2)^3 \tag{2.81}$$

and

$$\begin{aligned} Q(z_1, z_2) &= k_1^3(z_1 - a_1)^3 \left[\begin{array}{c} 0.5k_2^3(z_2 - a_2)^3+ \\ 1.414k_2^2(z_2 - a_2)^2(z_2 + b_2)+ \\ 1.5k_2(z_2 - a_2)(z_2 + b_2)^2+ \\ 0.707(z_2 + b_2)^3 \end{array}\right] \\ &+ k_1^2(z_1 - a_1)^2(z_1 + b_1) \left[\begin{array}{c} 1.414k_2^3(z_2 - a_2)^3+ \\ 4k_2^2(z_2 - a_2)^2(z_2 + b_2)+ \\ 4.24k_2(z_2 - a_2)(z_2 + b_2)^2+ \\ 2(z_2 + b_2)^3 \end{array}\right] \end{aligned}$$

$$
\begin{aligned}
&+ \quad k_1(z_1-a_1)(z_1+b_1)^2 \begin{bmatrix} 1.5k_2^3(z_2-a_2)^3+ \\ 4.24k_2^2(z_2-a_2)^2(z_2+b_2)+ \\ 4.5k_2(z_2-a_2)(z_2+b_2)^2+ \\ 2.12k_2^2(z_2+b_2)^3 \end{bmatrix} \\
&+ \quad (z_1+b_1)^3 \begin{bmatrix} 0.707k_2^3(z_2-a_2)^3+ \\ 2k_2^2(z_2-a_2)^2(z_2+b_2) \\ 2k_2(z_2-a_2)(z_2+b_2)^2 \\ (z_2+b_2)^3 \end{bmatrix}
\end{aligned} \tag{2.82}
$$

The transfer function of the all-pole 2-D lowpass filter in analog domain is given by eqn. (2.79) and the transfer function of the all-pole 2-D lowpass filter in digital domain is given by eqn. (2.80). As seen from the eqn. (2.79) and (2.80), we are getting the stable transfer functions of the all-pole 2-D lowpass filter in analog and digital domain.

N=Order of the Filter	Transfer Function of 2-D lowpass filter in Category A
3	$\dfrac{\begin{bmatrix} 1.37s_1^4s_2^4+0.40s_1^4s_2^2+2.34s_1^4+0.40s_1^2s_2^4+ \\ 0.12s_1^2s_2^2+0.68s_1^2+2.34s_2^4+0.68s_2^2+4 \end{bmatrix}}{\begin{bmatrix} s_1^5(s_2^5+3.41s_2^4+5.82s_2^3+5.82s_2^2+3.41s_2+1) \\ +s_1^4(3.41s_2^5+11.65s_2^4+19.89s_2^3++19.89s_2^2+11.65s_2+3.41) \\ +s_1^3(5.82s_2^5+19.89s_2^4+33.96s_2^3+33.96s_2^2+19.89s_2+5.82) \\ +s_1^2(5.82s_2^5+19.89s_2^4+33.96s_2^3+33.96s_2^2+19.89s_2+5.82) \\ +s_1(3.41s_2^5+11.65s_2^4+19.89s_2^3+19.89s_2^2+11.65s_2+3.41) \\ +1(s_2^5+3.41s_2^4+5.82s_2^3+5.82s_2^2+3.41s_2+1) \end{bmatrix}}$
4	$\dfrac{\begin{bmatrix} 0.09s_1^6s_2^6-0.72s_1^6s_2^4-1.99s_1^6s_2^2+0.61s_1^6-0.72s_1^4s_2^6+5.68s_1^4s_2^4+5.67s_1^4s_2^2-4.76s_1^4 \\ -1.99s_1^2s_2^6+15.67s_1^2s_2^4+43.22s_1^2s_2^2-13.15s_1^2+0.61s_2^6-4.76s_2^4-13.15s_2^2+4 \end{bmatrix}}{\begin{bmatrix} s_1^7(s_2^7+3.84s_2^6+8.46s_2^5+14.25s_2^4+16.439s_2^3+12.82s_2^2+6.03s_2+1)+ \\ s_1^6(3.84s_2^7+14.80s_2^6+32.56s_2^5+54.84s_2^4+63.22s_2^3+49.32s_2^2+23.2s_2+3.84)+ \\ s_1^5(8.46s_2^7+32.56s_2^6+71.58s_2^5+120.58s_2^4+139.01s_2^3+108.44s_2^2+50.98s_2+8.46)+ \\ s_1^4(14.25s_2^7+54.84s_2^6+120.58s_2^5+203.11s_2^4+234.16s_2^3+182.66s_2^2+85.88s_2+14.25)+ \\ s_1^3(16.43s_2^7+63.22s_2^6+139.01s_2^5+234.16s_2^4+269.94s_2^3+210.58s_2^2+99.01s_2+16.43)+ \\ s_1^2(12.82s_2^7+49.32s_2^6+108.44s_2^5+182.66s_2^4+210.58s_2^3+164.27s_2^2+77.23s_2++12.82)+ \\ s_1(6.01s_2^7+23.18s_2^6+50.98s_2^5+85.88s_2^4+99.01s_2^3+77.23s_2^2+36.31s_2+6.01)+ \\ 1(s_2^7+3.84s_2^6+8.46s_2^5+14.25s_2^4+16.43s_2^3+12.82s_2^2+6.01s+1) \end{bmatrix}}$

Table 2.2: Transfer Function of 2-D lowpass filter in analog domain for Category A up to fourth order

Similarly, using different order of Butterworth polynomials taken as the denominator of a network function, we can find the transfer function of the 2-D lowpass filter for the Category A and the transfer function of the all-pole 2-D lowpass filter for the Category B,

which is shown in the Table 2.2 and 2.3 up to fourth order in analog domain.

N=Order of the Filter	Transfer Function of the All-pole 2-D lowpass filter in Category B
3	$\frac{4}{\left[\begin{array}{c} s_1^5(0.44s_2^5+1.78s_2^4+3.33s_2^3+4.88s_2^2+2.22s_2+0.66)+ \\ s_1^4(1.78s_2^5+7.11s_2^4+13.33s_2^3+19.55s_2^2+8.88s_2+2.66)+ \\ s_1^3(3.33s_2^5+13.33s_2^4+25s_2^3+36.66s_2^2+16.66s_2+5)+ \\ s_1^2(4.88s_2^5+19.55s_2^4+36.66s_2^3+53.77s_2^2+24.44s_2+7.33)+ \\ s_1(2.22s_2^5+8.88s_2^4+16.66s_2^3+24.44s_2^2+11.08s_2+3.33)+ \\ +1(0.66s_2^5+2.66s_2^4+5s_2^3+7.33s_2^2+3.33s_2+1) \end{array}\right]}$
4	$\frac{4}{\left[\begin{array}{c} s_1^7(1.3s_2^7+4.81s_2^6+9.4s_2^5+15.55s_2^4+16.9s_2^3+11.1s_2^2+5.96s_2+1.14)+ \\ s_1^6(4.81s_2^7+17.8s_2^6+34.81s_2^5+57.56s_2^4+62.58s_2^3+41.10s_2^2+22.07s_2+4.22)+ \\ s_1^5(9.4s_2^7+34.8s_2^6+68.06s_2^5+112.5s_2^4+122.35s_2^3+80.35s_2^2+43.15s_2+8.25)+ \\ s_1^4(15.55s_2^7++57.56s_2^6+112.5s_2^5+186.05s_2^4+202.28s_2^3+132.85s_2^2+71.33s_2+13.64)+ \\ s_1^3(16.9s_2^7+62.58s_2^6+122.35s_2^5+202.28s_2^4+219.92s_2^3+144.44s_2^2+77.56s_2+14.83)+ \\ s_1^2(11.1s_2^7+41.10s_2^6+80.35s_2^5+132.85s_2^4+144.44s_2^3+94.86s_2^2+50.94s_2+9.74)+ \\ s_1(5.96s_2^7+22.07s_2^6+43.14s_2^5+71.33s_2^4+77.56s_2^3+50.94s_2^2+27.35s_2+5.23)+ \\ +1(1.14s_2^7+4.22s_2^6+8.25s_2^5+13.64s_2^4+14.83s_2^3+9.74s_2^2+5.23s+1) \end{array}\right]}$

Table 2.3: Transfer Function of the All-pole 2-D lowpass filter in analog domain for Category B up to fourth order

2.6 Frequency Response of 2-D Digital Lowpass Filters

2.6.1 Frequency Response of 2-D Digital Lowpass Filter in Category A

The transfer function for the lowpass filter is obtained by using the second order Butterworth polynomial connected in the all pass filter manner. The resultant transfer function eqn. (2.58) obtained is digitized by applying the generalized bilinear transformation eqn. (2.42). The digitized transfer function of 2-D digital lowpass filter is given by eqn. (2.60). With the input coefficient of generalized bilinear transformation we can obtain the contour and 3-D magnitude plots of the resulting 2-D digital lowpass filter [46].

To investigate the manner in which each coefficient of generalized bilinear transformation effects the magnitude response of the resulting 2-D digital lowpass filter, we change the values of some of the coefficients or fixing some of the coefficients to a specific values. It is possible to obtain a 2-D digital lowpass filter when the coefficients are in the limits of $k_i > 0, 0 < |a_i| < 1$ and taking $b_i = 1$ where $i = 1, 2$. Let us consider the coefficients of the

generalized bilinear transformation for the 2-D digital lowpass filter to be unity i.e., $a_1 = 1$, $a_2 = 1$, $k_1 = 1$, $k_2 = 1$, $b_1 = 1$, $b_2 = 1$. Under this condition, the 3-D amplitude-frequency response and contour plots of the 2-D digital filter are shown in the Figure 2.6.

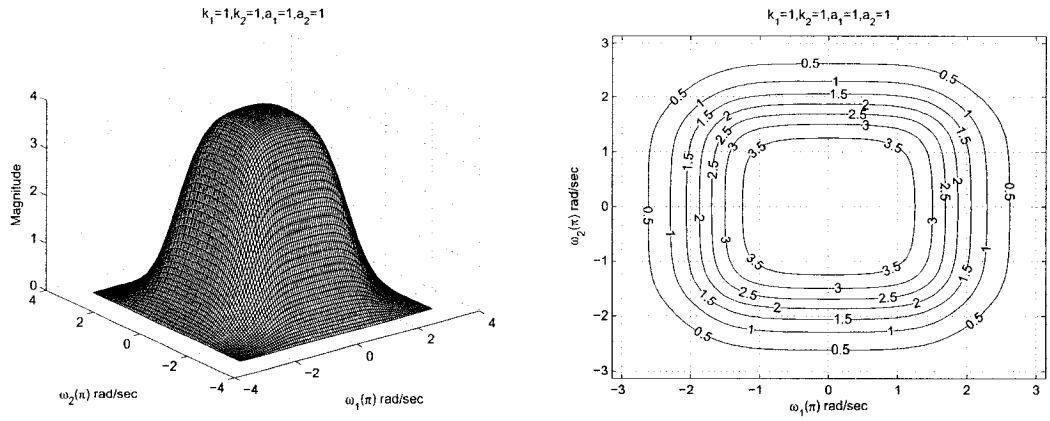

Figure 2.6: 3-D Amplitude frequency response and contour response of the 2-D digital lowpass filter with all the coefficient values as unity.

2.6.1.1 Frequency Response of 2-D Digital Lowpass Filter with different values of k_1

In this section, we study the manner in which k_1 effects the frequency response behavior of the resulting 2-D digital lowpass filter in Category A and to separate the effect of the other coefficients, we vary the values of k_1, and fixing all the other coefficient of the generalized bilinear transformation to be unity in order not to loose any generality and to make the situation simple, e.g. with $k_2 = 1$, $a_1 = 1$, $a_2 = 1$, $b_1 = 1$ and $b_2 = 1$. The values of k_1 are varied from 0.1 to 10 and the 3-D magnitude response and the contour plots for the lowpass filter with the values of $k_1 = 0.1$, $k_1 = 0.5$, $k_1 = 0.9$, $k_1 = 2$, $k_1 = 5$, and $k_1 = 10$ are shown in the Figures 2.7 and 2.8.

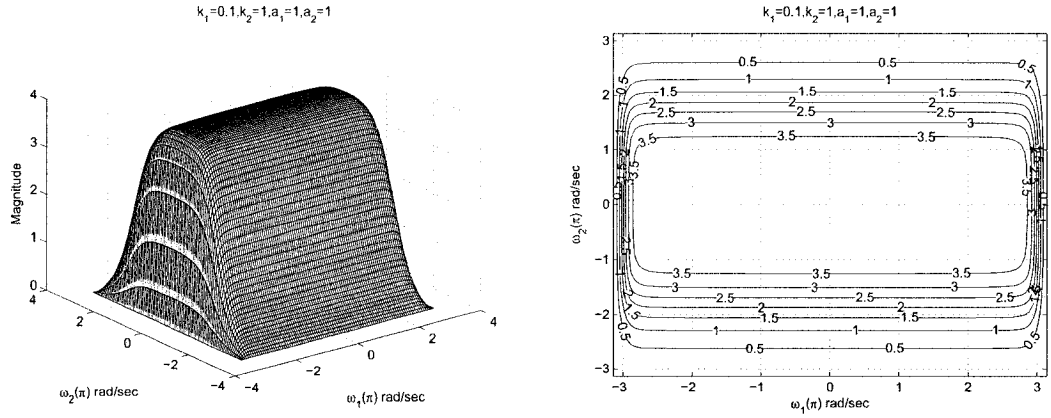

(a) $k_1 = 0.1$

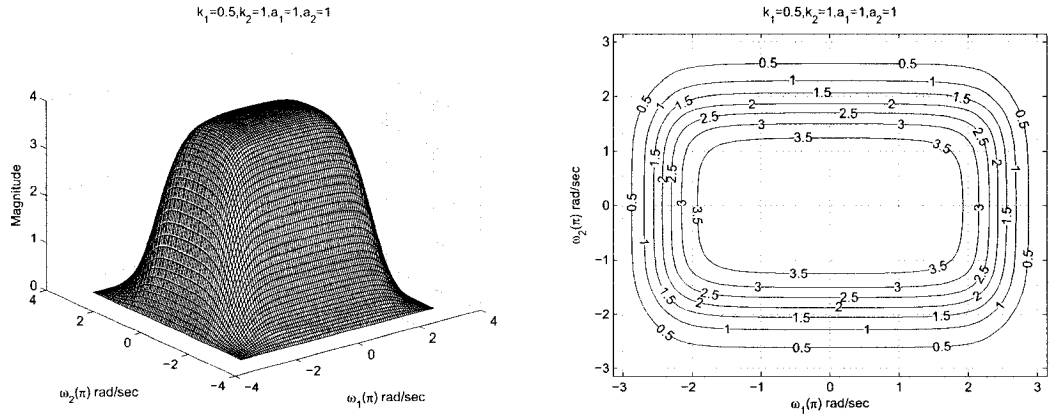

(b) $k_1 = 0.5$

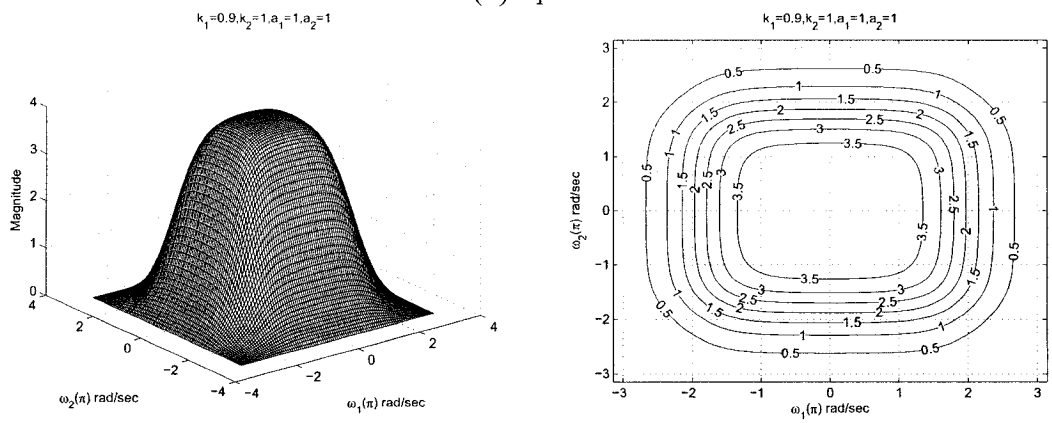

(c) $k_1 = 0.9$

Figure 2.7: 3-D amplitude frequency response and contour response of the 2-D digital lowpass filter for different values of k_1

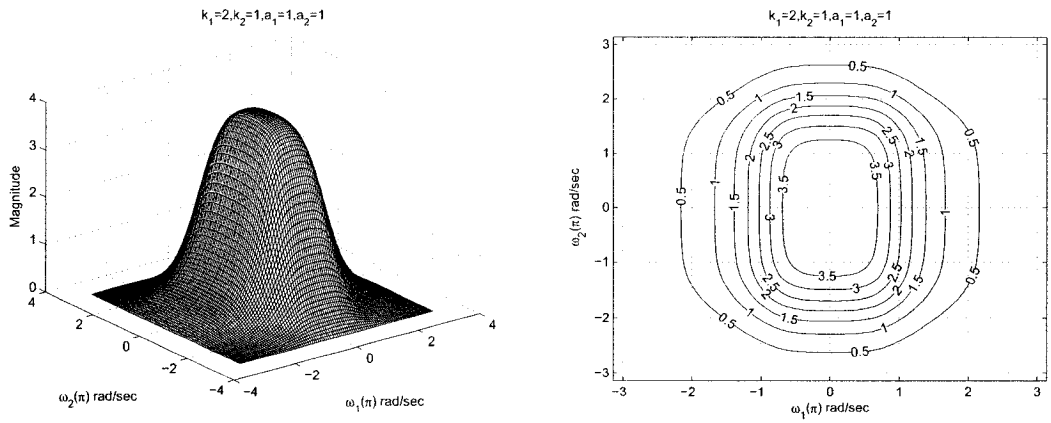

(a) $k_1 = 2$

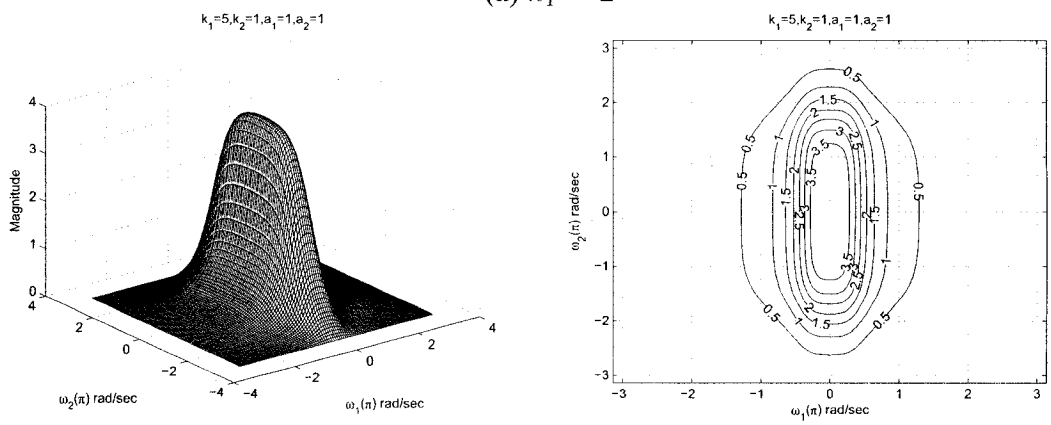

(b) $k_1 = 5$

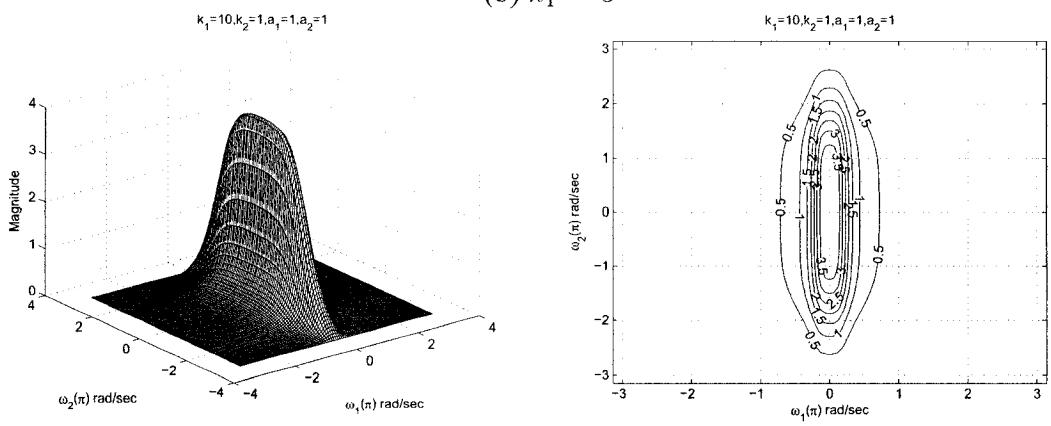

(c) $k_1 = 10$

Figure 2.8: 3-D amplitude frequency response and contour response of the 2-D digital lowpass filter for different values of k_1

It is observed that although the coefficient k_1 does not have any effect on the passband along the $\omega_2 - axis$, it affects the width of the passsband along the $\omega_1 - axis$. Initially when the value of the coefficient $k_1 = 0.1$ (see Figure 2.7 (a)) the width of the passband is maximum along the $\omega_1 - axis$. As we increase the value of k_1, the the bandwidth along the $\omega_1 - axis$ gradually decreases. Also, the amplitude of the frequency response remains constant for the same.

2.6.1.2 Frequency Response of 2-D Digital Lowpass Filter with different values of k_2

In Section 2.6.1.1, the effect of the coefficient of k_1 was analyzed. In this section, effect of the k_2 will be analyzed. To study the manner in which k_2 effects the frequency response behavior of the resulting 2-D digital lowpass filter in Category A and to separate the effect of the other coefficients, we vary the values of k_2, and fixing all the other coefficient of the generalized bilinear transformation to be unity in order not to loose any generality and to make the situation simple, e.g. with $k_1 = 1$, $a_1 = 1$, $a_2 = 1$, $b_1 = 1$ and $b_2 = 1$. The values of k_2 are varied from 0.1 to 10 and the 3-D magnitude response and the contour plots for the lowpass filter with the values of $k_2 = 0.1$, $k_2 = 0.5$ $k_2 = 0.9$, $k_2 = 2$, $k_2 = 5$, and $k_2 = 10$ are shown in the Figures 2.9 and 2.10.

It is observed that although the coefficient k_2 does not have any effect on the passband along the $\omega_1 - axis$, it affects the width of the passband along the $\omega_2 - axis$. Initially when the value of the coefficient $k_2 = 0.1$ (see Figure 2.9 (a)) the width of the passband is maximum along the $\omega_2 - axis$. As we increase the value of k_2, the passband width along the $\omega_2 - axis$ gradually decreases. Also, the amplitude of the frequency response remains constant for the same.

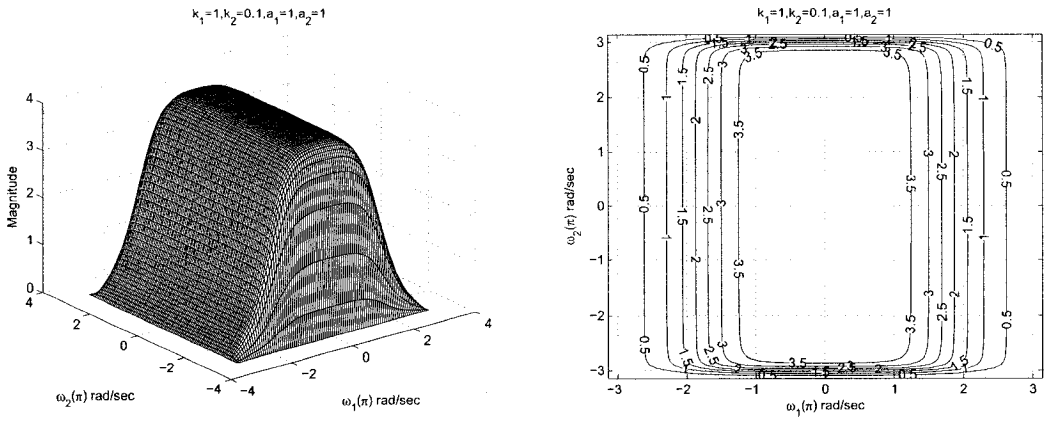

(a) $k_2 = 0.1$

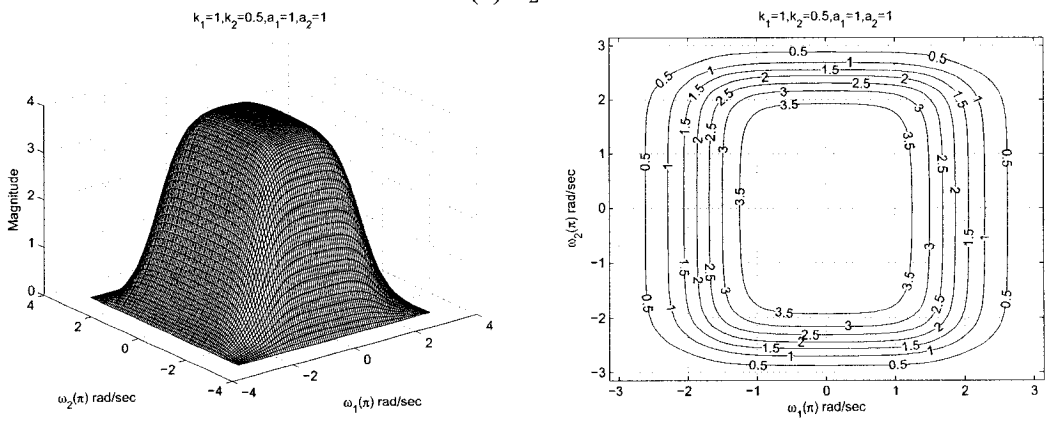

(b) $k_2 = 0.5$

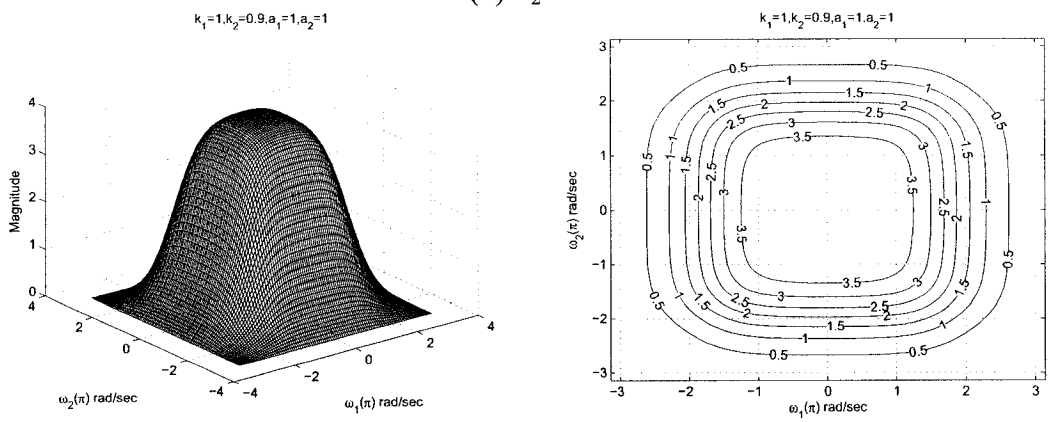

(c) $k_2 = 0.9$

Figure 2.9: 3-D amplitude frequency response and contour response of the 2-D digital lowpass filter for different values of k_2

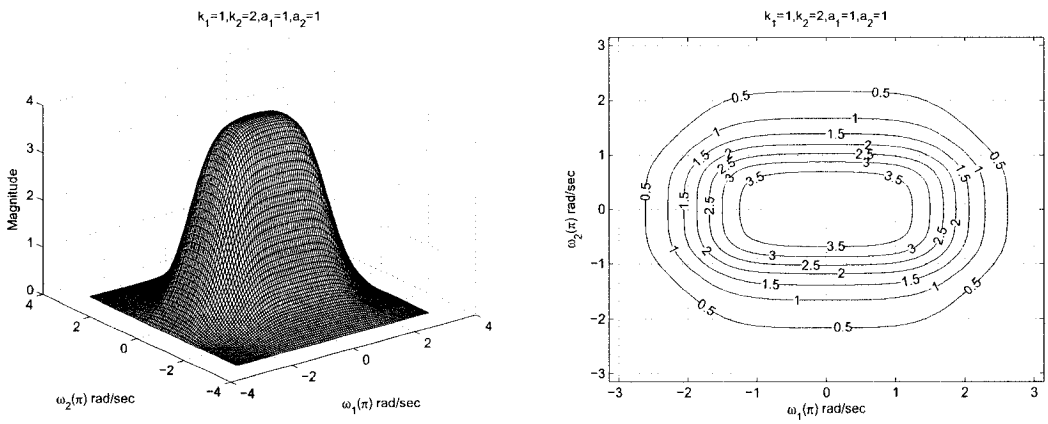

(a) $k_2 = 2$

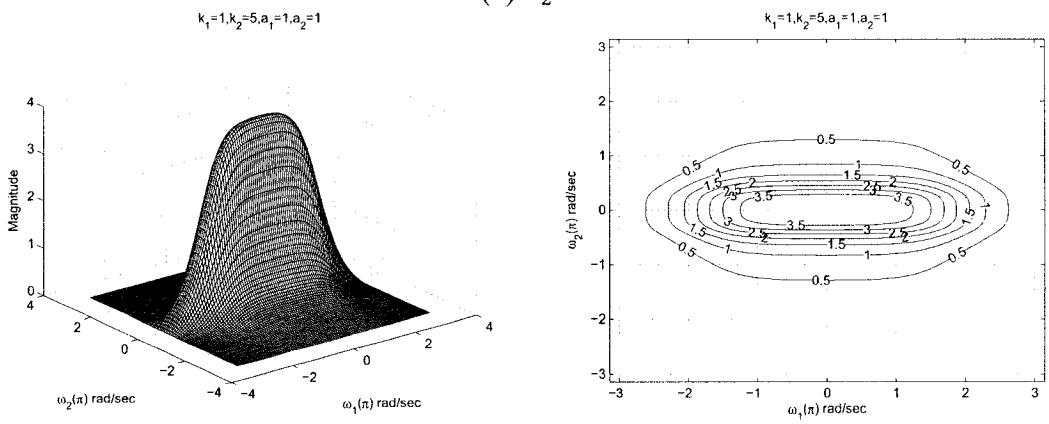

(b) $k_2 = 5$

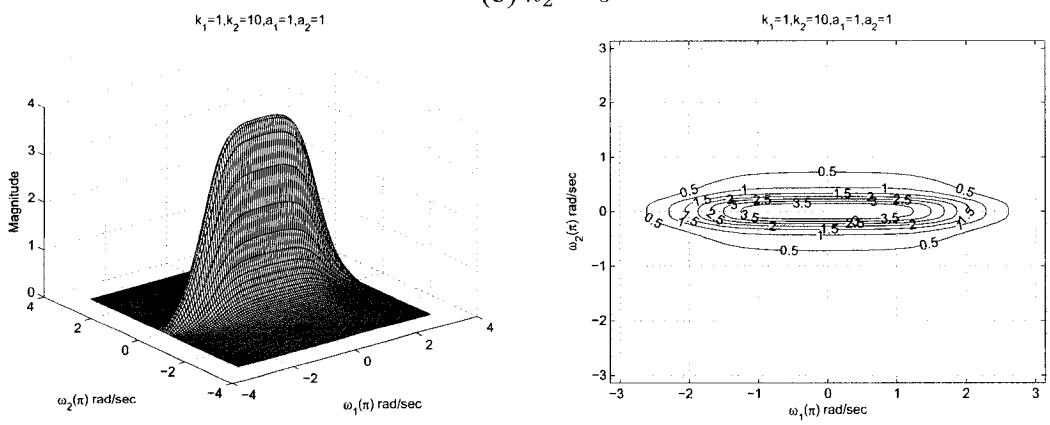

(c) $k_2 = 10$

Figure 2.10: 3-D amplitude frequency response and contour response of the 2-D digital lowpass filter for different values of k_2

2.6.1.3 Frequency Response of 2-D Digital Lowpass Filter with different values of a_1

In the Sections 2.6.1.1 and 2.6.1.2, the effect of the coefficient of k_1 and k_2 are studied. In this section, the effect of the coefficient a_1 will be studied. The stable range of a_1 can be obtained with other specified coefficient of the generalized bilinear transformation. There are many combinations possible for the coefficients. To study the response with different values of a_1, properly, we fix other coefficient values to be equal to unity. The range of a_1 varies from 0.1 to 1 and the other coefficient values are specified as unity, i.e., $k_1 = 1$, $k_2 = 1$, $a_2 = 1$, $b_1 = 1$ and $b_2 = 1$ in order to get 2-D digital lowpass filter response in Category A.

By varying the value of a_1, the 3-D magnitude response and contour plots which represents different values of a_1, i.e. $a_1 = 0.1$, $a_1 = 0.25$, $a_1 = 0.5$, $a_1 = 0.75$, and $a_1 = 0.9$ are shown in the Figures 2.11 and 2.12. By making the value of $a_1 = 1$, it resembles the standard lowpass filter as shown in the Figure 2.6. It is observed for the diagrams that the coefficient effects the gain of the amplitude-frequency response. At the lowest value of a_1 the gain of the passband will be less than 1. As the value of a_1 increases, the gain increases from 1.2 to 3.5 and reach the maximum value at $a_1 = 1$. In addition, the width of the passband increases and decreases periodically along the $\omega_1 - axis$ for different values of a_1. Also, the coefficient a_1 does not have any effect along the $\omega_2 - axis$.

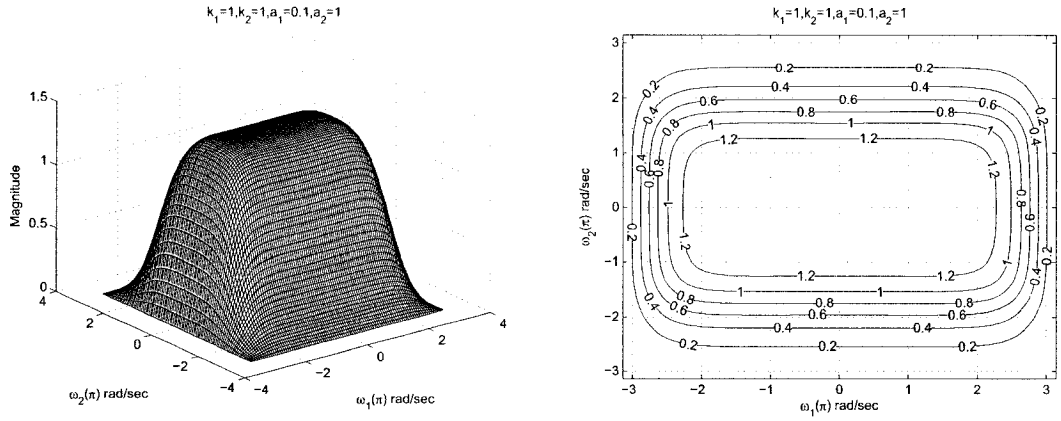

(a) $a_1 = 0.1$

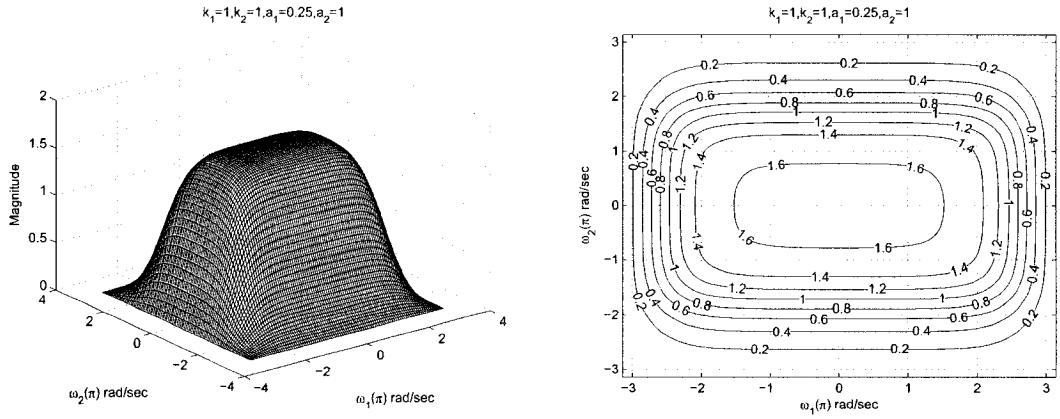

(b) $a_1 = 0.25$

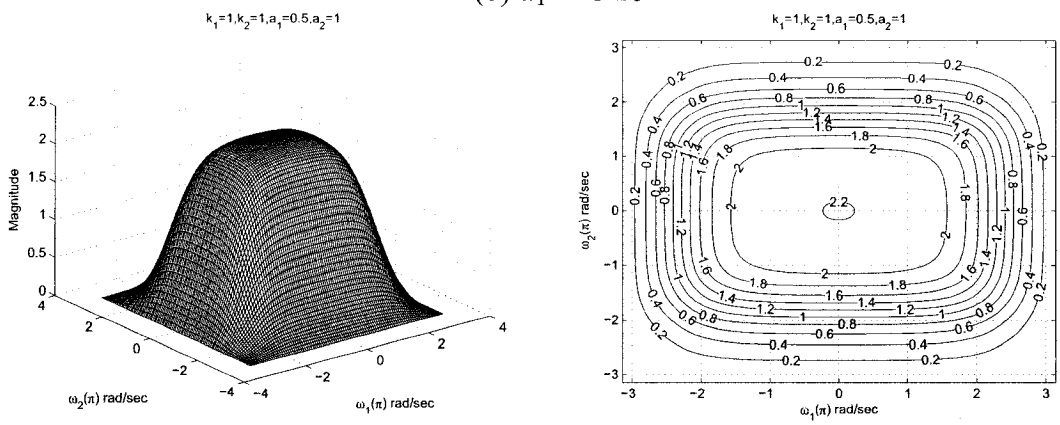

(c) $a_1 = 0.5$

Figure 2.11: 3-D amplitude frequency response and contour response of the 2-D digital lowpass filter for different values of a_1

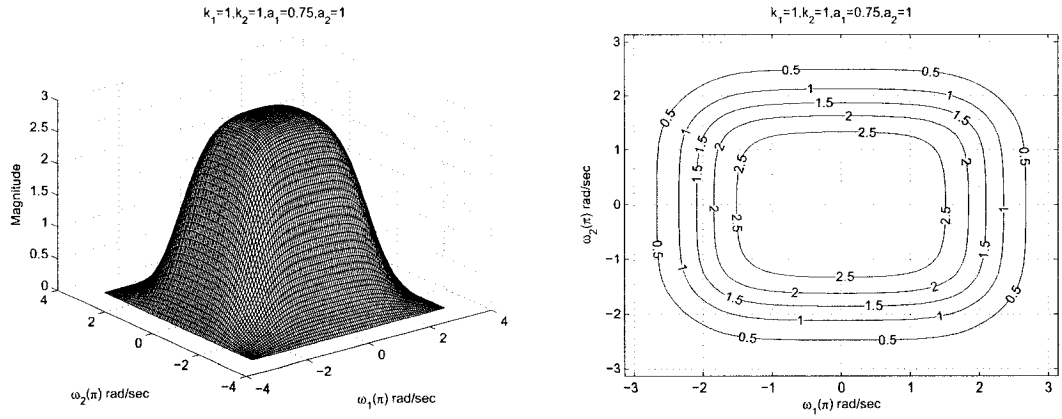

(a) $a_1 = 0.75$

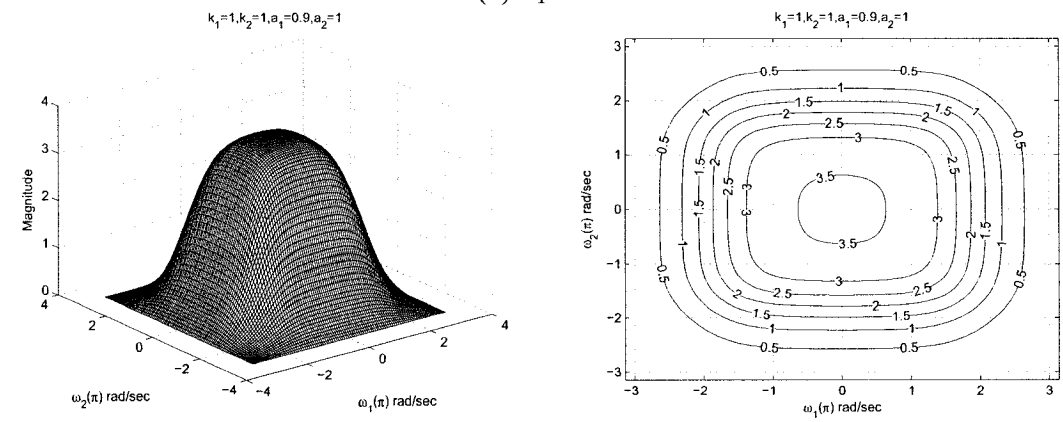

(b) $a_1 = 0.9$

Figure 2.12: 3-D amplitude frequency response and contour response of the 2-D digital lowpass filter for different values of a_1

2.6.1.4 Frequency Response of 2-D Digital Low Pass Filter with different values of a_2

In the Sections 2.6.1.3, the effect of the coefficient of a_1 was studied. In this section, the effect of the coefficient a_2 will be studied. The stable range of a_2 can be obtained with other specified coefficient of the generalized bilinear transformation. There are many combinations possible for the coefficients. To study the response with different values of a_2, properly, we fix other coefficient values to be equal to unity. The range of a_2 varies from 0.1 to 1 and the other coefficient values are specified as unity, i.e., $k_1 = 1$, $k_2 = 1$, $a_1 = 1$, $b_1 = 1$ and $b_2 = 1$ in order to get 2-D digital lowpass filter response in Category A.

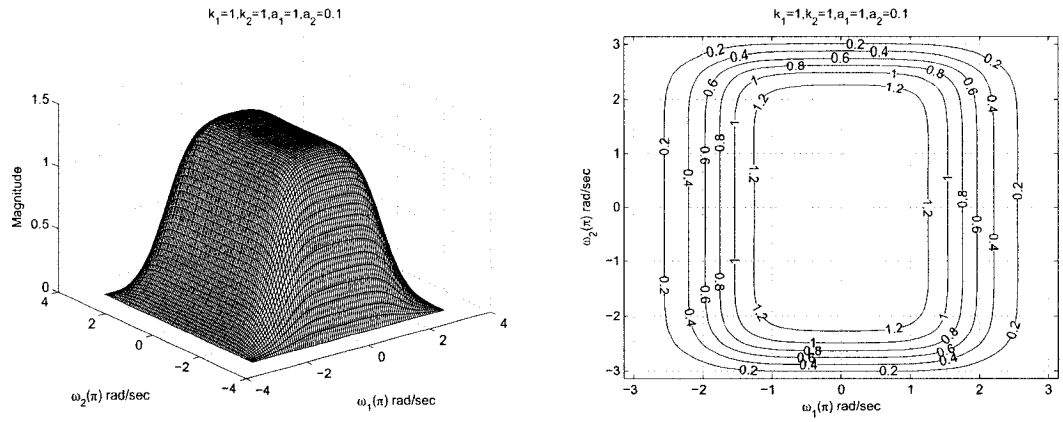

(a) $a_2 = 0.1$

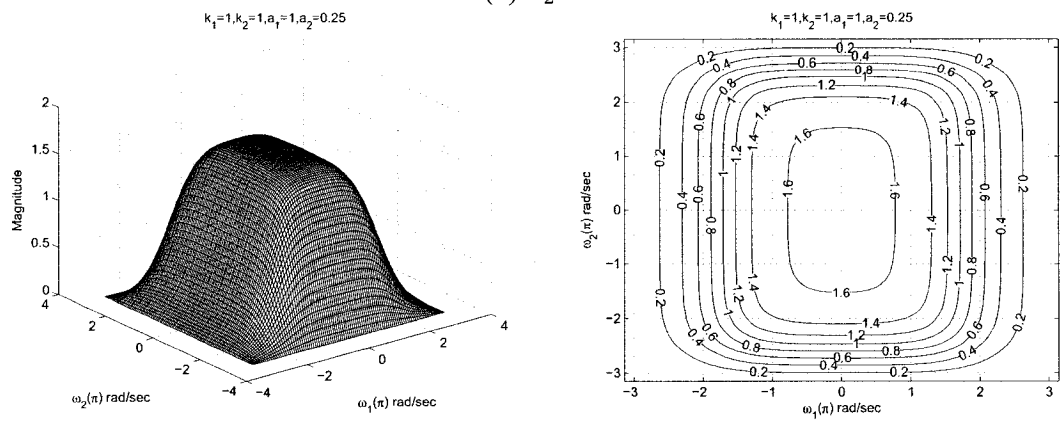

(b) $a_2 = 0.25$

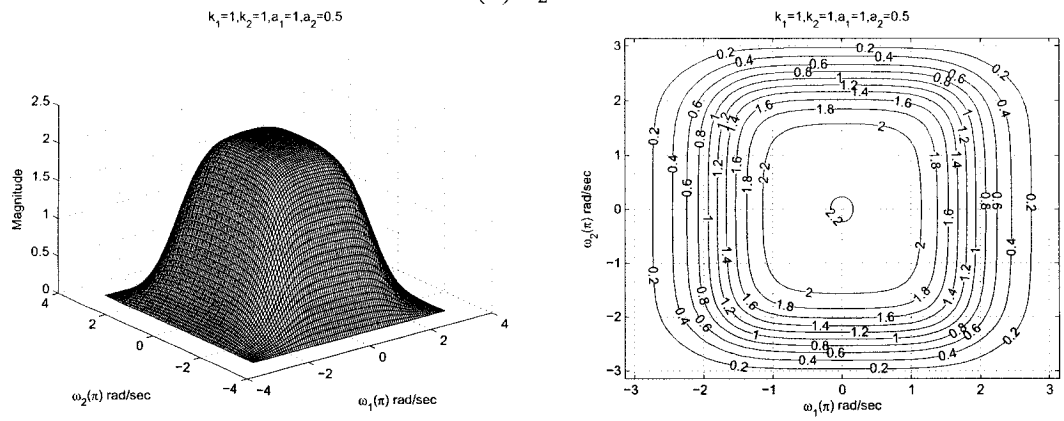

(c) $a_2 = 0.5$

Figure 2.13: 3-D amplitude frequency response and contour response of the 2-D lowpass digital filter for different values of a_2

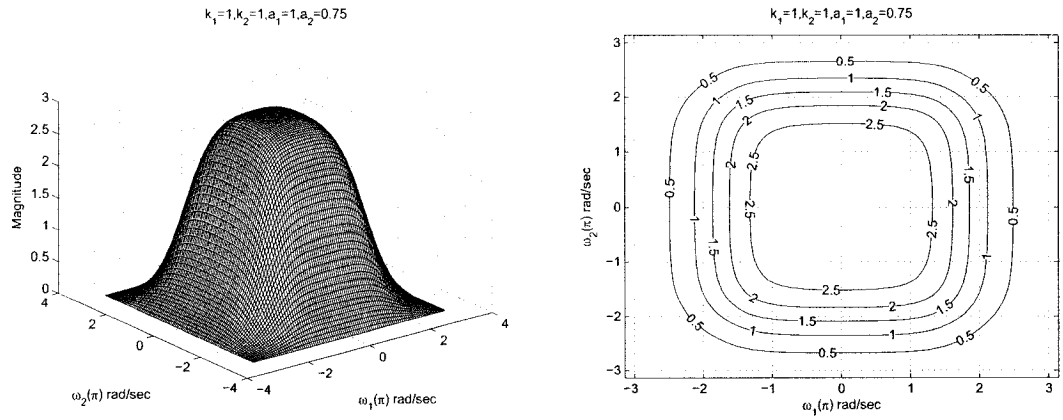

(a) $a_2 = 0.75$

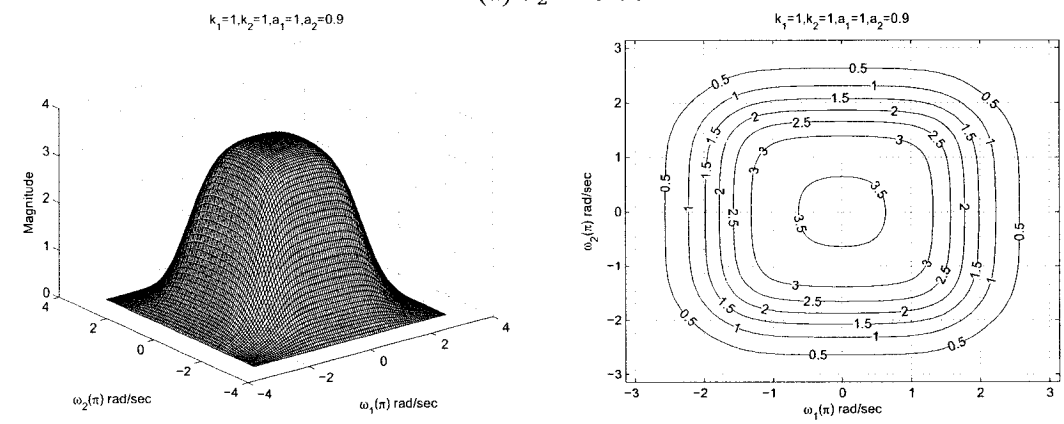

(b) $a_2 = 0.9$

Figure 2.14: 3-D amplitude frequency response and contour response of the 2-D digital lowpass filter for different values of a_2

By varying the value of a_2, the 3-D magnitude response and contour plots which represents different values of a_2, i.e., $a_2 = 0.1$, $a_2 = 0.25$, $a_2 = 0.5$, $a_2 = 0.75$, and $a_2 = 0.9$ are shown in the Figures 2.13 and 2.14. By making the value of $a_2 = 1$, it resembles the standard lowpass filter as shown in the Figure 2.6. It is observed for the diagrams that the coefficient effects the gain of the amplitude-frequency response. At the lowest value of a_2 the gain of the passband will be less than 1. As the value of a_2 increases, the gain increases from 1.2 to 3.5 and reach the maximum value at $a_2 = 1$. In addition, the width of the passband increases and decreases periodically along the $\omega_2 - axis$ for different values of a_2. Also, the coefficient a_2 does not have any effect on along the $\omega_1 - axis$.

2.6.1.5 Frequency Response of 2-D Digital Lowpass Filter with same values of a_1 and a_2 and same values of k_1 and k_2

In the Sections 2.6.1.1 to 2.6.1.4 the individual effect of the coefficients a_1, a_2, k_1 and k_2 were studied. In this section, we will study the effect of coefficients, where $a_1 = a_2$ and $k_1 = k_2$ and the remaining coefficient b_1 and b_2 are considered to be unity for the 2-D digital lowpass filter in Category A. The values of a_1 and a_2 ranges from 0 to 1 and the values of k_1 and k_2 ranges from 0 to 50.

As observed from the Figures 2.15 to 2.21, the coefficients k_1 and k_2 affect the passband width of the frequency response. In the Figures 2.15 (a), 2.16 (b), 2.17 (c), 2.19 (a) and 2.20 (b) there is a decrease in the passband width of the contour response as the values of k_1 and k_2 are increased from 0.5 to 50 for the same values of $a_1 = a_2 = 0.25$. At the same time there is also a decrease in the amplitude from 1.6 to 0.0014 for the same.

As observed from the Figures 2.15 to 2.21, the coefficients a_1 and a_2 affect the amplitude of the frequency response. It can be clearly observed from the Figures 2.15 (a), (b), (c) and 2.16 (a) that the amplitude of the contour response increases from 1.6 to 3.5 when the values of a_1 and a_2 are increased from 0.25 to 0.9 keeping the same value of $k_1 = k_2 = 0.5$. In addition, the width of the passband increases and decreases periodically for the same.

As observed for the Figure 2.17 (c), that when the values of $k_1 = k_2 > 1$ and $a_1 = a_2 \leq 0.5$, there are ripples in the amplitude and the contour response. As we increase the values of $a_1 = a_2 > 0.5$, the ripples tend to reduce, giving the response of the lowpass filter as seen from the Figures 2.17 (c) and 2.18 (a), (b), (c). When $1 < k_1, k_2 \leq 10$, and $a_1,\ a_2 \leq 0.5$ we see very strong ripples as seen from the Figures 2.19 (a), (b), (c) and 2.20 (a). As we increase the values of a_1 and $a_2 > 0.5$, the ripples tend to reduce and we get the response of a lowpass filter as seen from the Figure 2.20 (a). As we further increase the value of $k_1, k_2 > 10$, and also the values of a_1 and a_2 from 0.25 to 0.9, there are no ripples present in the amplitude and the contour response of the 2-D digital lowpass filter as seen from the Figures 2.20 (b), (c) and 2.21 (a), (b). Thus, it can be seen that there are ripples in

the passband when $1 < k_1,\ k_2 \leq 10$ and $a_1,\ a_2 \leq 0.5$.

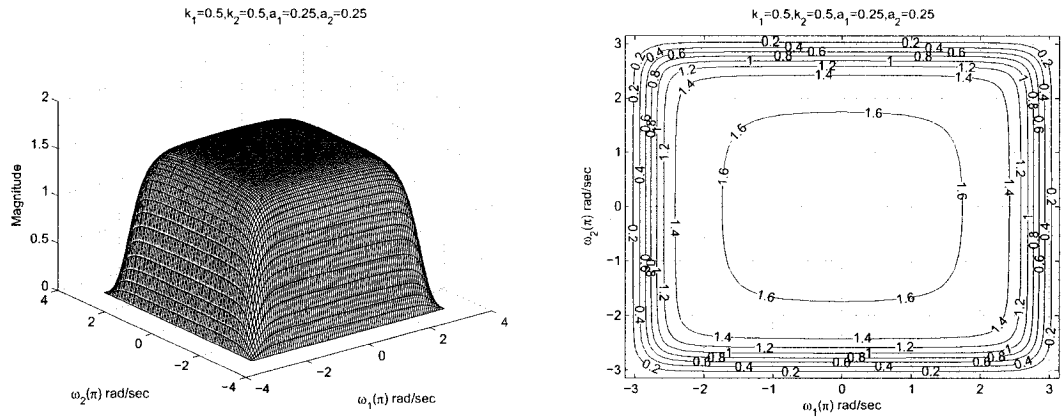

(a) $a_1 = a_2 = 0.25$ and $k_1 = k_2 = 0.5$

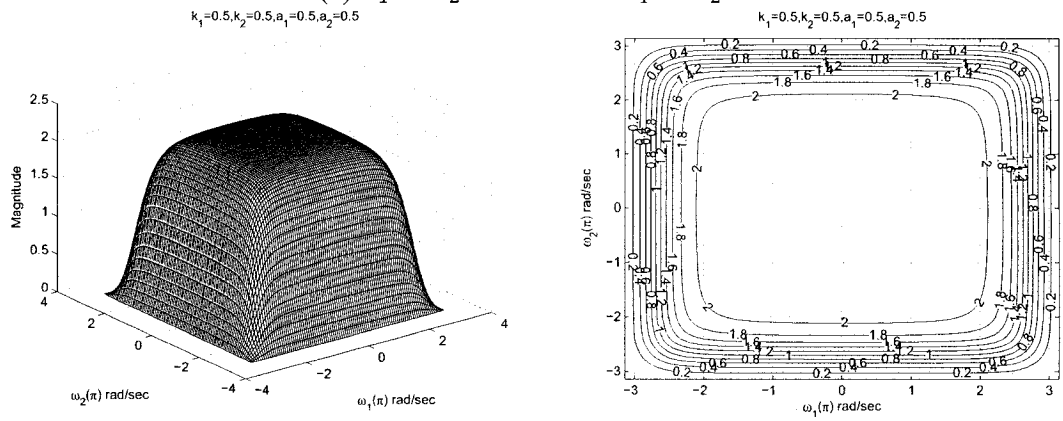

(b) $a_1 = a_2 = 0.5$ and $k_1 = k_2 = 0.5$

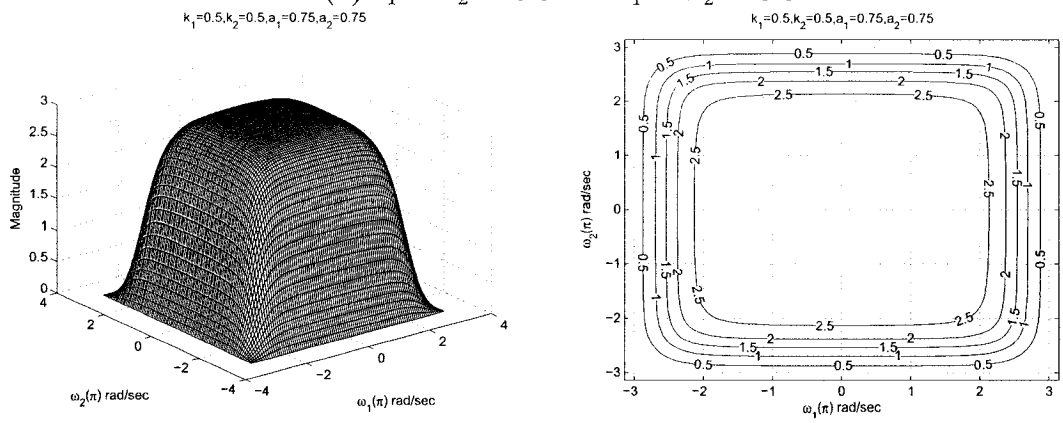

(c) $a_1 = a_2 = 0.75$ and $k_1 = k_2 = 0.5$

Figure 2.15: 3-D amplitude frequency response and contour response of the 2-D digital lowpass filter for $a_1 = a_2$ and $k_1 = k_2$

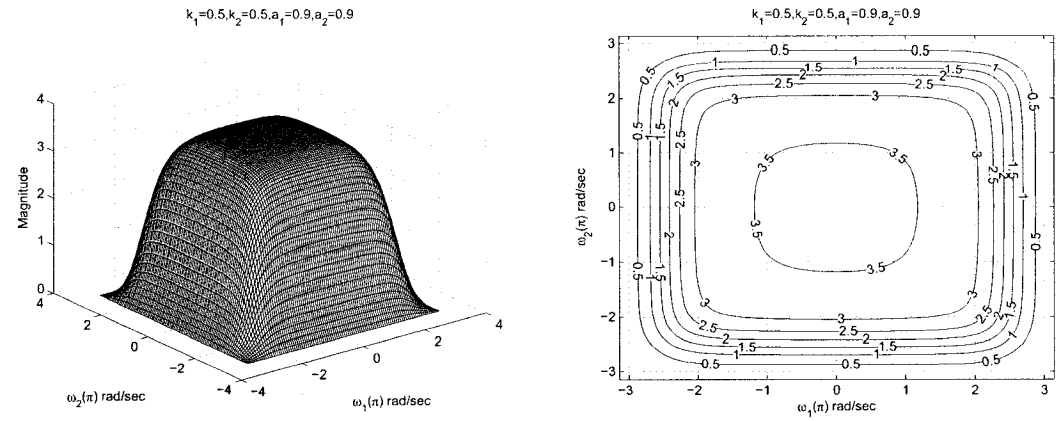

(a) $a_1 = a_2 = 0.9$ and $k_1 = k_2 = 0.5$

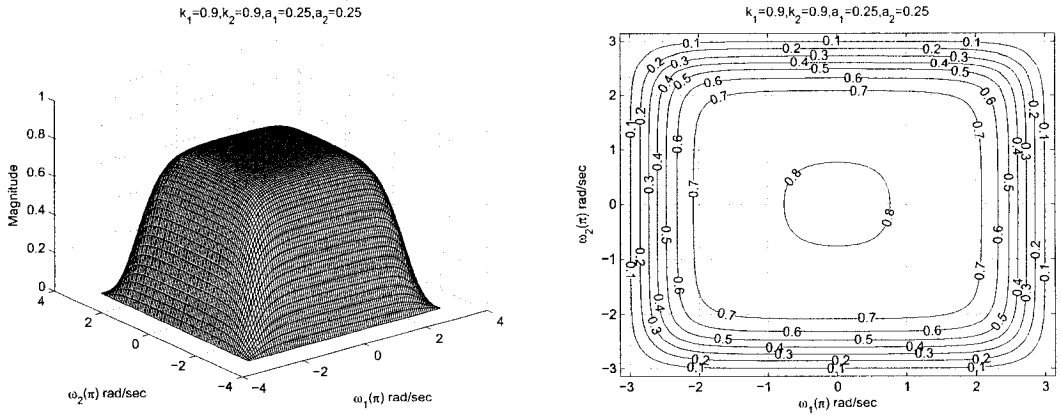

(b) $a_1 = a_2 = 0.25$ and $k_1 = k_2 = 0.9$

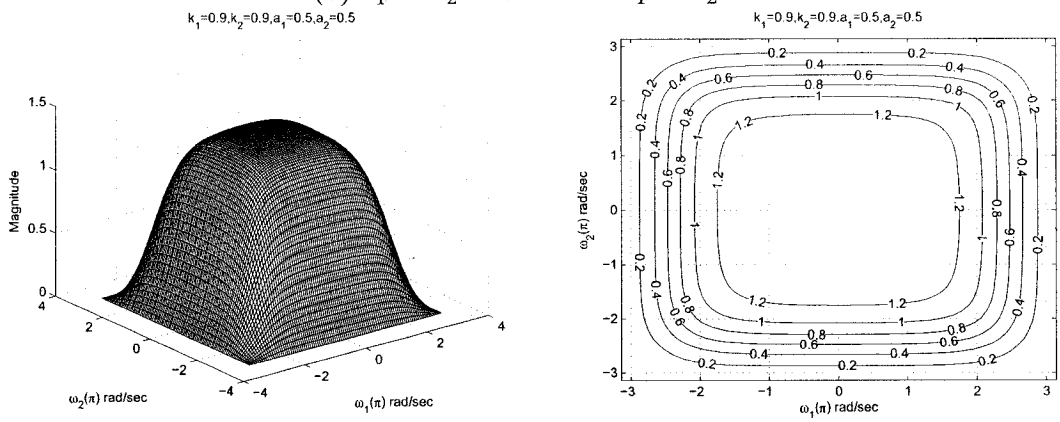

(c) $a_1 = a_2 = 0.5$ and $k_1 = k_2 = 0.9$

Figure 2.16: 3-D amplitude frequency response and contour response of the 2-D digital lowpass filter for $a_1 = a_2$ and $k_1 = k_2$

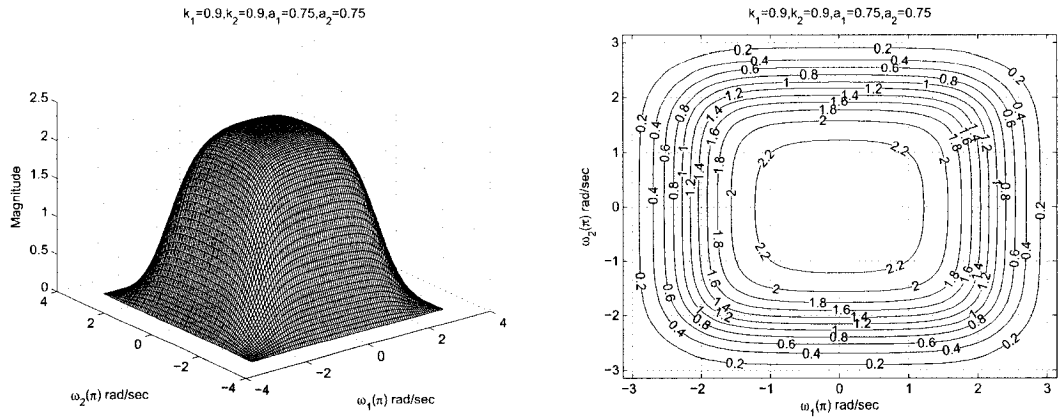

(a) $a_1 = a_2 = 0.75$ and $k_1 = k_2 = 0.9$

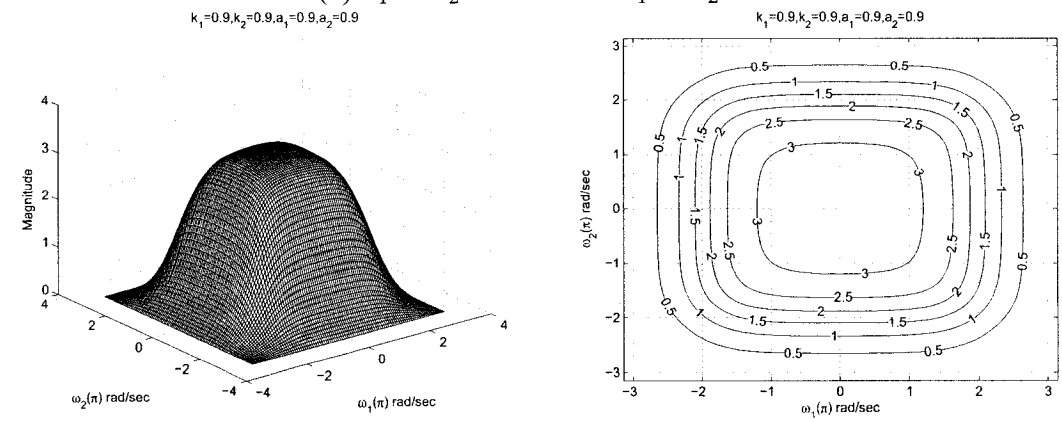

(b) $a_1 = a_2 = 0.9$ and $k_1 = k_2 = 0.9$

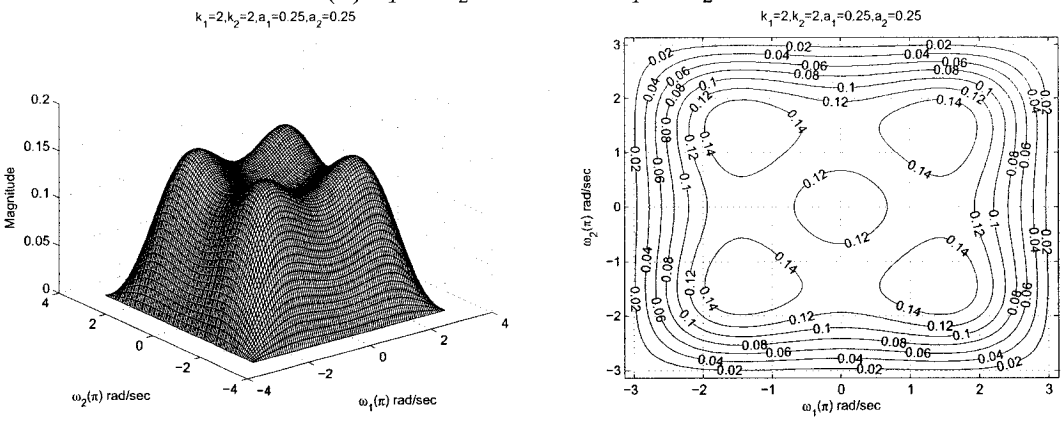

(c) $a_1 = a_2 = 0.25$ and $k_1 = k_2 = 2$

Figure 2.17: 3-D amplitude frequency response and contour response of the 2-D digital lowpass filter for $a_1 = a_2$ and $k_1 = k_2$

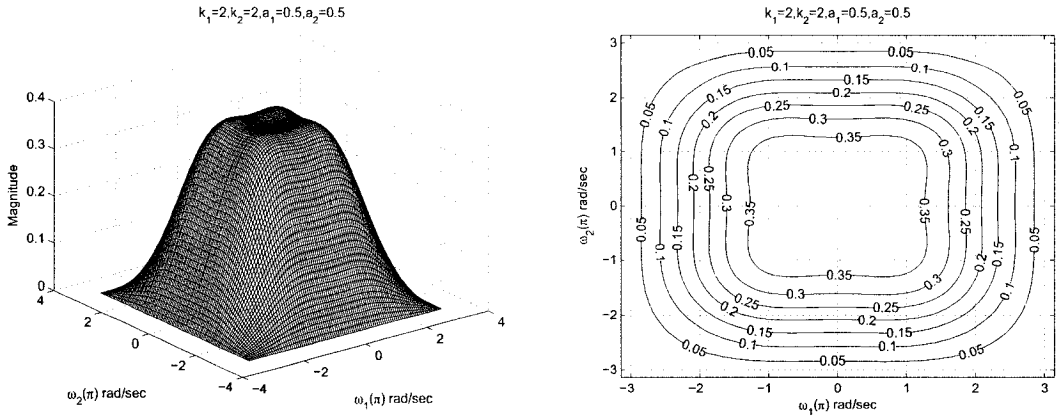

(a) $a_1 = a_2 = 0.5$ and $k_1 = k_2 = 2$

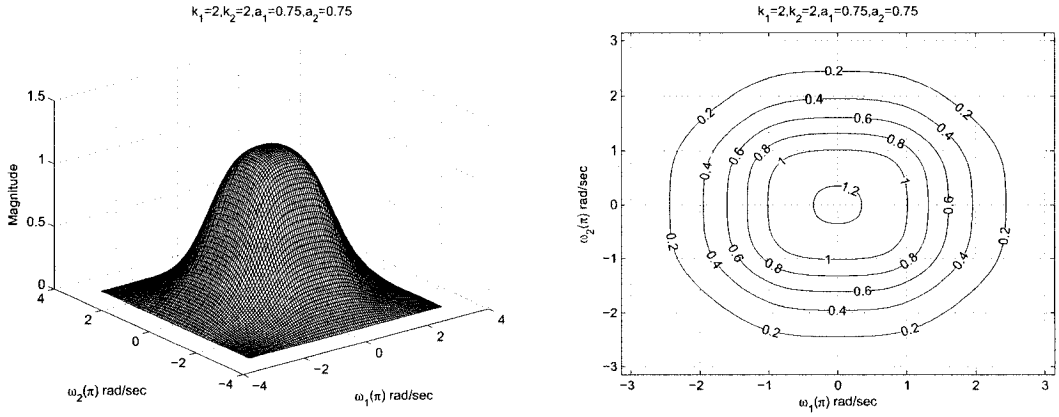

(b) $a_1 = a_2 = 0.75$ and $k_1 = k_2 = 2$

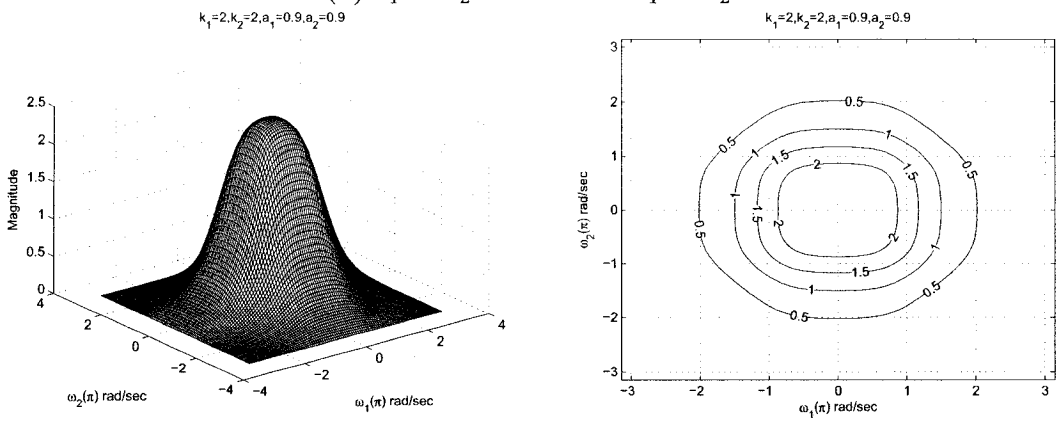

(c) $a_1 = a_2 = 0.9$ and $k_1 = k_2 = 2$

Figure 2.18: 3-D amplitude frequency response and contour response of the 2-D digital lowpass filter for $a_1 = a_2$ and $k_1 = k_2$

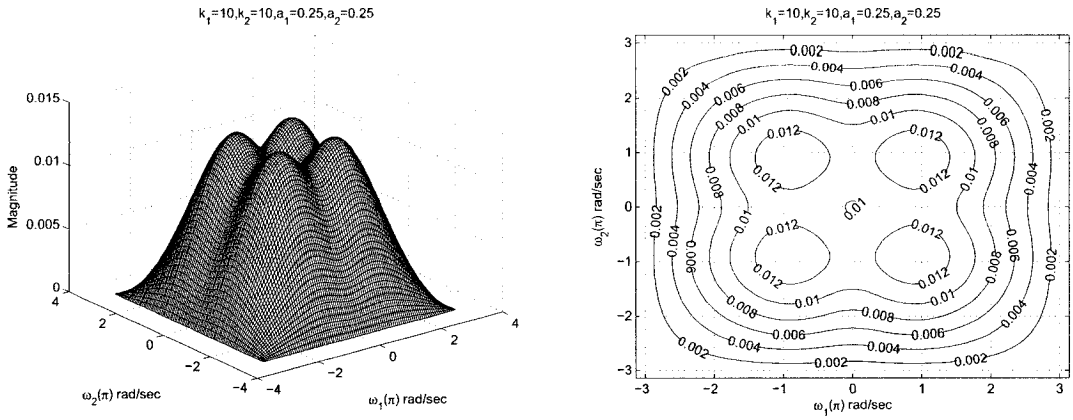

(a) $a_1 = a_2 = 0.25$ and $k_1 = k_2 = 10$

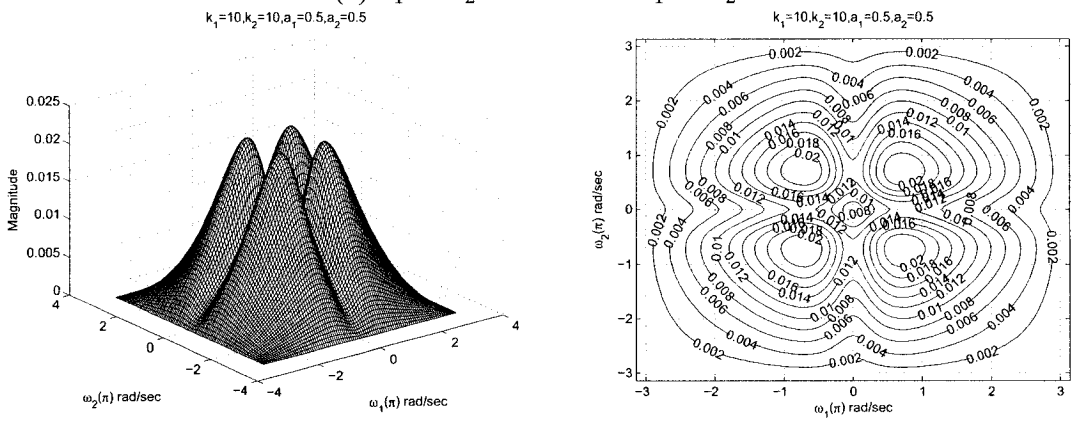

(b) $a_1 = a_2 = 0.5$ and $k_1 = k_2 = 10$

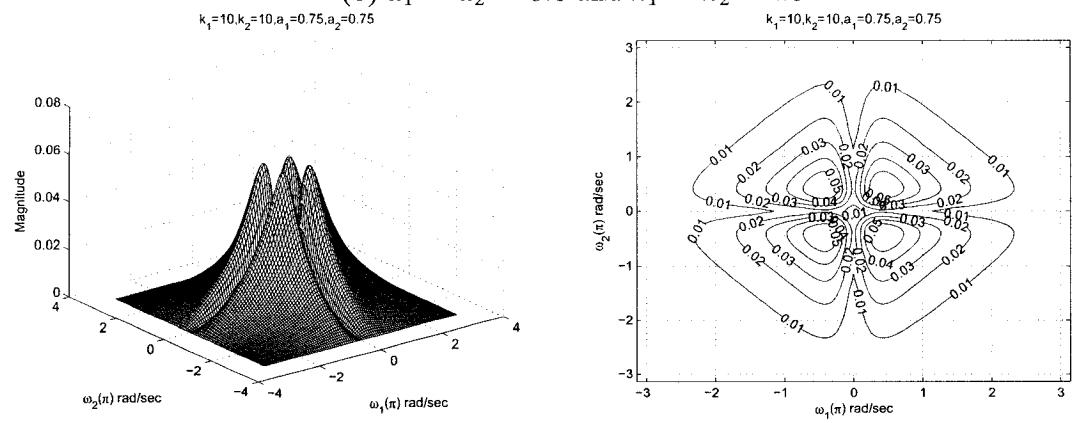

(c) $a_1 = a_2 = 0.75$ and $k_1 = k_2 = 10$

Figure 2.19: 3-D amplitude frequency response and contour response of the 2-D digital lowpass filter for $a_1 = a_2$ and $k_1 = k_2$

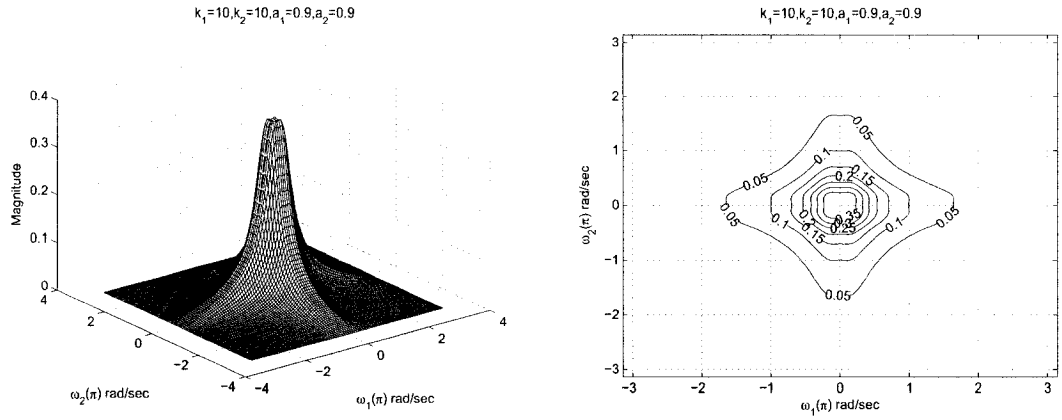

(a) $a_1 = a_2 = 0.9$ and $k_1 = k_2 = 10$

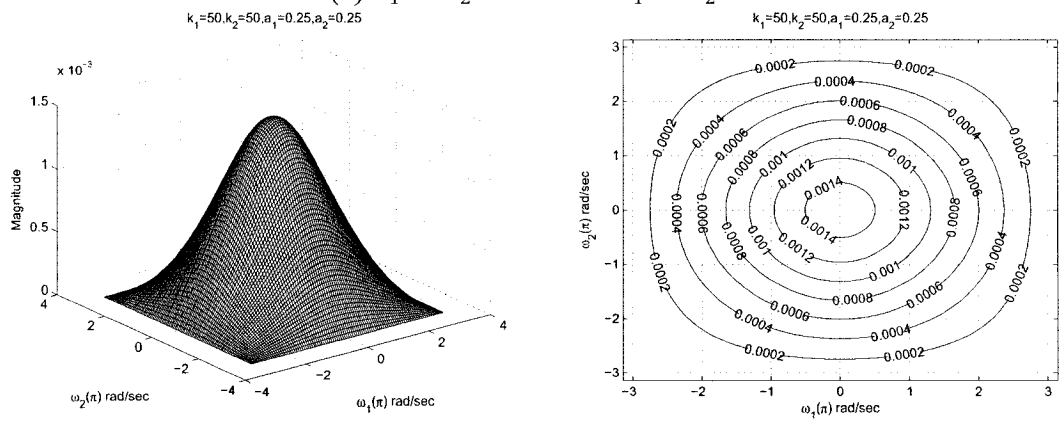

(b) $a_1 = a_2 = 0.25$ and $k_1 = k_2 = 50$

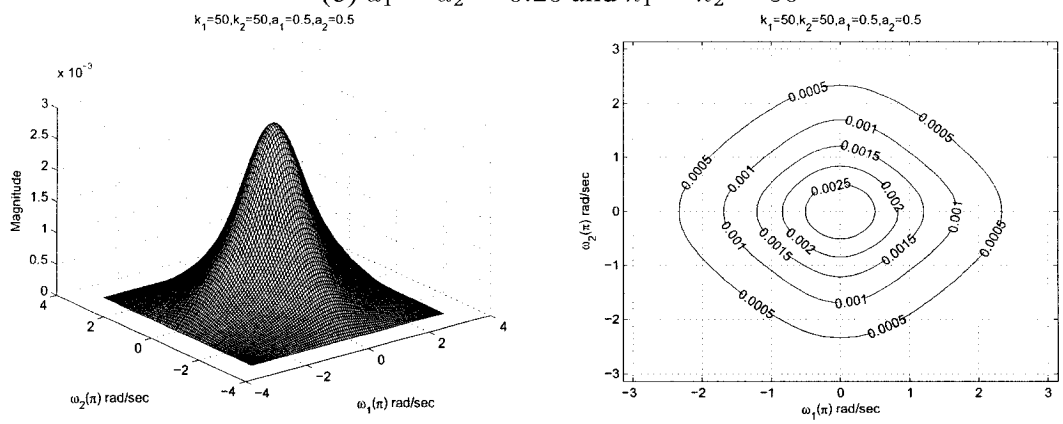

(c) $a_1 = a_2 = 0.5$ and $k_1 = k_2 = 50$

Figure 2.20: 3-D amplitude frequency response and contour response of the 2-D digital lowpass filter for $a_1 = a_2$ and $k_1 = k_2$

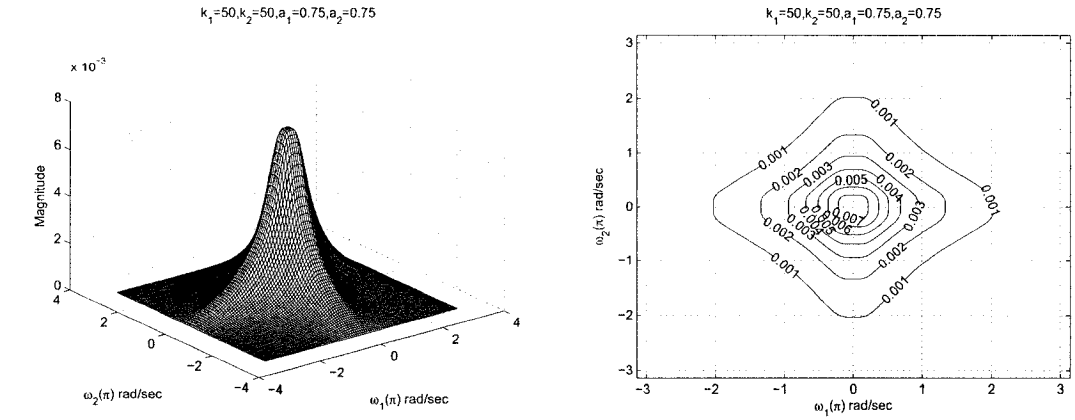

(a) $a_1 = a_2 = 0.75$ and $k_1 = k_2 = 50$

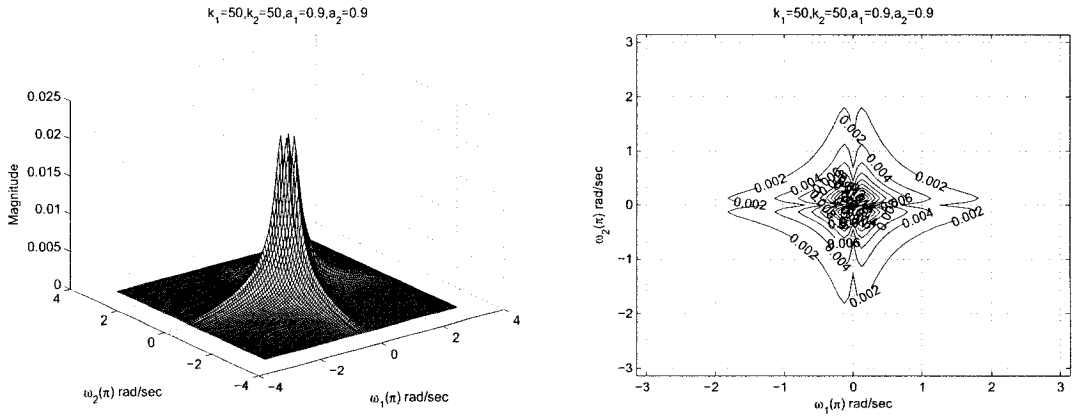

(b) $a_1 = a_2 = 0.9$ and $k_1 = k_2 = 50$

Figure 2.21: 3-D amplitude frequency response and contour response of the 2-D digital lowpass filter for $a_1 = a_2$ and $k_1 = k_2$

2.6.1.6 Frequency Response of 2-D Digital Lowpass Filter with different values of a_1 and a_2 and same values of k_1 and k_2

In this section, we will study the effect of coefficients, where $a_1 \neq a_2$ and $k_1 = k_2$ and the remaining coefficient b_1 and b_2 are considered to be unity for the 2-D digital lowpass filter in Category A. The values of a_1 and a_2 ranges from 0.25 to 0.5 and 0.5 to 0.75 respectively, and the values of k_1 and k_2 ranges from 0 to 50.

As observed from the Figures 2.22 to 2.27, that the coefficients k_1 and k_2 affect the passband width of the frequency response. In the Figures 2.22 (a), 2.23 (a), 2.24 (a), 2.25 (a), 2.26 (a) and 2.27 (a) there is a decrease in the passband width as the values of k_1 and

k_2 are increased from 0.5 to 50 for different values of $a_1 = 0.25$ and $a_2 = 0.5$. At the same time, there is also a decrease in the magnitude of the contour response from 1.8 to 0.002 for the same.

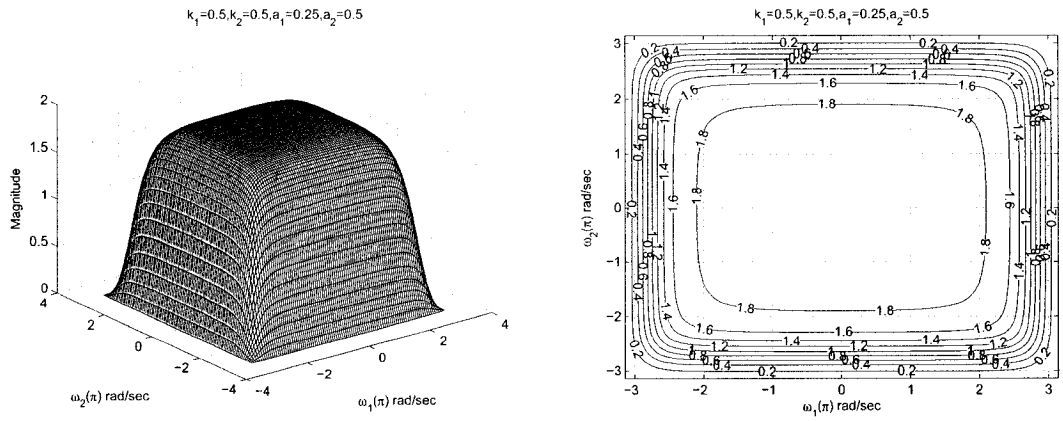

(a) $a_1 = 0.25,\ a_2 = 0.5$ and $k_1 = k_2 = 0.5$

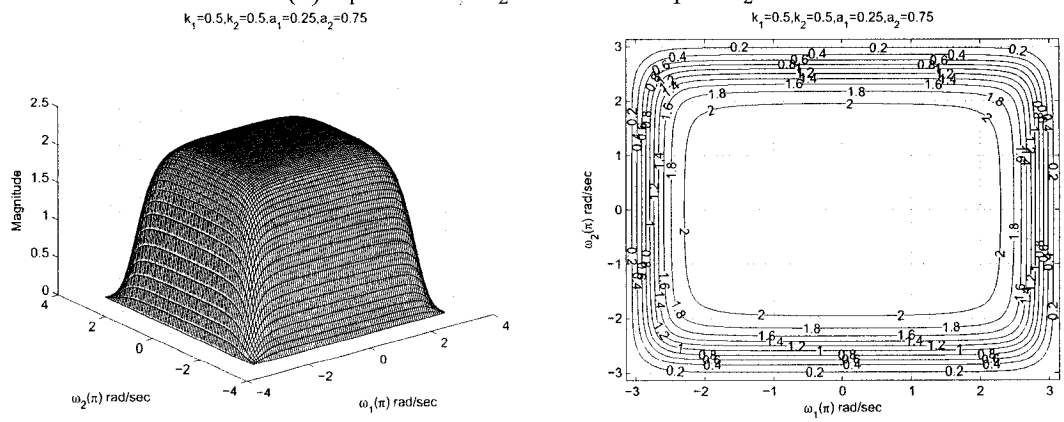

(b) $a_1 = 0.25,\ a_2 = 0.75$ and $k_1 = k_2 = 0.5$

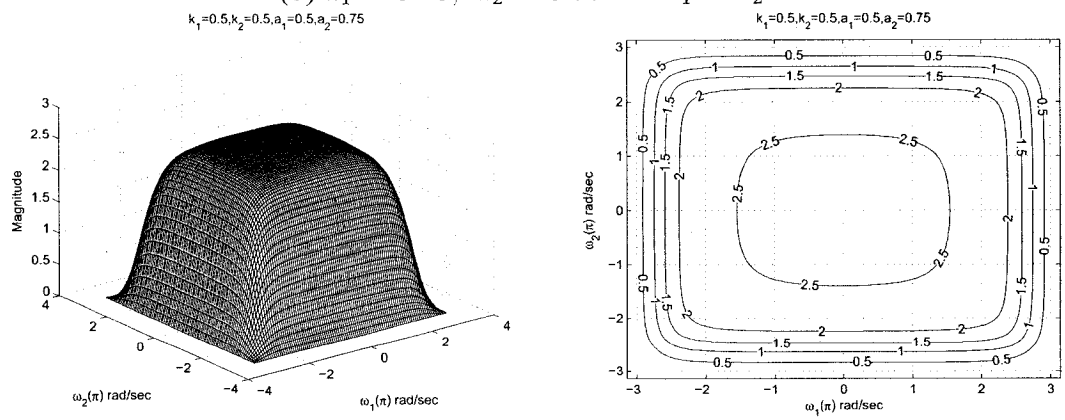

(c) $a_1 = 0.5,\ a_2 = 0.75$ and $k_1 = k_2 = 0.5$

Figure 2.22: 3-D amplitude frequency response and contour response of the 2-D digital lowpass filter for $a_1 \neq a_2$ and $k_1 = k_2$

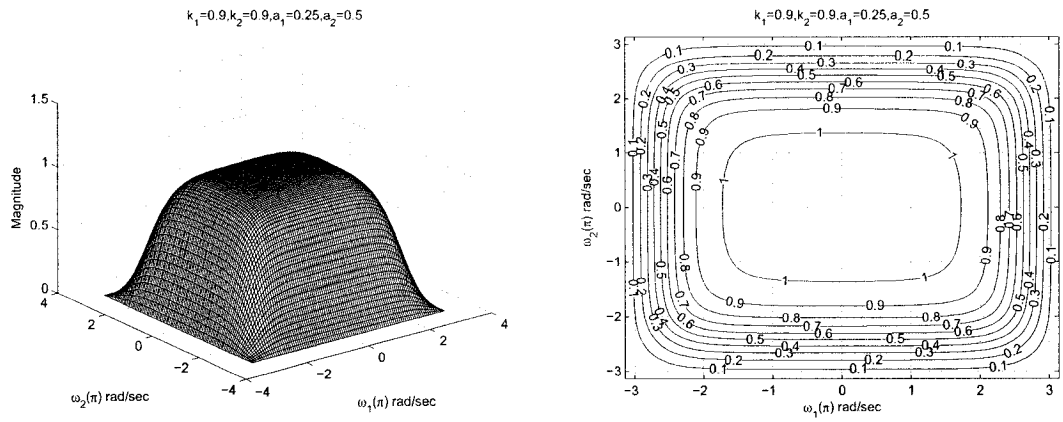

(a) $a_1 = 0.25,\ a_2 = 0.5$ and $k_1 = k_2 = 0.9$

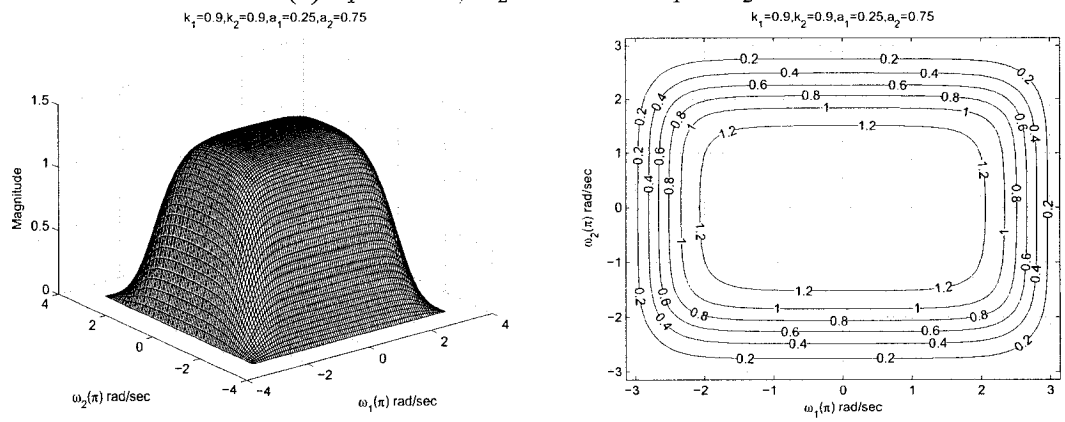

(b) $a_1 = 0.25,\ a_2 = 0.75$ and $k_1 = k_2 = 0.9$

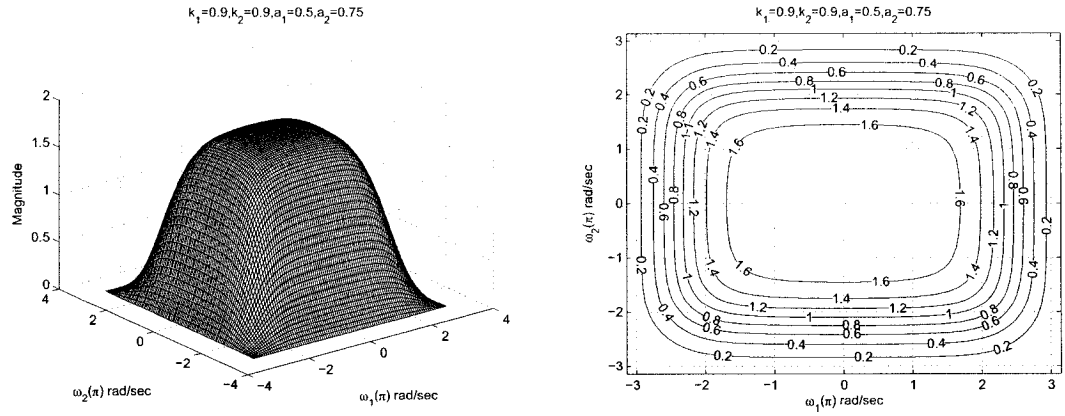

(c) $a_1 = 0.5,\ a_2 = 0.75$ and $k_1 = k_2 = 0.9$

Figure 2.23: 3-D amplitude frequency response and contour response of the 2-D digital lowpass filter for $a_1 \neq a_2$ and $k_1 = k_2$

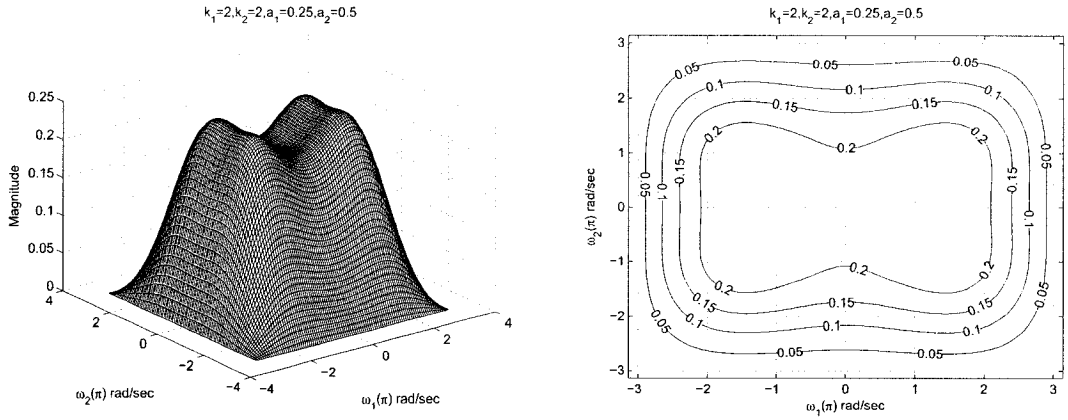

(a) $a_1 = 0.25,\ a_2 = 0.5$ and $k_1 = k_2 = 2$

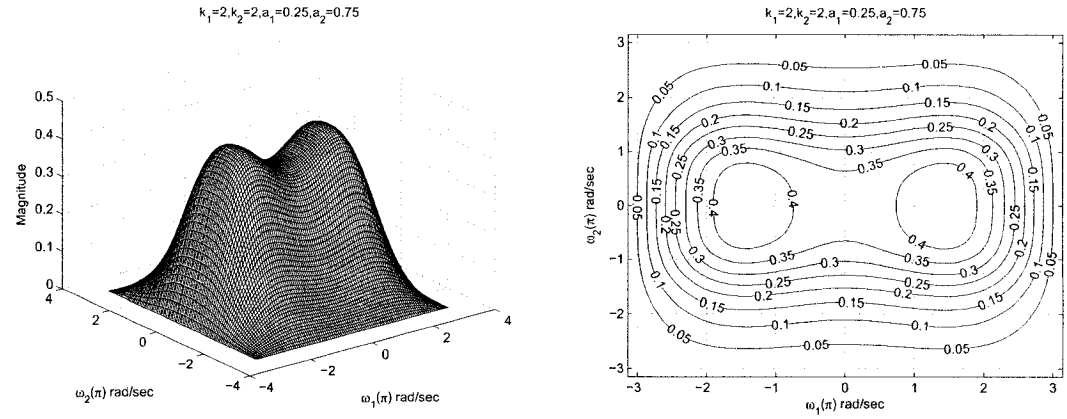

(b) $a_1 = 0.25,\ a_2 = 0.75$ and $k_1 = k_2 = 2$

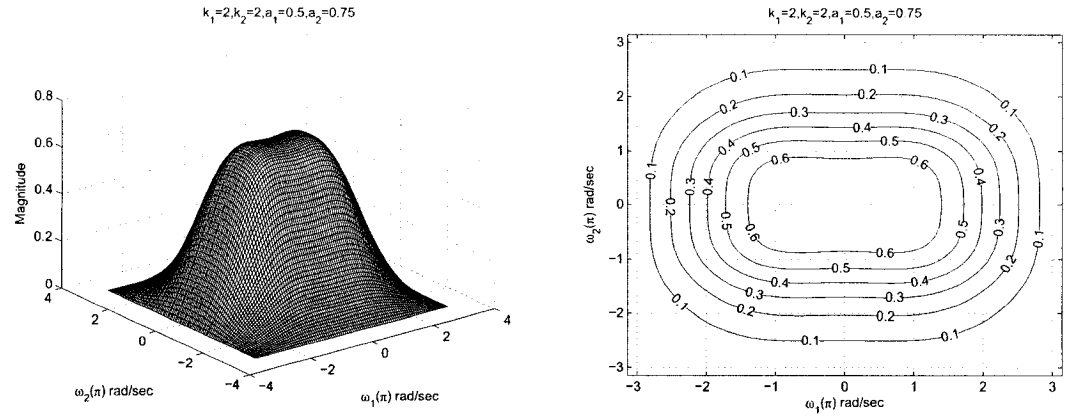

(c) $a_1 = 0.5,\ a_2 = 0.75$ and $k_1 = k_2 = 2$

Figure 2.24: 3-D amplitude frequency response and contour response of the 2-D digital lowpass filter for $a_1 \neq a_2$ and $k_1 = k_2$

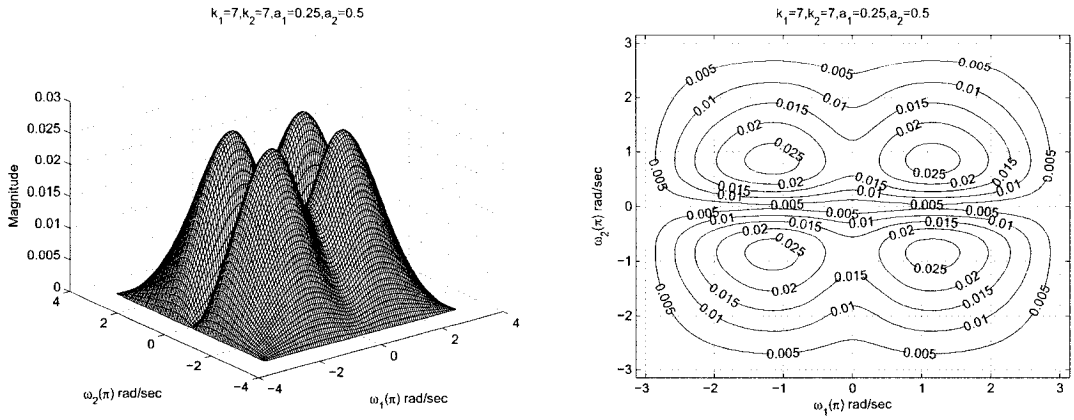

(a) $a_1 = 0.25,\ a_2 = 0.5$ and $k_1 = k_2 = 7$

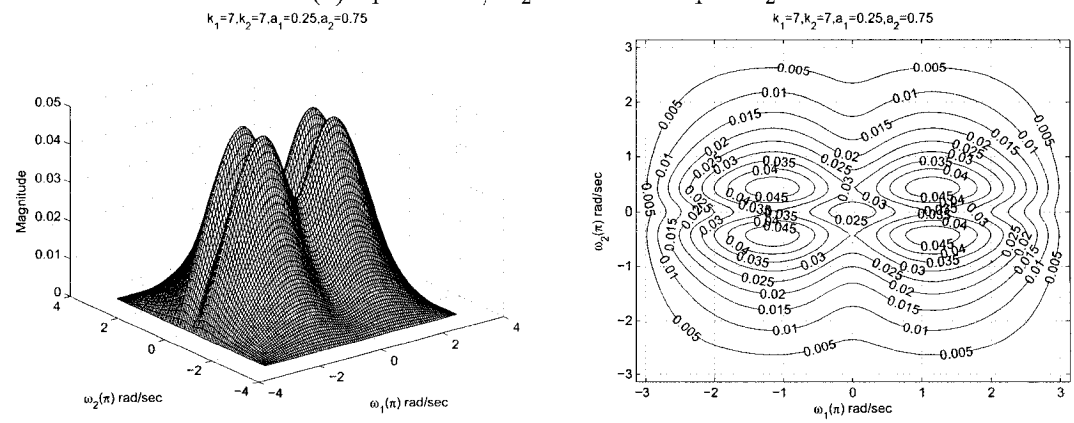

(b) $a_1 = 0.25,\ a_2 = 0.75$ and $k_1 = k_2 = 7$

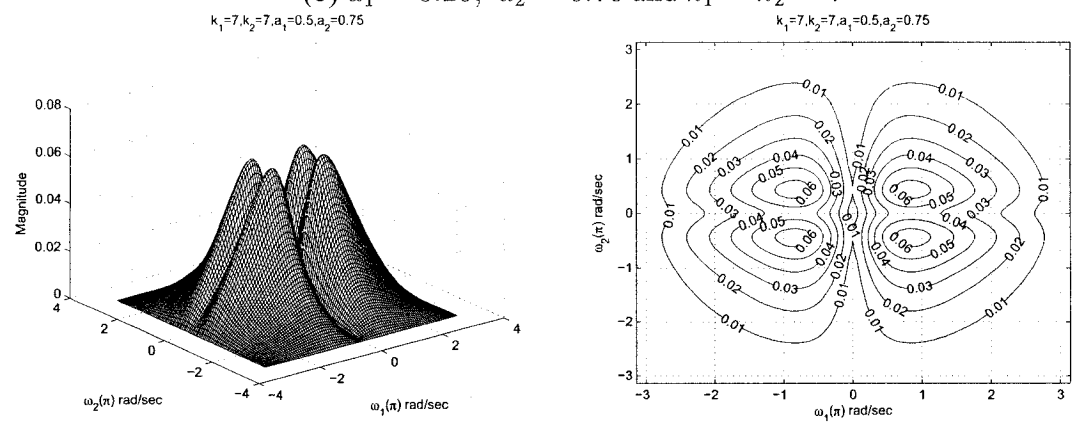

(c) $a_1 = 0.5,\ a_2 = 0.75$ and $k_1 = k_2 = 7$

Figure 2.25: 3-D amplitude frequency response and contour response of the 2-D digital lowpass filter for $a_1 \neq a_2$ and $k_1 = k_2$

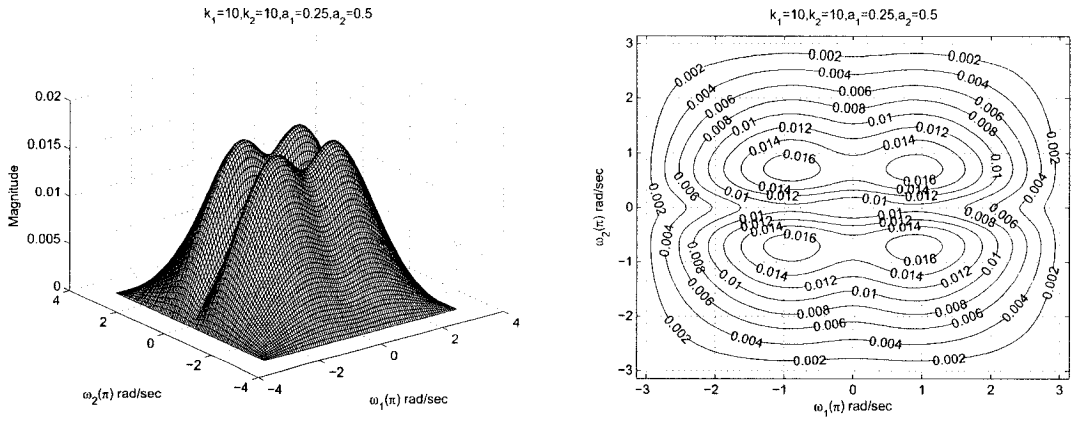

(a) $a_1 = 0.25,\ a_2 = 0.5$ and $k_1 = k_2 = 10$

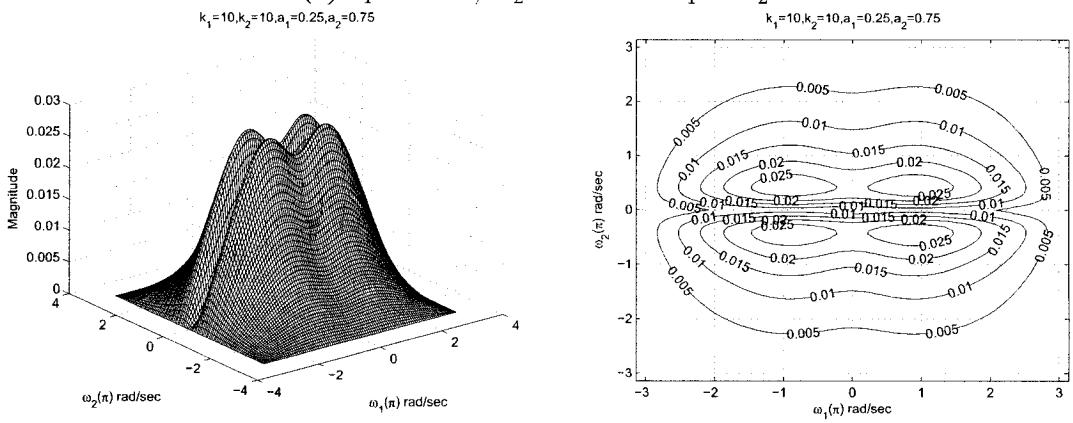

(b) $a_1 = 0.25,\ a_2 = 0.75$ and $k_1 = k_2 = 10$

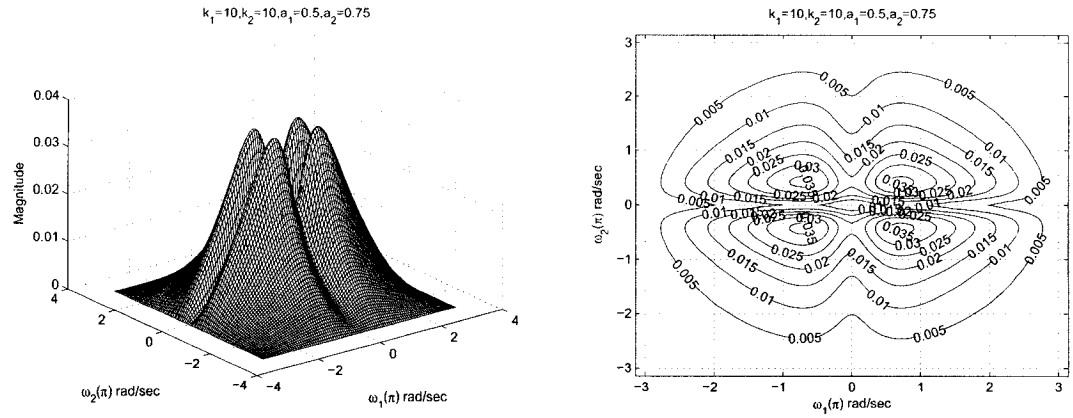

(c) $a_1 = 0.5,\ a_2 = 0.75$ and $k_1 = k_2 = 10$

Figure 2.26: 3-D amplitude frequency response and contour response of the 2-D digital lowpass filter for $a_1 \neq a_2$ and $k_1 = k_2$

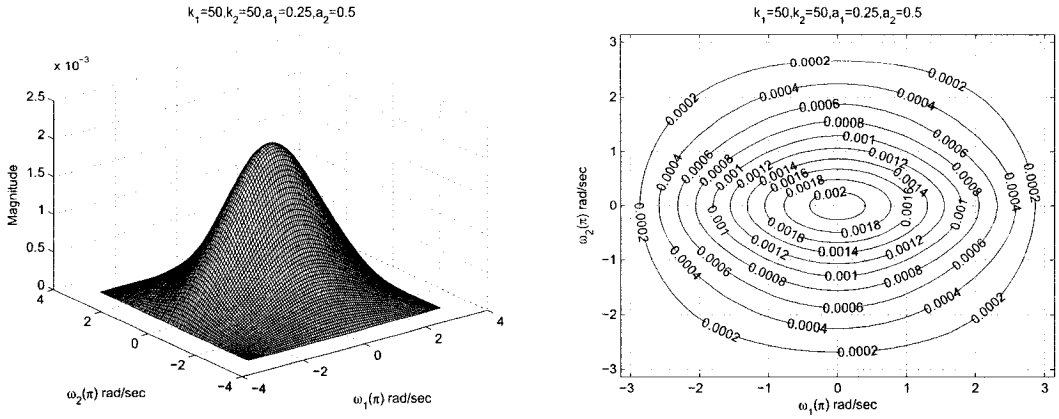

(a) $a_1 = 0.25,\ a_2 = 0.5$ and $k_1 = k_2 = 50$

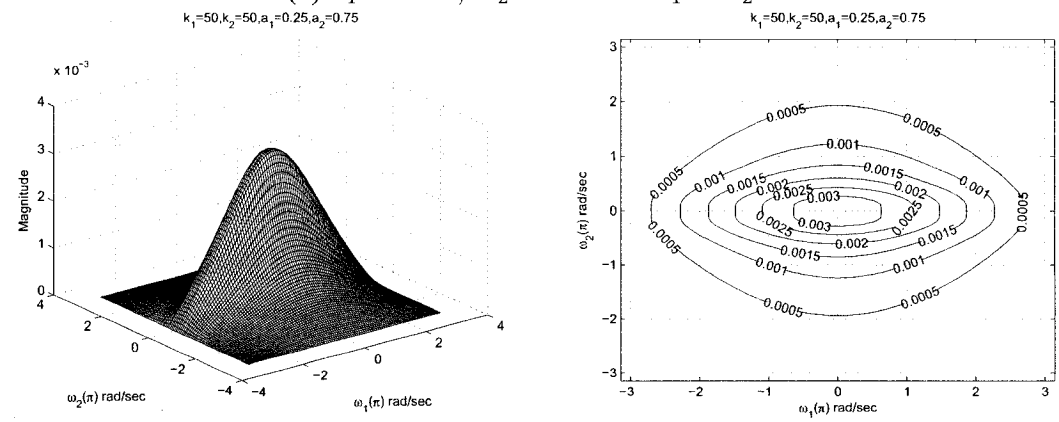

(b) $a_1 = 0.25,\ a_2 = 0.75$ and $k_1 = k_2 = 50$

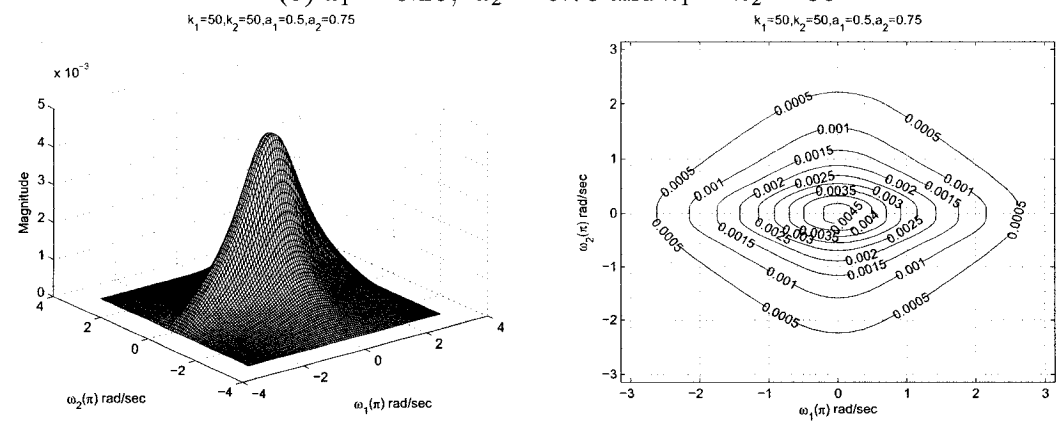

(c) $a_1 = 0.5,\ a_2 = 0.75$ and $k_1 = k_2 = 50$

Figure 2.27: 3-D amplitude frequency response and contour response of the 2-D digital lowpass filter for $a_1 \neq a_2$ and $k_1 = k_2$

As observed from the Figures 2.22 to 2.27, that the coefficients a_1 and a_2 affect the amplitude of the frequency response. It can be clearly observed from the Figures 2.22 (a), (b), (c) that the amplitude of the contour response increases from 1.8 to 2.5 when the

values of a_1 and a_2 are increased from 0.25 to 0.5 and 0.5 to 0.75 keeping the same value of $k_1 = k_2 = 0.5$. In addition, the width of the passband increases and decreases for the same.

As observed for the Figure 2.24 (a), when the values of $k_1, k_2 > 1$ and $a_1, a_2 \leq 0.5$, there are ripples in the amplitude and the contour response. As we increase the values of a_1 and a_2, the ripples tend to reduce, giving the response of the lowpass filter. When $k_1, k_2 \geq 2$, as seen from the Figures 2.24 to 2.26, we see very strong ripples in the passband. As we increase the values of a_1, a_2 and $2 \leq k_1,\ k_2 \leq 10$, the ripples tend to increase. As we further increase the value of $k_1, k_2 > 10$, and also the values of a_1 and a_2 from 0.25 to 0.5 and 0.5 to 0.75, these ripples tend to reduce, giving the response of the lowpass filter as seen from the Figures 2.27. Thus, it can be seen that there are ripples in the passband when $1 < k_1,\ k_2 \leq 10$ and $a_1,\ a_2 \leq 0.5$.

2.6.1.7 Frequency Response of 2-D Digital Lowpass Filter with different values of a_1 and a_2 and different values of k_1 and k_2

In this section, we study the effect of coefficients when $a_1 \neq a_2$ and $k_1 \neq k_2$, and the remaining coefficients b_1 and b_2 are considered to be unity for the 2-D digital lowpass filter in Category A. The values of a_1 and a_2 vary from 0.25 to 0.75 and 0.5 to 0.9 respectively, and the values of k_1 and k_2 vary from 0.5 to 50 and 1 to 75 respectively.

As observed from the Figures 2.28 to 2.31, the coefficients k_1 and k_2 affect the passband width of the frequency response. In the Figures 2.28 (a), (b), (c) and 2.29 (a) there is a decrease in the passband width as the values of k_1 and k_2 are increased from 0.5 to 50 and from 1 to 75 respectively, for the different values of $a_1 = 0.25$ and $a_2 = 0.5$. At the same time there is also a gradual decrease in the amplitude from 1.4 to 0.0014.

As observed from the Figures 2.28 to 2.31, the coefficients a_1 and a_2 affect the amplitude of the frequency response. It can be clearly observed from the Figures 2.28 (a), 2.29 (b) and 2.30 (c) that the amplitude of the contour response increases from 1.4 to 3 when the

values of a_1 and a_2 are increased from 0.25 to 0.75 and 0.5 to 0.9, respectively, keeping the same value of $k_1 = 0.5$ and $k_2 = 1$. In addition, the width of the passband increases and decreases for the same.

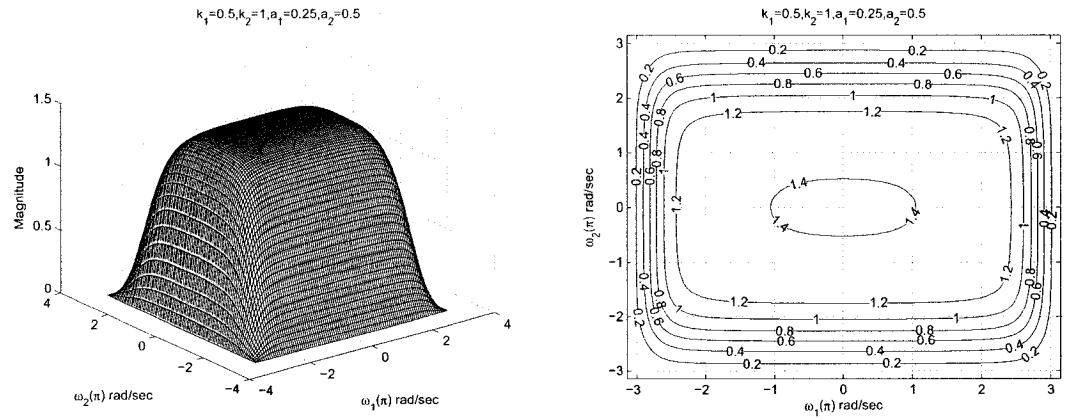

(a) $a_1 = 0.25,\ a_2 = 0.5$ and $k_1 = 0.5,\ k_2 = 1$

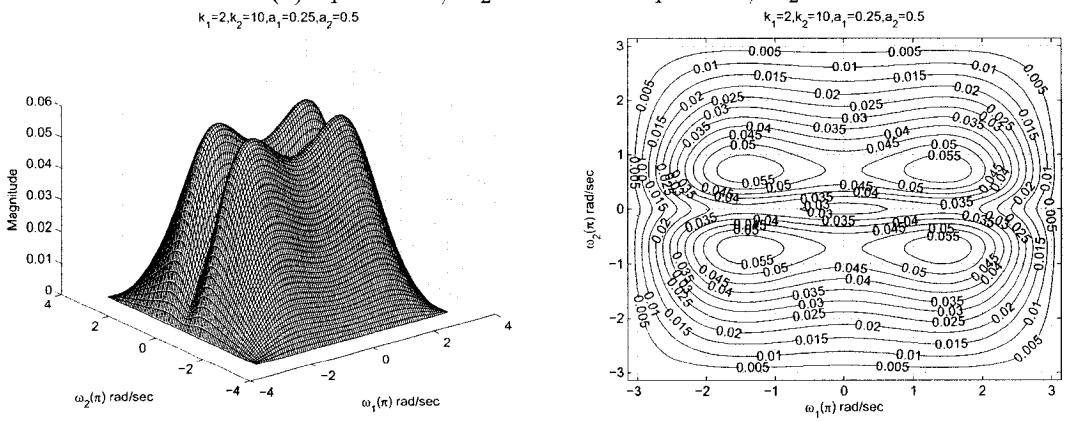

(b) $a_1 = 0.25,\ a_2 = 0.5$ and $k_1 = 2,\ k_2 = 10$

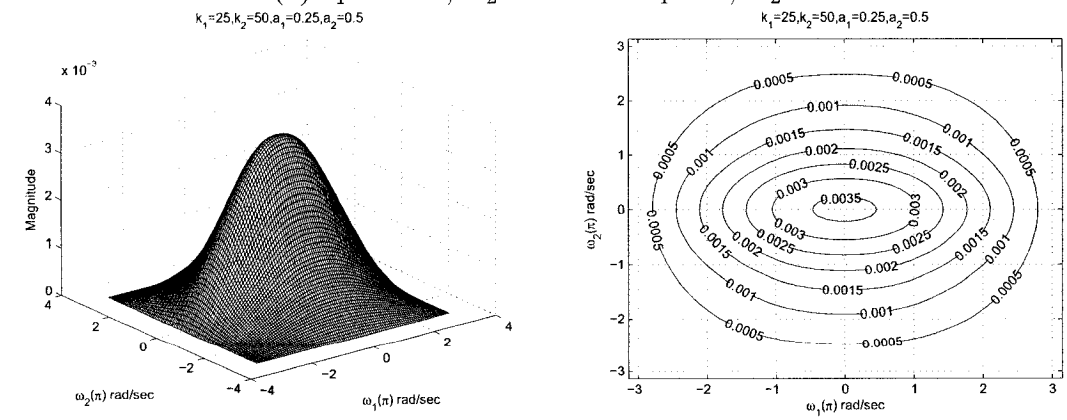

(c) $a_1 = 0.25,\ a_2 = 0.5$ and $k_1 = 25,\ k_2 = 50$

Figure 2.28: 3-D amplitude frequency response and contour response of the 2-D digital lowpass filter for $a_1 \neq a_2$ and $k_1 \neq k_2$

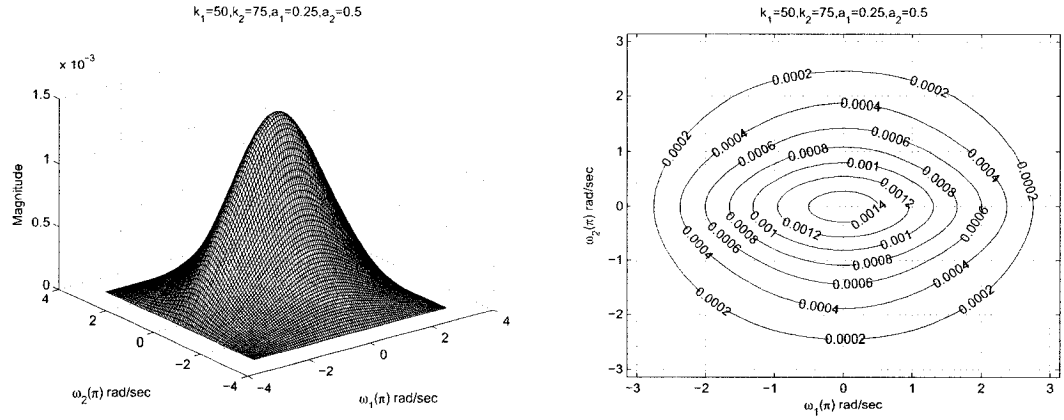

(a) $a_1 = 0.25,\ a_2 = 0.5$ and $k_1 = 50,\ k_2 = 75$

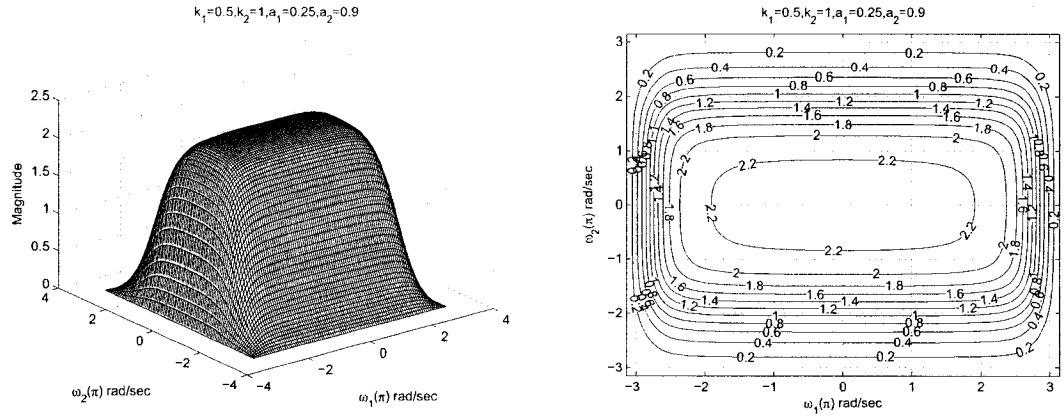

(b) $a_1 = 0.25,\ a_2 = 0.9$ and $k_1 = 0.5,\ k_2 = 1$

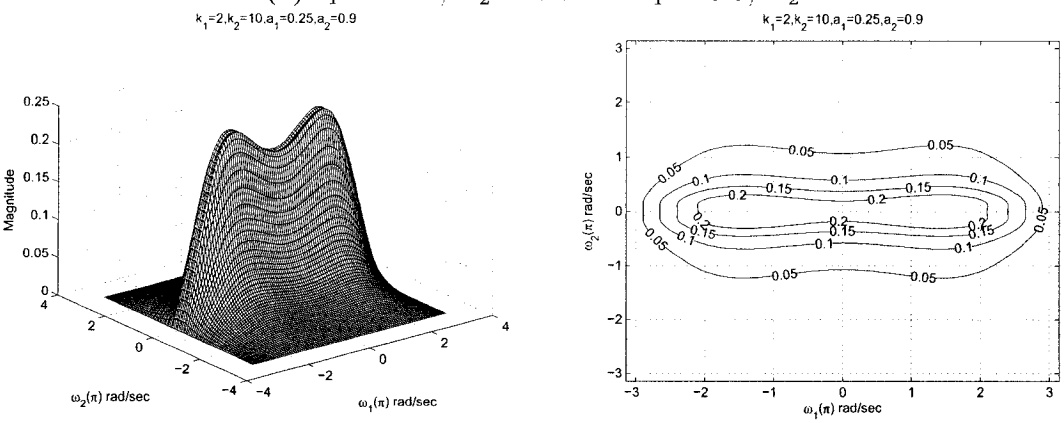

(c) $a_1 = 0.25,\ a_2 = 0.9$ and $k_1 = 2,\ k_2 = 10$

Figure 2.29: 3-D amplitude frequency response and contour response of the 2-D digital lowpass filter for $a_1 \neq a_2$ and $k_1 \neq k_2$

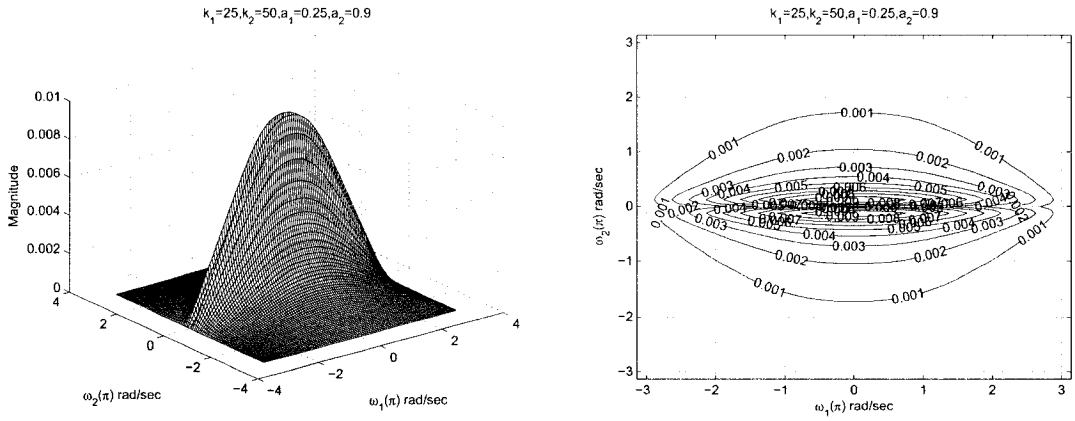

(a) $a_1 = 0.25,\ a_2 = 0.9$ and $k_1 = 25,\ k_2 = 50$

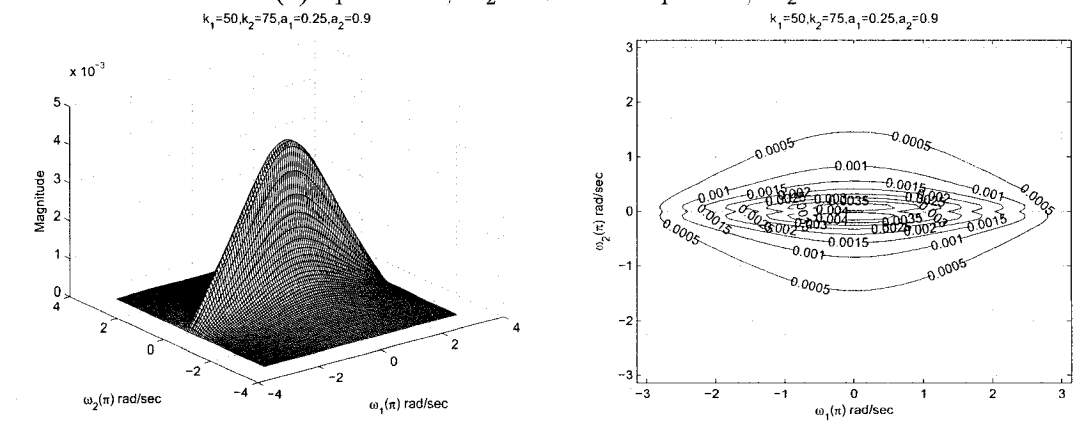

(b) $a_1 = 0.25,\ a_2 = 0.9$ and $k_1 = 50,\ k_2 = 75$

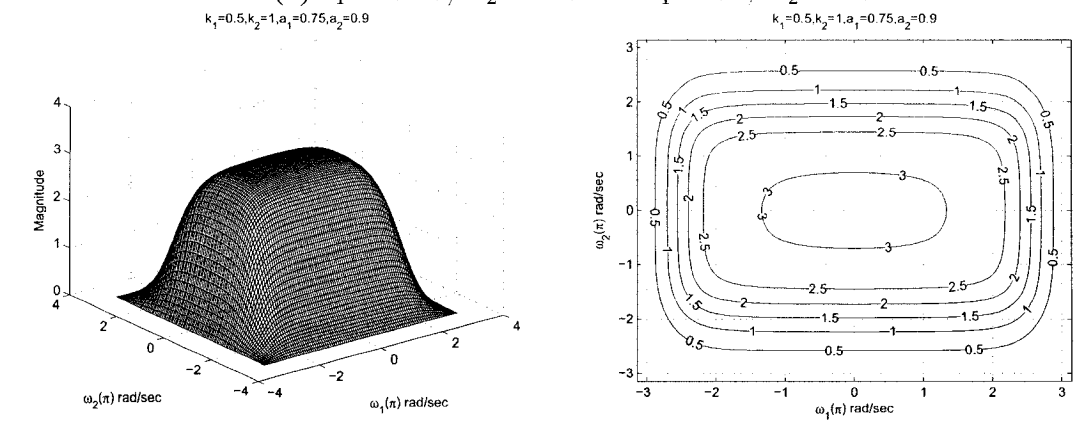

(c) $a_1 = 0.75,\ a_2 = 0.9$ and $k_1 = 0.5,\ k_2 = 1$

Figure 2.30: 3-D amplitude frequency response and contour response of the 2-D digital lowpass filter for $a_1 \neq a_2$ and $k_1 \neq k_2$

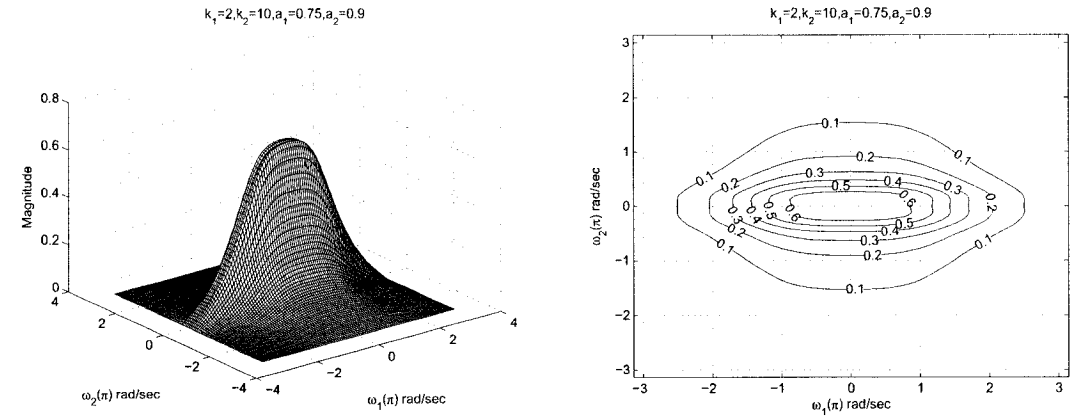

(a) $a_1 = 0.75,\ a_2 = 0.9$ and $k_1 = 2,\ k_2 = 10$

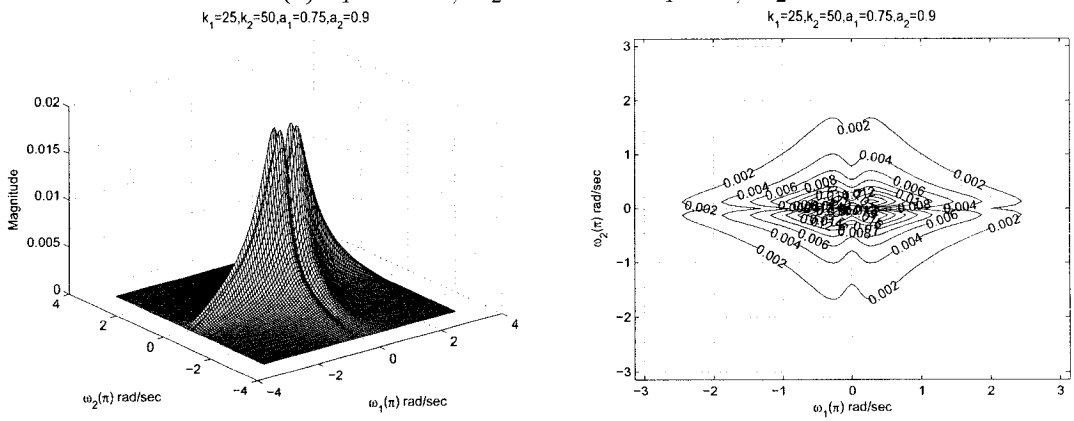

(b) $a_1 = 0.75,\ a_2 = 0.9$ and $k_1 = 25,\ k_2 = 50$

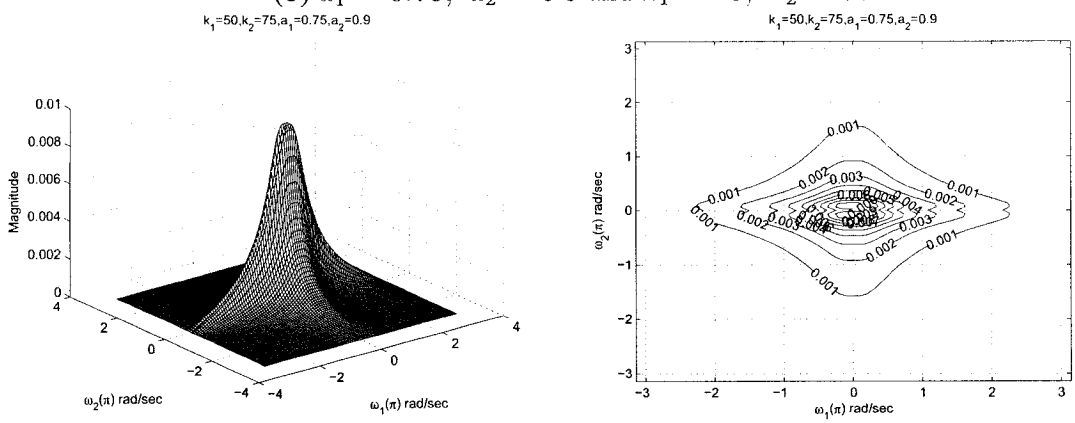

(c) $a_1 = 0.75,\ a_2 = 0.9$ and $k_1 = 50,\ k_2 = 75$

Figure 2.31: 3-D amplitude frequency response and contour response of the 2-D digital lowpass filter for $a_1 \neq a_2$ and $k_1 \neq k_2$

In the case $a_1 \neq a_2$ and $k_1 \neq k_2$, when the values of $k_1, k_2 > 1$ and $a_1, a_2 \leq 0.5$, there are ripples in the amplitude and the contour response. As we increase the values of a_1 and a_2, the ripples tend to reduce, giving the response of the lowpass filter. As we further increase the value of $k_1, k_2 > 10$, and also the values of a_1 and a_2 from 0.25 to 0.5 and 0.5 to 0.75, respectively, these ripples tend to reduce, giving the response of the low pass filter as seen from the Figures 2.28 to 2.31. Thus, it can be seen that there are ripples in the passband when one of k_1, k_2 values is $1 < k_1,\ k_2 \leq 10$ and when one of a_1, a_2 values is a_1, $a_2 \leq 0.5$.

2.6.1.8 Frequency Response of 2-D Digital Lowpass Filter with same values of a_1 and a_2 and different values of k_1 and k_2

In this section, we study the effect of coefficients, where $a_1 = a_2$ and $k_1 \neq k_2$ and the remaining coefficients b_1 and b_2 are considered to be unity for the 2-D digital lowpass filter in Category A. The values of a_1 and a_2 vary from 0 to 1 and the values of k_1 and k_2 vary from 0.5 to 50 and 1 to 75 respectively.

As observed from the Figures 2.32 to 2.37, the coefficients k_1 and k_2 affect the passband width of the frequency response. In the Figures 2.32 (a), (b), (c) and 2.33 (a) there is a decrease in the passband width as the values of k_1 and k_2 are increased from 0.5 to 75 for the same values of $a_1 = a_2 = 0.25$. At the same time there is also a gradual decrease in the amplitude from 1 to 0.001.

As observed from the Figures 2.32 to 2.37, the coefficients a_1 and a_2 affect the amplitude of the frequency response. It can be clearly observed from the Figures 2.32 (a), 2.33 (b), 2.34 (c) and 2.36 (a) that the amplitude of the contour response increases from 1 to 3 when the values of a_1 and a_2 are increased from 0.25 to 0.9 keeping the same value of $k_1 = 0.5$ and $k_2 = 1$. In addition, the width of the passband increases and decreases for the same.

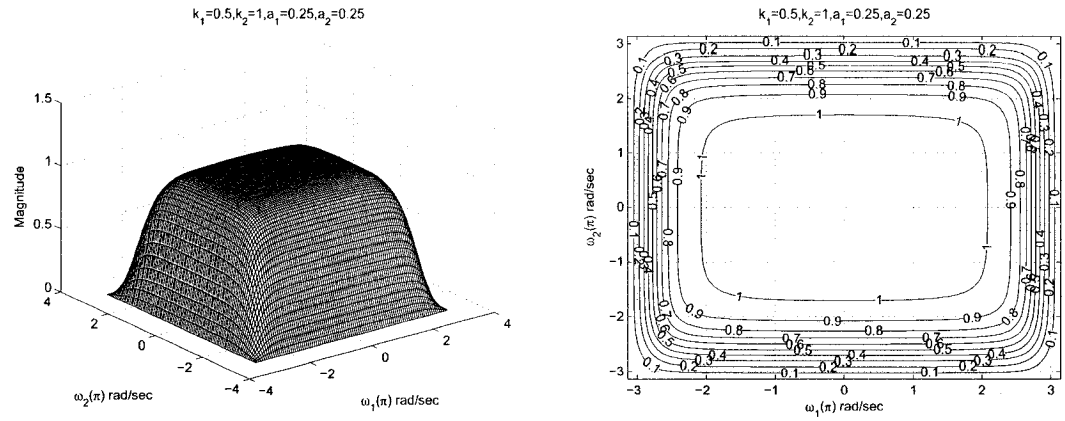

(a) $a_1 = a_2 = 0.25$ and $k_1 = 0.5,\ k_2 = 1$

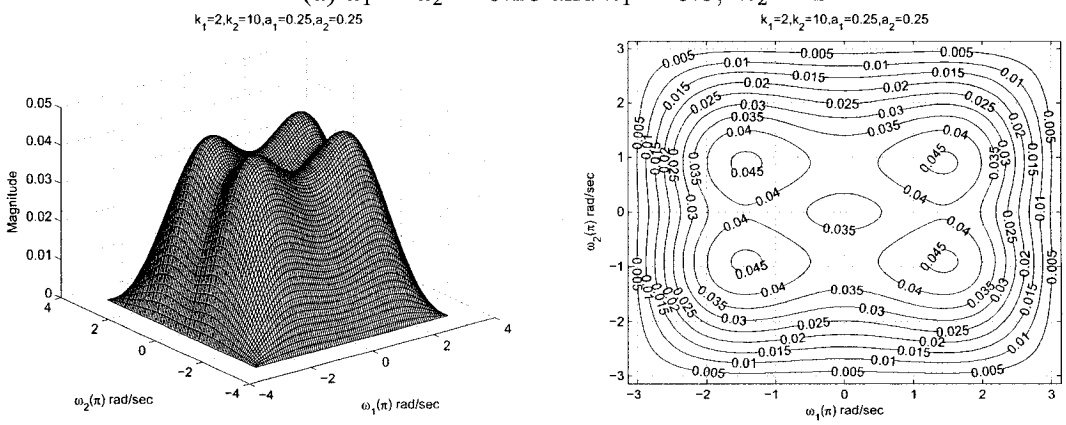

(b) $a_1 = a_2 = 0.25$ and $k_1 = 2,\ k_2 = 10$

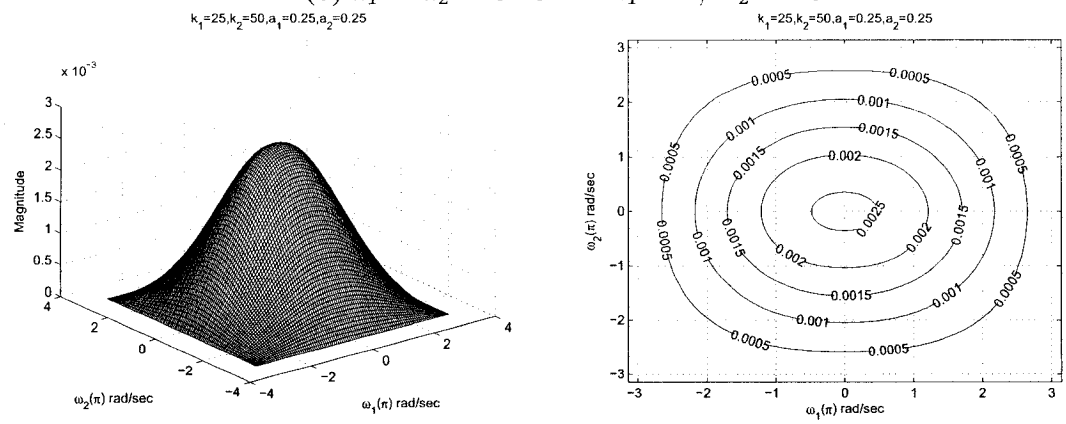

(c) $a_1 = a_2 = 0.25$ and $k_1 = 25,\ k_2 = 50$

Figure 2.32: 3-D amplitude frequency response and contour response of the 2-D digital lowpass filter for $a_1 = a_2$ and $k_1 \neq k_2$

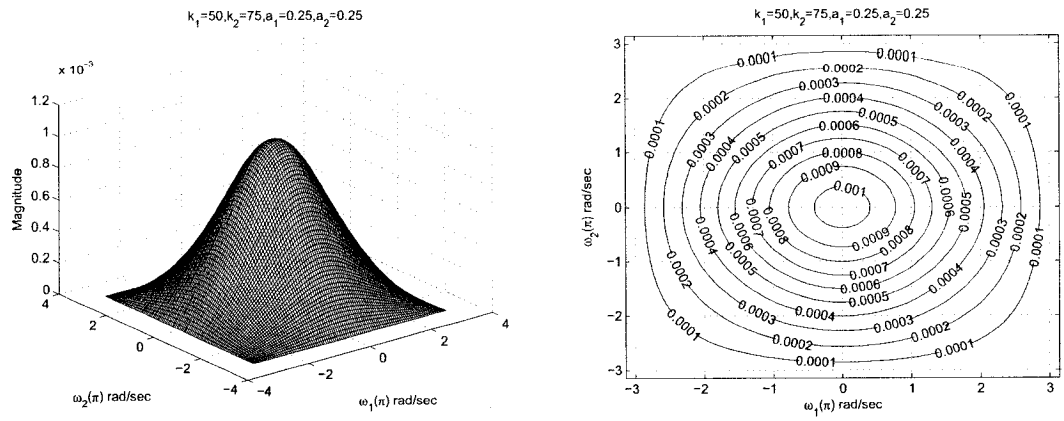

(a) $a_1 = a_2 = 0.25$ and $k_1 = 50$ $k_2 = 75$

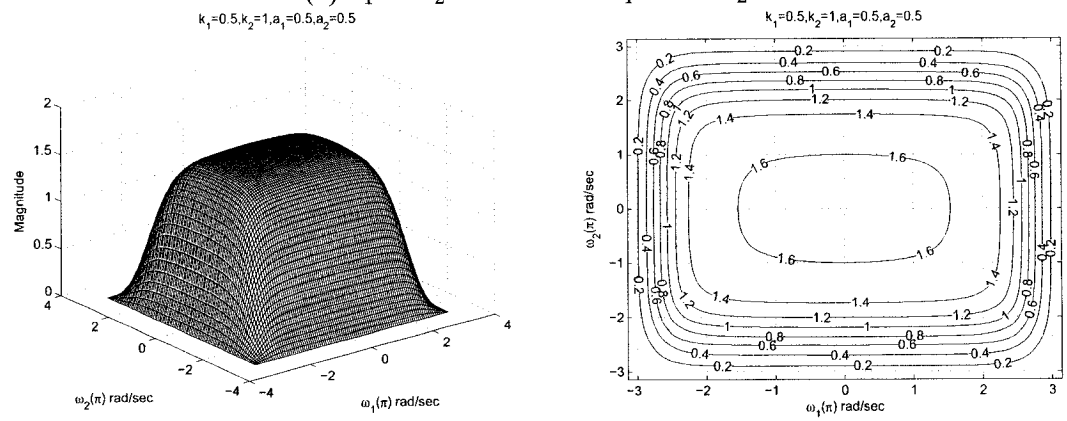

(b) $a_1 = a_2 = 0.5$ and $k_1 = 0.5$ $k_2 = 1$

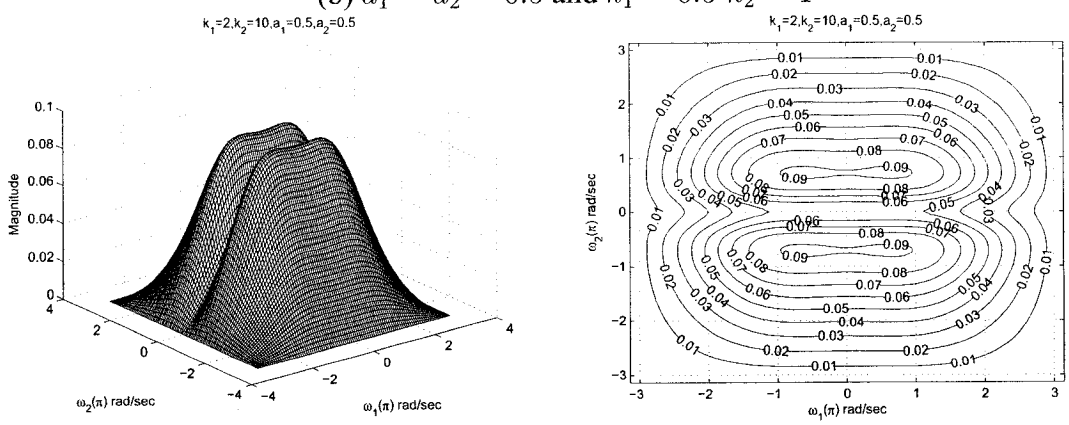

(c) $a_1 = a_2 = 0.5$ and $k_1 = 2$ $k_2 = 10$

Figure 2.33: 3-D amplitude frequency response and contour response of the 2-D digital lowpass filter for $a_1 = a_2$ and $k_1 \neq k_2$

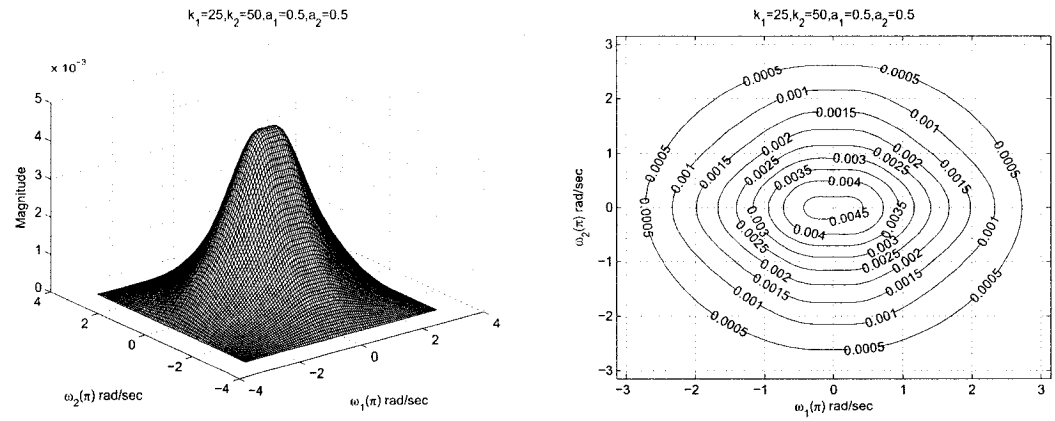

(a) $a_1 = a_2 = 0.5$ and $k_1 = 25$ $k_2 = 50$

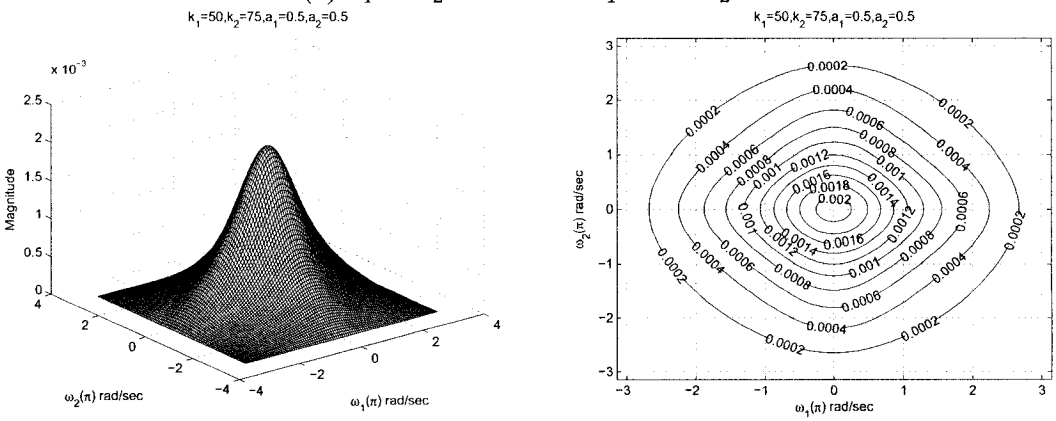

(b) $a_1 = a_2 = 0.5$ and $k_1 = 50$ $k_2 = 75$

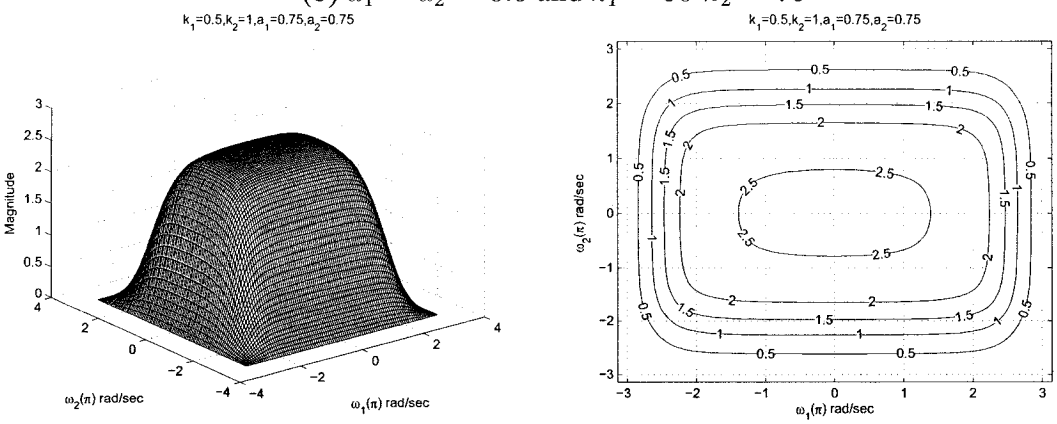

(c) $a_1 = a_2 = 0.75$ and $k_1 = 0.5$ $k_2 = 1$

Figure 2.34: 3-D amplitude frequency response and contour response of the 2-D digital lowpass filter for $a_1 = a_2$ and $k_1 \neq k_2$

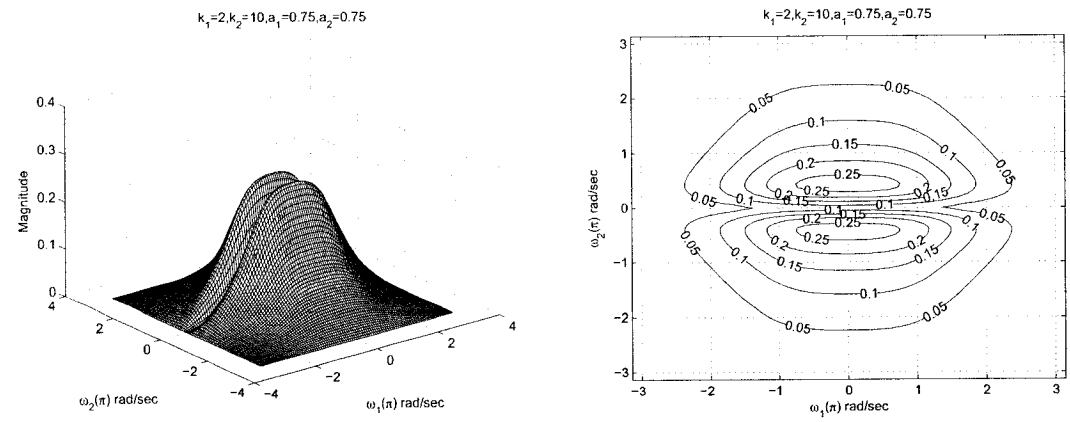

(a) $a_1 = a_2 = 0.75$ and $k_1 = 2\ k_2 = 10$

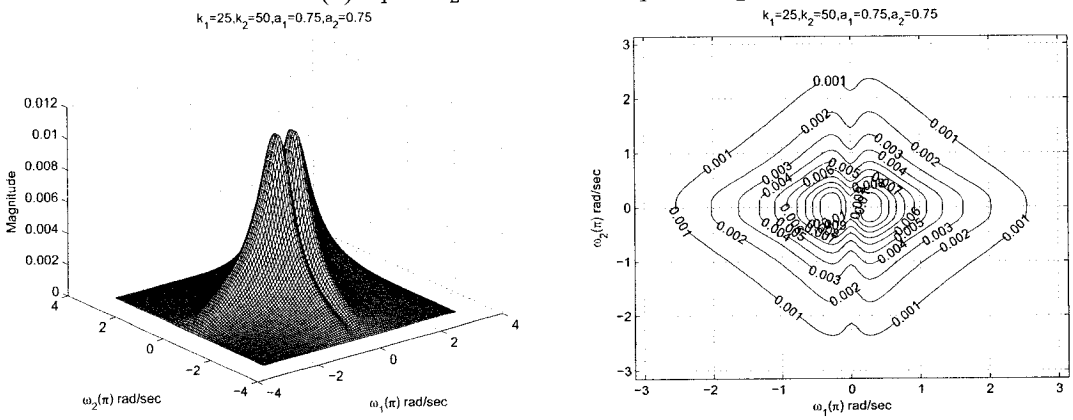

(b) $a_1 = a_2 = 0.75$ and $k_1 = 25\ k_2 = 50$

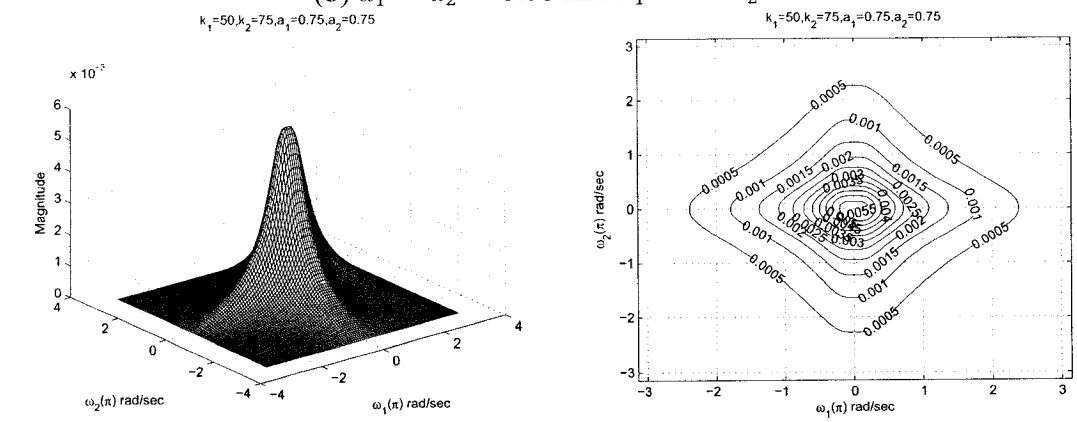

(c) $a_1 = a_2 = 0.75$ and $k_1 = 50\ k_2 = 75$

Figure 2.35: 3-D amplitude frequency response and contour response of the 2-D digital lowpass filter for $a_1 = a_2$ and $k_1 \neq k_2$

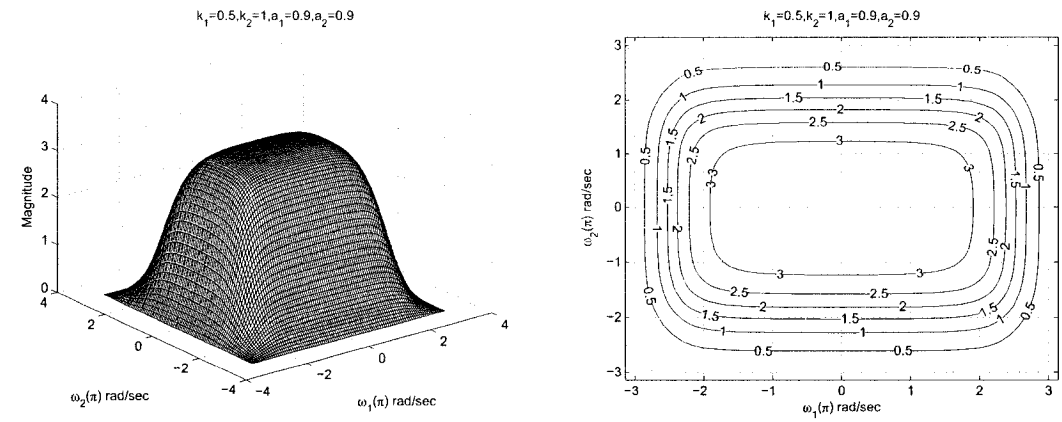

(a) $a_1 = a_2 = 0.9$ and $k_1 = 0.5$ $k_2 = 1$

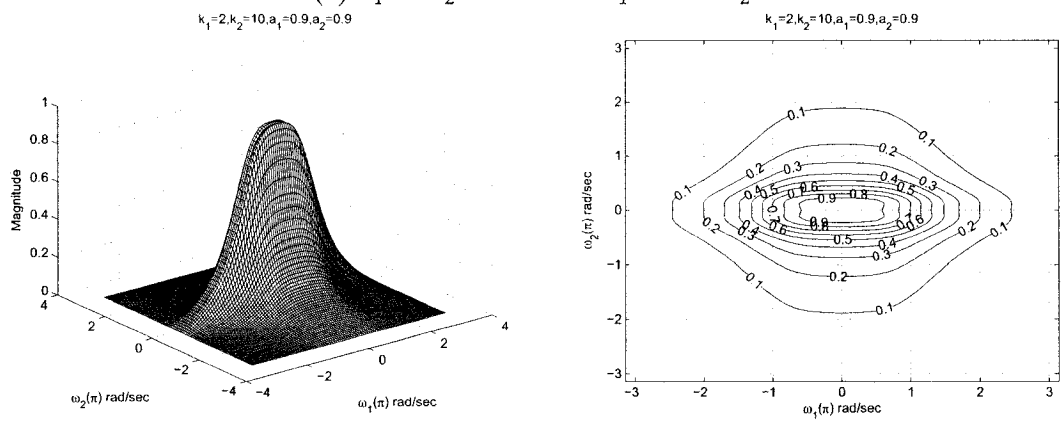

(b) $a_1 = a_2 = 0.9$ and $k_1 = 2$ $k_2 = 10$

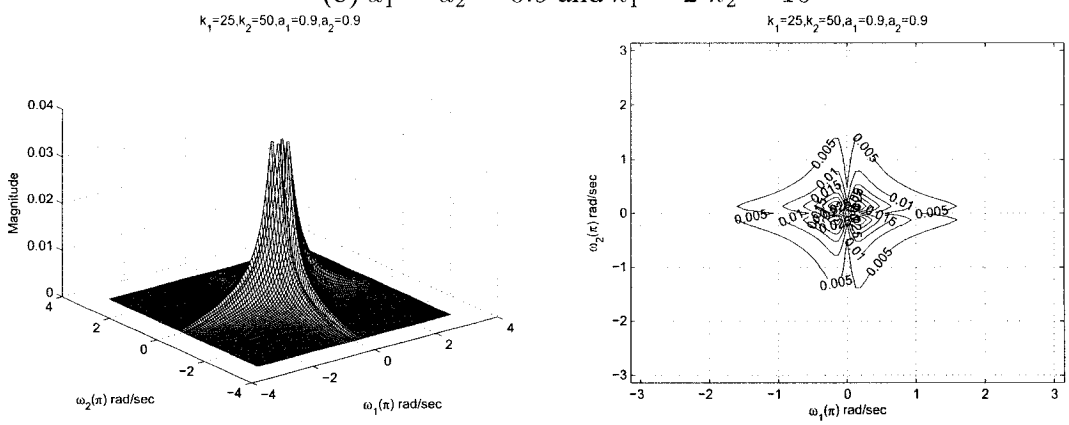

(c) $a_1 = a_2 = 0.9$ and $k_1 = 25$ $k_2 = 50$

Figure 2.36: 3-D amplitude frequency response and contour response of the 2-D digital lowpass filter for $a_1 = a_2$ and $k_1 \neq k_2$

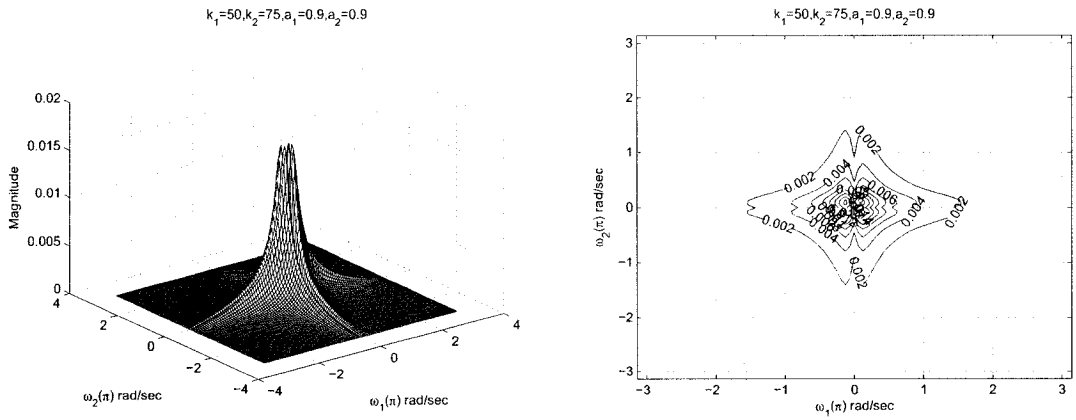

$a_1 = a_2 = 0.9$ and $k_1 = 50$ $k_2 = 75$

Figure 2.37: 3-D amplitude frequency response and contour response of the 2-D digital lowpass filter for $a_1 = a_2$ and $k_1 \neq k_2$

In this case $a_1 = a_2$ and $k_1 \neq k_2$, and when the values of $k_1, k_2 > 1$ and $a_1, a_2 \leq 0.5$, there are ripples in the amplitude and the contour response. As we increase the values of a_1 and a_2, the ripples tend to increase. Also the magnitude tends to increase from 0.045 to 0.9 for same values of $k_1 = 2$ and $k_2 = 10$ as we increase the values of a_1 and a_2 from 0.25 to 0.9 as seen from the Figures 2.32 (b), 2.33 (c), 2.35 (a) and 2.36 (b). As we further increase the value of $k_1, k_2 > 10$, and also the values of a_1 and a_2 from 0.25 to 0.9, these ripples tend to reduce, giving the response of the lowpass filter as seen from the Figures 2.32 to 2.37. Thus, it can be seen that there are ripples in the passband when $1 < k_1,\ k_2 \leq 10$ and when one of $a_1,\ a_2 \leq 0.5$.

2.6.2 Frequency Response of the All-pole 2-D Digital Lowpass Filter in Category B

The transfer function for the all-pole 2-D lowpass filter is obtained by using the second order Butterworth polynomial and its corresponding real part function connected in the all-pass filter manner. The resultant transfer function eqn. (2.79) obtained is digitized by applying the generalized bilinear transformation (eqn. (2.42)). The digitized transfer function of the all-pole 2-D digital lowpass filter is given by eqn. (2.80). With the input coefficient

of generalized bilinear transformation we can obtain the contour and 3-D magnitude plots of the resulting all-pole 2-D digital lowpass filter [46].

To investigate the manner in which each coefficient of the generalized bilinear transformation effects the magnitude response of the resulting all-pole 2-D digital lowpass filter, we change the values of some of the coefficients and fix some of the coefficients to specific values. It is possible to obtain the all-pole 2-D digital lowpass filter when the coefficients are in the limits of $k_i > 0$, $0 < |a_i| < 1$ and taking $b_i = 1$ where $i = 1, 2$. Let us consider the coefficients of the generalized bilinear transformation for the all-pole 2-D digital lowpass filter to be unity, i.e., $a_1 = 1$, $a_2 = 1$, $k_1 = 1$, $k_2 = 1$, $b_1 = 1$, $b_2 = 1$. Under this condition, the 3-D amplitude-frequency response and contour plots of the all-pole 2-D digital lowpass filter are shown in the Figure 2.38. In the following sections, we will see the effect of these coefficients on the frequency-responses of the all-pole 2-D digital lowpass filter.

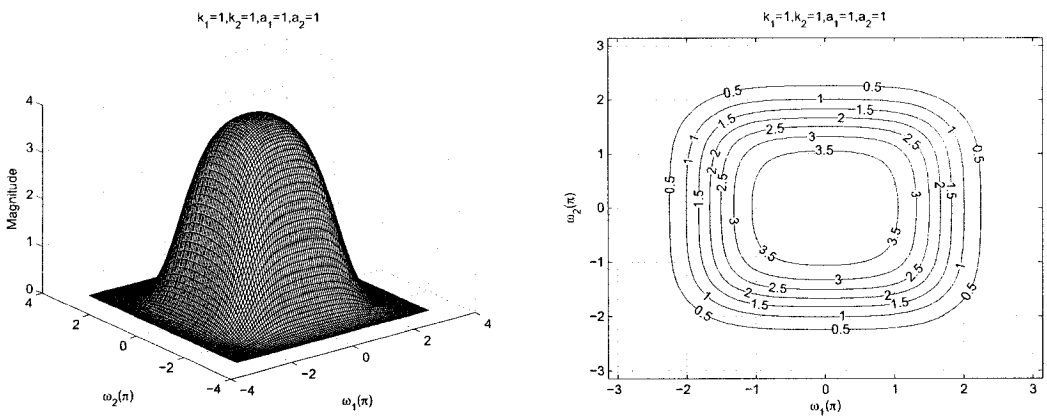

Figure 2.38: 3-D Amplitude frequency response and contour response of the All-pole 2-D digital lowpass filter with all the coefficient values as unity.

2.6.2.1 Frequency Response of the All-pole 2-D Digital Lowpass Filter with different values of k_1

In this section, we study the manner in which k_1 effects the frequency response behavior of the resulting all-pole 2-D lowpass filter in Category B and to separate the effect of the other coefficients, we vary the value of k_1, and fix all the other coefficients of the generalized bilinear transformation to be unity in order not to lose any generality and to make the situation simple, e.g. with $k_2 = 1$, $a_1 = 1$, $a_2 = 1$, $b_1 = 1$ and $b_2 = 1$. The value of k_1 is varied from 0.1 to 10 and the 3-D magnitude response and the contour plots for the lowpass filter with the values of $k_1 = 0.1$, $k_1 = 0.5$ $k_1 = 0.9$, $k_1 = 2$, $k_1 = 5$,and $k_1 = 10$ are shown in the Figures 2.39 and 2.40.

It is observed that although the coefficient k_1 does not have any effect on the passband width along the $\omega_2 - axis$, it affects the width of the passband along the $\omega_1 - axis$. Initially when the value of the coefficient $k_1 = 0.1$ (see Figure 2.39 (a)) the passband width is maximum along the $\omega_1 - axis$. As we increase the value of k_1, the passband width along the $\omega_1 - axis$ gradually decreases. Also, the amplitude of the frequency response remains constant for the same.

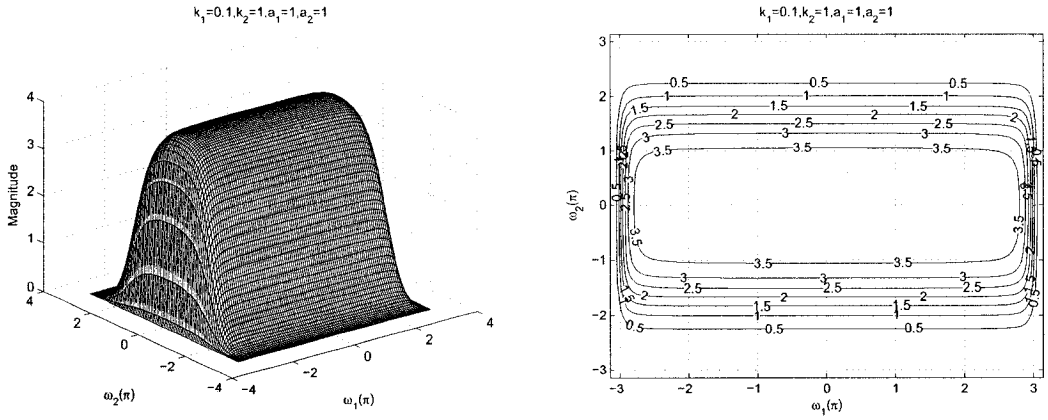

(a) $k_1 = 0.1$

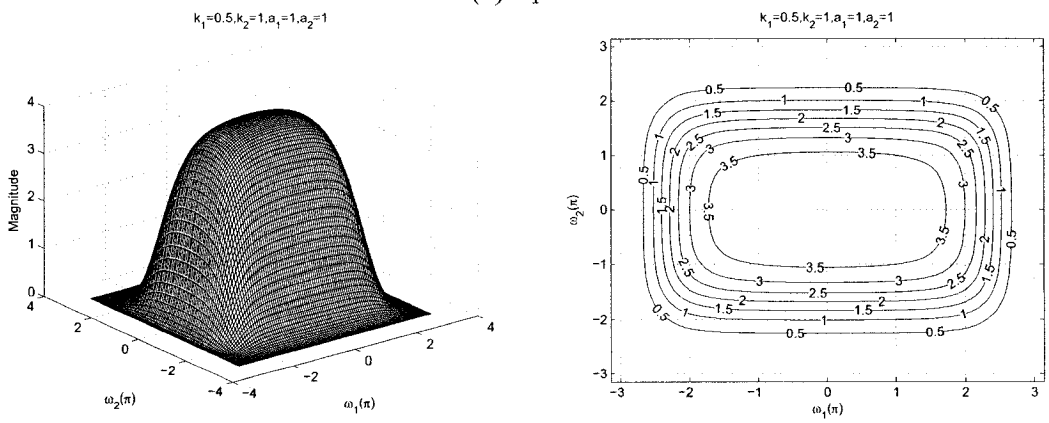

(b) $k_1 = 0.5$

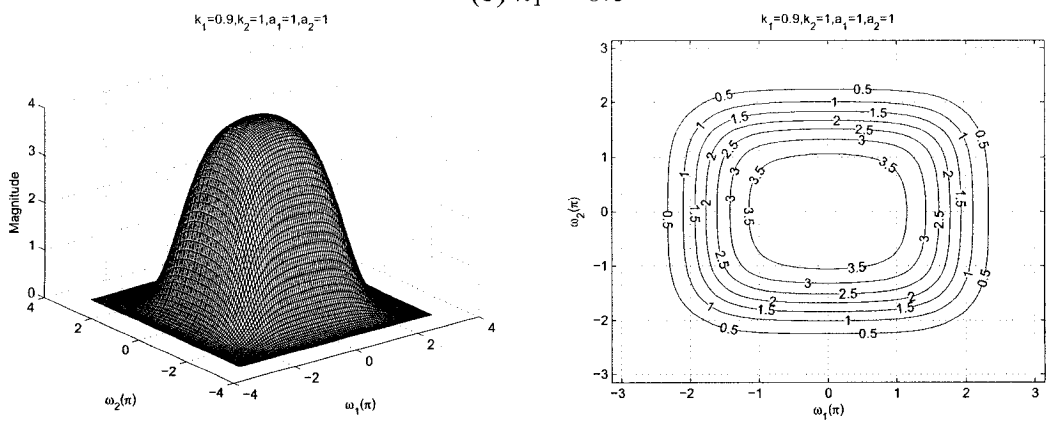

(c) $k_1 = 0.9$

Figure 2.39: 3-D amplitude frequency response and contour response of the All-pole 2-D digital lowpass filter for different values of k_1

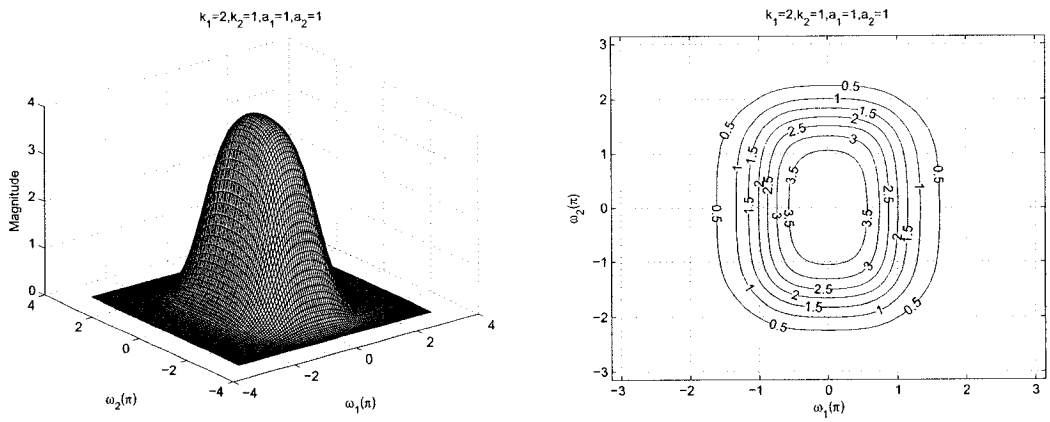

(a) $k_1 = 2$

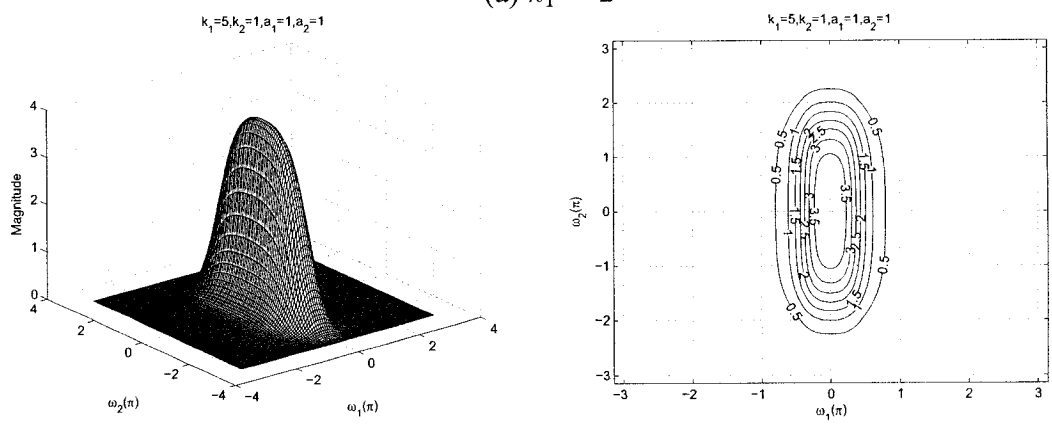

(b) $k_1 = 5$

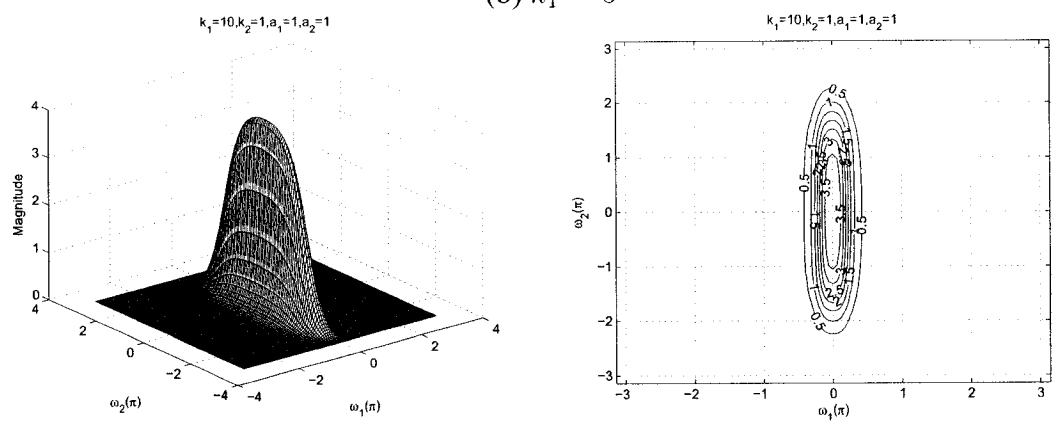

(c) $k_1 = 10$

Figure 2.40: 3-D amplitude frequency response and contour response of the All-pole 2-D digital lowpass filter for different values of k_1

2.6.2.2 Frequency Response of the All-pole 2-D Digital Lowpass Filter with different values of k_2

In Section 2.6.2.1, the effect of the coefficient k_1 was analyzed. In this section, effect of k_2 will be analyzed. To study the manner in which k_2 affects the frequency response behavior of the resulting all-pole 2-D digital lowpass filter in Category B and to separate the effect of the other coefficients, we vary the value of k_2, and fix all the other coefficients of the generalized bilinear transformation to be unity in order not to loose any generality and to make the situation simple, e.g. with $k_1 = 1$, $a_1 = 1$, $a_2 = 1$, $b_1 = 1$ and $b_2 = 1$. The value of k_2 is varied from 0.1 to 10 and the 3-D magnitude response and the contour plots for the all-pole 2-D digital lowpass filter with the values of $k_2 = 0.1$, $k_2 = 0.5$ $k_2 = 0.9$, $k_2 = 2$, $k_2 = 5$, and $k_2 = 10$ are shown in the Figures 2.41 and 2.42.

It is observed that although the coefficient k_2 does not have any effect on the passband width along the $\omega_1 - axis$, it affects the width of the passband along the $\omega_2 - axis$. Initially when the value of the coefficient $k_2 = 0.1$ (see Figure 2.41 (a)) the width of the passband is maximum along the $\omega_2 - axis$. As we increase the value of k_2, the passband width along the $\omega_2 - axis$ gradually decreases. Also, the amplitude remains constant for the same.

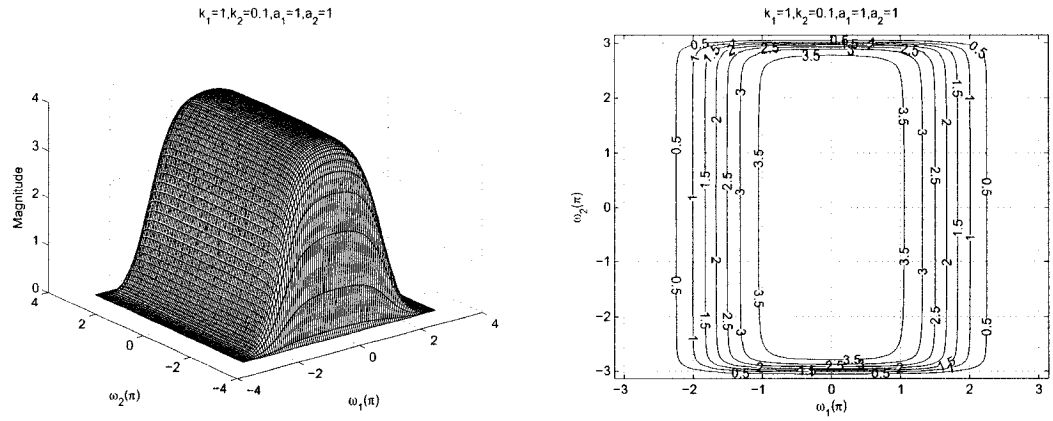

(a) $k_2 = 0.1$

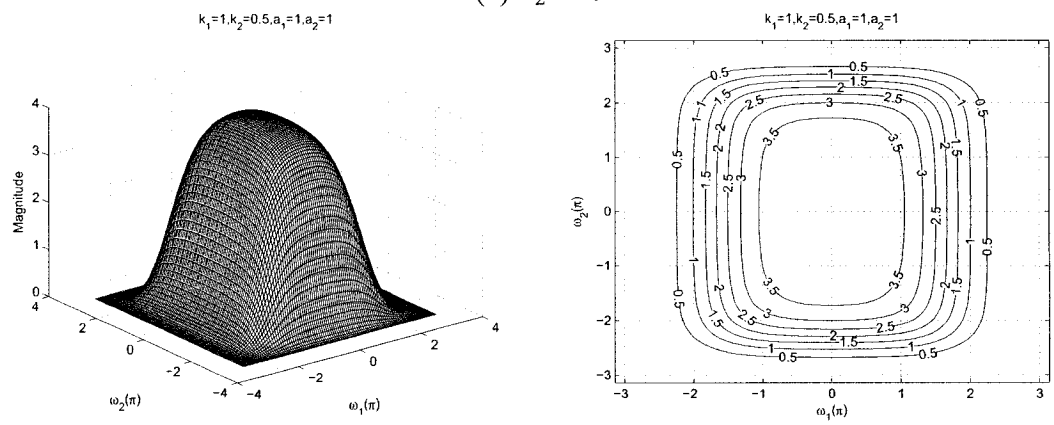

(b) $k_2 = 0.5$

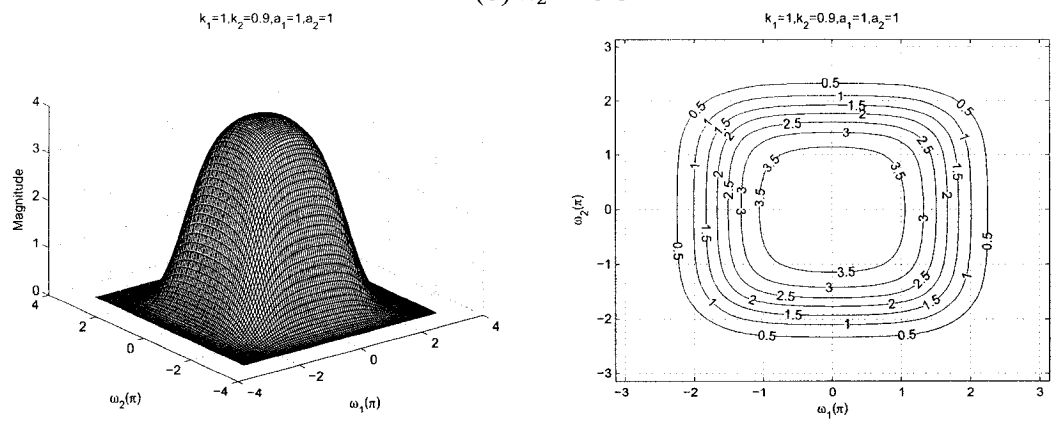

(c) $k_2 = 0.9$

Figure 2.41: 3-D amplitude frequency response and contour response of the All-pole 2-D digital lowpass filter for different values of k_2

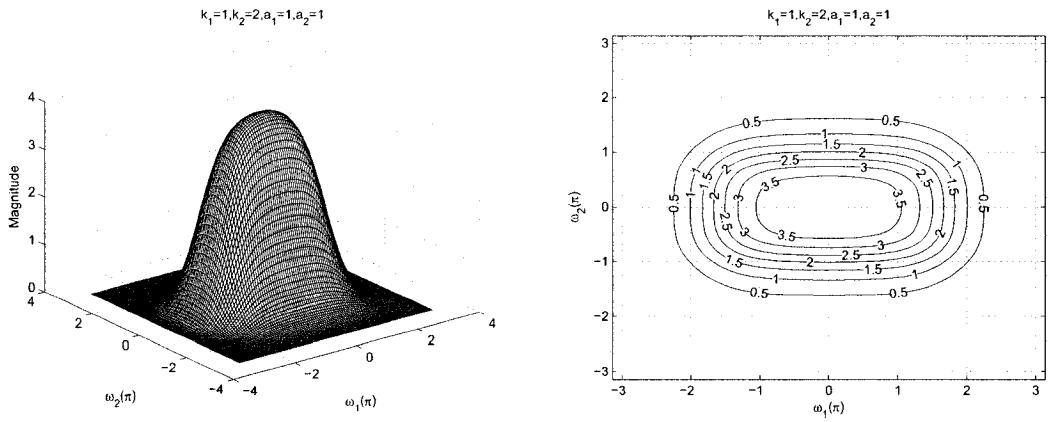

(a) $k_2 = 2$

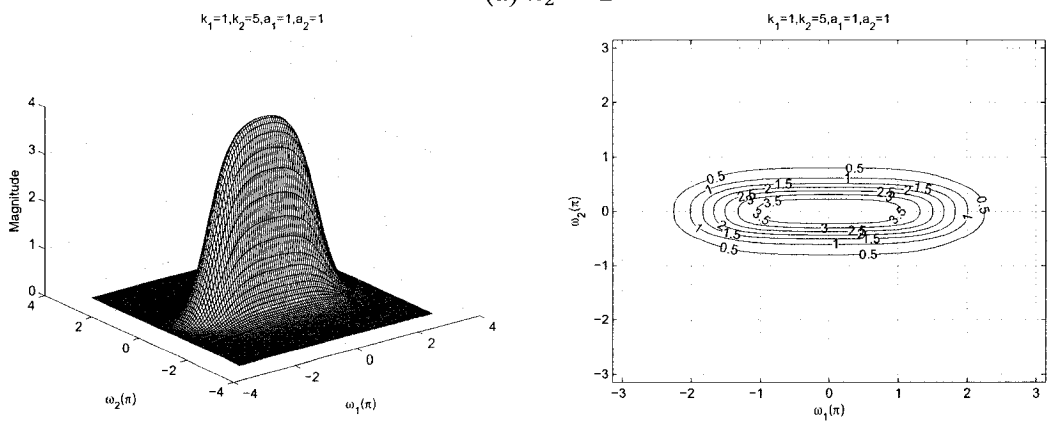

(b) $k_2 = 5$

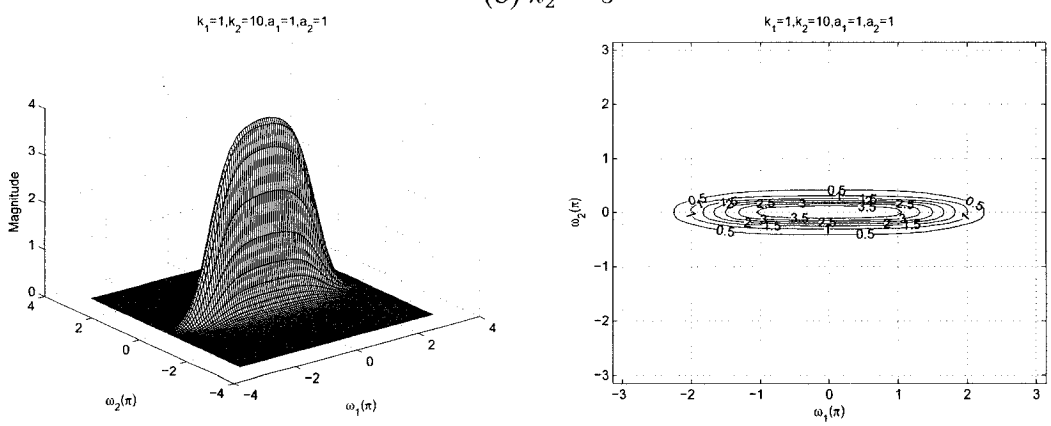

(c) $k_2 = 10$

Figure 2.42: 3-D amplitude frequency response and contour response of the All-pole 2-D digital lowpass filter for different values of k_2

2.6.2.3 Frequency Response of the All-pole 2-D Digital Lowpass Filter with different values of a_1

In the Sections 2.6.2.1 and 2.6.2.2, the effect of the coefficients k_1 and k_2 was studied. In this section, the effect of the coefficient a_1 will be studied. The stable range of a_1 can be obtained with other specified coefficient of the generalized bilinear transformation. There are many combinations possible for the coefficients. To study the response with different values of a_1 properly, we fix other coefficient values to be equal to unity. The range of a_1 varies from 0.1 to 1 and the other coefficient values are specified as unity, i.e., $k_1 = 1$, $k_2 = 1$, $a_2 = 1$, $b_1 = 1$ and $b_2 = 1$ in order to get the all-pole 2-D digital lowpass filter in Category B.

By varying the value of a_1, the 3-D magnitude response and contour plots which represents different values of a_1, i.e. $a_1 = 0.1$, $a_1 = 0.25$, $a_1 = 0.5$, $a_1 = 0.75$, and $a_1 = 0.9$ are shown in the Figures 2.43 and 2.44. By making the value of $a_1 = 1$, it resembles the standard all-pole 2-D digital lowpass filter as shown in the Figure 2.38. It is observed for the diagrams that the coefficient a_1 affects the gain of the amplitude response. At the lowest value of a_1 the gain of the passband will be less than 1. As the value of a_1 increases, the gain increases from 1.6 to 3.5 and reaches the maximum value at $a_1 = 1$. At the same time the passband width increases when the value of $a_1 \leq 0.5$ and then decreases along $\omega_1 - axis$. Also, the coefficient a_1 does not have any effect along the $\omega_2 - axis$.

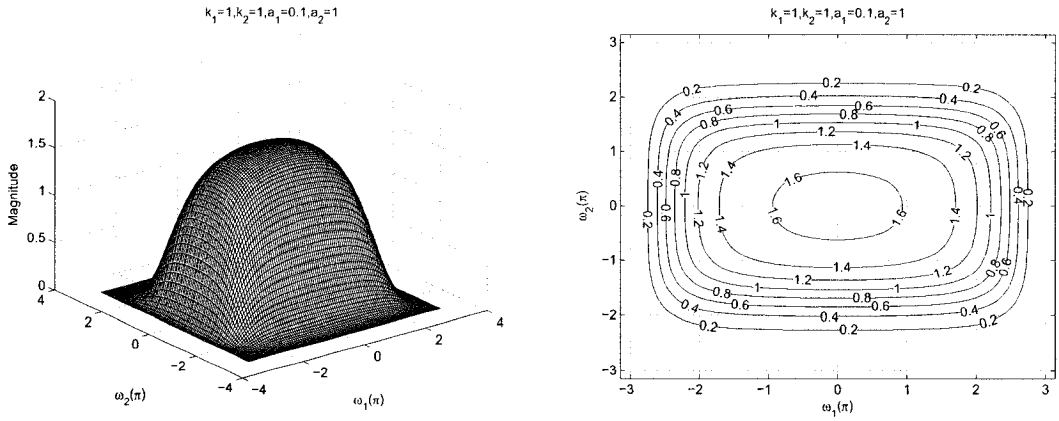

(a) $a_1 = 0.1$

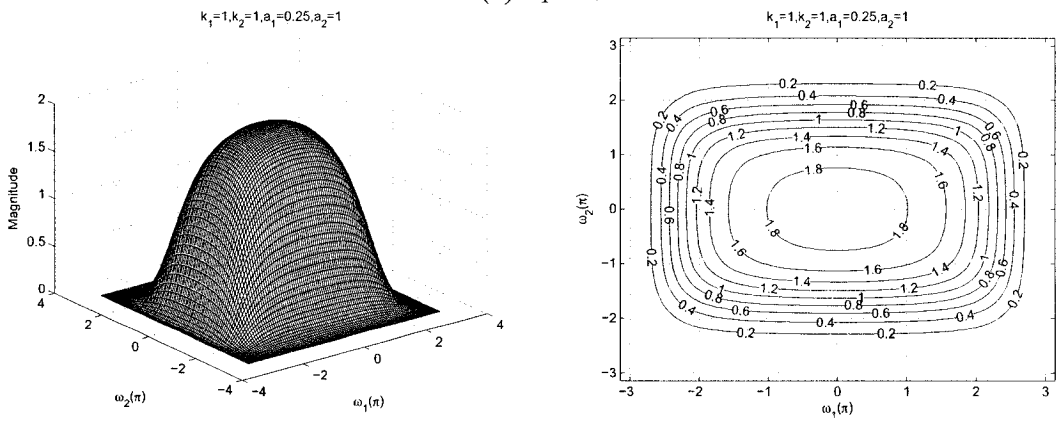

(b) $a_1 = 0.25$

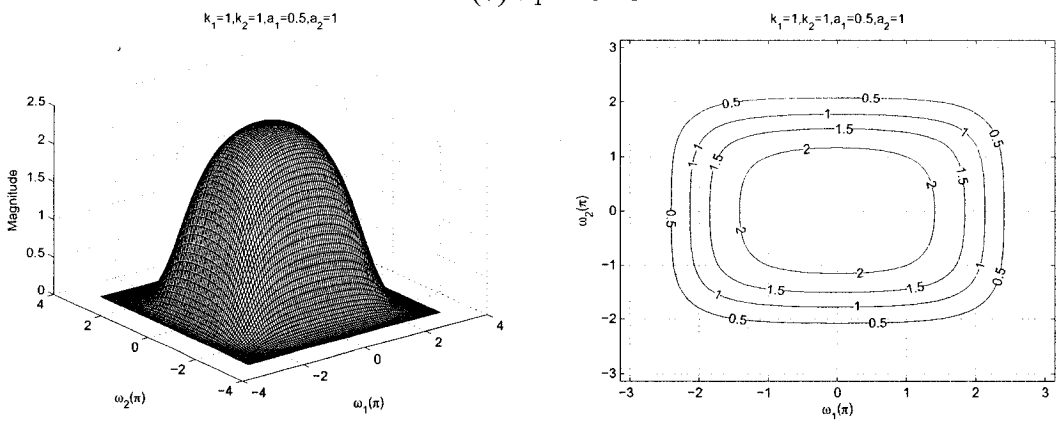

(c) $a_1 = 0.5$

Figure 2.43: 3-D amplitude frequency response and contour response of the All-pole 2-D digital lowpass filter for different values of a_1

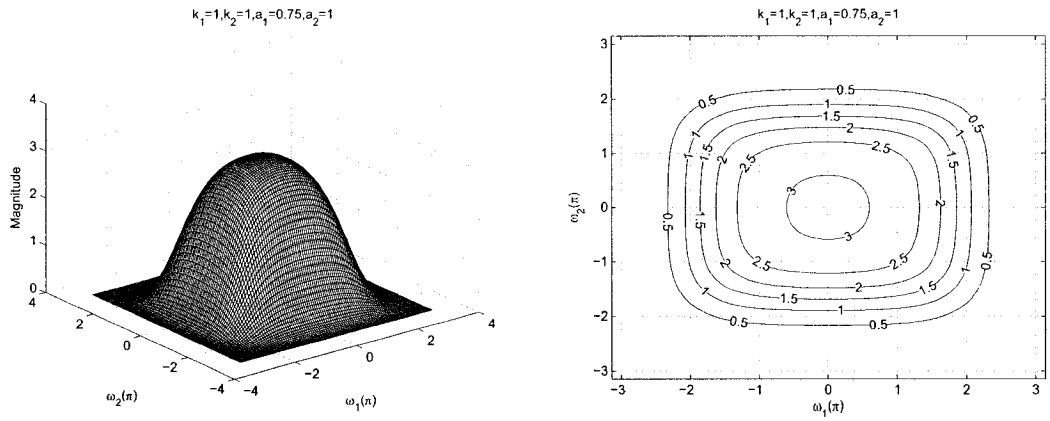

(a) $a_1 = 0.75$

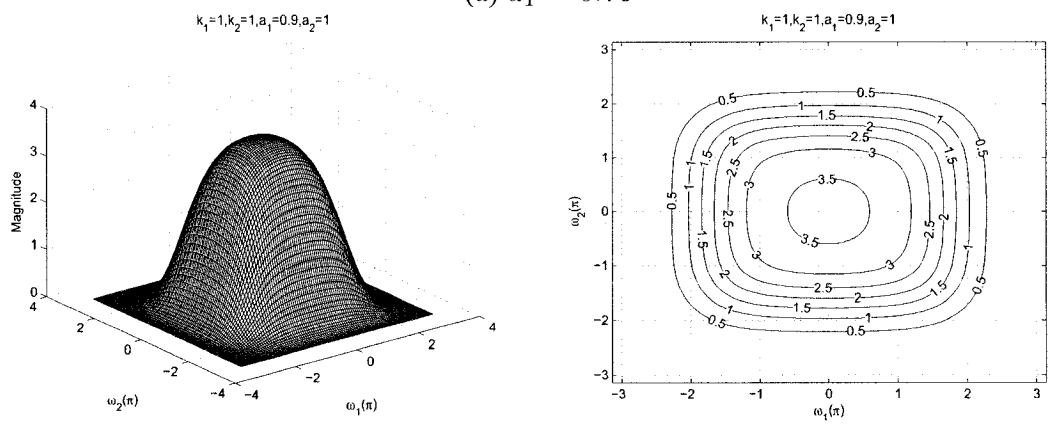

(b) $a_1 = 0.9$

Figure 2.44: 3-D amplitude frequency response and contour response of the All-pole 2-D digital lowpass filter for different values of a_1

2.6.2.4 Frequency Response of the All-pole 2-D Digital Lowpass Filter with different values of a_2

In the Section 2.6.2.3, the effect of the coefficient a_1 was studied. In this Section, the effect of the coefficient a_2 will be studied. The stable range of a_2 can be obtained with other specified coefficient of the generalized bilinear transformation. There are many combinations possible for the coefficients. To study the response with different values of a_2 properly, we fix other coefficient values to be equal to unity. The range of a_2 varies from 0.1 to 1 and the other coefficient values are specified as unity, i.e., $k_1 = 1$, $k_2 = 1$, $a_1 = 1$, $b_1 = 1$ and $b_2 = 1$ in order to get the all-pole 2-D digital lowpass filter in Category B.

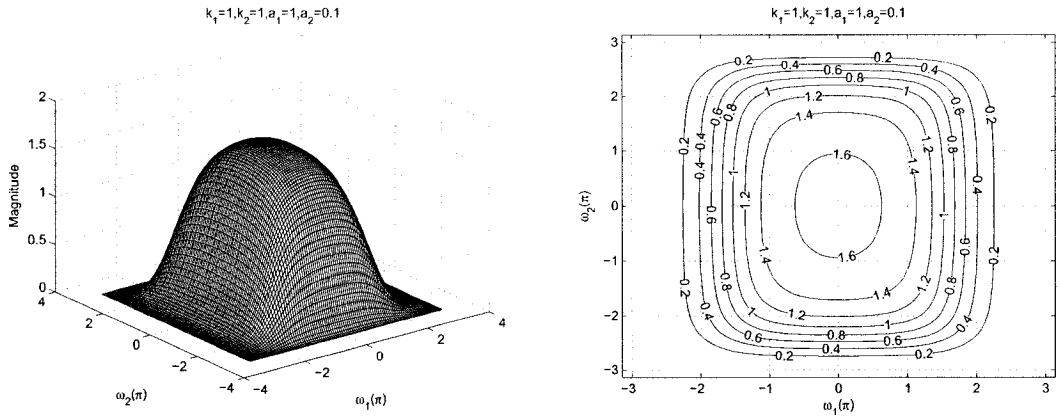

(a) $a_2 = 0.1$

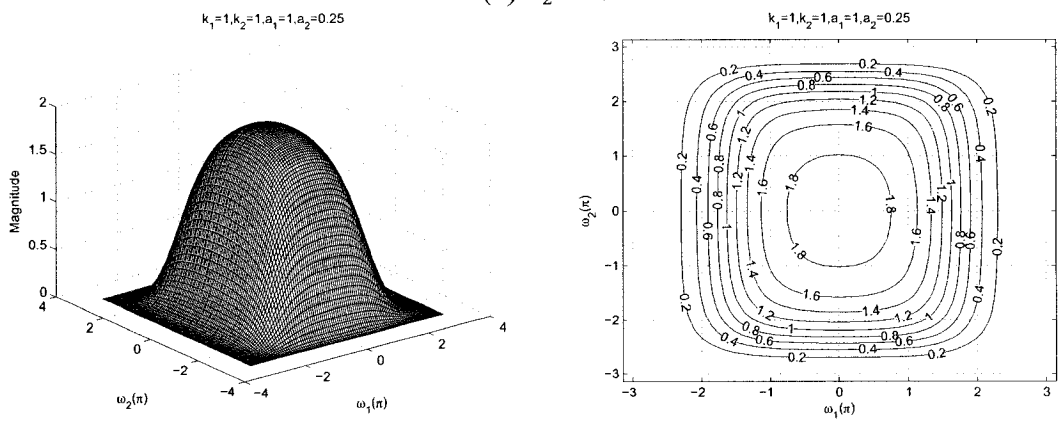

(b) $a_2 = 0.25$

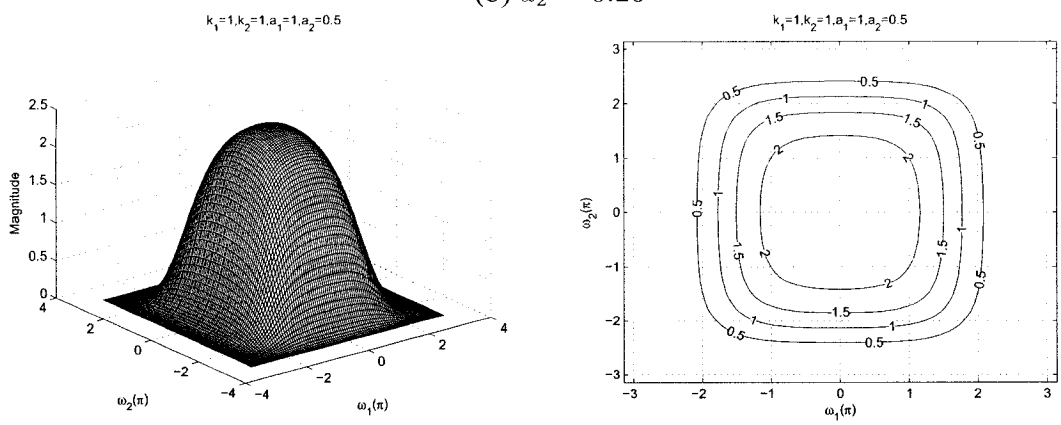

(c) $a_2 = 0.5$

Figure 2.45: 3-D amplitude frequency response and contour response of the All-pole 2-D digital lowpass filter for different values of a_2

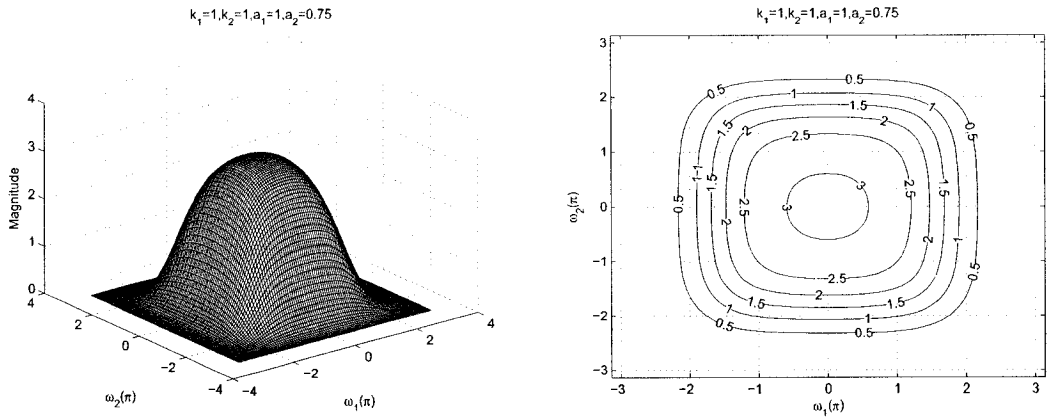

(a) $a_2 = 0.75$

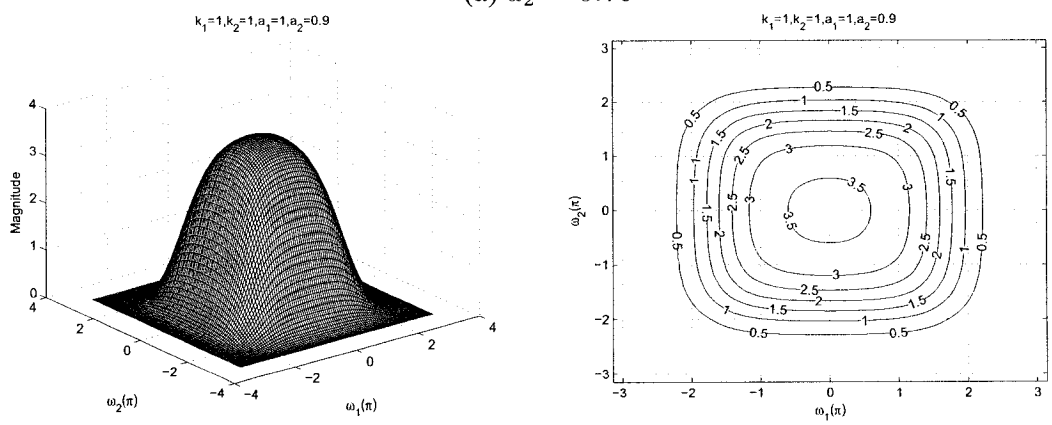

(b) $a_2 = 0.9$

Figure 2.46: 3-D amplitude frequency response and contour response of the All-pole 2-D digital lowpass filter for different values of a_2

By varying the value of a_2, the 3-D magnitude response and contour plots which represents different values of a_2, i.e., $a_2 = 0.1$, $a_2 = 0.25$, $a_2 = 0.5$, $a_2 = 0.75$, and $a_2 = 0.9$ are shown in the Figures 2.45 and 2.46. By making the value of $a_2 = 1$, it resembles the standard all-pole 2-D digital lowpass filter as shown in the Figure 2.38. It is observed for the diagrams that the coefficient effects the gain of the amplitude response. At the lowest value of a_2 the gain of the passband will be less than 1. As the value of a_2 increases, the gain increases from 1.6 to 3.5 and reaches the maximum value at $a_2 = 1$. At the same time the passband width increases as we increase when the value of $a_2 \leq 0.5$ and then decreases along the $\omega_2 - axis$. Also, the coefficient a_2 does not have any effect on along the $\omega_1 - axis$.

2.6.2.5 Frequency Response of the All-pole 2-D Digital Lowpass Filter with same values of a_1 and a_2 and same values of k_1 and k_2

In the Sections 2.6.2.1 to 2.6.2.4 the individual effect of the coefficients a_1, a_2, k_1 and k_2 was studied. In this section, we will study the effect of coefficients where $a_1 = a_2$ and $k_1 = k_2$ and the remaining coefficient b_1 and b_2 are considered to be unity for the all-pole 2-D digital lowpass filter in Category B. The values of a_1 and a_2 ranges from 0 to 1 and the values of k_1 and k_2 ranges from 0 to 50.

As observed from the Figures 2.47 to 2.53, that the coefficients k_1 and k_2 affect the passband width of the frequency response. In the Figures 2.47 (a), 2.48 (b), 2.49 (c), 2.51 (a) and 2.52 (b), there is a decrease in the passband width of the contour response as the values of k_1 and k_2 are increased from 0.5 to 50 for the same values of $a_1 = a_2 = 0.25$. At the same time, there is also a decrease in the amplitude of the contour response from 1.8 to 1.6×10^{-7} for the same. It is also observed that for very high values of k_1 and k_2, the passband width of the frequency response becomes very narrow as shown in the Figure 2.53 (b).

As observed from the Figures 2.47 to 2.53, the coefficients a_1 and a_2 affect the magnitude of the amplitude-frequency response. It can be clearly observed from the Figures 2.47 (a), (b), (c) and 2.48 (a) that the amplitude of the frequency response increases from 1.8 to 3.5 when the values of a_1 and a_2 are increased from 0.25 to 0.9 keeping the same value of $k_1 = k_2 = 0.5$. In addition, the width of the passband increases and decreases for the same.

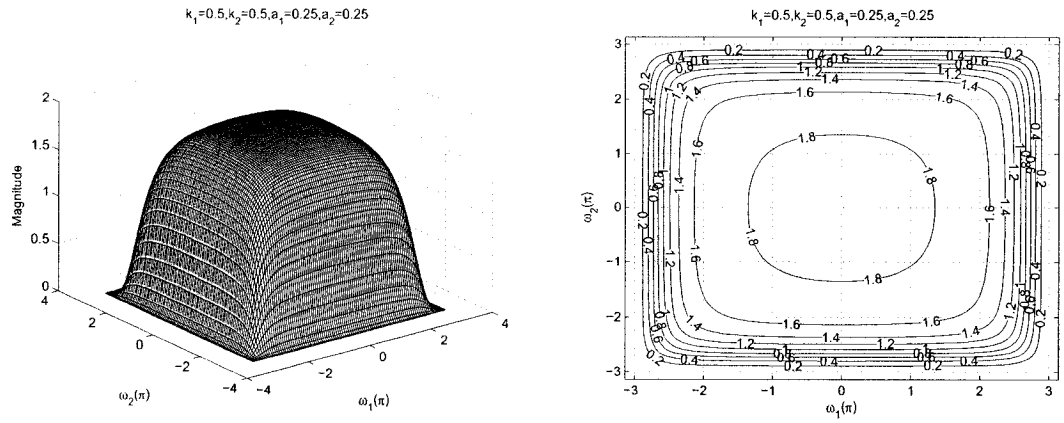

(a) $a_1 = a_2 = 0.25$ and $k_1 = k_2 = 0.5$

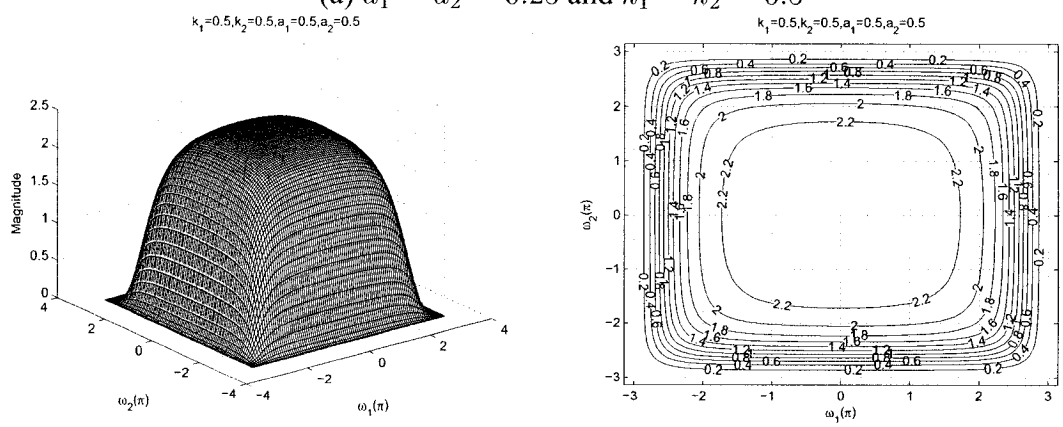

(b) $a_1 = a_2 = 0.5$ and $k_1 = k_2 = 0.5$

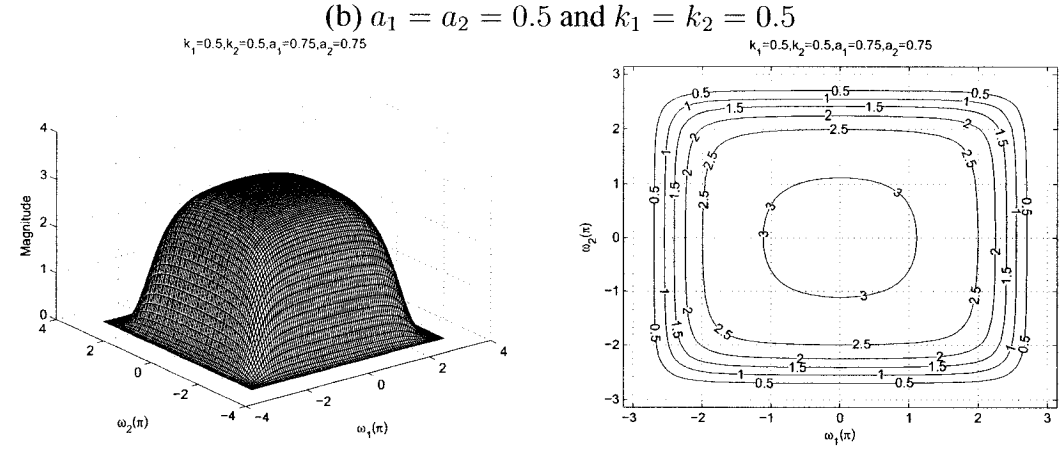

(c) $a_1 = a_2 = 0.75$ and $k_1 = k_2 = 0.5$

Figure 2.47: 3-D amplitude frequency response and contour response of the All-pole 2-D digital lowpass filter for $a_1 = a_2$ and $k_1 = k_2$

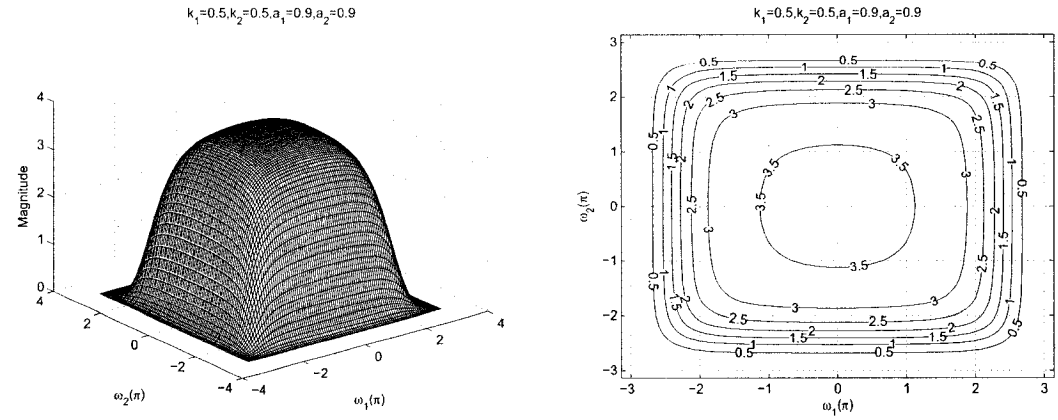

(a) $a_1 = a_2 = 0.9$ and $k_1 = k_2 = 0.5$

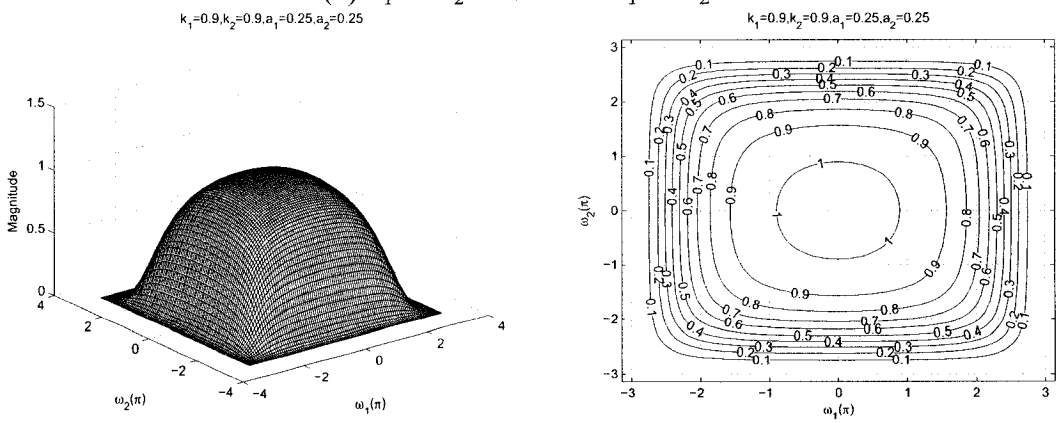

(b) $a_1 = a_2 = 0.25$ and $k_1 = k_2 = 0.9$

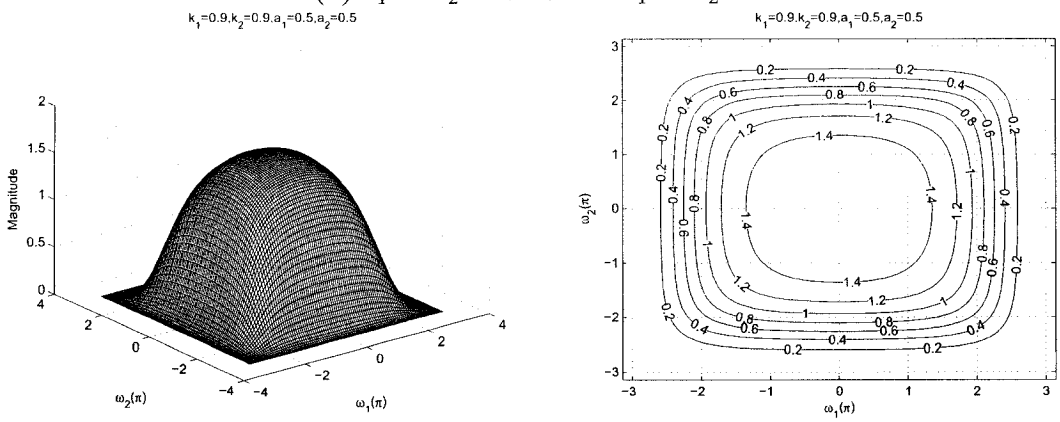

(c) $a_1 = a_2 = 0.5$ and $k_1 = k_2 = 0.9$

Figure 2.48: 3-D amplitude frequency response and contour response of the All-pole 2-D digital lowpass filter for $a_1 = a_2$ and $k_1 = k_2$

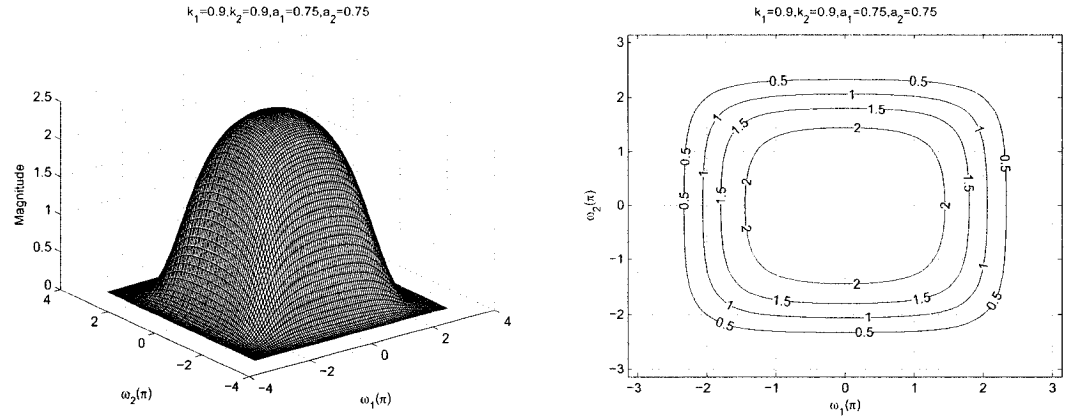

(a) $a_1 = a_2 = 0.75$ and $k_1 = k_2 = 0.9$

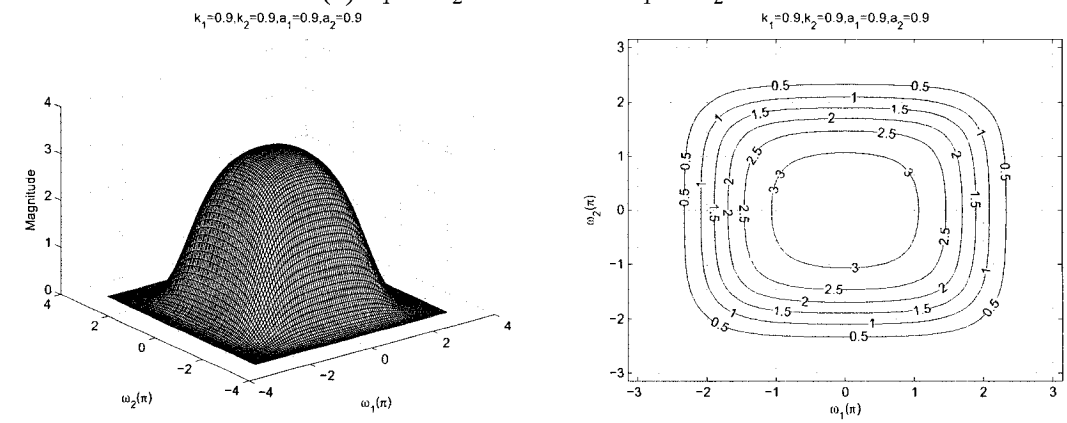

(b) $a_1 = a_2 = 0.9$ and $k_1 = k_2 = 0.9$

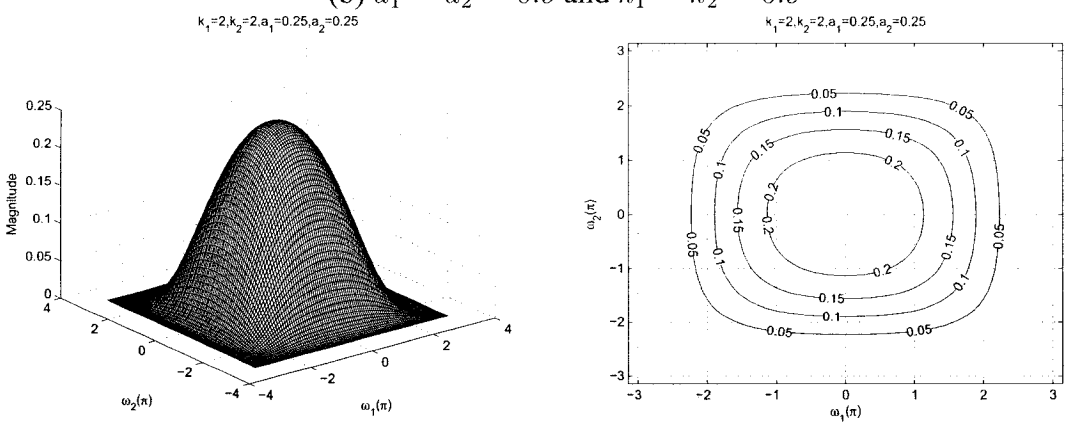

(c) $a_1 = a_2 = 0.25$ and $k_1 = k_2 = 2$

Figure 2.49: 3-D amplitude frequency response and contour response of the All-pole 2-D digital lowpass filter for $a_1 = a_2$ and $k_1 = k_2$

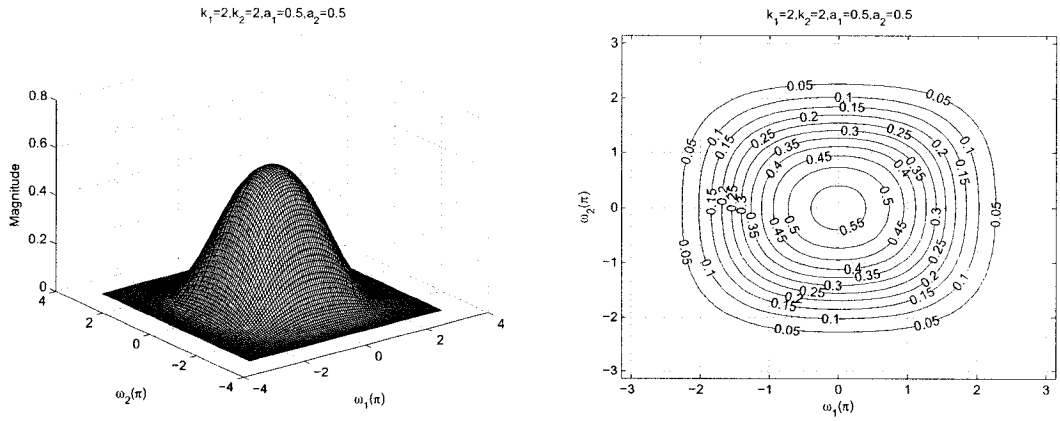

(a) $a_1 = a_2 = 0.5$ and $k_1 = k_2 = 2$

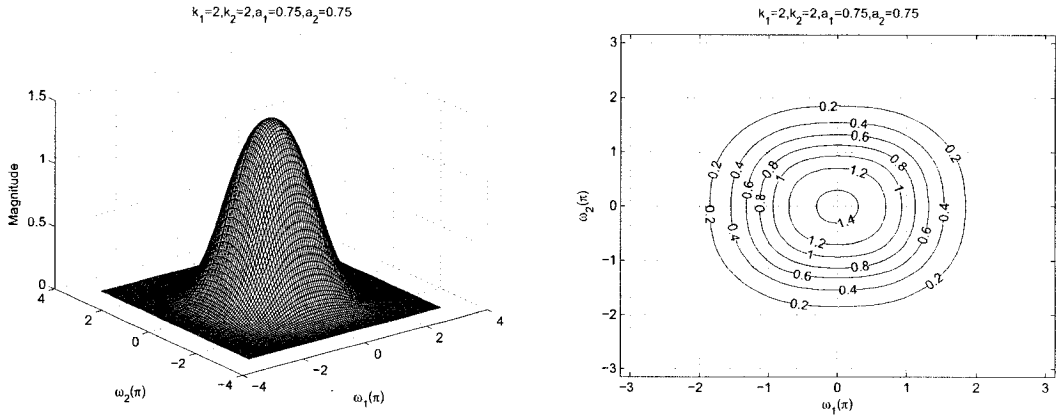

(b) $a_1 = a_2 = 0.75$ and $k_1 = k_2 = 2$

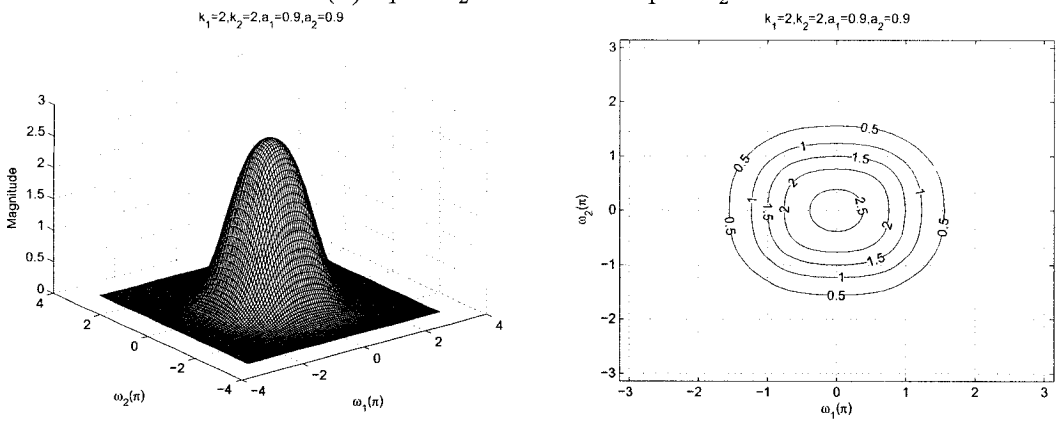

(c) $a_1 = a_2 = 0.9$ and $k_1 = k_2 = 2$

Figure 2.50: 3-D amplitude frequency response and contour response of the All-pole 2-D digital lowpass filter for $a_1 = a_2$ and $k_1 = k_2$

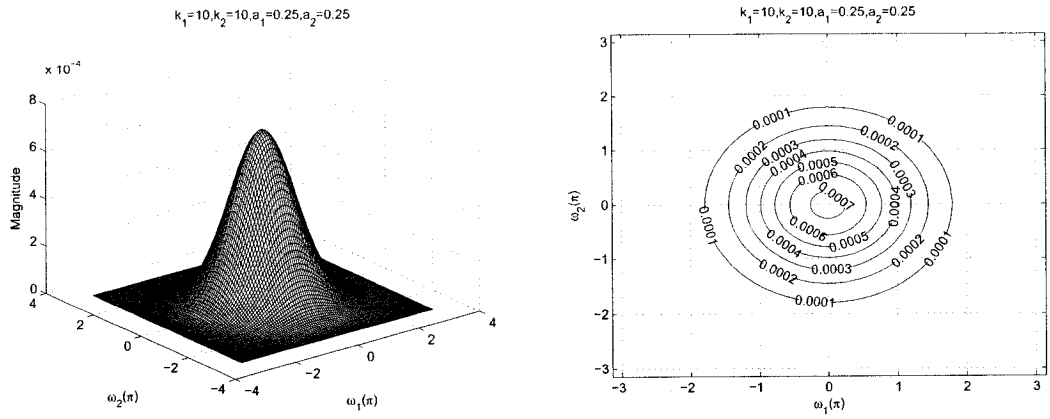

(a) $a_1 = a_2 = 0.25$ and $k_1 = k_2 = 10$

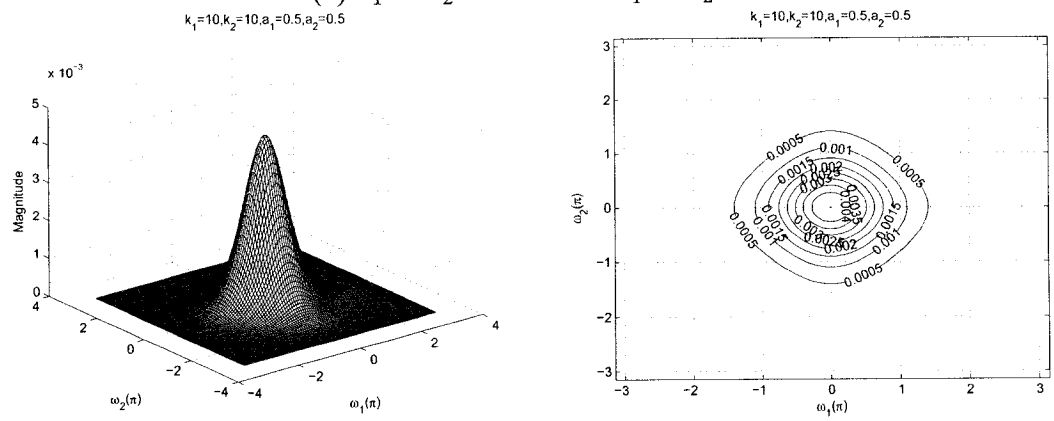

(b) $a_1 = a_2 = 0.5$ and $k_1 = k_2 = 10$

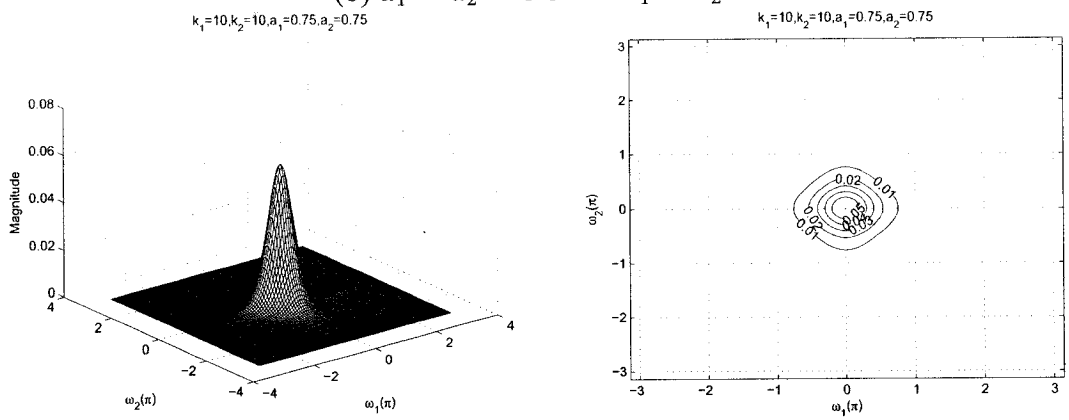

(c) $a_1 = a_2 = 0.75$ and $k_1 = k_2 = 10$

Figure 2.51: 3-D amplitude frequency response and contour response of the All-pole 2-D digital lowpass filter for $a_1 = a_2$ and $k_1 = k_2$

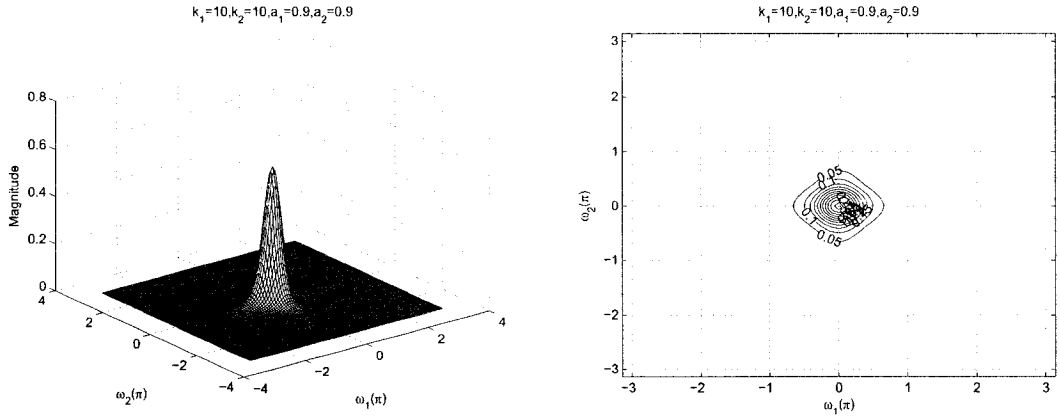

(a) $a_1 = a_2 = 0.9$ and $k_1 = k_2 = 10$

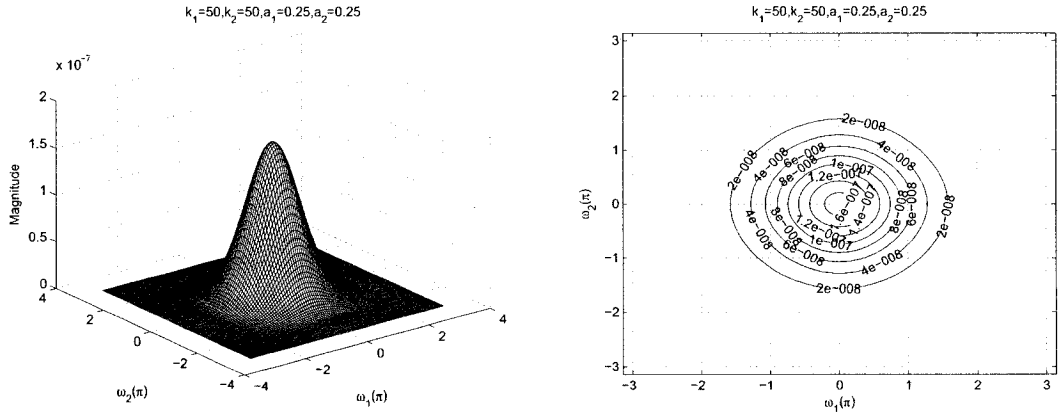

(b) $a_1 = a_2 = 0.25$ and $k_1 = k_2 = 50$

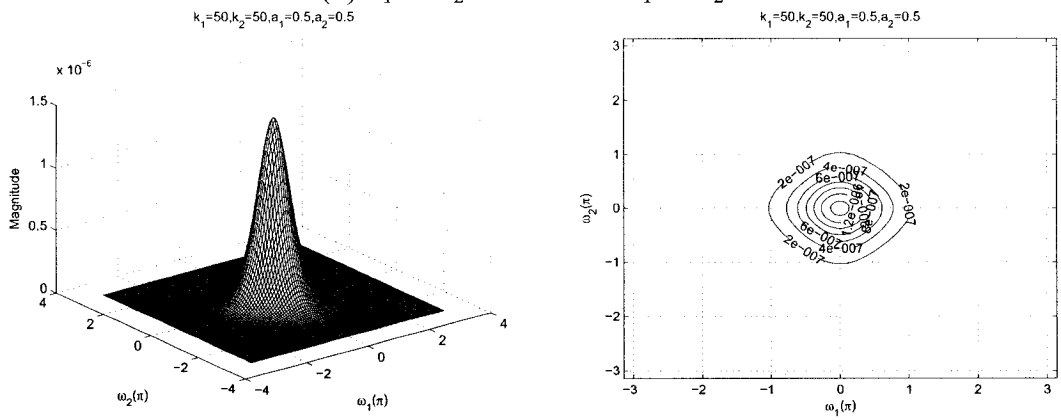

(c) $a_1 = a_2 = 0.5$ and $k_1 = k_2 = 50$

Figure 2.52: 3-D amplitude frequency response and contour response of the All-pole 2-D digital lowpass filter for $a_1 = a_2$ and $k_1 = k_2$

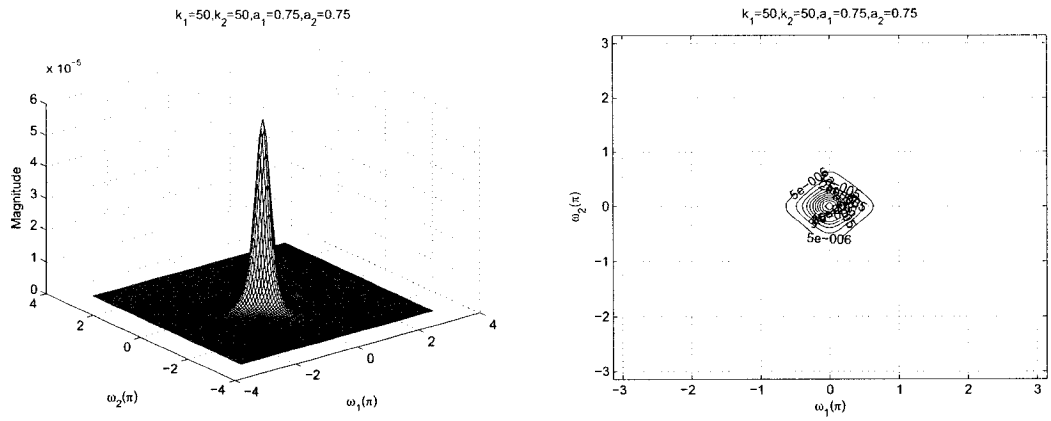

(a) $a_1 = a_2 = 0.75$ and $k_1 = k_2 = 50$

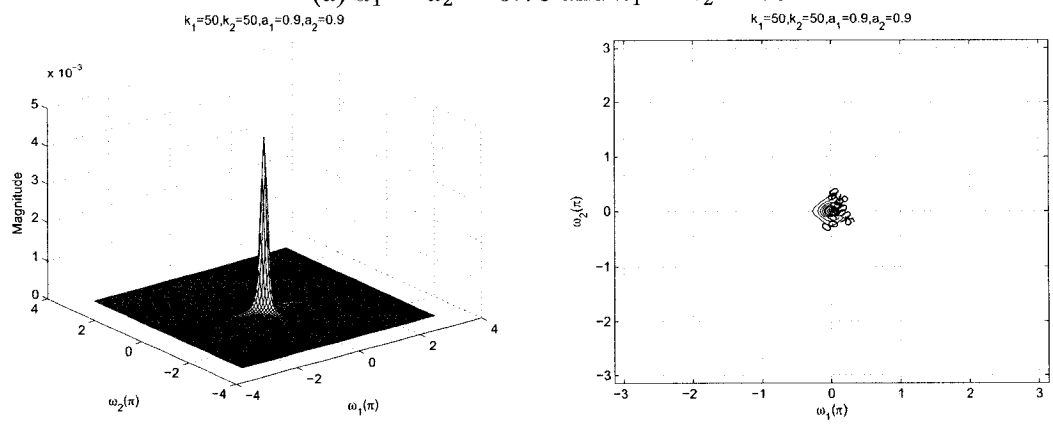

(b) $a_1 = a_2 = 0.9$ and $k_1 = k_2 = 50$

Figure 2.53: 3-D amplitude frequency response and contour response of the All-pole 2-D digital lowpass filter for $a_1 = a_2$ and $k_1 = k_2$

2.6.2.6 Frequency Response of the All-pole 2-D Digital Lowpass Filter with different values of a_1 and a_2 and same values of k_1 and k_2

In this section, we will study the effect of coefficients where $a_1 \neq a_2$ and $k_1 = k_2$ and the remaining coefficient b_1 and b_2 are considered to be unity for the all-pole 2-D digital lowpass filter in Category B. The values of a_1 and a_2 ranges from 0.25 to 0.5 and 0.5 to 0.75 respectively and the values of k_1 and k_2 ranges from 0 to 50.

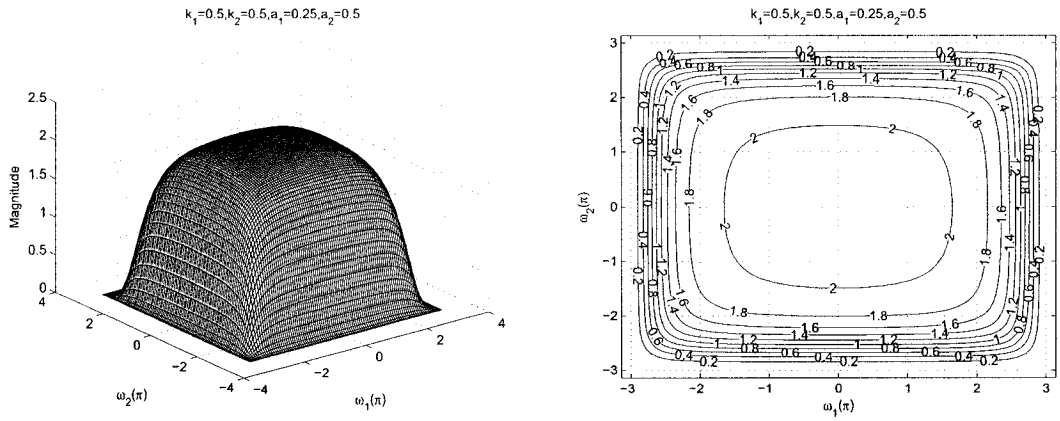

(a) $a_1 = 0.25,\ a_2 = 0.5$ and $k_1 = k_2 = 0.5$

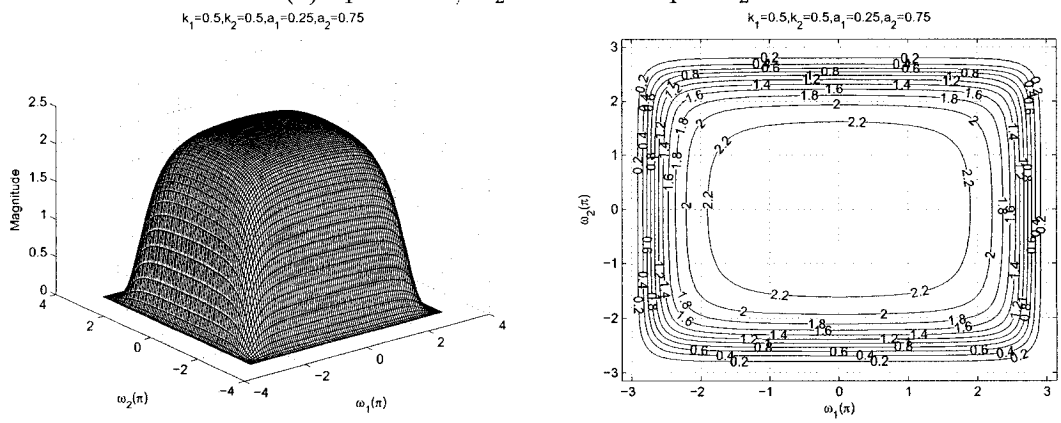

(b) $a_1 = 0.25,\ a_2 = 0.75$ and $k_1 = k_2 = 0.5$

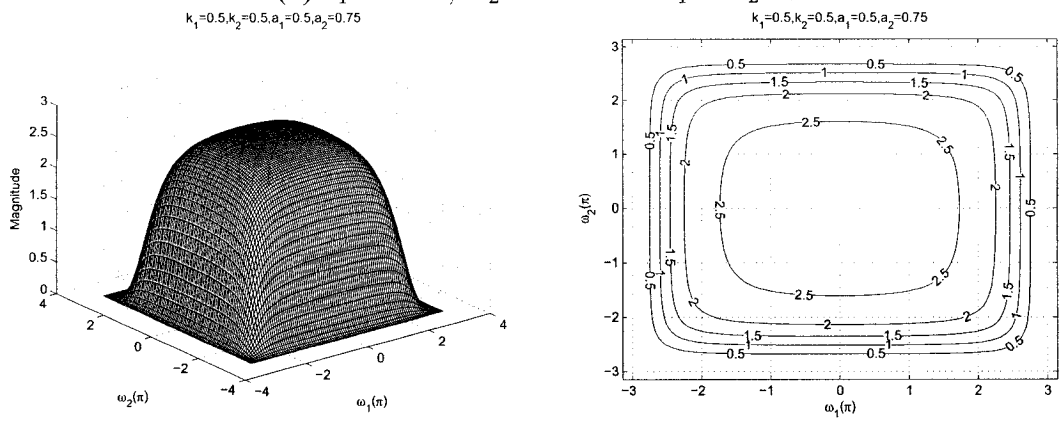

(c) $a_1 = 0.5,\ a_2 = 0.75$ and $k_1 = k_2 = 0.5$

Figure 2.54: 3-D amplitude frequency response and contour response of the All-pole 2-D digital lowpass filter for $a_1 \neq a_2$ and $k_1 = k_2$

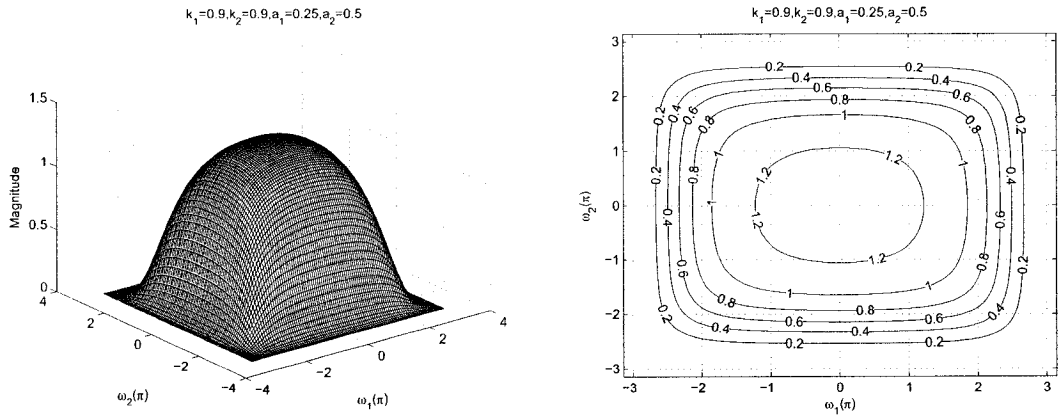

(a) $a_1 = 0.25,\ a_2 = 0.5$ and $k_1 = k_2 = 0.9$

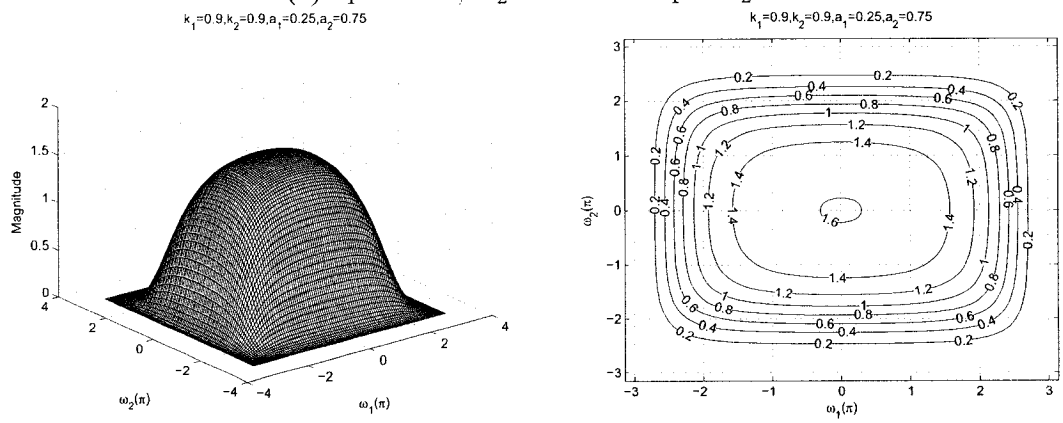

(b) $a_1 = 0.25,\ a_2 = 0.75$ and $k_1 = k_2 = 0.9$

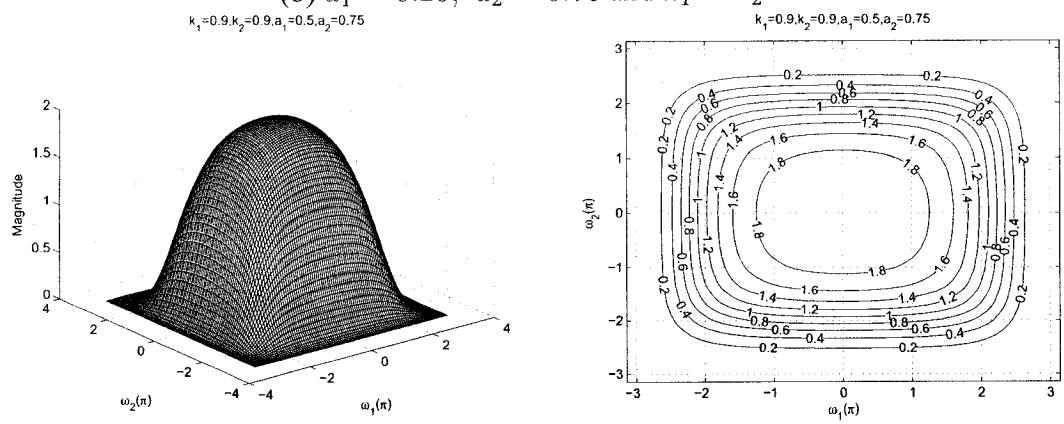

(c) $a_1 = 0.5,\ a_2 = 0.75$ and $k_1 = k_2 = 0.9$

Figure 2.55: 3-D amplitude frequency response and contour response of the All-pole 2-D digital lowpass filter for $a_1 \neq a_2$ and $k_1 = k_2$

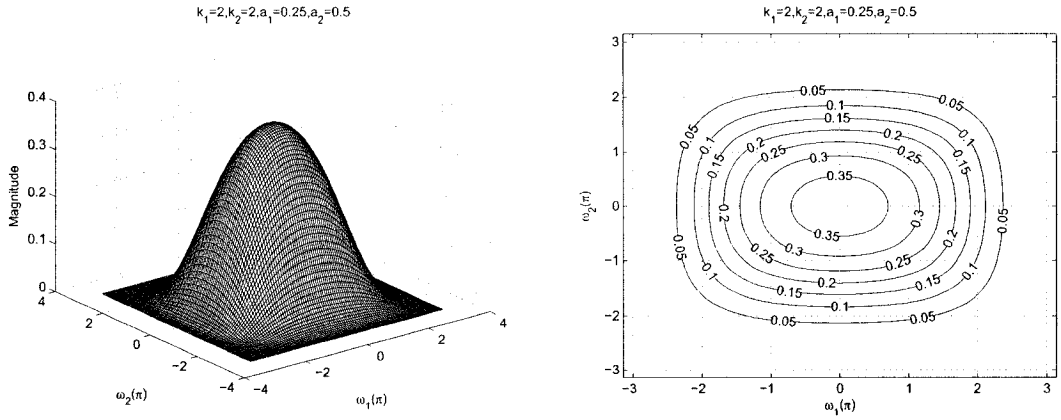

(a) $a_1 = 0.25,\ a_2 = 0.5$ and $k_1 = k_2 = 2$

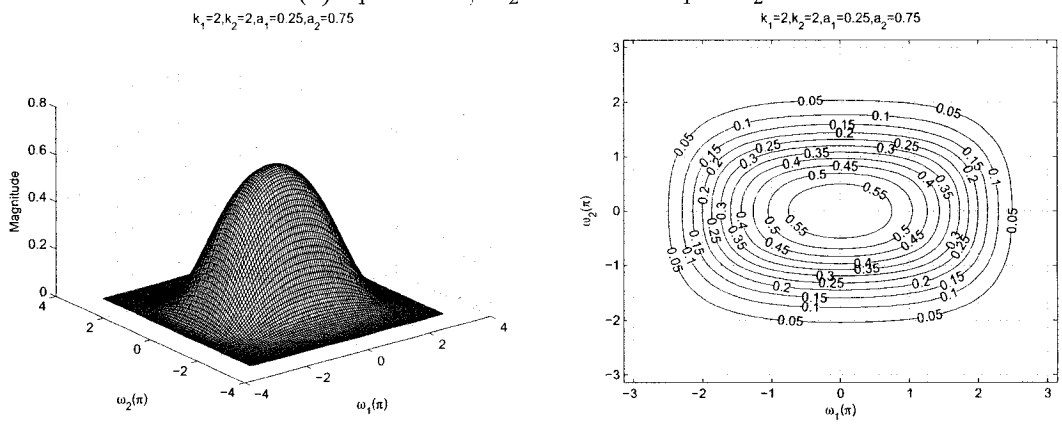

(b) $a_1 = 0.25,\ a_2 = 0.75$ and $k_1 = k_2 = 2$

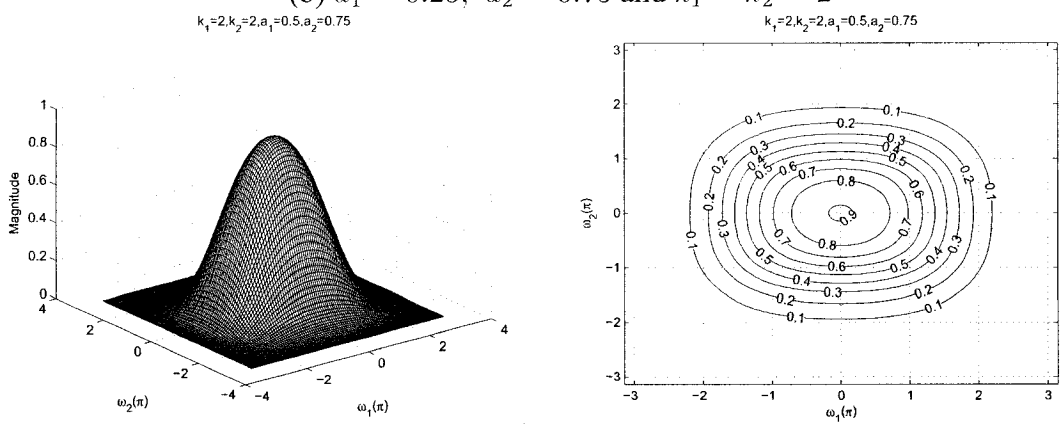

(c) $a_1 = 0.5,\ a_2 = 0.75$ and $k_1 = k_2 = 2$

Figure 2.56: 3-D amplitude frequency response and contour response of the All-pole 2-D digital lowpass filter for $a_1 \neq a_2$ and $k_1 = k_2$

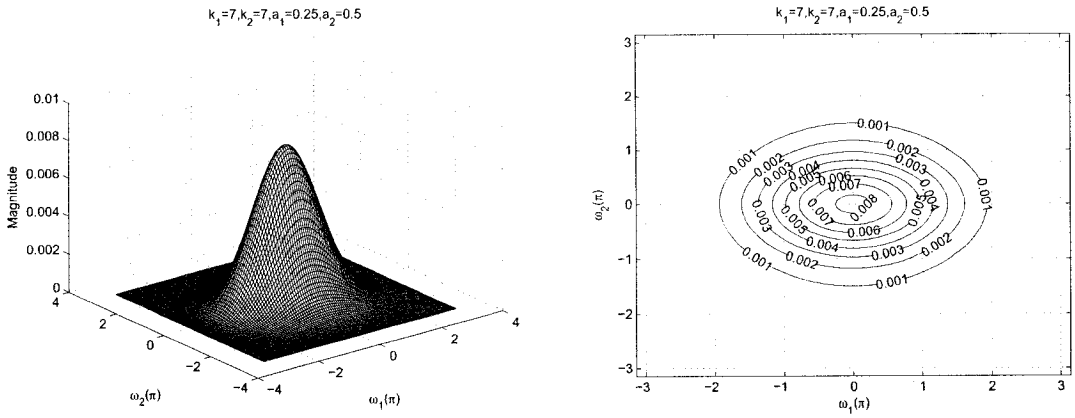

(a) $a_1 = 0.25,\ a_2 = 0.5$ and $k_1 = k_2 = 7$

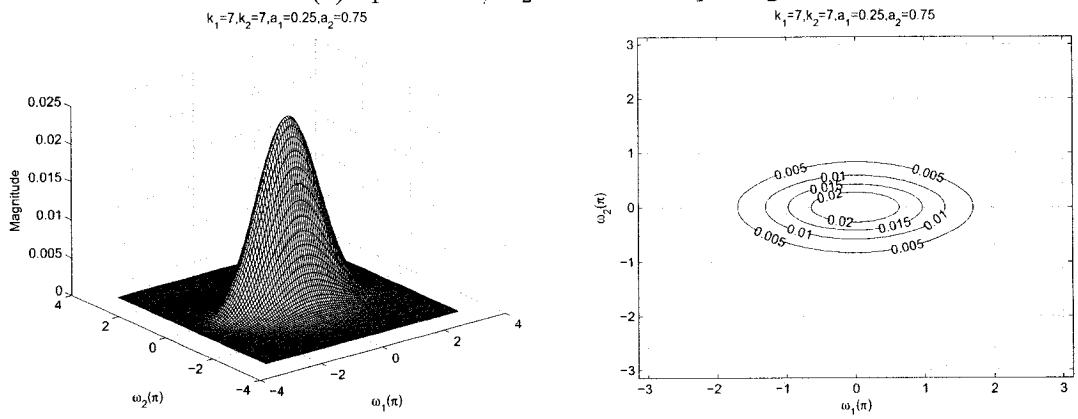

(b) $a_1 = 0.25,\ a_2 = 0.75$ and $k_1 = k_2 = 7$

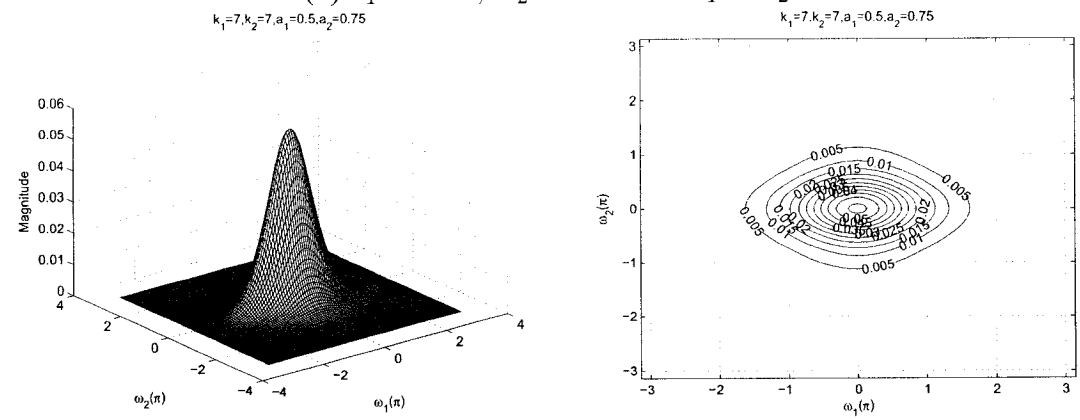

(c) $a_1 = 0.5,\ a_2 = 0.75$ and $k_1 = k_2 = 7$

Figure 2.57: 3-D amplitude frequency response and contour response of the All-pole 2-D digital lowpass filter for $a_1 \neq a_2$ and $k_1 = k_2$

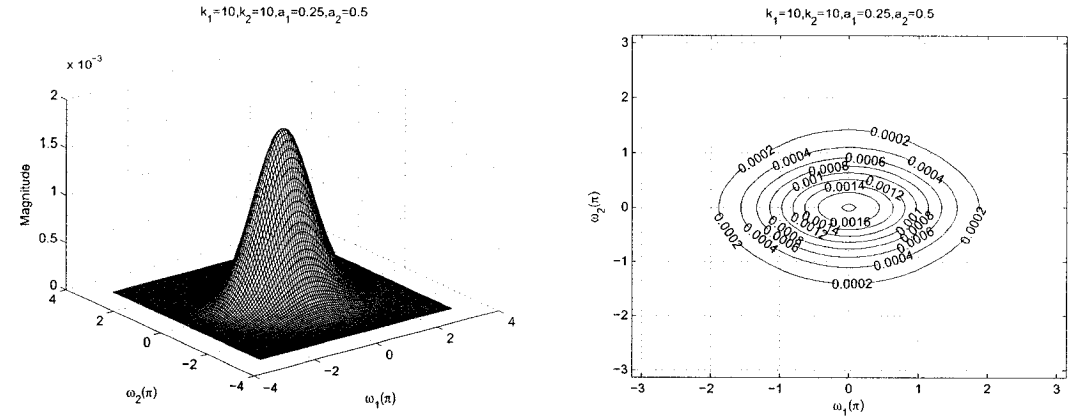

(a) $a_1 = 0.25,\ a_2 = 0.5$ and $k_1 = k_2 = 10$

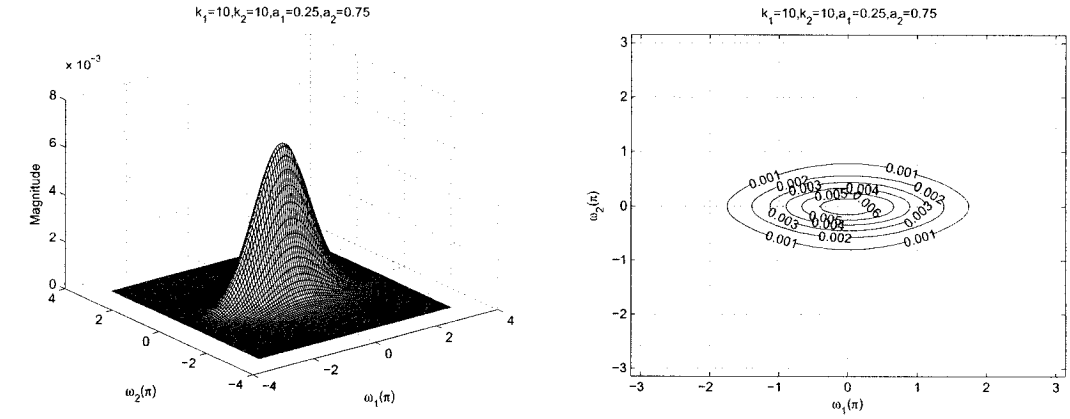

(b) $a_1 = 0.25,\ a_2 = 0.75$ and $k_1 = k_2 = 10$

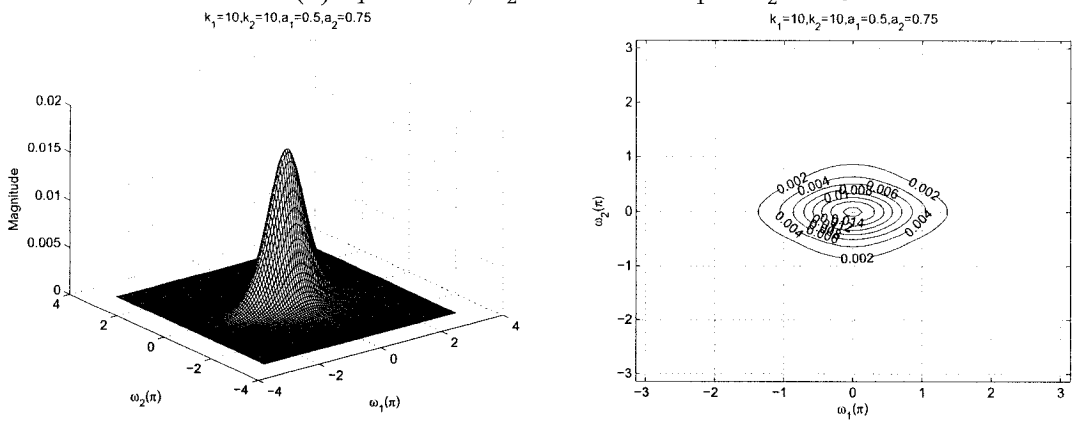

(c) $a_1 = 0.5,\ a_2 = 0.75$ and $k_1 = k_2 = 10$

Figure 2.58: 3-D amplitude frequency response and contour response of the All-pole 2-D digital lowpass filter for $a_1 \neq a_2$ and $k_1 = k_2$

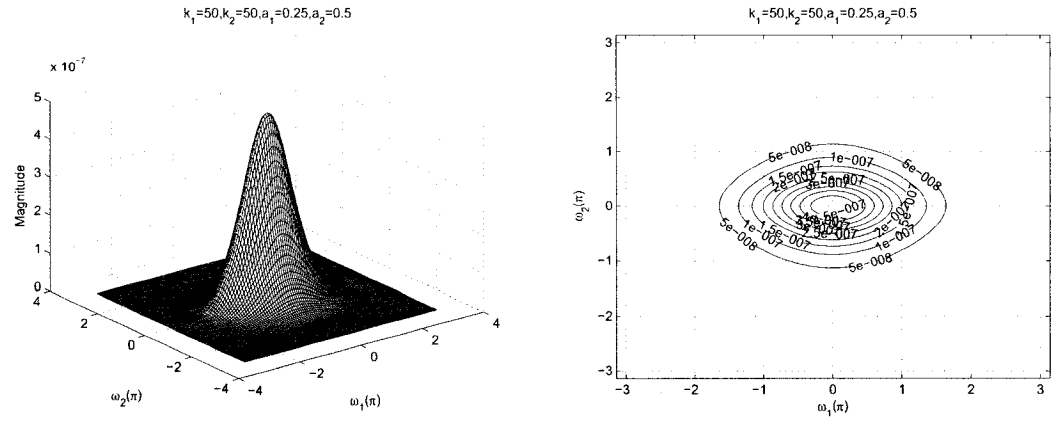

(a) $a_1 = 0.25,\ a_2 = 0.5$ and $k_1 = k_2 = 50$

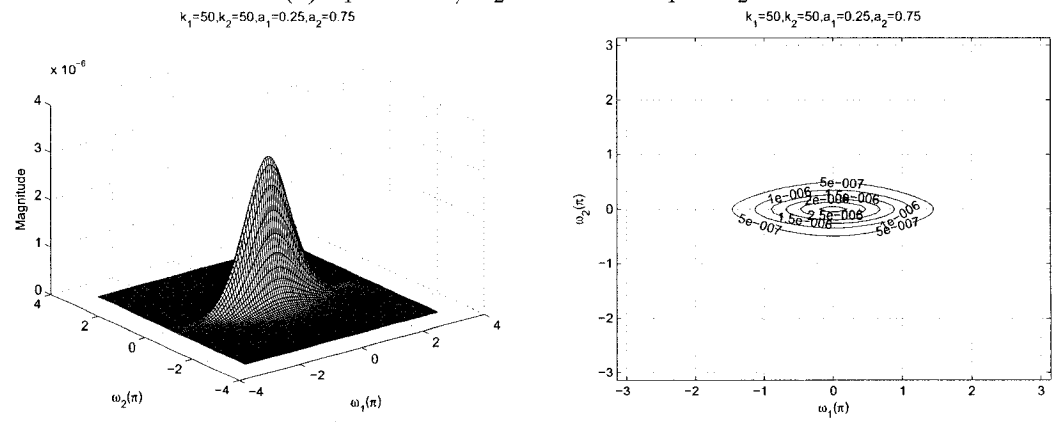

(b) $a_1 = 0.25,\ a_2 = 0.75$ and $k_1 = k_2 = 50$

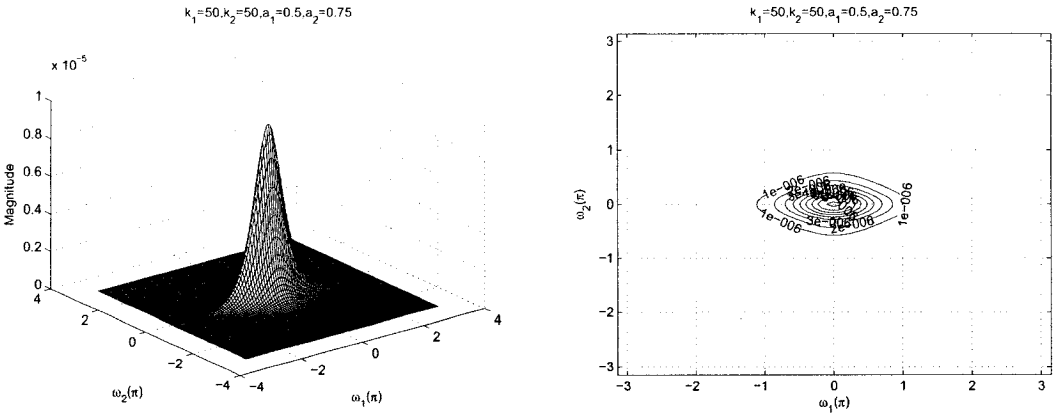

(c) $a_1 = 0.5,\ a_2 = 0.75$ and $k_1 = k_2 = 50$

Figure 2.59: 3-D amplitude frequency response and contour response of the All-pole 2-D digital lowpass filter for $a_1 \neq a_2$ and $k_1 = k_2$

As observed from the Figures 2.54 to 2.59, that the coefficients k_1 and k_2 affect the passband width of the frequency response. In the Figures 2.54 (a), 2.55 (a), 2.56 (a), 2.57 (a), 2.58 (a) and 2.59 (a), there is a decrease in the passband width as the values of k_1

and k_2 are increased from 0.5 to 50 for different values of $a_1 = 0.25$ and $a_2 = 0.5$. In addition, there is also a decrease in the amplitude from 2 to 4.5×10^{-7} for the same. It is also observed that for very high values of k_1 and k_2, the passband width of the frequency response becomes very narrow as shown in the Figure 2.59 (c).

As observed from the Figures 2.54 to 2.59, the coefficients a_1 and a_2 affect the gain of the frequency response. It can be clearly observed from the Figures 2.54 (a), (b), (c), that the amplitude of the frequency response increases from 2 to 2.5 when the values of a_1 and a_2 are increased from 0.25 to 0.5 and 0.5 to 0.75 respectively, keeping the same value of $k_1 = k_2 = 0.5$. In addition, the width of the passband increases and decreases for the same.

2.6.2.7 Frequency Response of the All-pole 2-D Digital Lowpass Filter with different values of a_1 and a_2 and different values of k_1 and k_2

In this section, we study the effect of coefficients when $a_1 \neq a_2$ and $k_1 \neq k_2$, and the remaining coefficients b_1 and b_2 are considered to be unity for the all-pole 2-D digital lowpass filter. The values of a_1 and a_2 vary from 0.25 to 0.75 and 0.5 to 0.9 respectively and the values of k_1 and k_2 vary from 0.5 to 50 and 1 to 75, respectively.

As observed from the Figures 2.60 to 2.63, that the coefficients k_1 and k_2 affect the passband width of the frequency response. In the Figures 2.60 (a), (b), (c) and 2.61 (a), there is a decrease in the passband width as the values of k_1 and k_2 are increased from 0.5 to 50 and from 1 to 75 respectively, for the different values of a_1 and a_2 0.25 and 0.5 respectively. At the same time there is also a gradual decrease in the amplitude from 1.6 to 1.4×10^{-7} for the same. Also it is observed that for very high values of k_1 and k_2, the passband width of the frequency response becomes very narrow as shown in the Figure 2.63 (c).

As observed from the Figures 2.60 to 2.63, the coefficients a_1 and a_2 affect the magnitude of the frequency response. It can be clearly observed from the Figures 2.60 (a), 2.61 (b) and 2.62 (c), that the amplitude of the frequency response increases from 1.6 to 3 when

the values of a_1 and a_2 are increased from 0.25 to 0.75 and 0.5 to 0.9, respectively, keeping the same value of $k_1 = 0.5$ and $k_2 = 1$. In addition, the passband width of the passband increases and decreases for the same.

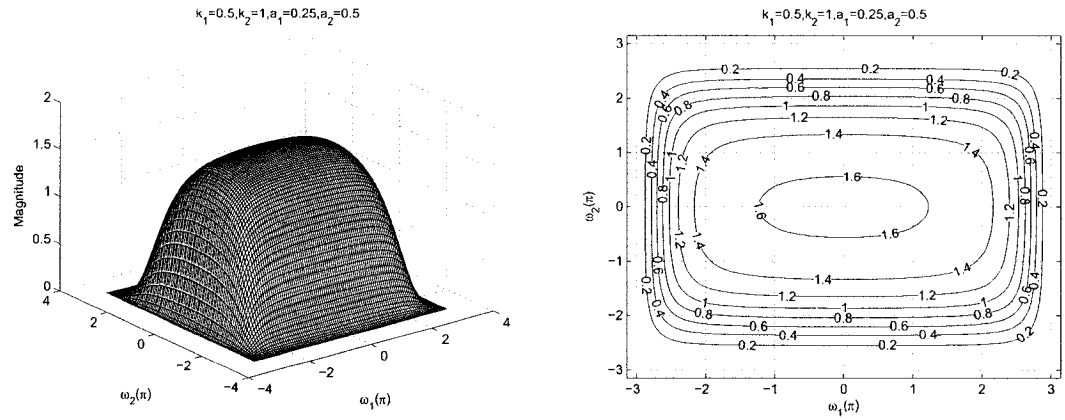

(a) $a_1 = 0.25,\ a_2 = 0.5$ and $k_1 = 0.5,\ k_2 = 1$

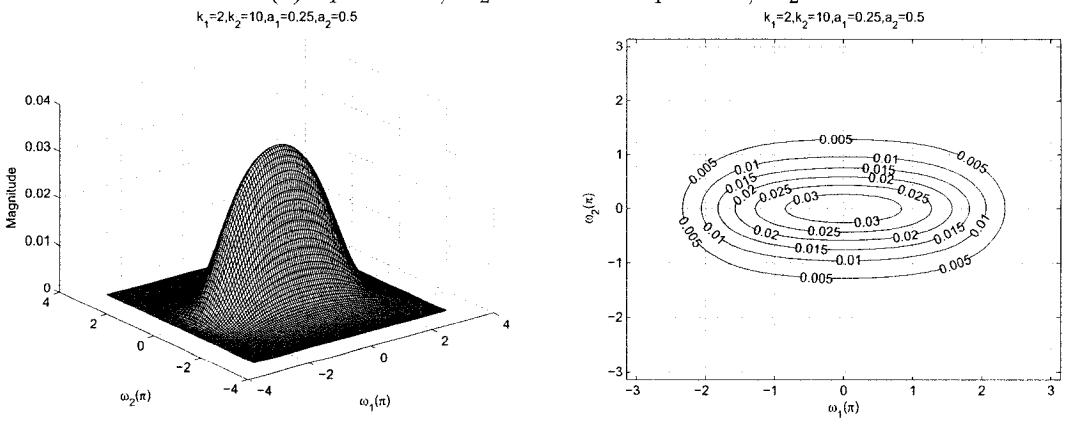

(b) $a_1 = 0.25,\ a_2 = 0.5$ and $k_1 = 2,\ k_2 = 10$

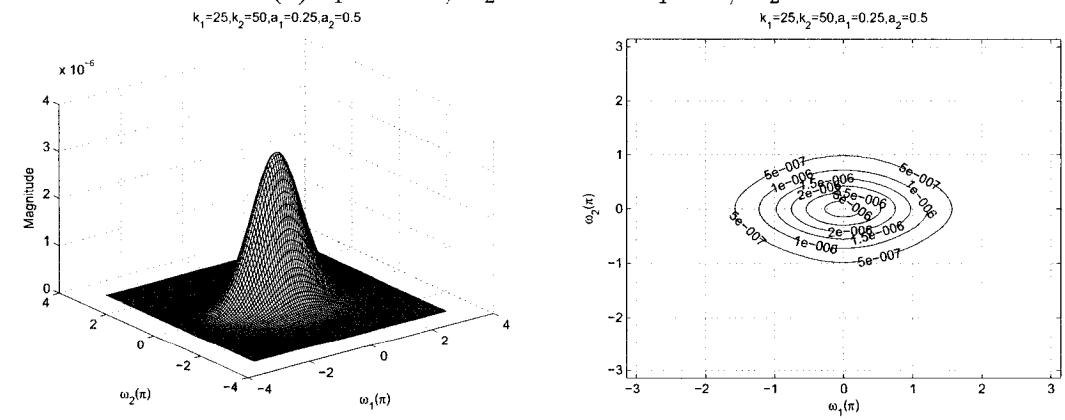

(c) $a_1 = 0.25,\ a_2 = 0.5$ and $k_1 = 25,\ k_2 = 50$

Figure 2.60: 3-D amplitude frequency response and contour response of the All-pole 2-D digital lowpass filter for $a_1 \neq a_2$ and $k_1 \neq k_2$

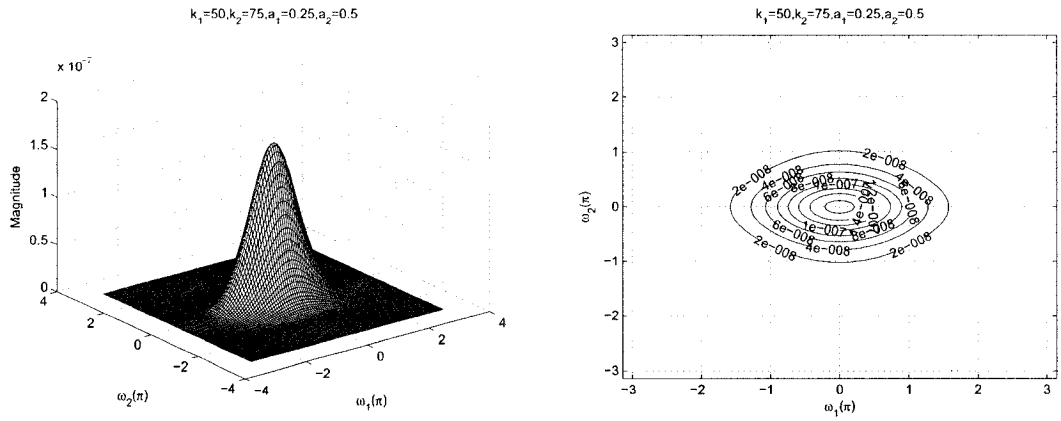

(a) $a_1 = 0.25,\ a_2 = 0.5$ and $k_1 = 50,\ k_2 = 75$

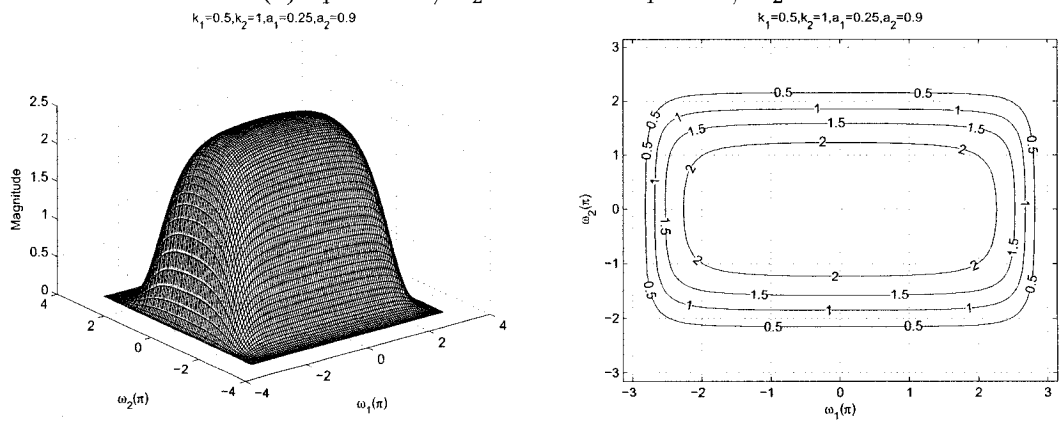

(b) $a_1 = 0.25,\ a_2 = 0.9$ and $k_1 = 0.5,\ k_2 = 1$

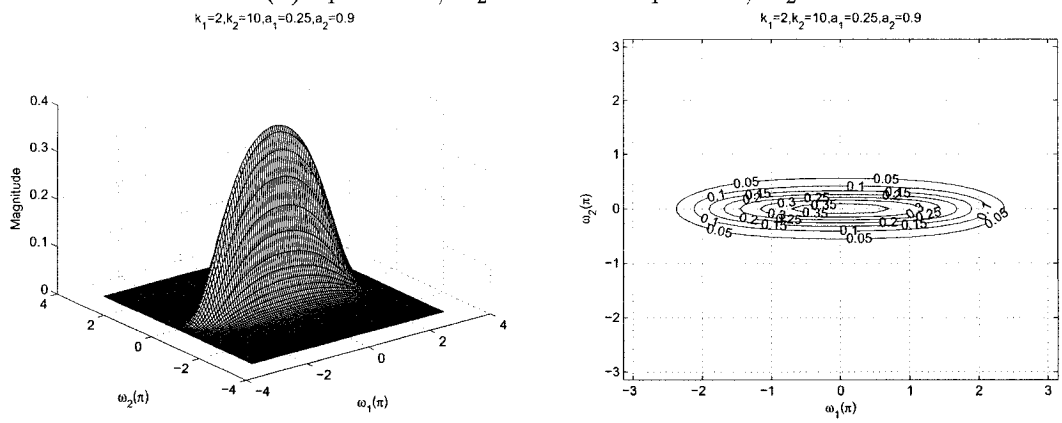

(c) $a_1 = 0.25,\ a_2 = 0.9$ and $k_1 = 2,\ k_2 = 10$

Figure 2.61: 3-D amplitude frequency response and contour response of the All-pole 2-D digital lowpass filter for $a_1 \neq a_2$ and $k_1 \neq k_2$

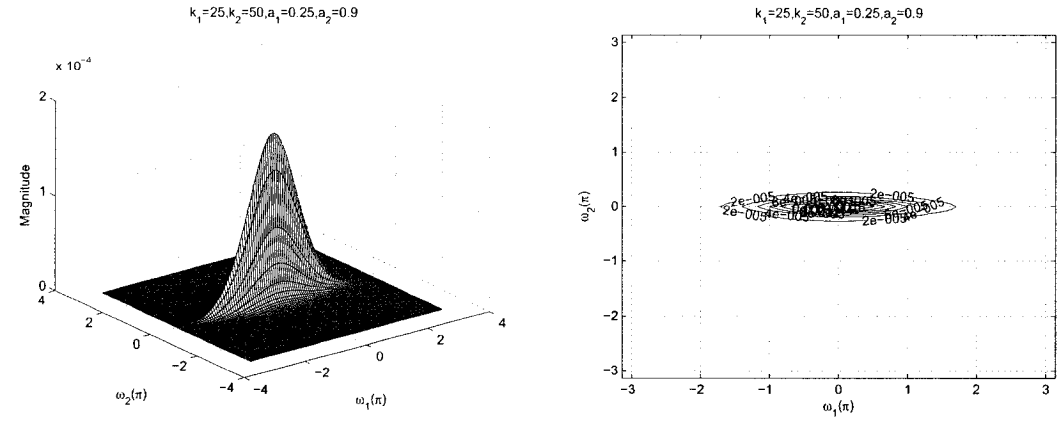

(a) $a_1 = 0.25,\ a_2 = 0.9$ and $k_1 = 25,\ k_2 = 50$

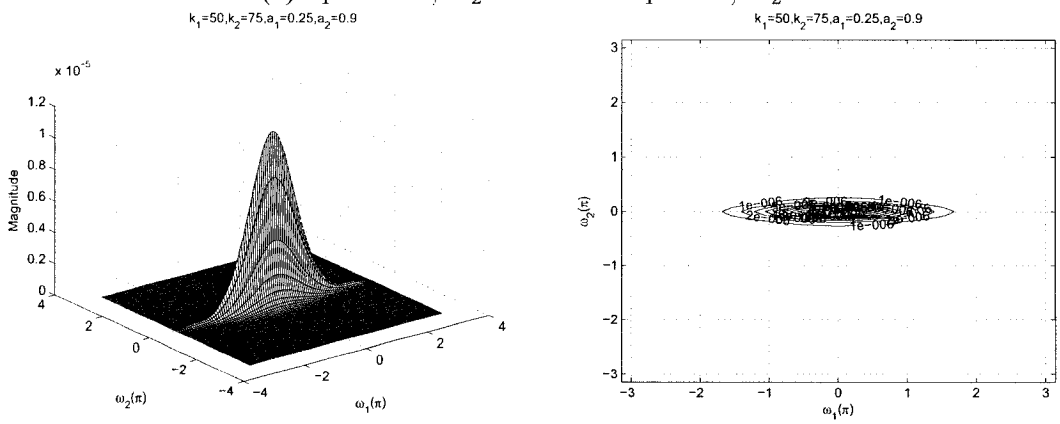

(b) $a_1 = 0.25,\ a_2 = 0.9$ and $k_1 = 50,\ k_2 = 75$

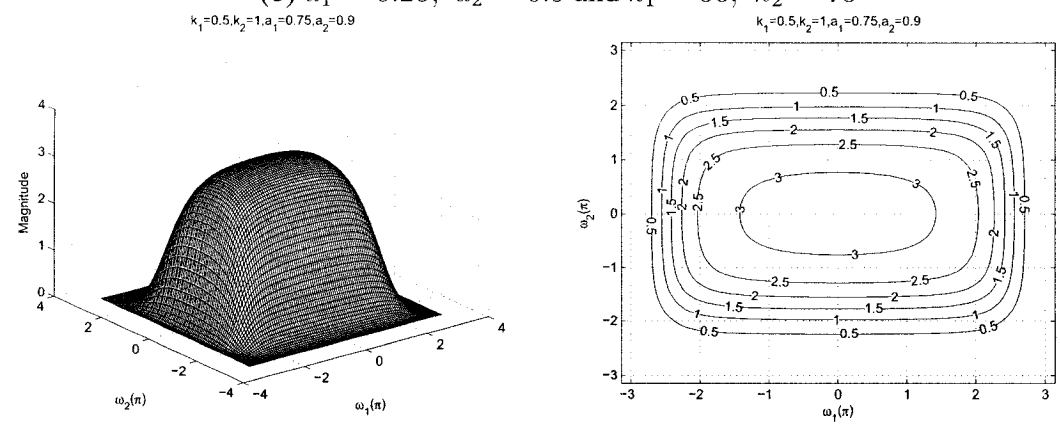

(c) $a_1 = 0.75,\ a_2 = 0.9$ and $k_1 = 0.5,\ k_2 = 1$

Figure 2.62: 3-D amplitude frequency response and contour response of the All-pole 2-D digital lowpass filter for $a_1 \neq a_2$ and $k_1 \neq k_2$

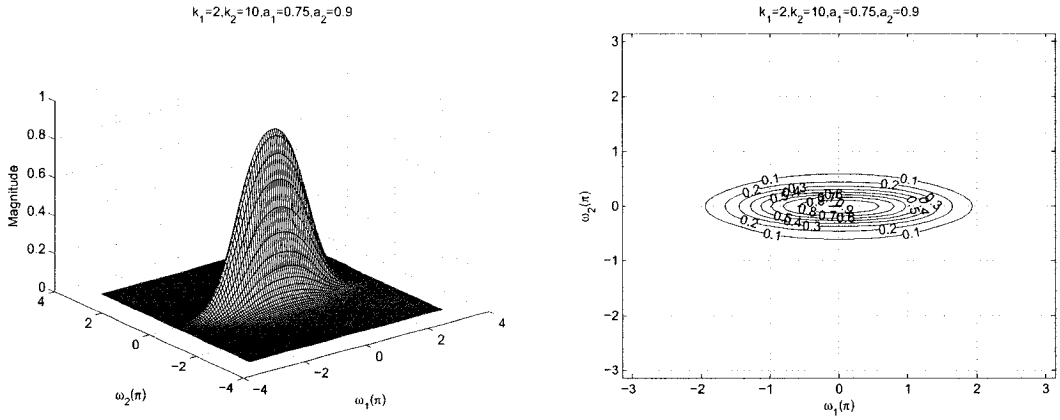

(a) $a_1 = 0.75,\ a_2 = 0.9$ and $k_1 = 2,\ k_2 = 10$

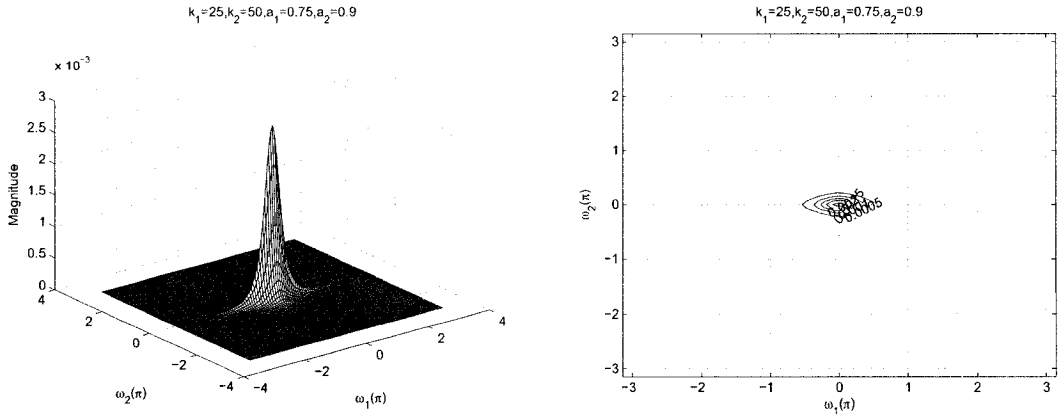

(b) $a_1 = 0.75,\ a_2 = 0.9$ and $k_1 = 25,\ k_2 = 50$

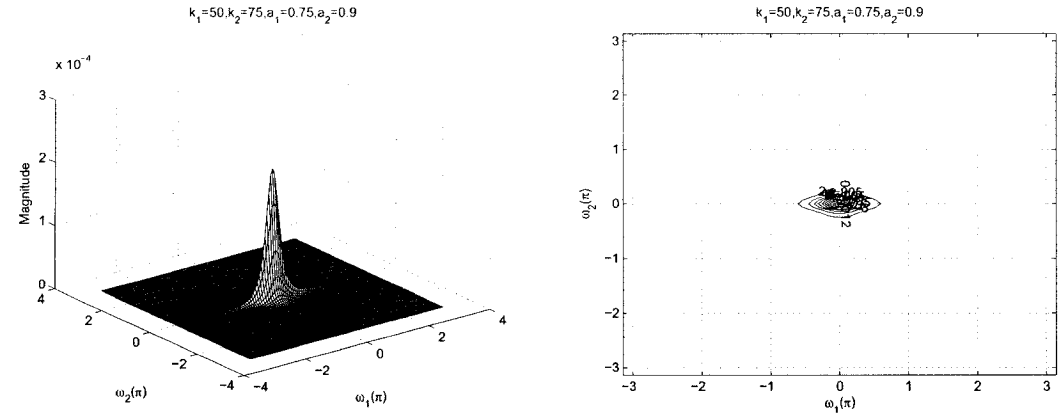

(c) $a_1 = 0.75,\ a_2 = 0.9$ and $k_1 = 50,\ k_2 = 75$

Figure 2.63: 3-D amplitude frequency response and contour response of the All-pole 2-D digital lowpass filter for $a_1 \neq a_2$ and $k_1 \neq k_2$

2.6.2.8 Frequency Response of the All-pole 2-D Digital Lowpass Filter with same values of a_1 and a_2 and different values of k_1 and k_2

In this section, we study the effect of coefficients where $a_1 = a_2$ and $k_1 \neq k_2$ and the remaining coefficients b_1 and b_2 are considered to be unity for the all-pole 2-D digital lowpass filter in Category B. The values of a_1 and a_2 vary from 0 to 1 and the values of k_1 and k_2 vary from 0.5 to 50 and 1 to 75 respectively.

As observed from the Figures 2.64 to 2.69, the coefficients k_1 and k_2 affect the passband width of the frequency response. In the Figures 2.64 (a), (b), (c) and 2.65 (a), there is a decrease in the passband width as the values of k_1 and k_2 are increased from 0.5 to 75 for the same values of $a_1 = a_2 = 0.25$. At the same time there is also a gradual decrease in the amplitude from 1.2 to 1×10^{-6} for the same. Also it is observed that for very high values of k_1 and k_2, the passband width of the frequency response becomes very narrow as shown in the Figure 2.69.

As observed from the Figures 2.64 to 2.69, the coefficients a_1 and a_2 affect the amplitude of the frequency response. It can be clearly observed from the Figures 2.64 (a), 2.65 (b), 2.66 (c) and 2.68 (a), that the amplitude of the frequency response increases from 1.2 to 3 when the values of a_1 and a_2 are increased from 0.25 to 0.9 keeping the same value of $k_1 = 0.5$ and $k_2 = 1$. In addition, there is also an increase in the passband width of the contour response for the same.

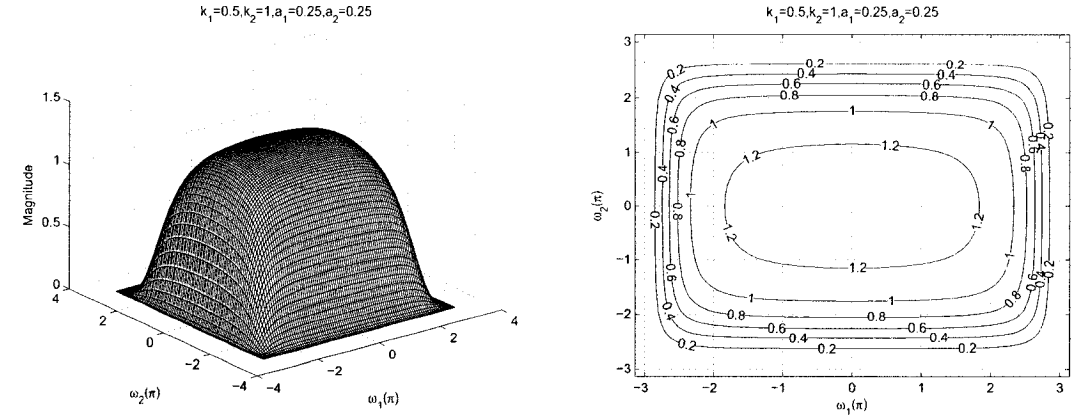

(a) $a_1 = a_2 = 0.25$ and $k_1 = 0.5,\ k_2 = 1$

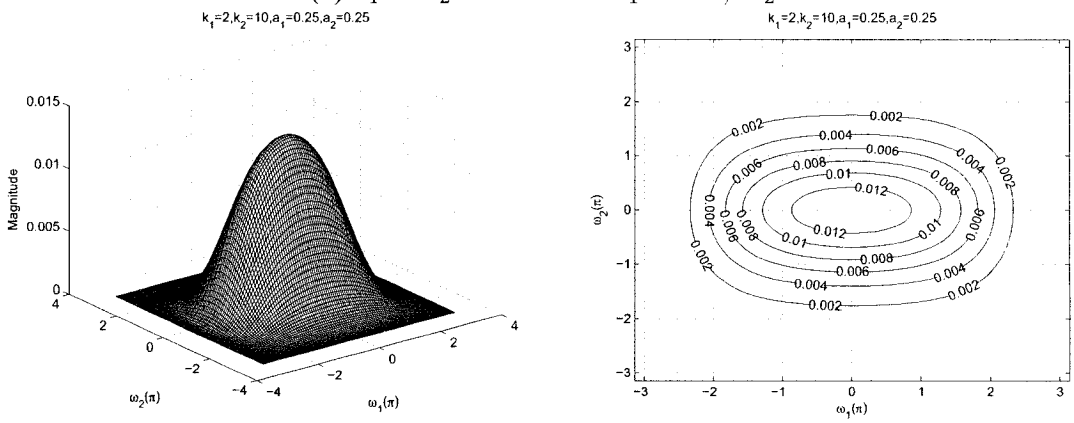

(b) $a_1 = a_2 = 0.25$ and $k_1 = 2,\ k_2 = 10$

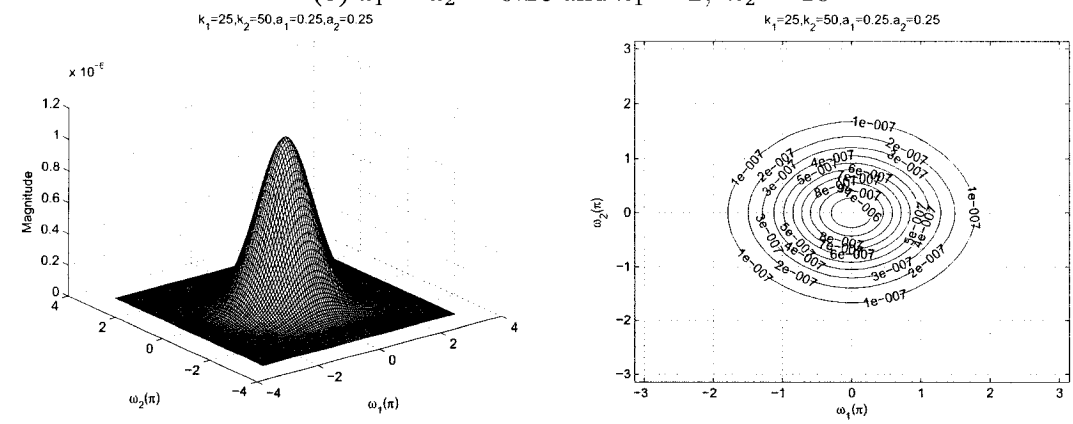

(c) $a_1 = a_2 = 0.25$ and $k_1 = 25,\ k_2 = 50$

Figure 2.64: 3-D amplitude frequency response and contour response of the All-pole 2-D digital lowpass filter for $a_1 = a_2$ and $k_1 \neq k_2$

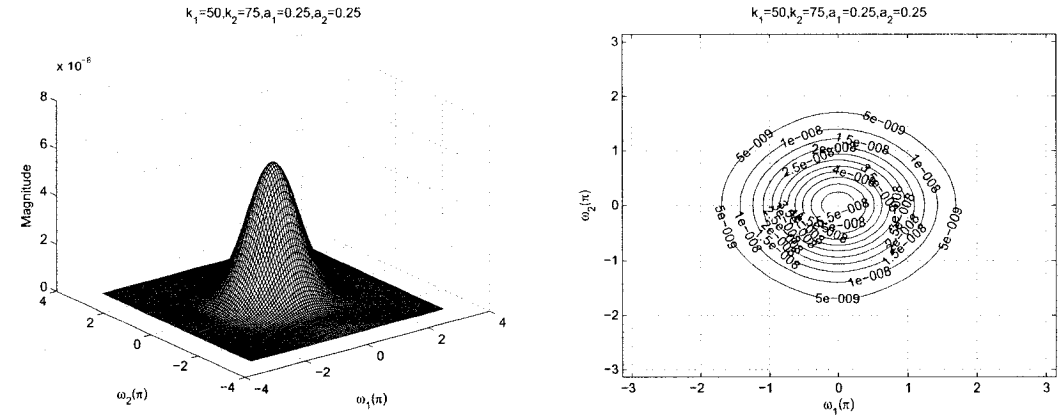

(a) $a_1 = a_2 = 0.25$ and $k_1 = 50$ $k_2 = 75$

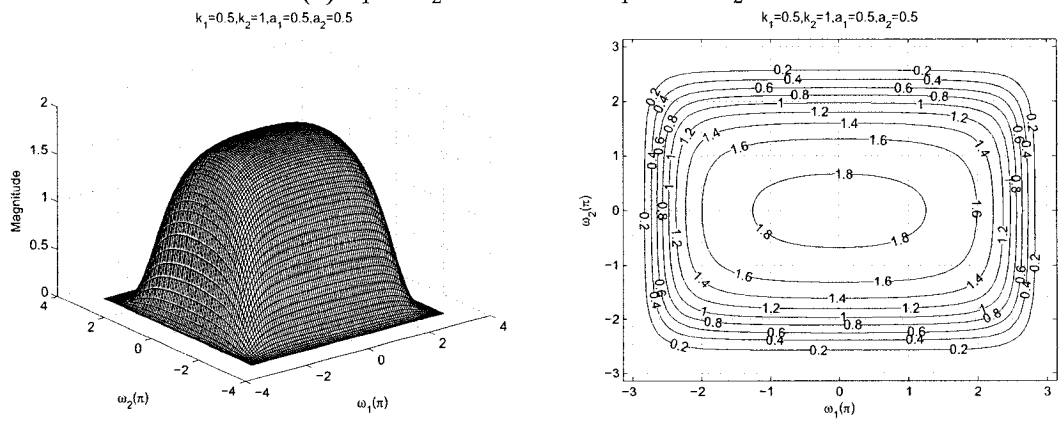

(b) $a_1 = a_2 = 0.5$ and $k_1 = 0.5$ $k_2 = 1$

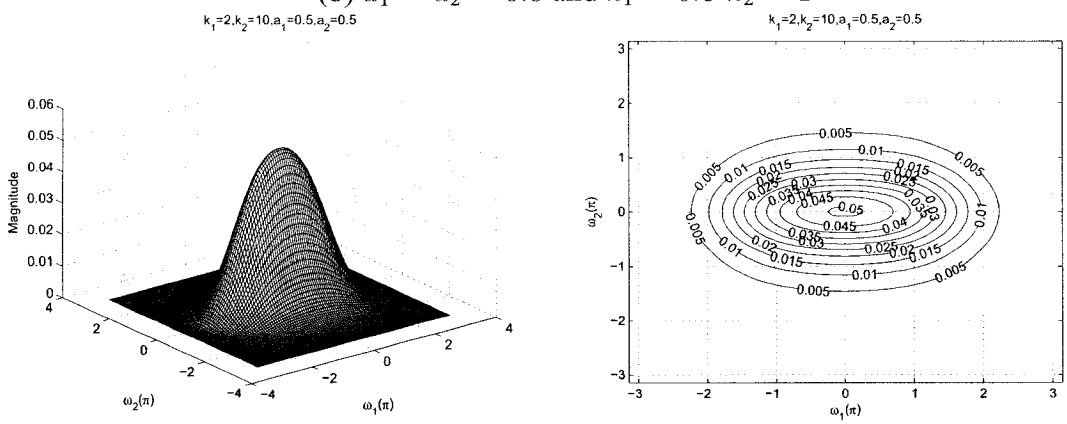

(c) $a_1 = a_2 = 0.5$ and $k_1 = 2$ $k_2 = 10$

Figure 2.65: 3-D amplitude frequency response and contour response of the All-pole 2-D digital lowpass filter for $a_1 = a_2$ and $k_1 \neq k_2$

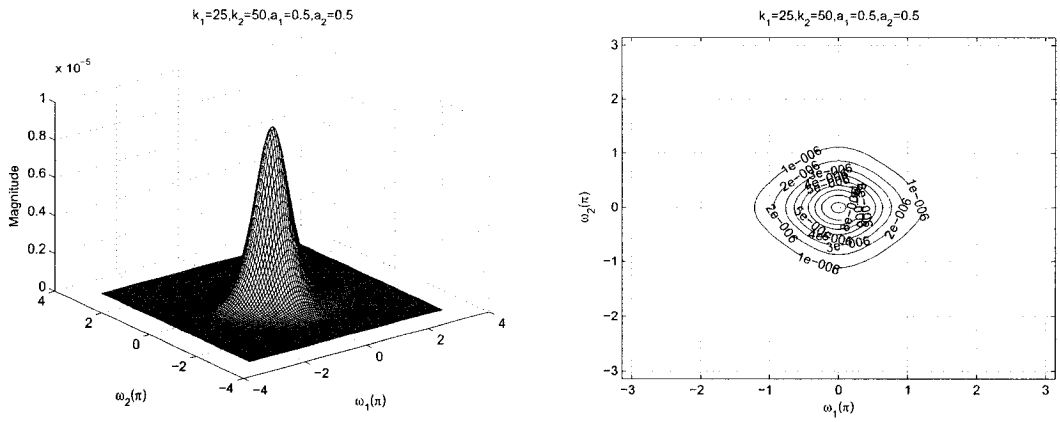

(a) $a_1 = a_2 = 0.5$ and $k_1 = 25$ $k_2 = 50$

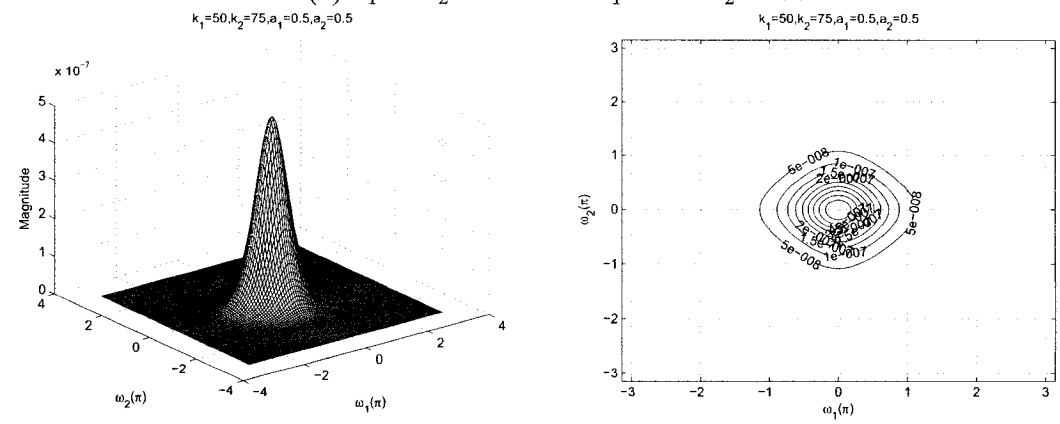

(b) $a_1 = a_2 = 0.5$ and $k_1 = 50$ $k_2 = 75$

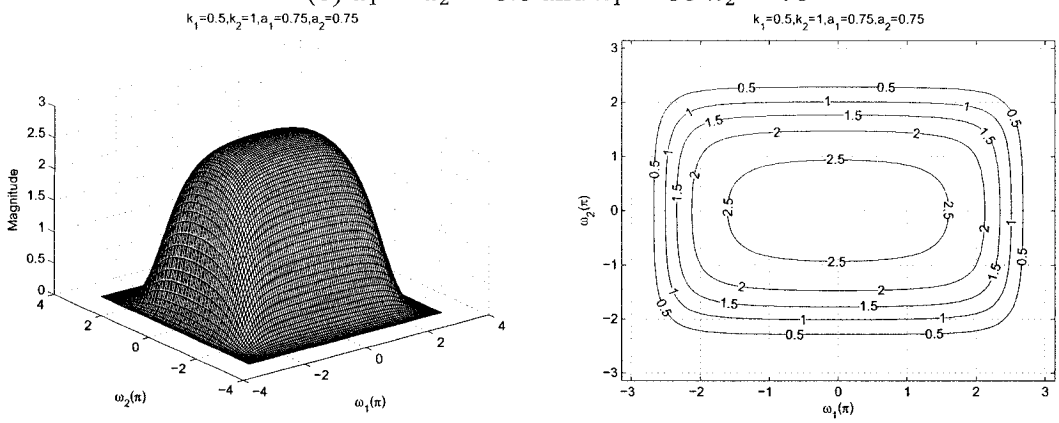

(c) $a_1 = a_2 = 0.75$ and $k_1 = 0.5$ $k_2 = 1$

Figure 2.66: 3-D amplitude frequency response and contour response of the All-pole 2-D digital lowpass filter for $a_1 = a_2$ and $k_1 \neq k_2$

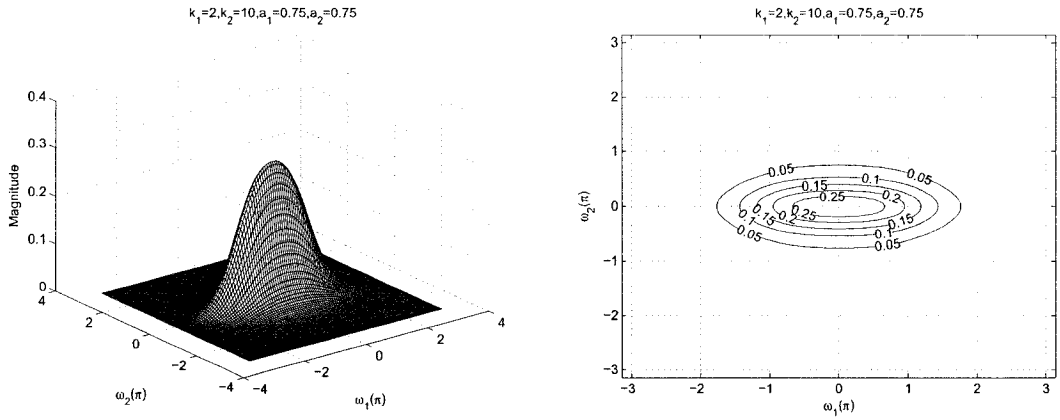

(a) $a_1 = a_2 = 0.75$ and $k_1 = 2$ $k_2 = 10$

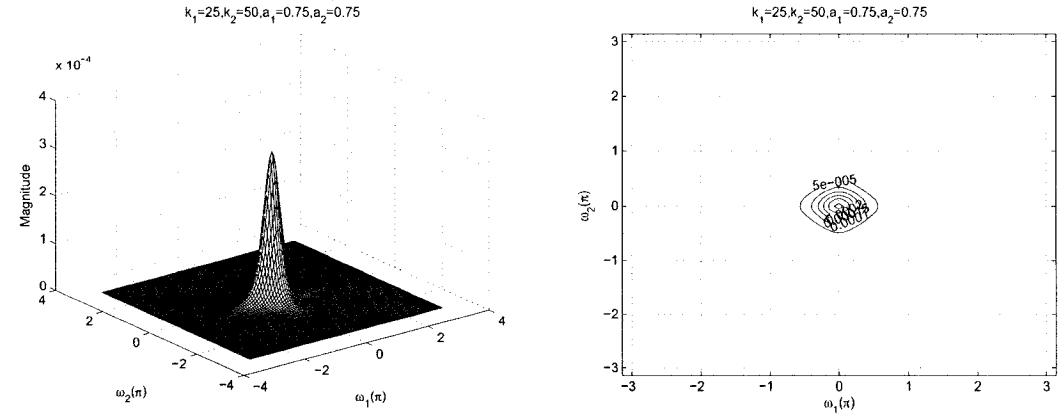

(b) $a_1 = a_2 = 0.75$ and $k_1 = 25$ $k_2 = 50$

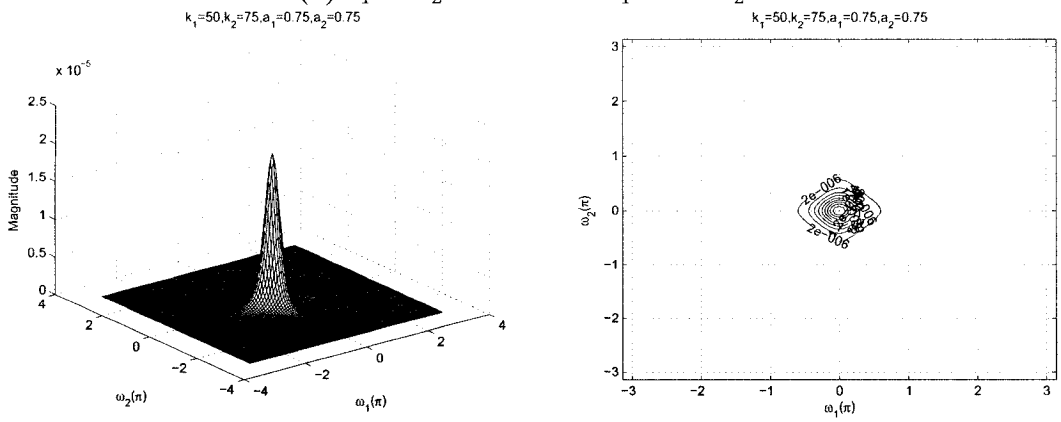

(c) $a_1 = a_2 = 0.75$ and $k_1 = 50$ $k_2 = 75$

Figure 2.67: 3-D amplitude frequency response and contour response of the All-pole 2-D digital lowpass filter for $a_1 = a_2$ and $k_1 \neq k_2$

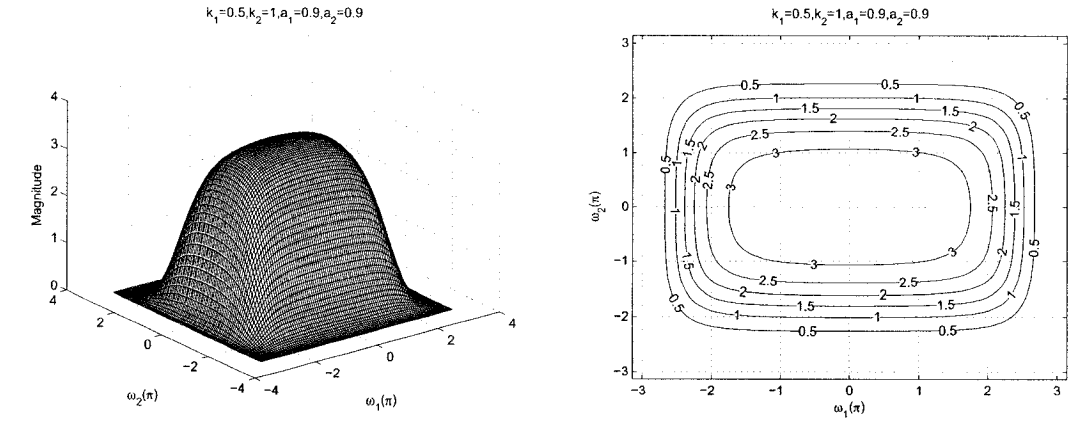

(a) $a_1 = a_2 = 0.9$ and $k_1 = 0.5$ $k_2 = 1$

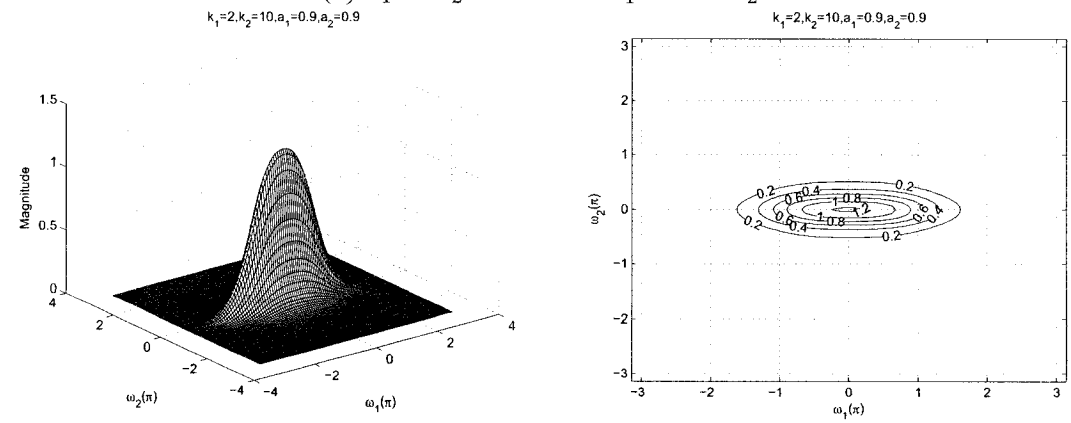

(b) $a_1 = a_2 = 0.9$ and $k_1 = 2$ $k_2 = 10$

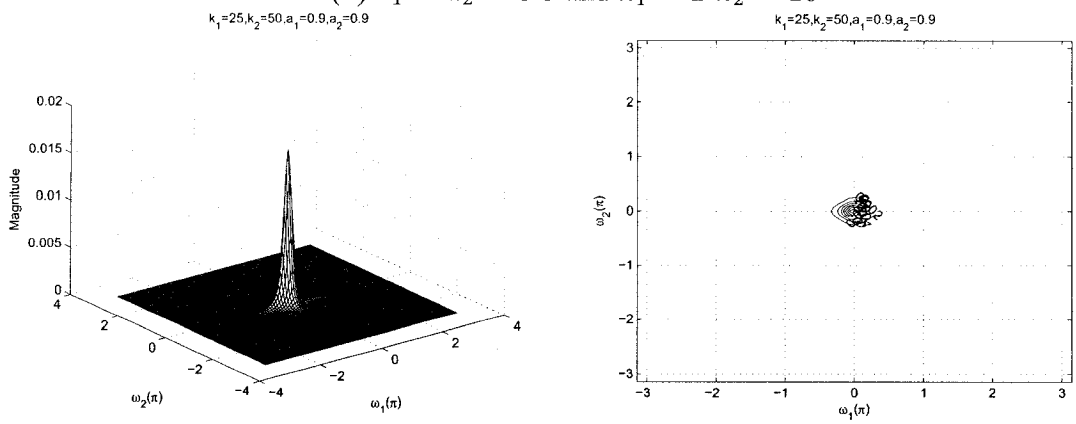

(c) $a_1 = a_2 = 0.9$ and $k_1 = 25$ $k_2 = 50$

Figure 2.68: 3-D amplitude frequency response and contour response of the All-pole 2-D digital lowpass filter for $a_1 = a_2$ and $k_1 \neq k_2$

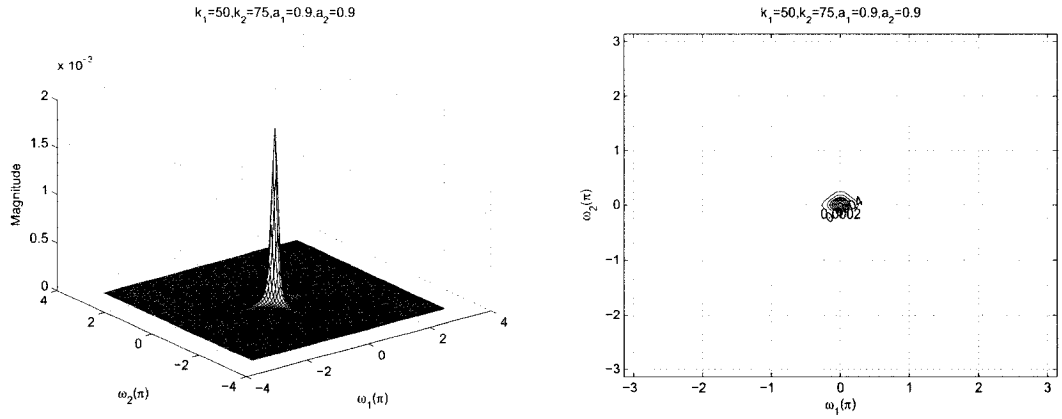

$a_1 = a_2 = 0.9$ and $k_1 = 50$ $k_2 = 75$

Figure 2.69: 3-D amplitude frequency response and contour response of the All-pole 2-D digital lowpass filter for $a_1 = a_2$ and $k_1 \neq k_2$

2.7 Summary

In this chapter, we have presented a new approach to obtain a transfer function for the 2-D analog and digital lowpass filters from a combination of the 2-D all-pass filter structures in the analog domain in Category A and Category B mentioned in Section 2.5. The 2-D digital transfer function has been derived from the analog transfer function using the generalized bilinear transformation and the stability conditions have been satisfied. By changing the values of the generalized bilinear transformation coefficients we can change the type and the frequency response of the 2-D digital lowpass filters. Also, we have discussed the effect of the coefficients of the 2-D digital lowpass filter obtained by applying generalized bilinear transformation on the amplitude-frequency response in Category A and Category B mentioned in Section 2.5. The detailed analysis of the effect of each of the coefficient is discussed in Section 2.6.

The summary of the effect of the coefficient of the generalized bilinear transformation in Category A are as follows.

On increasing the values of k_1 and k_2, as discussed in Sections 2.6.1.1 and 2.6.1.2 respectively, it is observed that when we increase the values of k_1 and k_2 from 0.1 to 10,

the passband width along the $\omega_1 - axis$ and $\omega_2 - axis$, respectively, gradually decreases keeping the amplitude constant. On increasing the values of a_1 and a_2, as discussed in Sections 2.6.1.3 and 2.6.1.4, respectively, it is observed that when we increase the values of a_1 and a_2 from 0.1 to 1, the gain of the amplitude response increases from 1.2 to 3.5 along the $\omega_1 - axis$ and $\omega_2 - axis$, respectively.

Sections 2.6.1.5 to 2.6.1.8 discuss the effect of the coefficients on the frequency response of the 2-D digital lowpass filter, viz. $a_1 = a_2$ and $k_1 = k_2$, $a_1 \neq a_2$ and $k_1 = k_2$, $a_1 \neq a_2$ and $k_1 \neq k_2$, and $a_1 = a_2$ and $k_1 \neq k_2$ respectively. It is observed in all the four cases that the coefficients k_1, k_2 affect the pass band width and a_1, a_2 affect the gain of the amplitude response. As the values of the coefficients k_1 and k_2 are increased, the pass bandwidth and the amplitude of the contour response of the 2-D digital lowpass filter decreases. As the values of the coefficients a_1 and a_2 are increased, the magnitude of the frequency response of the 2-D digital lowpass filter increases. Also it can be seen that there are ripples in the passband of the amplitude and the contour response when the values of the coefficients of the generalized bilinear transformation are in the range $1 < k_1,\ k_2 \leq 10$ and $a_1,\ a_2 \leq 0.5$.

The summary of the effect of the coefficient of the generalized bilinear transformation in Category B are as follows.

On increasing the values of k_1 and k_2, as discussed in Sections 2.6.2.1 and 2.6.2.2 respectively, it is observed that when we increase the values of k_1 and k_2 from 0.1 to 10, the passband width along the $\omega_1 - axis$ and $\omega_2 - axis$, respectively, gradually decreases keeping the amplitude constant. On increasing the values of a_1 and a_2, as discussed in Sections 2.6.2.3 and 2.6.2.4, respectively, it is observed that when we increase the values of a_1 and a_2 from 0.1 to 1, the magnitude of amplitude-frequency response of the all-pole 2-D lowpass filter increases from 1.6 to 3.5 along the $\omega_1 - axis$ and $\omega_2 - axis$ respectively.

Sections 2.6.2.5 to 2.6.2.8 discuss the effect of the coefficients on the frequency response of the all-pole 2-D digital lowpass filter, viz. $a_1 = a_2$ and $k_1 = k_2$, $a_1 \neq a_2$ and

$k_1 = k_2$, $a_1 \neq a_2$ and $k_1 \neq k_2$, and $a_1 = a_2$ and $k_1 \neq k_2$ respectively. It is observed in all the four cases that the coefficients k_1, k_2 affect the passband width and a_1, a_2 affect the gain of the amplitude response. As the values of the coefficients k_1 and k_2 are increased, the passband width and the amplitude of the contour response of the all-pole 2-D digital lowpass filter decreases. As the values of the coefficients a_1 and a_2 are increased, the magnitude of the frequency response of the all-pole 2-D digital lowpass filter increases .

The comparison of the amplitude-frequency response of the 2-D lowpass filter in Category A and the all-pole 2-D lowpass filter in Category B is as follows:

It is observed in both the categories that the coefficients of the generalized bilinear transformation k_1, k_2 affect the passband width and a_1, a_2 affect the gain of the amplitude-frequency response. When we observe the effect of the coefficients on the frequency response of the 2-D digital lowpass filter in Sections 2.6.1.5 to 2.6.1.8 and all-pole 2-D digital lowpass filter in Sections 2.6.2.5 to 2.6.2.8, viz. $a_1 = a_2$ and $k_1 = k_2$, $a_1 \neq a_2$ and $k_1 = k_2$, $a_1 \neq a_2$ and $k_1 \neq k_2$, and $a_1 = a_2$ and $k_1 \neq k_2$ in both the categories, it can be seen that for the values of $1 < k_1, k_2 \leq 10$, and $a_1, a_2 \leq 0.5$ in category A, there are ripples present in the amplitude-frequency response. Further increasing the values of $k_1, k_2 > 10$ and $a_1, a_2 > 0.5$, the ripples tend to reduce, giving the response of the 2-D digital lowpass filter. Whereas for the same values of k_1, k_2 and a_1, a_2 in category B there are no ripples present in the amplitude-frequency response of the all-pole 2-D digital lowpass filter.

Thus, this chapter contributes towards the study of the 2-D digital lowpass filters which are derived from the 2-D all-pass filters in both categories. The effect of the various combinations of the coefficients of the generalized bilinear transformation on the proposed 2-D digital lowpass filters in Category A and the proposed all-pole 2-D digital lowpass filter in Category B was analyzed and compared, and the selective 3-D magnitude and contour responses of the proposed 2-D digital lowpass filter and all-pole 2-D digital lowpass filter were plotted.

Chapter 3

All-pole 2-D Highpass Filters Using All-Pass Filters

3.1 Introduction

In Chapter 2, 2-D lowpass filter has been derived from the combination of all-pass filters. The analog transfer function for the 2-D lowpass filter in Category A and Category B, which is obtained from the combination of all-pass filters, is transformed to a 2-D digital filter by using generalized bilinear transfer function which is explained in Chapter 2 and we have discussed and analyzed the 2-D digital lowpass filter in both the categories. There are different filters, such as highpass, bandpass and bandstop filters which can be obtained from the equivalent lowpass and all-pole lowpass filters. In this chapter we will propose, discuss and analyze the 2-D digital highpass filters in Category A and Category B, which are derived from the equivalent lowpass filter and all-pole lowpass filter in Category A and Category B respectively proposed in Chapter 2.

In Section 3.2, we will proposed the transfer function for the 2-D highpass filter and the all-pole 2-D highpass filter from the proposed equivalent 2-D lowpass filter and the all-pole 2-D lowpass filter in Category A and Category B respectively, proposed earlier in Chapter 2.

In Section 3.3, we will discuss and analyze the effects of the coefficients of the generalized bilinear transformation of the 2-D highpass filter on the amplitude-frequency response in both the categories. Section 3.4 gives the summary, discussions and comparisons of the analysis presented in this chapter.

3.2 Transfer Function of the 2-D Highpass Filter

In this section, we derive the transfer function for the 2-D highpass filter in digital domain by considering the transfer function obtained by its equivalent analog 2-D lowpass filter in Category A and Category B.

3.2.1 Transfer Function of the 2-D Highpass Filter in Category A

In this section, we will derive the transfer function for the 2-D highpass filter in digital domain by considering the transfer function obtained by its equivalent analog 2-D lowpass filter in Category A. One method of designing a 2-D digital highpass filter is to start from the analog 2-D lowpass filter transfer function in Category A proposed in Chapter 2 and then apply generalized transfer function [8], which is given by

$$s_i \rightarrow k_i \frac{z_i + a_i}{z_i + b_i} \tag{3.1}$$

where $i = 1, 2$ for 2-D filters. For the resulting 2-D digital highpass filter to be stable, it is required that $k_i > 0$, $0 \leq |a_i| \leq 1$ and $-1 \leq b_i \leq 0$. The values of the coefficients $b_i's$ in the generalized bilinear transformation are taken to be -1 in order to get the desired 2-D digital highpass filter.

The analog transfer function for the 2-D highpass filter obtained from its equivalent analog 2-D lowpass filter is given by

$$H(s_1, s_2) = \frac{4 - 1.656s_1^2 - 1.656s_2^2 + 0.685584s_1^2 s_2^2}{\left[\begin{array}{c} s_1^3(s_2^3 + 2.414s_2^2 + 2.414s_2 + 1)+ \\ s_1^2(2.414s_2^3 + 5.827396s_2^2 + 5.827396s_2 + 2.414)+ \\ s_1(2.414s_2^3 + 5.827396s_2^2 + 5.827396s_2 + 2.414)+ \\ 1(s_2^3 + 2.414s_2^2 + 2.414s_2 + 1) \end{array}\right]} \tag{3.2}$$

By applying the generalized bilinear transformation, i.e. (eqn. (3.1)) to the analog transfer function for the 2-D lowpass filter obtained by the combination of the all pass filter, i.e., (eqn. (3.2)), we get,

$$H(z_1, z_2) = \frac{P(z_1, z_2)}{Q(z_1, z_2)} \tag{3.3}$$

where

$$P(z_1, z_2) = \left[\begin{array}{c} 4(z_1 + b_1)^3(z_2 + b_2)^3 - 1.656k_1^2(z_1 + b_1)(z_1 + a_1)^2(z_2 + b_2)^3 \\ -1.656k_2^2(z_2 + b_2)(z_2 + a_2)^2(z_1 + b_1)+ \\ 0.6855k_1^2k_2^2(z_1 + b_1)(z_2 + b_2)(z_1 + a_1)^2(z_2 + a_2)^2 \end{array}\right] \tag{3.4}$$

and

$$Q(z_1, z_2) = k_1^3(z_1 + a_1)^3 \left[\begin{array}{c} k_2^3(z_2 + a_2)^3+ \\ 2.414k_2^2(z_2 + b_2)(z_2 + a_2)^2+ \\ 2.414k_2(z_2 + b_2)^2(z_2 + a_2)+ \\ (z_2 + 1)^3 \end{array}\right]$$

$$
\begin{aligned}
&+ \quad k_1^2(z_1+a_1)^2(z_1+b_1)\begin{bmatrix} 2.414k_2^3(z_2+a_2)^3+ \\ 5.8274k_2^2(z_2+b_2)(z_2+a_2)^2+ \\ 5.8274k_2(z_2+b_2)^2(z_2+a_2)+ \\ 2.414(z_2+b_2)^3 \end{bmatrix} \\
&+ \quad k_1(z_1+a_1)(z_1+b_1)^2\begin{bmatrix} 2.414k_2^3(z_2+a_2)^3+ \\ 5.8274k_2^2(z_2+b_2)(z_2+a_2)^2+ \\ 5.8274k_2(z_2+b_2)^2(z_2+a_2)+ \\ 2.414(z_2+b_2)^3 \end{bmatrix} \\
&+ \quad (z_1+b_1)^3\begin{bmatrix} k_2^3(z_2+a_2)^3+ \\ 2.414k_2^2(z_2+b_2)(z_2+a_2)^2+ \\ 2.414k_2(z_2+b_2)^2(z_2+a_2)+ \\ (z_2+b_2)^3 \end{bmatrix}
\end{aligned} \tag{3.5}
$$

which is the transfer function for 2-D digital highpass filter in Category A.

3.2.2 Transfer Function of the All-pole 2-D Highpass Filter in Category B

In this section, we will derive the transfer function for the all-pole 2-D highpass filter in digital domain by considering the transfer function obtained by its equivalent analog all-pole 2-D low pass filter in Category B. One method of designing the all-pole 2-D digital highpass filter is to start from the analog all-pole 2-D lowpass filter transfer function in Category B proposed in Chapter 2 and then apply generalized transfer function [8], which is given by eqn. (3.1), where $i = 1, 2$ for 2-D filters. For the resulting all-pole 2-D digital highpass filter to be stable, it is required that $k_i > 0, 0 \leq |a_i| \leq 1$ and $-1 \leq b_i \leq 0$. The values of the coefficients $b_i's$ in the generalized bilinear transformation are taken to be -1 in order to get the desired all-pole 2-D digital highpass filter.

The analog transfer function for the all-pole 2-D highpass filter obtained from its equiv-

alent analog all-pole 2-D lowpass filter is given by

$$H(s_1, s_2) = \frac{4}{\left[\begin{array}{c} s_1^3(0.5s_2^3 + 1.414s_2^2 + 1.5s_2 + 0.707) + \\ s_1^2(1.414s_2^3 + 4s_2^2 + 4.24s_2 + 2) + \\ s_1(1.5s_2^3 + 4.24s_2^2 + 4.5s_2 + 2.12) + \\ 1(0.707s_2^3 + 2s_2^2 + 2.12s_2 + 1) \end{array}\right]} \tag{3.6}$$

By applying the generalized bilinear transformation, i.e. (eqn. (3.1)) to the analog transfer function for the all-pole 2-D low pass filter obtained by the combination of the all pass filter, i.e., (eqn. (3.6)), we get,

$$H(z_1, z_2) = \frac{P(z_1, z_2)}{Q(z_1, z_2)} \tag{3.7}$$

where

$$P(z_1, z_2) = 4(z_1 + b_1)^3(z_2 + b_2)^3 \tag{3.8}$$

and

$$\begin{aligned} Q(z_1, z_2) &= k_1^3(z_1 + a_1)^3 \left[\begin{array}{c} 0.5k_2^3(z_2 + a_2)^3 + \\ 1.414k_2^2(z_2 + a_2)^2(z_2 + b_2) + \\ 1.5k_2(z_2 + a_2)(z_2 + b_2)^2 + \\ 0.707(z_2 + b_2)^3 \end{array}\right] \\ &+ k_1^2(z_1 + a_1)^2(z_1 + b_1) \left[\begin{array}{c} 1.414k_2^3(z_2 + a_2)^3 + \\ 4k_2^2(z_2 + a_2)^2(z_2 + b_2) + \\ 4.24k_2(z_2 + a_2)(z_2 + b_2)^2 + \\ 2(z_2 + b_2)^3 \end{array}\right] \end{aligned}$$

$$
\begin{aligned}
+ \quad & k_1(z_1+a_1)(z_1+b_1)^2 \left[\begin{array}{c} 1.5k_2^3(z_2+a_2)^3+ \\ 4.24k_2^2(z_2+a_2)^2(z_2+b_2)+ \\ 4.5k_2(z_2+a_2)(z_2+b_2)^2+ \\ 2.12k_2^2(z_2+b_2)^3 \end{array}\right] \\
+ \quad & (z_1+b_1)^3 \left[\begin{array}{c} 0.707k_2^3(z_2+a_2)^3+ \\ 2k_2^2(z_2+a_2)^2(z_2+b_2) \\ 2k_2(z_2+a_2)(z_2+b_2)^2 \\ (z_2+b_2)^3 \end{array}\right]
\end{aligned} \tag{3.9}
$$

which is the transfer function for the all-pole 2-D digital highpass filter in Category B.

3.3 Frequency Response of the 2-D Digital Highpass Filter

3.3.1 Frequency Response of 2-D Digital Highpass Filter in Category A

The transfer function for the 2-D highpass filter is obtained by using the transfer function of 2-D lowpass filter in the analog domain in Category A. This transfer function for 2-D lowpass filter is obtained by using the second order Butterworth polynomial connected in the all-pass filters manner in Category A. The resultant transfer function (eqn. (3.2)) obtained is digitized by applying generalized bilinear transformation (eqn. (3.1)). The digitized transfer function of 2-D digital highpass filter is given by eqn. (3.3). With the input coefficients of the generalized bilinear transformation we can obtain the contour and 3-D magnitude plots of the resulting 2-D digital highpass filter [46].

To investigate the manner in which each coefficient of the generalized bilinear transformation effects the magnitude response of the resulting 2-D digital highpass filter, we change the values of some of the coefficients or fix some of the coefficients to specific values. It is possible to obtain a 2-D digital highpass filter when the coefficients have the

following limits: $k_i > 0$, $0 \leq |a_i| \leq 1$ and taking $b_i = -1$, where $i = 1, 2$. Let us consider the coefficients of the generalized bilinear transformation for the 2-D digital highpass filter to be unity, i.e., $a_1 = 1$, $a_2 = 1$, $k_1 = 1$, $k_2 = 1$ and $b_1 = -1$, $b_2 = -1$. Under this condition, the 3-D amplitude-frequency response and the contour plots of the 2-D digital filter are shown in the Figure 3.1

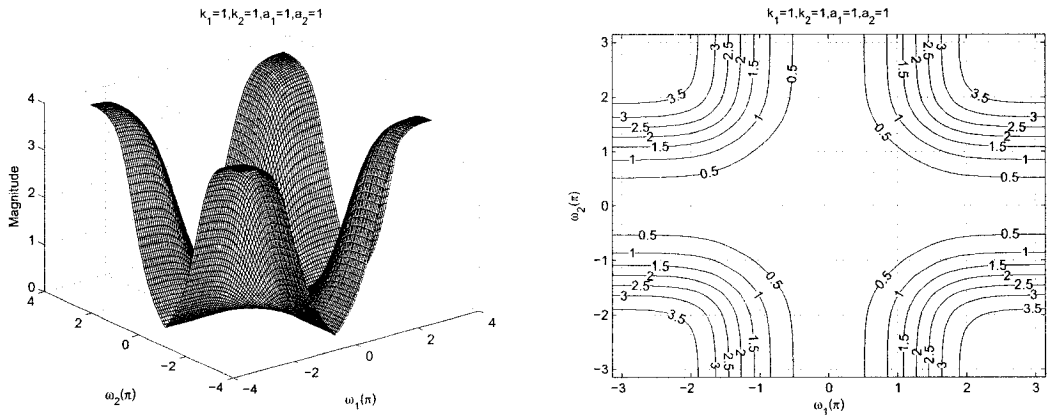

Figure 3.1: 3-D Amplitude-Frequency response and contour response of the 2-D Digital Highpass Filter with all the coefficients values as unity

3.3.1.1 Frequency Response of 2-D Digital Highpass Filter with different values of k_1

In this section, we study the manner in which k_1 effects the frequency response behavior of the resulting 2-D digital highpass filter in Category A and to separate the effect of the other coefficients, we vary the values of k_1, and fixing all the other coefficient of the generalized bilinear transformation to be unity in order not to loose any generality and to make the situation situation simple, e.g. with $k_2 = 1$, $a_1 = 1$, $a_2 = 1$, $b_1 = -1$ and $b_2 = -1$.The values of k_1 are varied from 0.1 to 10 and the 3-D magnitude response and the contour plots for the 2-D digital highpass filter with the values of $k_1 = 0.1$, $k_1 = 0.5$ $k_1 = 0.9$, $k_1 = 2$, $k_1 = 5$ and $k_1 = 10$ are shown in the Figures 3.2 and 3.3.

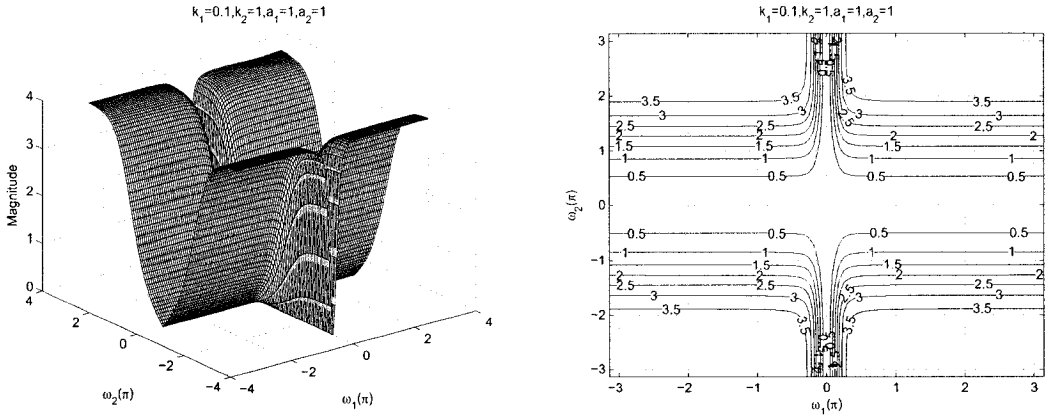

(a) $k_1 = 0.1$

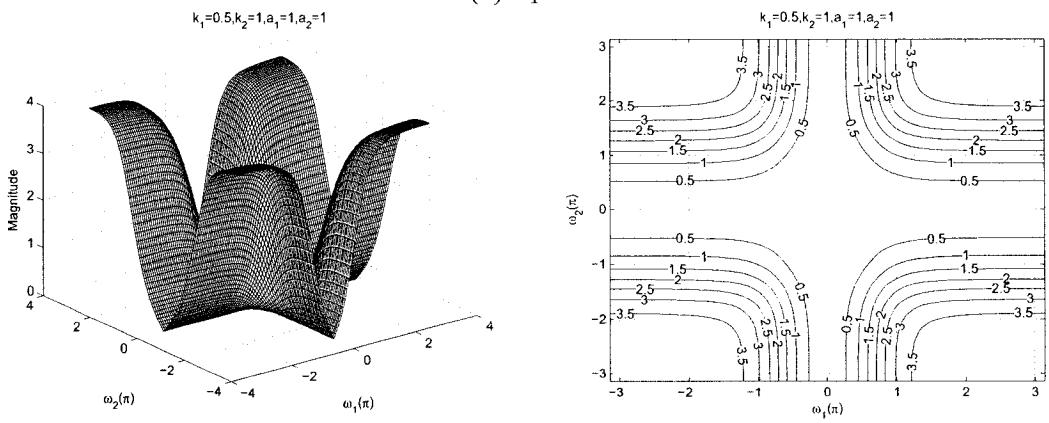

(b) $k_1 = 0.5$

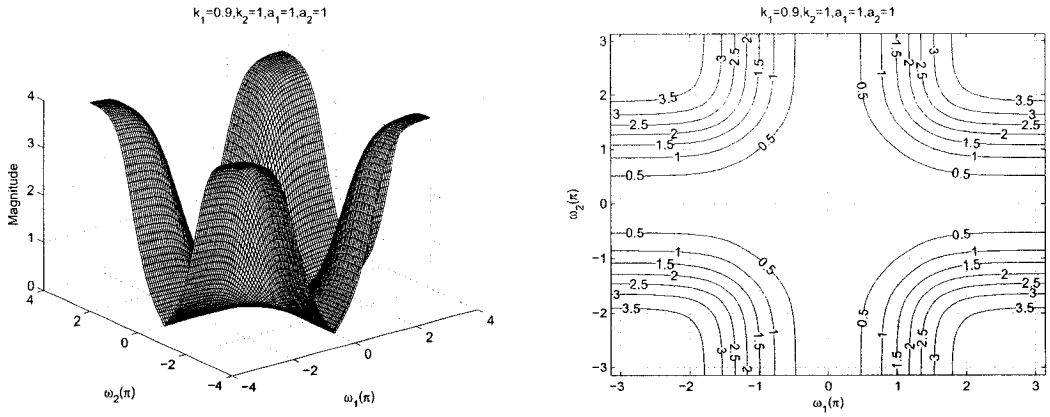

(c) $k_1 = 0.9$

Figure 3.2: 3-D amplitude frequency response and the contour response of the 2-D digital highpass filter for different values of k_1

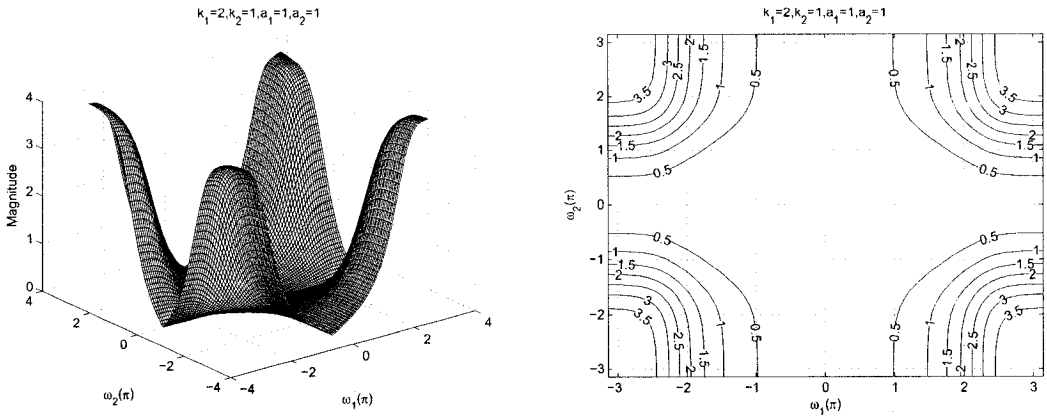

(a) $k_1 = 2$

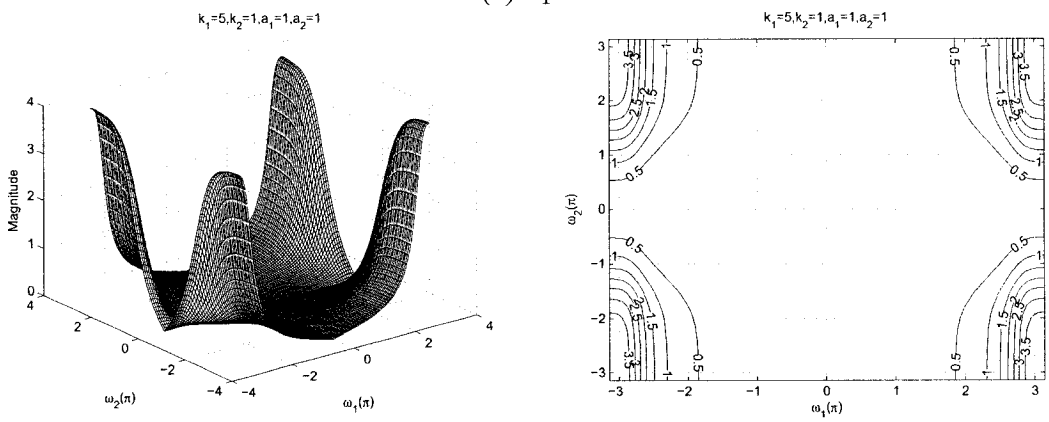

(b) $k_1 = 5$

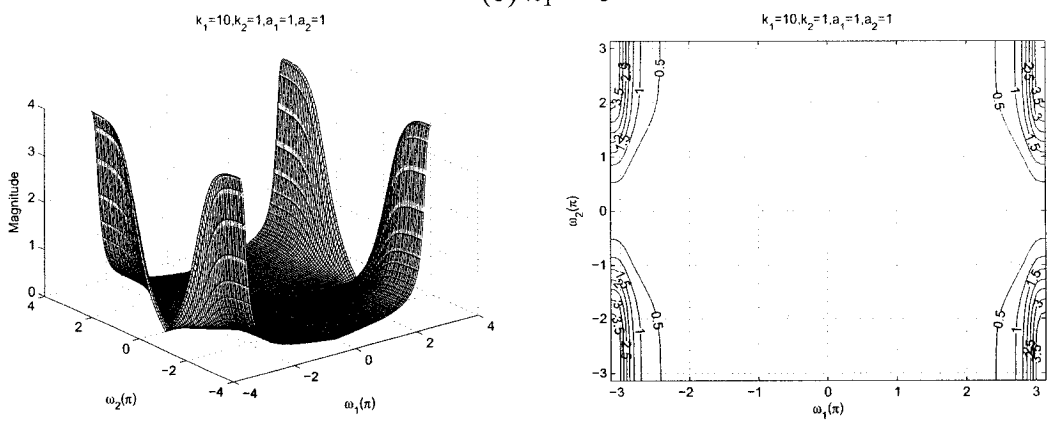

(c) $k_1 = 10$

Figure 3.3: 3-D amplitude frequency response and the contour response of the 2-D digital highpass filter for different values of k_1

It is observed that although the coefficient k_1 does not have any effect on stopband width along the $\omega_2 - axis$, it affects the width of the stopband along the $\omega_1 - axis$. Initially when the value of the coefficient $k_1 = 0.1$ (see Figure 3.2 (a)) the stopband width is minimum along the $\omega_1 - axis$. As we increase the value of k_1, the stop bandwidth gradually increases. Also the amplitude of the frequency response remains constant for the same.

3.3.1.2 Frequency Response of 2-D Digital Highpass Filter with different values of k_2

In this section, we study the manner in which k_2 effects the frequency response behavior of the resulting 2-D digital highpass filter in Category A and to separate the effect of the other coefficients, we vary the values of k_2, and fix all the other coefficients of the generalized bilinear transformation to unity in order not to loose any generality and to make the situation simple, e.g. with $k_1 = 1$, $a_1 = 1$, $a_2 = 1$, $b_1 = -1$ and $b_2 = -1$. The values of k_2 are varied from 0.1 to 10 and the 3-D magnitude response and the contour plots for the 2-D digital highpass filter with the values of $k_2 = 0.1$, $k_2 = 0.5$ $k_2 = 0.9$, $k_2 = 2$, $k_2 = 5$ and $k_2 = 10$ are shown in the Figures 3.4 and 3.5.

It is observed that although the coefficient k_2 does not have any effect on the stopband width along the $\omega_1 - axis$, it affects the width of the stopband along the $\omega_2 - axis$. Initially when the value of the coefficient $k_1 = 0.1$ (see Figure 3.4 (a)) the stopband width is minimum along the $\omega_2 - axis$. As we increase the value of k_2, the stopband width gradually increases. Also the amplitude of the frequency response remains constant for the same.

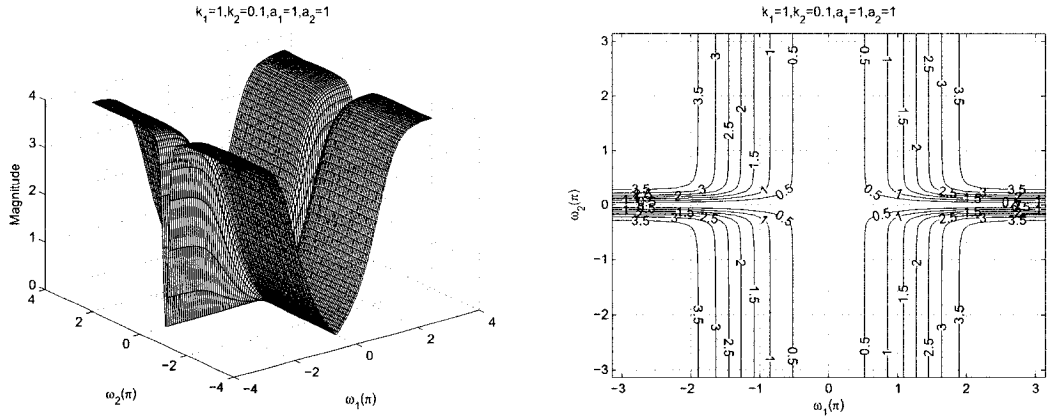

(a) $k_2 = 0.1$

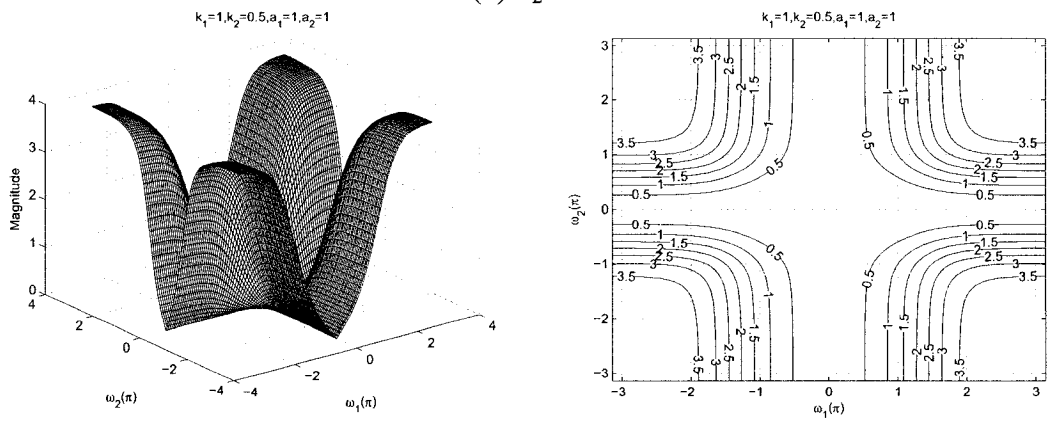

(b) $k_2 = 0.5$

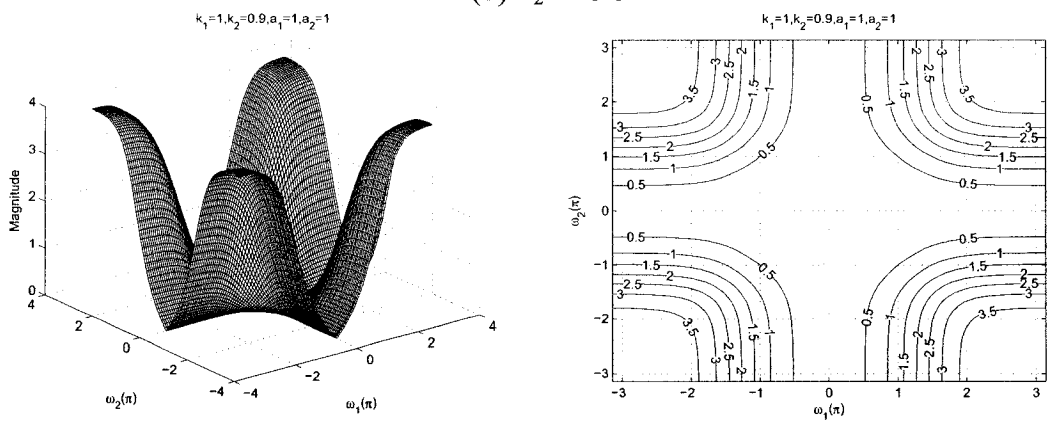

(c) $k_2 = 0.9$

Figure 3.4: 3-D amplitude frequency response and the contour response of the 2-D digital highpass filter for different values of k_2

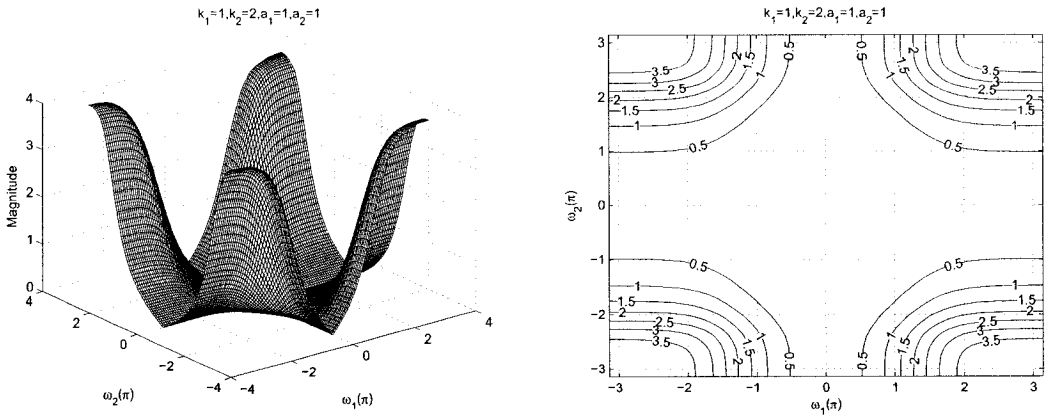

(a) $k_2 = 2$

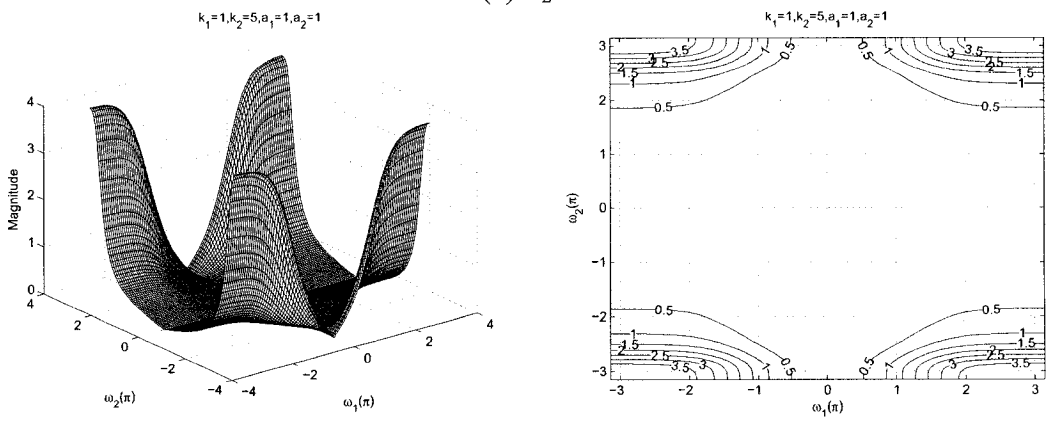

(b) $k_2 = 5$

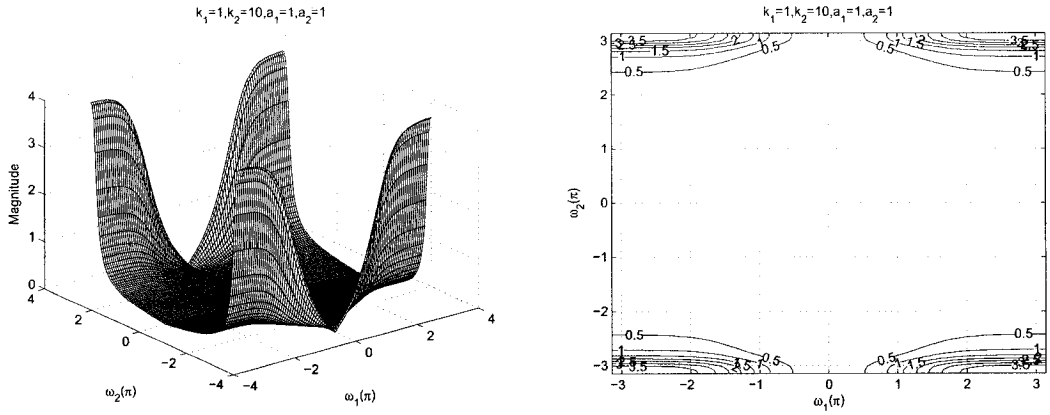

(c) $k_2 = 10$

Figure 3.5: 3-D amplitude frequency response and the contour response of the 2-D digital highpass filter for different values of k_2

3.3.1.3 Frequency Response of 2-D Digital Highpass Filter with different values of a_1

In the Sections 3.3.1.1 and 3.3.1.2, the effect of the coefficient of k_1 and k_2 are studied. In this section, the effect of the coefficient a_1 will be studied. The stable range of a_1 can be obtained with other specified coefficients of the generalized bilinear transformation. There are many combinations possible for the coefficients. To study the response with different values of a_1 properly, we fix other coefficient values to be equal to unity. The range of a_1 varies from 0.1 to 1 and the other coefficient values are specified as unity, i.e., $k_1 = 1$, $k_2 = 1$, $a_2 = 1$, and $b_1 = -1$ and $b_2 = -1$ in order to get 2-D digital highpass filter response in Category A.

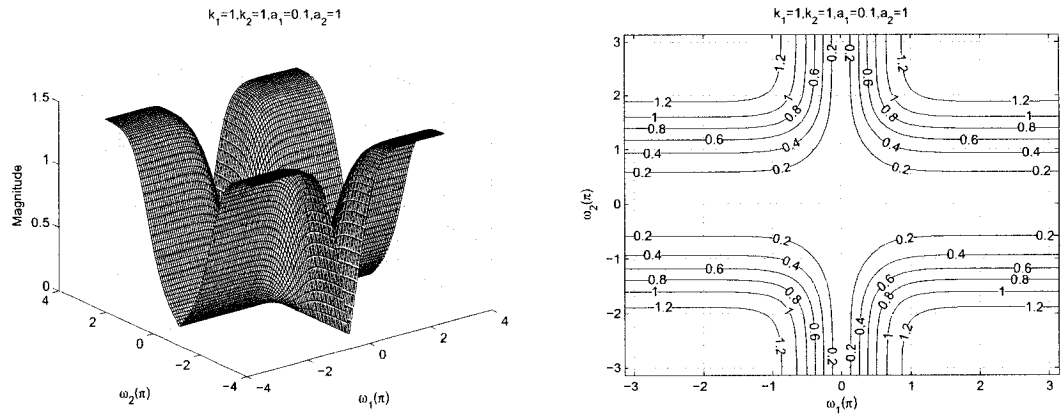

(a) $a_1 = 0.1$

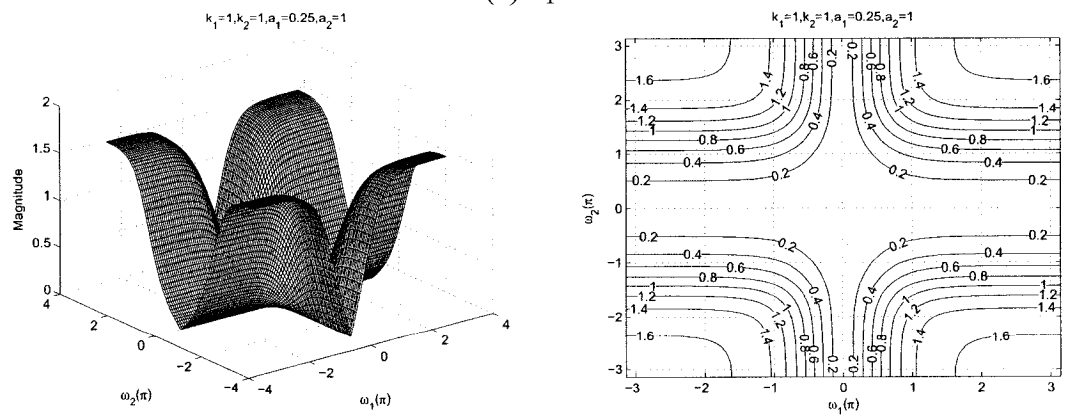

(b) $a_1 = 0.25$

Figure 3.6: 3-D amplitude frequency response and the contour response of the 2-D digital highpass filter for different values of a_1

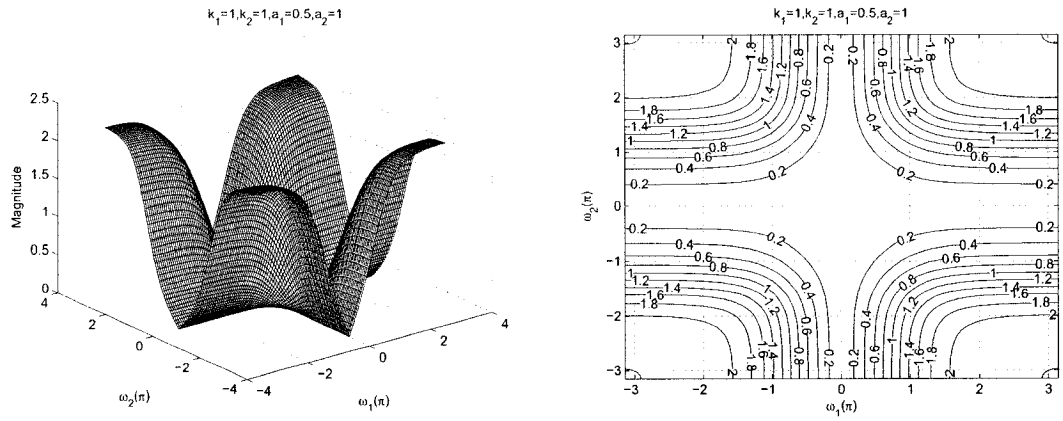

(a) $a_1 = 0.5$

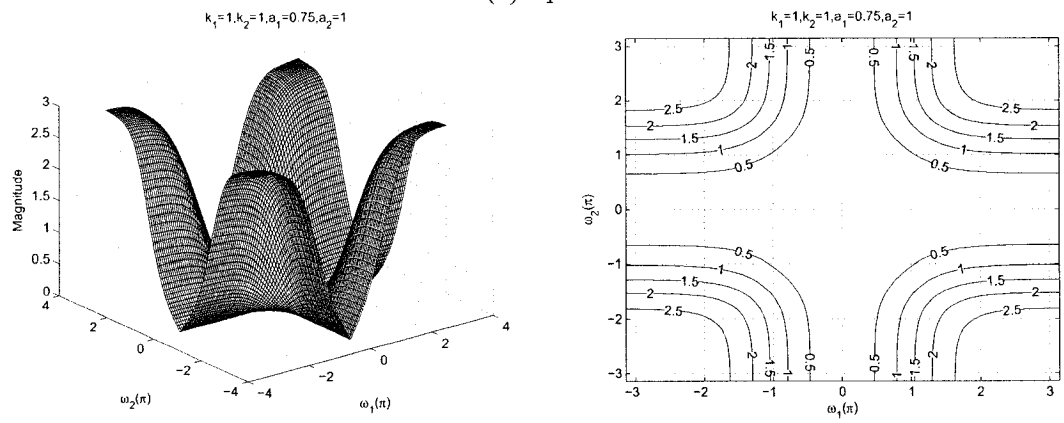

(b) $a_1 = 0.75$

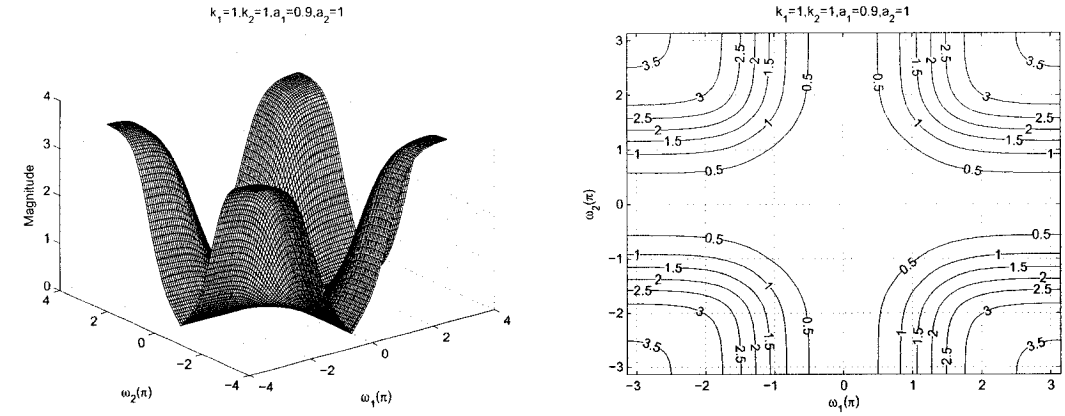

(c) $a_1 = 0.9$

Figure 3.7: 3-D amplitude frequency response and the contour response of the 2-D digital highpass filter for different values of a_1

By varying the value of a_1, the 3-D magnitude response and contour plots which represents different values of a_1, i.e. $a_1 = 0.1$, $a_1 = 0.25$, $a_1 = 0.5$, $a_1 = 0.75$, and $a_1 = 0.9$ are shown in the Figures 3.6 and 3.7. By making the value of $a_1 = 1$, it resembles the standard highpass filter as shown in the Figure 3.1. It is observed for the diagrams that the coefficient effects the gain of the amplitude-frequency response. At the lowest value of a_1 the gain of the stopband will be less than 1. As we increase the value of a_1 from 0.1 to 1, the gain of the amplitude-frequency increases from 1.2 to 3.5. As the value of a_1 increases, the gain increases and reach the maximum value at $a_1 = 1$. Also, the width of the stopband remains constant for the same.

3.3.1.4 Frequency Response of 2-D Digital Highpass Filter with different values of a_2

In the Section 3.3.1.3, the effect of the coefficient of a_1 was studied. In this section, the effect of the coefficient a_2 is studied. The stable range of a_2 can be obtained with other specified coefficients of the generalized bilinear transformation. There are many combinations possible for the coefficients. To study the response with different values of a_2 properly, we fix other coefficient values to be equal to unity. The range of a_2 varies from 0.1 to 1 and the other coefficient values are specified as unity, i.e., $k_1 = 1$, $k_2 = 1$, $a_1 = 1$, $b_1 = -1$ and $b_2 = -1$ in order to get 2-D digital highpass filter response in Category A.

By varying the value of a_2, the 3-D magnitude response and contour plots which represents different values of a_2, i.e. $a_2 = 0.1$, $a_2 = 0.25$, $a_2 = 0.5$, $a_2 = 0.75$, and $a_2 = 0.9$ are shown in the Figures 3.8 and 3.9. By making the value of $a_2 = 1$, it resembles the standard highpass filter as shown in the Figure 3.1. It is observed for the diagrams that the coefficient effects the gain of the amplitude response. At the lowest value of a_2 the gain of the stopband will be less than 1. As the value of a_2 increases from 0.1 to 1, the gain of the amplitude-response increases from 1.2 to 3.5. As the value of a_2 increases, the gain

increases and reach the maximum value at $a_2 = 1$. Also, the width of the stopband remains constant for the same.

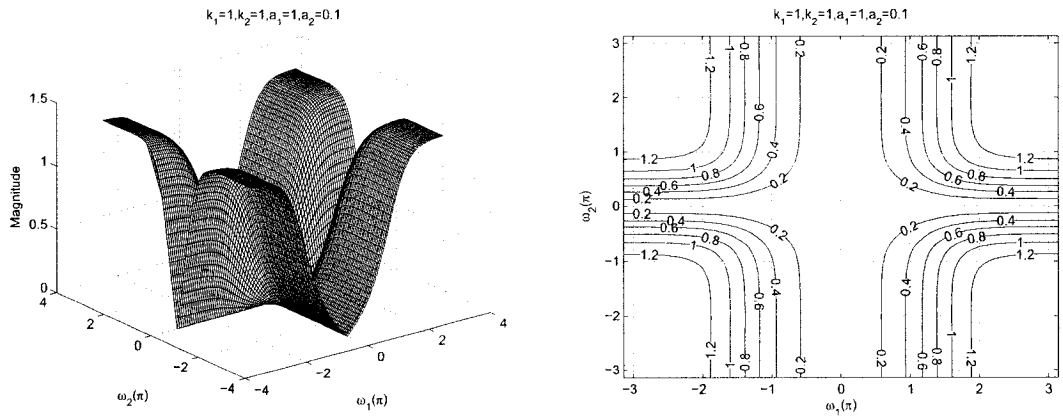

(a) $a_2 = 0.1$

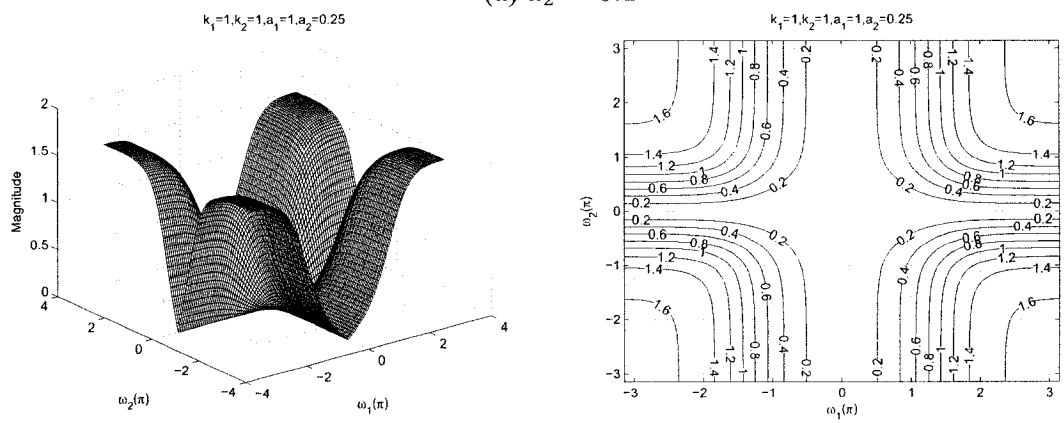

(b) $a_2 = 0.25$

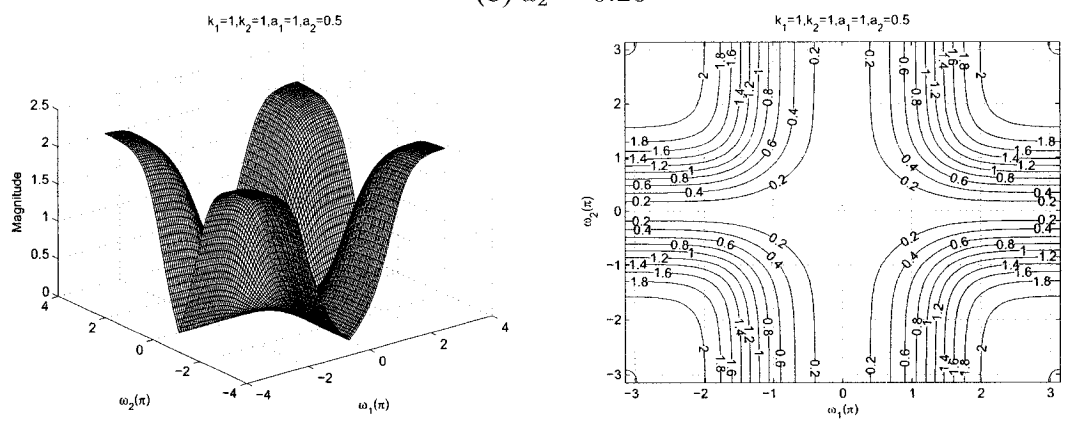

(c) $a_2 = 0.5$

Figure 3.8: 3-D amplitude frequency response and the contour response of the 2-D digital highpass filter for different values of a_2

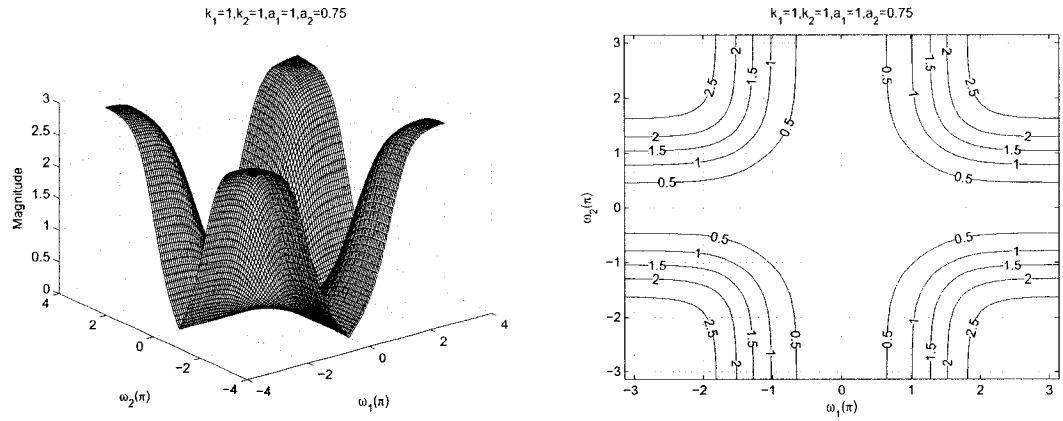

(a) $a_2 = 0.75$

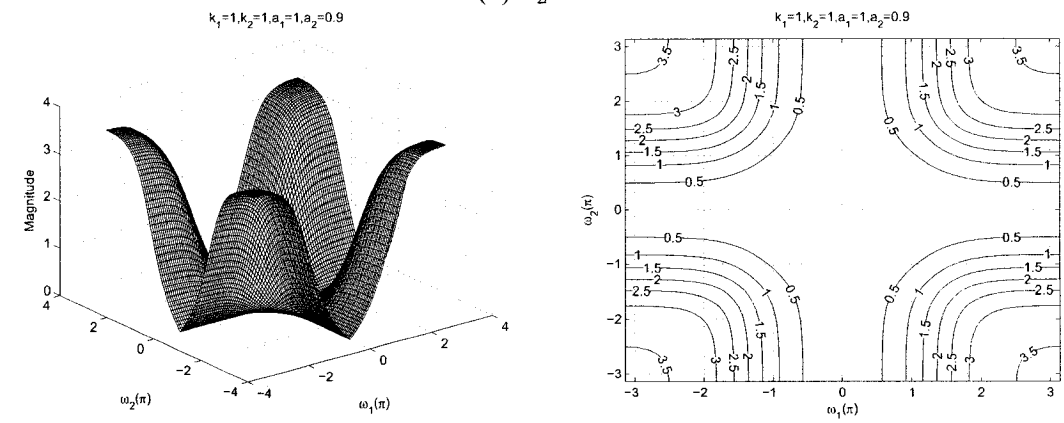

(b) $a_2 = 0.9$

Figure 3.9: 3-D amplitude frequency response and the contour response of the 2-D digital highpass filter for different values of a_2

3.3.1.5 Frequency Response of 2-D Digital Highpass Filter with same values of a_1 and a_2 and same values of k_1 and k_2

In the Sections 3.3.1.1 to 3.3.1.4 the individual effect of the coefficients a_1, a_2, k_1 and k_2 was studied. In this section, we will study the effect of coefficients where $a_1 = a_2$ and $k_1 = k_2$ and the remaining coefficients $b_1 = b_2 = -1$ in order to get the 2-D digital highpass filter in Category A. The values of a_1 and a_2 range from 0 to 1 and the values of k_1 and k_2 range from 0 to 50.

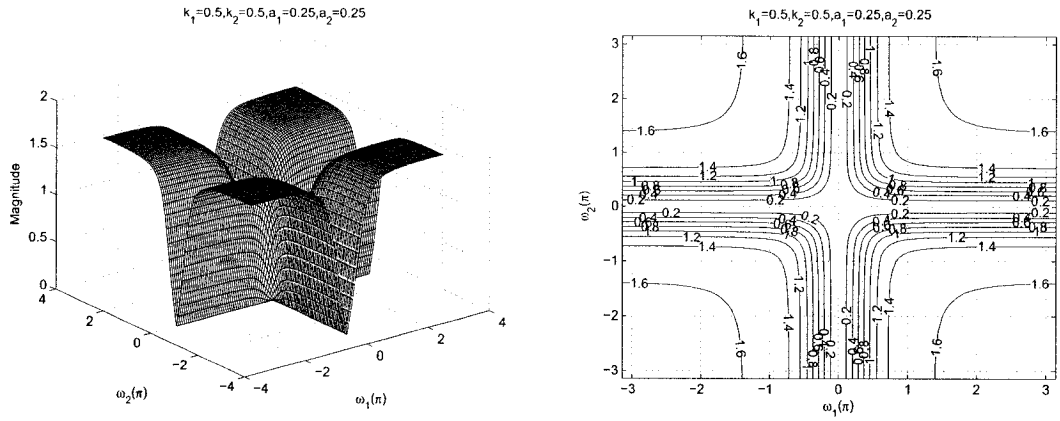

(a) $a_1 = a_2 = 0.25$ and $k_1 = k_2 = 0.5$

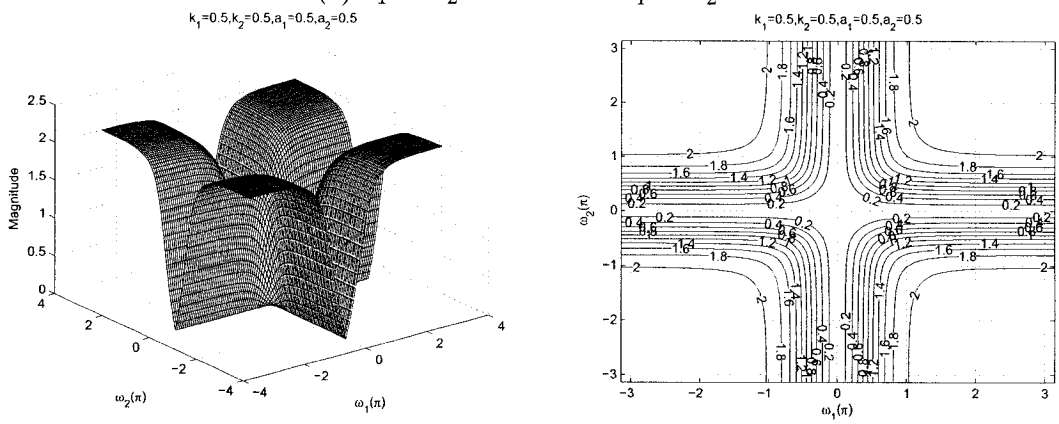

(b) $a_1 = a_2 = 0.5$ and $k_1 = k_2 = 0.5$

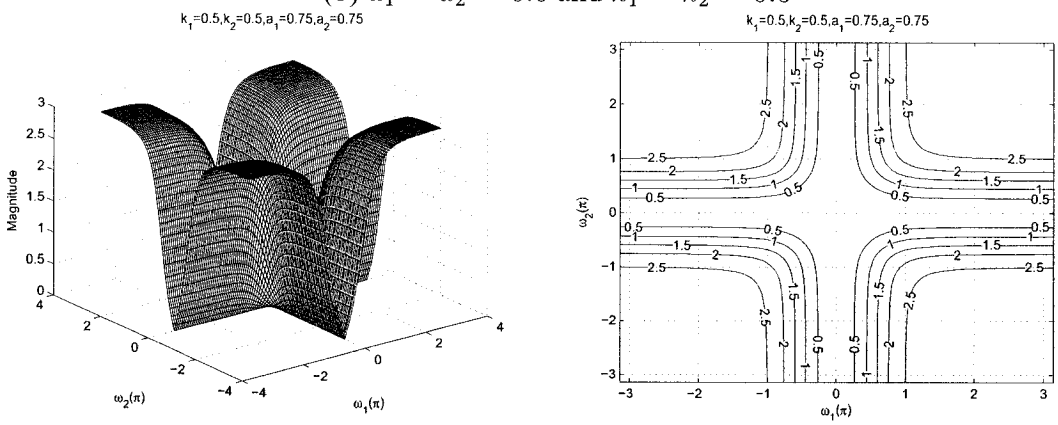

(c) $a_1 = a_2 = 0.75$ and $k_1 = k_2 = 0.5$

Figure 3.10: 3-D amplitude frequency response and the contour response of the 2-D digital highpass filter for $a_1 = a_2$ and $k_1 = k_2$

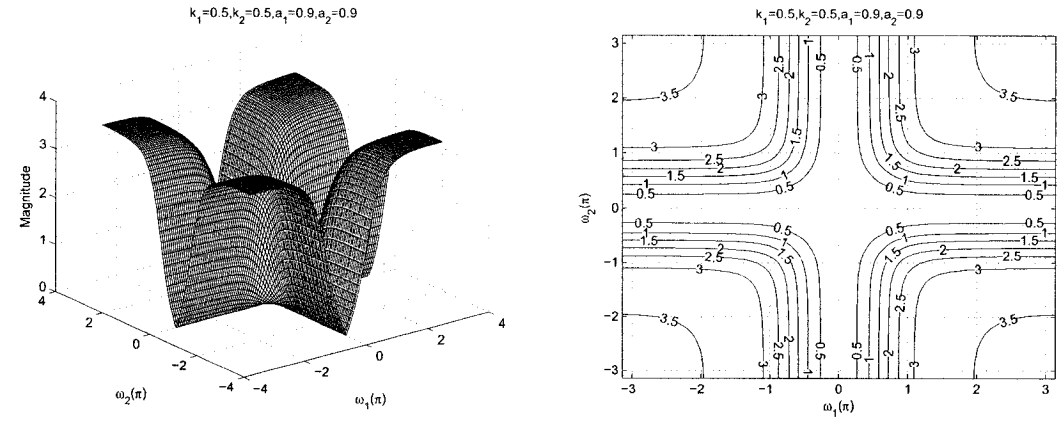

(a) $a_1 = a_2 = 0.9$ and $k_1 = k_2 = 0.5$

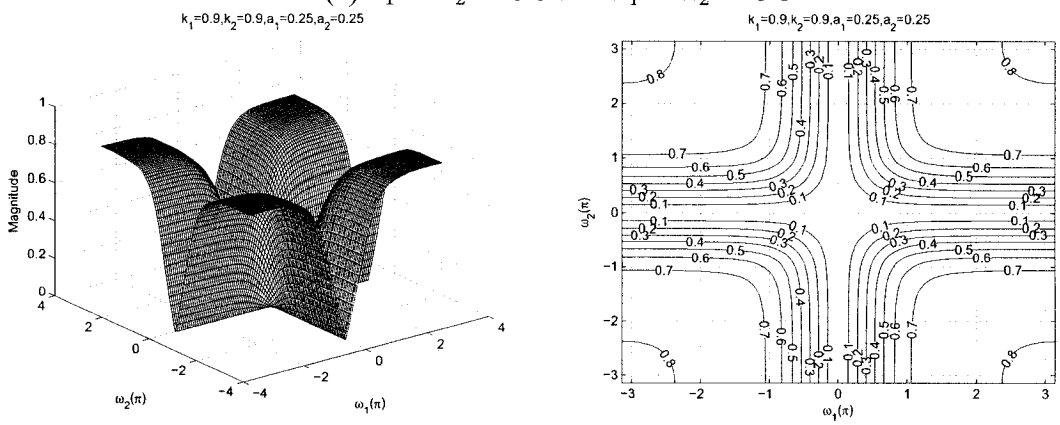

(b) $a_1 = a_2 = 0.25$ and $k_1 = k_2 = 0.9$

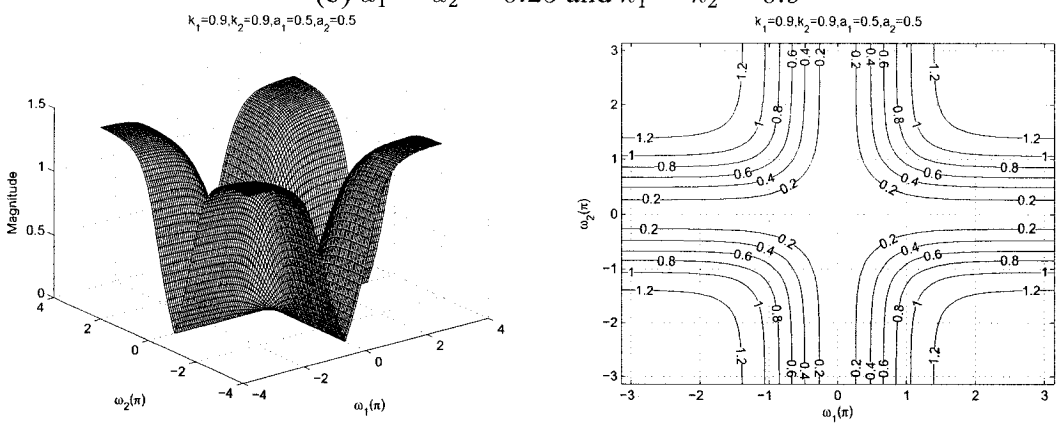

(c) $a_1 = a_2 = 0.5$ and $k_1 = k_2 = 0.9$

Figure 3.11: 3-D amplitude frequency response and the contour response of the 2-D digital highpass filter for $a_1 = a_2$ and $k_1 = k_2$

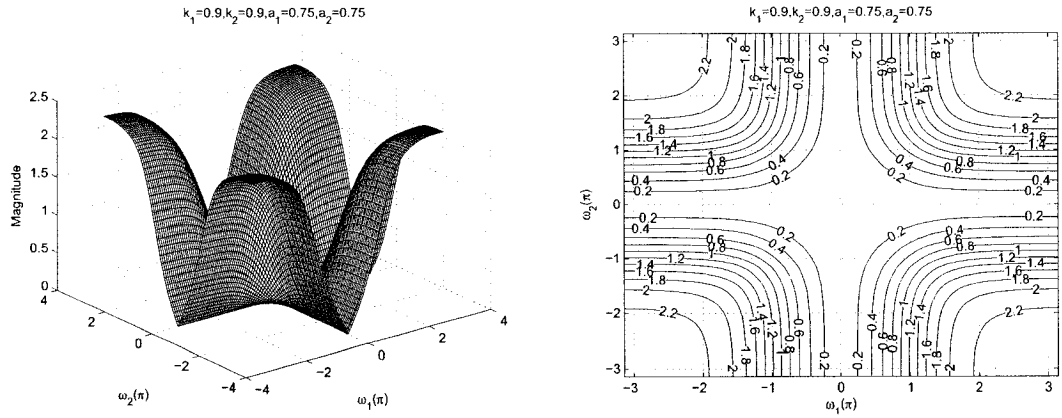

(a) $a_1 = a_2 = 0.75$ and $k_1 = k_2 = 0.9$

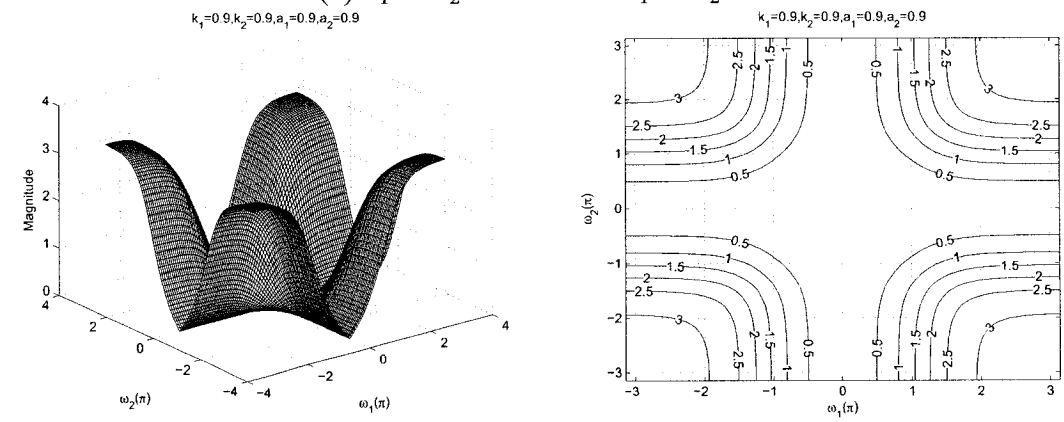

(b) $a_1 = a_2 = 0.9$ and $k_1 = k_2 = 0.9$

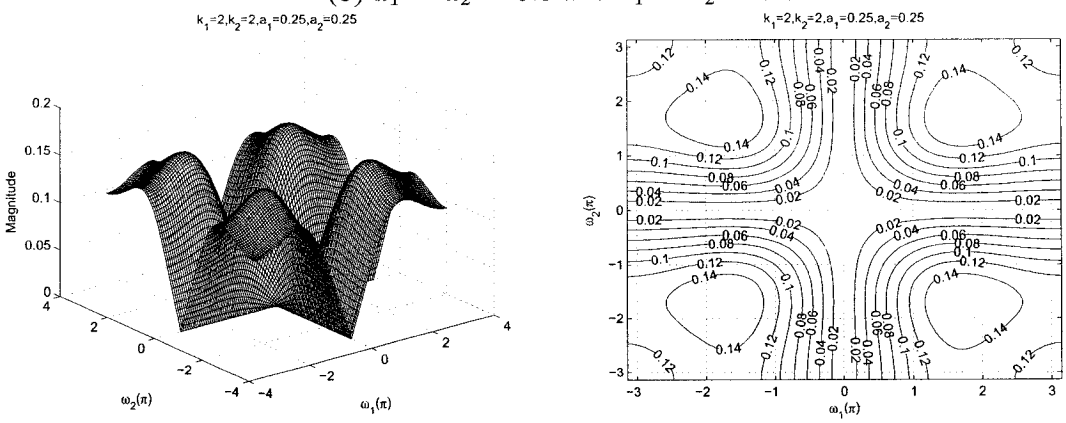

(c) $a_1 = a_2 = 0.25$ and $k_1 = k_2 = 2$

Figure 3.12: 3-D amplitude frequency response and the contour response of the 2-D digital highpass filter for $a_1 = a_2$ and $k_1 = k_2$

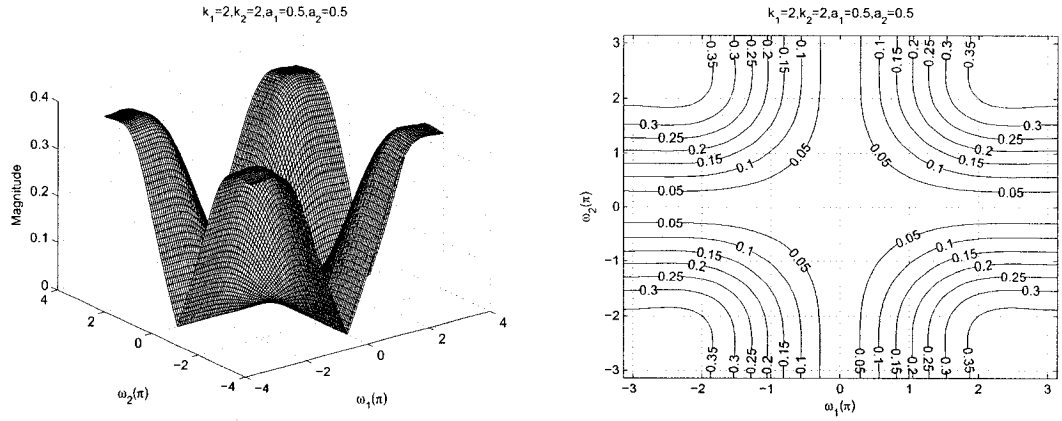

(a) $a_1 = a_2 = 0.5$ and $k_1 = k_2 = 2$

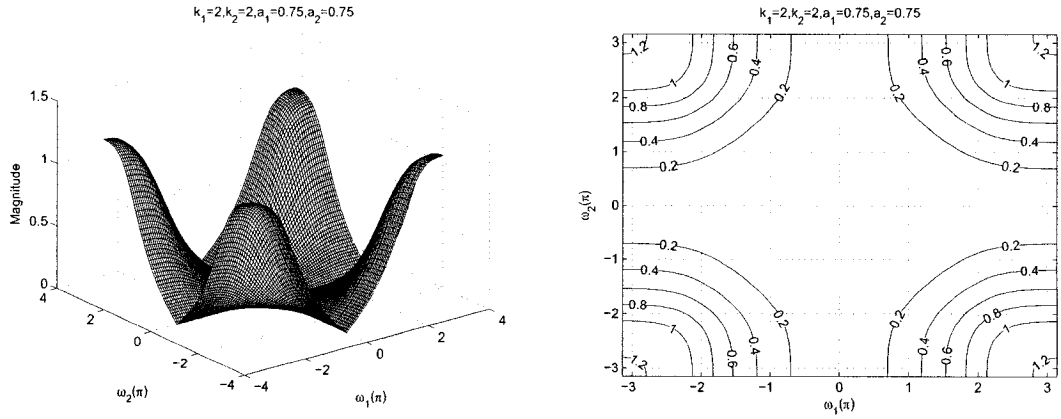

(b) $a_1 = a_2 = 0.75$ and $k_1 = k_2 = 2$

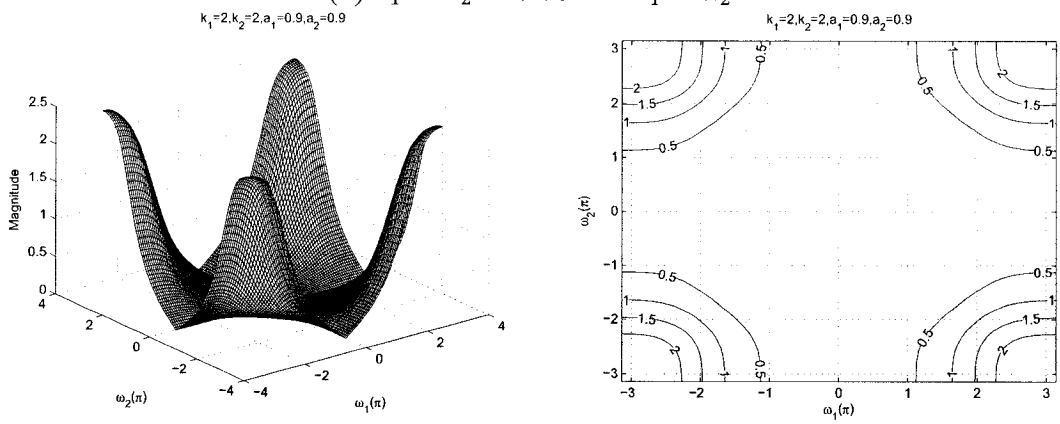

(c) $a_1 = a_2 = 0.9$ and $k_1 = k_2 = 2$

Figure 3.13: 3-D amplitude frequency response and the contour response of the 2-D digital highpass filter for $a_1 = a_2$ and $k_1 = k_2$

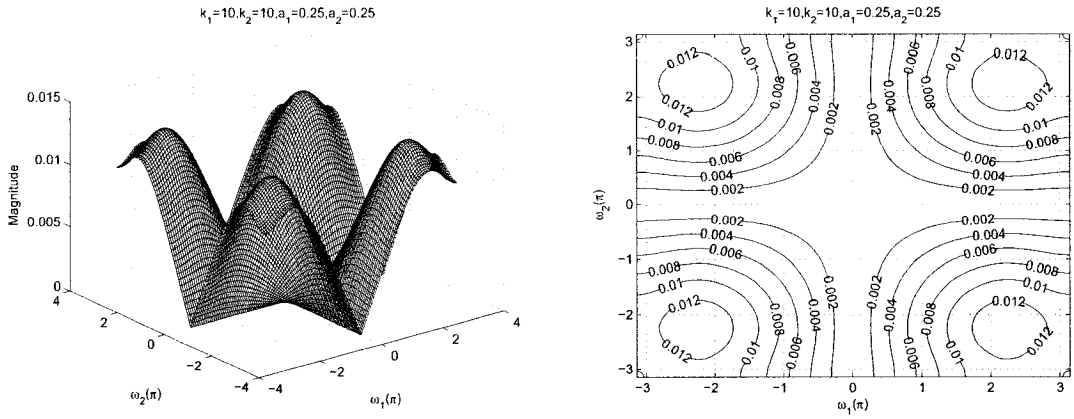

(a) $a_1 = a_2 = 0.25$ and $k_1 = k_2 = 10$

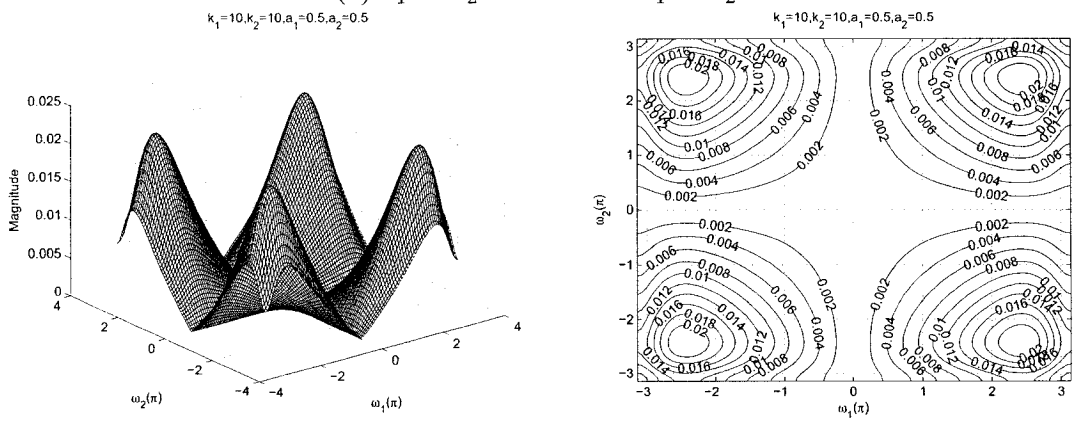

(b) $a_1 = a_2 = 0.5$ and $k_1 = k_2 = 10$

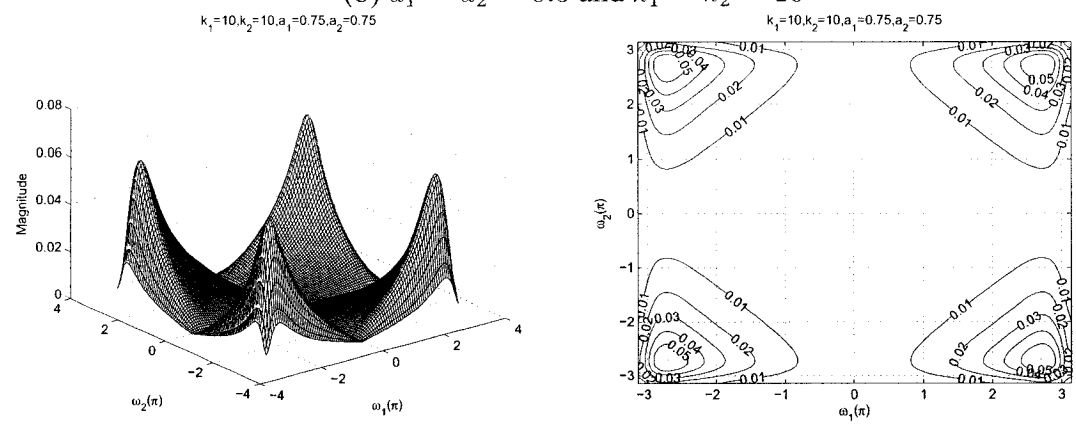

(c) $a_1 = a_2 = 0.75$ and $k_1 = k_2 = 10$

Figure 3.14: 3-D amplitude frequency response and the contour response of the 2-D digital highpass filter for $a_1 = a_2$ and $k_1 = k_2$

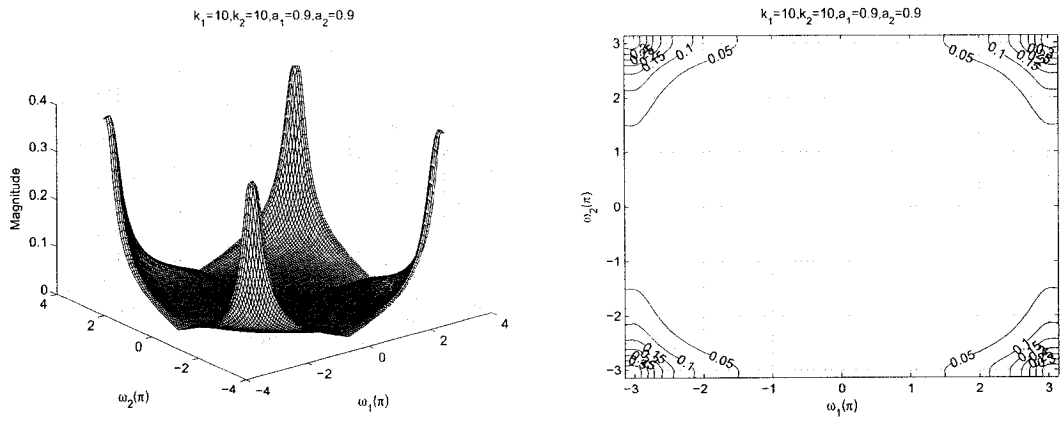

(a) $a_1 = a_2 = 0.9$ and $k_1 = k_2 = 10$

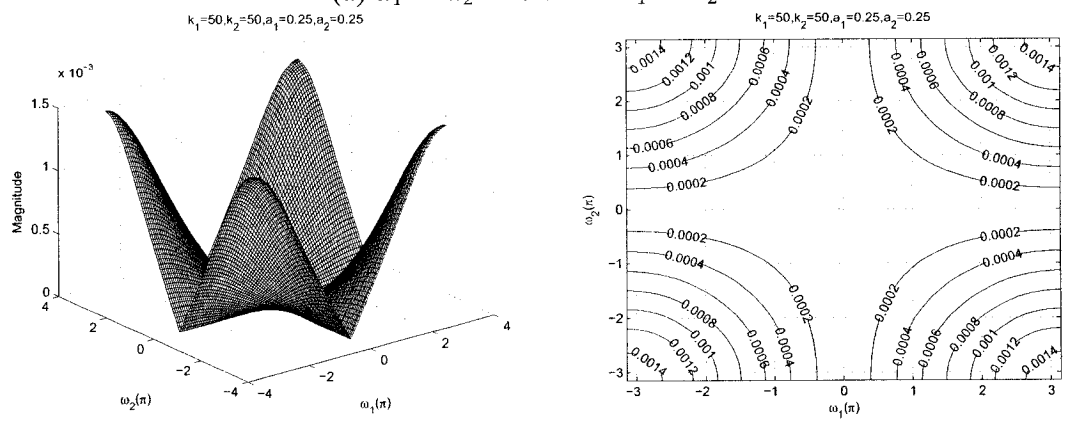

(b) $a_1 = a_2 = 0.25$ and $k_1 = k_2 = 50$

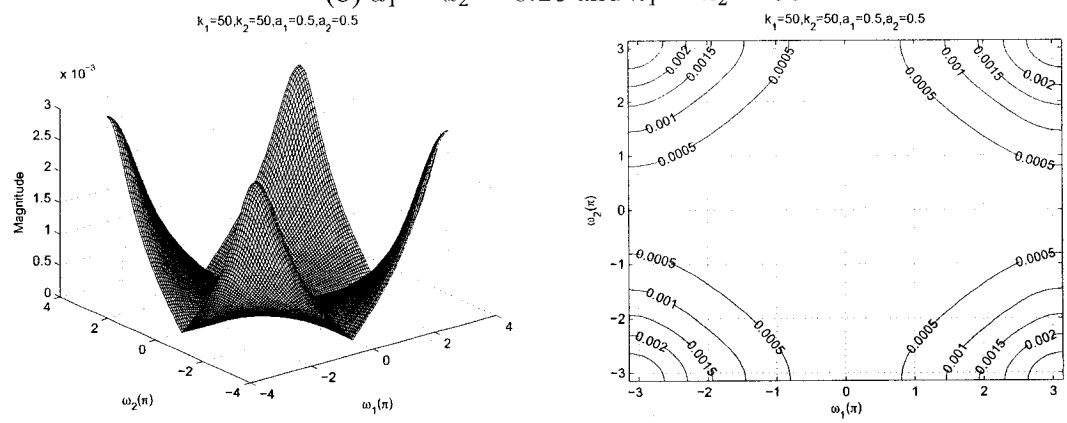

(c) $a_1 = a_2 = 0.5$ and $k_1 = k_2 = 50$

Figure 3.15: 3-D amplitude frequency response and the contour response of the 2-D digital highpass filter for $a_1 = a_2$ and $k_1 = k_2$

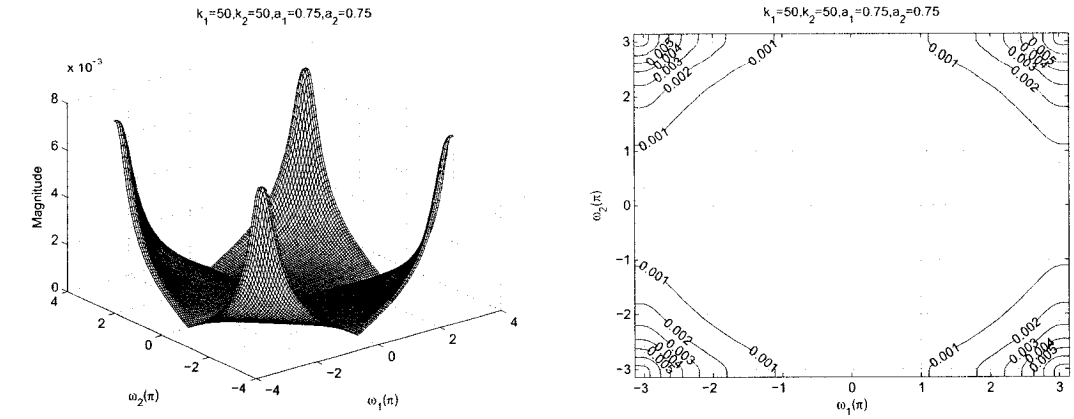

(a) $a_1 = a_2 = 0.75$ and $k_1 = k_2 = 50$

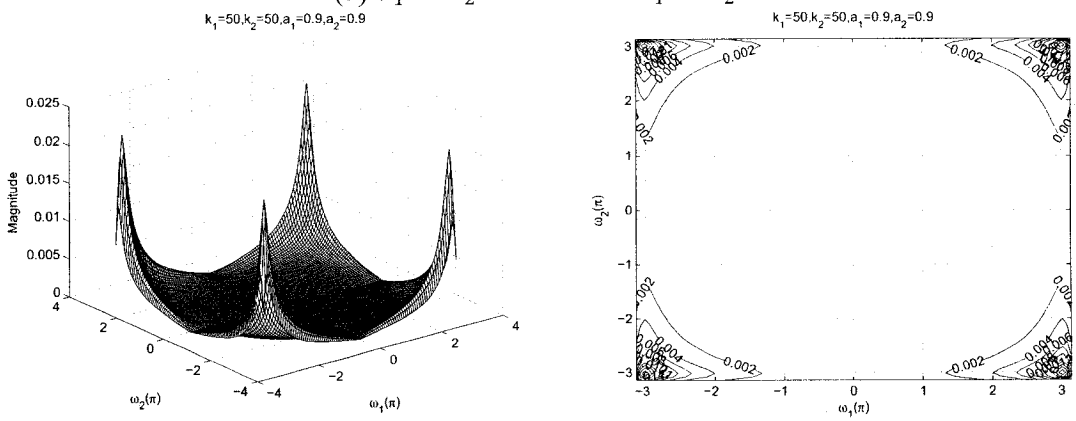

(b) $a_1 = a_2 = 0.9$ and $k_1 = k_2 = 50$

Figure 3.16: 3-D amplitude frequency response and the contour response of the 2-D digital highpass filter for $a_1 = a_2$ and $k_1 = k_2$

As observed from the Figures 3.10 to 3.16, the coefficients k_1 and k_2 affect the stopband width of the frequency response. In the Figures 3.10 (a), 3.11 (b), 3.12 (c), 3.14 (a), and 3.15 (b), there is an increase in the stopband width of the contour response as the values of k_1 and k_2 are increased from 0.5 to 50 for the same values of $a_1 = a_2 = 0.25$. It is also observed that there is a decrease in the magnitude of the contour response from 1.6 to 0.0014 for the same values.

As observed from the Figures 3.10 to 3.16, the coefficients a_1 and a_2 affect the gain of the amplitude-frequency response. It can be clearly observed from the Figures 3.10 (a), (b), (c) and 3.11 (a), that the amplitude of the contour response increases from 1.6 to 3.5 when the values of a_1 and a_2 are increased from 0.25 to 0.9 keeping the same value of

$k_1 = k_2 = 0.5$.

As observed from the Figure 3.12 (c), when the values of $k_1, k_2 > 1$ and $a_1, a_2 \leq 0.5$, there are ripples in the amplitude and the contour response. As we increase the values of a_1 and a_2, the ripples tend to reduce, giving the response of the 2-D digital highpass filter as seen from the Figures 3.12 (c) and 3.13 (a), (b) and (c) . When $k_1, k_2 > 2$, (Figures 3.14, 3.15 (a)) we see very strong ripples. As we further increase the values of a_1 and a_2, the ripples tend to increase in the range of $k_1, k_2 \geq 2$. As we further increase the value of $k_1, k_2 > 10$, and also the values of a_1 and a_2 from 0.25 to 0.9, these ripples tend to reduce, giving the response of the 2-D digital highpass filter as seen from the Figures 3.15(a), (b), 3.16 (a) and (b). Thus, it can be seen that there are ripples in the stopband when $1 < k_1,\ k_2 \leq 10$ and $a_1,\ a_2 \leq 0.5$.

3.3.1.6 Frequency Response of 2-D Digital Highpass Filter with different values of a_1 and a_2 and same values of k_1 and k_2

In this section, we will study the effect of coefficients, where $a_1 \neq a_2$ and $k_1 = k_2$ and the remaining coefficients $b_1 = b_2 = -1$ in order to get the 2-D digital highpass filter in Category A. The values of a_1 and a_2 ranges from 0.25 to 0.5 and 0.5 to 0.75, respectively and the values of k_1 and k_2 ranges from 0 to 50.

As observed from the Figures 3.17 to 3.22 , the coefficients k_1 and k_2 affect the stopband width of the frequency response of the 2-D digital highpass filter. In the Figures 3.17 (a), 3.18 (a), 3.19 (a), 3.20 (a), 3.21 (a) and 3.22 (a), there is a gradual increase in the stopband width as the values of k_1 and k_2 are increased from 0.5 to 50 for different values of $a_1 = 0.25$ and $a_2 = 0.5$. At the same time there is a gradual decrease in the magnitude of the contour response from 1.8 to 0.0018.

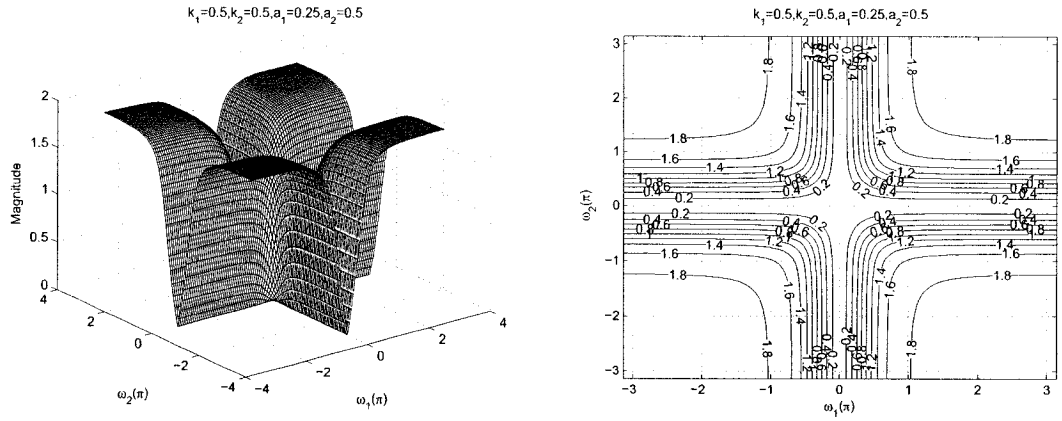

(a) $a_1 = 0.25$, $a_2 = 0.5$ and $k_1 = k_2 = 0.5$

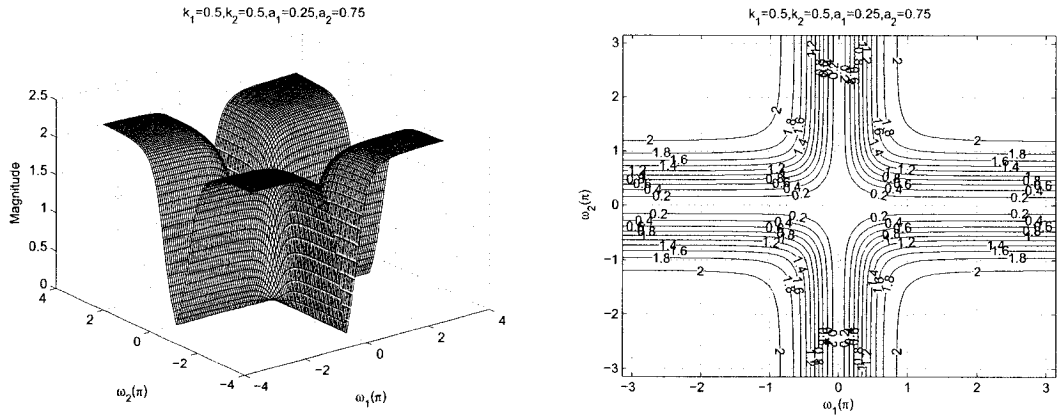

(b) $a_1 = 0.25$, $a_2 = 0.75$ and $k_1 = k_2 = 0.5$

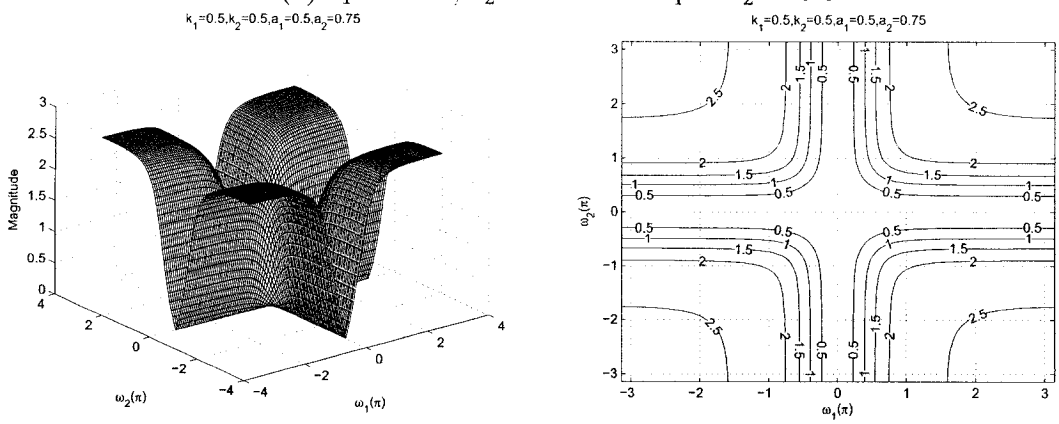

(c) $a_1 = 0.5$, $a_2 = 0.75$ and $k_1 = k_2 = 0.5$

Figure 3.17: 3-D amplitude frequency response and the contour response of the 2-D digital highpass filter for $a_1 \neq a_2$ and $k_1 = k_2$

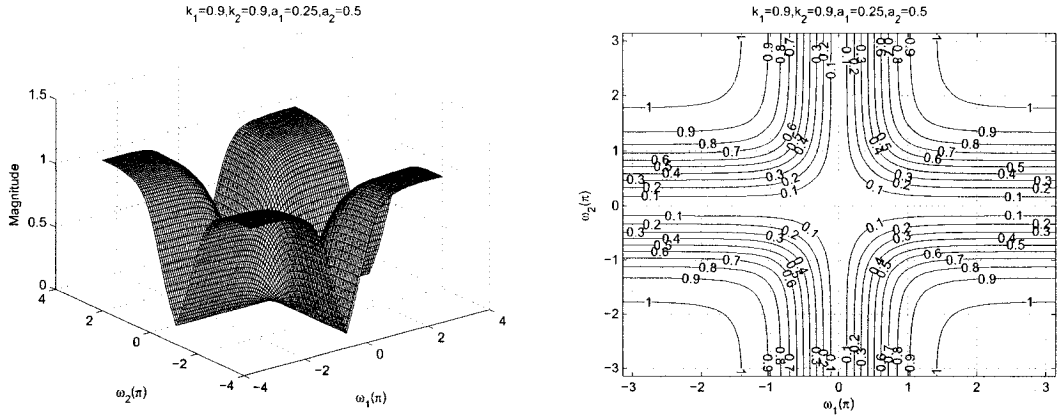

(a) $a_1 = 0.25$, $a_2 = 0.5$ and $k_1 = k_2 = 0.9$

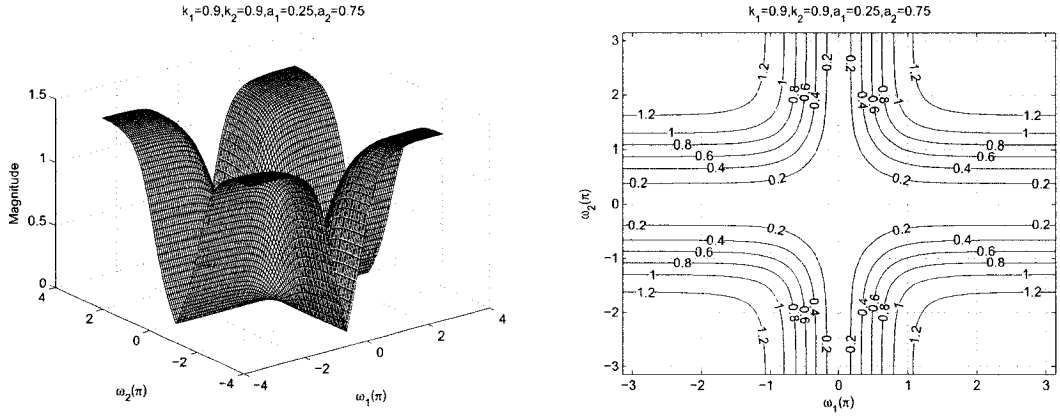

(b) $a_1 = 0.25$, $a_2 = 0.75$ and $k_1 = k_2 = 0.9$

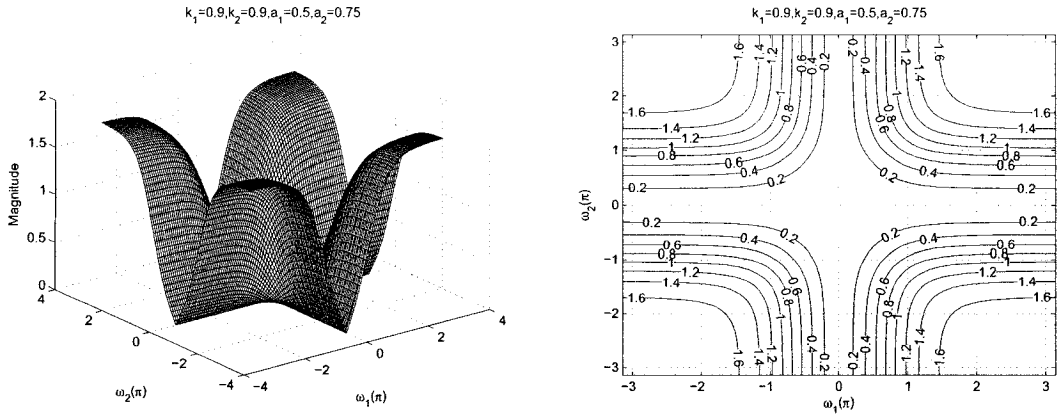

(c) $a_1 = 0.5$, $a_2 = 0.75$ and $k_1 = k_2 = 0.9$

Figure 3.18: 3-D amplitude frequency response and the contour response of the 2-D digital highpass filter for $a_1 \neq a_2$ and $k_1 = k_2$

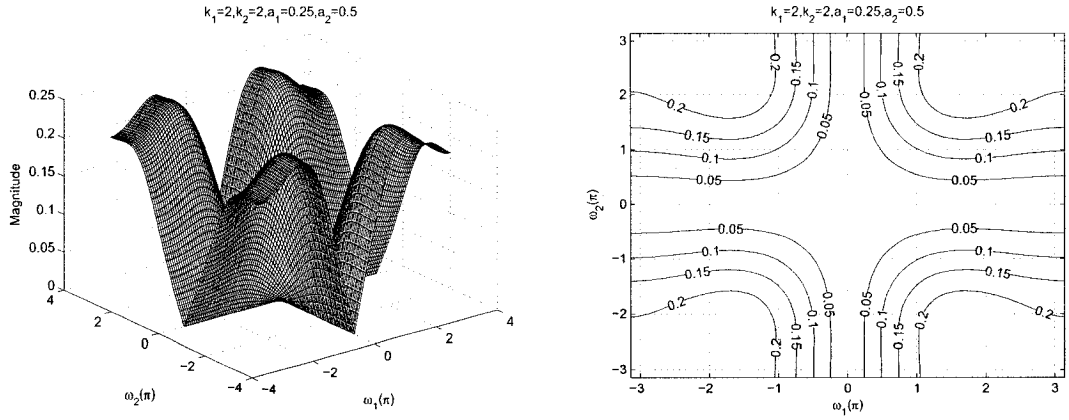

(a) $a_1 = 0.25$, $a_2 = 0.5$ and $k_1 = k_2 = 2$

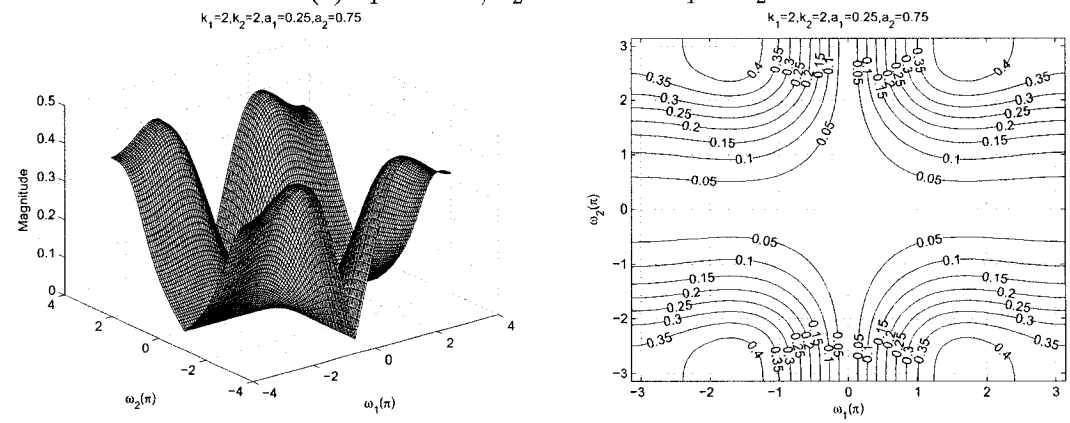

(b) $a_1 = 0.25$, $a_2 = 0.75$ and $k_1 = k_2 = 2$

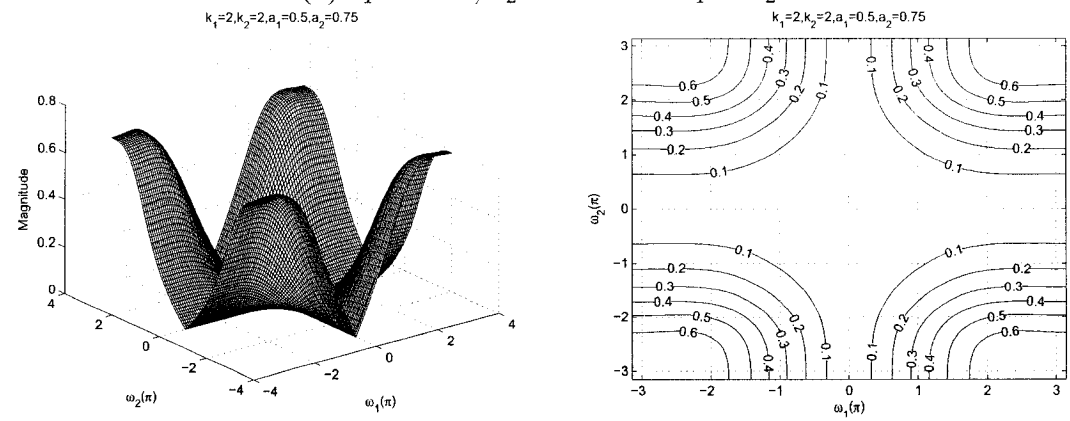

(c) $a_1 = 0.5$, $a_2 = 0.75$ and $k_1 = k_2 = 2$

Figure 3.19: 3-D amplitude frequency response and the contour response of the 2-D digital highpass filter for $a_1 \neq a_2$ and $k_1 = k_2$

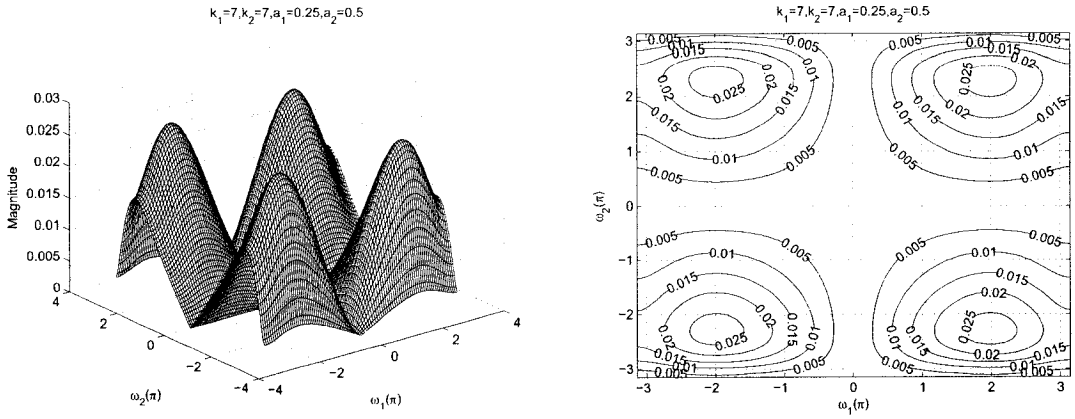

(a) $a_1 = 0.25$, $a_2 = 0.5$ and $k_1 = k_2 = 7$

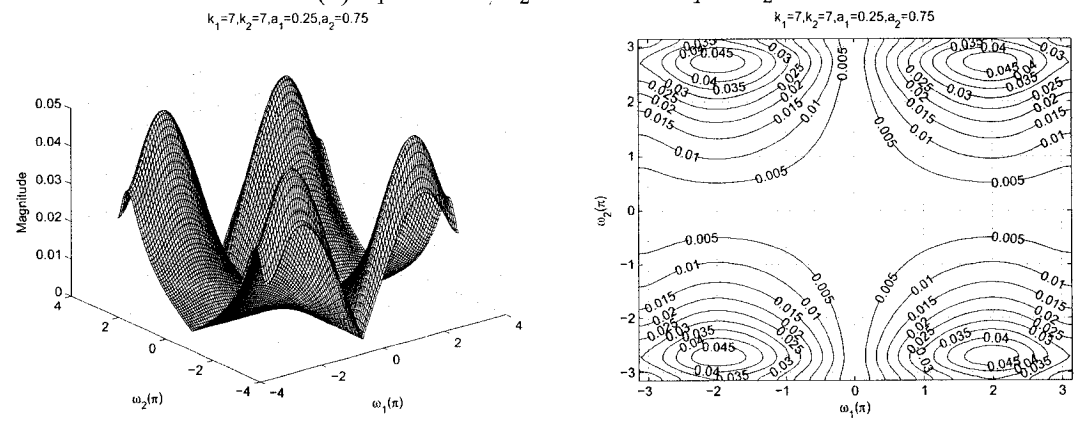

(b) $a_1 = 0.25$, $a_2 = 0.75$ and $k_1 = k_2 = 7$

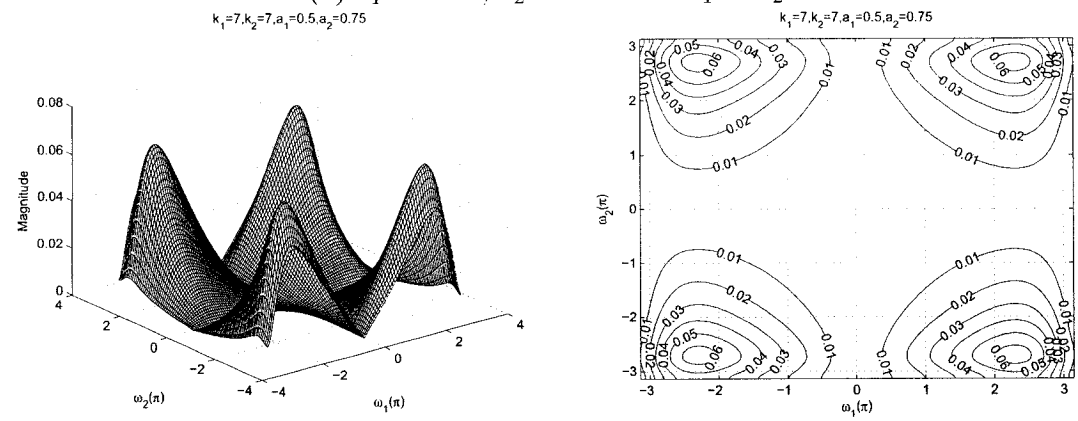

(c) $a_1 = 0.5$, $a_2 = 0.75$ and $k_1 = k_2 = 7$

Figure 3.20: 3-D amplitude frequency response and the contour response of the 2-D digital highpass filter for $a_1 \neq a_2$ and $k_1 = k_2$

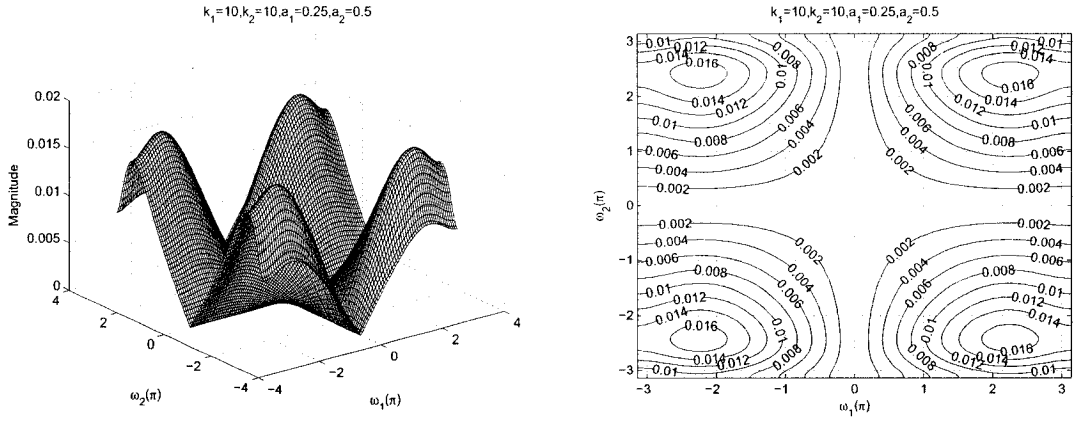

(a) $a_1 = 0.25$, $a_2 = 0.5$ and $k_1 = k_2 = 10$

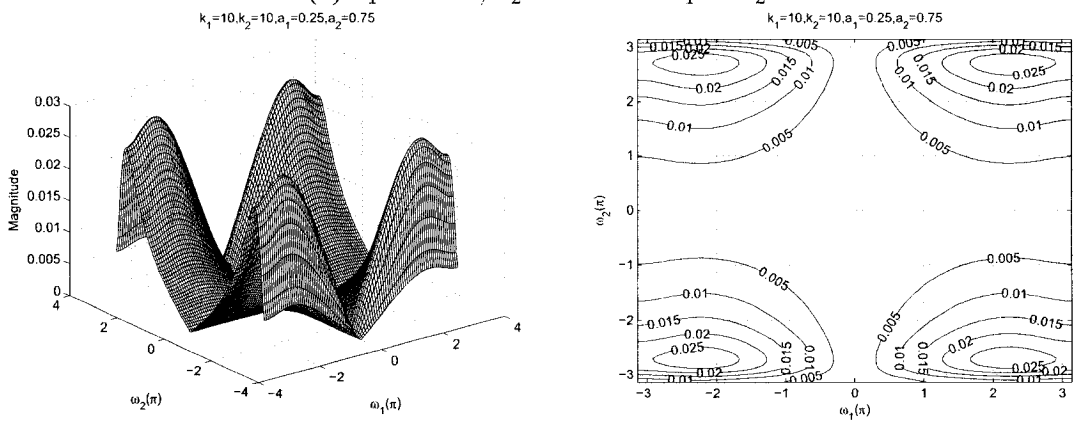

(b) $a_1 = 0.25$, $a_2 = 0.75$ and $k_1 = k_2 = 10$

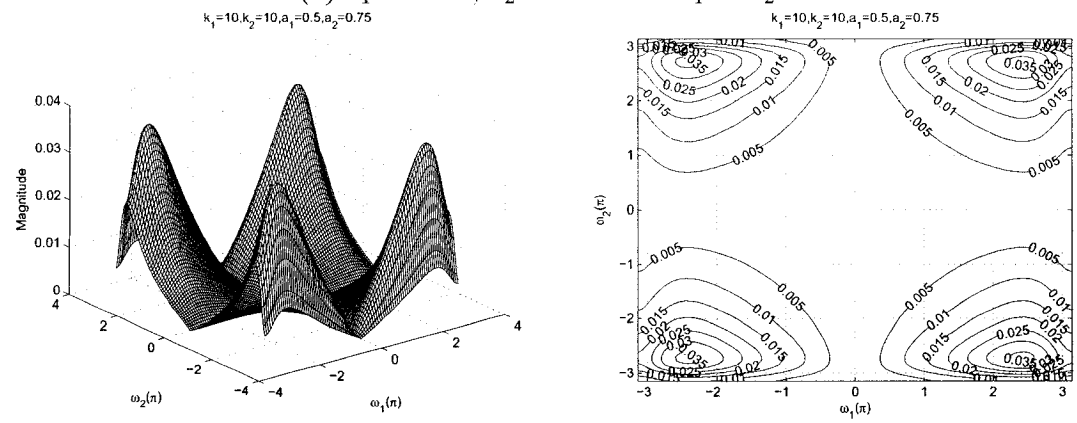

(c) $a_1 = 0.5$, $a_2 = 0.75$ and $k_1 = k_2 = 10$

Figure 3.21: 3-D amplitude frequency response and the contour response of the 2-D digital highpass filter for $a_1 \neq a_2$ and $k_1 = k_2$

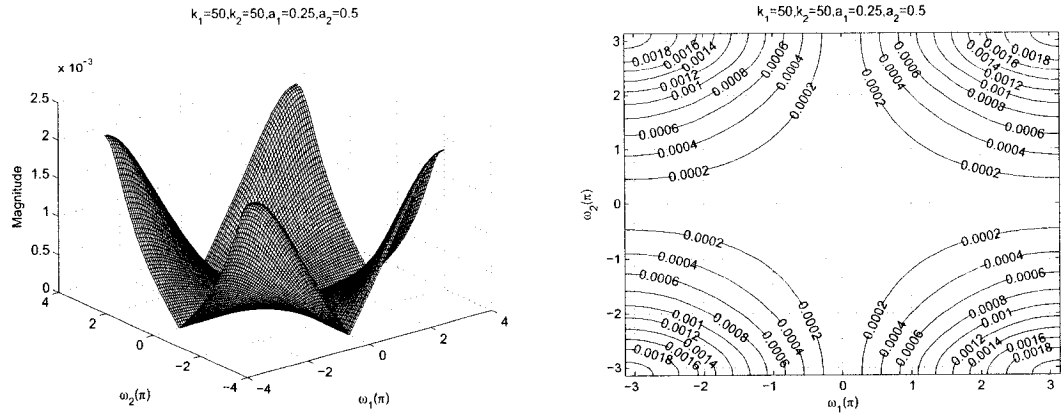

(a) $a_1 = 0.25$, $a_2 = 0.5$ and $k_1 = k_2 = 50$

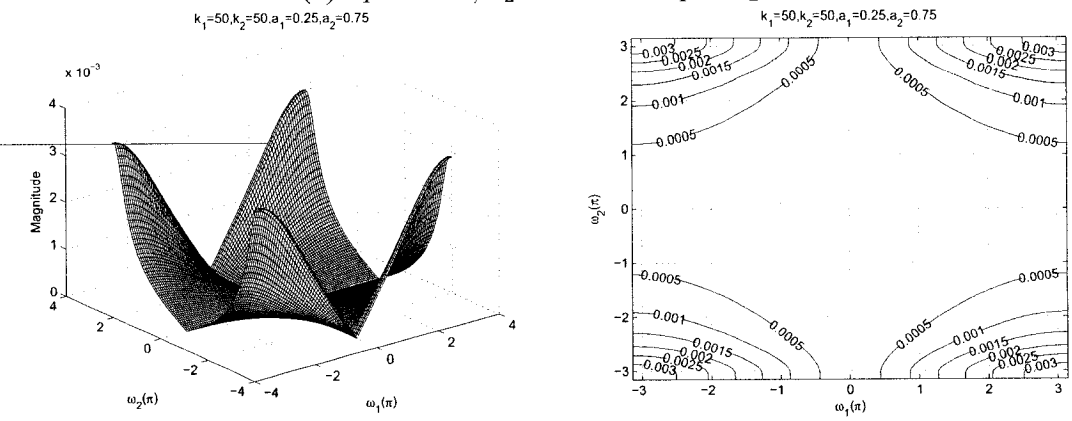

(b) $a_1 = 0.25$, $a_2 = 0.75$ and $k_1 = k_2 = 50$

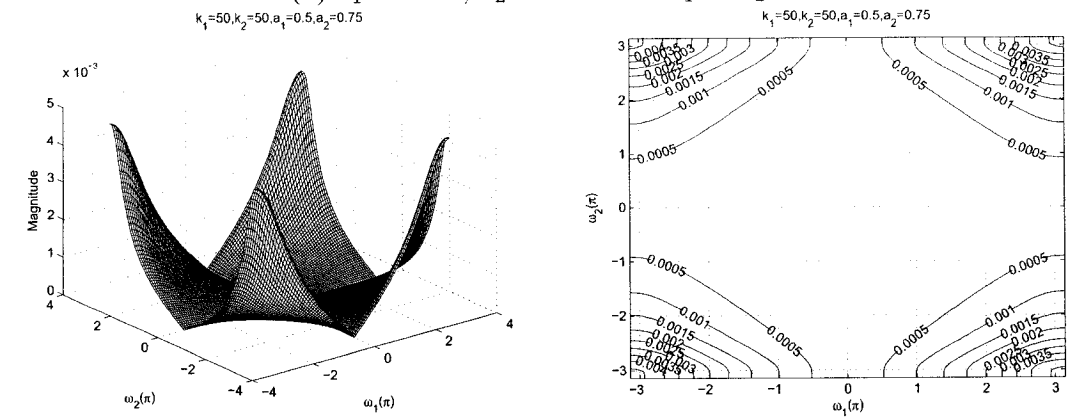

(c) $a_1 = 0.5$, $a_2 = 0.75$ and $k_1 = k_2 = 50$

Figure 3.22: 3-D amplitude frequency response and the contour response of the 2-D digital highpass filter for $a_1 \neq a_2$ and $k_1 = k_2$

As observed from the Figures 3.17 to 3.22, the coefficients a_1 and a_2 affect the gain of the amplitude-frequency response. It can be clearly observed from the Figures 3.17 (a), (b) and (c), that the amplitude of the contour response increases from 1.8 to 2.5 when the values of a_1 and a_2 are increased from 0.25 to 0.5 and 0.5 to 0.75 while keeping the same value of $k_1 = k_2 = 0.5$.

As observed for the Figure 3.19 (c), when the values of $k_1, k_2 > 1$ and $a_1, a_2 \leq 0.5$, there are ripples in the amplitude and the contour response. As we increase the values of a_1 and a_2, the ripples tend to reduce, giving the response of the 2-D digital highpass filter. When $k_1, k_2 \geq 2$, as seen from the Figures 3.19 to 3.21, we see very strong ripples. As we increase the values of a_1 and a_2, the ripples tend to increase in the range of $k_1, k_2 \geq 5$. As we further increase the value of k_1, $k_2 > 10$, and also the values of a_1 and a_2 from 0.25 to 0.5 and 0.5 to 0.75, these ripples tend to reduce, giving the response of the 2-D digital highpass filter as seen from the Figures 3.22. Thus, it can be seen that there are ripples in the stopband when $1 < k_1$, $k_2 \leq 10$ and a_1, $a_2 \leq 0.5$.

3.3.1.7 Frequency Response of 2-D Digital Highpass Filter with different values of a_1 and a_2 and different values of k_1 and k_2

In this section, we study the effect of coefficients when $a_1 \neq a_2$ and $k_1 \neq k_2$, and the remaining coefficients $b_1 = b_2 = -1$ in order to get the 2-D digital highpass filter in Category A. The values of a_1 and a_2 vary from 0.25 to 0.75 and 0.5 to 0.9, respectively and the values of k_1 and k_2 vary from 0.5 to 50 and 1 to 75, respectively.

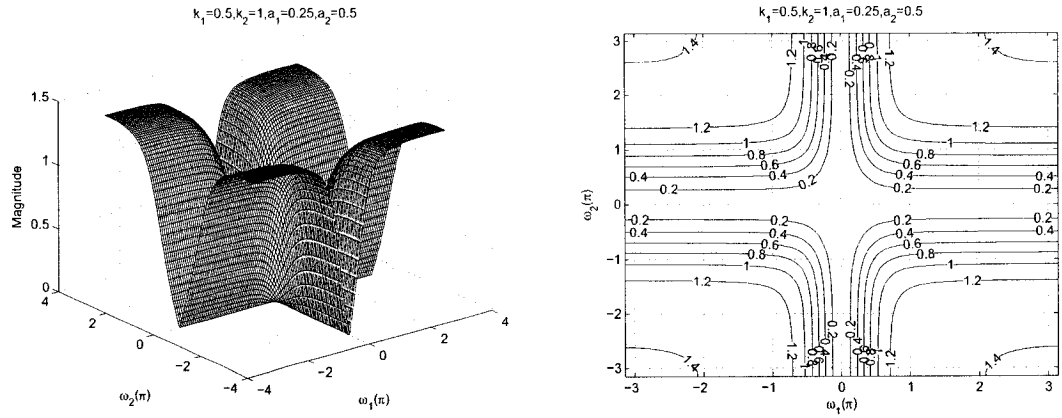

(a) $a_1 = 0.25$, $a_2 = 0.5$ and $k_1 = 0.5$, $k_2 = 1$

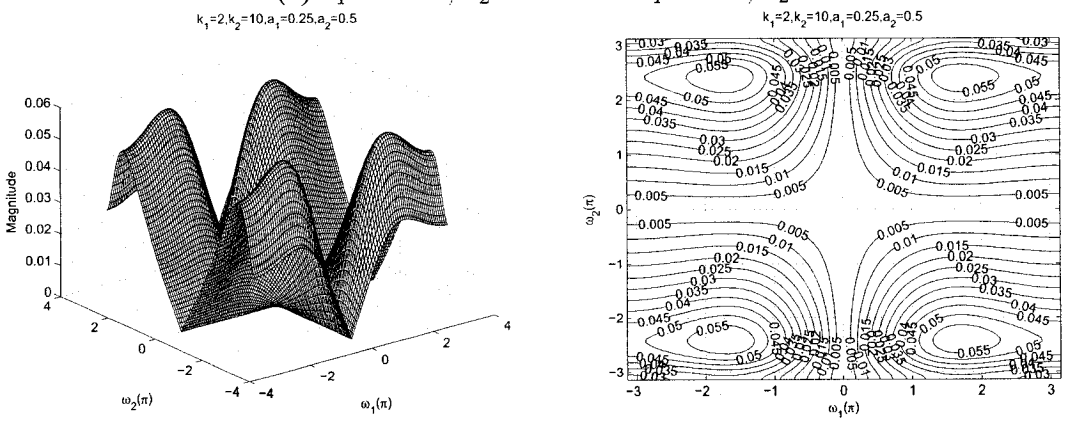

(b) $a_1 = 0.25$, $a_2 = 0.5$ and $k_1 = 2$, $k_2 = 10$

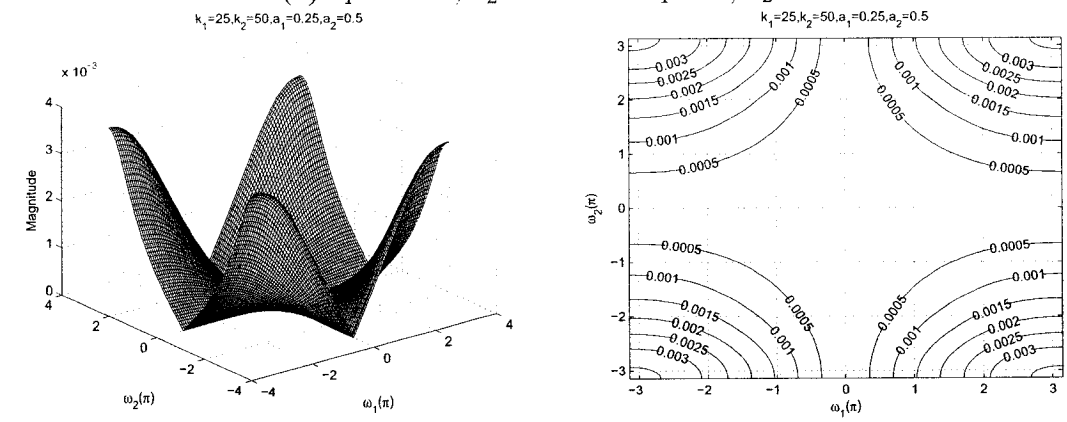

(c) $a_1 = 0.25$, $a_2 = 0.5$ and $k_1 = 25$, $k_2 = 50$

Figure 3.23: 3-D amplitude frequency response and the contour response of the 2-D digital highpass filter for $a_1 \neq a_2$ and $k_1 \neq k_2$

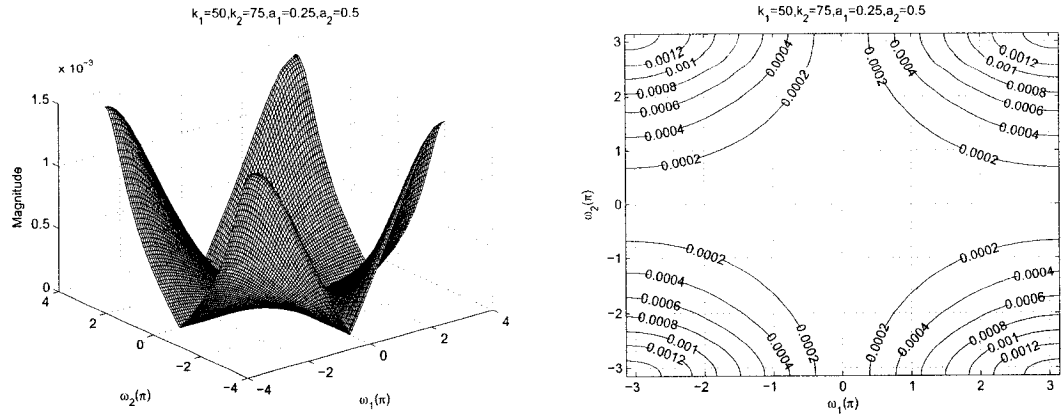

(a) $a_1 = 0.25$, $a_2 = 0.5$ and $k_1 = 50$, $k_2 = 75$

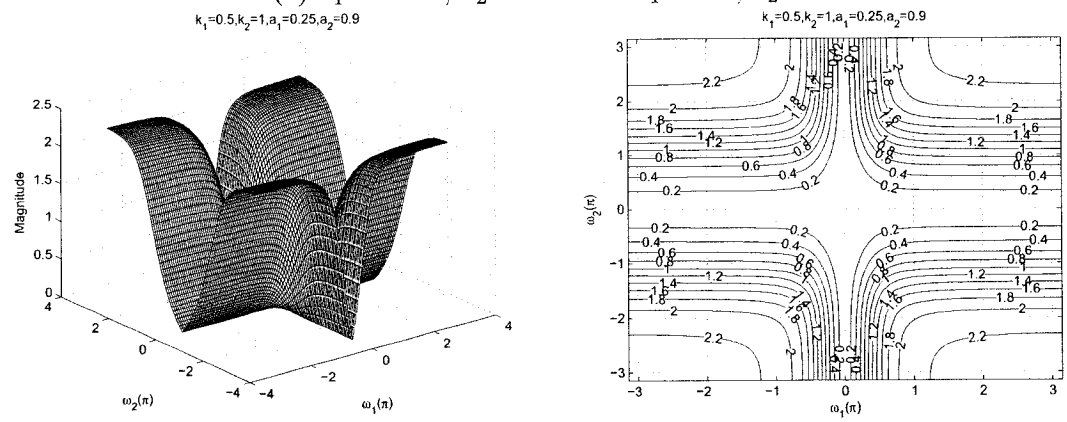

(b) $a_1 = 0.25$, $a_2 = 0.9$ and $k_1 = 0.5$, $k_2 = 1$

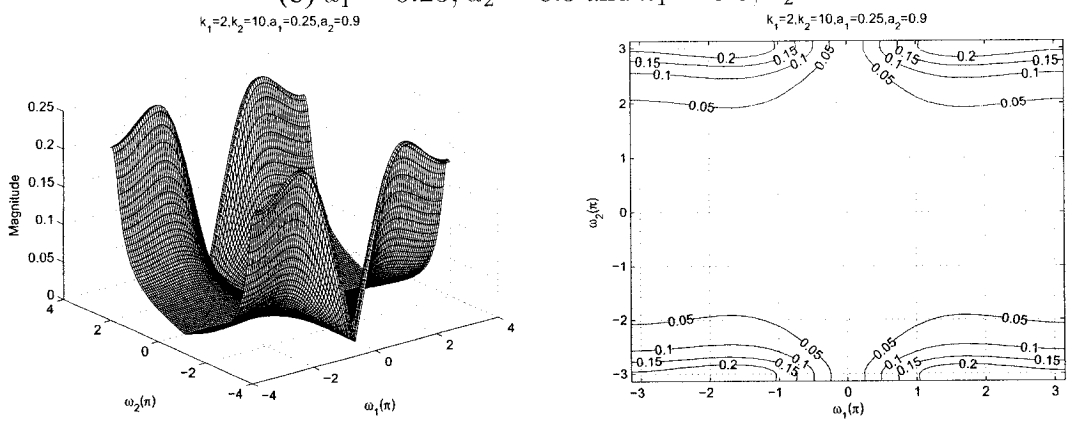

(c) $a_1 = 0.25$, $a_2 = 0.9$ and $k_1 = 2$, $k_2 = 10$

Figure 3.24: 3-D amplitude frequency response and the contour response of the 2-D digital highpass filter for $a_1 \neq a_2$ and $k_1 \neq k_2$

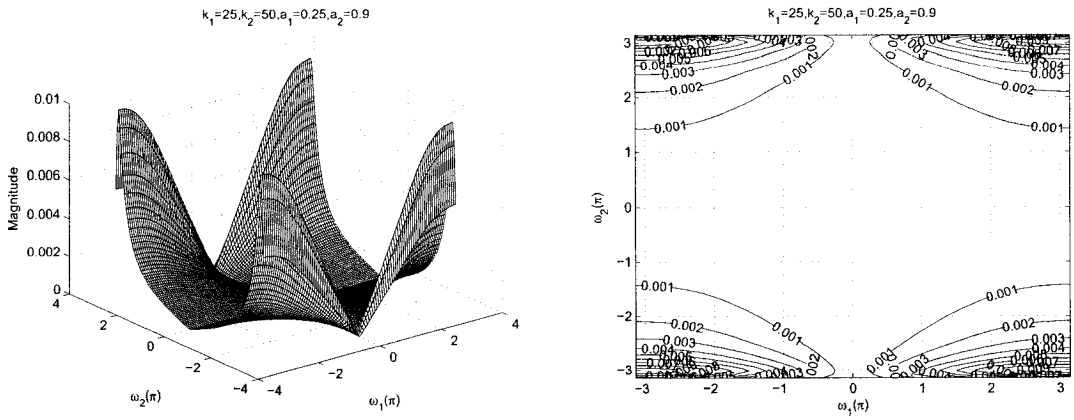

(a) $a_1 = 0.25$, $a_2 = 0.9$ and $k_1 = 25$, $k_2 = 50$

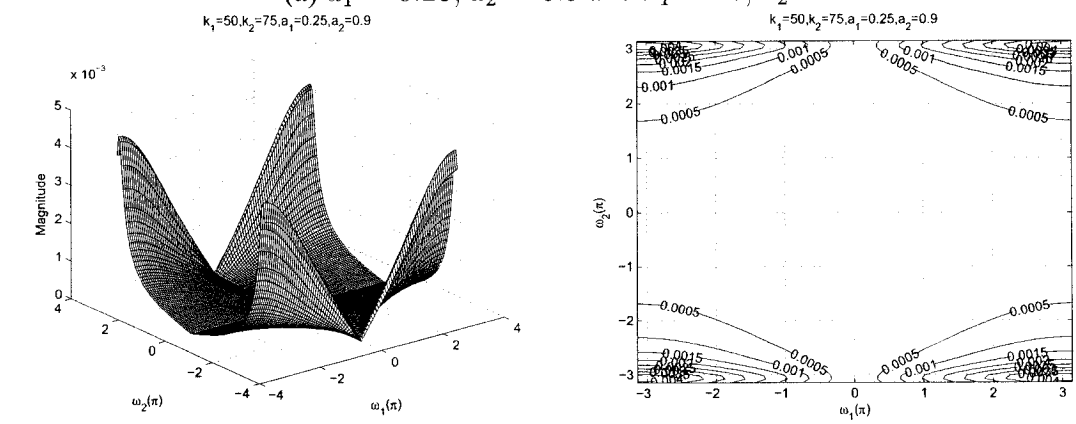

(b) $a_1 = 0.25$, $a_2 = 0.9$ and $k_1 = 50$, $k_2 = 75$

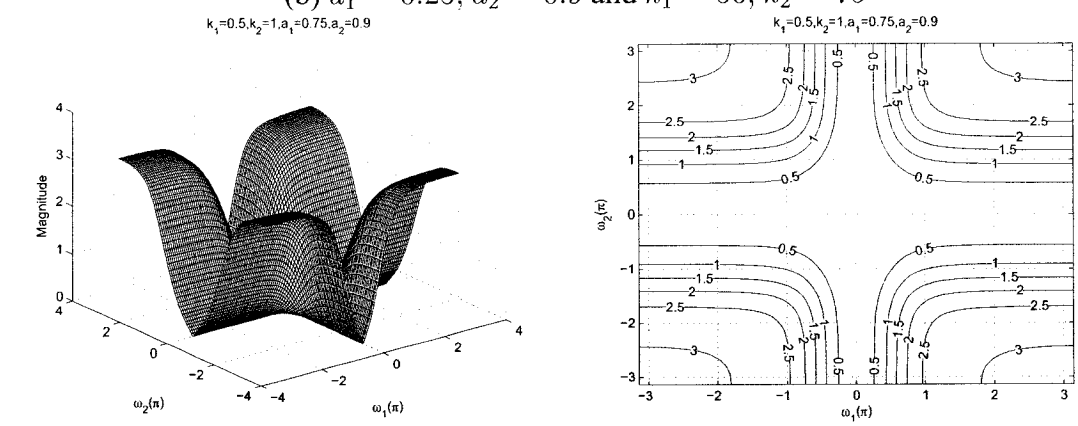

(c) $a_1 = 0.75$, $a_2 = 0.9$ and $k_1 = 0.5$, $k_2 = 1$

Figure 3.25: 3-D amplitude frequency response and the contour response of the 2-D digital highpass filter for $a_1 \neq a_2$ and $k_1 \neq k_2$

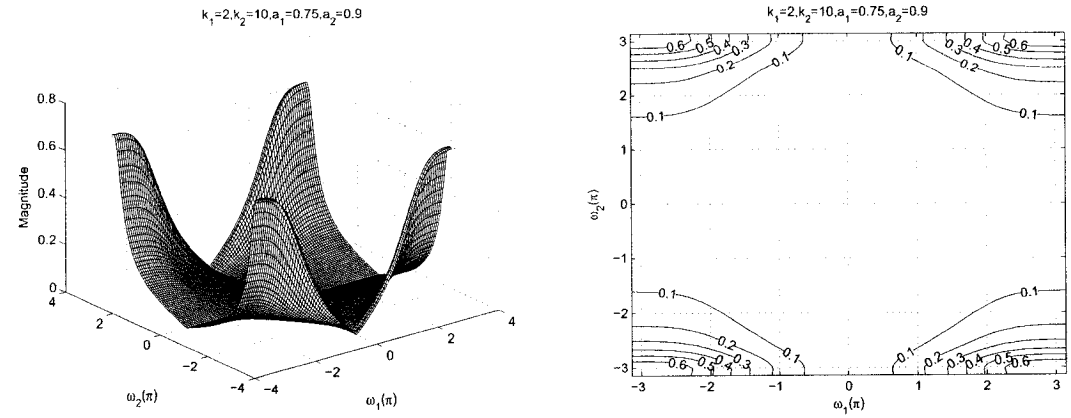

(a) $a_1 = 0.75$, $a_2 = 0.9$ and $k_1 = 2$, $k_2 = 10$

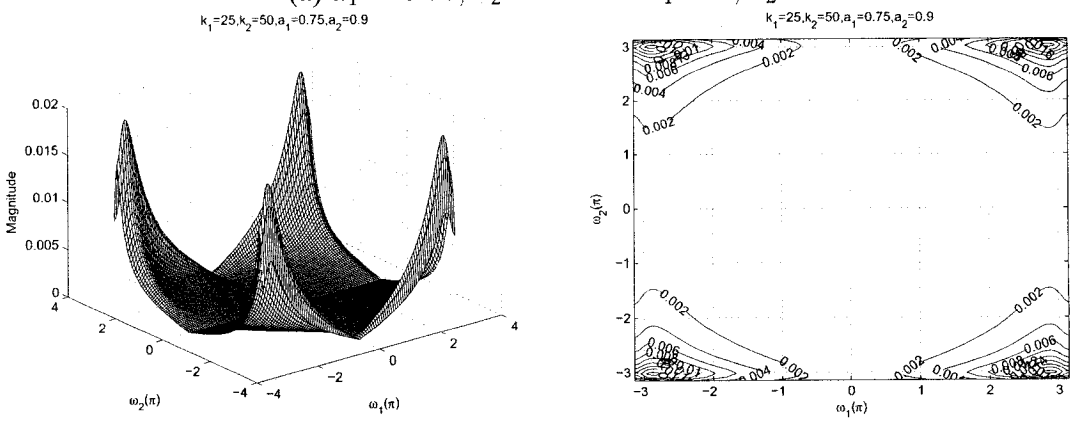

(b) $a_1 = 0.75$, $a_2 = 0.9$ and $k_1 = 25$, $k_2 = 50$

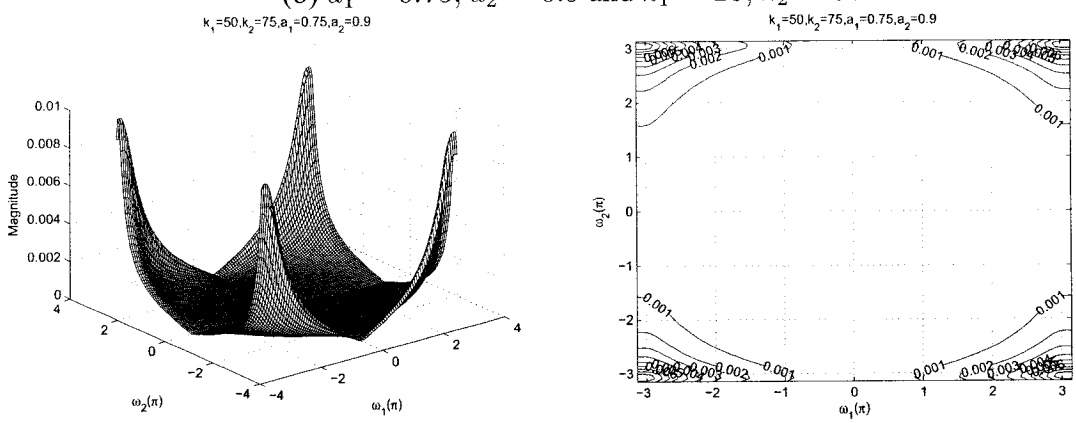

(c) $a_1 = 0.75$, $a_2 = 0.9$ and $k_1 = 50$, $k_2 = 75$

Figure 3.26: 3-D amplitude frequency response and the contour response of the 2-D digital highpass filter for $a_1 \neq a_2$ and $k_1 \neq k_2$

As observed from the Figures 3.23 to 3.26, the coefficients k_1 and k_2 affect the stopband width of the frequency response. In the Figures 3.23 (a), (b), (c) and 3.24 (a), there is a gradual increase in the stopband width as the values of k_1 and k_2 are increased from 0.5 to 50 and from 1 to 75 respectively, for the different values of a_1 and a_2 0.25 and 0.5, respectively. At the same time there is also a gradual decrease in the amplitude from 1.4 to 0.0012.

As observed from the Figures 3.23 to 3.26, the coefficients a_1 and a_2 affect the amplitude-frequency response. It can be clearly observed from the Figures 3.23 (a), 3.24 (b) and 3.25 (c), that the amplitude of the contour response increases from 1.4 to 3 when the values of a_1 and a_2 are increased from 0.25 to 0.75 and 0.5 to 0.9, respectively, keeping the same value of $k_1 = 0.5$ and $k_2 = 1$.

In the case $a_1 \neq a_2$ and $k_1 \neq k_2$, when the values of $k_1, k_2 > 1$ and $a_1, a_2 \leq 0.5$, there are ripples in the amplitude and the contour response. As we increase the values of a_1 and a_2, the ripples tend to reduce, giving the response of the highpass filter. As we further increase the value of $k_1, k_2 > 10$, and also the values of a_1 and a_2 from 0.25 to 0.5 and 0.5 to 0.75, respectively, these ripples tend to reduce, giving the response of the highpass filter as seen from the Figures 3.23 to 3.26. Thus, it can be seen that there are ripples in the stopband when $1 < k_1, k_2 \leq 10$ and $a_1, a_2 \leq 0.5$.

3.3.1.8 Frequency Response of 2-D Digital Highpass Filter with same values of a_1 and a_2 and different values of k_1 and k_2

In this section, we study the effect of coefficients, where $a_1 = a_2$ and $k_1 \neq k_2$ and the remaining coefficients $b_1 = b_2 = -1$ in order to get the 2-D digital highpass filter in Category A. The values of a_1 and a_2 vary from 0 to 1 and the values of k_1 and k_2 vary from 0.5 to 50 and 1 to 75, respectively.

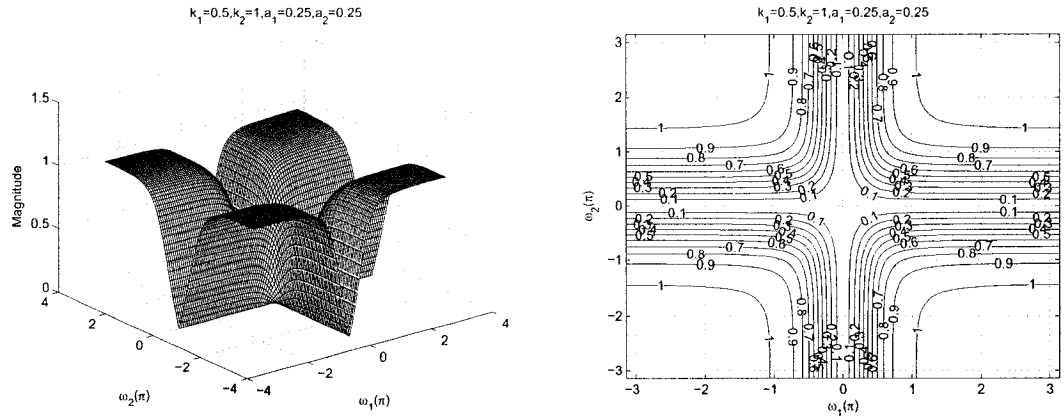

(a) $a_1 = a_2 = 0.25$ and $k_1 = 0.5$, $k_2 = 1$

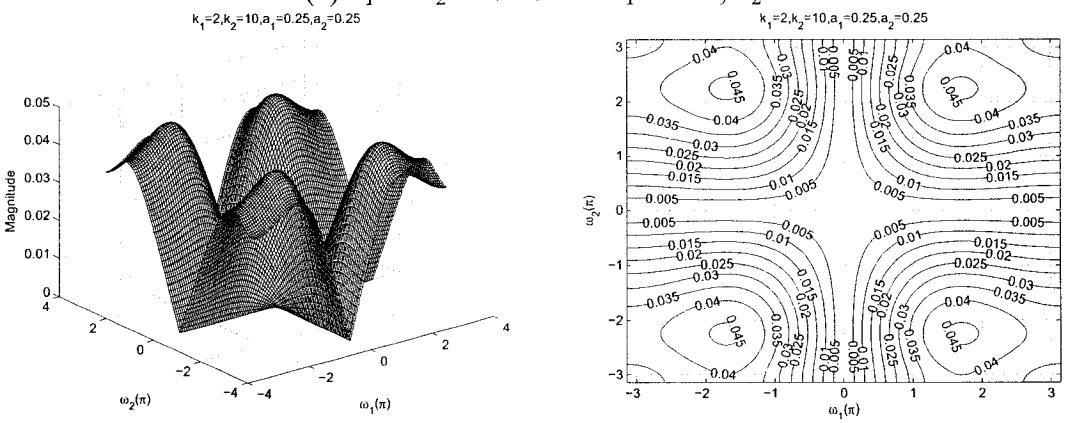

(b) $a_1 = a_2 = 0.25$ and $k_1 = 2$, $k_2 = 10$

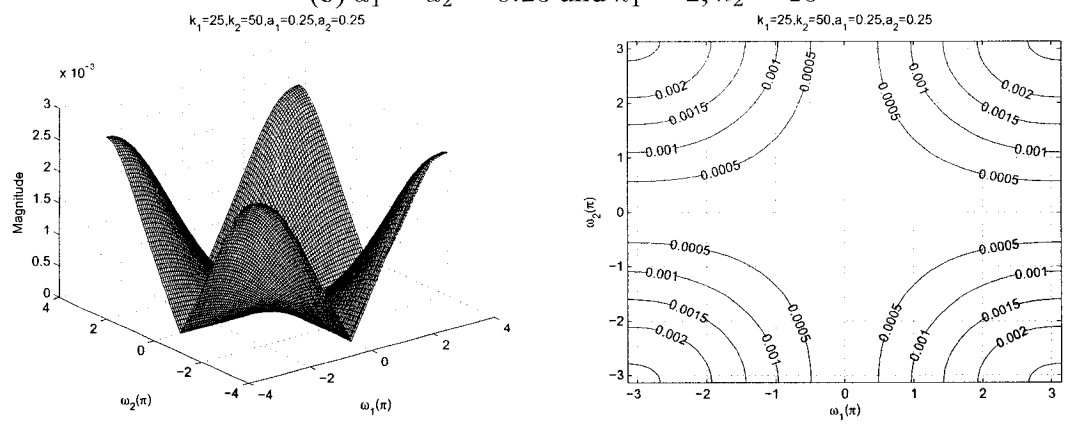

(c) $a_1 = a_2 = 0.25$ and $k_1 = 25$, $k_2 = 50$

Figure 3.27: 3-D amplitude frequency response and the contour response of the 2-D digital highpass filter for $a_1 = a_2$ and $k_1 \neq k_2$

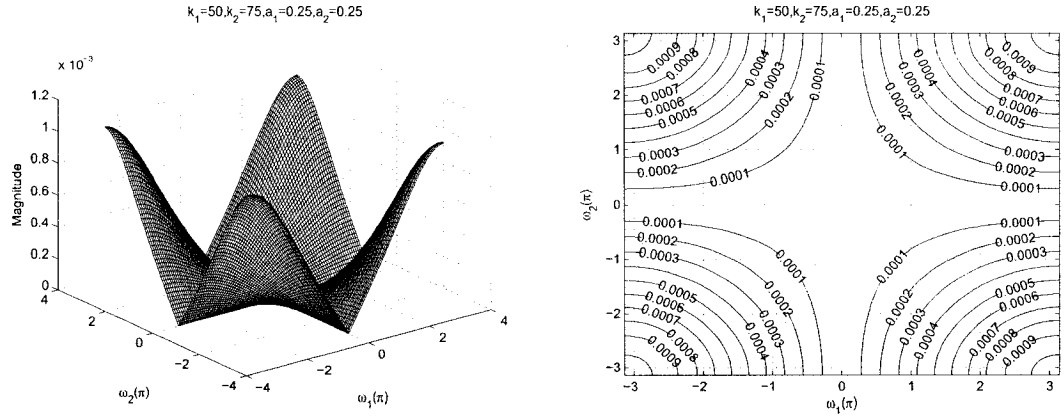

(a) $a_1 = a_2 = 0.25$ and $k_1 = 50$, $k_2 = 75$

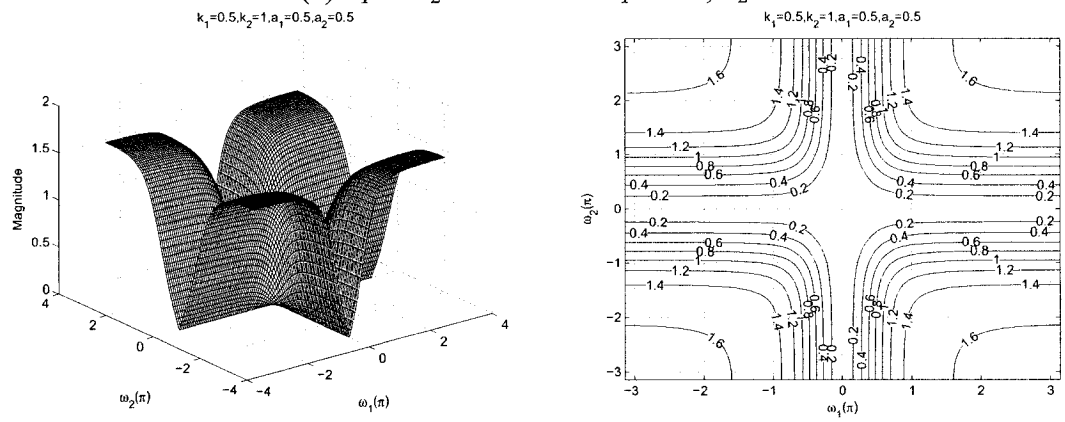

(b) $a_1 = a_2 = 0.5$ and $k_1 = 0.5$, $k_2 = 1$

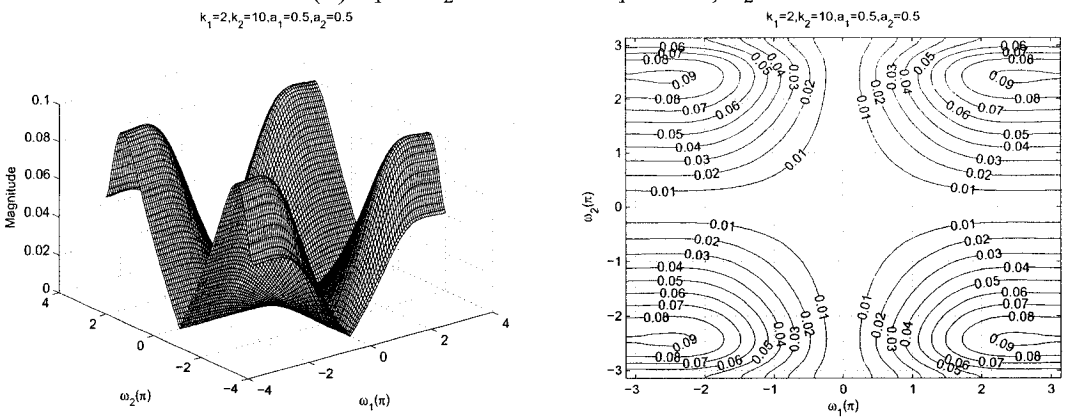

(c) $a_1 = a_2 = 0.5$ and $k_1 = 2$, $k_2 = 10$

Figure 3.28: 3-D amplitude frequency response and the contour response of the 2-D digital highpass filter for $a_1 = a_2$ and $k_1 \neq k_2$

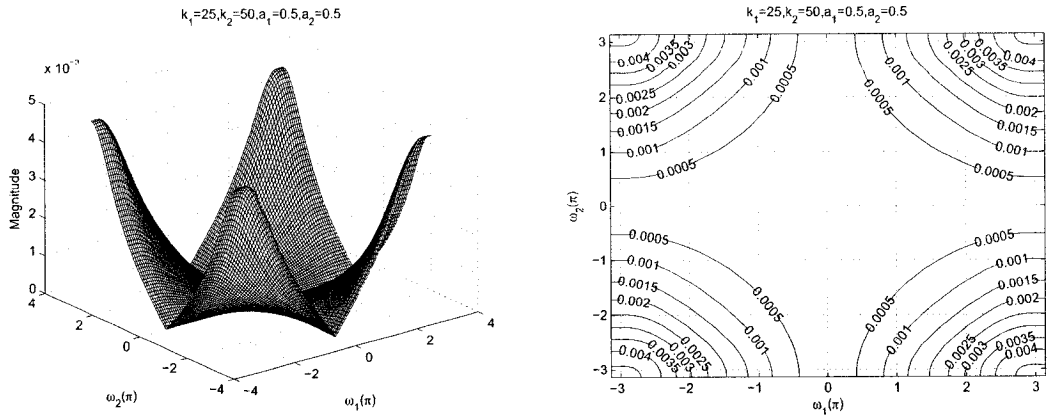

(a) $a_1 = a_2 = 0.5$ and $k_1 = 25$, $k_2 = 50$

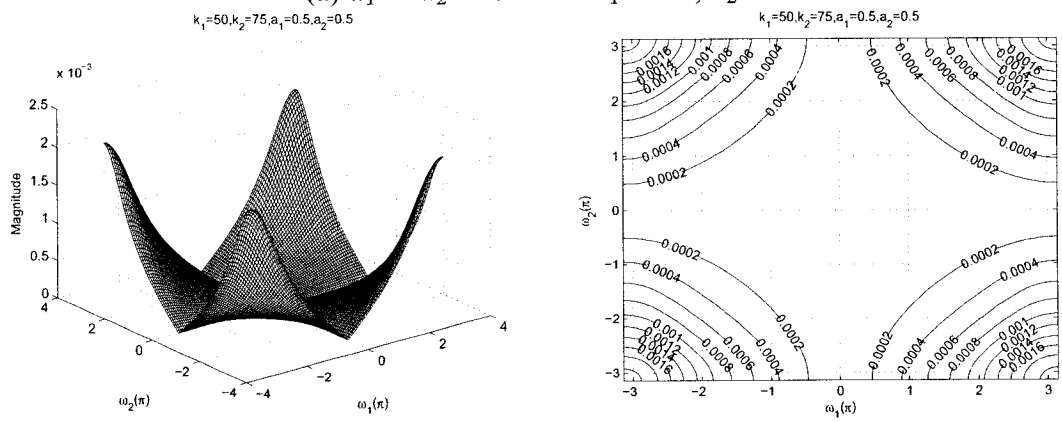

(b) $a_1 = a_2 = 0.5$ and $k_1 = 50$, $k_2 = 75$

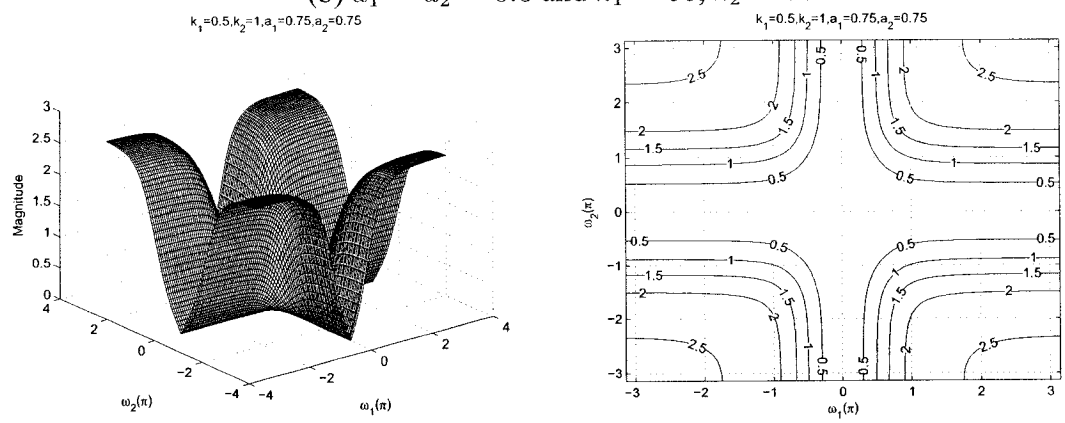

(c) $a_1 = a_2 = 0.75$ and $k_1 = 0.5$, $k_2 = 1$

Figure 3.29: 3-D amplitude frequency response and the contour response of the 2-D digital highpass filter for $a_1 = a_2$ and $k_1 \neq k_2$

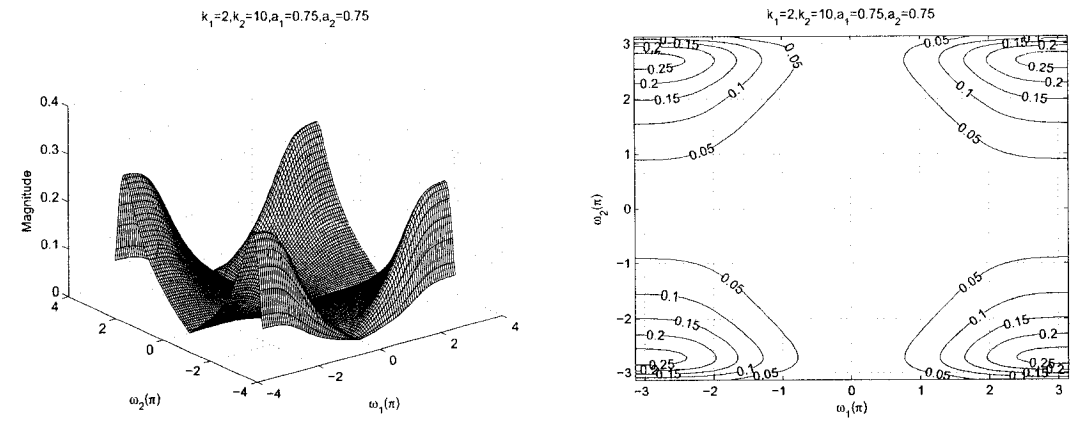

(a) $a_1 = a_2 = 0.75$ and $k_1 = 2$, $k_2 = 10$

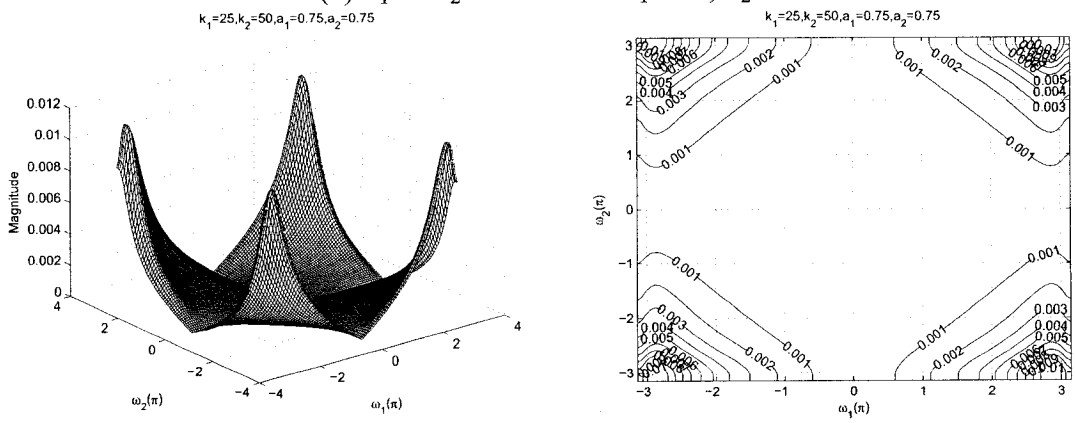

(b) $a_1 = a_2 = 0.75$ and $k_1 = 25$, $k_2 = 50$

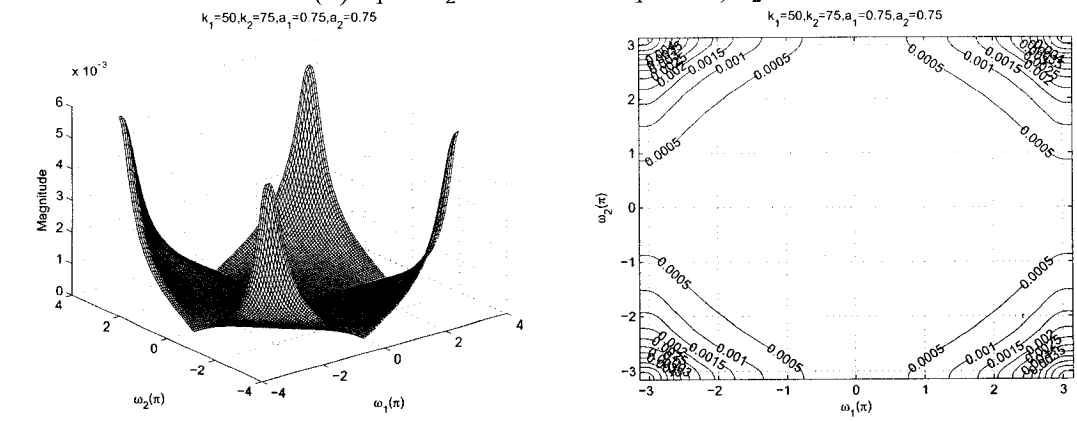

(c) $a_1 = a_2 = 0.75$ and $k_1 = 50$, $k_2 = 75$

Figure 3.30: 3-D amplitude frequency response and the contour response of the 2-D digital highpass filter for $a_1 = a_2$ and $k_1 \neq k_2$

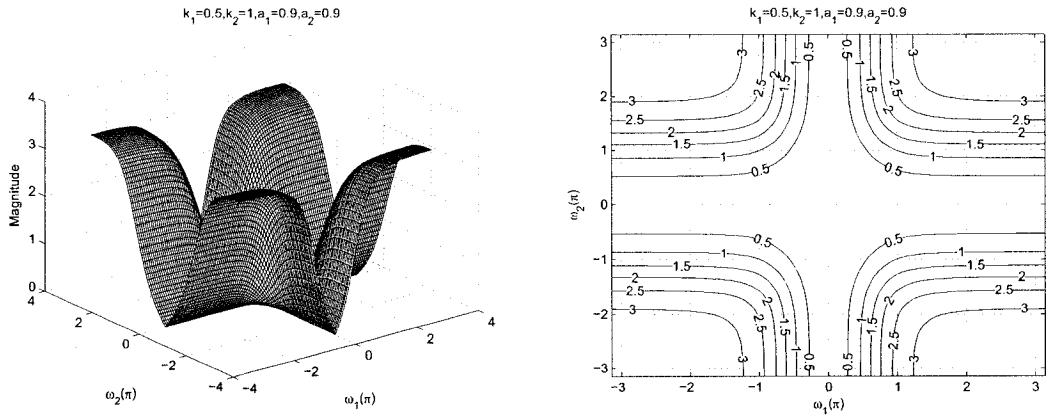

(a) $a_1 = a_2 = 0.9$ and $k_1 = 0.5$, $k_2 = 1$

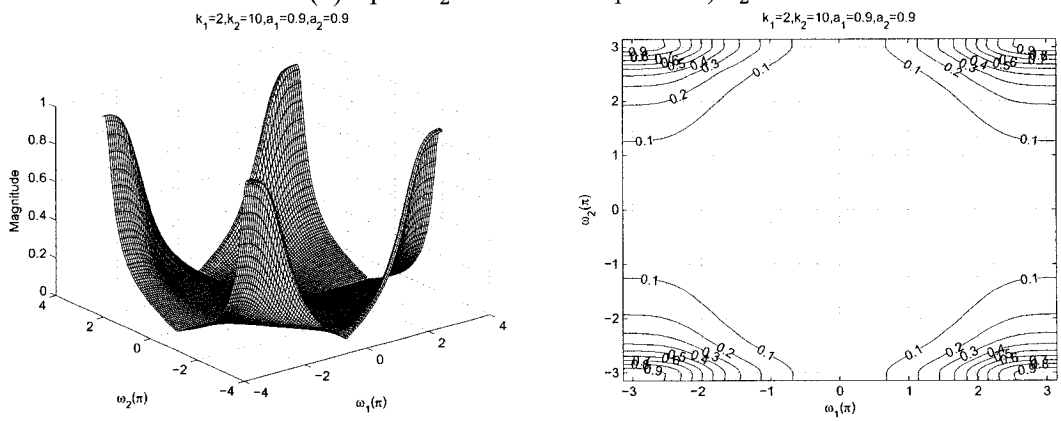

(b) $a_1 = a_2 = 0.9$ and $k_1 = 2$, $k_2 = 10$

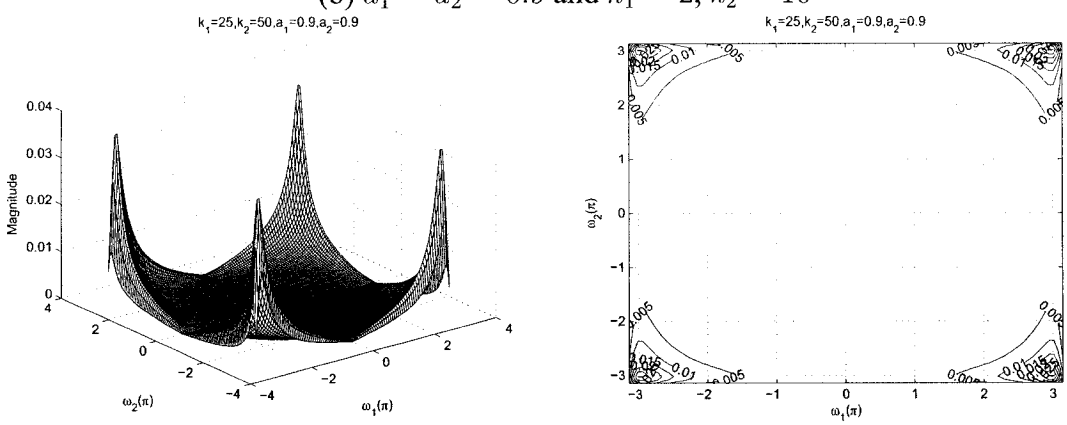

(c) $a_1 = a_2 = 0.9$ and $k_1 = 25$, $k_2 = 50$

Figure 3.31: 3-D amplitude frequency response and the contour response of the 2-D digital highpass filter for $a_1 = a_2$ and $k_1 \neq k_2$

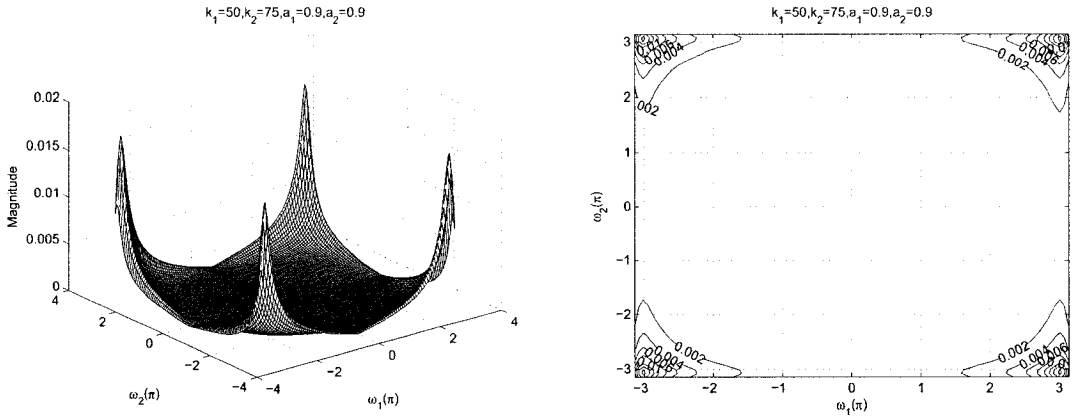

$a_1 = a_2 = 0.9$ and $k_1 = 25$, $k_2 = 75$

Figure 3.32: 3-D amplitude frequency response and the contour response of the 2-D digital highpass filter for $a_1 = a_2$ and $k_1 \neq k_2$

As observed from the Figures 3.27 to 3.32, the coefficients k_1 and k_2 affect the stopband width of the frequency response. In the Figures 3.27 (a), (b) ,(c) and 3.28 (a), there is an increase in the stopband width as the values of k_1 and k_2 are increased from 0.5 to 75 for the same values of $a_1 = a_2 = 0.25$. At the same time there is also a gradual decrease in the amplitude from 1 to 0.0009.

As observed from the Figures 3.27 to 3.32, the coefficients a_1 and a_2 affect the gain of the amplitude-frequency response. It can be clearly observed from the Figures 3.27 (a), 3.28 (b), 3.29 (c) and 3.31 (a), that the amplitude of the contour response increases from 1 to 3 when the values of a_1 and a_2 are increased from 0.25 to 0.9 keeping the same value of $k_1 = 0.5$ and $k_2 = 1$.

In this case $a_1 = a_2$ and $k_1 \neq k_2$, and when the values of $k_1, k_2 > 1$ and $a_1, a_2 \leq 0.5$, there are ripples in the amplitude and the contour response. As we increase the values of a_1 and a_2, the ripples tend to increase. Also the magnitude tends to increase from 0.045 to 0.9 for same values of $k_1 = 2$ and $k_2 = 10$ as we increase the values of a_1 and a_2 from 0.25 to 0.9 as seen from the Figures 3.27 (b), 3.28 (c), 3.30 (a) and 3.31 (b). As we further increase the value of k_1, $k_2 > 10$, and also the values of a_1 and a_2 from 0.25 to 0.9, these ripples tend to reduce, giving the response of the highpass filter as seen from the Figures 3.27 to

3.32. Thus, it can be seen that there are ripples in the stopband when $1 < k_1,\ k_2 \leq 10$ and $a_1,\ a_2 \leq 0.5$.

3.3.2 Frequency Response of the All-pole 2-D Digital Highpass Filter in Category B

The transfer function for the all-pole 2-D highpass filter is obtained by using the transfer function of the all-pole 2-D lowpass filter in the analog domain in Category B. This transfer function for the all-pole 2-D low pass filter is obtained by using the second order Butterworth polynomial and its equivalent real part which is connected in the all pass filters manner in Category B. The resultant transfer function (eqn. (3.6)) obtained is digitized by applying generalized bilinear transformation (eqn. (3.1)). The digitized transfer function of the all-pole 2-D digital highpass filter is given by eqn. (3.7). With the input coefficients of the generalized bilinear transformation we can obtain the contour and 3-D magnitude plots of the resulting all-pole 2-D digital highpass filter [46].

To investigate the manner in which each coefficient of the generalized bilinear transformation effects the magnitude response of the resulting all-pole 2-D digital highpass filter, we vary the values of the coefficients or fix some of the coefficients to specific values. It is possible to obtain the all-pole 2-D digital highpass filter when the coefficients have the following limits: $k_i > 0,\ 0 \leq |a_i| \leq 1$ and taking $b_i = -1$,where $i = 1,\ 2$. Let us consider the coefficients of the generalized bilinear transformation for the 2-D digital highpass filter to be unity, i.e., $a_1 = 1,\ a_2 = 1,\ k_1 = 1,\ k_2 = 1$ and $b_1 = -1,\ b_2 = -1$. Under this condition, the 3-D amplitude-frequency response and the contour plots of the 2-D digital filter are shown in the Figure 3.33. In the following sections, we will see the effect of these coefficients on the frequency-responses of the all-pole 2-D digital highpass filter.

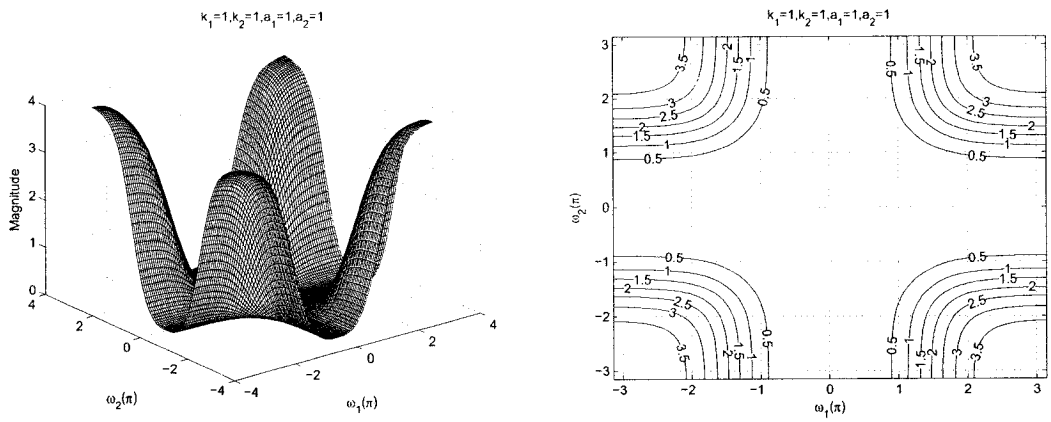

Figure 3.33: 3-D Amplitude-Frequency Response and contour response of the All-pole 2-D Digital Highpass Filter with all the coefficients values as unity

3.3.2.1 Frequency Response of the All-pole 2-D Digital Highpass Filter with different values of k_1

In this section, we study the manner in which k_1 effects the frequency response behavior of the resulting all-pole 2-D digital highpass filter in Category B and to separate the effect of the other coefficients, we vary the values of k_1, and fixing all the other coefficient of the generalized bilinear transformation to be unity in order not to loose any generality and to make the situation simple, e.g. with $k_2 = 1$, $a_1 = 1$, $a_2 = 1$, $b_1 = -1$ and $b_2 = -1$. The values of k_1 are varied from 0.1 to 10 and the 3-D magnitude response and the contour plots for the all-pole 2-D digital highpass filter with the values of $k_1 = 0.1$, $k_1 = 0.5$, $k_1 = 0.9$, $k_1 = 2$, $k_1 = 5$ and $k_1 = 10$ are shown in the Figures 3.34 and 3.35.

It is observed that although the coefficient k_1 does not have any effect on stopband width along the $\omega_2 - axis$, it affects the width of the stopband along the $\omega_1 - axis$. Initially when the value of the coefficient $k_1 = 0.1$ (see Figure 3.34 (a)) the stopband width is minimum along the $\omega_1 - axis$. As we increase the value of k_1, the stop bandwidth gradually increases. It is also observed that for very high values of k_1 and k_2, the stopband width of the frequency response becomes maximum along the $\omega_1 - axis$. Thus, as we increase the

value of k_1 from 0.1 to 10, the stopband width of the all-pole 2-D highpass filter increases and the amplitude remains constant.

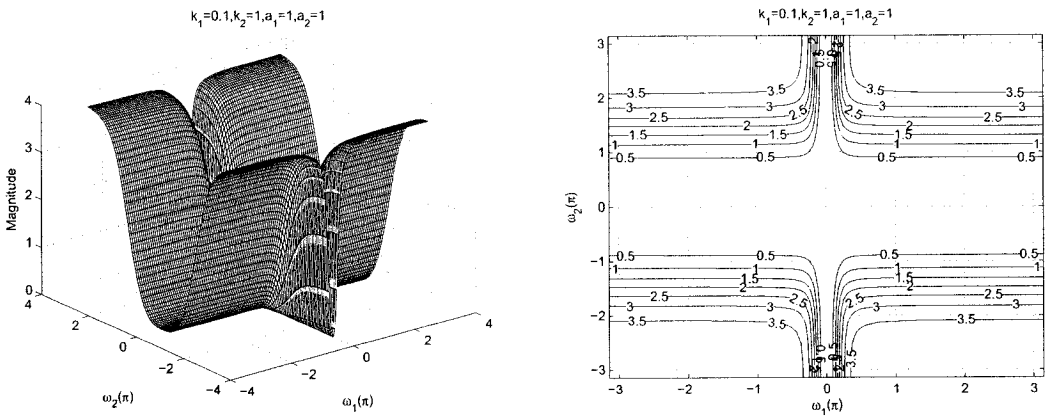

(a) $k_1 = 0.1$

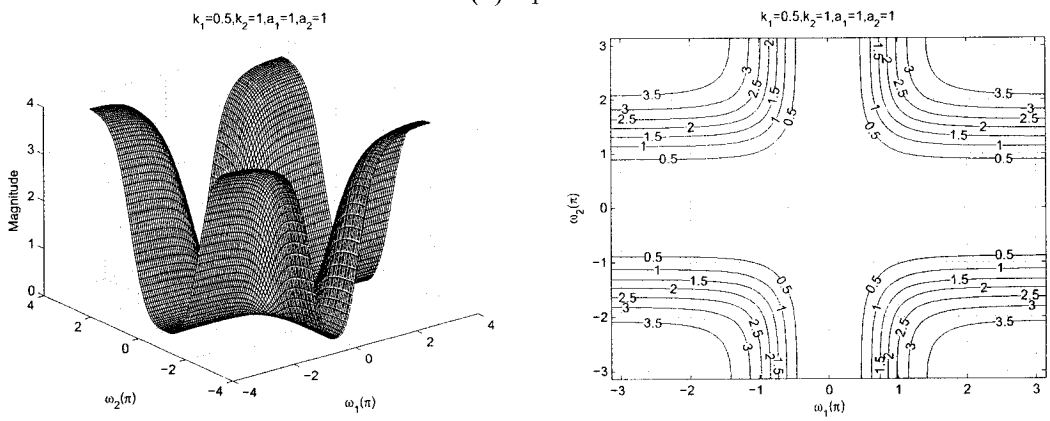

(b) $k_1 = 0.5$

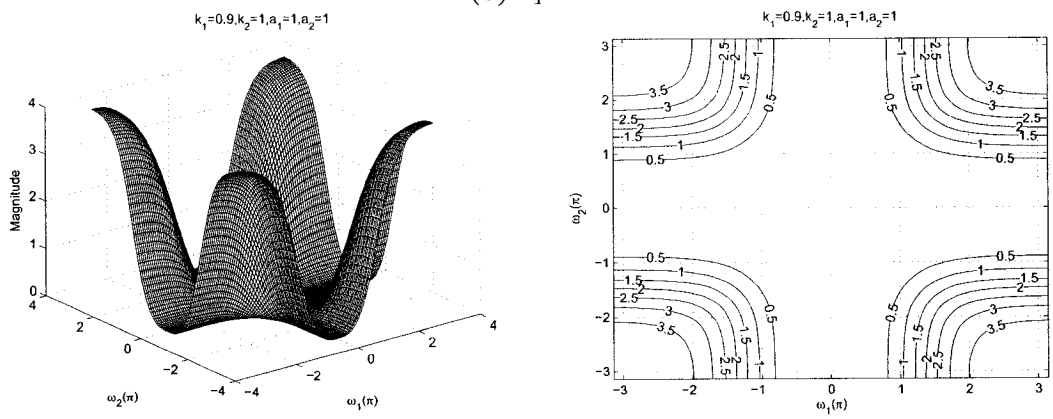

(c) $k_1 = 0.9$

Figure 3.34: 3-D amplitude frequency response and the contour response of the All-pole 2-D digital highpass filter for different values of k_1

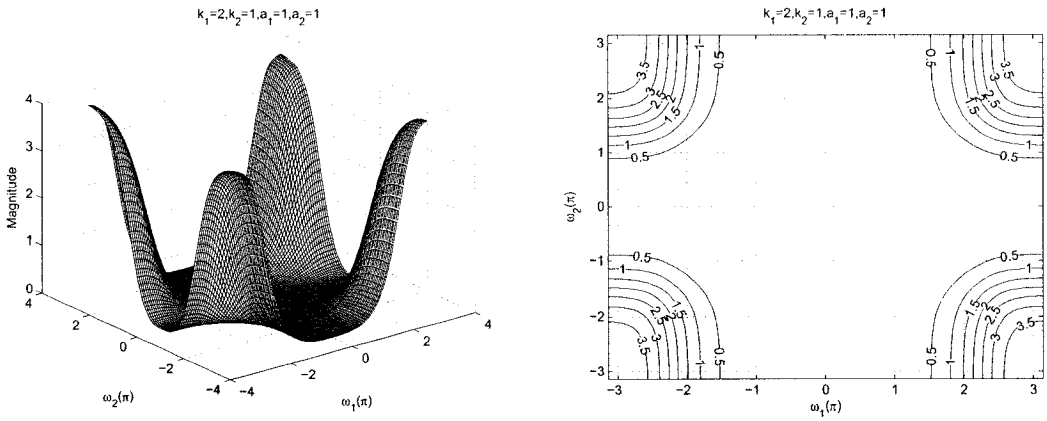

(a) $k_1 = 2$

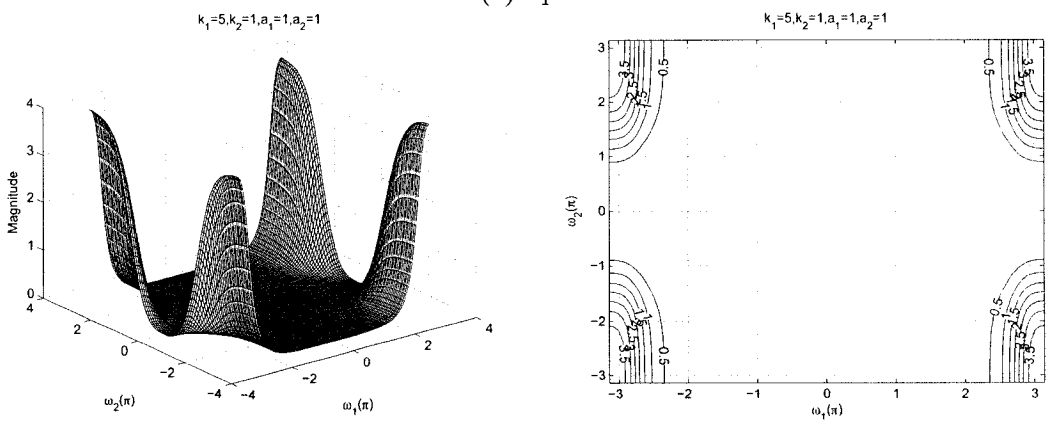

(b) $k_1 = 5$

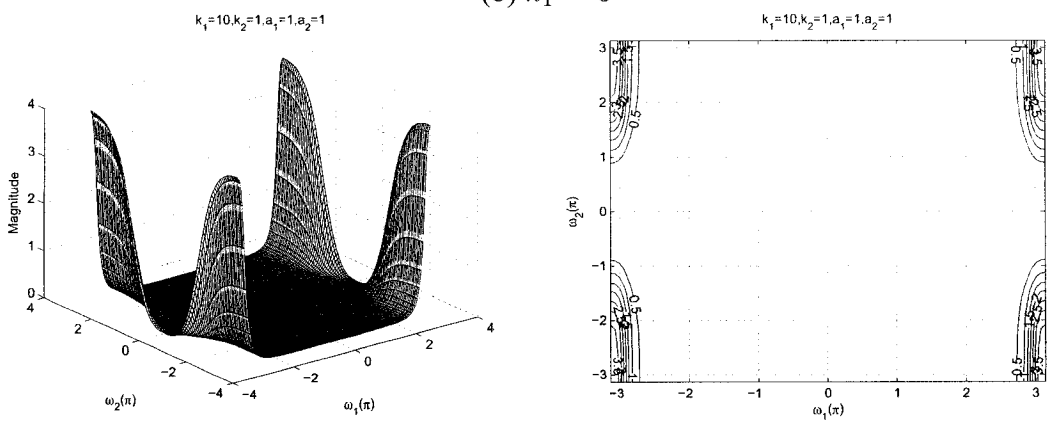

(c) $k_1 = 10$

Figure 3.35: 3-D amplitude frequency response and the contour response of the All-pole 2-D digital highpass filter for different values of k_1

3.3.2.2 Frequency Response of the All-pole 2-D Digital Highpass Filter with different values of k_2

In this section, we study the manner in which k_2 effects the frequency response behavior of the resulting all-pole 2-D digital highpass filter in Category B and to separate the effect of the other coefficients, we vary the values of k_2, and fix all the other coefficients of the generalized bilinear transformation to unity in order not to loose any generality and to make the situation simple, e.g. with $k_1 = 1, a_1 = 1, a_2 = 1, b_1 = -1$ and $b_2 = -1$. The values of k_2 are varied from 0.1 to 10 and the 3-D magnitude response and the contour plots for the all-pole 2-D digital highpass filter with the values of $k_2 = 0.1$, $k_2 = 0.5$ $k_2 = 0.9$, $k_2 = 2$, $k_2 = 5$ and $k_2 = 10$ are shown in the Figures 3.36 and 3.37.

It is observed that although the coefficient k_2 does not have any effect on the stopband width along the $\omega_1 - axis$, it affects the width of the stopband along the $\omega_2 - axis$. Initially when the value of the coefficient $k_2 = 0.1$ (see Figure 3.36 (a)) the width of the stopband is minimum along the $\omega_2 - axis$. As we increase the value of k_2, the stopband width gradually increases. It is also observed that for very high values of k_1 and k_2, the stopband width of the frequency response becomes maximum along the $\omega_2 - axis$. Thus as we increase the value of k_2 from 0.1 to 10, the stopband width of the all-pole 2-D digital highpass filter increases and the amplitude remains constant.

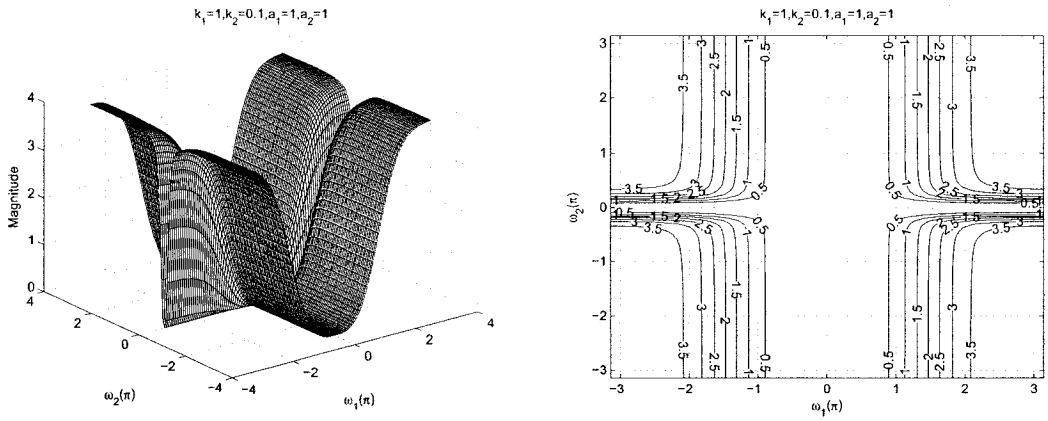

(a) $k_2 = 0.1$

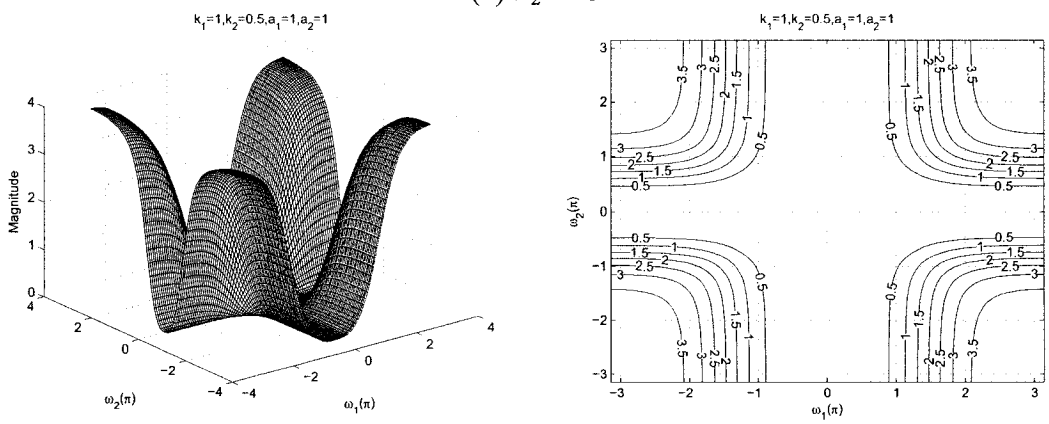

(b) $k_2 = 0.5$

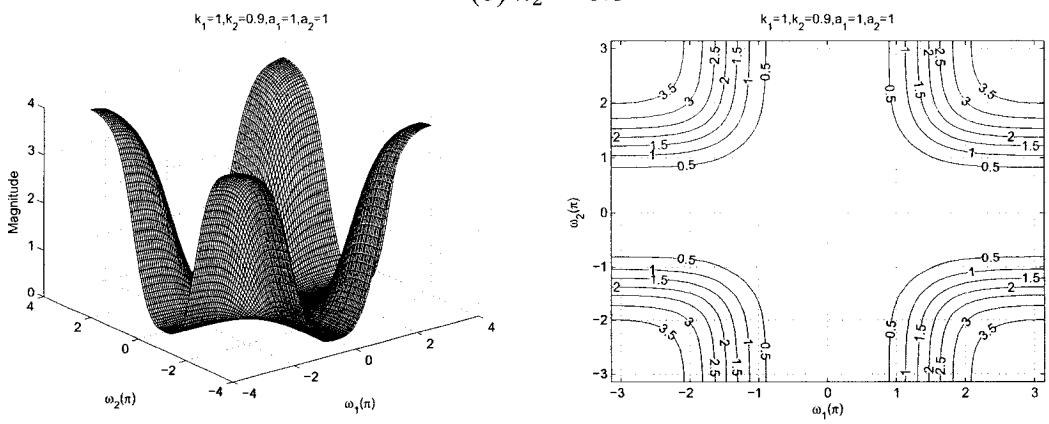

(c) $k_2 = 0.9$

Figure 3.36: 3-D amplitude frequency response and the contour response of the All-pole 2-D digital highpass filter for different values of k_2

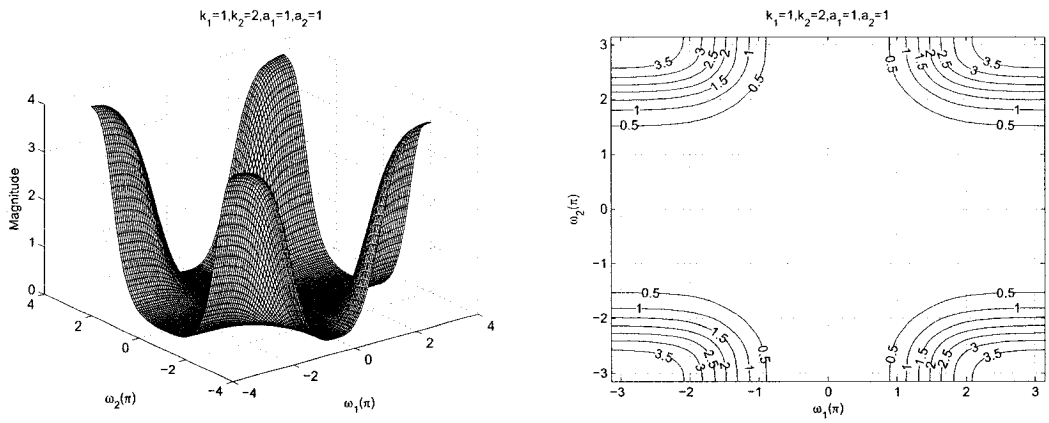

(a) $k_2 = 2$

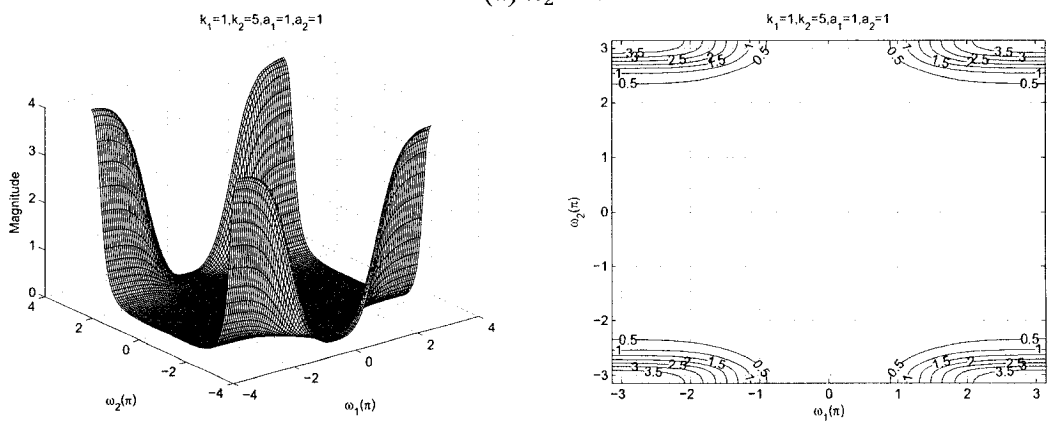

(b) $k_2 = 5$

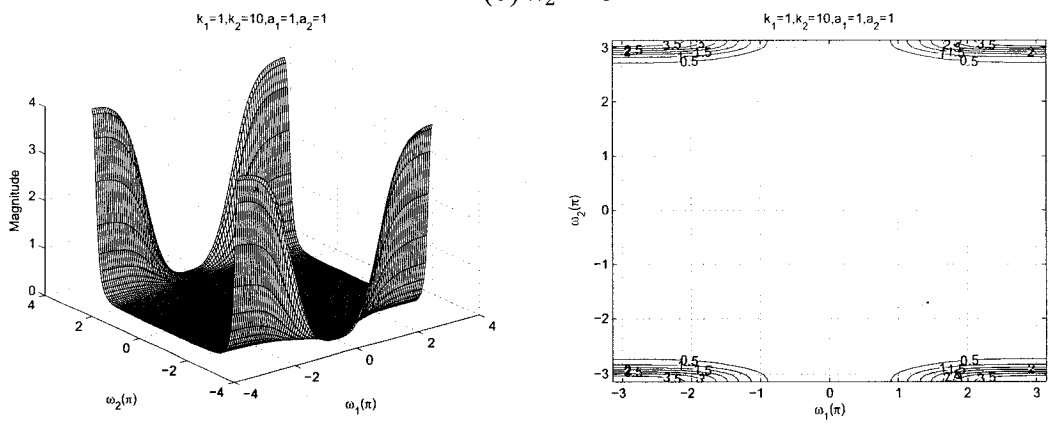

(c) $k_2 = 10$

Figure 3.37: 3-D amplitude frequency response and the contour response of the 2-D digital highpass filter for different values of k_2

3.3.2.3 Frequency Response of the All-pole 2-D Digital Highpass Filter with different values of a_1

In the Sections 3.3.2.1 and 3.3.2.2, the effect of the coefficient of k_1 and k_2 are studied. In this section, the effect of the coefficient a_1 will be studied. The stable range of a_1 can be obtained with other specified coefficients of the generalized bilinear transformation. There are many combinations possible for the coefficients. To study the response with different values of a_1 properly, we fix other coefficient values to be equal to unity. The range of a_1 varies from 0.1 to 1 and the other coefficient values are specified as unity, i.e., $k_1 = 1$, $k_2 = 1$, $a_2 = 1$, and $b_1 = -1$ and $b_2 = -1$ in order to get the all-pole 2-D digital highpass filter response in Category B.

By varying the value of a_1, the 3-D magnitude response and contour plots which represents different values of a_1, i.e. $a_1 = 0.1$, $a_1 = 0.25$, $a_1 = 0.5$, $a_1 = 0.75$, and $a_1 = 0.9$ are shown in the Figures 3.38 and 3.39. By making the value of $a_1 = 1$, it resembles the standard highpass filter as shown in the Figure 3.33. It is observed for the diagrams that the coefficient effects the gain of the amplitude-frequency response. As we increase the value of a_1 from 0.1 to 1 the gain of the amplitude-frequency increases from 1.6 to 3.5. As the value of a_1 increases, the gain increases and reach the maximum value at $a_1 = 1$. In addition, the width of stopband increases for the same. Also it is evident from the diagrams that the coefficient a_1 does not have any effect along the $\omega_2 - axis$.

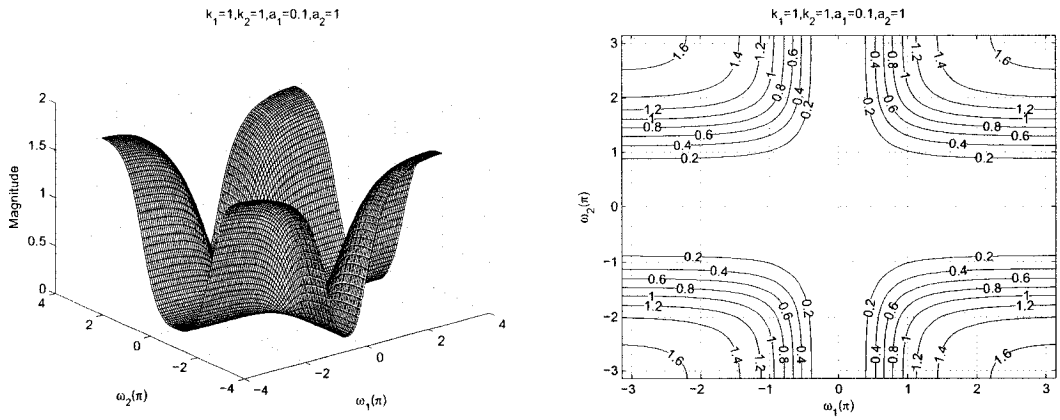

(a) $a_1 = 0.1$

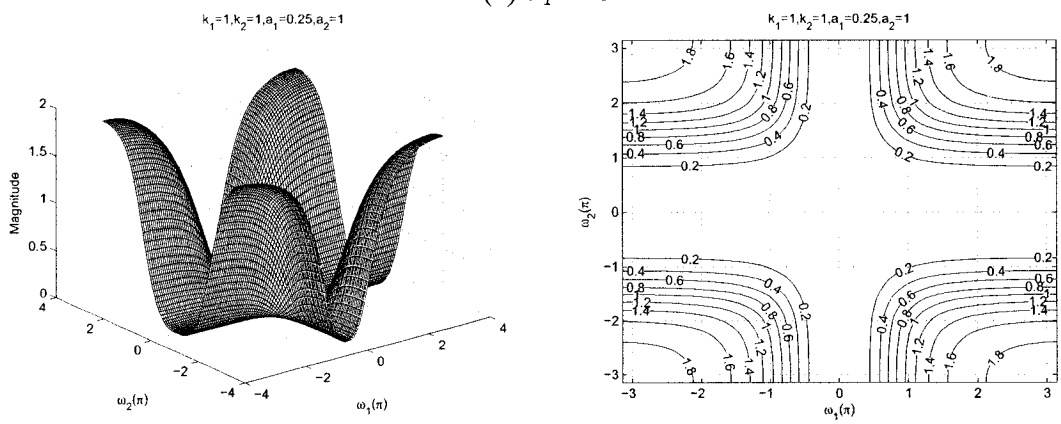

(b) $a_1 = 0.25$

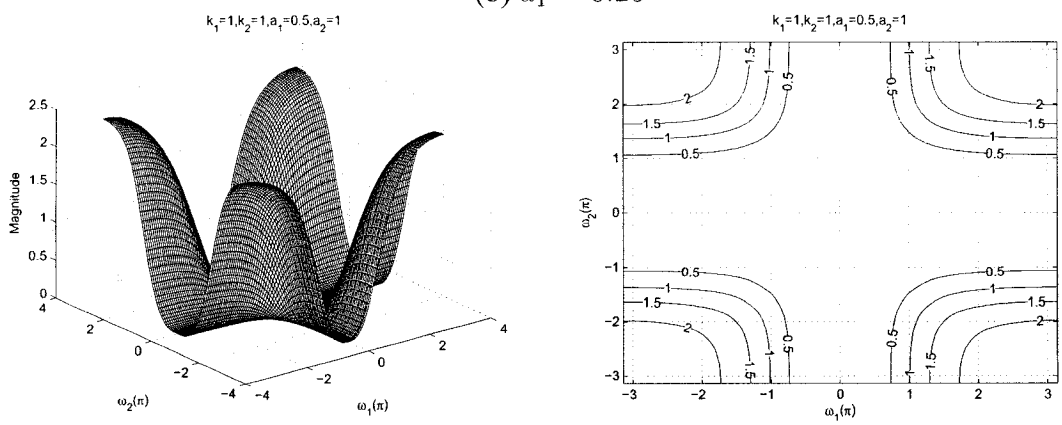

(c) $a_1 = 0.5$

Figure 3.38: 3-D amplitude frequency response and the contour response of the All-pole 2-D digital highpass filter for different values of a_1

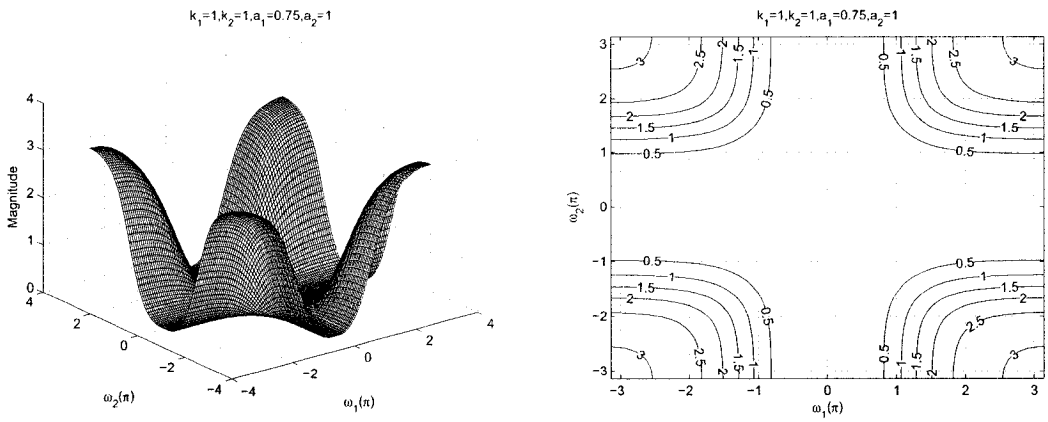

(a) $a_1 = 0.75$

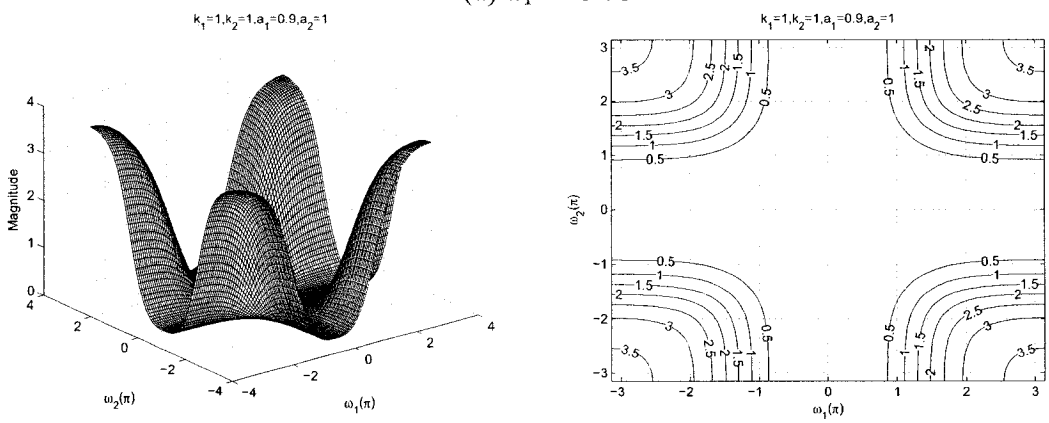

(b) $a_1 = 0.9$

Figure 3.39: 3-D amplitude frequency response and the contour response of the All-pole 2-D digital highpass filter for different values of a_1

3.3.2.4 Frequency Response of the All-pole 2-D Digital Highpass Filter with different values of a_2

In the Section 3.3.2.3, the effect of the coefficient of a_1 was studied. In this section, the effect of the coefficient a_2 is studied. The stable range of a_2 can be obtained with other specified coefficients of the generalized bilinear transformation. There are many combinations possible for the coefficients. To study the response with different values of a_2 properly, we fix other coefficient values to be equal to unity. The range of a_2 varies from 0.1 to 1 and the other coefficient values are specified as unity, i.e., $k_1 = 1$, $k_2 = 1$, $a_1 = 1$,

$b_1 = -1$ and $b_2 = -1$ in order to get the all-pole 2-D digital highpass filter response in Category B.

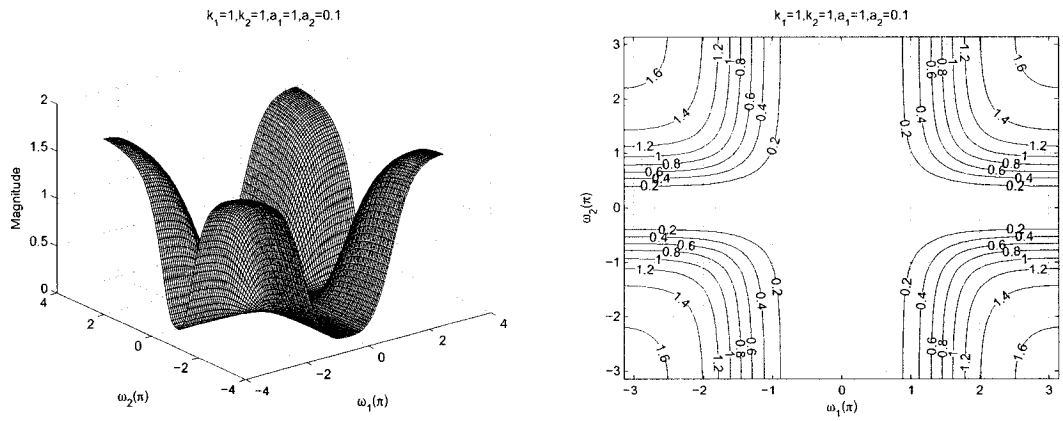

(a) $a_2 = 0.1$

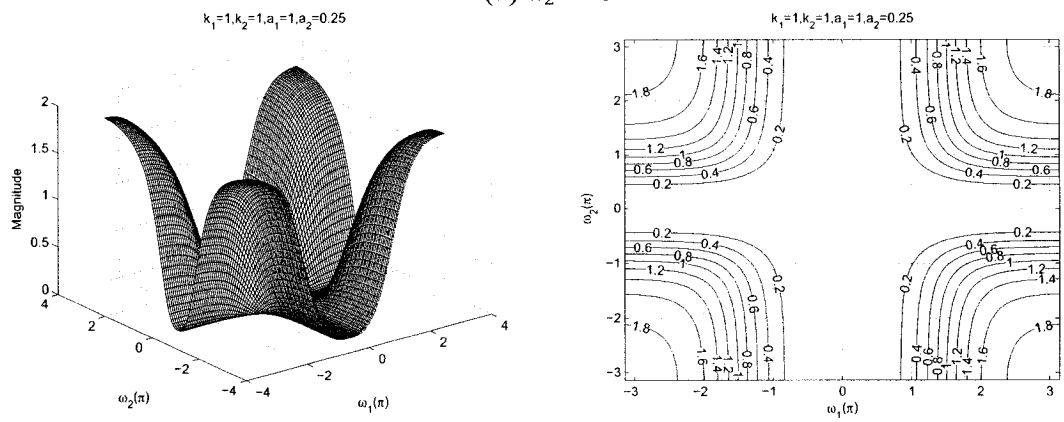

(b) $a_2 = 0.25$

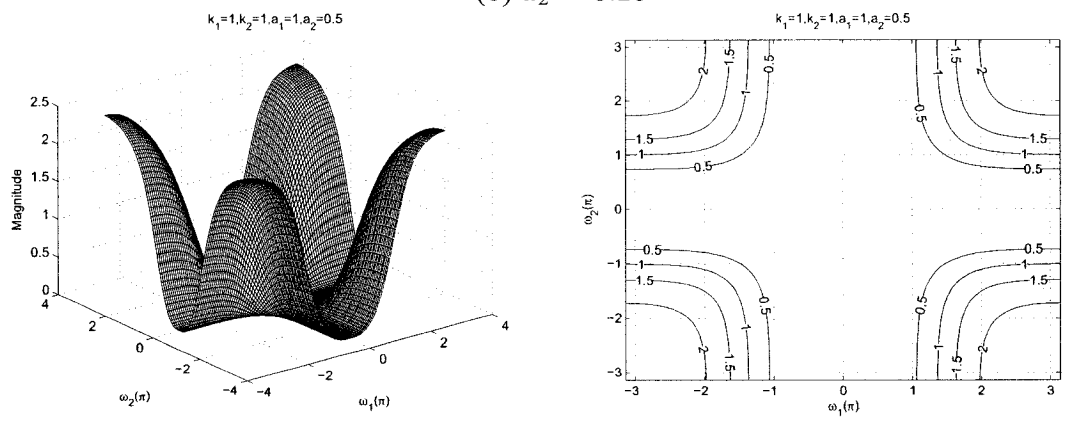

(c) $a_2 = 0.5$

Figure 3.40: 3-D amplitude frequency response and the contour response of the All-pole 2-D digital highpass filter for different values of a_2

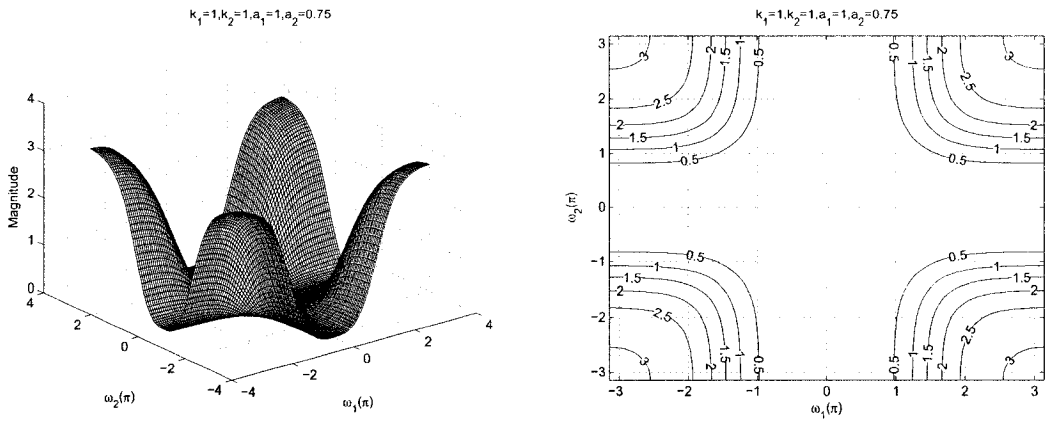

(a) $a_2 = 0.75$

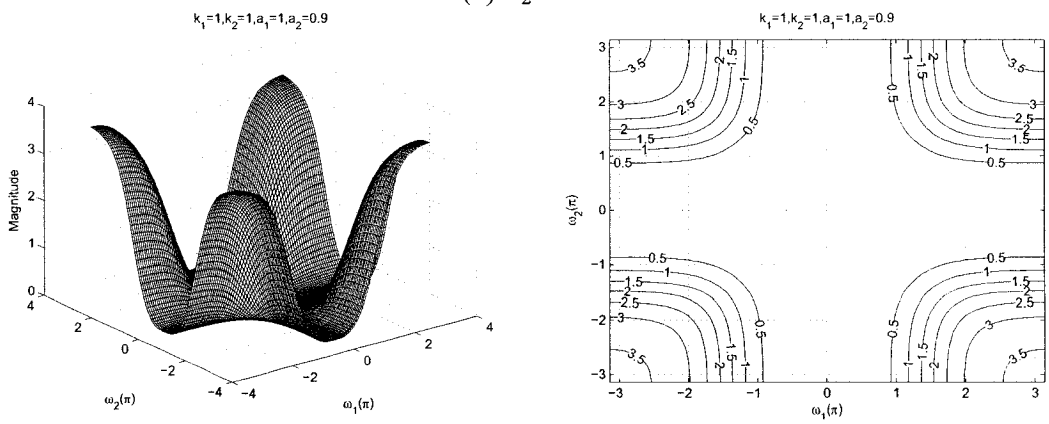

(b) $a_2 = 0.9$

Figure 3.41: 3-D amplitude frequency response and the contour response of the All-pole 2-D digital highpass filter for different values of a_2

By varying the value of a_2, the 3-D magnitude response and contour plots which represents different values of a_2, i.e. $a_2 = 0.1$, $a_2 = 0.25$, $a_2 = 0.5$, $a_2 = 0.75$, and $a_2 = 0.9$ are shown in the Figures 3.40 and 3.41. By making the value of $a_2 = 1$, it resembles the standard highpass filter as shown in the Figure 3.33. It is observed for the diagrams that the coefficient effects the gain of the amplitude response. As the value of a_2 increases from 0.1 to 1 the gain of the amplitude-response increases from 1.6 to 3.5. As the value of a_2 increases, the gain increases and reach the maximum value at $a_2 = 1$. In addition, the stop-band width increases for the same. Also it is evident from the diagrams that the coefficient a_2 does not have any effect on along the $\omega_1 - axis$.

3.3.2.5 Frequency Response of the All-pole 2-D Digital Highpass Filter with same values of a_1 and a_2 and same values of k_1 and k_2

In the Sections 3.3.2.1 to 3.3.2.4 the individual effect of the coefficients a_1, a_2, k_1 and k_2 was studied. In this section, we will study the effect of coefficients where $a_1 = a_2$ and $k_1 = k_2$ and the remaining coefficients $b_1 = b_2 = -1$ in order to get the all-pole 2-D digital highpass filter in Category B. The values of a_1 and a_2 range from 0 to 1 and the values of k_1 and k_2 range from 0 to 50.

As observed from the Figures 3.42 to 3.48, the coefficients k_1 and k_2 affect the stopband width of the frequency response. In the Figures 3.42 (a), 3.43 (b), 3.44 (c), 3.46 (a), and 3.47 (b), there is an increase in the stopband width of the contour response as the values of k_1 and k_2 are increased from 0.5 to 50 for the same values of $a_1 = a_2 = 0.25$. It is also observed that there is a decrease in the magnitude of the contour response from 1.8 to 1.5×10^{-7} for the same values. It is also observed that for very high values of k_1 and k_2, the stopband width of the frequency response becomes maximum as shown in the Figure 3.48 (b).

As observed from the Figures 3.42 to 3.48, the coefficients a_1 and a_2 affect the gain of the amplitude-frequency response. It can be clearly observed from the Figures 3.42 (a), (b, (c) and 3.43 (a), that the amplitude of the contour response increases from 1.8 to 3.5 when the values of a_1 and a_2 are increased from 0.25 to 0.9 keeping the same value of $k_1 = k_2 = 0.5$. In addition, the width of the stopband increases for the same.

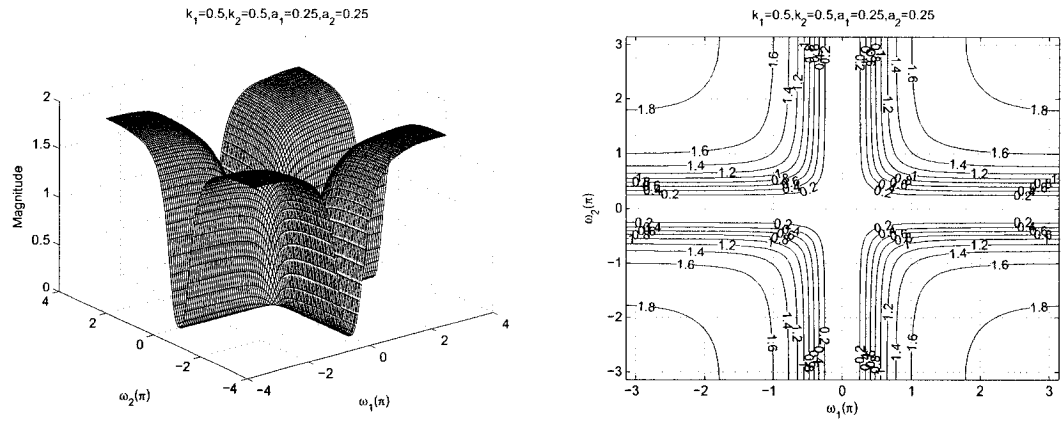

(a) $a_1 = a_2 = 0.25$ and $k_1 = k_2 = 0.5$

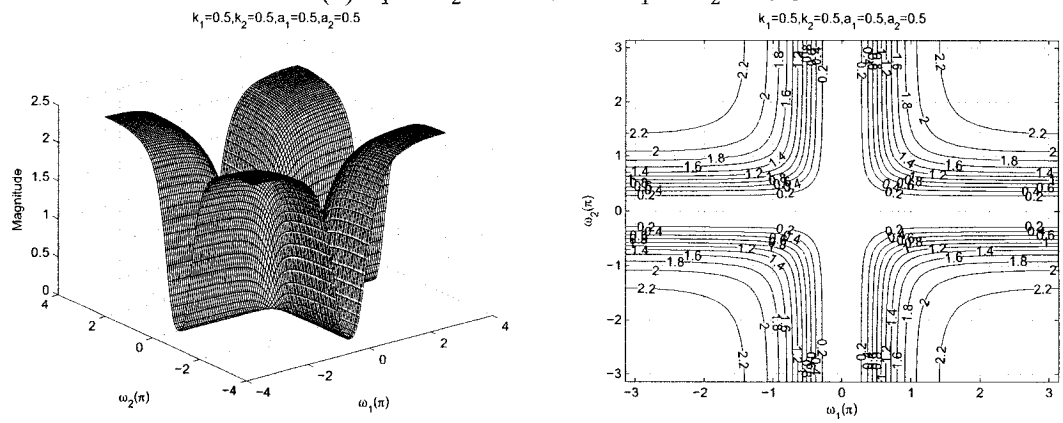

(b) $a_1 = a_2 = 0.5$ and $k_1 = k_2 = 0.5$

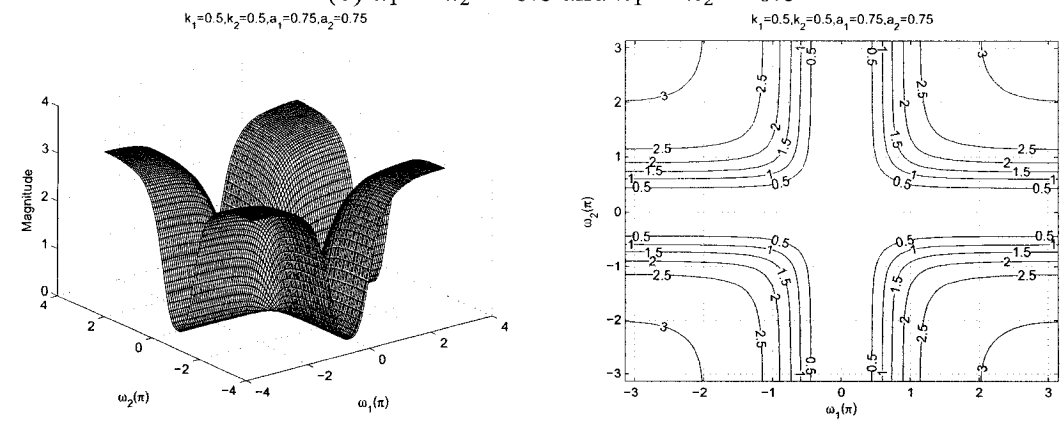

(c) $a_1 = a_2 = 0.75$ and $k_1 = k_2 = 0.5$

Figure 3.42: 3-D amplitude frequency response and the contour response of the All-pole 2-D digital highpass filter for $a_1 = a_2$ and $k_1 = k_2$

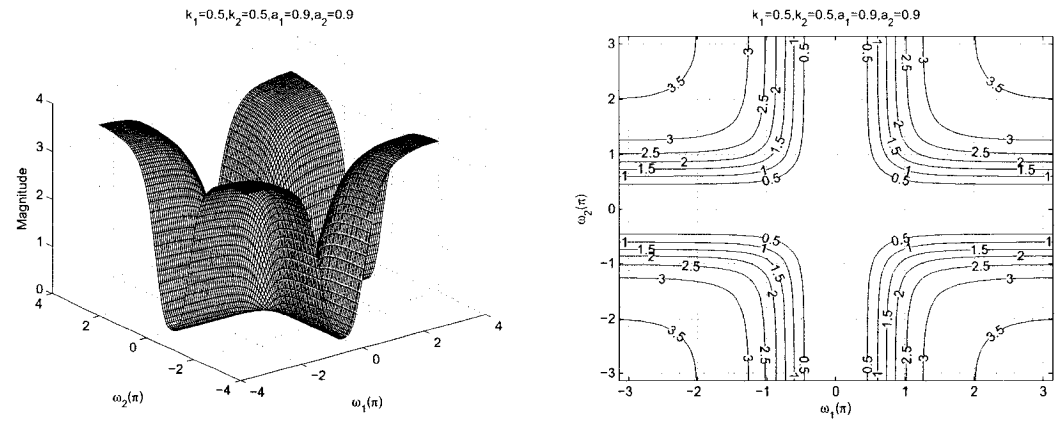

(a) $a_1 = a_2 = 0.9$ and $k_1 = k_2 = 0.5$

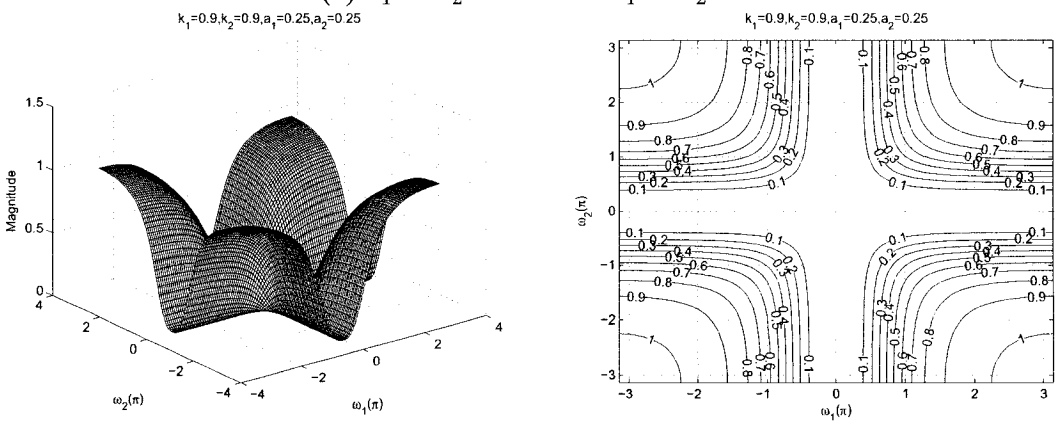

(b) $a_1 = a_2 = 0.25$ and $k_1 = k_2 = 0.9$

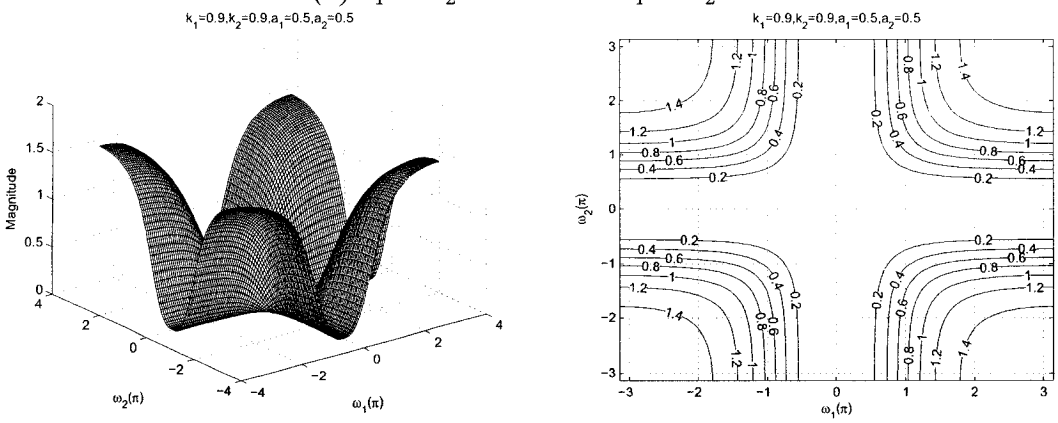

(c) $a_1 = a_2 = 0.5$ and $k_1 = k_2 = 0.9$

Figure 3.43: 3-D amplitude frequency response and the contour response of the All-pole 2-D digital highpass filter for $a_1 = a_2$ and $k_1 = k_2$

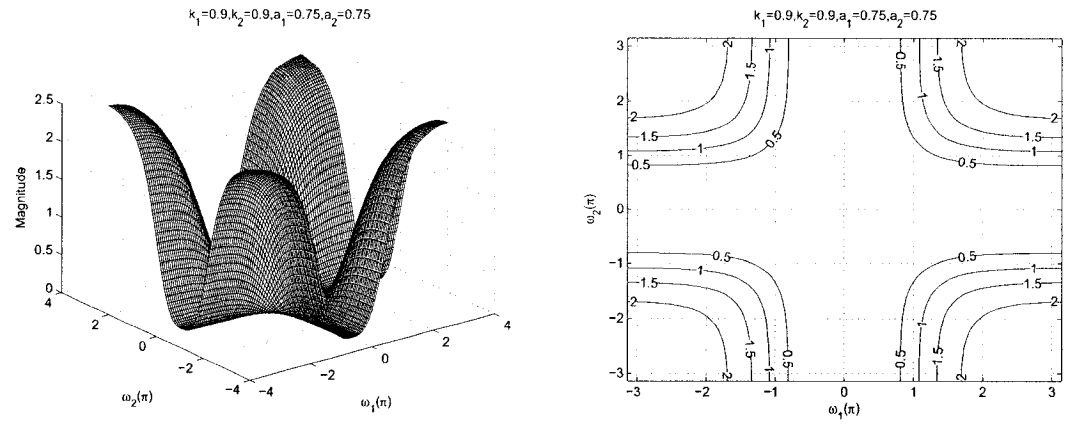

(a) $a_1 = a_2 = 0.75$ and $k_1 = k_2 = 0.9$

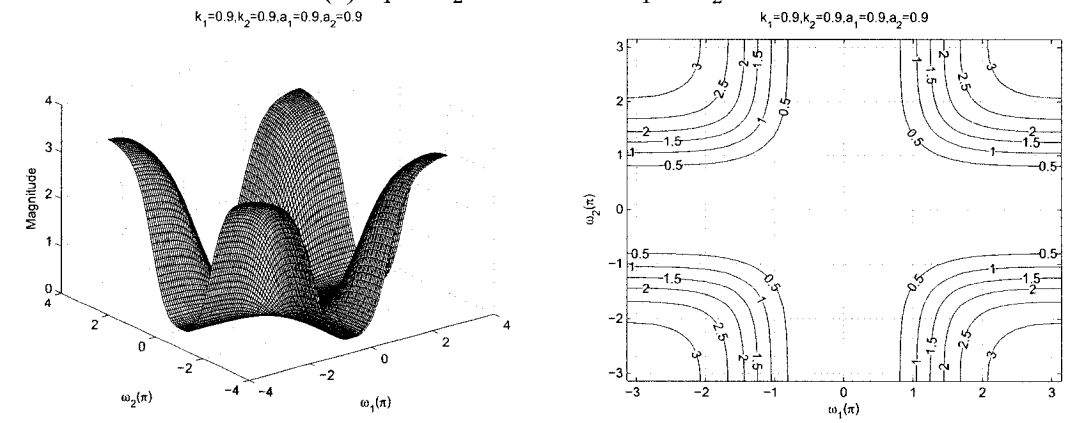

(b) $a_1 = a_2 = 0.9$ and $k_1 = k_2 = 0.9$

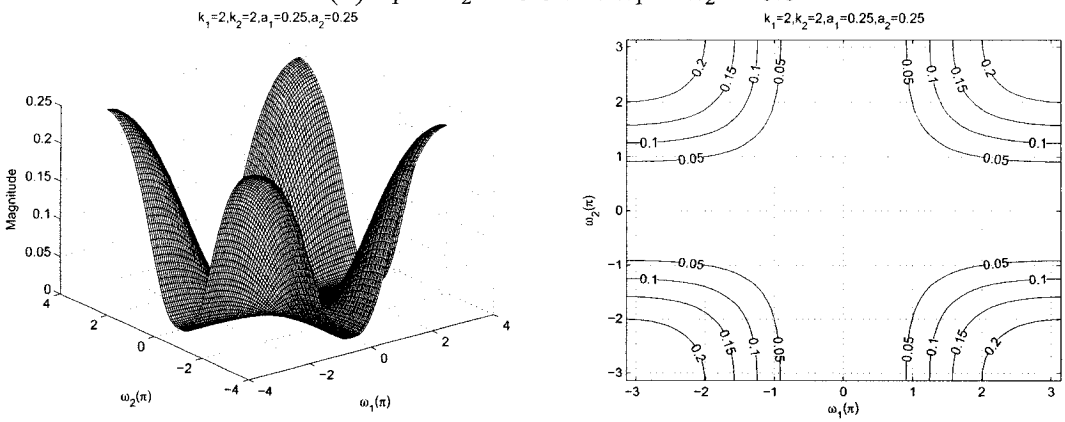

(c) $a_1 = a_2 = 0.25$ and $k_1 = k_2 = 2$

Figure 3.44: 3-D amplitude frequency response and the contour response of the All-pole 2-D digital highpass filter for $a_1 = a_2$ and $k_1 = k_2$

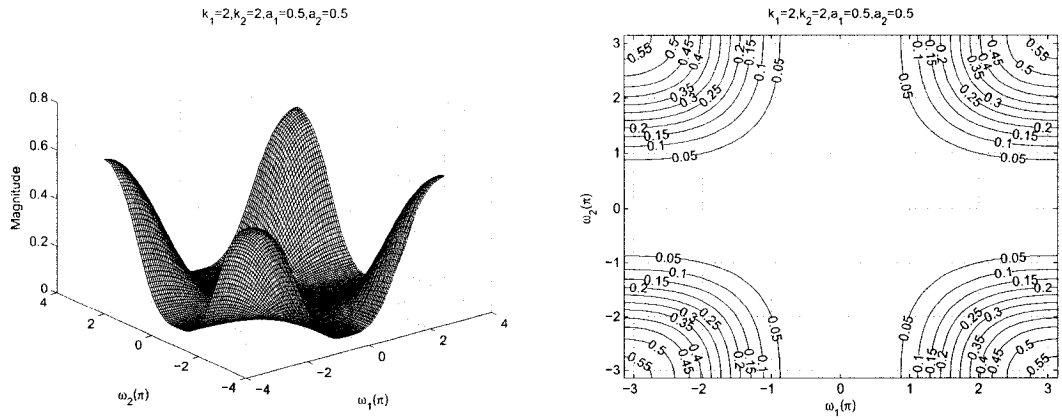

(a) $a_1 = a_2 = 0.5$ and $k_1 = k_2 = 2$

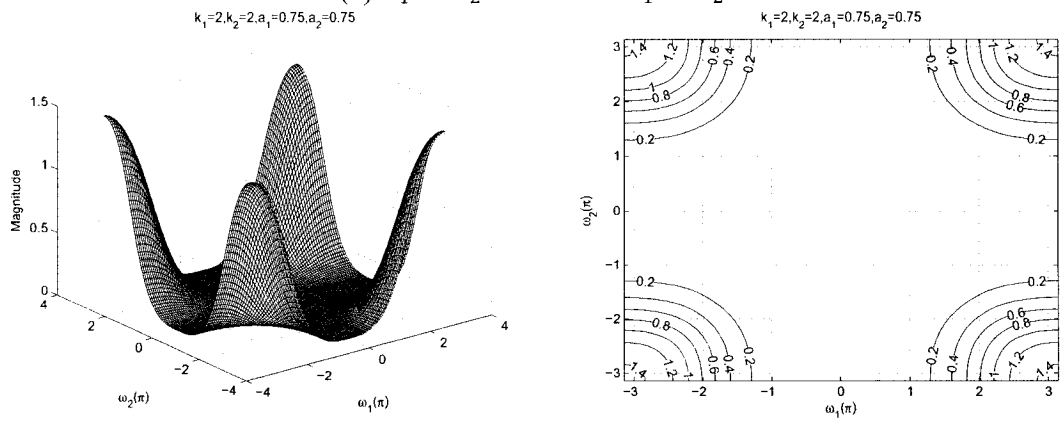

(b) $a_1 = a_2 = 0.75$ and $k_1 = k_2 = 2$

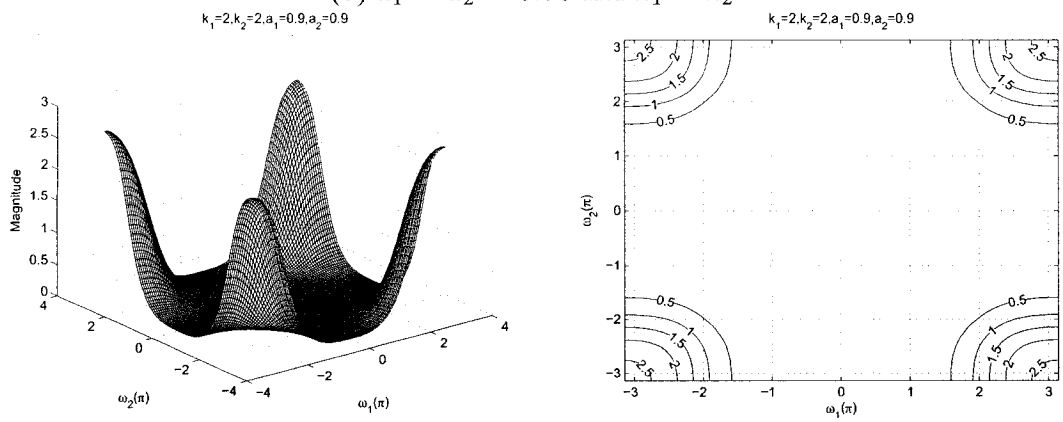

(c) $a_1 = a_2 = 0.9$ and $k_1 = k_2 = 2$

Figure 3.45: 3-D amplitude frequency response and the contour response of the All-pole 2-D digital highpass filter for $a_1 = a_2$ and $k_1 = k_2$

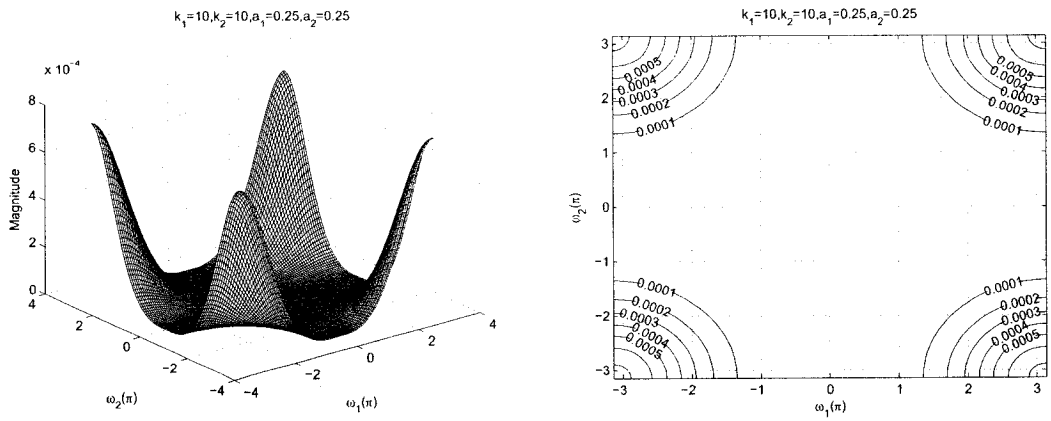

(a) $a_1 = a_2 = 0.25$ and $k_1 = k_2 = 10$

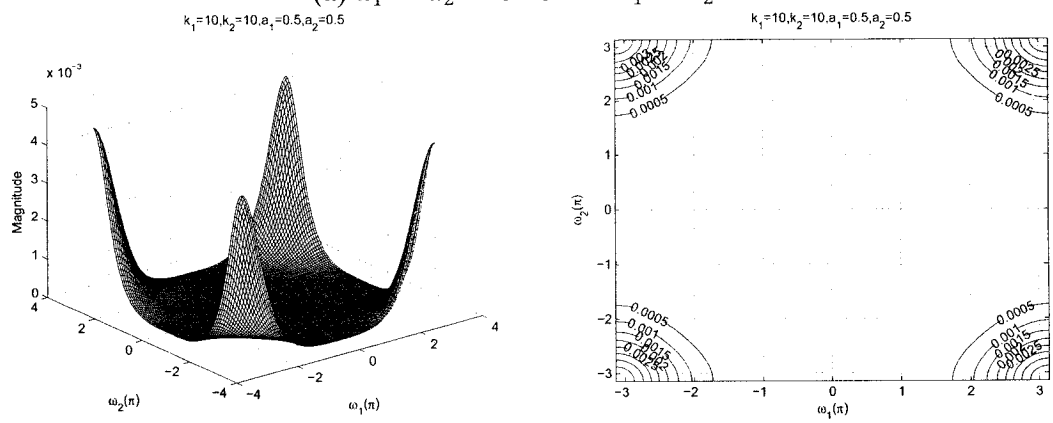

(b) $a_1 = a_2 = 0.5$ and $k_1 = k_2 = 10$

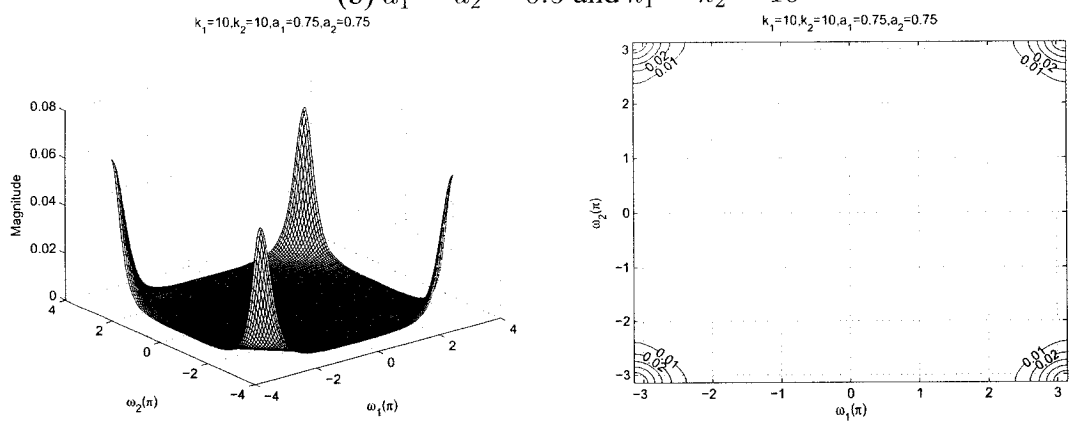

(c) $a_1 = a_2 = 0.75$ and $k_1 = k_2 = 10$

Figure 3.46: 3-D amplitude frequency response and the contour response of the All-pole 2-D digital highpass filter for $a_1 = a_2$ and $k_1 = k_2$

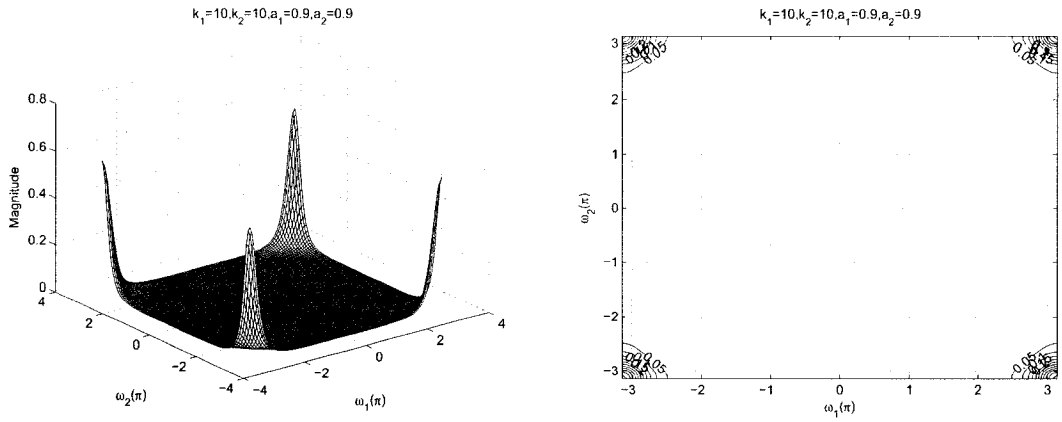

(a) $a_1 = a_2 = 0.9$ and $k_1 = k_2 = 10$

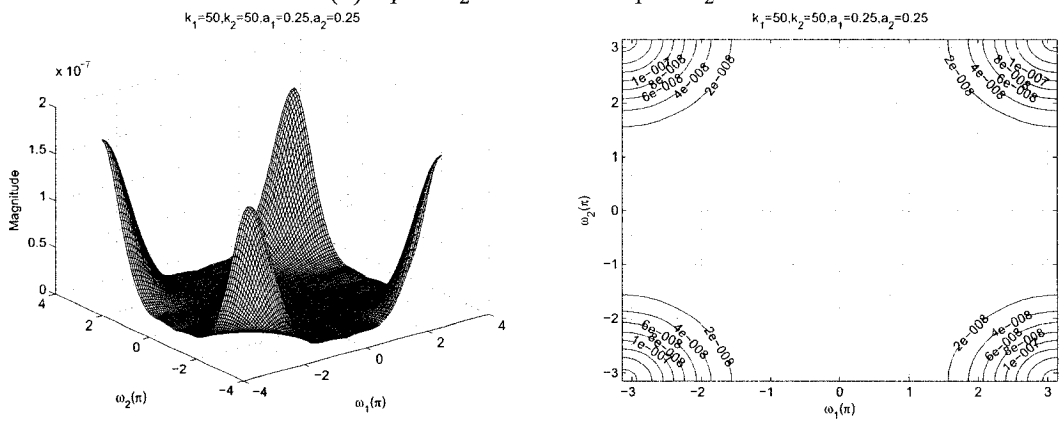

(b) $a_1 = a_2 = 0.25$ and $k_1 = k_2 = 50$

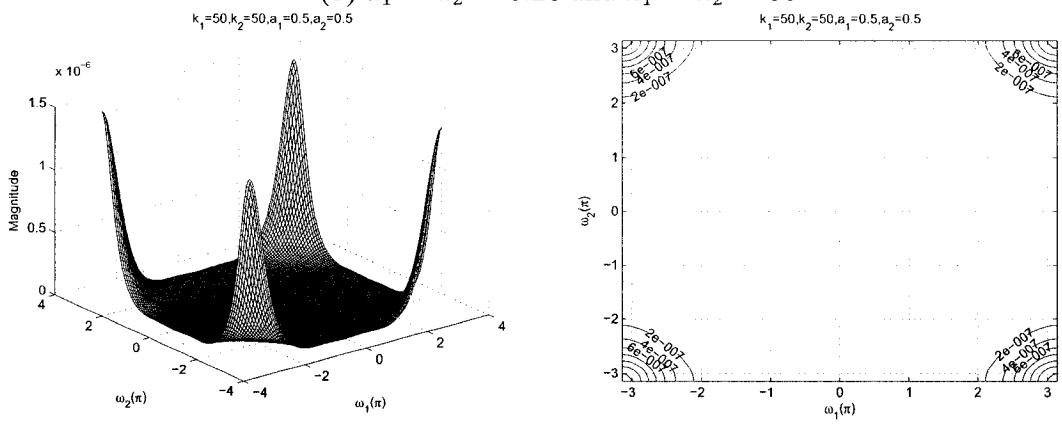

(c) $a_1 = a_2 = 0.5$ and $k_1 = k_2 = 50$

Figure 3.47: 3-D amplitude frequency response and the contour response of the All-pole 2-D digital highpass filter for $a_1 = a_2$ and $k_1 = k_2$

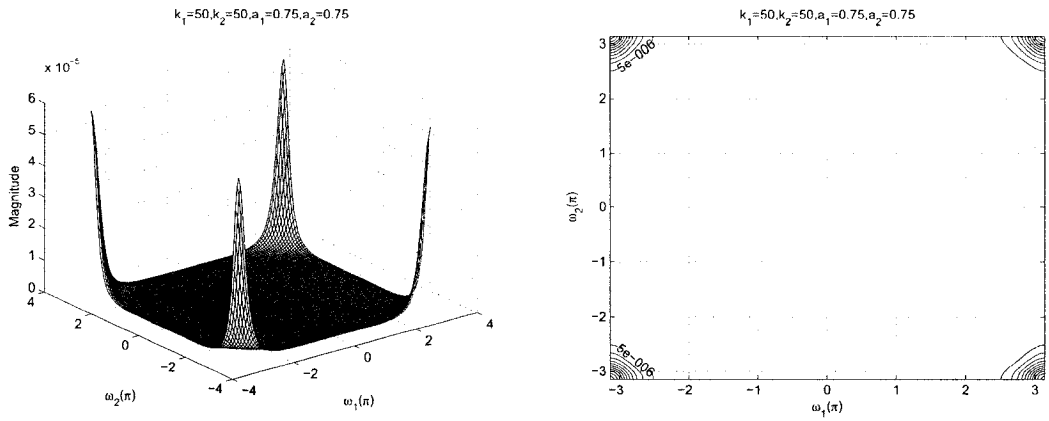

(a) $a_1 = a_2 = 0.75$ and $k_1 = k_2 = 50$

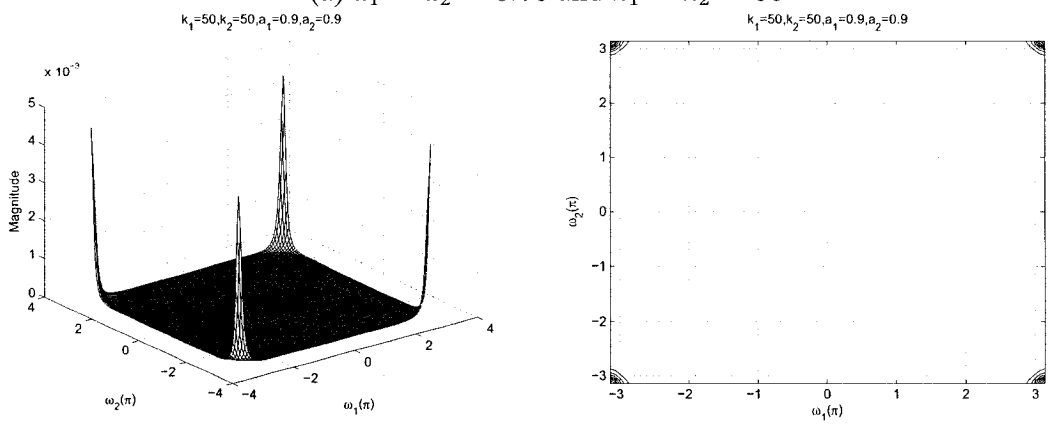

(b) $a_1 = a_2 = 0.9$ and $k_1 = k_2 = 50$

Figure 3.48: 3-D amplitude frequency response and the contour response of the All-pole 2-D digital highpass filter for $a_1 = a_2$ and $k_1 = k_2$

3.3.2.6 Frequency Response of the All-pole 2-D Digital Highpass Filter with different values of a_1 and a_2 and same values of k_1 and k_2

In this section, we will study the effect of coefficients, where $a_1 \neq a_2$ and $k_1 = k_2$ and the remaining coefficients $b_1 = b_2 = -1$ in order to get the all-pole 2-D digital highpass filter Category B. The values of a_1 and a_2 ranges from 0.25 to 0.5 and 0.5 to 0.75, respectively and the values of k_1 and k_2 ranges from 0 to 50.

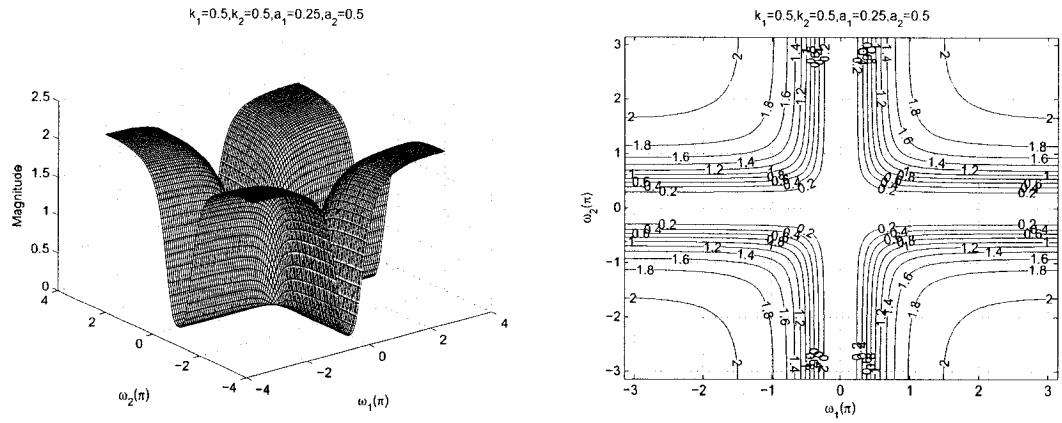

(a) $a_1 = 0.25$, $a_2 = 0.5$ and $k_1 = k_2 = 0.5$

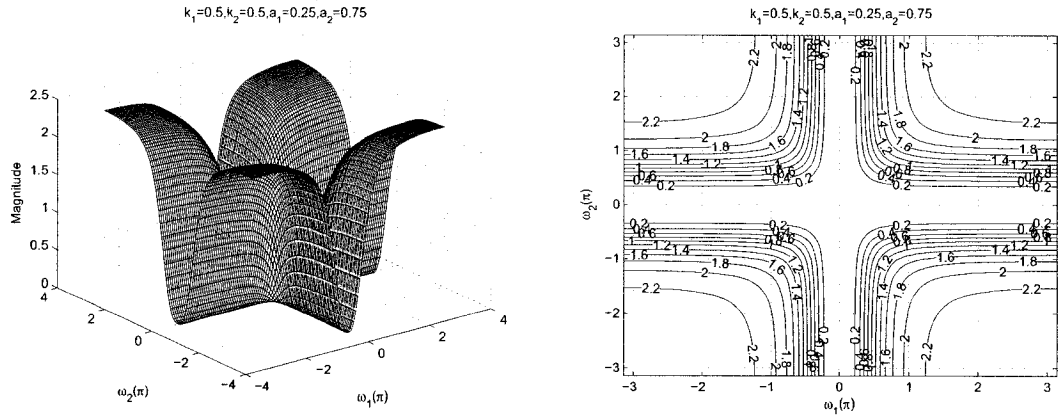

(b) $a_1 = 0.25$, $a_2 = 0.75$ and $k_1 = k_2 = 0.5$

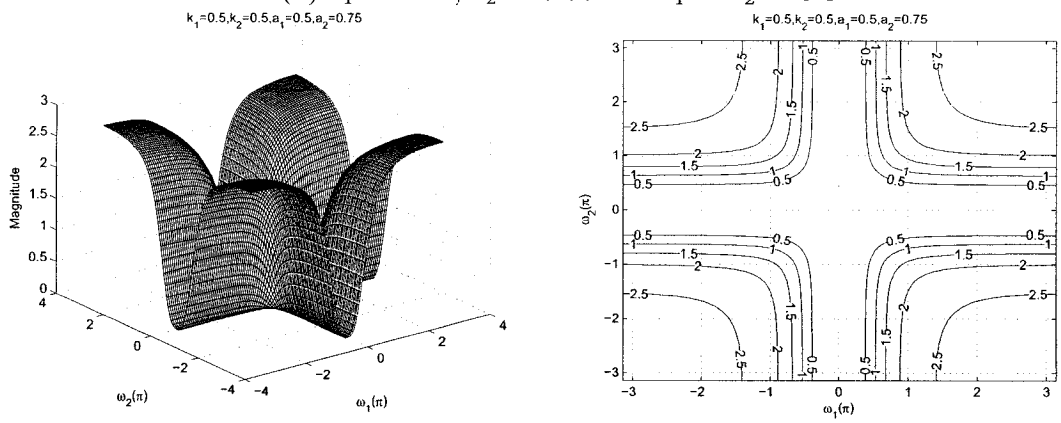

(c) $a_1 = 0.5$, $a_2 = 0.75$ and $k_1 = k_2 = 0.5$

Figure 3.49: 3-D amplitude frequency response and the contour response of the All-pole 2-D digital highpass filter for $a_1 \neq a_2$ and $k_1 = k_2$

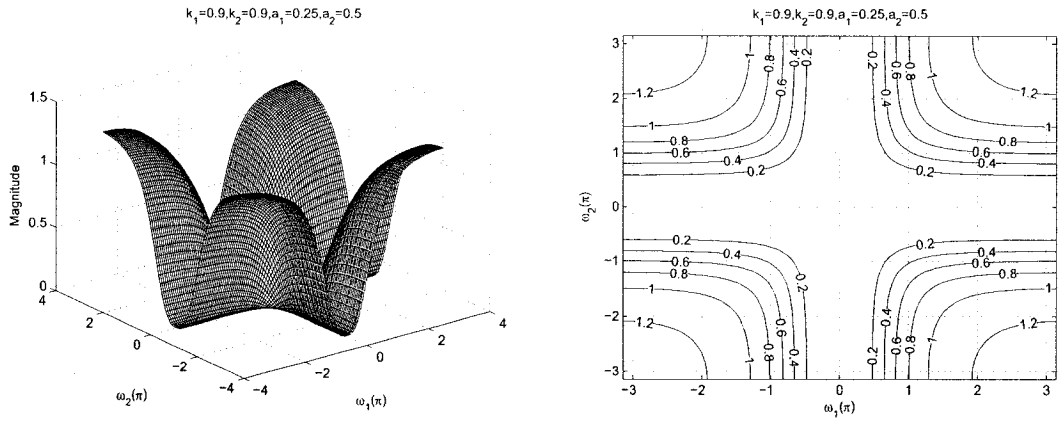

(a) $a_1 = 0.25$, $a_2 = 0.5$ and $k_1 = k_2 = 0.9$

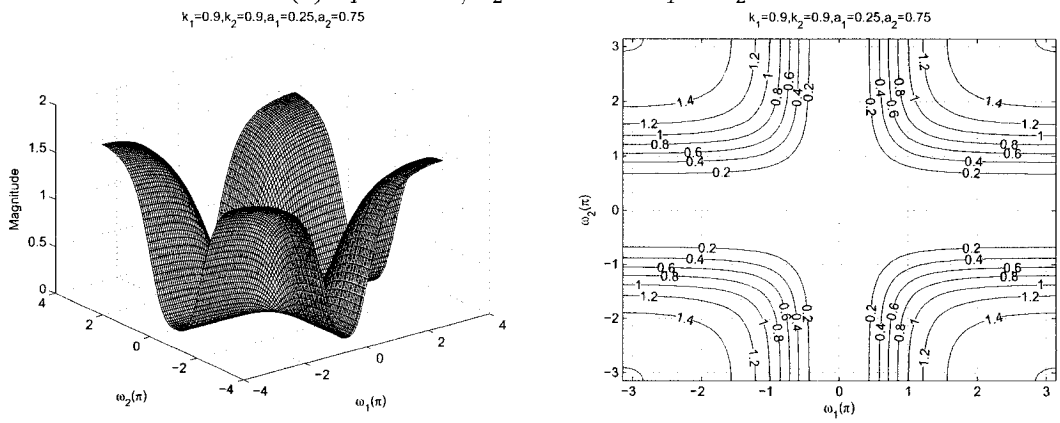

(b) $a_1 = 0.25$, $a_2 = 0.75$ and $k_1 = k_2 = 0.9$

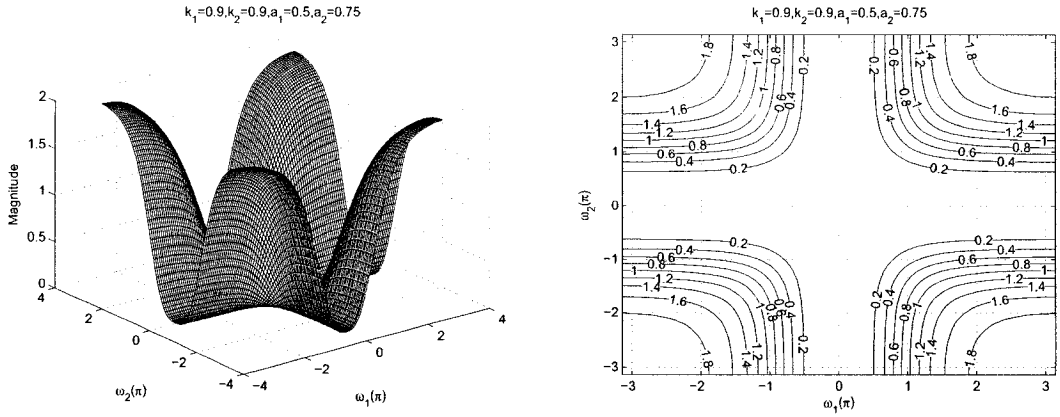

(c) $a_1 = 0.5$, $a_2 = 0.75$ and $k_1 = k_2 = 0.9$

Figure 3.50: 3-D amplitude frequency response and the contour response of the All-pole 2-D digital highpass filter for $a_1 \neq a_2$ and $k_1 = k_2$

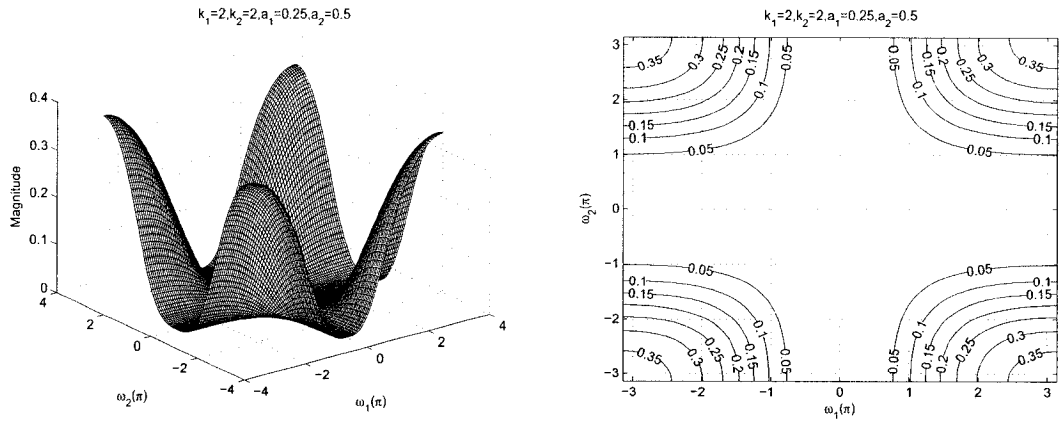

(a) $a_1 = 0.25$, $a_2 = 0.5$ and $k_1 = k_2 = 2$

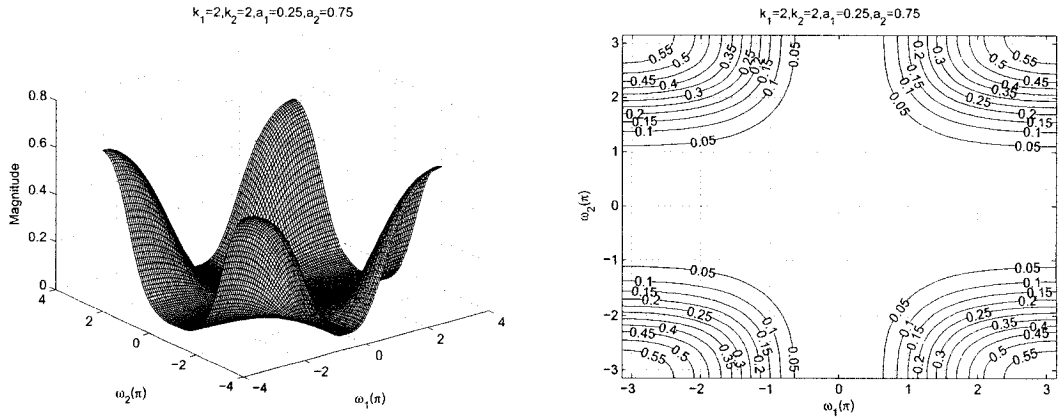

(b) $a_1 = 0.25$, $a_2 = 0.75$ and $k_1 = k_2 = 2$

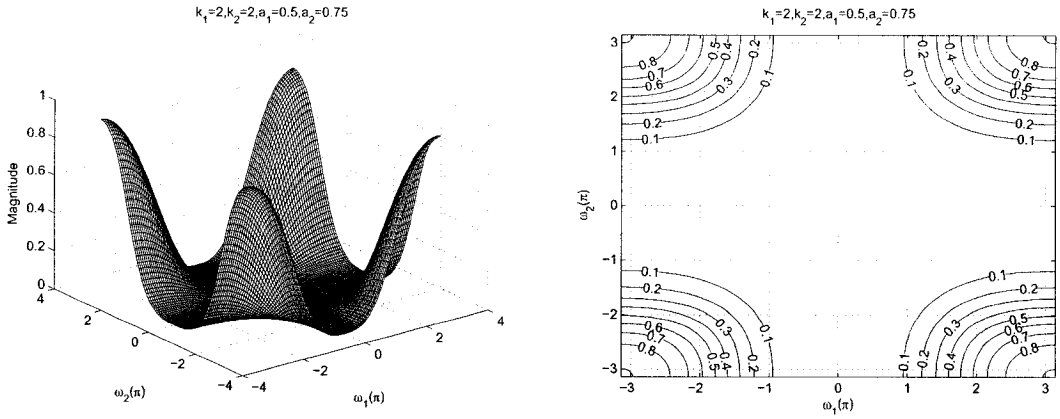

(c) $a_1 = 0.5$, $a_2 = 0.75$ and $k_1 = k_2 = 2$

Figure 3.51: 3-D amplitude frequency response and the contour response of the All-pole 2-D digital highpass filter for $a_1 \neq a_2$ and $k_1 = k_2$

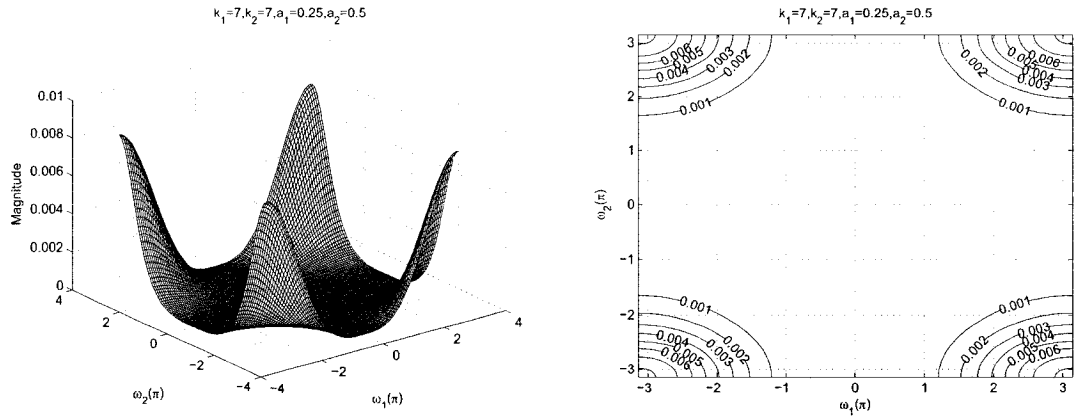

(a) $a_1 = 0.25$, $a_2 = 0.5$ and $k_1 = k_2 = 7$

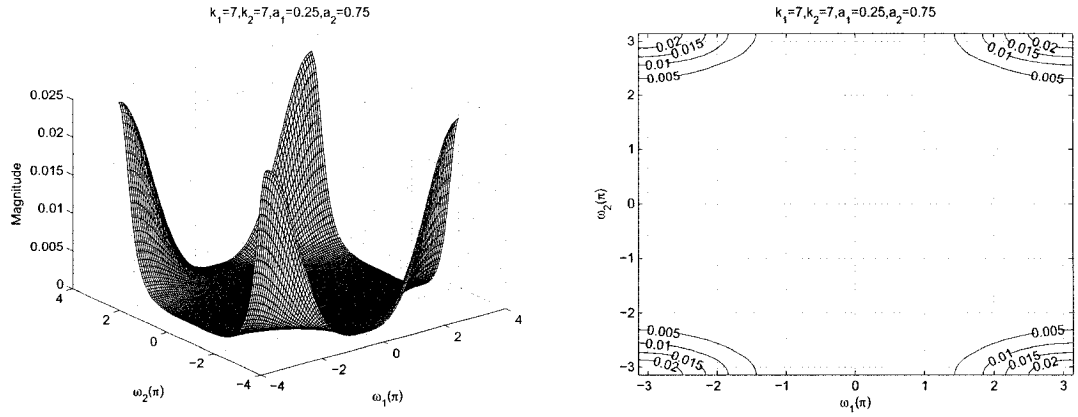

(b) $a_1 = 0.25$, $a_2 = 0.75$ and $k_1 = k_2 = 7$

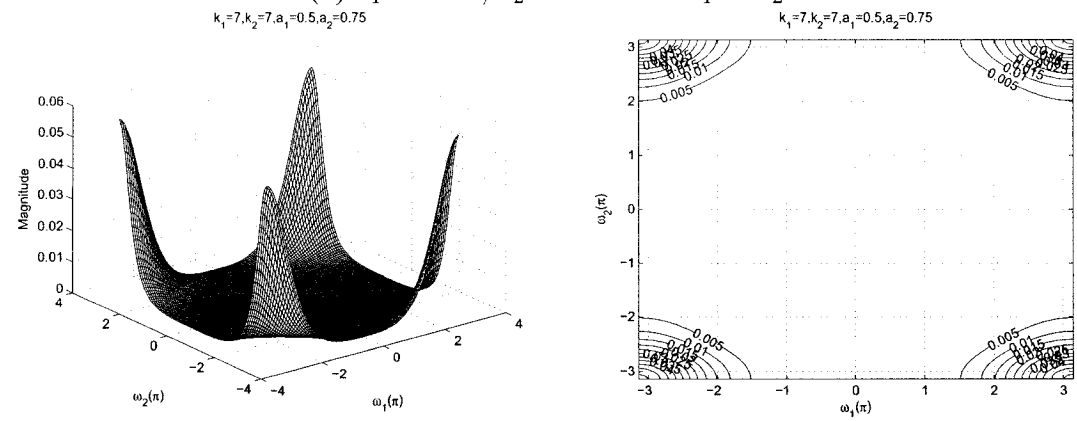

(c) $a_1 = 0.5$, $a_2 = 0.75$ and $k_1 = k_2 = 7$

Figure 3.52: 3-D amplitude frequency response and the contour response of the All-pole 2-D digital highpass filter for $a_1 \neq a_2$ and $k_1 = k_2$

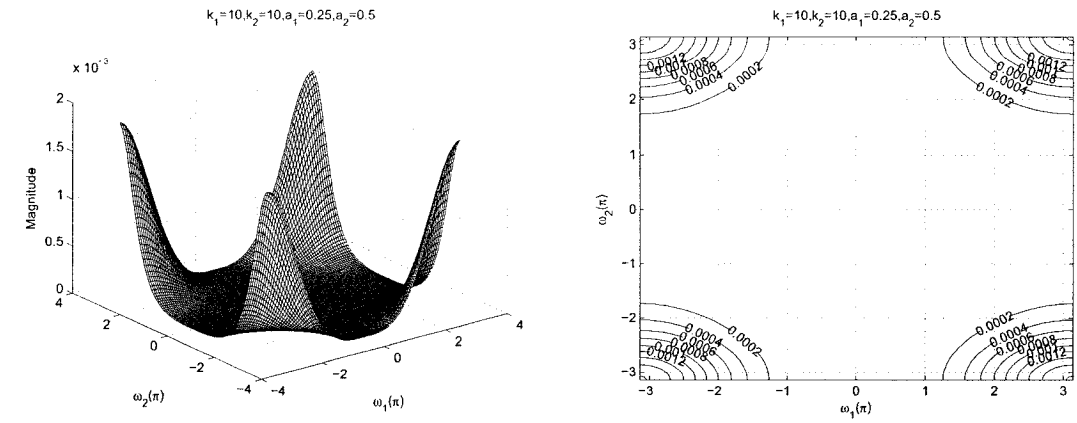

(a) $a_1 = 0.25$, $a_2 = 0.5$ and $k_1 = k_2 = 10$

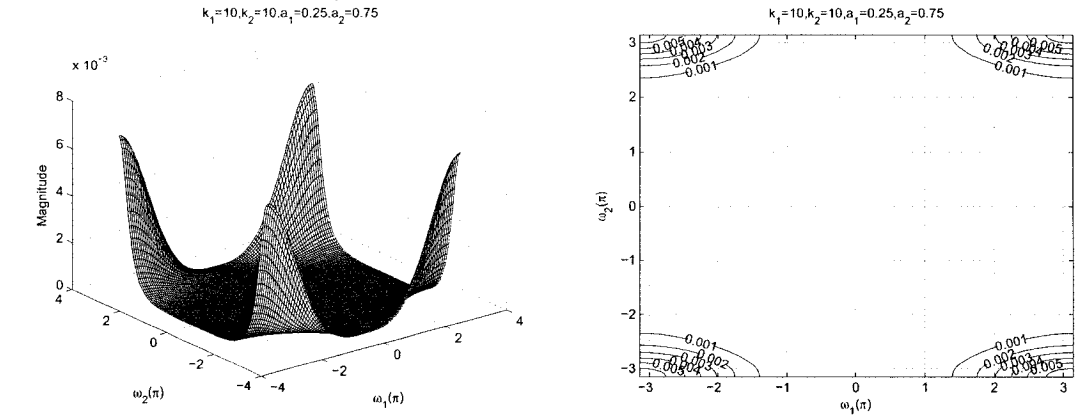

(b) $a_1 = 0.25$, $a_2 = 0.75$ and $k_1 = k_2 = 10$

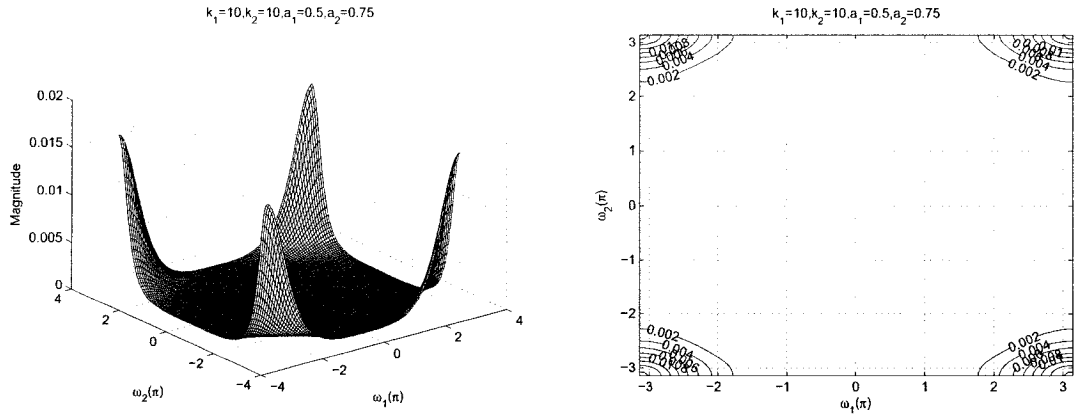

(c) $a_1 = 0.5$, $a_2 = 0.75$ and $k_1 = k_2 = 10$

Figure 3.53: 3-D amplitude frequency response and the contour response of the All-pole 2-D digital highpass filter for $a_1 \neq a_2$ and $k_1 = k_2$

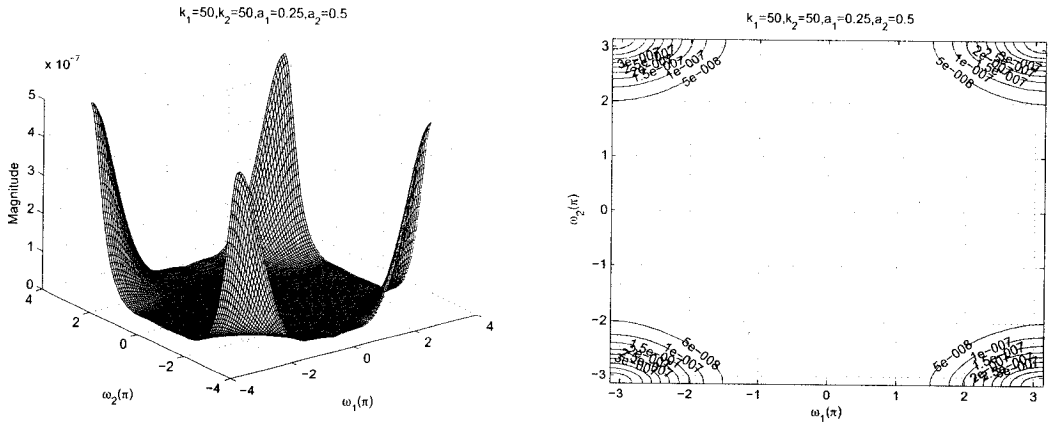

(a) $a_1 = 0.25$, $a_2 = 0.5$ and $k_1 = k_2 = 50$

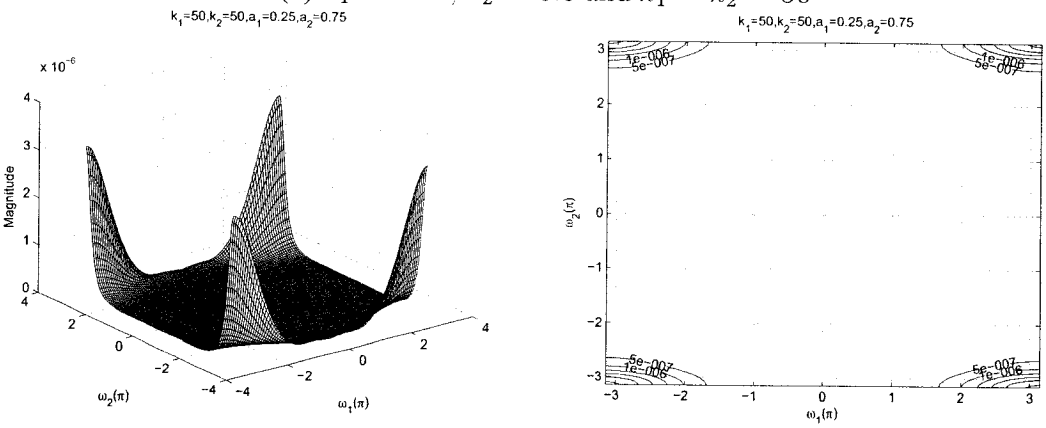

(b) $a_1 = 0.25$, $a_2 = 0.75$ and $k_1 = k_2 = 50$

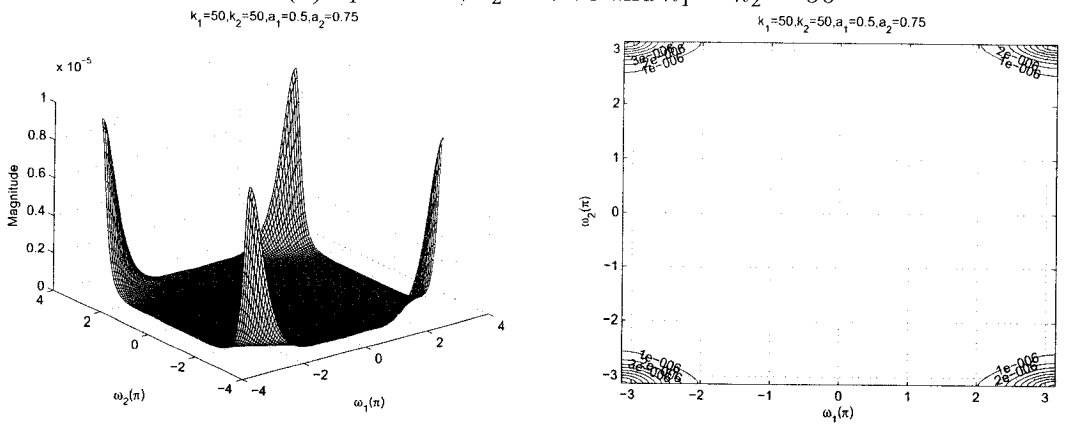

(c) $a_1 = 0.5$, $a_2 = 0.75$ and $k_1 = k_2 = 50$

Figure 3.54: 3-D amplitude frequency response and the contour response of the All-pole 2-D digital highpass filter for $a_1 \neq a_2$ and $k_1 = k_2$

As observed from the Figures 3.49 to 3.54, the coefficients k_1 and k_2 affect the stopband width of the frequency response of the all-pole 2-D digital highpass filter. In the Figures 3.49 (a), 3.50 (a), 3.51 (a), 3.52 (a), 3.53 (a) and 3.54 (a), there is a gradual increase in the stopband width as the values of k_1 and k_2 are increased from 0.5 to 50 for different values of $a_1 = 0.25$ and $a_2 = 0.5$. At the same time there is a gradual decrease in the magnitude of the contour response from 2 to 4.5×10^{-7}. It is also observed that for very high values of k_1 and k_2, the stopband width of the frequency response becomes maximum as shown in the Figure 3.54 (c).

As observed from the Figures 3.49 to 3.54, the coefficients a_1 and a_2 affect the gain of the amplitude-frequency response. It can be clearly observed from the Figures 3.49 (a), (b) and (c), that the amplitude of the contour response increases from 2 to 2.5 when the values of a_1 and a_2 are increased from 0.25 to 0.5 and 0.5 to 0.75 while keeping the same value of $k_1 = k_2 = 0.5$. In addition, the width of the stopband increases for the same.

3.3.2.7 Frequency Response of the All-pole 2-D Digital Highpass Filter with different values of a_1 and a_2 and different values of k_1 and k_2

In this section, we study the effect of coefficients when $a_1 \neq a_2$ and $k_1 \neq k_2$, and the remaining coefficients $b_1 = b_2 = -1$ in order to get the all-pole 2-D digital highpass filter in Category B. The values of a_1 and a_2 vary from 0.25 to 0.75 and 0.5 to 0.9, respectively and the values of k_1 and k_2 vary from 0.5 to 50 and 1 to 75, respectively.

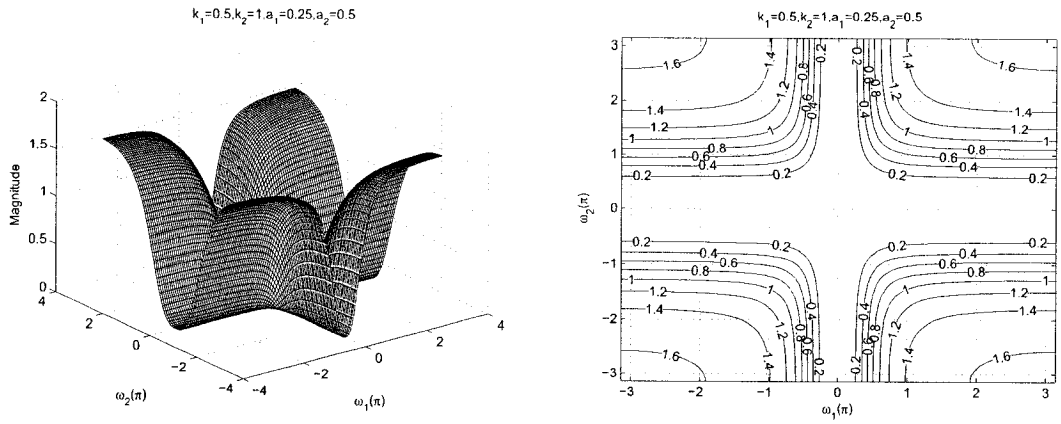

(a) $a_1 = 0.25$, $a_2 = 0.5$ and $k_1 = 0.5$, $k_2 = 1$

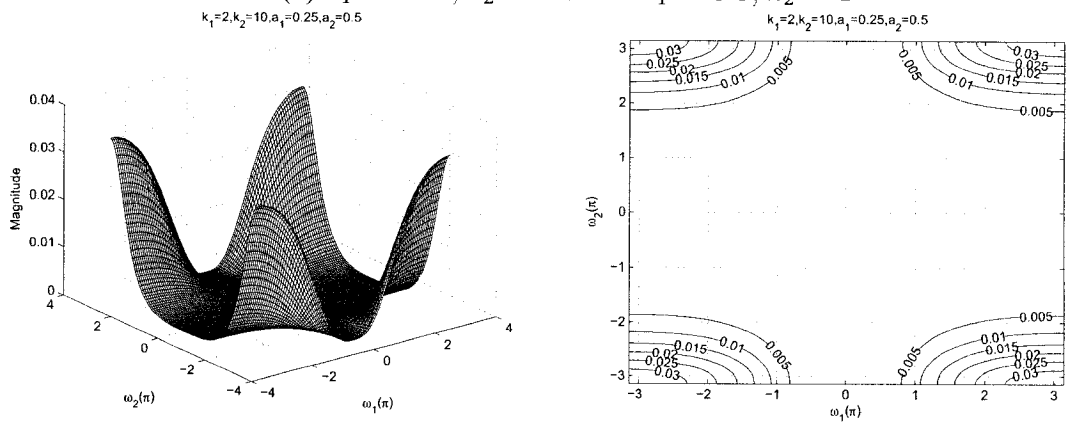

(b) $a_1 = 0.25$, $a_2 = 0.5$ and $k_1 = 2$, $k_2 = 10$

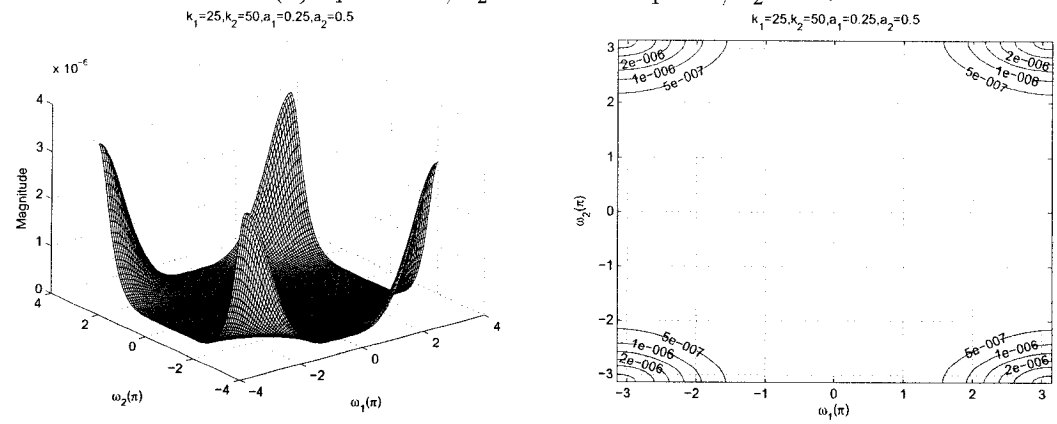

(c) $a_1 = 0.25$, $a_2 = 0.5$ and $k_1 = 25$, $k_2 = 50$

Figure 3.55: 3-D amplitude frequency response and the contour response of the All-pole 2-D digital highpass filter for $a_1 \neq a_2$ and $k_1 \neq k_2$

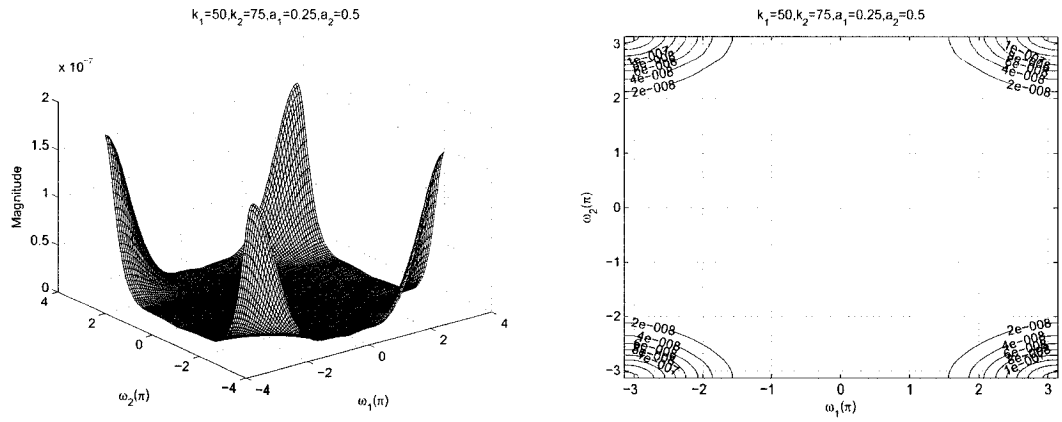

(a) $a_1 = 0.25$, $a_2 = 0.5$ and $k_1 = 50$, $k_2 = 75$

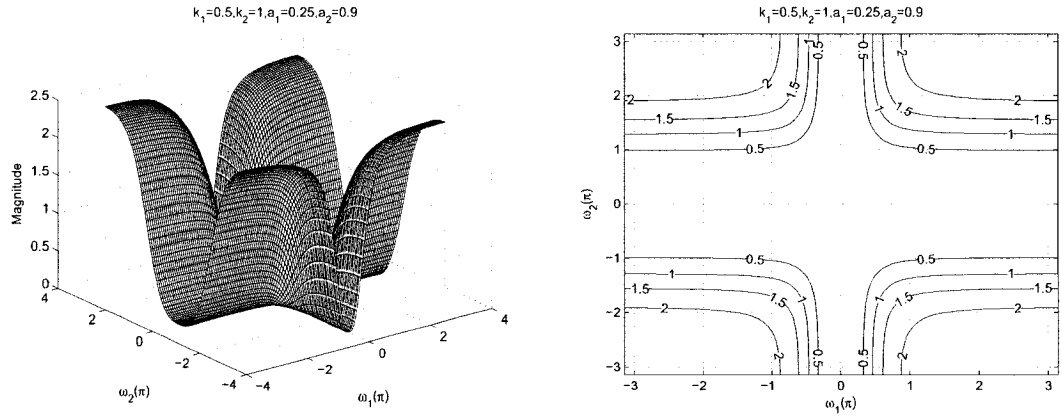

(b) $a_1 = 0.25$, $a_2 = 0.9$ and $k_1 = 0.5$, $k_2 = 1$

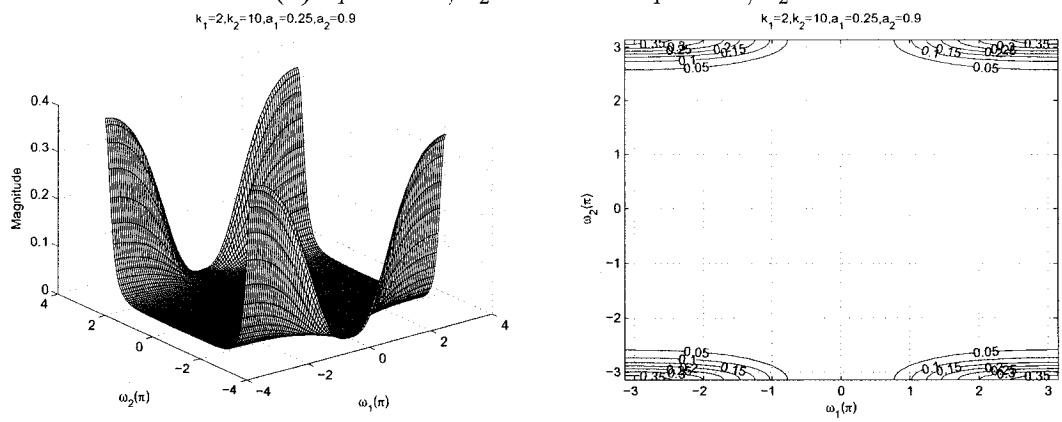

(c) $a_1 = 0.25$, $a_2 = 0.9$ and $k_1 = 2$, $k_2 = 10$

Figure 3.56: 3-D amplitude frequency response and the contour response of the All-pole 2-D digital highpass filter for $a_1 \neq a_2$ and $k_1 \neq k_2$

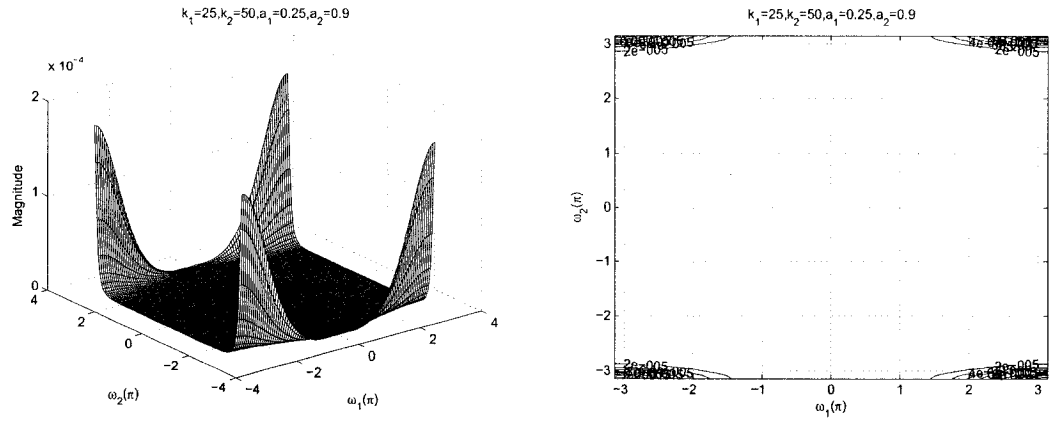

(a) $a_1 = 0.25$, $a_2 = 0.9$ and $k_1 = 25$, $k_2 = 50$

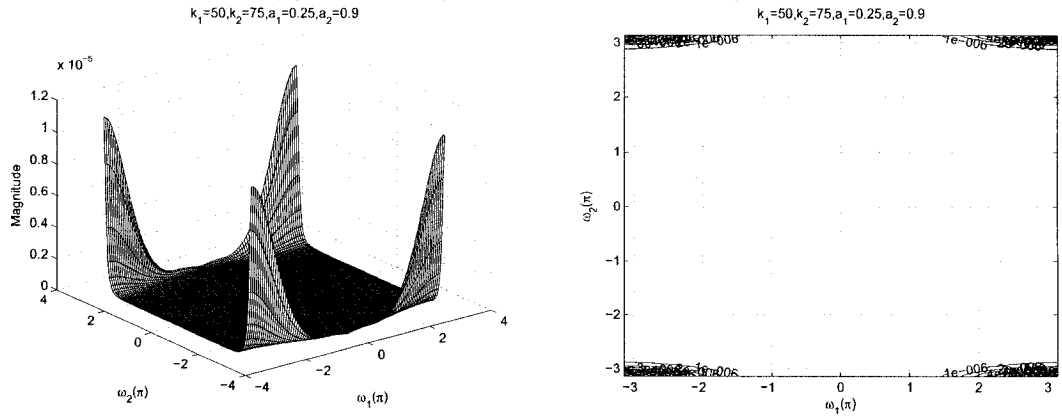

(b) $a_1 = 0.25$, $a_2 = 0.9$ and $k_1 = 50$, $k_2 = 75$

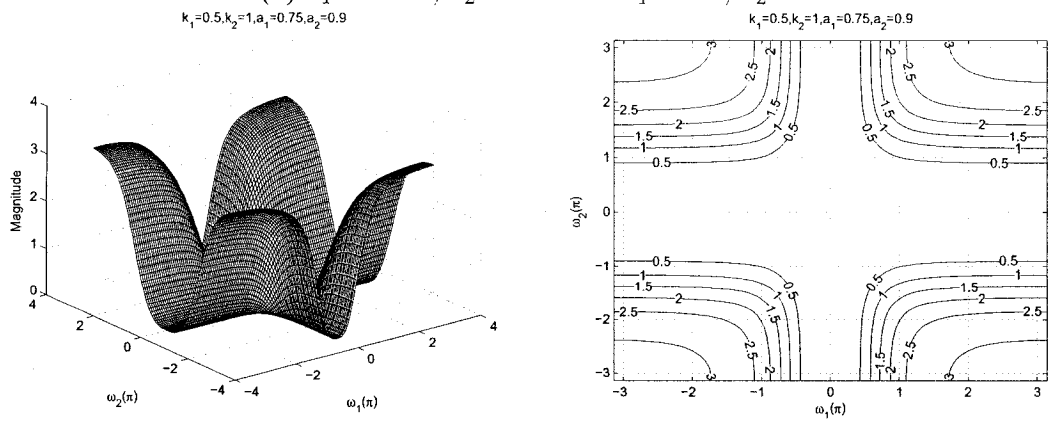

(c) $a_1 = 0.75$, $a_2 = 0.9$ and $k_1 = 0.5$, $k_2 = 1$

Figure 3.57: 3-D amplitude frequency response and the contour response of the All-pole 2-D digital highpass filter for $a_1 \neq a_2$ and $k_1 \neq k_2$

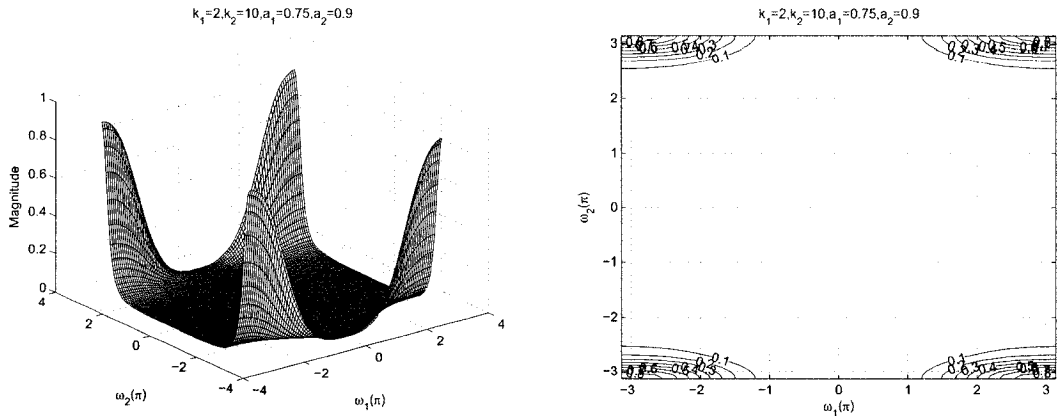

(a) $a_1 = 0.75$, $a_2 = 0.9$ and $k_1 = 2$, $k_2 = 10$

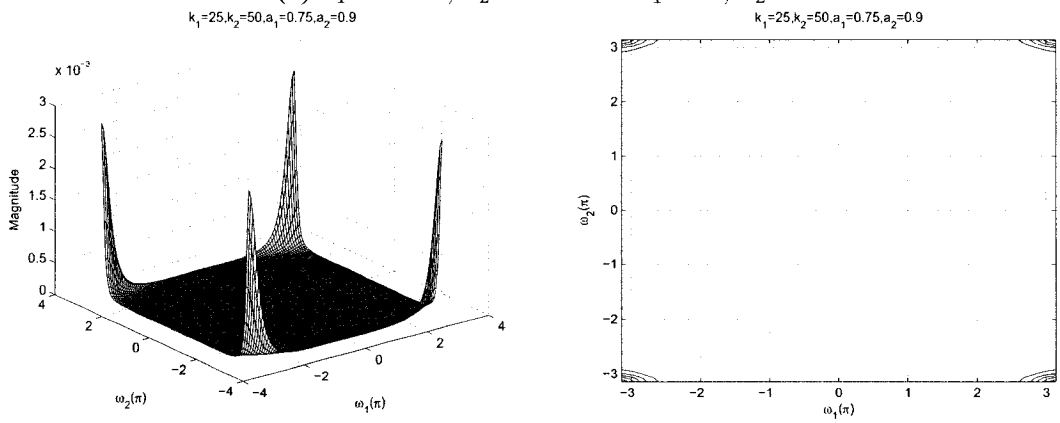

(b) $a_1 = 0.75$, $a_2 = 0.9$ and $k_1 = 25$, $k_2 = 50$

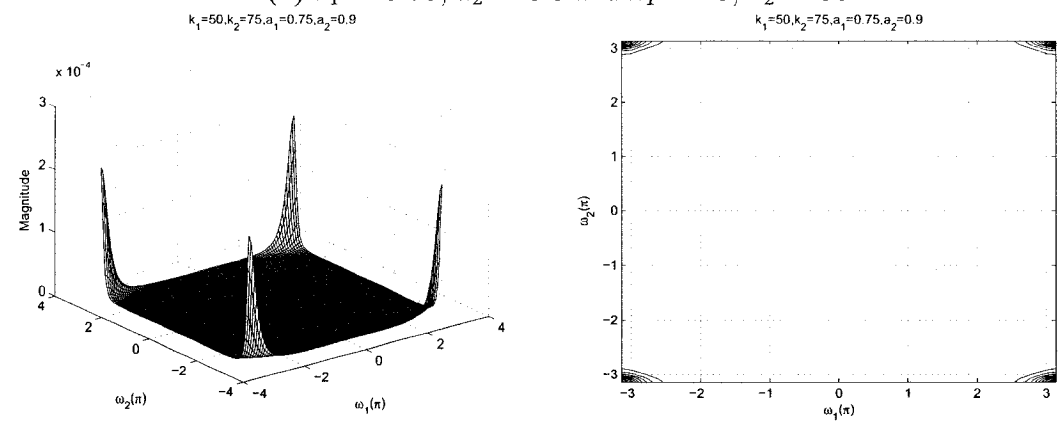

(c) $a_1 = 0.75$, $a_2 = 0.9$ and $k_1 = 50$, $k_2 = 75$

Figure 3.58: 3-D amplitude frequency response and the contour response of the All-pole 2-D digital highpass filter for $a_1 \neq a_2$ and $k_1 \neq k_2$

As observed from the Figures 3.55 to 3.58, the coefficients k_1 and k_2 affect the stopband width of the frequency response. In the Figures 3.55 (a), (b), (c) and 3.56 (a), there is a gradual increase in the stopband width as the values of k_1 and k_2 are increased from 0.5

to 50 and from 1 to 75 respectively, for the different values of $a_1 = 0.25$ and $a_2 = 0.5$. In addition there is also a gradual decrease in the amplitude from 1.6 to $1.5 \times 10^{-7}$for the same. It is also observed that for very high values of k_1 and k_2, the stopband width of the frequency response becomes maximum.

As observed from the Figures 3.55 to 3.58, the coefficients a_1 and a_2 affect the amplitude-frequency response. It can be clearly observed from the Figures 3.55 (a), 3.56 (b), and 3.57 (c), that the amplitude of the contour response increases from 1.6 to 3 when the values of a_1 and a_2 are increased from 0.25 to 0.75 and 0.5 to 0.9, respectively, keeping the same value of $k_1 = 0.5$ and $k_2 = 1$. In addition, the width of the stopband increases for the same.

3.3.2.8 Frequency Response of the All-pole 2-D Digital Highpass Filter with same values of a_1 and a_2 and different values of k_1 and k_2

In this section, we study the effect of coefficients, where $a_1 = a_2$ and $k_1 \neq k_2$ and the remaining coefficients $b_1 = b_2 = -1$ in order to get the all-pole 2-D digital highpass filter in Category B. The values of a_1 and a_2 vary from 0 to 1 and the values of k_1 and k_2 vary from 0.5 to 50 and 1 to 75, respectively.

As observed from the Figures 3.59 to 3.64, the coefficients k_1 and k_2 affect the stopband width of the frequency response. In the Figures 3.59 (a), (b), (c) and 3.60 (a), there is a increase in the stopband width as the values of k_1 and k_2 are increased from 0.5 to 75 for the same values of $a_1 = a_2 = 0.25$. At the same time there is also a gradual decrease in the amplitude from 1.2 to 5×10^{-8}. It is also observed that for very high values of k_1 and k_2, the stopband width of the frequency response becomes maximum.

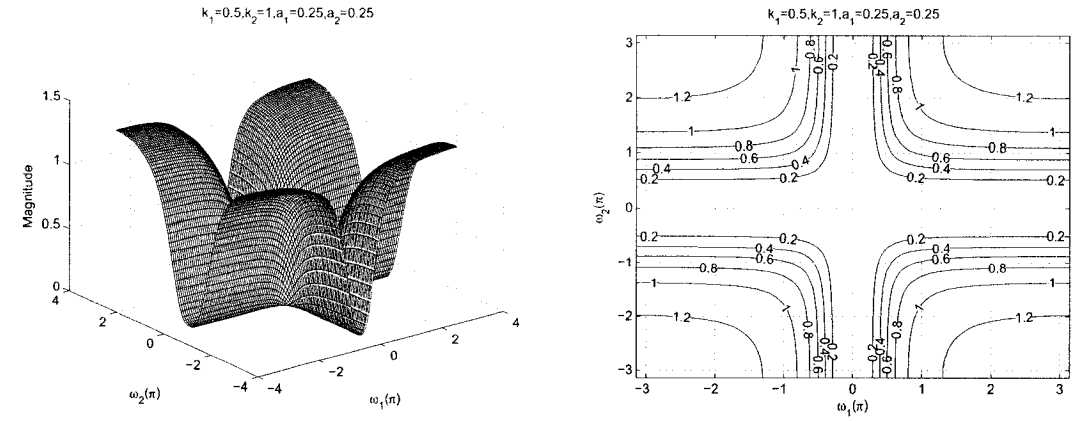

(a) $a_1 = a_2 = 0.25$ and $k_1 = 0.5$, $k_2 = 1$

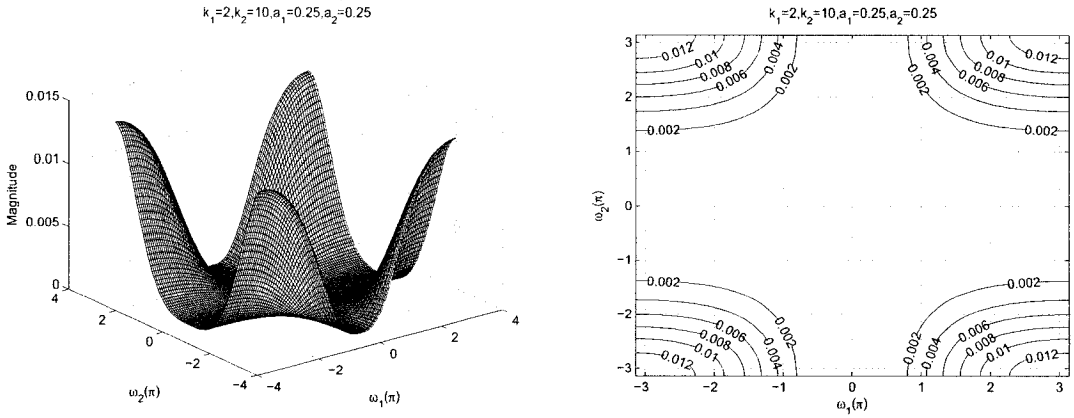

(b) $a_1 = a_2 = 0.25$ and $k_1 = 2$, $k_2 = 10$

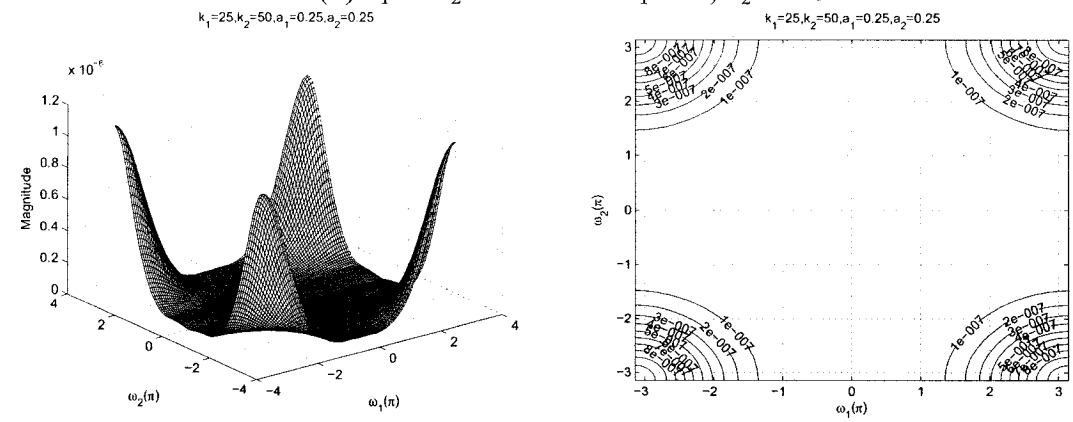

(c) $a_1 = a_2 = 0.25$ and $k_1 = 25$, $k_2 = 50$

Figure 3.59: 3-D amplitude frequency response and the contour response of the All-pole 2-D digital highpass filter for $a_1 = a_2$ and $k_1 \neq k_2$

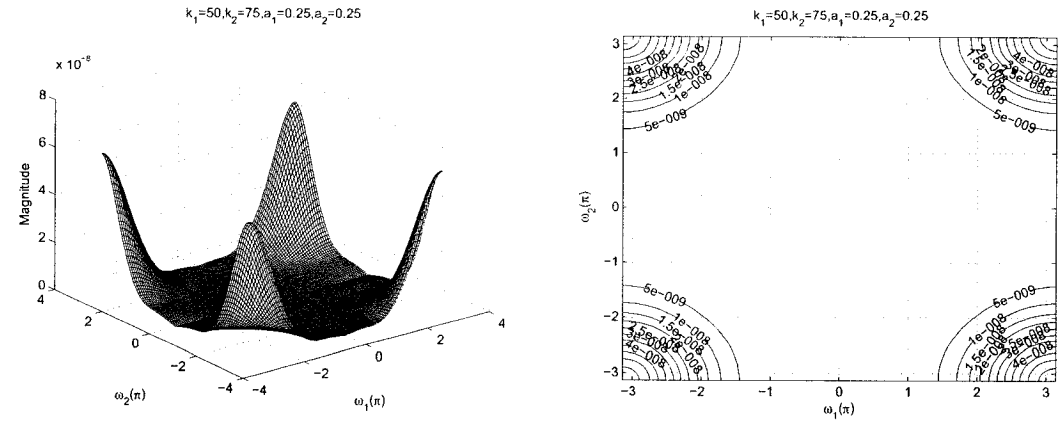

(a) $a_1 = a_2 = 0.25$ and $k_1 = 50$, $k_2 = 75$

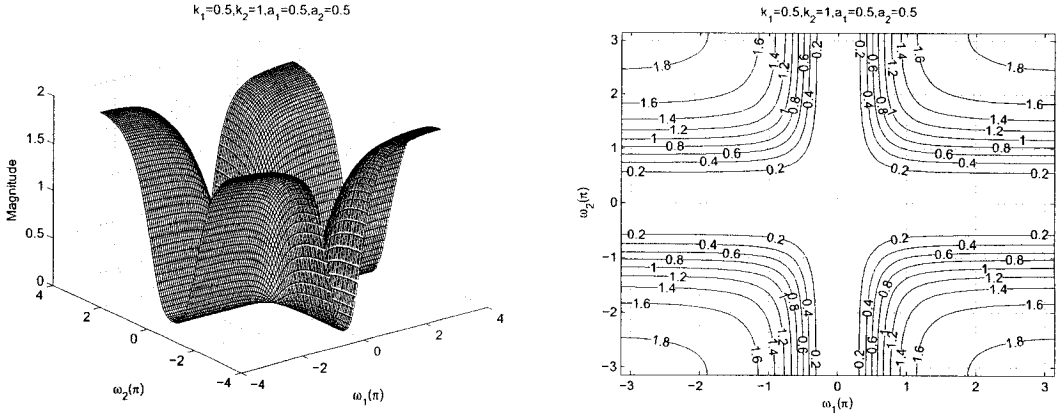

(b) $a_1 = a_2 = 0.5$ and $k_1 = 0.5$, $k_2 = 1$

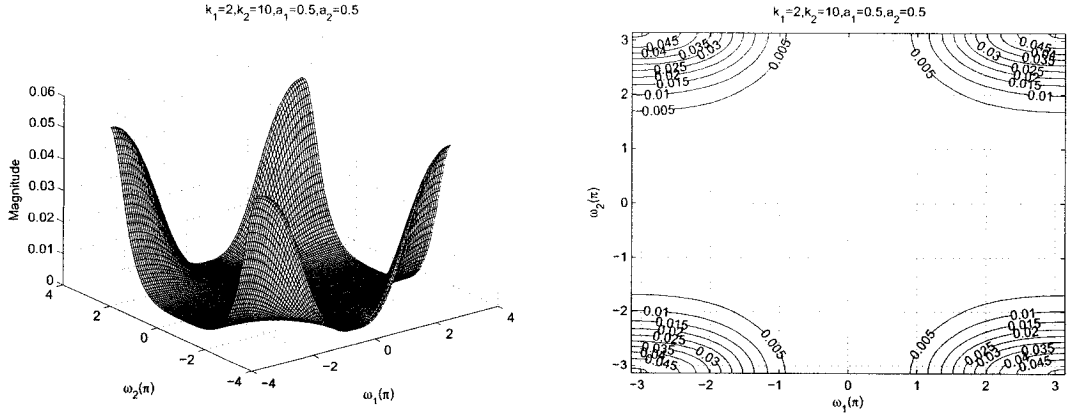

(c) $a_1 = a_2 = 0.5$ and $k_1 = 2$, $k_2 = 10$

Figure 3.60: 3-D amplitude frequency response and the contour response of the All-pole 2-D digital highpass filter for $a_1 = a_2$ and $k_1 \neq k_2$

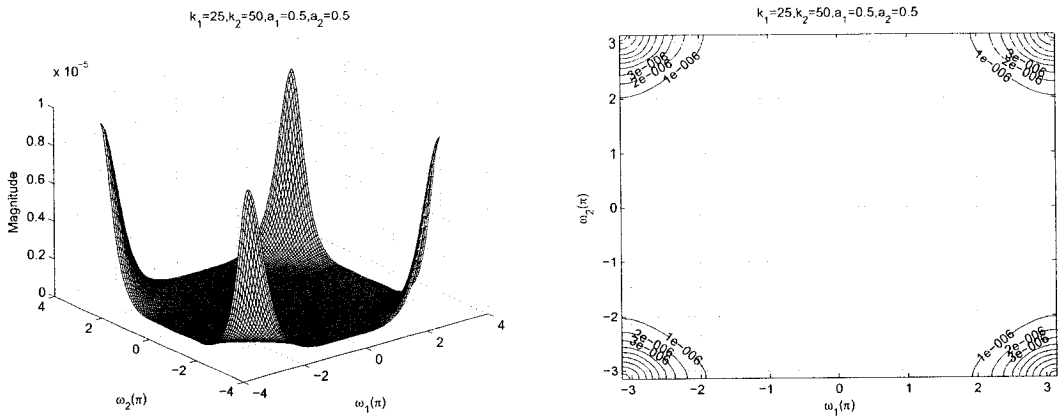

(a) $a_1 = a_2 = 0.5$ and $k_1 = 25$, $k_2 = 50$

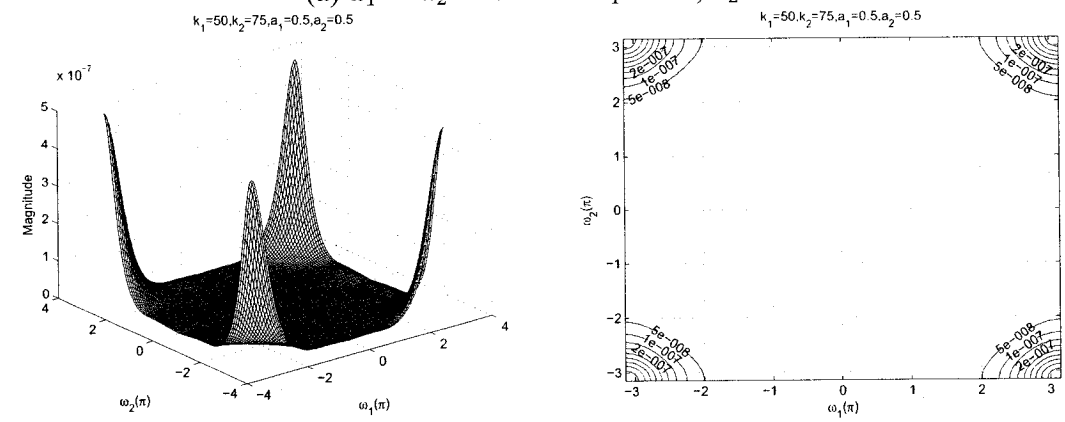

(b) $a_1 = a_2 = 0.5$ and $k_1 = 50$, $k_2 = 75$

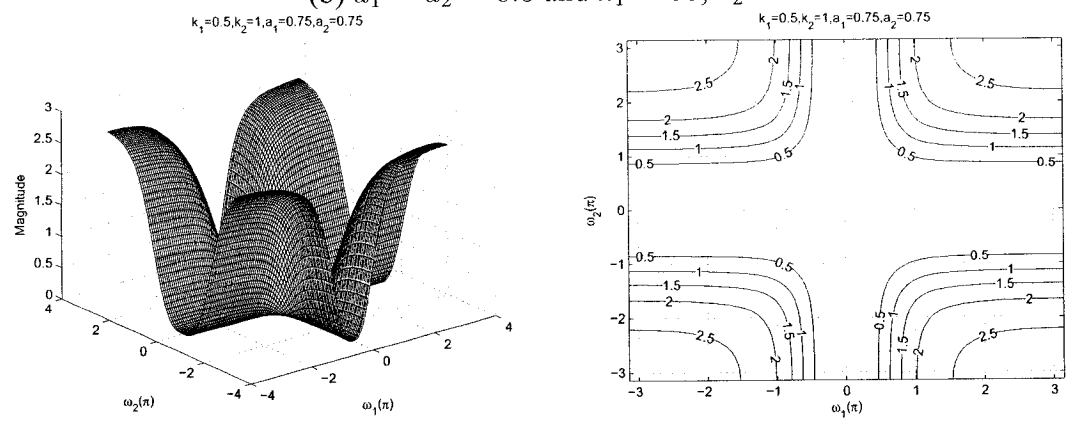

(c) $a_1 = a_2 = 0.75$ and $k_1 = 0.5$, $k_2 = 1$

Figure 3.61: 3-D amplitude frequency response and the contour response of the All-pole 2-D digital highpass filter for $a_1 = a_2$ and $k_1 \neq k_2$

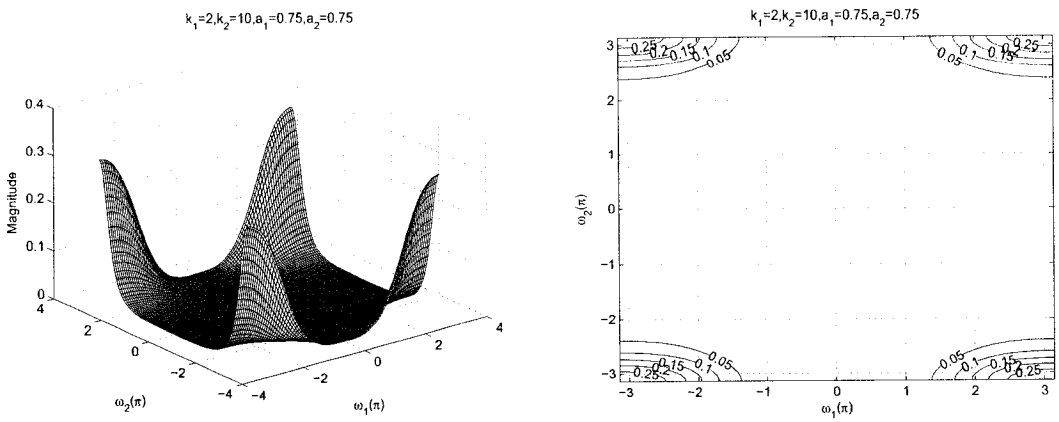

(a) $a_1 = a_2 = 0.75$ and $k_1 = 2$, $k_2 = 10$

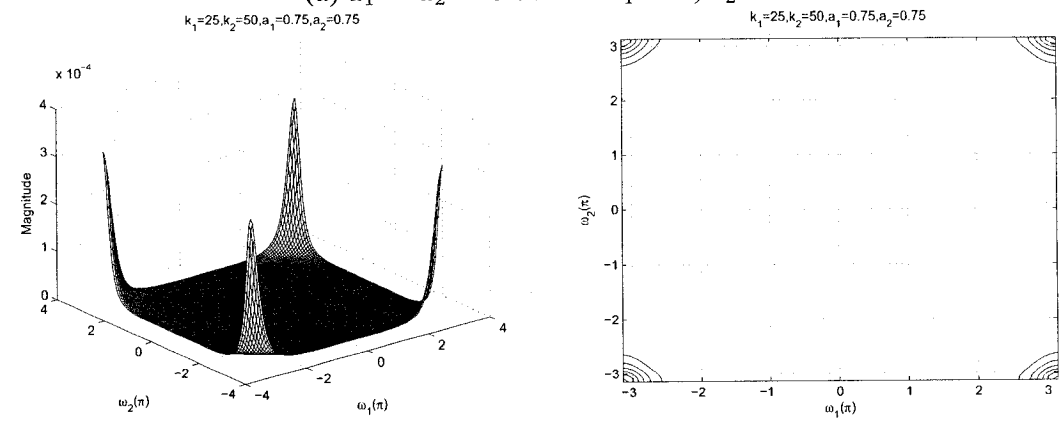

(b) $a_1 = a_2 = 0.75$ and $k_1 = 25$, $k_2 = 50$

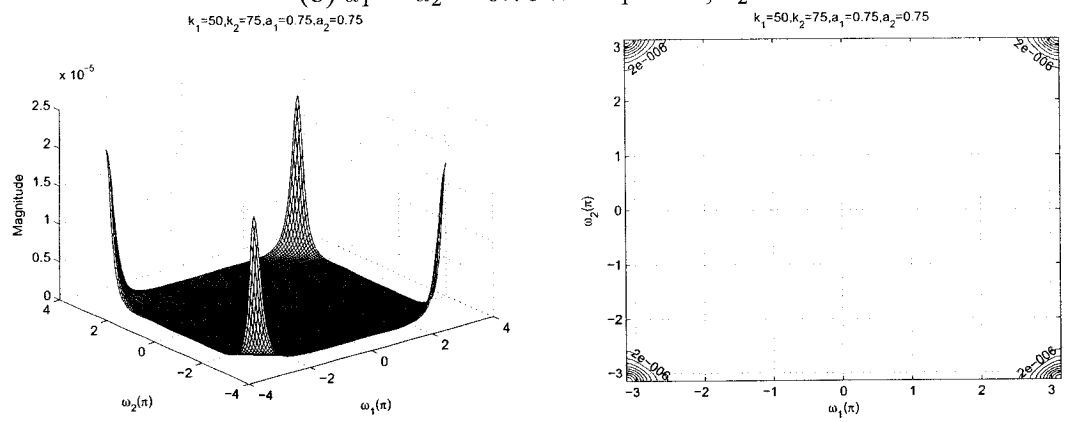

(c) $a_1 = a_2 = 0.75$ and $k_1 = 50$, $k_2 = 75$

Figure 3.62: 3-D amplitude frequency response and the contour response of the All-pole 2-D digital highpass filter for $a_1 = a_2$ and $k_1 \neq k_2$

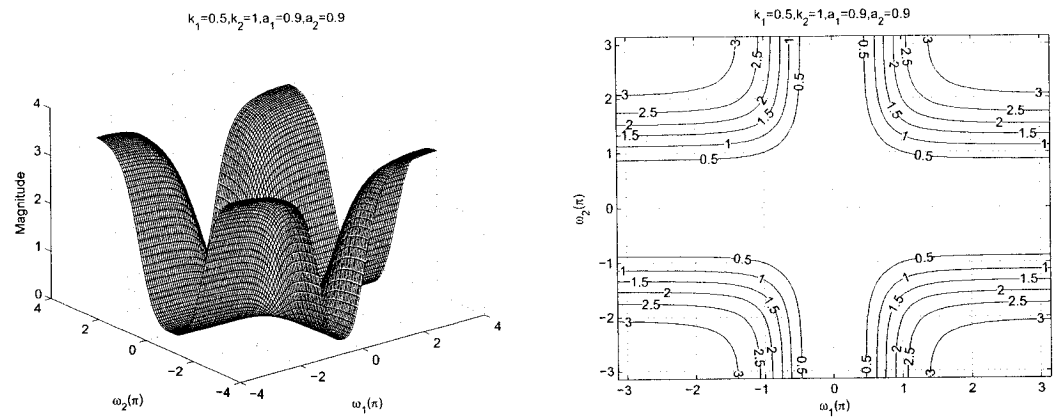

(a) $a_1 = a_2 = 0.9$ and $k_1 = 0.5$, $k_2 = 1$

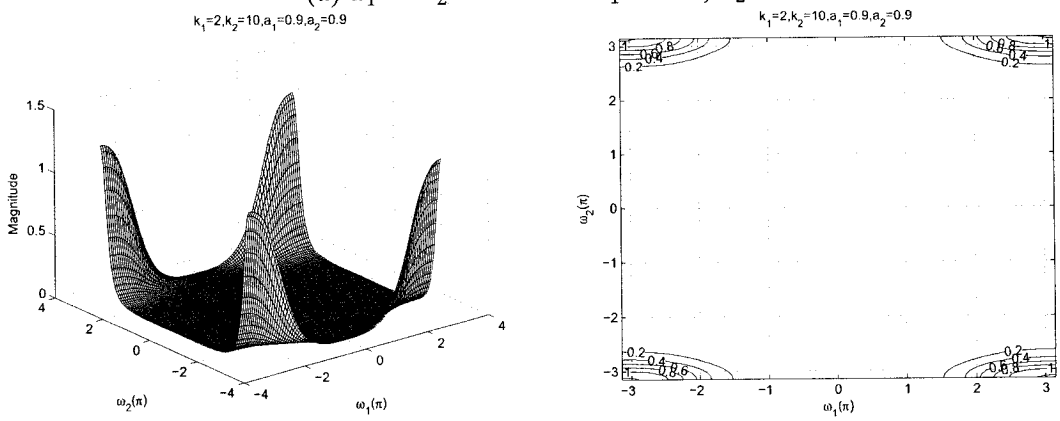

(b) $a_1 = a_2 = 0.9$ and $k_1 = 2$, $k_2 = 10$

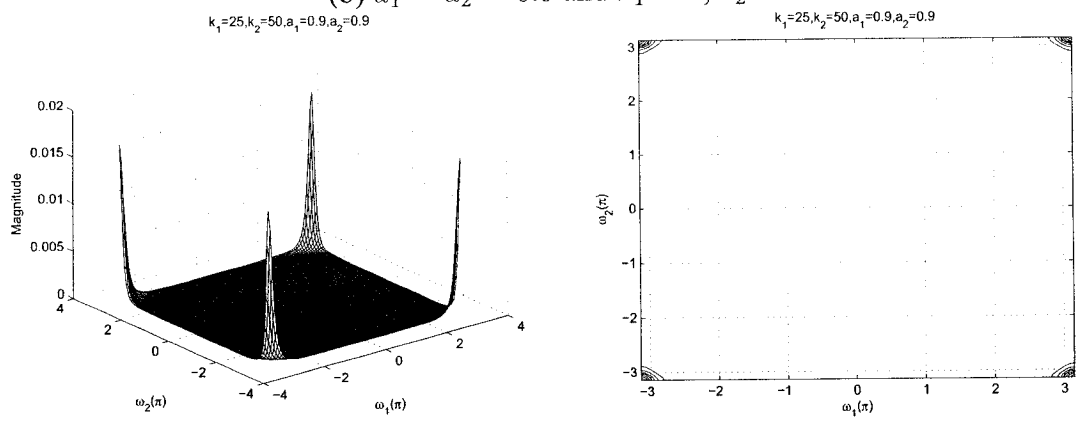

(c) $a_1 = a_2 = 0.9$ and $k_1 = 25$, $k_2 = 50$

Figure 3.63: 3-D amplitude frequency response and the contour response of the All-pole 2-D digital highpass filter for $a_1 = a_2$ and $k_1 \neq k_2$

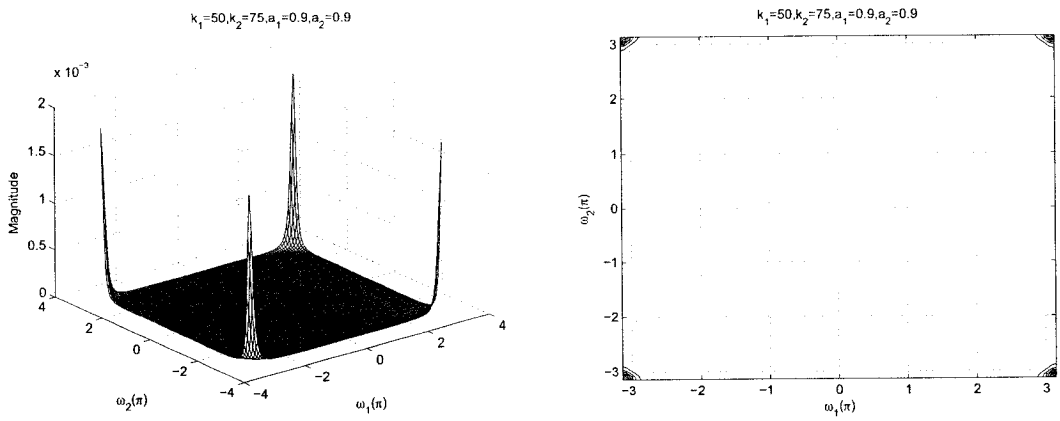

$a_1 = a_2 = 0.9$ and $k_1 = 50$, $k_2 = 75$

Figure 3.64: 3-D amplitude frequency response and the contour response of the All-pole 2-D digital highpass filter for $a_1 = a_2$ and $k_1 \neq k_2$

As observed from the Figures 3.59 to 3.64, the coefficients a_1 and a_2 affect the gain of the amplitude-frequency response. It can be clearly observed from the Figures 3.59 (a), 3.60 (b), 3.61 (c) and 3.63 (a), that the amplitude of the contour response increases from 1.2 to 3 when the values of a_1 and a_2 are increased from 0.25 to 0.9 keeping the same value of $k_1 = 0.5$ and $k_2 = 1$. In addition the width of the stopband increases for the same.

3.4 Summary

In this Chapter, we have obtain a transfer function for the 2-D analog and digital highpass filters form its equivalent 2-D lowpass filter which is obtained from the combination of the 2-D all-pass filter structures in the analog domain in Category A and B mentioned in Section 3.2. The 2-D digital transfer function has been derived from the analog transfer function using the generalized bilinear transformation and the stability conditions have been satisfied. By changing the values of the generalized bilinear transformation coefficients we can change the type and the frequency response of the 2-D digital highpass filters. Also, we have discussed the effect of the coefficients of the 2-D digital highpass

filter obtained by applying generalized bilinear transformation on the amplitude-frequency response in Category A and B mentioned in Section 3.2. The detailed analysis of the effect of each of the coefficient is discussed in Section 3.3.

In this chapter, we have discussed the effect of the coefficients of the 2-D digital high-pass filter obtained by applying generalized bilinear transformation. The detailed analysis on each of the coefficient is discussed in section 3.3.

The summary of the effect of the coefficient of the generalized bilinear transformation on 2-D digital bandpass filter in Category A are as follows:

On increasing the values of k_1 and k_2, as discussed in Sections 3.3.1.1 and 3.3.1.2 respectively, it is observed that when we increase the values of k_1 and k_2 from 0.1 to 10, the stopband width along the $\omega_1 - axis$ and $\omega_2 - axis$, respectively, gradually increases keeping the amplitude constant. On increasing the values of a_1 and a_2, as discussed in Sections 3.3.1.3 and 3.3.1.4, respectively, it is observed that when we increase the values of a_1 and a_2 from 0.1 to 1, the gain of the amplitude-response increases from 1.2 to 3.5 along the $\omega_1 - axis$ and $\omega_2 - axis$, respectively.

Sections 3.3.1.5 to 3.3.1.8 discuss the effect of the coefficients on the frequency response of the 2-D digital highpass filter, viz. $a_1 = a_2$ and $k_1 = k_2$, $a_1 \neq a_2$ and $k_1 = k_2$, $a_1 \neq a_2$ and $k_1 \neq k_2$, and $a_1 = a_2$ and $k_1 \neq k_2$ respectively. It is observed in all the four cases that the coefficients k_1, k_2 affect the stopband width and a_1, a_2 affect the gain of the amplitude-frequency response. As the values of the coefficients k_1 and k_2 are increased, the stop bandwidth increases and the amplitude of the contour response of the 2-D digital highpass filter decreases. As the values of the coefficients a_1 and a_2 are increased, the magnitude of the frequency response of the 2-D digital highpass filter increases. Also it can be seen that there are ripples in the stopband of the amplitude and the contour response when the values of the coefficients of the generalized bilinear transformation are in the range $1 < k_1,\ k_2 \leq 10$ and $a_1,\ a_2 \leq 0.5$.

The summary of the effect of the coefficient of the generalized bilinear transformation

in Category B are as follows:

On increasing the values of k_1 and k_2, as discussed in Sections 3.3.2.1 and 3.3.2.2 respectively, it is observed that when we increase the values of k_1 and k_2 from 0.1 to 10, the stopband width along the $\omega_1 - axis$ and $\omega_2 - axis$, respectively, gradually increases keeping the amplitude constant. On increasing the values of a_1 and a_2, as discussed in Sections 3.3.2.3 and 3.3.2.4, respectively, it is observed that when we increase the values of a_1 and a_2 from 0.1 to 1, the gain of the amplitude-response increases from 1.6 to 3.5 along the $\omega_1 - axis$ and $\omega_2 - axis$, respectively. At the same time the stopband width increases as we increase the values of a_1 and a_2 from 0.1 to 1 along the $\omega_1 - axis$ and $\omega_2 - axis$ respectively.

Sections 3.3.2.5 to 3.3.2.8 discuss the effect of the coefficients on the frequency response of the all-pole 2-D digital highpass filter, viz. $a_1 = a_2$ and $k_1 = k_2$, $a_1 \neq a_2$ and $k_1 = k_2$, $a_1 \neq a_2$ and $k_1 \neq k_2$, and $a_1 = a_2$ and $k_1 \neq k_2$ respectively. It is observed in all the four cases that the coefficients k_1, k_2 affect the stopband width and a_1, a_2 affect the gain of the amplitude-frequency response. As the values of the coefficients k_1 and k_2 are increased, the stop bandwidth increases and the amplitude of the contour response of the all-pole 2-D digital highpass filter decreases. As the values of the coefficients a_1 and a_2 are increased, the magnitude and the width of the stopband of the amplitude-frequency response of the all-pole 2-D digital highpass filter increases.

The comparison of the amplitude-frequency response of the 2-D highpass filter in Category A and the all-pole 2-D highpass filter in Category B is as follows:

It is observed in both the categories that the coefficients of the generalized bilinear transformation k_1, k_2 affect the stopband width and a_1, a_2 affect the gain of the amplitude-frequency response. When we observe the effect of the coefficients on the frequency response of the 2-D digital highpass filter in Sections 3.3.1.5 to 3.3.1.8 and all-pole 2-D highpass filter in Sections 3.3.2.5 to 3.3.2.8, viz. $a_1 = a_2$ and $k_1 = k_2$, $a_1 \neq a_2$ and $k_1 = k_2$, $a_1 \neq a_2$ and $k_1 \neq k_2$, and $a_1 = a_2$ and $k_1 \neq k_2$ in both the categories, it can

be seen that for the values of $1 < k_1,\ k_2 \leq 10$, and $a_1,\ a_2 \leq 0.5$ in category A, there are ripples present in the amplitude-frequency response of 2-D digital highpass in this range. Further increasing the values of $k_1,\ k_2 > 10$, the ripples tend to reduce, giving the response of the 2-D digital highpass filter. Whereas for the same values of $k_1,\ k_2$ and $a_1,\ a_2$ in category B there are no ripples present in the amplitude-frequency response of the all-pole 2-D digital highpass filter.

Thus the effect of the various combinations of the coefficients of the generalized bilinear transformation on the proposed 2-D digital highpass filters in Category A and Category B was analyzed and compared, and the selective 3-D magnitude and contour responses of the proposed 2-D digital highpass filter and all-pole 2-D digital highpass filter were plotted.

Chapter 4

All-pole 2-D Bandpass Filters using All-pass Filters

4.1 Introduction

In this chapter, the 2-D bandpass filters are analyzed. There are various methods to obtain 2-D bandpass filter from its equivalent 2-D lowpass filter. One method of obtaining 2-D digital bandpass filter is by using the combination of 2-D digital lowpass filter and 2-D digital highpass filter proposed in the previous chapters. We can obtain 2-D digital bandpass filter by cascading 2-D digital low pass filter and 2-D digital high pass filter in Category A, provided that the passband of both the filters, i.e., lowpass filter and highpass filter, overlap. Similarly, all-pole 2-D digital bandpass filter can be obtained by cascading all-pole 2-D digital lowpass filter and all-pole 2-D digital highpass filter in Category B, provided that the passband of both the filters, i.e., lowpass filter and highpass filter, overlap. In this chapter, we will propose 2-D digital bandpass filter by using the transfer functions of the 2-D digital lowpass filter and 2-D digital highpass filter proposed in Chapter 2 and Chapter 3 for both the Category A and Category B respectively.

In Section 4.2, we will proposed the transfer function for 2-D digital bandpass filters

by cascading the transfer functions of the proposed 2-D digital lowpass filters and 2-D digital highpass filters in Category A and Category B explained earlier in Chapter 2. In Section 4.3, we will discuss and analyze the effects of the coefficients of the generalized transformation of the 2-D digital bandpass filter in Category A and all-pole 2-D digital bandpass filter in Category B on the amplitude-frequency response. Section 4.4 gives the summary, discussions and comparisons of the analysis presented in this chapter.

4.2 Transfer Function of 2-D Digital Bandpass Filter

In this section, we will derive the transfer function for the 2-D bandpass filter in digital domain by cascading the transfer function of the 2-D digital lowpass filter and 2-D digital highpass filter in Category A and Category B.

4.2.1 Transfer Function of the 2-D Bandpass Filter in Category A

The analog and digital lowpass filters in Category A are proposed in Chapter 2 and are given by eqn. (2.58) and eqn. (2.60) respectively. The 2-D digital highpass filter in Category A is proposed in Chapter 3 and is given by eqn. (3.3).

The transfer function of the resultant 2-D digital bandpass filter which is obtain by cascading the 2-D digital lowpass filter (eqn. (2.60)) and 2-D digital highpass filter (eqn. (3.3)) in Category A, is given by

$$H_{BPF}(z_1, z_2) = H_{LPF}(z_1, z_2).H_{HPF}(z_1, z_2) \tag{4.1}$$

For the resulting 2-D digital bandpass filter in Category A (i.e. eqn. (4.1) to be stable, it is required that $k_i > 0$ and $0 \leq |a_i| \leq 1$. [8, 47].

4.2.2 Transfer Function of the All-pole 2-D Bandpass Filter in Category B

The all-pole analog and digital lowpass filters in Category B are proposed in Chapter 2 and are given by eqn. (2.79) and eqn. (2.80) respectively. The all-pole 2-D digital highpass filter in Category B is proposed in Chapter 3 and is given by eqn. (3.7).

The transfer function of the resultant 2-D digital bandpass filter which is obtain by cascading the 2-D digital lowpass filter (eqn. (2.80)) and 2-D digital highpass filter (eqn. (3.7)) in Category B, is given by

$$H_{BPF}(z_1, z_2) = H_{LPF}(z_1, z_2).H_{HPF}(z_1, z_2) \tag{4.2}$$

For the resulting all-pole 2-D digital bandpass filter in Category B (i.e. eqn. (4.2) to be stable, it is required that $k_i > 0$ and $0 \leq |a_i| \leq 1$. [8, 47].

4.3 Frequency Response of 2-D Digital Bandpass Filters

4.3.1 Frequency Response of 2-D Digital Bandpass Filter in Category A

The transfer function of 2-D digital bandpass filter is obtained by cascading the 2-D digital lowpass filter and 2-D digital high pass filter in Category A. With the input coefficient of the generalized bilinear transformation, we can obtain the 3-D magnitude and contour plots of the resulting 2-D digital bandpass filter [46]. In this, the stability is taken care such that the 2-D bandpass is stable with these input arguments.

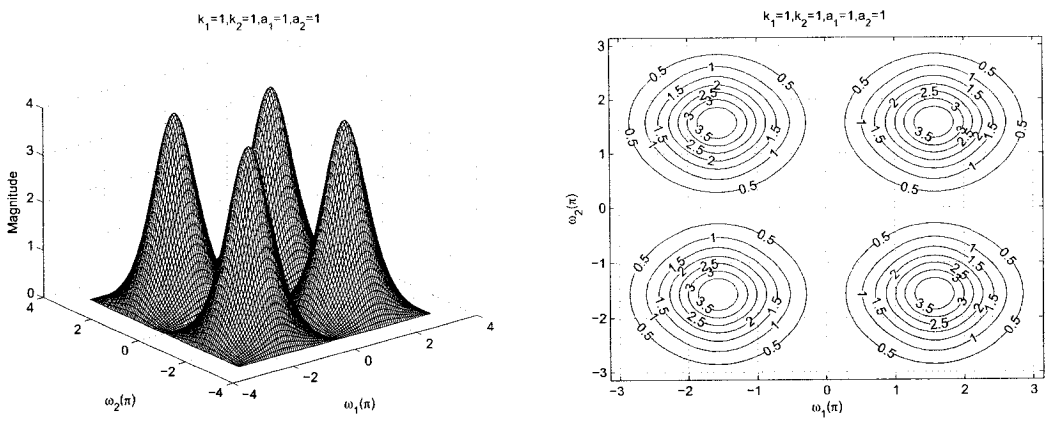

Figure 4.1: 3-D Amplitude-Frequency response and contour response of the 2-D Digital Band-pass Filter with all the coefficients values as unity

To investigate the manner in which each coefficient of the generalized bilinear transformation effects the magnitude response of the resulting 2-D digital bandpass filter, we vary the values of the coefficients or fix some of the coefficients to specific values. It is possible to obtain a 2-D digital bandpass filter when the coefficients have the following limits: $k_i > 0$, $0 \leq |b_i| \leq 1$ and $0 \leq |a_i| \leq 1$ where $i = 1, 2$. Let us consider the coefficients of the generalized bilinear transformation for the 2-D digital bandpass filter to be unity, i.e., $a_1 = 1$, $a_2 = 1$, $k_1 = 1$, and $k_2 = 1$. Under this condition, the 3-D amplitude-frequency response and the contour plots of the 2-D digital bandpass filter are shown in the Figure 4.1

In the following, we will study the effects of these coefficients to the frequency responses of the 2-D digital bandpass filter [33, 48].

4.3.1.1 Frequency Response of 2-D Digital Bandpass Filter with different values of k_1

In this section, we study the manner in which k_1 affects the frequency response behavior of the resulting 2-D digital bandpass filter in Category A and to separate the effect of the other coefficients, we vary the value of k_1, and fix all the other coefficients of the generalized bilinear transformation to unity, e.g. with $k_2 = 1$, $a_1 = 1$, $a_2 = 1$. This was done so that no generality is lost and to make the situation simple. The values of k_1 are varied from 0.1 to

5 and the 3-D magnitude response and the contour plots for the 2-D digital bandpass filter with the values of $k_1 = 0.1$, $k_1 = 0.5$, $k_1 = 0.9$, $k_1 = 2$, and $k_1 = 5$, are shown in the Figures 4.2 and 4.3.

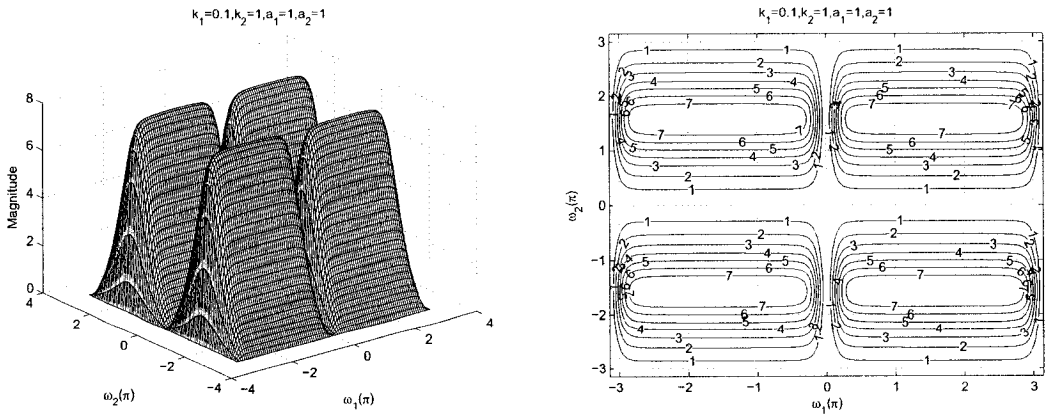

(a) $k_1 = 0.1$

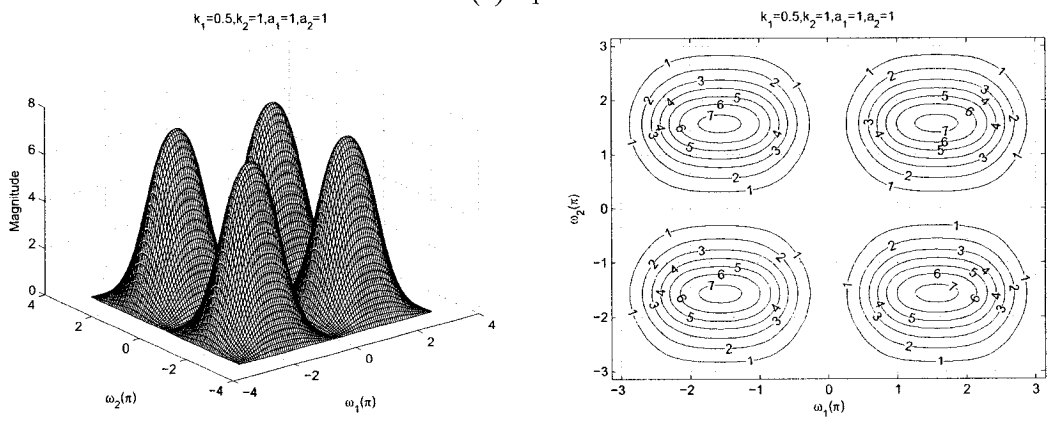

(b) $k_1 = 0.5$

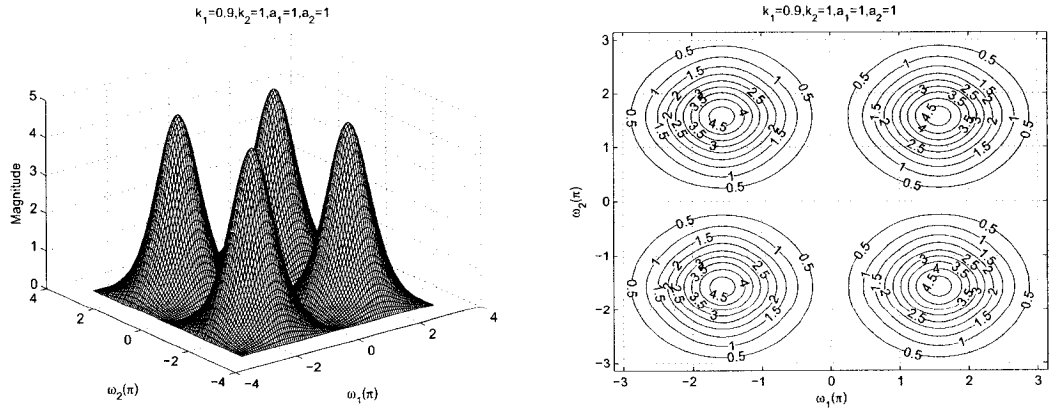

(c) $k_1 = 0.9$

Figure 4.2: 3-D amplitude frequency response and the contour response of the 2-D digital bandpass filter for different values of k_1

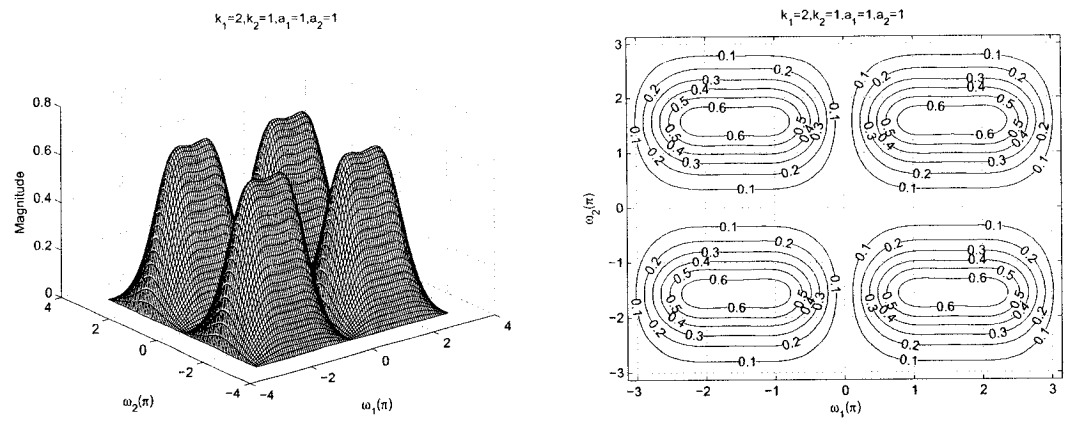

(a) $k_1 = 2$

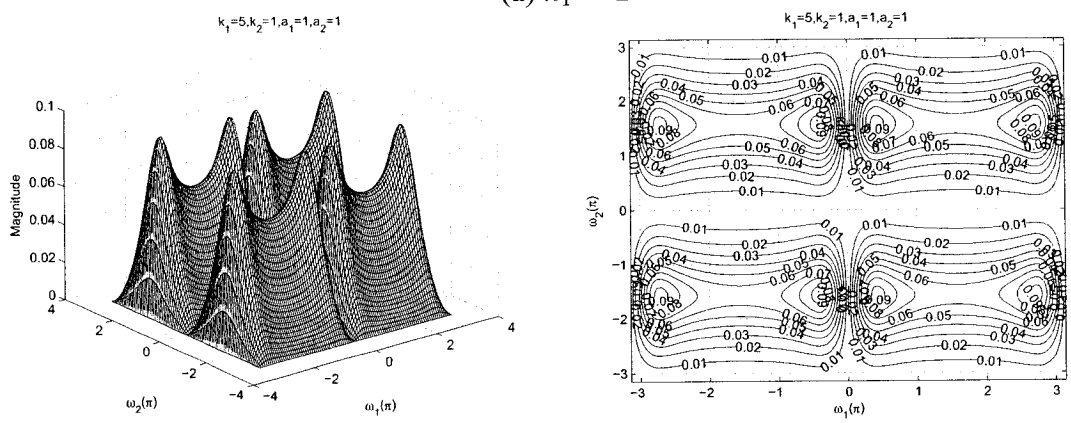

(b) $k_1 = 5$

Figure 4.3: 3-D amplitude frequency response and the contour response of the 2-D digital bandpass filter for different values of k_1

It is observed that although the coefficient k_1 does not have any effect on the passband width along the $\omega_2 - axis$, it affects the passsband width along the $\omega_1 - axis$. Initially when the value of the coefficient $k_1 = 0.1$ (see Figure 4.2(a)) the passband width is maximum along $\omega_1 - axis$ and at the same time it has maximum magnitude. As we increase the value of k_1 from 0.1 to 5, the passband width along the $\omega_1 - axis$ gradually decreases and at the same time the magnitude of the contour response also decreases from 7 to 0.09. Also, it can be seen that there are ripples in the passband of the amplitude and contour response when the values of $1 < k_1 \leq 5$.

4.3.1.2 Frequency Response of 2-D Digital Bandpass Filter with different values of k_2

In this section, we study the manner in which k_2 affects the frequency response behavior of the resulting 2-D digital bandpass filter in Category A and to separate the effect of the other coefficients, we vary the value of k_2, and fix all the other coefficients of the generalized bilinear transformation to unity, e.g. with $k_1 = 1, a_1 = 1, a_2 = 1$. This was done so that no generality is lost and to make the situation simple. The values of k_2 are varied from 0.1 to 5 and the 3-D magnitude response and the contour plots for the 2-D digital bandpass filter with the values of $k_2 = 0.1$, $k_2 = 0.5$, $k_2 = 0.9$, $k_2 = 2$, and $k_2 = 5$, are shown in the Figures 4.4 and 4.5.

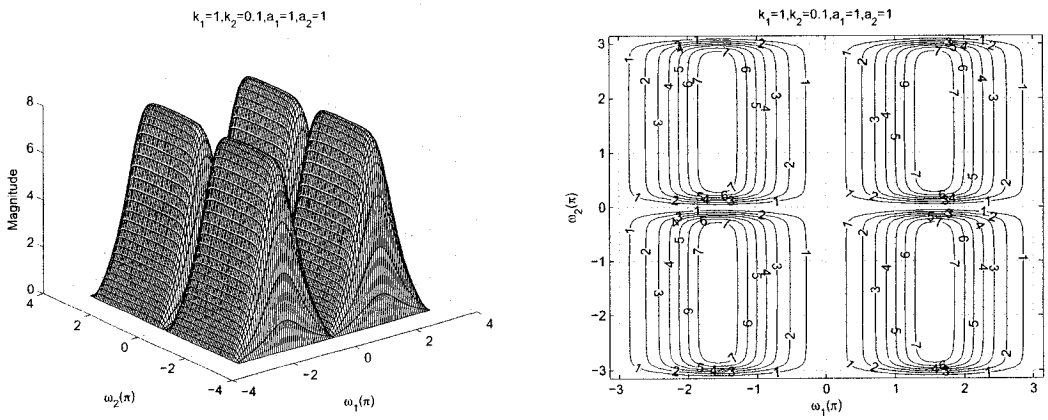

(a) $k_2 = 0.1$

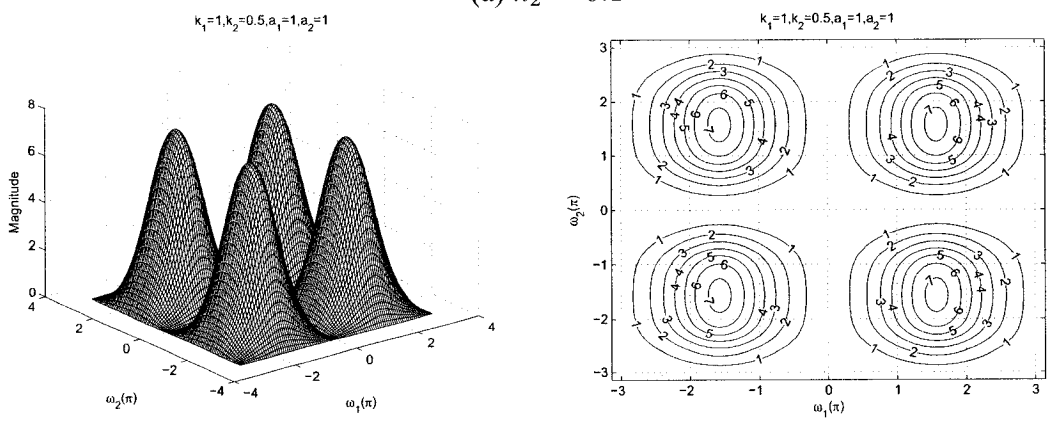

(b) $k_2 = 0.5$

Figure 4.4: 3-D amplitude frequency response and the contour response of the 2-D digital bandpass filter for different values of k_2

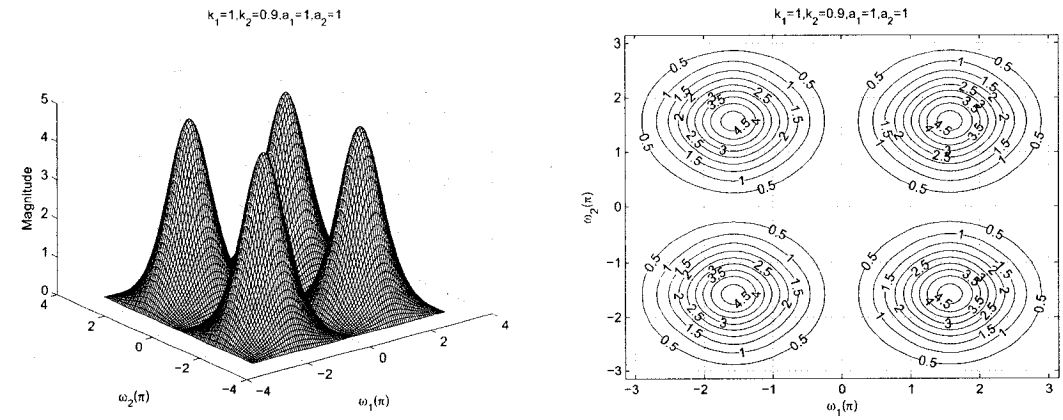

(a) $k_2 = 0.9$

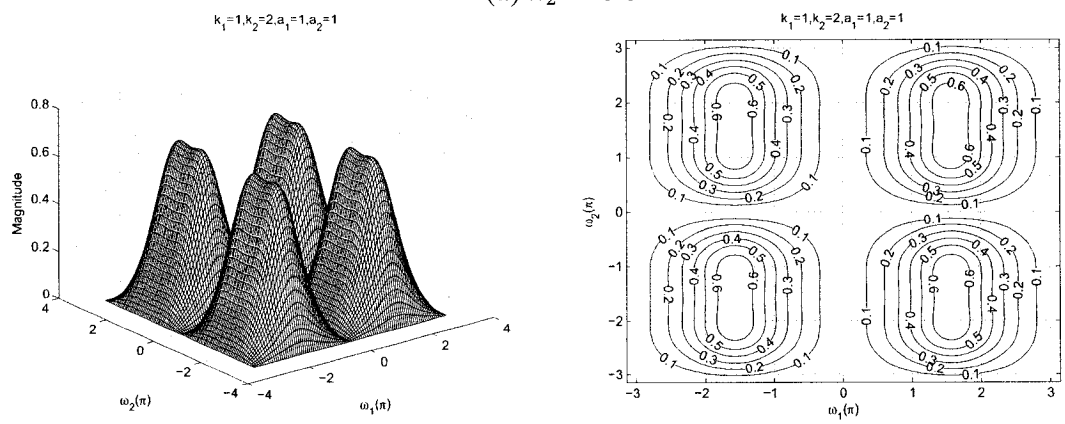

(b) $k_2 = 2$

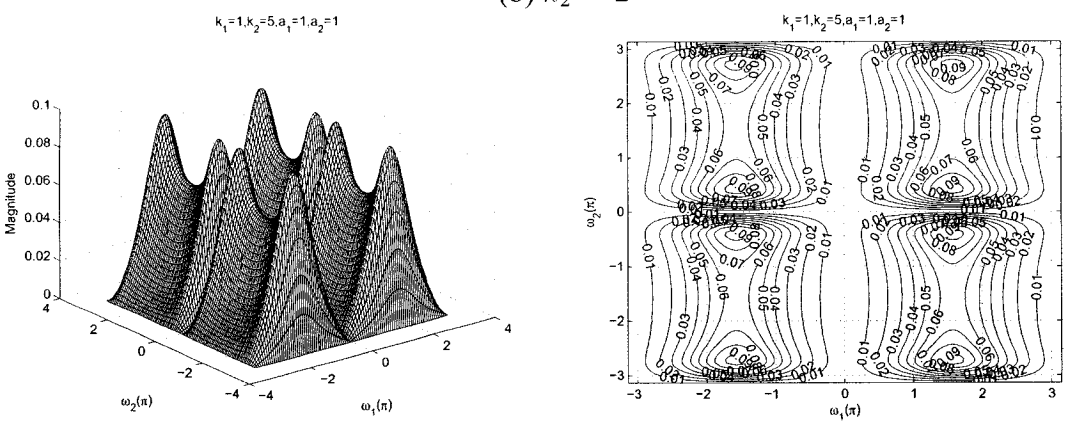

(c) $k_2 = 5$

Figure 4.5: 3-D amplitude frequency response and the contour response of the 2-D digital bandpass filter for different values of k_2

It is observed that although the coefficient k_2 does not have any effect on the passband width along the $\omega_1 - axis$, it affects the passsband width along the $\omega_2 - axis$. Initially when the value of the coefficient $k_2 = 0.1$ (see Figure 4.4 (a)) the passband width is maximum

along $\omega_2 - axis$ and at the same time it has maximum magnitude. As we increase the value of k_2 from 0.1 to 5, the passband width along the $\omega_2 - axis$ gradually decreases and at the same time the magnitude of the contour response also decreases from 7 to 0.09 . Also, it can be seen that there are ripples in the passband of the amplitude and contour response when the values of $1 < k_2 \leq 5$.

4.3.1.3 Frequency Response of 2-D Digital Bandpass Filter with different values of a_1

In the Sections 4.3.1.1 and 4.3.1.2, the effect of the coefficient of k_1 and k_2 are studied. In this section, the effect of the coefficient a_1 is studied. The stable range of a_1 can be obtained with other specified coefficients of the generalized bilinear transformation. There are many combinations possible for the coefficients. To study the response with different values of a_1 properly, we fix other coefficients values to be equal to unity. The range of a_1 varies from 0.1 to 1 and the other coefficient values are specified as unity, i.e., $k_1 = 1$, $k_2 = 1$, $a_2 = 1$, $b_1 = 1$ and $b_2 = 1$ in order to get 2-D digital bandpass filter response in Category A.

By varying the value of a_1, the 3-D magnitude response and contour plots which represents different values of a_1, i.e. $a_1 = 0.1$, $a_1 = 0.25$, $a_1 = 0.5$, $a_1 = 0.75$, and $a_1 = 0.9$ are shown in the Figures 4.6 and 4.7. By making the value of $a_1 = 1$, it resembles the standard 2-D digital bandpass filter as shown in the Figure 4.1. It is observed from the diagrams that the coefficient a_1 affects the gain of the amplitude-frequency response. At the lowest value of $a_1 = 0.1$, the gain of the amplitude-frequency response is 0.9. As the value of a_1 increases, the gain increases and reach the maximum value at $a_1 = 1$. As seen from the diagrams that as we increase the value of a_1 from 0.1 to 0.9, the gain of the amplitude-frequency response increases from 0.9 to 3.5. Also, the coefficient a_1 does not have any effect along the $\omega_2 - axis$.

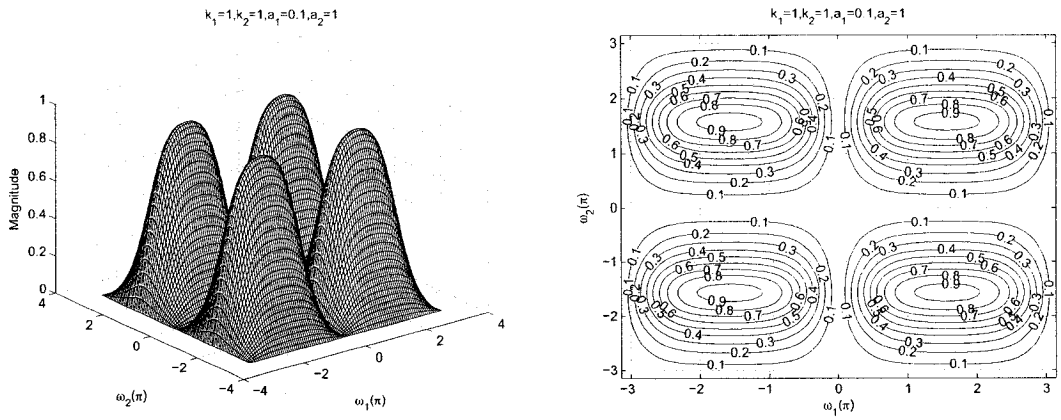

(a) $a_1 = 0.1$

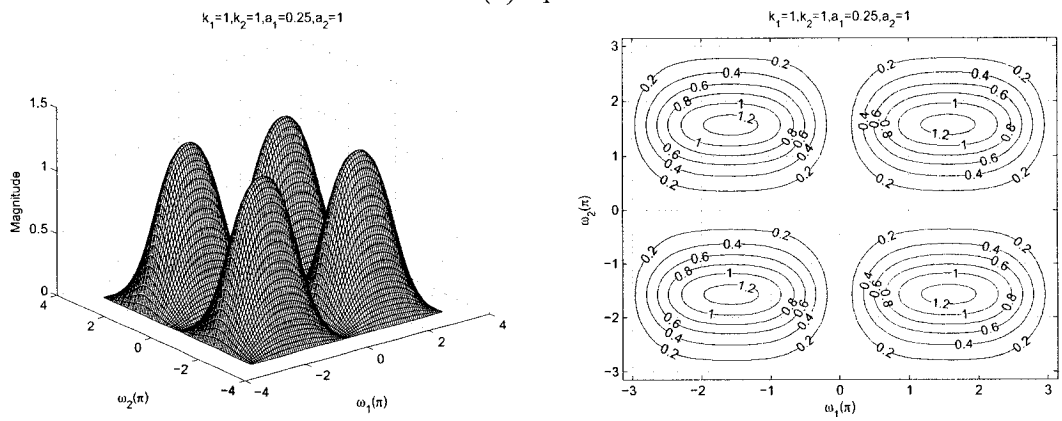

(b) $a_1 = 0.25$

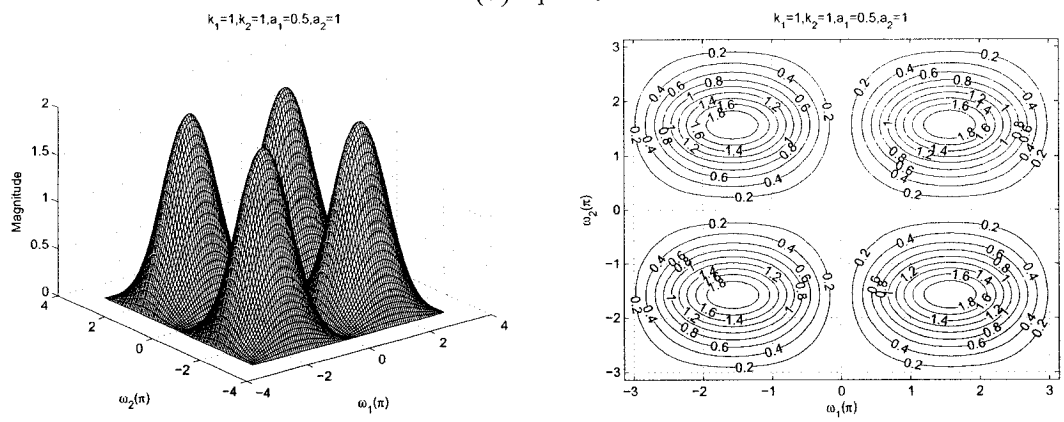

(c) $a_1 = 0.5$

Figure 4.6: 3-D amplitude frequency response and the contour response of the 2-D digital bandpass filter for different values of a_1

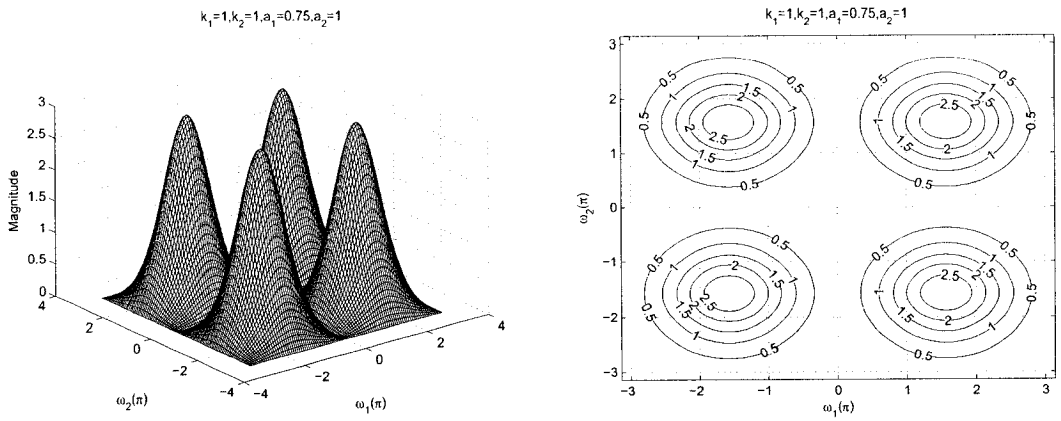

(a) $a_1 = 0.75$

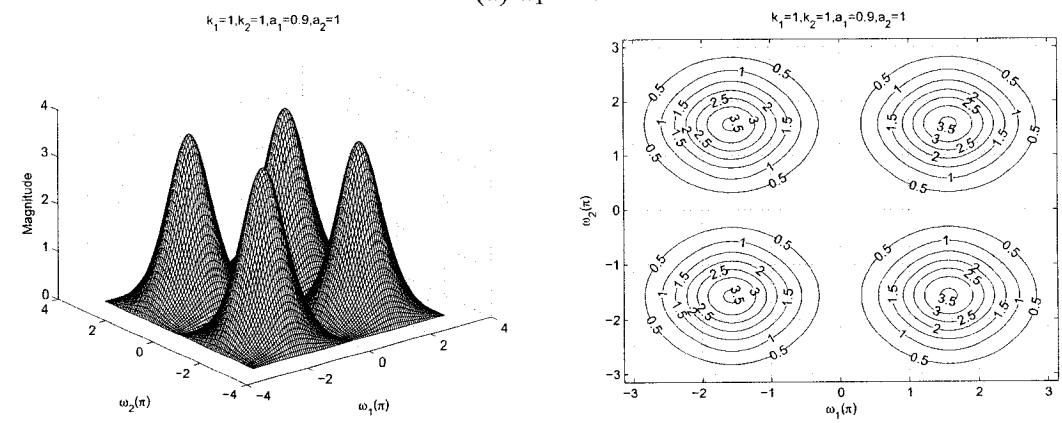

(b) $a_1 = 0.9$

Figure 4.7: 3-D amplitude frequency response and the contour response of the 2-D digital bandpass filter for different values of a_1

4.3.1.4 Frequency Response of 2-D Digital Bandpass Filter with different values of a_2

In the Section 4.3.1.3, the effect of the coefficient of a_1 was studied. In this section, the effect of the coefficient a_2 will be studied. The stable range of a_2 can be obtained with other specified coefficients of the generalized bilinear transformation. There are many combinations possible for the coefficients. To study the response with different values of a_2 properly, we fix other coefficient values to be equal to unity. The range of a_2 varies from 0.1 to 1 and the other coefficient values are specified as unity, i.e., $k_1 = 1$, $k_2 = 1$, $a_1 = 1$, $b_1 = 1$ and $b_2 = 1$ in order to get 2-D digital bandpass filter response in Category A.

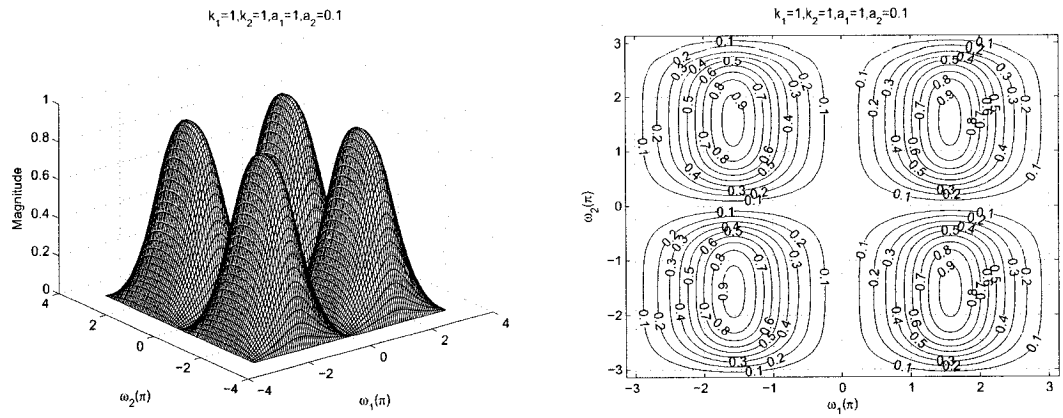

(a) $a_2 = 0.1$

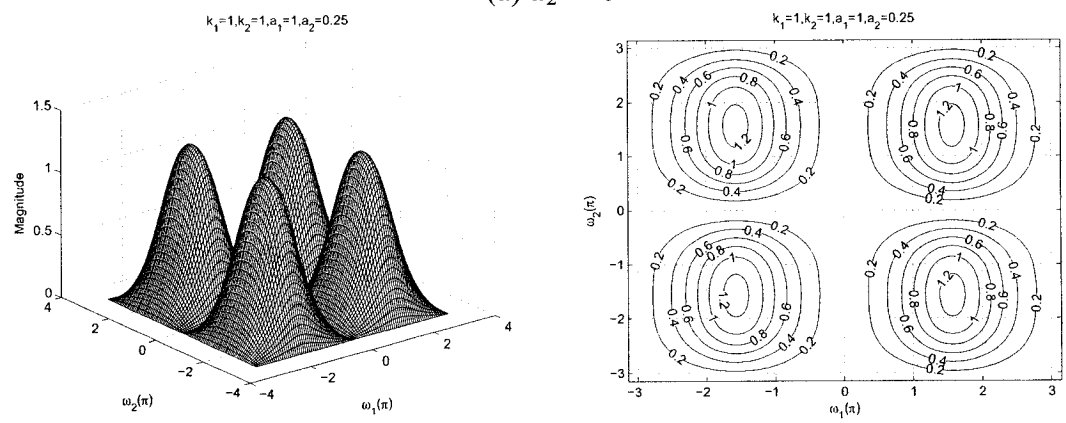

(b) $a_2 = 0.25$

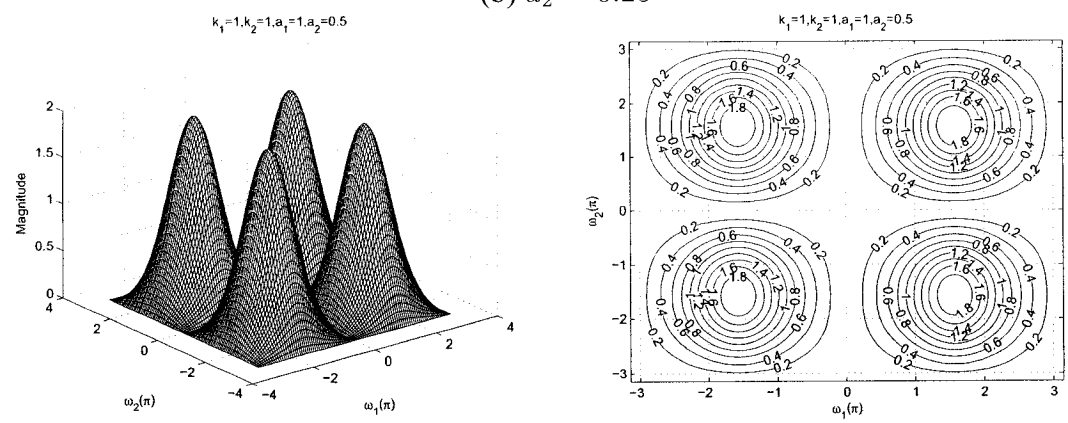

(c) $a_2 = 0.5$

Figure 4.8: 3-D amplitude frequency response and the contour response of the 2-D digital bandpass filter for different values of a_2

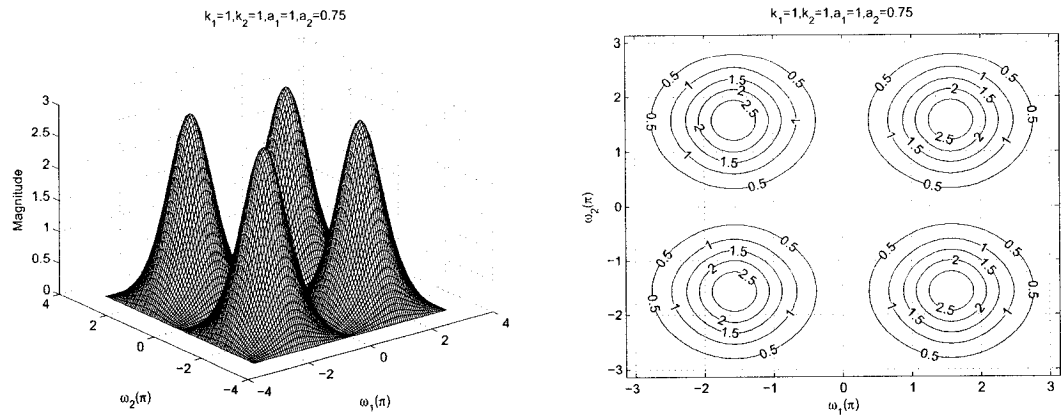

(a) $a_2 = 0.75$

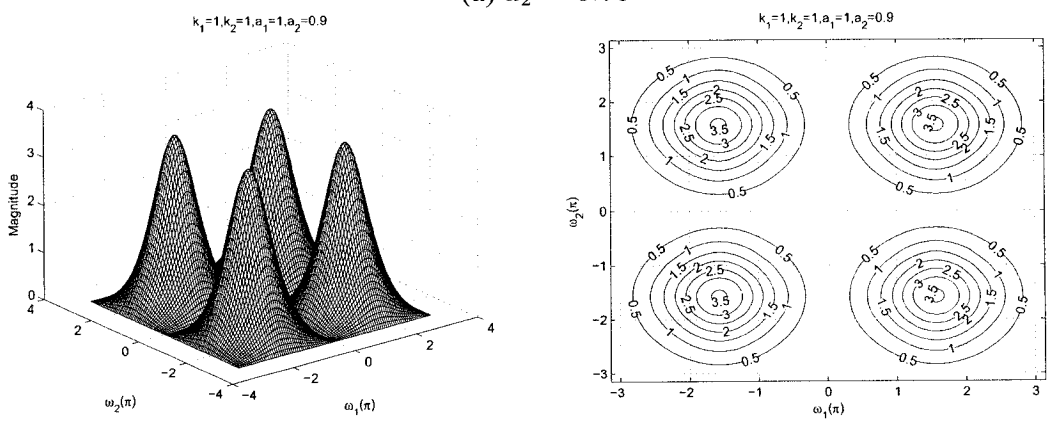

(b) $a_2 = 0.9$

Figure 4.9: 3-D amplitude frequency response and the contour response of the 2-D digital bandpass filter for different values of a_2

By varying the value of a_2, the 3-D magnitude response and contour plots which represents different values of a_2, i.e., $a_2 = 0.1$, $a_2 = 0.25$, $a_2 = 0.5$, $a_2 = 0.75$, and $a_2 = 0.9$ are shown in the Figures 4.8 and 4.9. By making the value of $a_2 = 1$, it resembles the standard 2-D digital bandpass filter as shown in the Figure 4.1. It is observed from the diagrams that the coefficient a_2 affects the gain of the amplitude-frequency response. At the lowest value of $a_2 = 0.1$, the gain of the amplitude-frequency response is 0.9. As the value of a_2 increases, the gain increases and reach the maximum value at $a_2 = 1$. As seen from the diagrams that as we increase the value of a_2 from 0.1 to 0.9, the gain of the amplitude-frequency response increases from 0.9 to 3.5. Also, the coefficient a_2 does not have any effect along the $\omega_1 - axis$.

4.3.1.5 Frequency Response of 2-D Digital Bandpass Filter with same values of a_1 and a_2 and same values of k_1 and k_2

In the Sections 4.3.1.1 to 4.3.1.4 the individual effect of the coefficients a_1, a_2, k_1 and k_2 were studied. In this section, we will study the effect of coefficients, where $a_1 = a_2$ and $k_1 = k_2$ and the remaining coefficients b_1 and b_2 are considered to be unity for the 2-D digital bandpass filter in Category A. The values of a_1 and a_2 ranges from 0 to 1 and the values of k_1 and k_2 ranges from 0 to 5.

As observed from the Figures 4.10 to 4.13, the coefficients k_1 and k_2 affect the passband width of the frequency response. In the Figures 4.10 (a), 4.11 (b) and 4.12 (c), there is a gradual decrease in the passband width of the contour response as the values of k_1 and k_2 are increased from 0.5 to 5 for the same values of $a_1 = a_2 = 0.25$. It is also observed that there is also a decrease in the magnitude of the contour response for the same.

As observed from the Figures 4.10 to 4.13, the coefficients a_1 and a_2 affect the gain of the amplitude-frequency response. It can be clearly observed from the Figures 4.10 (a), (b), (c) and 4.11 (a), that the gain of the amplitude-frequency response increases from 2.5 to 10 when the values of a_1 and a_2 are increased from 0.25 to 0.9 keeping the same value of $k_1 = k_2 = 0.5$. In addition, the width of the passband increases and decreases periodically for the same. There are ripples in the contour response for the values of a_1, $a_2 = 0.9$ and k_1, $k_2 = 5$ as shown in the Figure 4.13 (c).

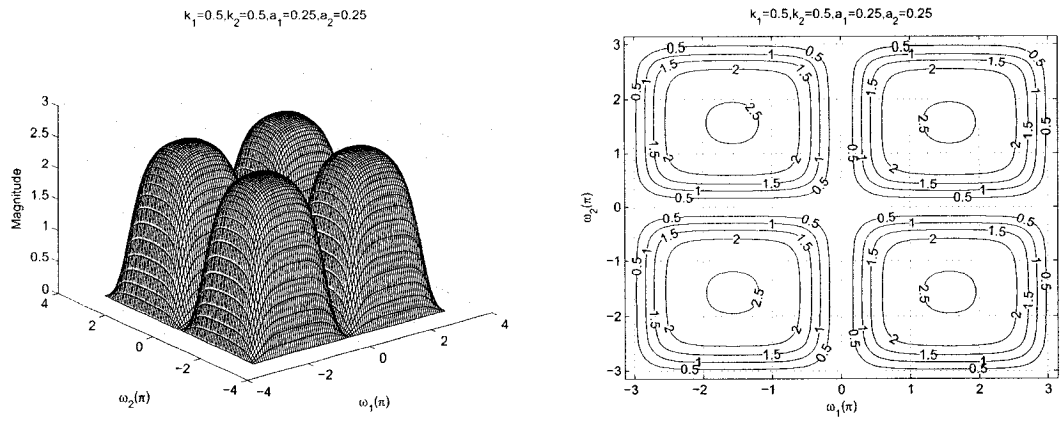

(a) $a_1 = a_2 = 0.25$ and $k_1 = k_2 = 0.5$

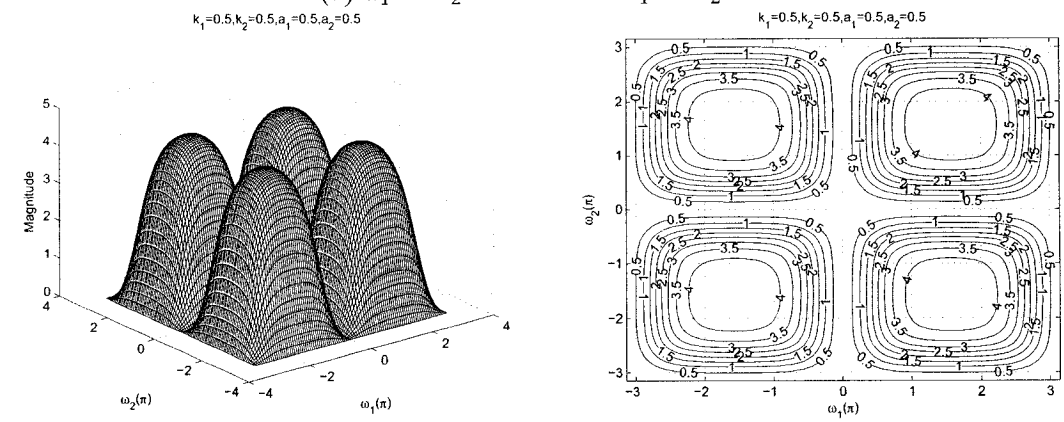

(b) $a_1 = a_2 = 0.5$ and $k_1 = k_2 = 0.5$

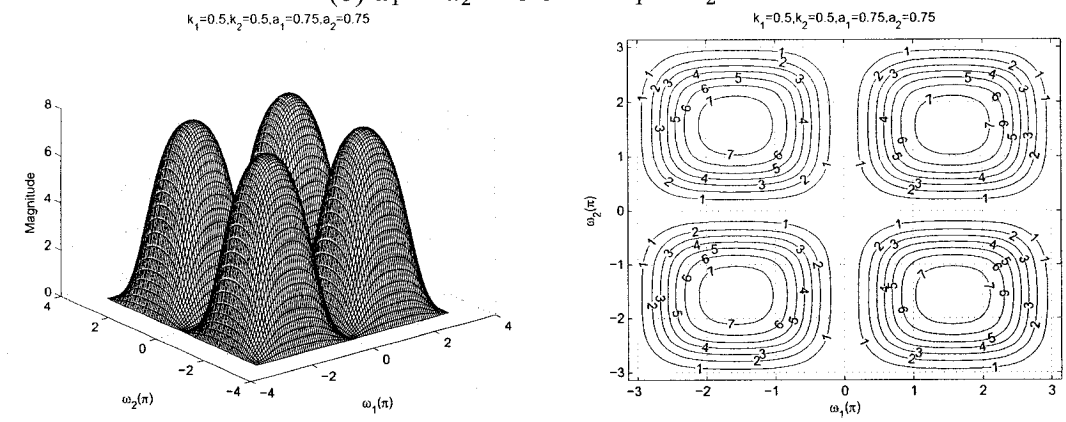

(c) $a_1 = a_2 = 0.75$ and $k_1 = k_2 = 0.5$

Figure 4.10: 3-D amplitude frequency response and the contour response of the 2-D digital bandpass filter for $a_1 = a_2$ and $k_1 = k_2$

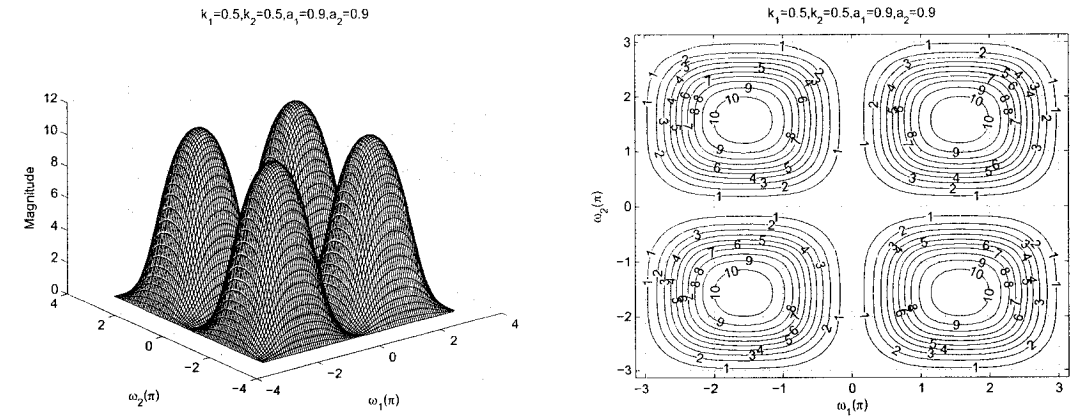

(a) $a_1 = a_2 = 0.9$ and $k_1 = k_2 = 0.9$

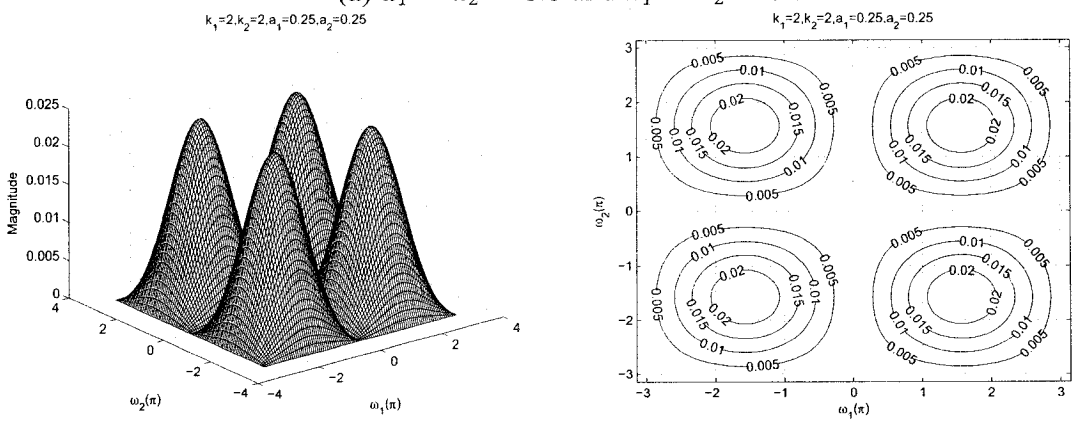

(a) $a_1 = a_2 = 0.25$ and $k_1 = k_2 = 2$

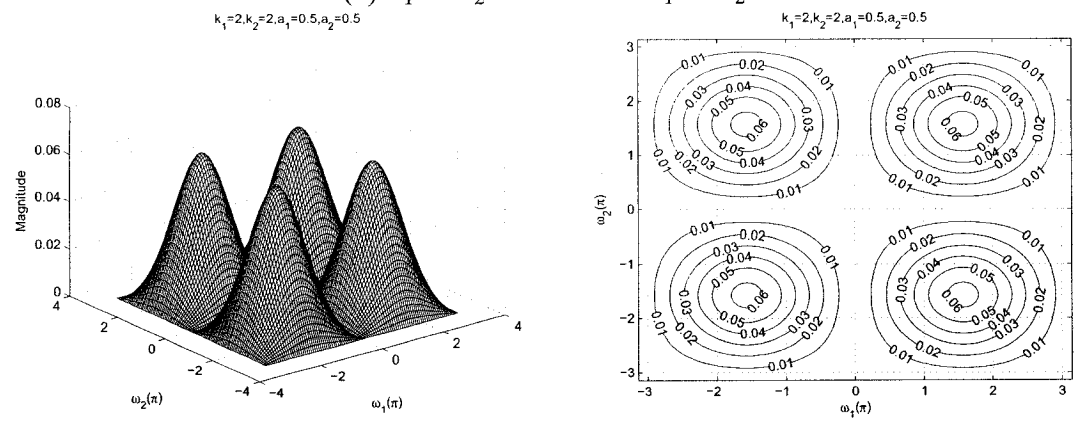

(c) $a_1 = a_2 = 0.5$ and $k_1 = k_2 = 2$

Figure 4.11: amplitude 3-D frequency response and the contour response of the 2-D digital bandpass filter for $a_1 = a_2$ and $k_1 = k_2$

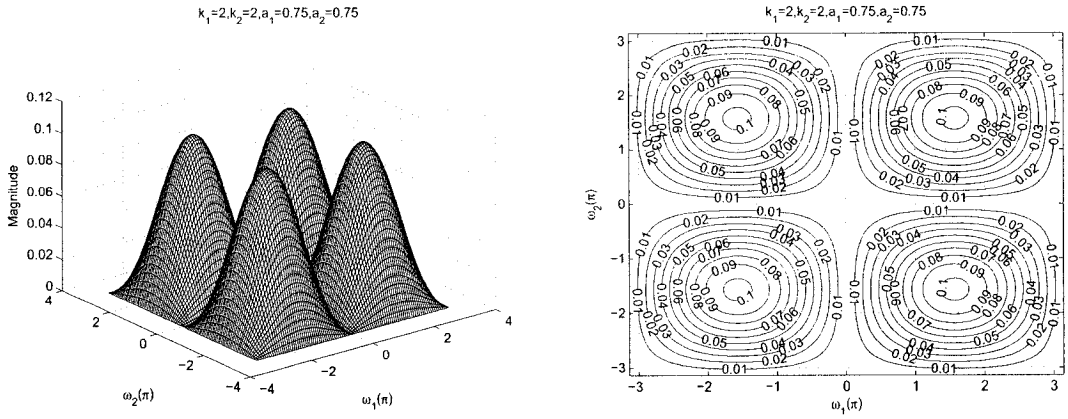

(a) $a_1 = a_2 = 0.75$ and $k_1 = k_2 = 2$

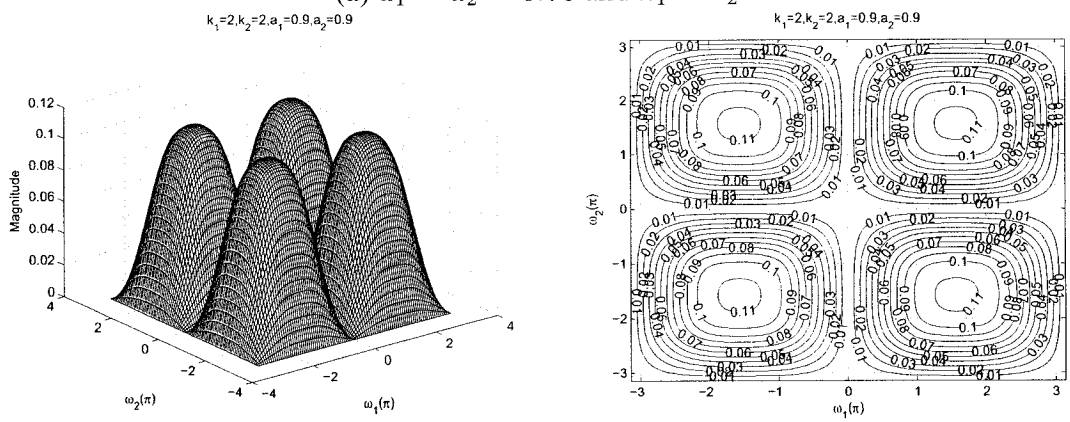

(b) $a_1 = a_2 = 0.9$ and $k_1 = k_2 = 2$

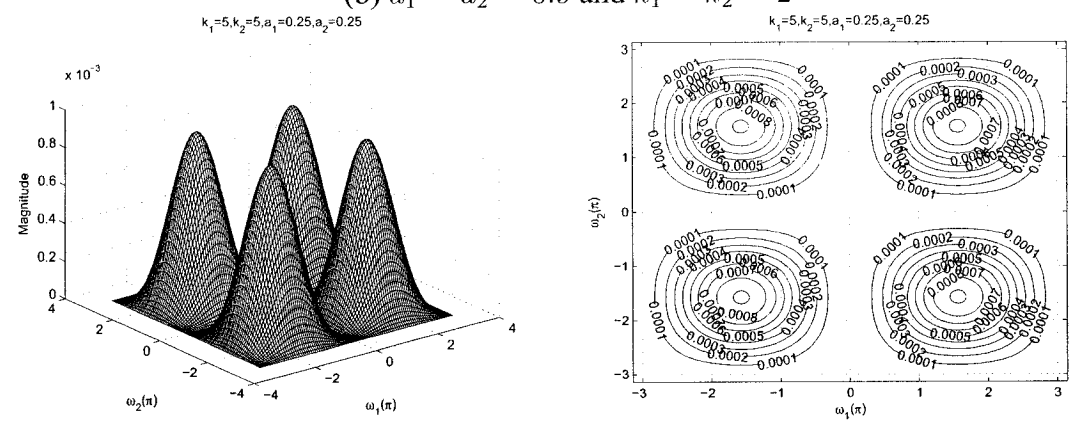

(c) $a_1 = a_2 = 0.25$ and $k_1 = k_2 = 5$

Figure 4.12: 3-D amplitude frequency response and the contour response of the 2-D digital bandpass filter for $a_1 = a_2$ and $k_1 = k_2$

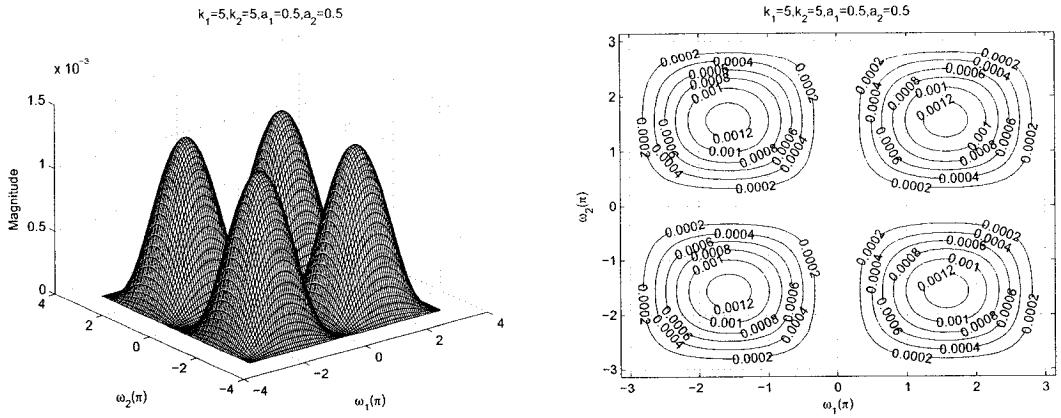

(a) $a_1 = a_2 = 0.5$ and $k_1 = k_2 = 5$

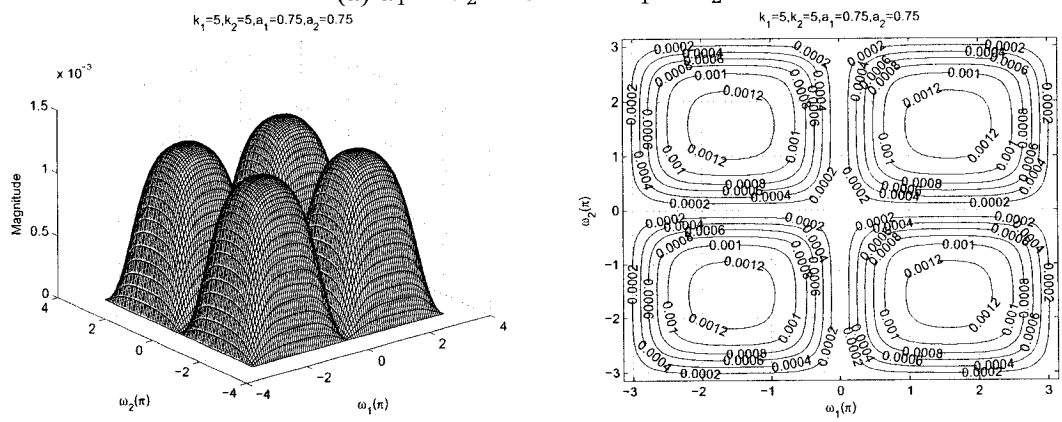

(b) $a_1 = a_2 = 0.75$ and $k_1 = k_2 = 5$

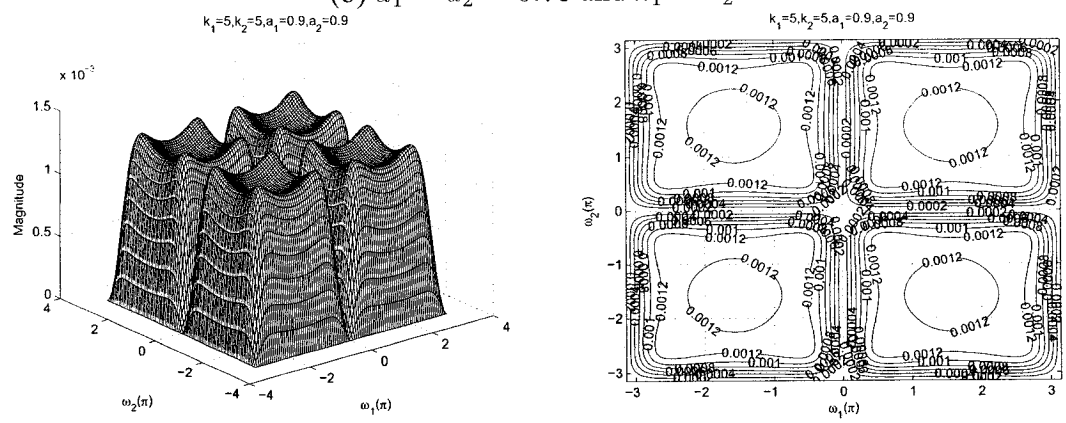

(c) $a_1 = a_2 = 0.9$ and $k_1 = k_2 = 5$

Figure 4.13: 3-D amplitude frequency response and the contour response of the 2-D digital bandpass filter for $a_1 = a_2$ and $k_1 = k_2$

4.3.1.6 Frequency Response of 2-D Digital Bandpass Filter with different values of a_1 and a_2 and same values of k_1 and k_2

In this section, we will study the effect of coefficients, where $a_1 \neq a_2$ and $k_1 = k_2$ and the remaining coefficients b_1 and b_2 are considered to be unity for the 2-D digital band-pass filter in Category A. The values of a_1 ranges from 0.25 to 0.5 and a_2 ranges from 0.5 to 0.75, and the values of k_1 and k_2 ranges from 0.5 to 5.

As observed from the Figures 4.14 to 4.17, the coefficients k_1 and k_2 affect the passband width of the frequency response of the 2-D digital bandpass filter. In the Figures 4.14 (a), 4.15 (a), 4.16 (a) and 4.17 (a), there is a gradual decrease in the passband width of the contour response as the values of k_1 and k_2 are increased from 0.5 to 5 for different values of $a_1 = 0.25$ and $a_2 = 0.5$. At the same time there is a gradual decrease in the magnitude of the contour response for the same values.

As observed from the Figures 4.14 to 4.17, the coefficients a_1 and a_2 affect the gain of the amplitude-frequency response. It can be clearly observed from the Figures 4.14 (a), (b) and (c), that the gain of the amplitude-frequency response increases from 3 to 5.5 when the values of a_1 and a_2 are increased from 0.25 to 0.5 and 0.5 to 0.75 while keeping the same value of $k_1 = k_2 = 0.5$. In addition, the width of the passband decreases for the same. In this case, it is observed that there are no ripples in the contour response of the 2-D digital bandpass filter.

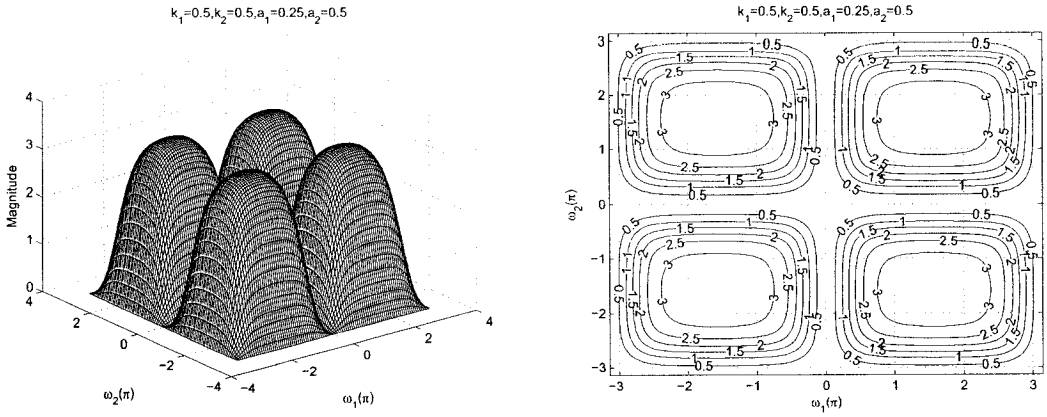

(a) $a_1 = 0.25,\ a_2 = 0.5$ and $k_1 = k_2 = 0.5$

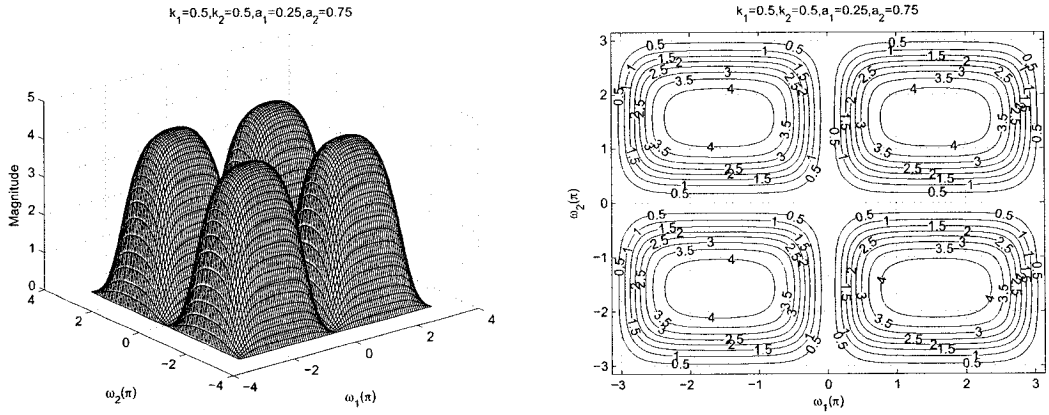

(b) $a_1 = 0.25,\ a_2 = 0.75$ and $k_1 = k_2 = 0.5$

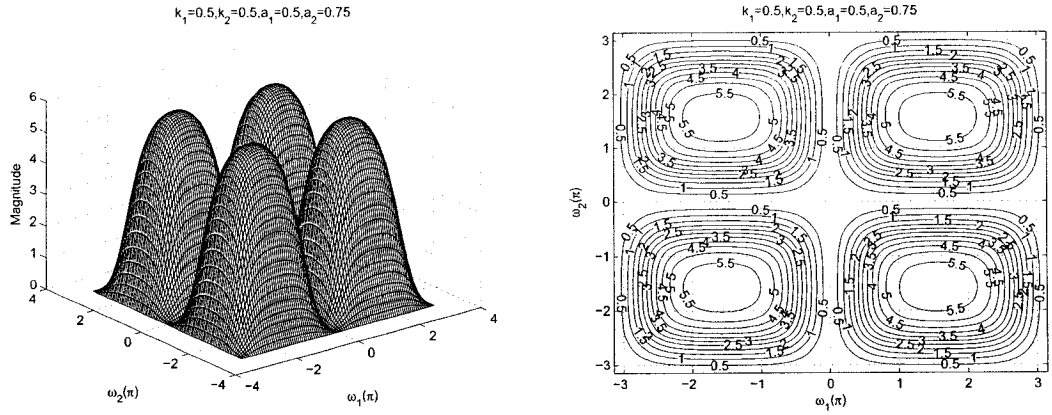

(c) $a_1 = 0.25,\ a_2 = 0.75$ and $k_1 = k_2 = 0.5$

Figure 4.14: 3-D amplitude frequency response and the contour response of the 2-D digital bandpass filter for $a_1 \neq a_2$ and $k_1 = k_2$

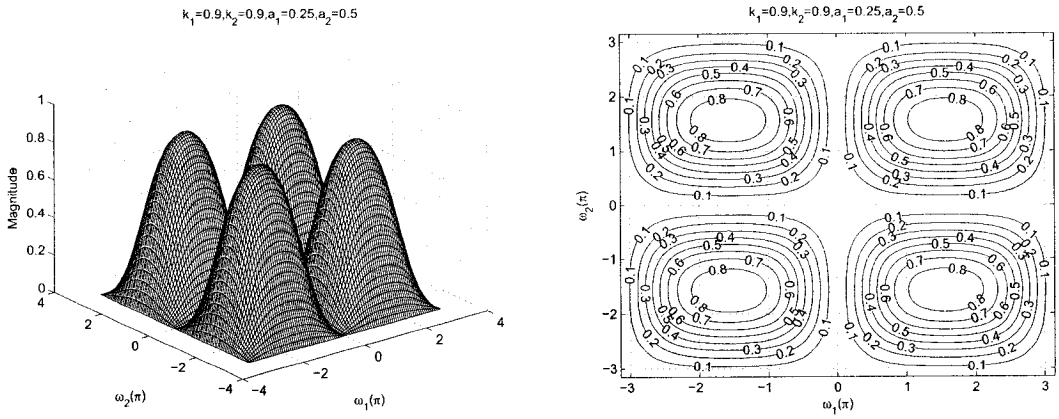

(a) $a_1 = 0.25,\ a_2 = 0.5$ and $k_1 = k_2 = 0.9$

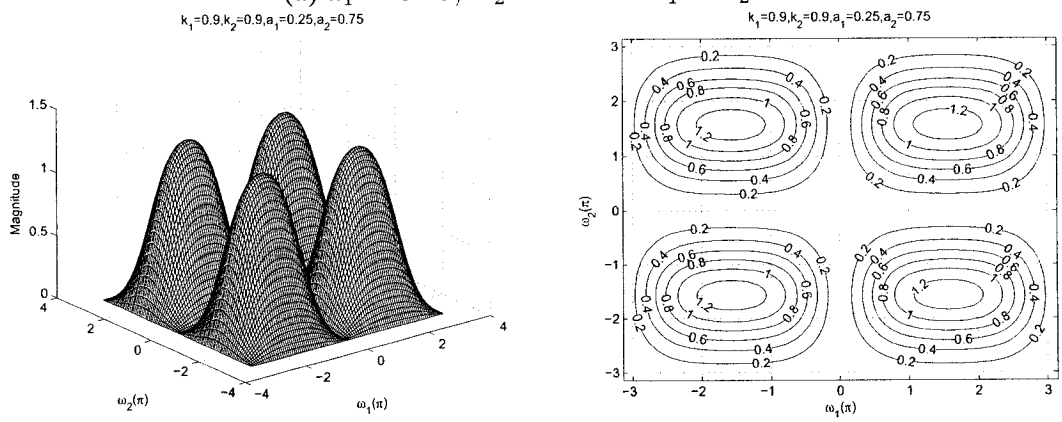

(b) $a_1 = 0.25,\ a_2 = 0.75$ and $k_1 = k_2 = 0.9$

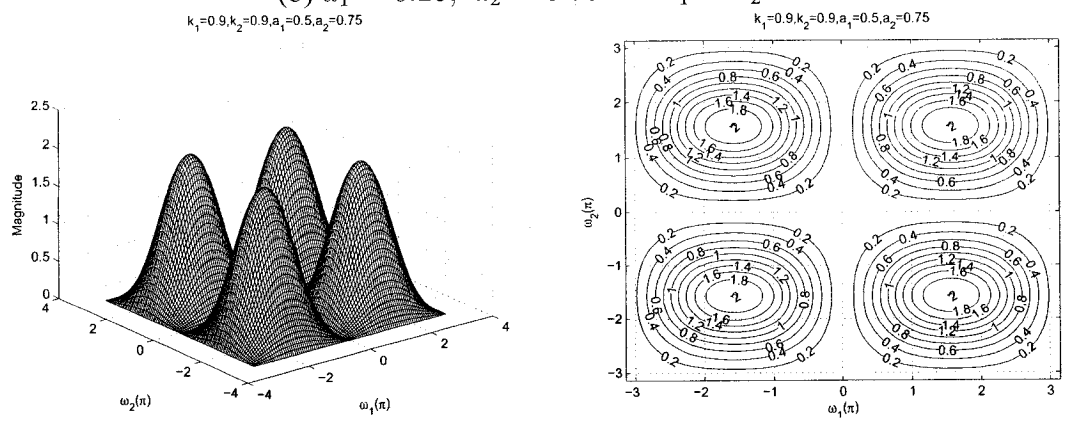

(c) $a_1 = 0.5,\ a_2 = 0.75$ and $k_1 = k_2 = 0.9$

Figure 4.15: 3-D amplitude frequency response and the contour response of the 2-D digital bandpass filter for $a_1 \neq a_2$ and $k_1 = k_2$

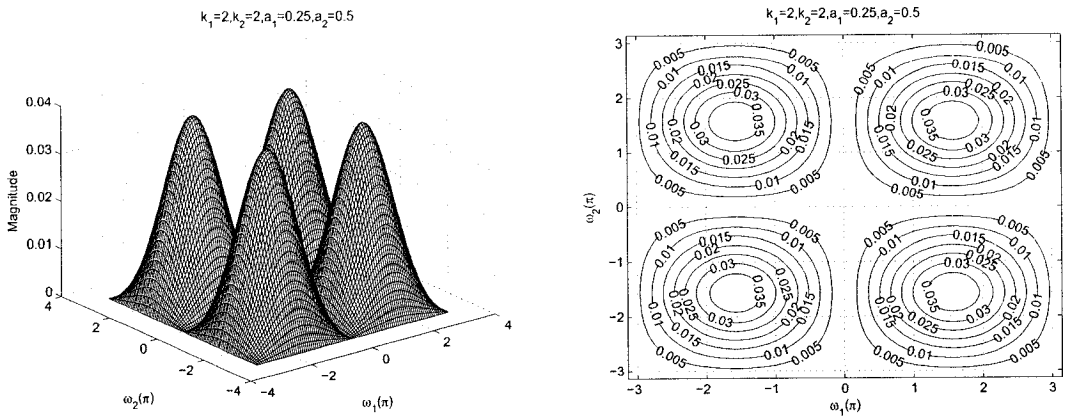

(a) $a_1 = 0.25,\ a_2 = 0.5$ and $k_1 = k_2 = 2$

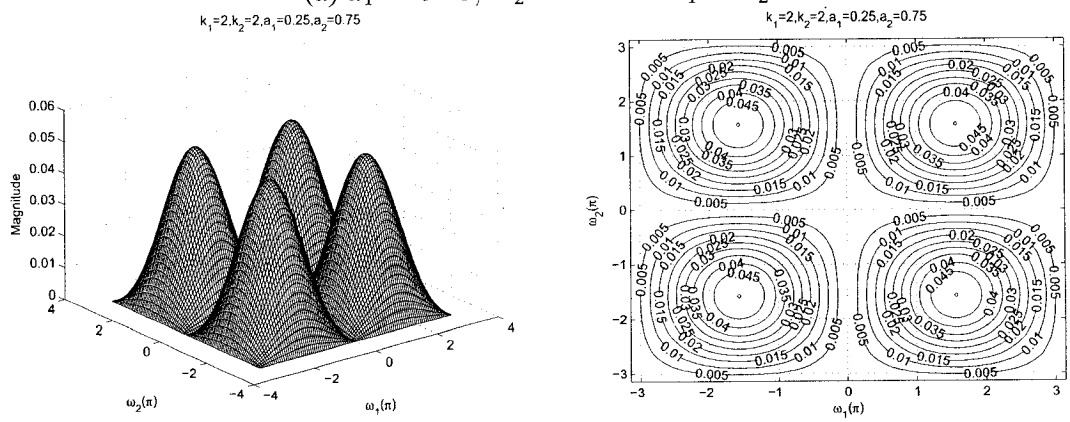

(b) $a_1 = 0.25,\ a_2 = 0.75$ and $k_1 = k_2 = 2$

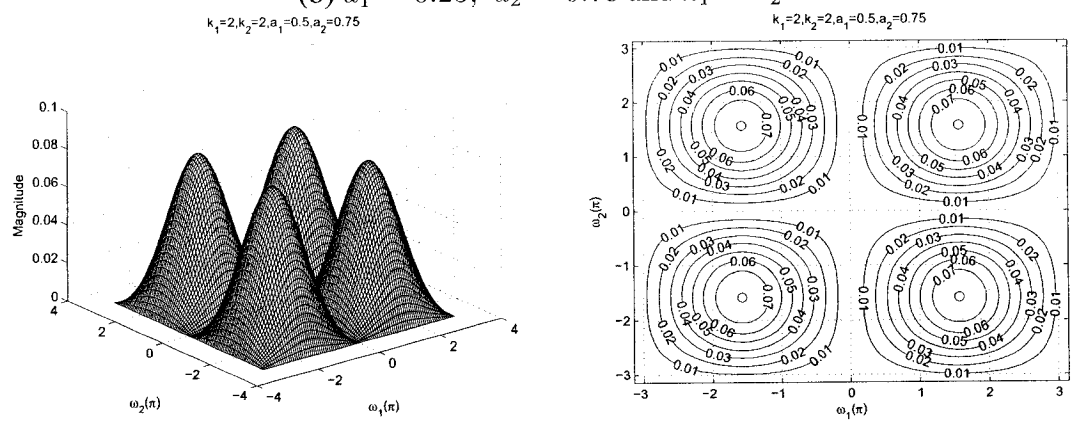

(c) $a_1 = 0.5,\ a_2 = 0.75$ and $k_1 = k_2 = 2$

Figure 4.16: 3-D amplitude frequency response and the contour response of the 2-D digital bandpass filter for $a_1 \neq a_2$ and $k_1 = k_2$

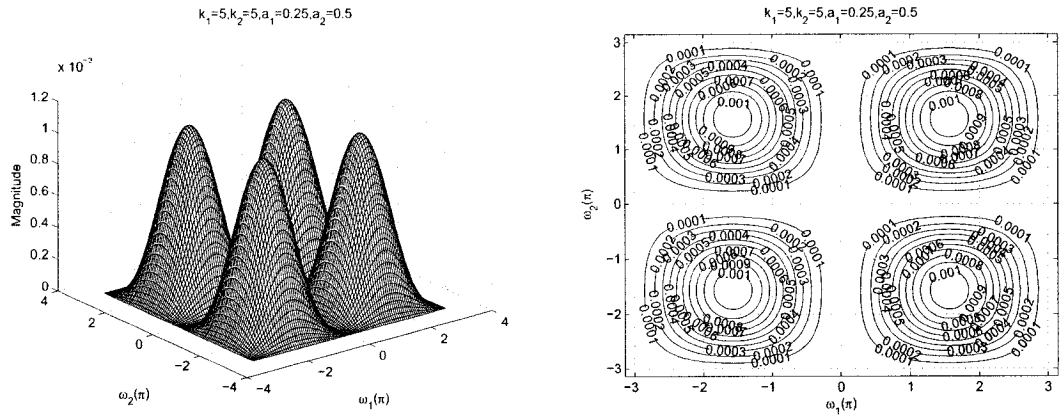

(a) $a_1 = 0.25,\ a_2 = 0.5$ and $k_1 = k_2 = 5$

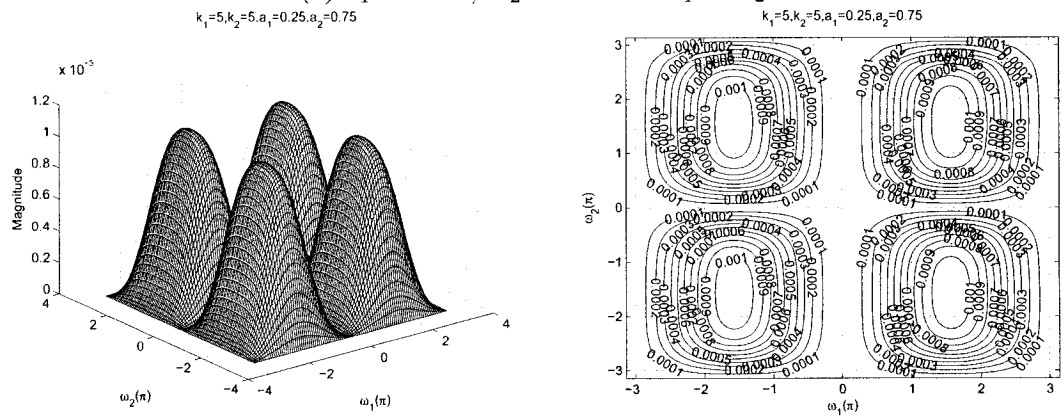

(b) $a_1 = 0.25,\ a_2 = 0.75$ and $k_1 = k_2 = 5$

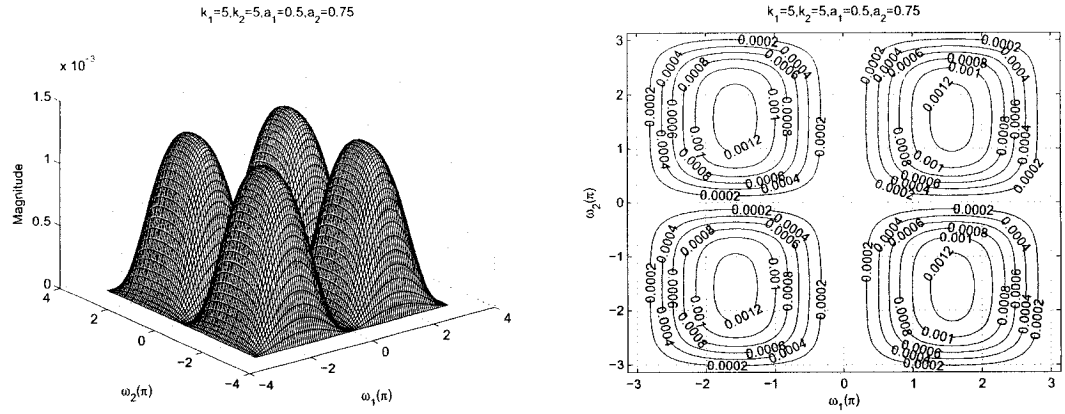

(c) $a_1 = 0.5,\ a_2 = 0.75$ and $k_1 = k_2 = 5$

Figure 4.17: 3-D amplitude frequency response and the contour response of the 2-D digital bandpass filter for $a_1 \neq a_2$ and $k_1 = k_2$

4.3.1.7 Frequency Response of 2-D Digital Bandpass Filter with different values of a_1 and a_2 and different values of k_1 and k_2

In this section, we study the effect of coefficients when $a_1 \neq a_2$ and $k_1 \neq k_2$, and the remaining coefficients b_1 and b_2 are considered to be unity for the 2-D digital bandpass filter in Category A. The values of a_1 and a_2 vary from 0.25 to 0.75 and 0.5 to 0.9 respectively, and the values of k_1 and k_2 vary from 0.25 to 5 and 0.5 to 8 respectively.

As observed from the Figures 4.18 to 4.21, the coefficients k_1 and k_2 affect the passband width of the frequency response. In the Figures 4.18 (a), (b), (c) and 4.19 (a), there is a gradual decrease in the passband width of the contour response as the values of k_1 and k_2 are increased from 0.25 to 5 and from 0.5 to 8 respectively, for the different values of a_1 and a_2 as 0.25 and 0.5, respectively. At the same time there is also a gradual decrease in the amplitude of the contour response for the same values.

As observed from the Figures 4.18 to 4.21, the coefficients a_1 and a_2 affect the gain of the amplitude-frequency response. It can be clearly observed from the Figures 4.18 (a), 4.19 (b) and 4.20 (c), that the gain of the amplitude-frequency response increases from 5 to 11 when the values of a_1 and a_2 are increased from 0.25 to 0.75 and 0.5 to 0.9, respectively, keeping the same value of $k_1 = 0.25$ and $k_2 = 0.5$. At the same time there is a decrease in the passband width for the same. It is observed that there are ripples in the contour response when the values of $a_1,\ a_2 \geq 0.75$ and $1 < k_1,\ k_2 \leq 5$.

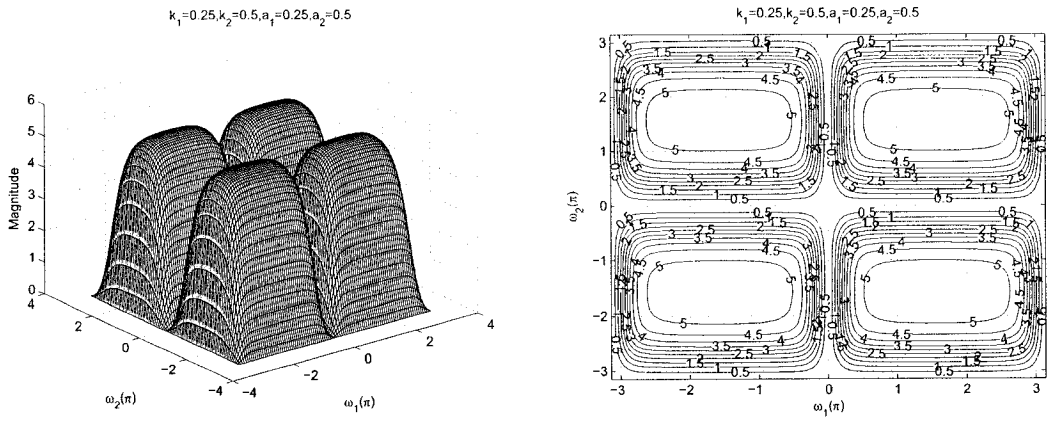

(a) $a_1 = 0.25,\ a_2 = 0.5$ and $k_1 = 0.25,\ k_2 = 0.5$

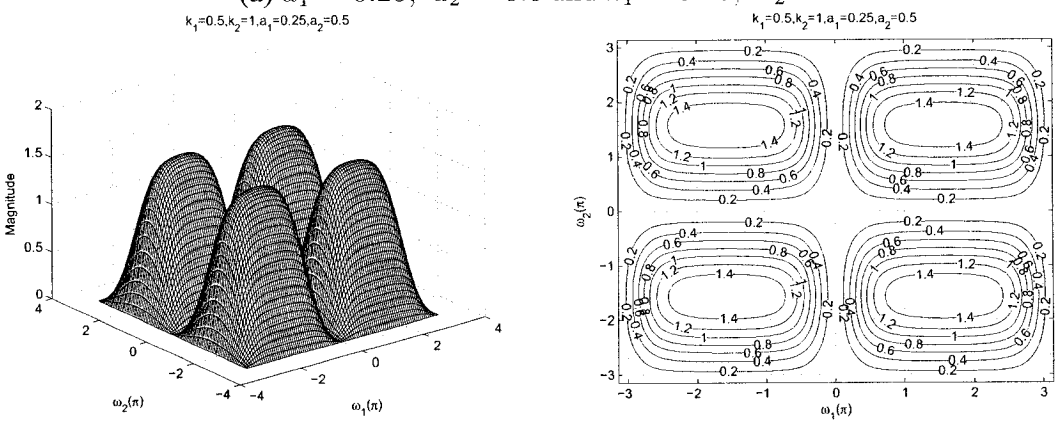

(b) $a_1 = 0.25,\ a_2 = 0.5$ and $k_1 = 0.5,\ k_2 = 1$

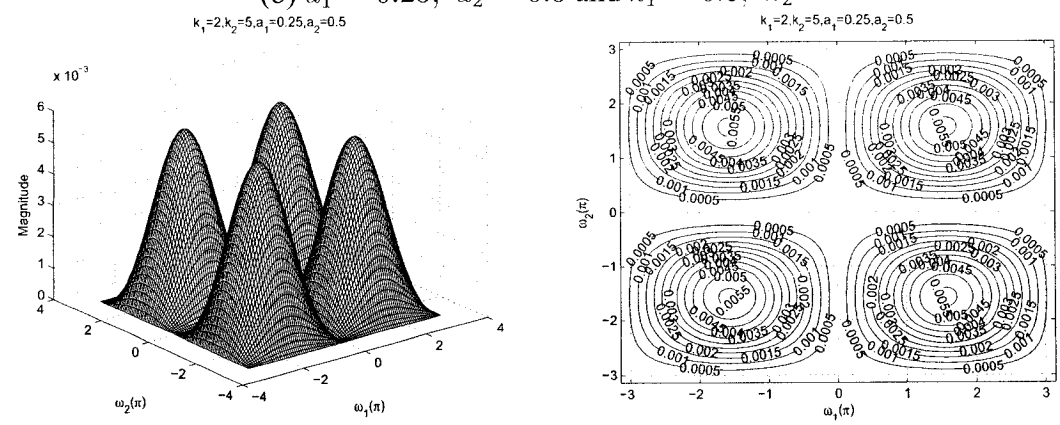

(c) $a_1 = 0.25,\ a_2 = 0.5$ and $k_1 = 2,\ k_2 = 5$

Figure 4.18: 3-D amplitude frequency response and the contour response of the 2-D digital bandpass filter for $a_1 \neq a_2$ and $k_1 \neq k_2$

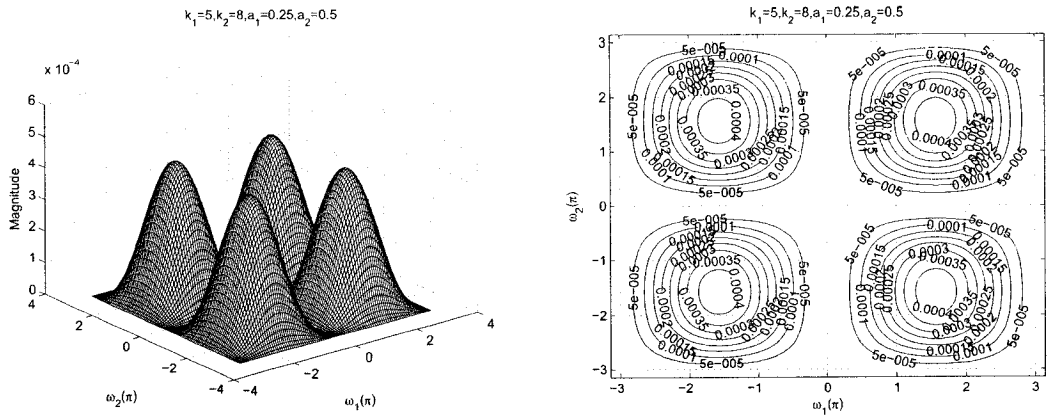

(a) $a_1 = 0.25,\ a_2 = 0.5$ and $k_1 = 5,\ k_2 = 8$

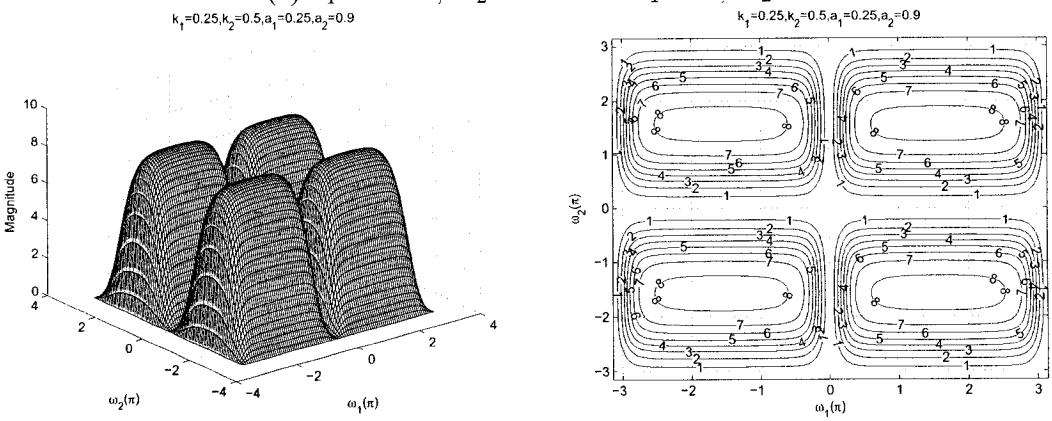

(b) $a_1 = 0.25,\ a_2 = 0.9$ and $k_1 = 0.25,\ k_2 = 0.5$

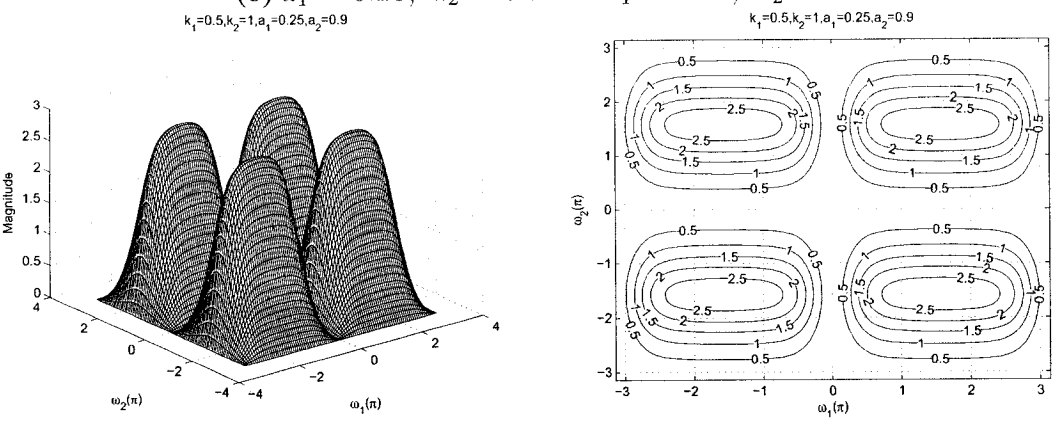

(c) $a_1 = 0.25,\ a_2 = 0.9$ and $k_1 = 0.5,\ k_2 = 1$

Figure 4.19: 3-D amplitude frequency response and the contour response of the 2-D digital bandpass filter for $a_1 \neq a_2$ and $k_1 \neq k_2$

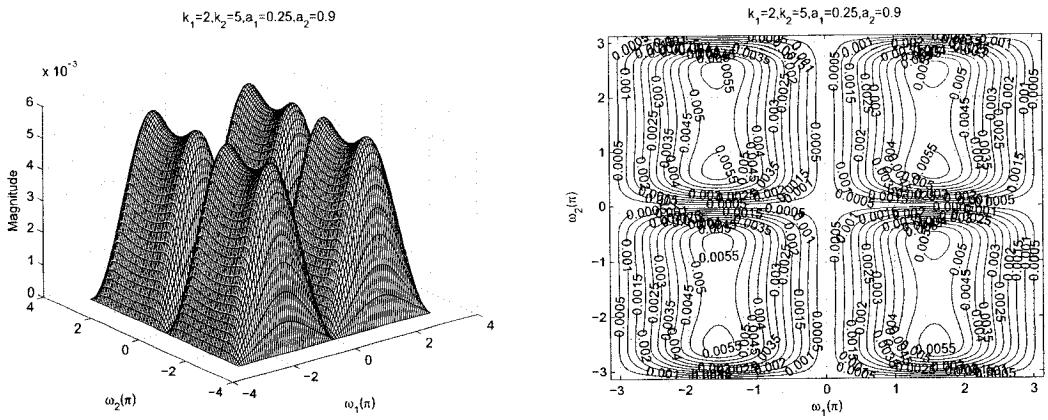

(a) $a_1 = 0.25,\ a_2 = 0.9$ and $k_1 = 2,\ k_2 = 5$

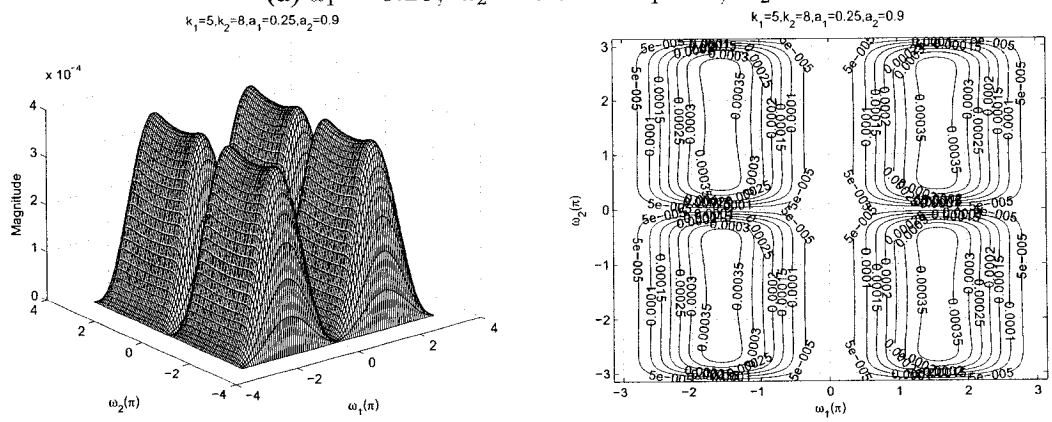

(b) $a_1 = 0.25,\ a_2 = 0.9$ and $k_1 = 5,\ k_2 = 8$

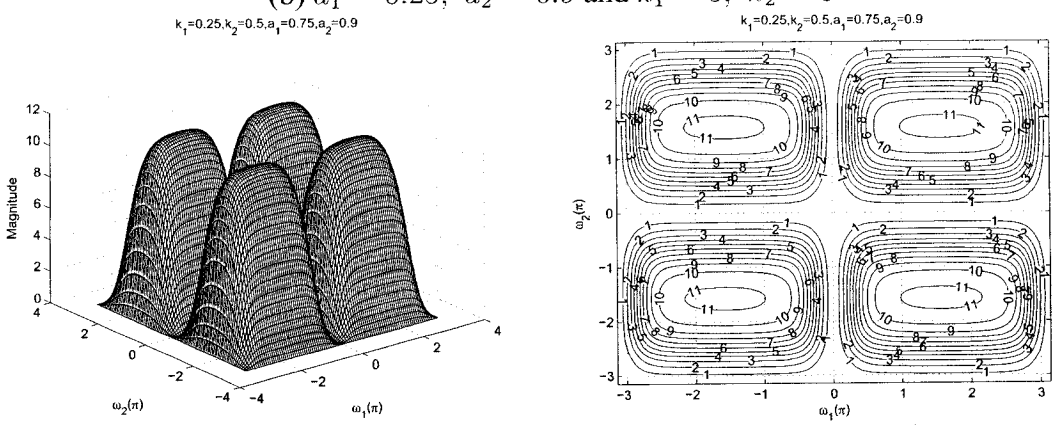

(c) $a_1 = 0.75,\ a_2 = 0.9$ and $k_1 = 0.25,\ k_2 = 0.5$

Figure 4.20: 3-D amplitude frequency response and the contour response of the 2-D digital bandpass filter for $a_1 \neq a_2$ and $k_1 \neq k_2$

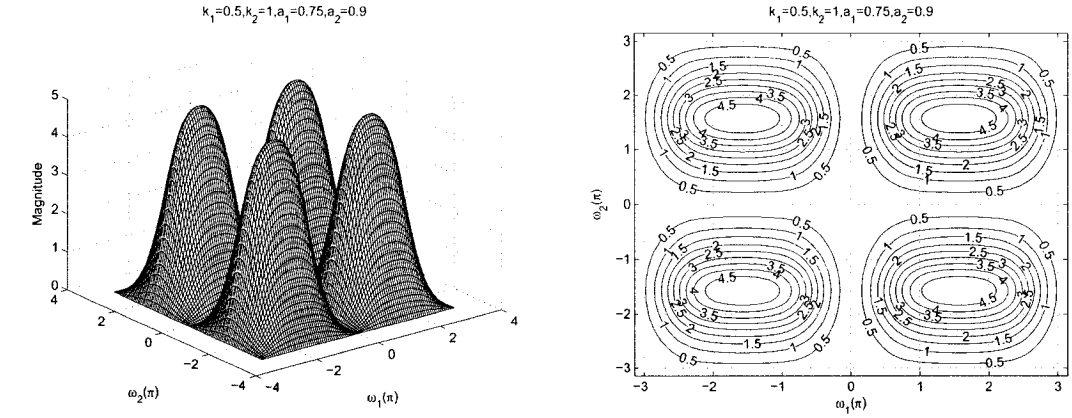

(a) $a_1 = 0.75,\ a_2 = 0.9$ and $k_1 = 0.5,\ k_2 = 1$

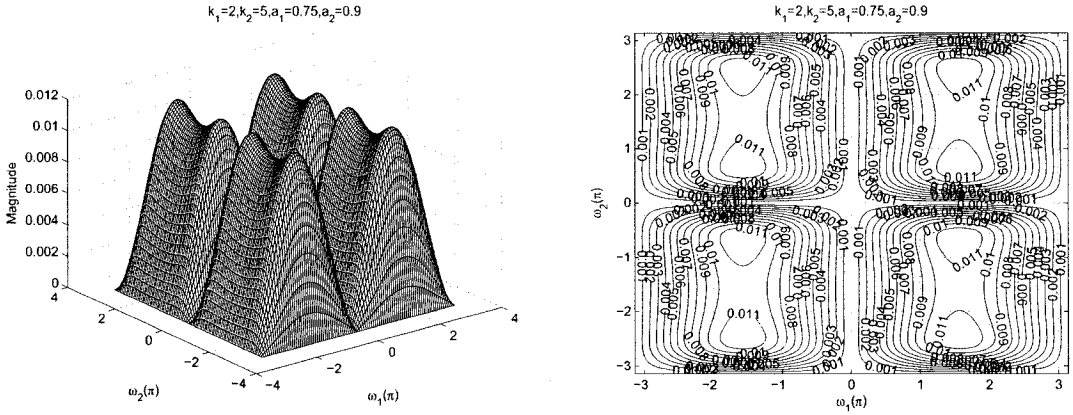

(b) $a_1 = 0.75,\ a_2 = 0.9$ and $k_1 = 2,\ k_2 = 5$

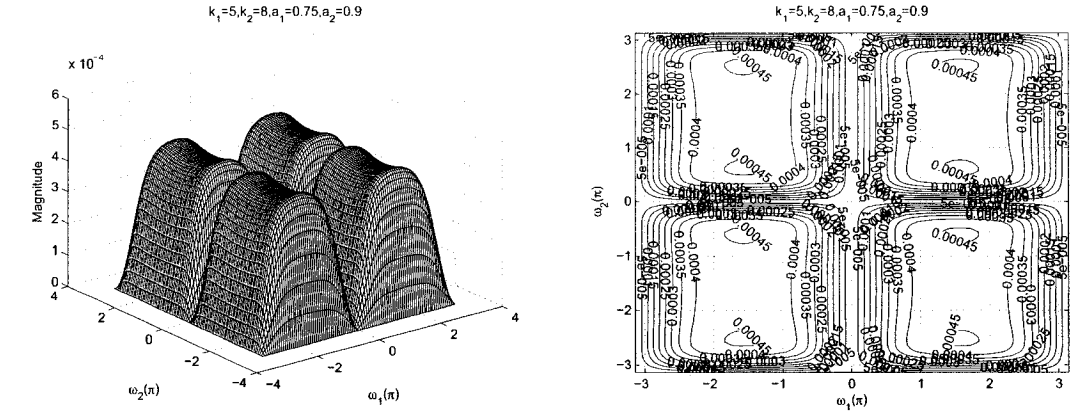

(c) $a_1 = 0.75,\ a_2 = 0.9$ and $k_1 = 5,\ k_2 = 8$

Figure 4.21: 3-D amplitude frequency response and the contour response of the 2-D digital bandpass filter for $a_1 \neq a_2$ and $k_1 \neq k_2$

4.3.1.8 Frequency Response of 2-D Digital Bandpass Filter with same values of a_1 and a_2 and different values of k_1 and k_2

In this section, we study the effect of coefficients, where $a_1 = a_2$ and $k_1 \neq k_2$ and the remaining coefficients b_1 and b_2 are considered to be unity for the 2-D digital band-pass filter in Category A. The values of a_1 and a_2 vary from 0 to 1 and the values of k_1 and k_2 vary from 0.25 to 2 and 0.5 to 5 respectively.

As observed from the Figures 4.22 to 4.25, the coefficients k_1 and k_2 affect the passband width of the frequency response. In the Figures 4.22 (a), (b) and (c), there is a gradual decrease in the passband width of the contour response when the values of k_1 and k_2 are increased from 0.25 to 2 and 0.5 to 5 respectively, for the same values of $a_1 = a_2 = 0.25$. At the same time there is also a gradual decrease in the amplitude of the contour response.

As observed from the Figures 4.22 to 4.25, the coefficients a_1 and a_2 affect the gain of the amplitude-frequency response. It can be clearly observed from the Figures 4.22 (a), 4.23 (a), 4.24 (a) and 4.25 (a), that the amplitude of the contour response increases from 4 to 12 when the values of a_1 and a_2 are increased from 0.25 to 0.9 keeping the same value of $k_1 = 0.25$ and $k_2 = 0.5$. In addition, the width of the passband increases and decreases periodically for the same. It is observed that there are ripples in the contour response when the values of $a_1,\ a_2 > 0.75$ and $1 < k_1,\ k_2 \leq 5$.

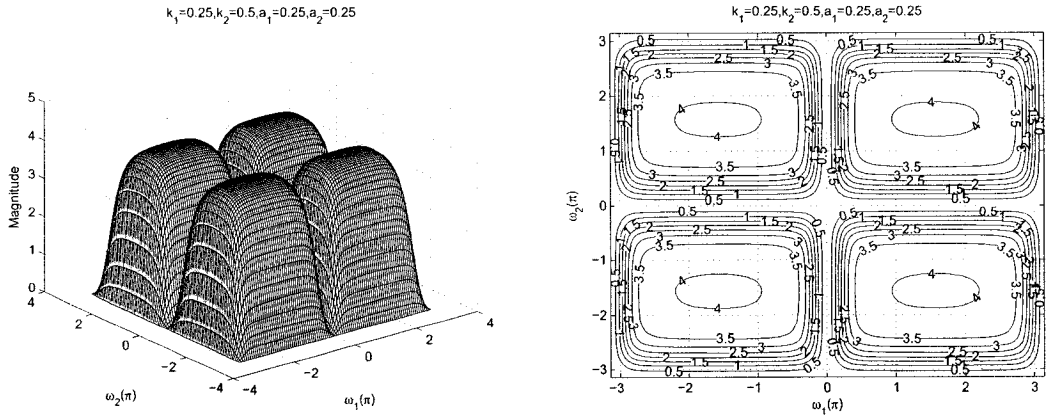

(a) $a_1 = a_2 = 0.25$ and $k_1 = 0.25,\ k_2 = 0.5$

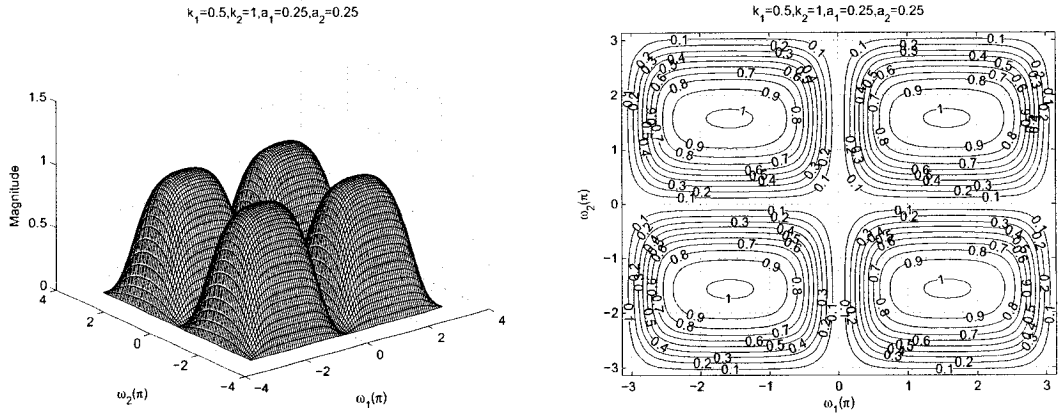

(b) $a_1 = a_2 = 0.25$ and $k_1 = 0.5,\ k_2 = 1$

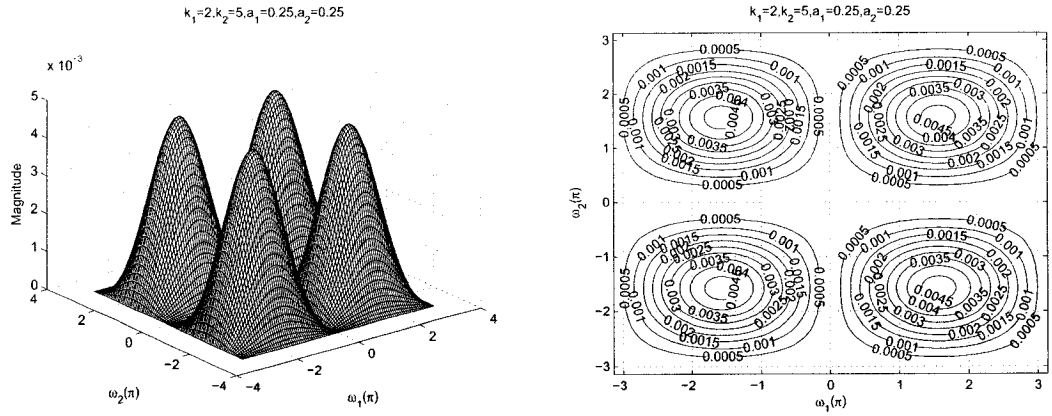

(c) $a_1 = a_2 = 0.25$ and $k_1 = 2,\ k_2 = 5$

Figure 4.22: 3-D amplitude frequency response and the contour response of the 2-D digital bandpass filter for $a_1 = a_2$ and $k_1 \neq k_2$

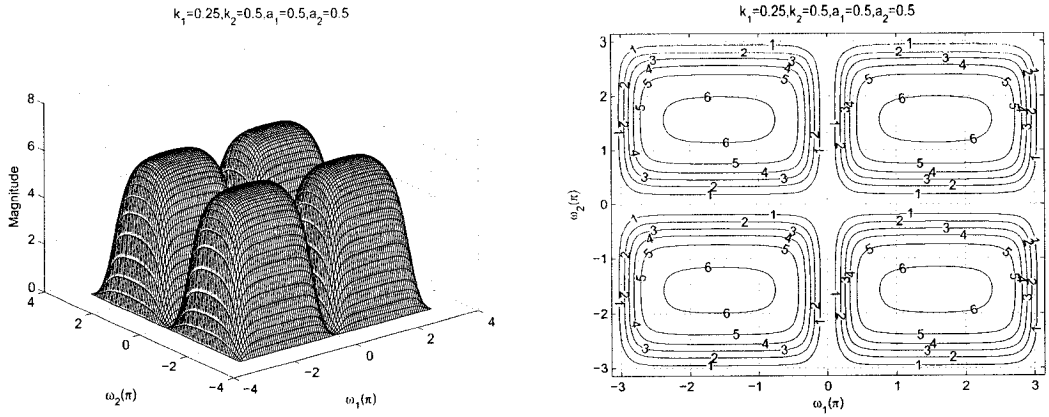

(a) $a_1 = a_2 = 0.5$ and $k_1 = 0.25,\ k_2 = 0.5$

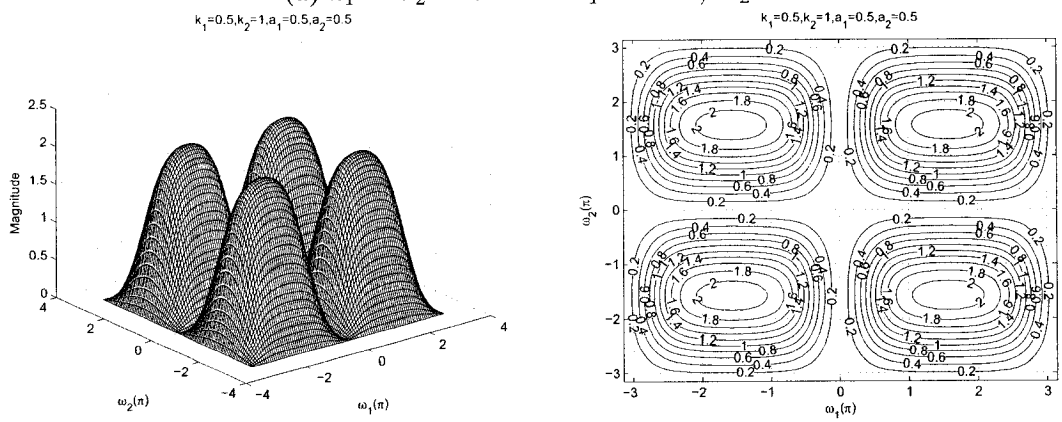

(b) $a_1 = a_2 = 0.5$ and $k_1 = 0.5,\ k_2 = 1$

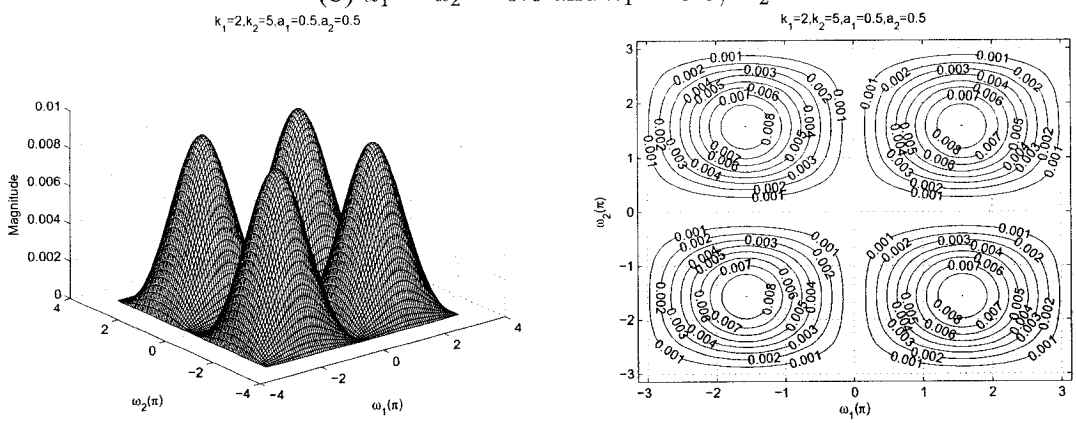

(c) $a_1 = a_2 = 0.5$ and $k_1 = 2,\ k_2 = 5$

Figure 4.23: 3-D amplitude frequency response and the contour response of the 2-D digital bandpass filter for $a_1 = a_2$ and $k_1 \neq k_2$

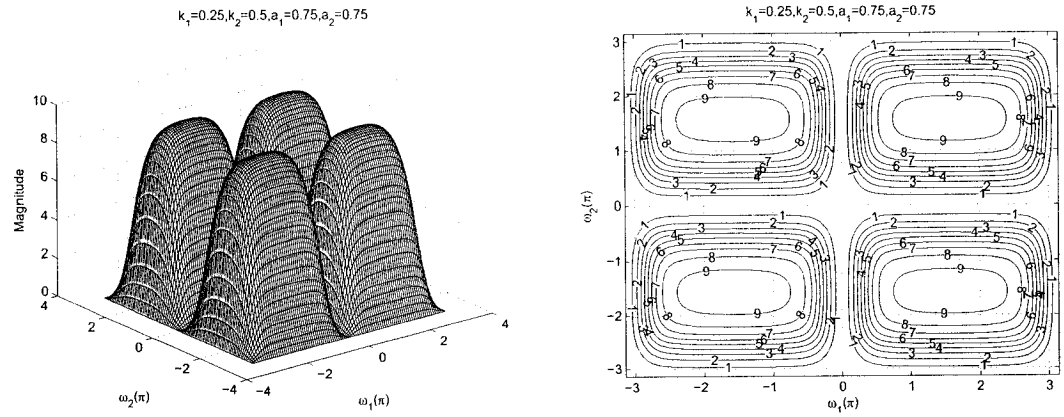

(a) $a_1 = a_2 = 0.75$ and $k_1 = 0.25,\ k_2 = 0.5$

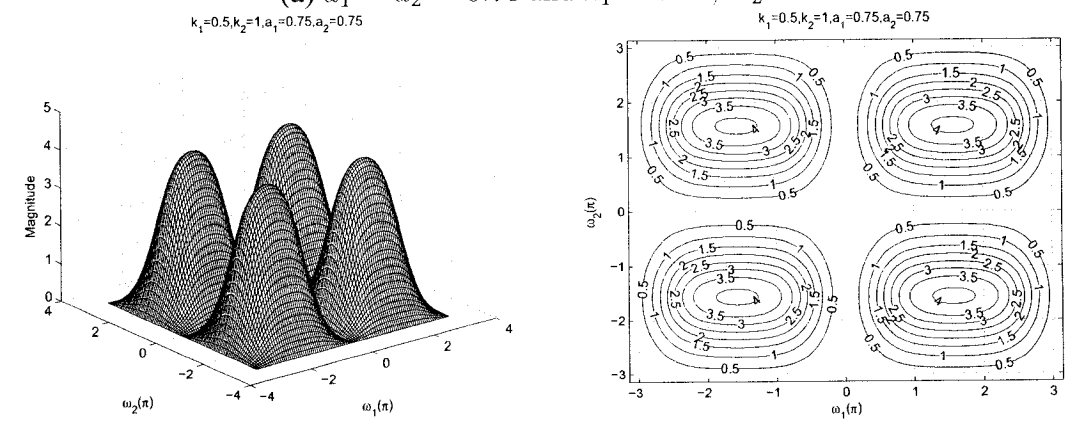

(b) $a_1 = a_2 = 0.75$ and $k_1 = 0.5,\ k_2 = 1$

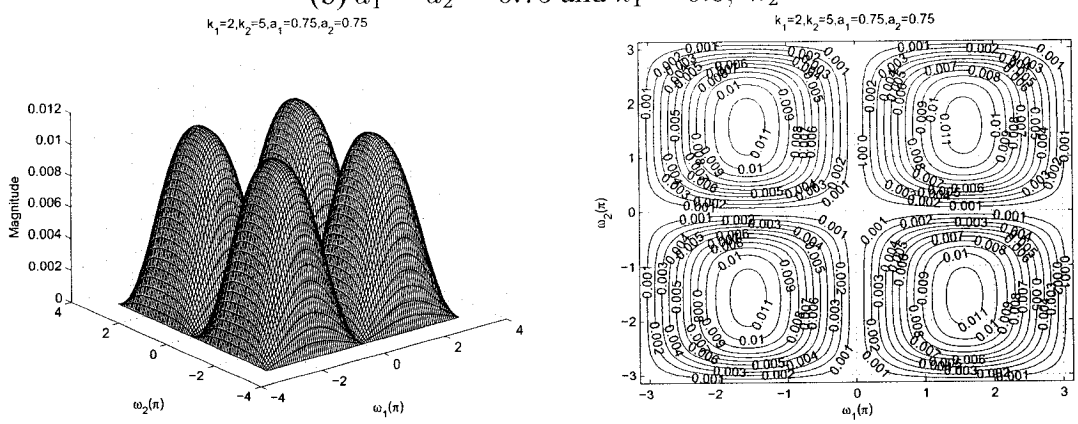

(c) $a_1 = a_2 = 0.75$ and $k_1 = 2,\ k_2 = 5$

Figure 4.24: 3-D amplitude frequency response and the contour response of the 2-D digital bandpass filter for $a_1 = a_2$ and $k_1 \neq k_2$

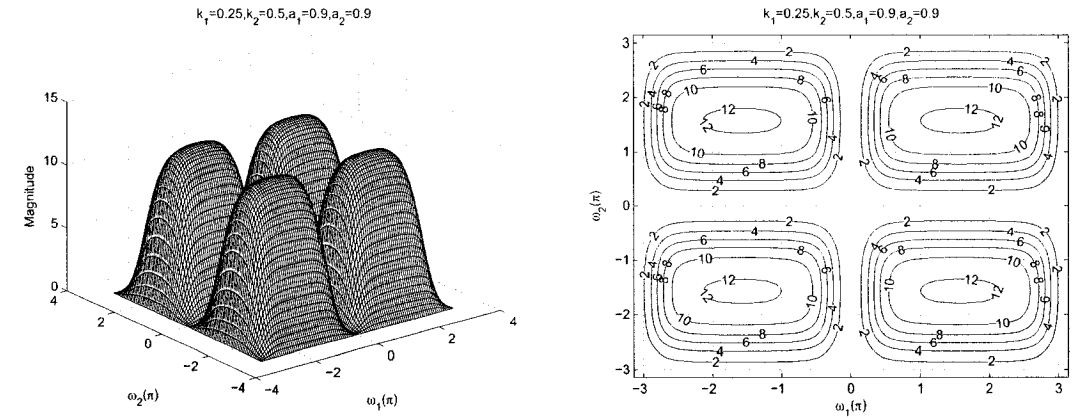

(a) $a_1 = a_2 = 0.9$ and $k_1 = 0.25,\ k_2 = 0.5$

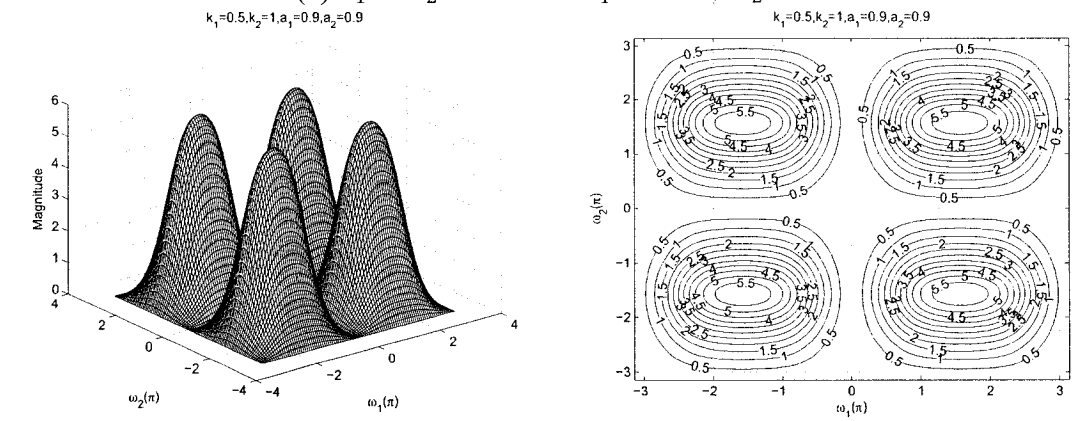

(b) $a_1 = a_2 = 0.9$ and $k_1 = 0.5,\ k_2 = 1$

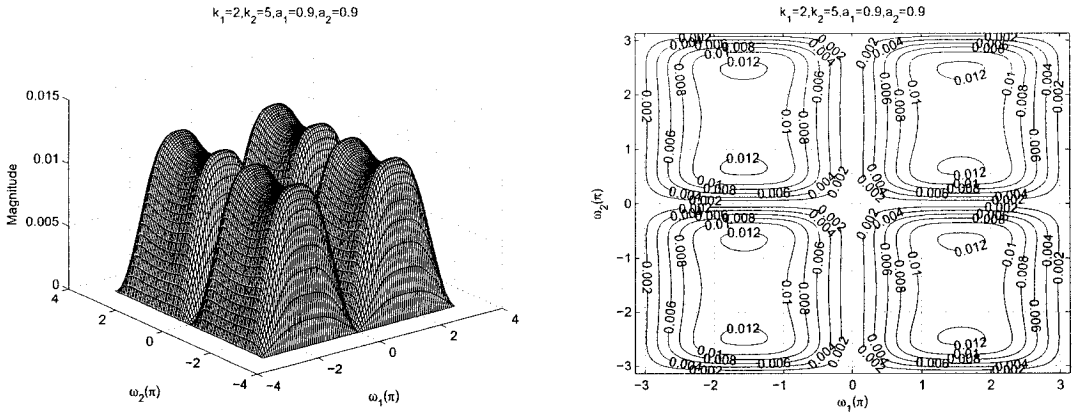

(c) $a_1 = a_2 = 0.9$ and $k_1 = 2,\ k_2 = 5$

Figure 4.25: 3-D amplitude frequency response and the contour response of the 2-D digital bandpass filter for $a_1 = a_2$ and $k_1 \neq k_2$

4.3.2 Frequency Response of the All-pole 2-D Digital Bandpass Filter in Category B

The transfer function of the all-pole 2-D digital bandpass filter is obtained by cascading the all-pole 2-D digital lowpass filter and the all-pole 2-D digital high pass filter in Category B. With the input coefficient of the generalized bilinear transformation, we can obtain the 3-D magnitude and contour plots of the resulting all-pole 2-D digital bandpass filter [46]. In this, the stability is taken care such that the all-pole 2-D bandpass is stable with these input arguments.

To investigate the manner in which each coefficient of the generalized bilinear transformation effects the magnitude response of the resulting all-pole 2-D digital bandpass filter, we vary the values of the coefficients or fix some of the coefficients to specific values. It is possible to obtain the all-pole 2-D digital bandpass filter when the coefficients have the following limits: $k_i > 0, 0 \leq |b_i| \leq 1$ and $0 \leq |a_i| \leq 1$ where $i = 1, 2$. Let us consider the coefficients of the generalized bilinear transformation for the all-pole 2-D digital bandpass filter to be unity, i.e., $a_1 = 1$, $a_2 = 1$, $k_1 = 1$, and $k_2 = 1$. Under this condition, the 3-D amplitude-frequency response and the contour plots of the all-pole 2-D digital bandpass filter are shown in the Figure 4.26

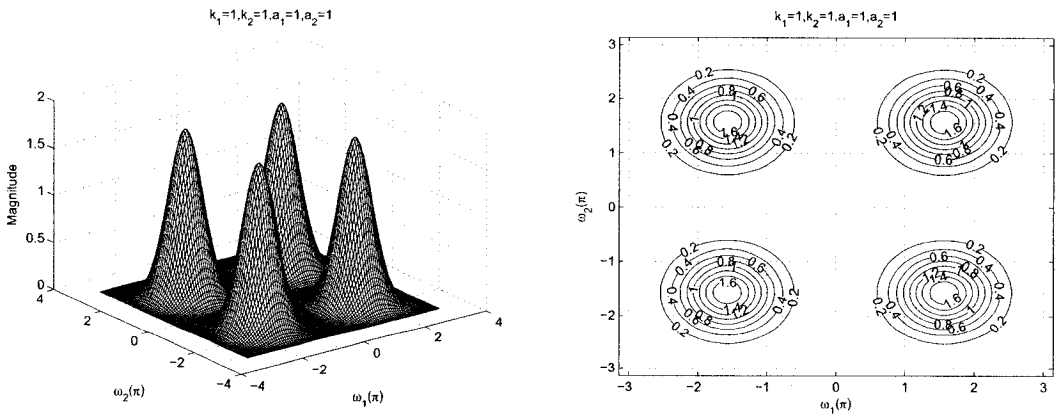

Figure 4.26: 3-D Amplitude-Frequency response and contour response of the All-pole 2-D Digital Bandpass Filter with all the coefficients values as unity

In the following, we will study the effects of these coefficients to the frequency responses of the all-pole 2-D digital bandpass filter [33, 48].

4.3.2.1 Frequency Response of the All-pole 2-D Digital Bandpass Filter with different values of k_1

In this section, we study the manner in which k_1 affects the frequency response behavior of the resulting all-pole 2-D digital bandpass filter in Category B and to separate the effect of the other coefficients, we vary the value of k_1, and fix all the other coefficients of the generalized bilinear transformation to unity, e.g. with $k_2 = 1$, $a_1 = 1$, $a_2 = 1$. This was done so that no generality is lost and to make the situation simple. The values of k_1 are varied from 0.1 to 5 and the 3-D magnitude response and the contour plots for the all-pole 2-D digital bandpass filter with the values of $k_1 = 0.1$, $k_1 = 0.5$, $k_1 = 0.9$, $k_1 = 2$, and $k_1 = 5$, are shown in the Figures 4.27 and 4.28.

It is observed that although the coefficient k_1 does not have any effect on the passband width along the $\omega_2 - axis$, it affects the passsband width along the $\omega_1 - axis$. Initially when the value of the coefficient $k_1 = 0.1$ (see Figure 4.27 (a)) the passband width is maximum along $\omega_1 - axis$ and at the same time it has maximum magnitude. As we increase the value of k_1 from 0.1 to 5, the passband width gradually decreases and also the magnitude of the contour response decreases from 5 to 0.0006 along the $\omega_1 - axis$.

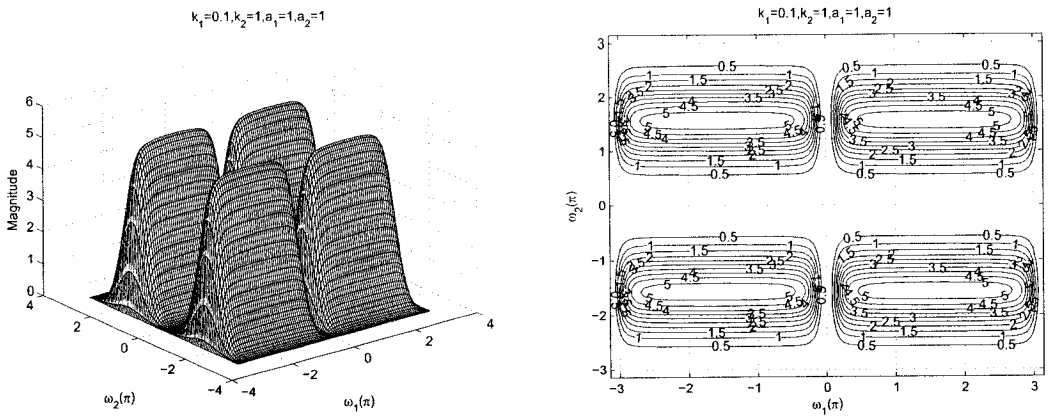

(a) $k_1 = 0.1$

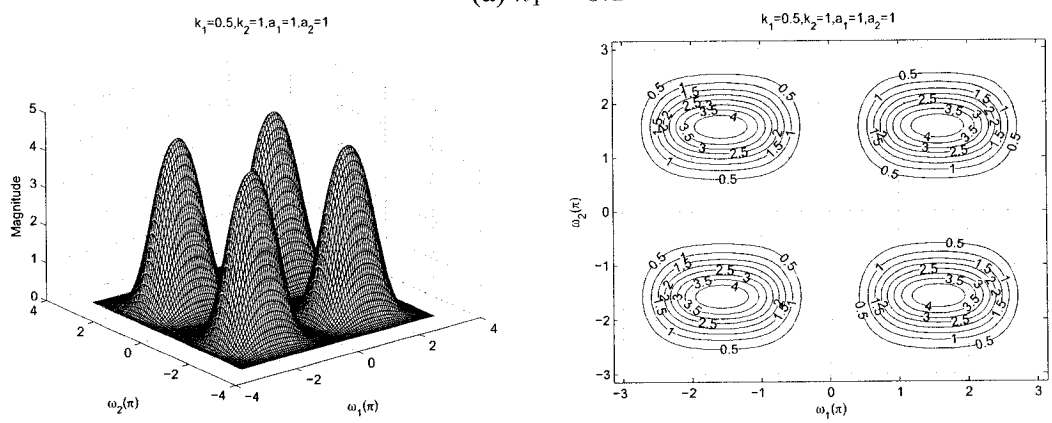

(b) $k_1 = 0.5$

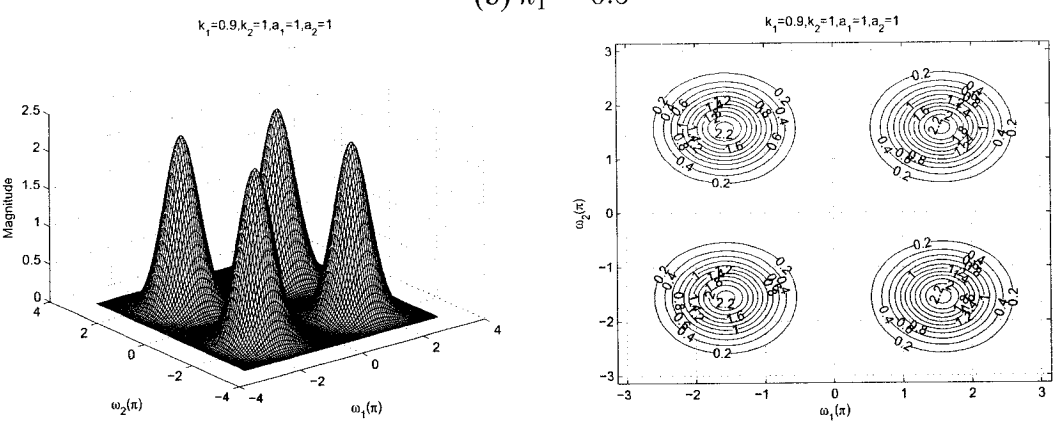

(c) $k_1 = 0.9$

Figure 4.27: 3-D amplitude frequency response and the contour response of the All-pole 2-D digital bandpass filter for different values of k_1

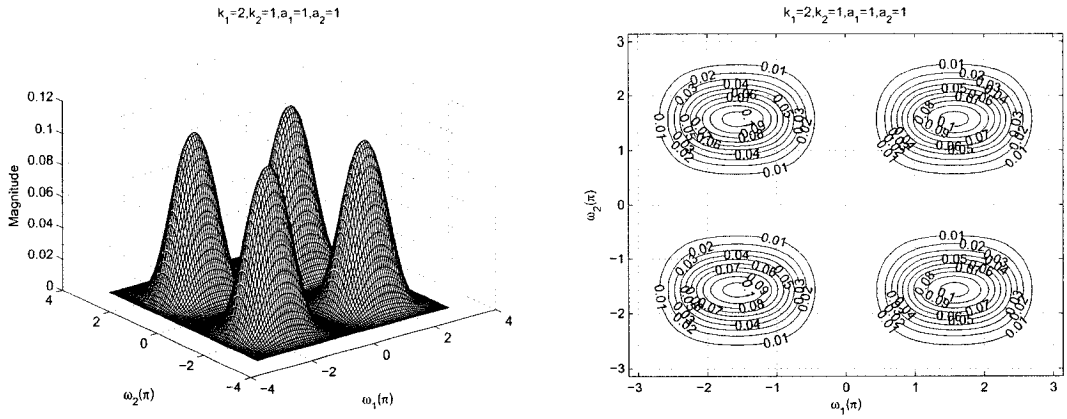

(a) $k_1 = 2$

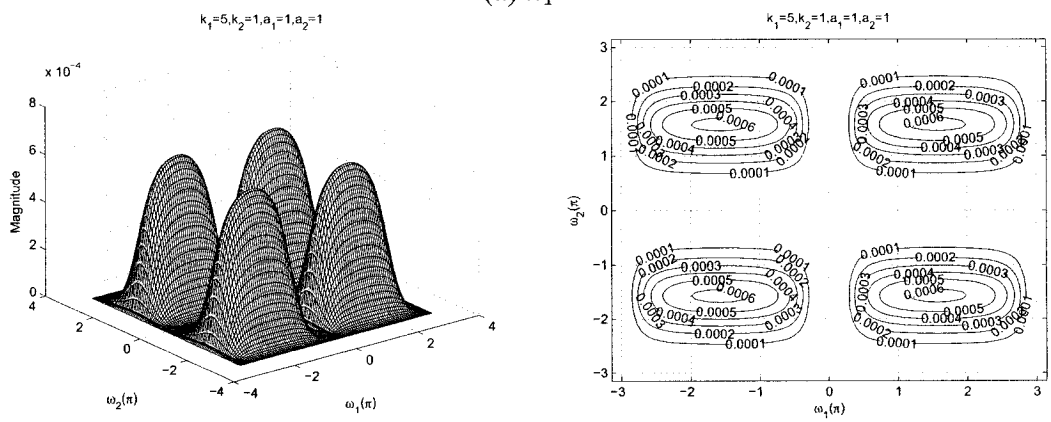

(b) $k_1 = 5$

Figure 4.28: 3-D amplitude frequency response and the contour response of the All-pole 2-D digital bandpass filter for different values of k_1

4.3.2.2 Frequency Response of the All-pole 2-D Digital Bandpass Filter with different values of k_2

In this section, we study the manner in which k_2 affects the frequency response behavior of the resulting all-pole 2-D digital bandpass filter in Category B and to separate the effect of the other coefficients, we vary the value of k_2, and fix all the other coefficients of the generalized bilinear transformation to unity, e.g. with $k_1 = 1$, $a_1 = 1$, $a_2 = 1$. This was done so that no generality is lost and to make the situation simple. The values of k_2 are varied from 0.1 to 5 and the 3-D magnitude response and the contour plots for the all-pole 2-D digital bandpass filter with the values of $k_2 = 0.1$, $k_2 = 0.5$, $k_2 = 0.9$, $k_2 = 2$, and

$k_2 = 5$, are shown in the Figures 4.29 and 4.30.

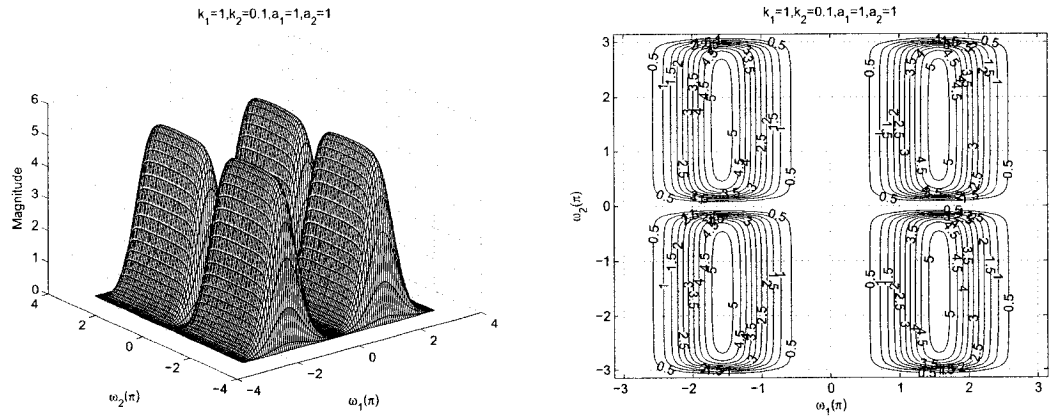

(a) $k_2 = 0.1$

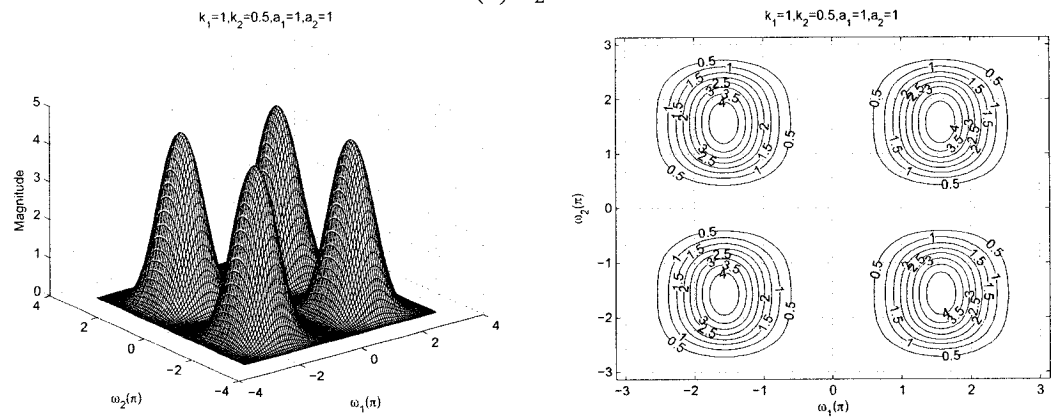

(b) $k_2 = 0.5$

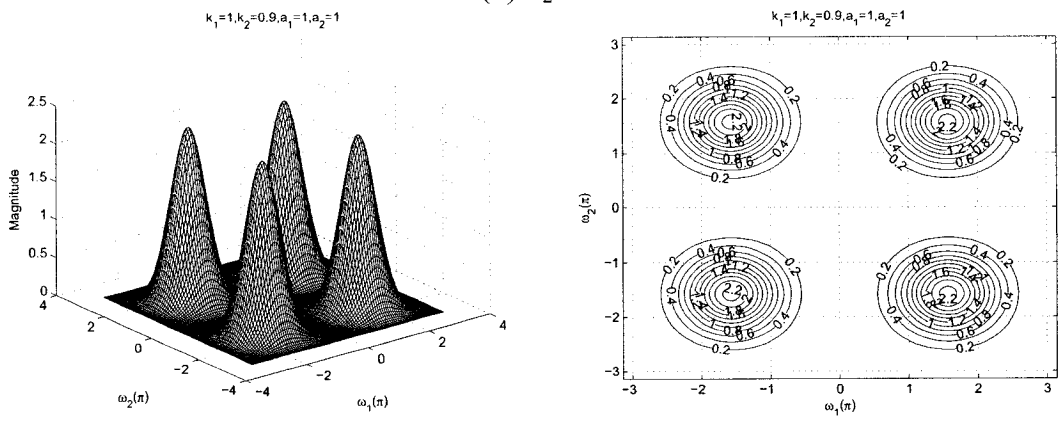

(c) $k_2 = 0.9$

Figure 4.29: 3-D amplitude frequency response and the contour response of the All-pole 2-D digital bandpass filter for different values of k_2

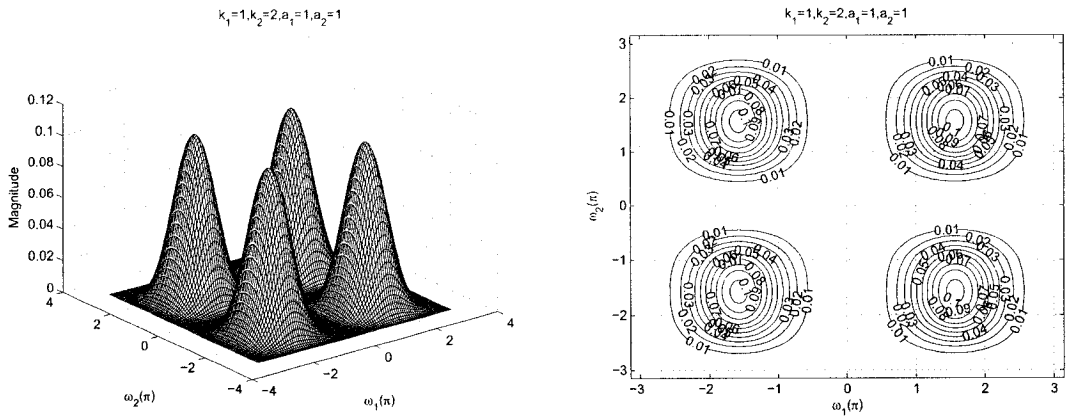

(a) $k_2 = 2$

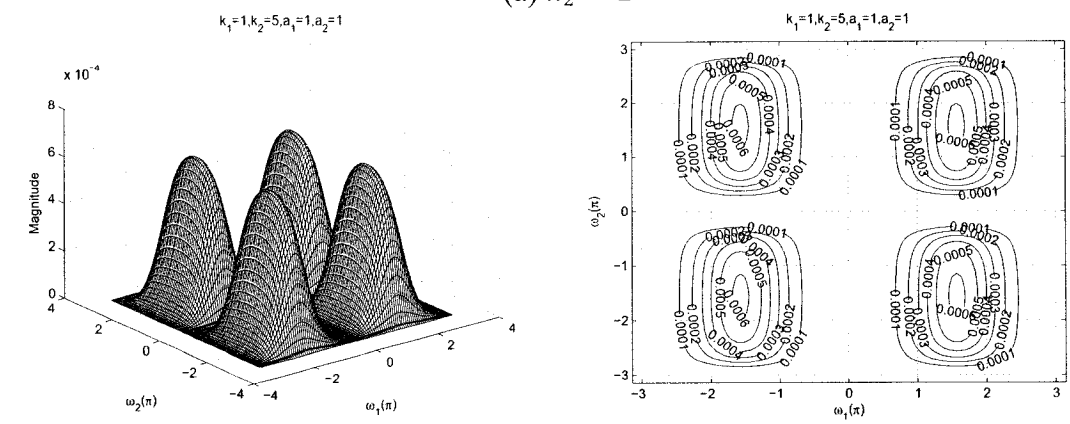

(b) $k_2 = 5$

Figure 4.30: 3-D amplitude frequency response and the contour response of the All-pole 2-D digital bandpass filter for different values of k_2

It is observed that although the coefficient k_2 does not have any effect on the passband width along the $\omega_1 - axis$, it affects the passsband width along the $\omega_2 - axis$. Initially when the value of the coefficient $k_2 = 0.1$ (see Figure 4.29 (a)) the passband width is maximum along $\omega_2 - axis$ and at the same time it has maximum magnitude. As we increase the value of k_2 from 0.1 to 5, the passband width gradually decreases and also the magnitude of the contour response decreases from 5 to 0.0006 along the $\omega_2 - axis$.

4.3.2.3 Frequency Response of the All-pole 2-D Digital Bandpass Filter with different values of a_1

In the Sections 4.3.2.1 and 4.3.2.2, the effect of the coefficient of k_1 and k_2 are studied. In this section, the effect of the coefficient a_1 is studied. The stable range of a_1 can be obtained with other specified coefficients of the generalized bilinear transformation. There are many combinations possible for the coefficients. To study the response with different values of a_1 properly, we fix other coefficients values to be equal to unity. The range of a_1 varies from 0.1 to 1 and the other coefficient values are specified as unity, i.e., $k_1 = 1$, $k_2 = 1$, $a_2 = 1$, $b_1 = 1$ and $b_2 = 1$ in order to get the all-pole 2-D digital bandpass filter response in Category B.

By varying the value of a_1, the 3-D magnitude response and contour plots which represents different values of a_1, i.e. $a_1 = 0.1$, $a_1 = 0.25$, $a_1 = 0.5$, $a_1 = 0.75$, and $a_1 = 0.9$ are shown in the Figures 4.31 and 4.32. By making the value of $a_1 = 1$, it resembles the standard all-pole 2-D digital bandpass filter as shown in the Figure 4.26. It is observed from the diagrams that the coefficient a_1 affects the gain of the amplitude-frequency response. At the lowest value of $a_1 = 0.1$, the gain of the amplitude-frequency response is 0.7. As the value of a_1 increases, the gain increases and reach the maximum value at $a_1 = 1$. As seen from the diagrams, that as we increase the value of a_1 from 0.1 to 0.9, the gain of the amplitude-frequency response increases from 0.7 to 1.6. Also, the coefficient a_1 does not have any effect along the $\omega_2 - axis$.

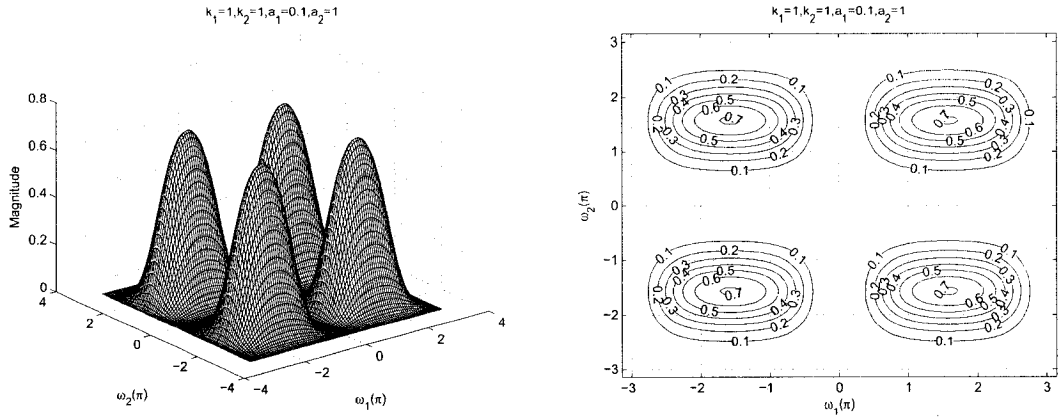

(a) $a_1 = 0.1$

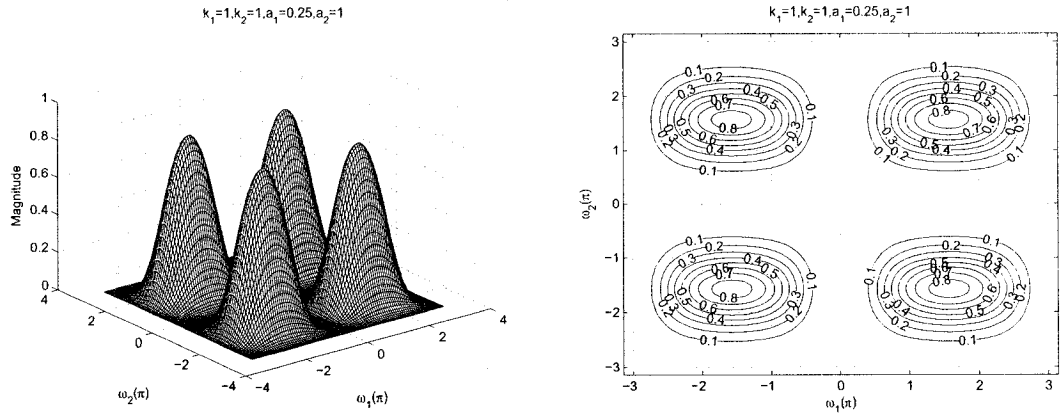

(b) $a_1 = 0.25$

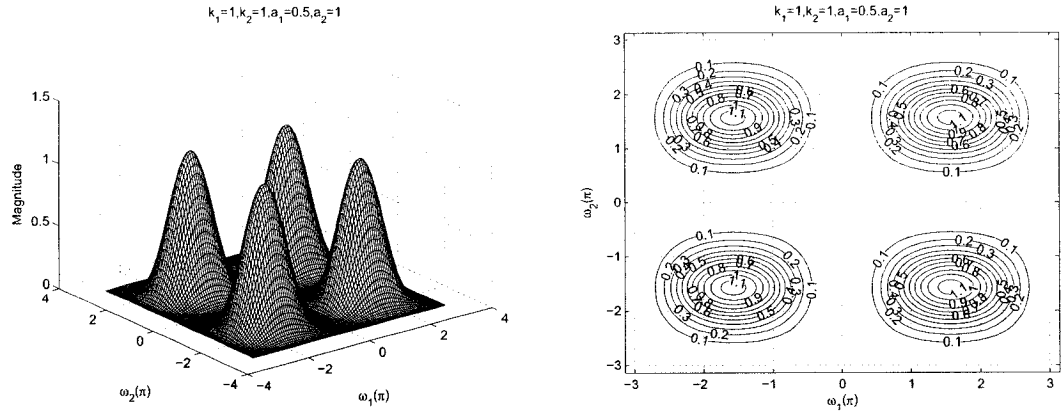

(c) $a_1 = 0.5$

Figure 4.31: 3-D amplitude frequency response and the contour response of the All-pole2-D digital bandpass filter for different values of a_1

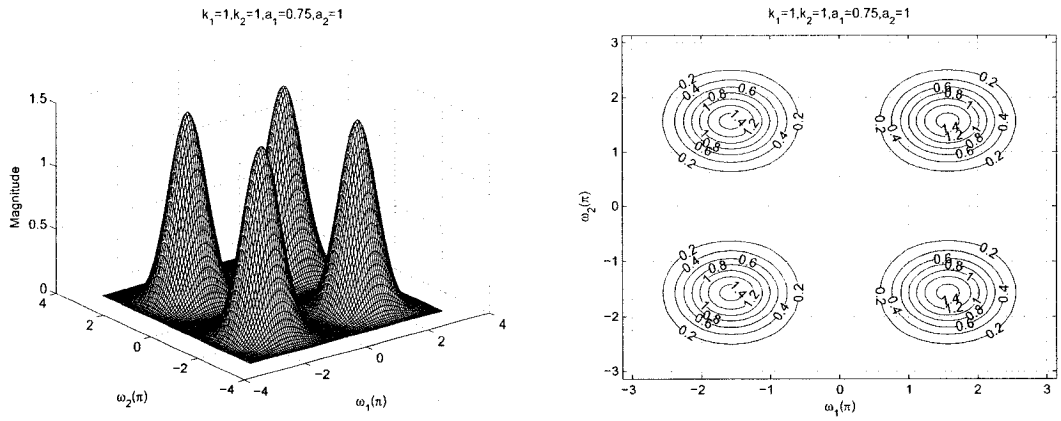

(a) $a_1 = 0.75$

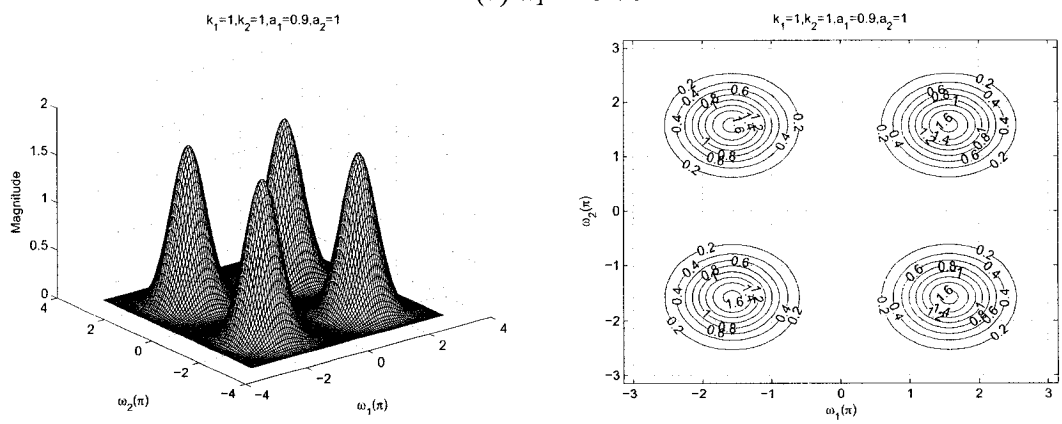

(b) $a_1 = 0.9$

Figure 4.32: 3-D amplitude frequency response and the contour response of the All-pole 2-D digital bandpass filter for different values of a_1

4.3.2.4 Frequency Response of the All-pole 2-D Digital Bandpass Filter with different values of a_2

In the Section 4.3.2.3, the effect of the coefficient of a_1 was studied. In this section, the effect of the coefficient a_2 will be studied. The stable range of a_2 can be obtained with other specified coefficients of the generalized bilinear transformation. There are many combinations possible for the coefficients. To study the response with different values of a_2 properly, we fix other coefficient values to be equal to unity. The range of a_2 varies from 0.1 to 1 and the other coefficient values are specified as unity, i.e., $k_1 = 1$, $k_2 = 1$, $a_1 = 1$, $b_1 = 1$ and $b_2 = 1$ in order to get the all-pole 2-D digital bandpass filter response

in Category B.

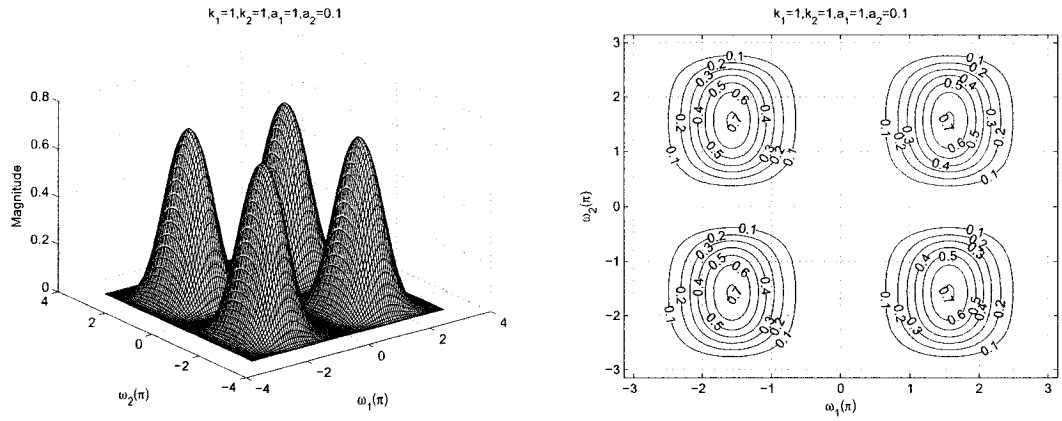

(a) $a_2 = 0.1$

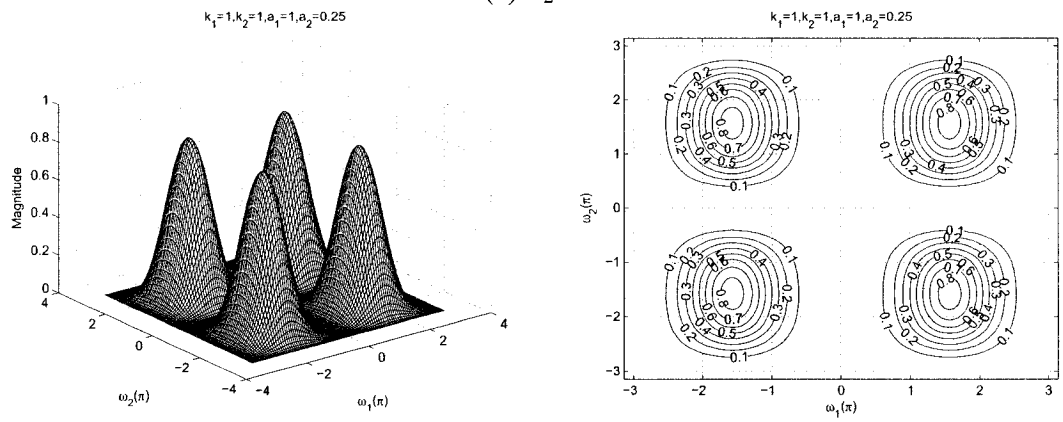

(b) $a_2 = 0.25$

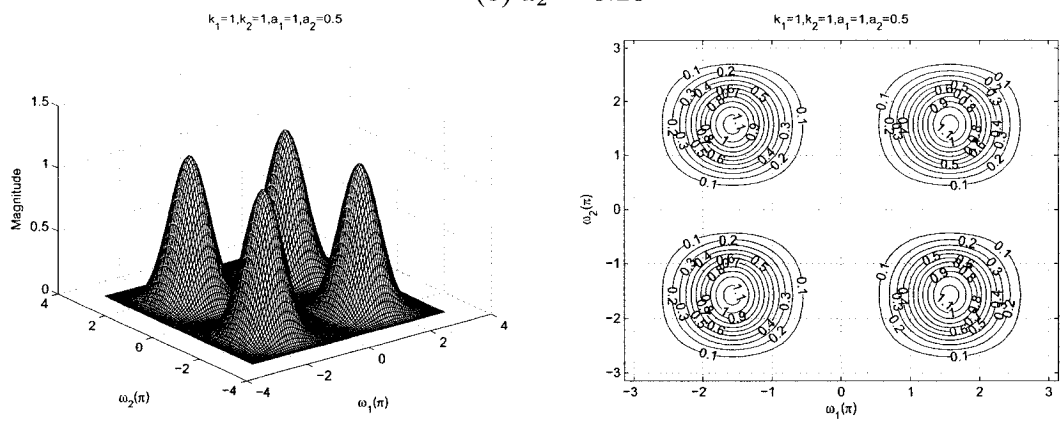

(c) $a_2 = 0.5$

Figure 4.33: 3-D amplitude frequency response and the contour response of the All-pole2-D digital bandpass filter for different values of a_2

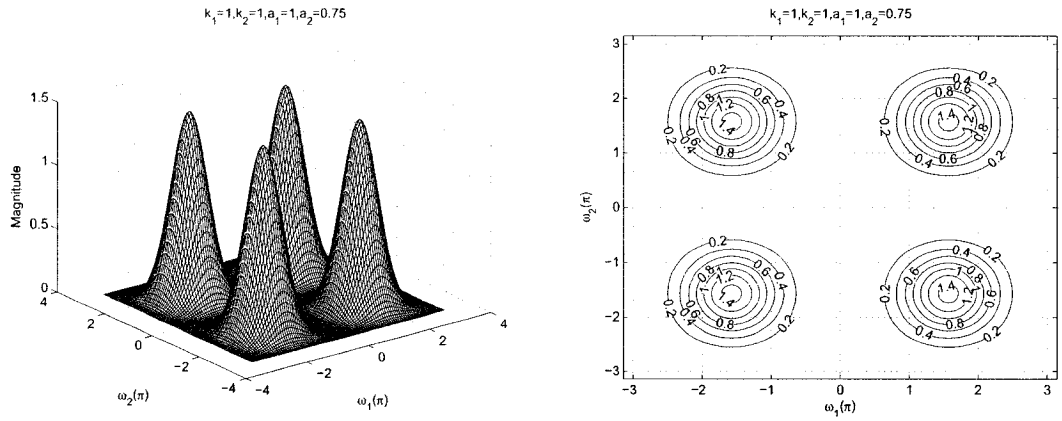

(a) $a_2 = 0.75$

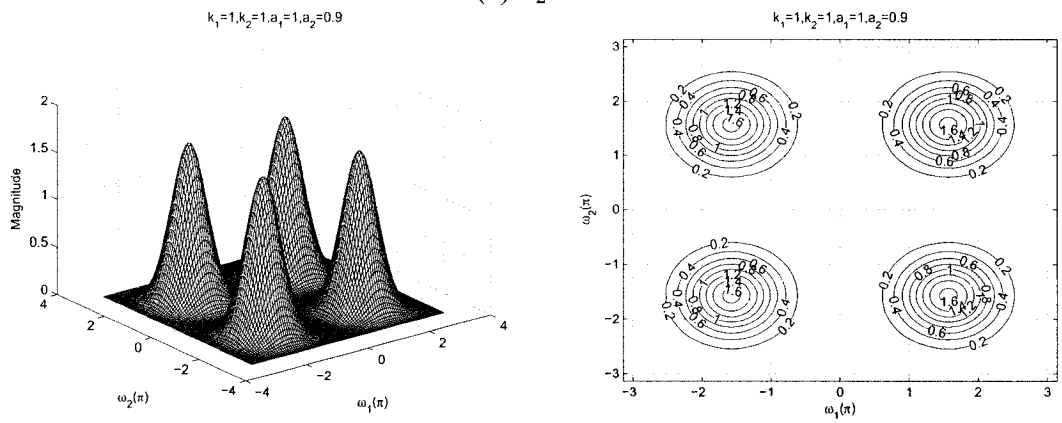

(b) $a_2 = 0.9$

Figure 4.34: 3-D amplitude frequency response and the contour response of the All-pole 2-D digital bandpass filter for different values of a_2

By varying the value of a_2, the 3-D magnitude response and contour plots which represents different values of a_2, i.e., $a_2 = 0.1$, $a_2 = 0.25$, $a_2 = 0.5$, $a_2 = 0.75$, and $a_2 = 0.9$ are shown in the Figures 4.33 and 4.34. By making the value of $a_2 = 1$, it resembles the standard all-pole 2-D digital bandpass filter as shown in the Figure 4.26. It is observed from the diagrams that the coefficient a_2 affects the gain of the amplitude-frequency response. At the lowest value of $a_2 = 0.1$, the gain of the amplitude-frequency response is 0.7. As the value of a_2 increases, the gain increases and reach the maximum value at $a_2 = 1$. As seen from the diagrams, that as we increase the value of a_1 from 0.1 to 0.9, the gain of the amplitude-frequency response increases from 0.7 to 1.6. Also, the coefficient a_2 does not have any effect along the $\omega_2 - axis$.

4.3.2.5 Frequency Response of the All-pole 2-D Digital Bandpass Filter with same values of a_1 and a_2 and same values of k_1 and k_2

In the Sections 4.3.2.1 to 4.3.2.4 the individual effect of the coefficients a_1, a_2, k_1 and k_2 were studied. In this section, we will study the effect of coefficients, where $a_1 = a_2$ and $k_1 = k_2$ and the remaining coefficients b_1 and b_2 are considered to be unity for the all-pole 2-D digital bandpass filter in Category B. The values of a_1 and a_2 ranges from 0 to 1 and the values of k_1 and k_2 ranges from 0 to 5.

As observed from the Figures 4.35 to 4.38, the coefficients k_1 and k_2 affect the passband width of the frequency response. In the Figures 4.35 (a), 4.36 (b) and 4.37 (c), there is a gradual decrease in the passband width of the contour response as the values of k_1 and k_2 are increased from 0.5 to 5 for the same values of $a_1 = a_2 = 0.25$. It is also observed that there is also a decrease in the magnitude of the contour response for the same.

As observed from the Figures 4.35 to 4.38, the coefficients a_1 and a_2 affect the gain of the amplitude-frequency response. It can be clearly observed from the Figures 4.35 (a), (b), (c) and 4.36 (a), that the gain of the amplitude-frequency response increases from 2.5 to 9 when the values of a_1 and a_2 are increased from 0.25 to 0.9 keeping the same value of $k_1 = k_2 = 0.5$. In addition, the width of the passband increases and decreases periodically for the same.

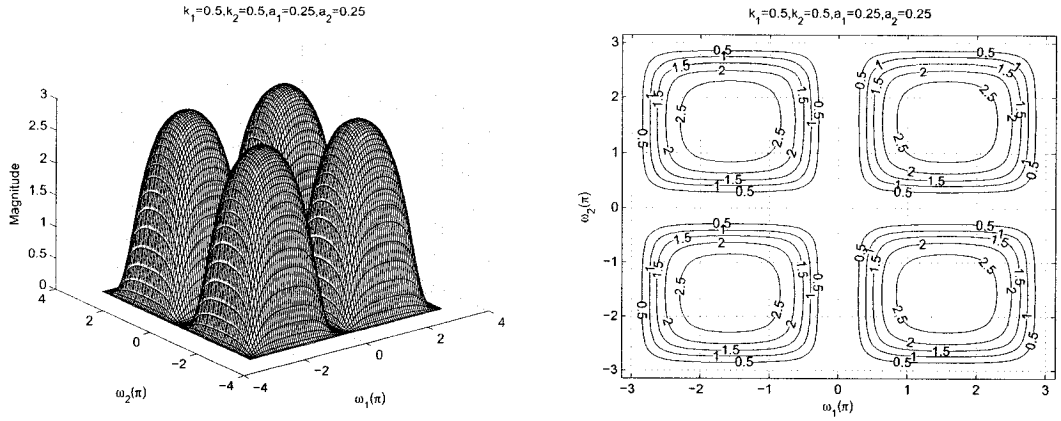

(a) $a_1 = a_2 = 0.25$ and $k_1 = k_2 = 0.5$

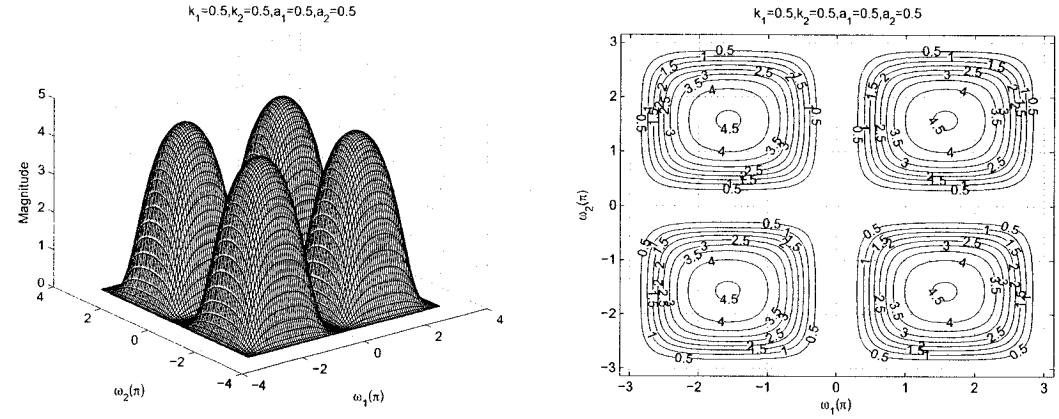

(b) $a_1 = a_2 = 0.5$ and $k_1 = k_2 = 0.5$

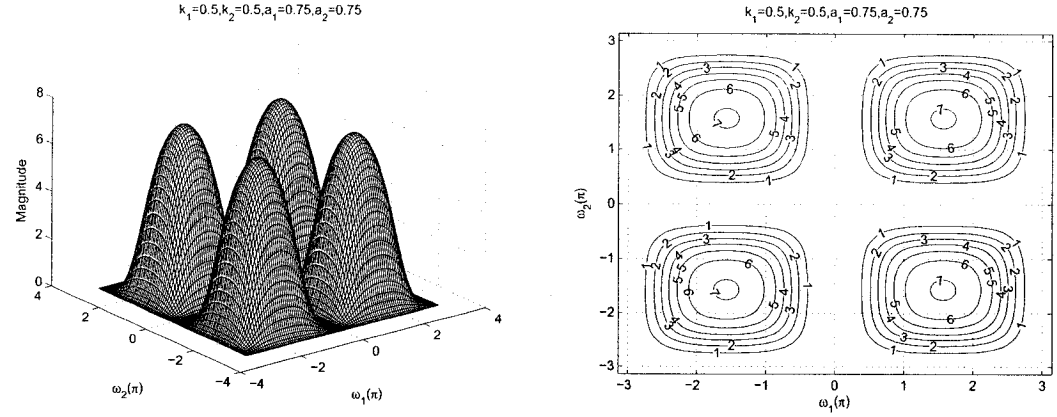

(c) $a_1 = a_2 = 0.75$ and $k_1 = k_2 = 0.5$

Figure 4.35: 3-D amplitude frequency response and the contour response of the All-pole 2-D digital bandpass filter for $a_1 = a_2$ and $k_1 = k_2$

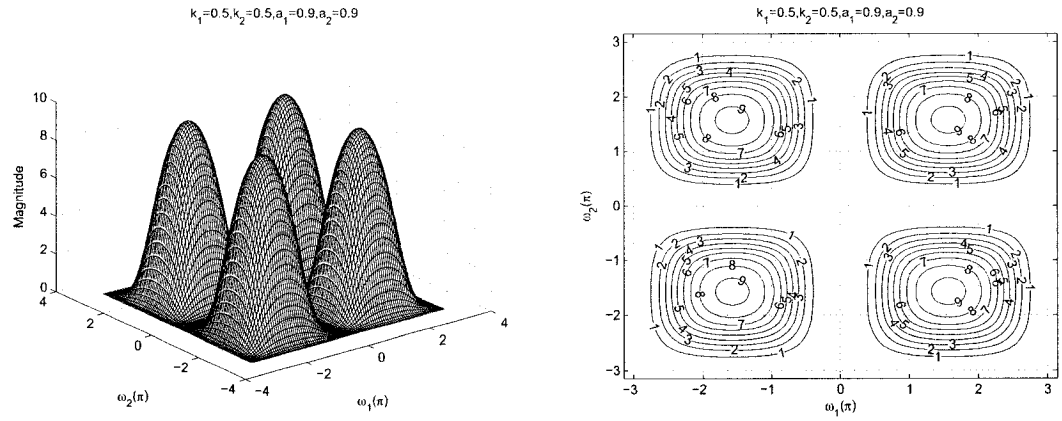

(a) $a_1 = a_2 = 0.9$ and $k_1 = k_2 = 0.5$

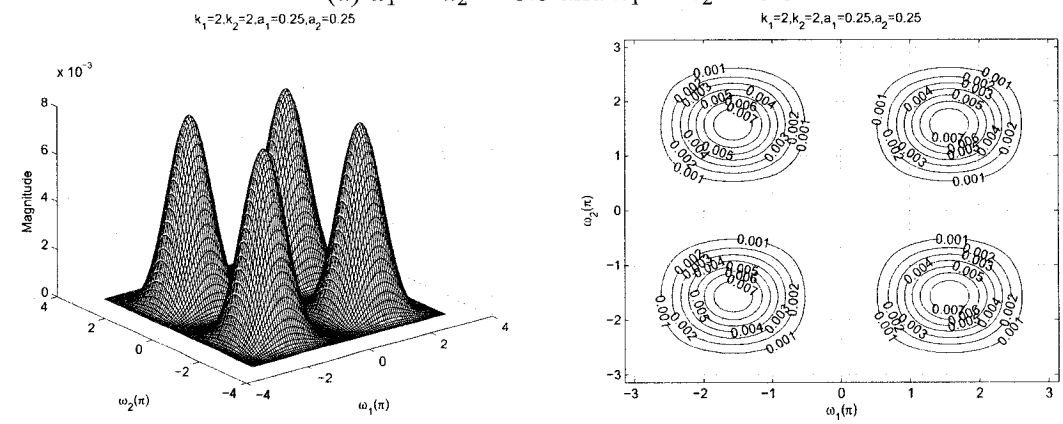

(b) $a_1 = a_2 = 0.25$ and $k_1 = k_2 = 2$

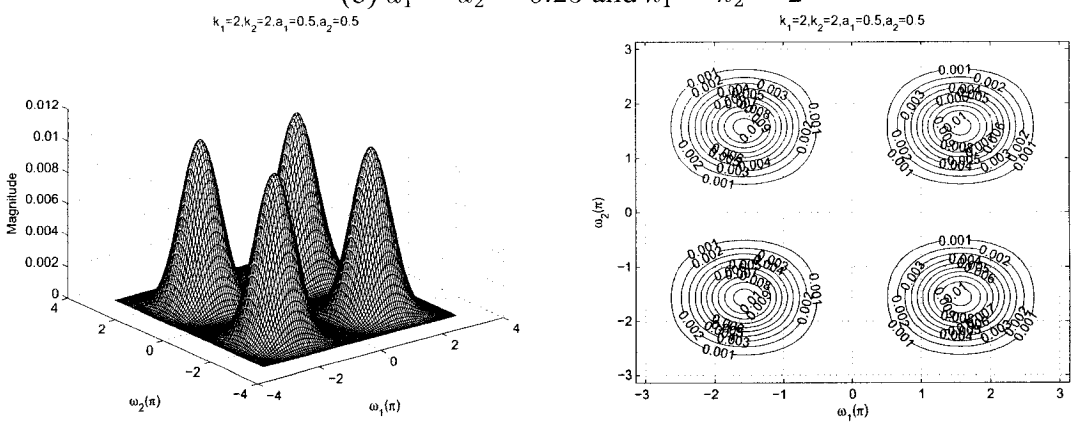

(c) $a_1 = a_2 = 0.5$ and $k_1 = k_2 = 2$

Figure 4.36: 3-D amplitude frequency response and the contour response of the All-pole 2-D digital bandpass filter for $a_1 = a_2$ and $k_1 = k_2$

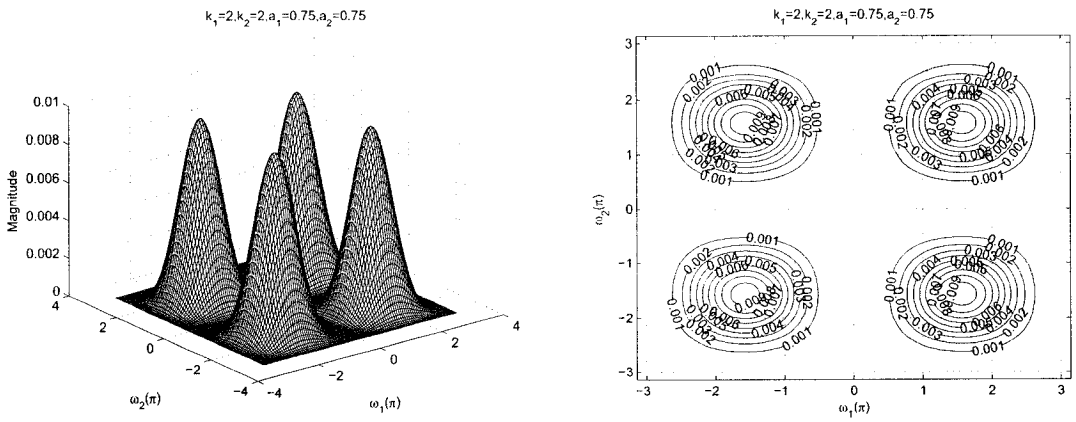

(a) $a_1 = a_2 = 0.75$ and $k_1 = k_2 = 2$

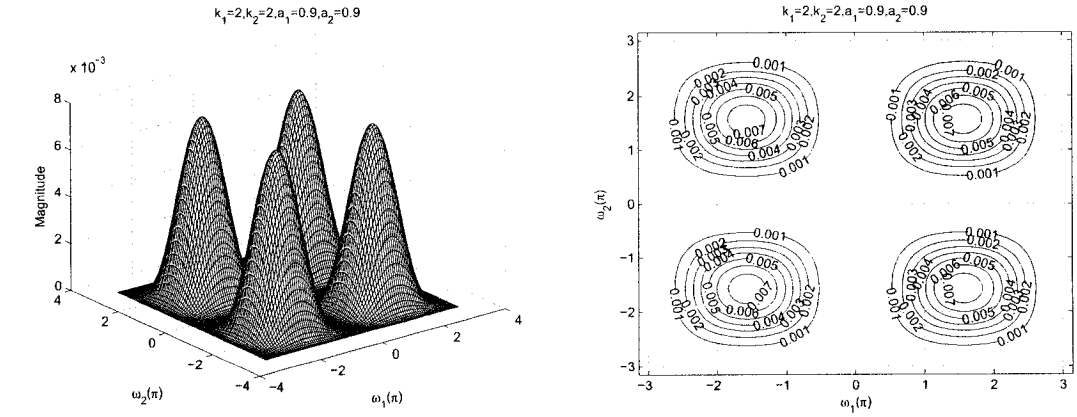

(b) $a_1 = a_2 = 0.9$ and $k_1 = k_2 = 2$

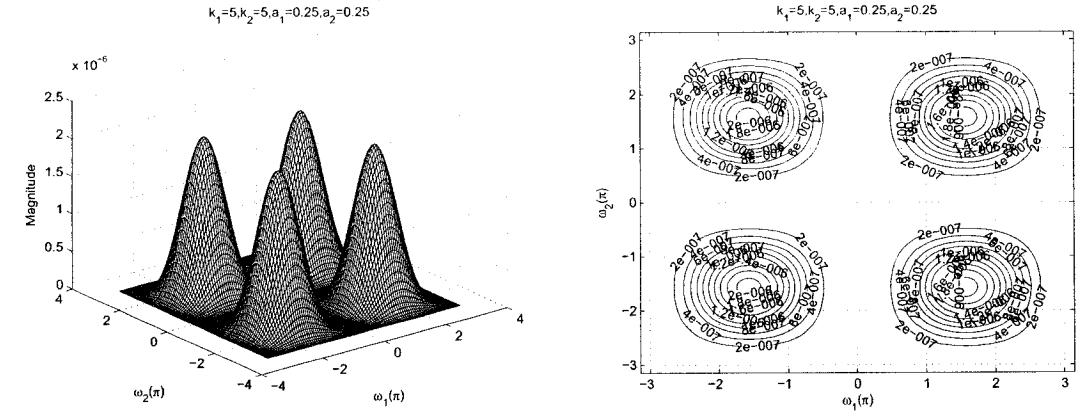

(c) $a_1 = a_2 = 0.25$ and $k_1 = k_2 = 5$

Figure 4.37: 3-D amplitude frequency response and the contour response of the All-pole 2-D digital bandpass filter for $a_1 = a_2$ and $k_1 = k_2$

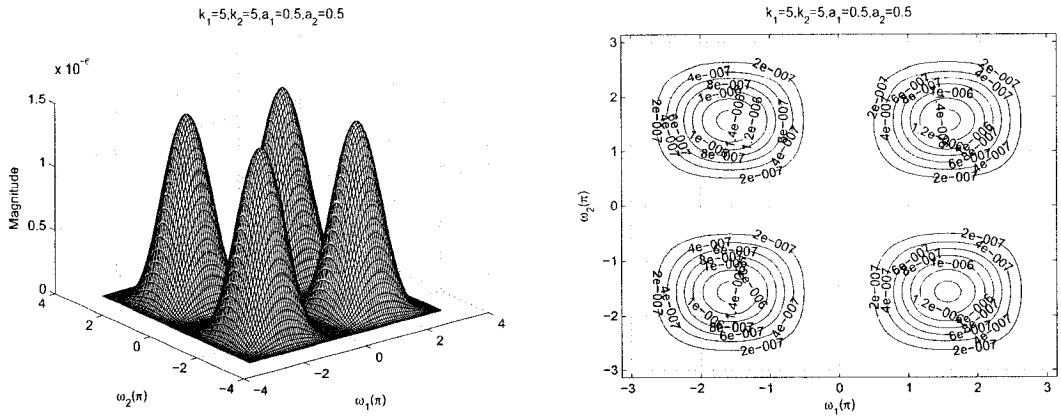

(a) $a_1 = a_2 = 0.5$ and $k_1 = k_2 = 5$

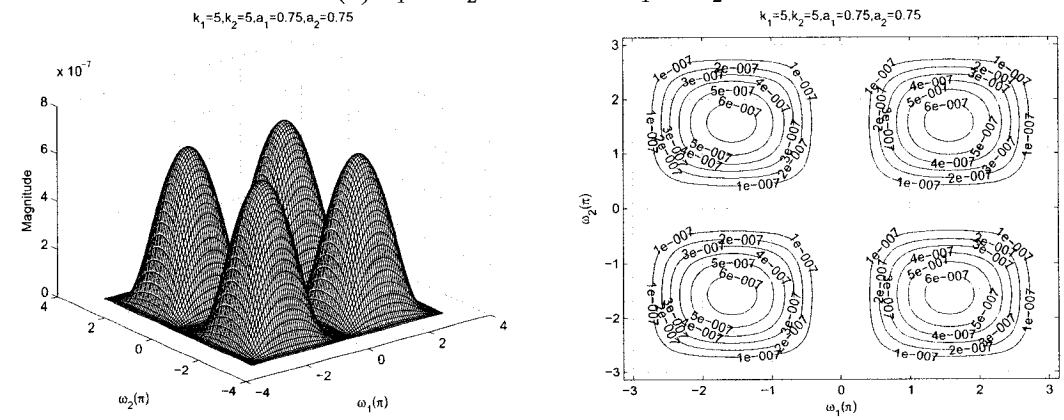

(b) $a_1 = a_2 = 0.75$ and $k_1 = k_2 = 5$

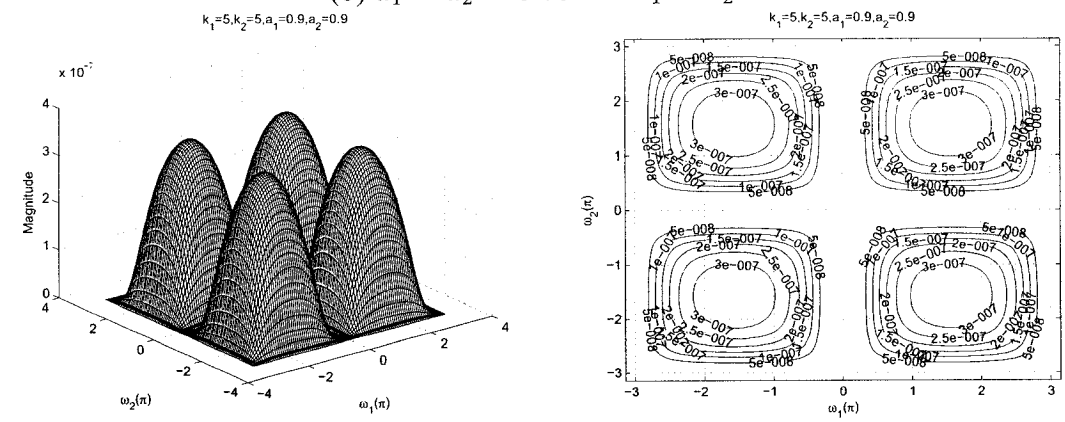

(c) $a_1 = a_2 = 0.9$ and $k_1 = k_2 = 5$

Figure 4.38: 3-D amplitude frequency response and the contour response of the All-pole 2-D digital bandpass filter for $a_1 = a_2$ and $k_1 = k_2$

4.3.2.6 Frequency Response of the All-pole 2-D Digital Bandpass Filter with different values of a_1 and a_2 and same values of k_1 and k_2

In this section, we will study the effect of coefficients, where $a_1 \neq a_2$ and $k_1 = k_2$ and the remaining coefficients b_1 and b_2 are considered to be unity for the all-pole 2-D digital band-pass filter in Category B. The values of a_1 ranges from 0.25 to 0.5 and a_2 ranges from 0.5 to 0.75, and the values of k_1 and k_2 ranges from 0.5 to 5.

As observed from the Figures 4.39 to 4.42, the coefficients k_1 and k_2 affect the passband width of the frequency response of the all-pole 2-D digital bandpass filter. In the Figures 4.39 (a), 4.40 (a), 4.41 (a) and 4.42 (a), there is a gradual decrease in the passband width as the values of k_1 and k_2 are increased from 0.5 to 5 for different values of $a_1 = 0.25$ and $a_2 = 0.5$. At the same time there is a gradual decrease in the magnitude of the contour response for the same values.

As observed from the Figures 4.39 to 4.42, the coefficients a_1 and a_2 affect the gain of the amplitude-frequency response. It can be clearly observed from the Figures 4.39 (a), (b), and (c), that the gain of the amplitude-frequency response increases from 3.5 to 5.5 when the values of a_1 and a_2 are increased from 0.25 to 0.5 and 0.5 to 0.75 while keeping the same value of $k_1 = k_2 = 0.5$. In addition, the width of the passband increases and decreases periodically for the same.

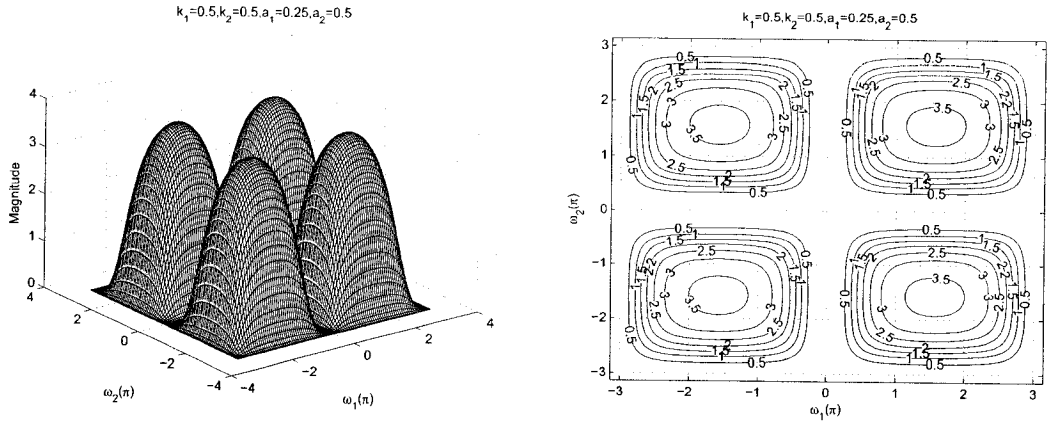

(a) $a_1 = 0.25$, $a_2 = 0.5$ and $k_1 = k_2 = 0.5$

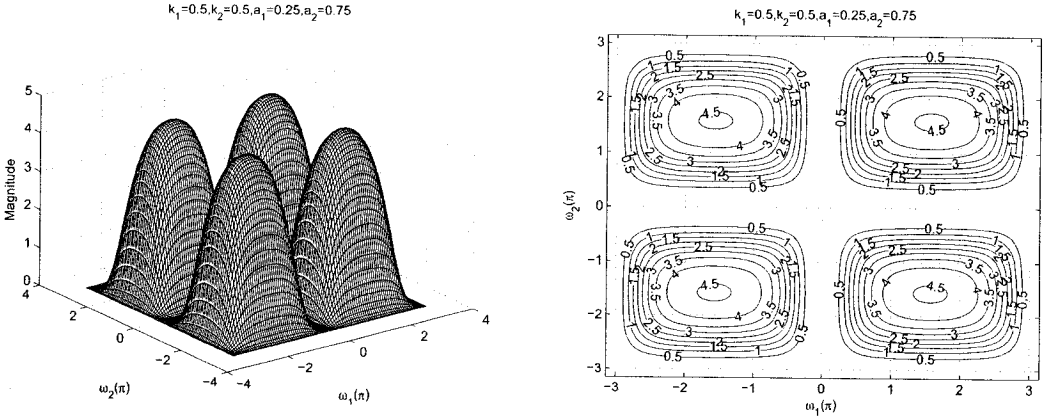

(b) $a_1 = 0.25$, $a_2 = 0.75$ and $k_1 = k_2 = 0.5$

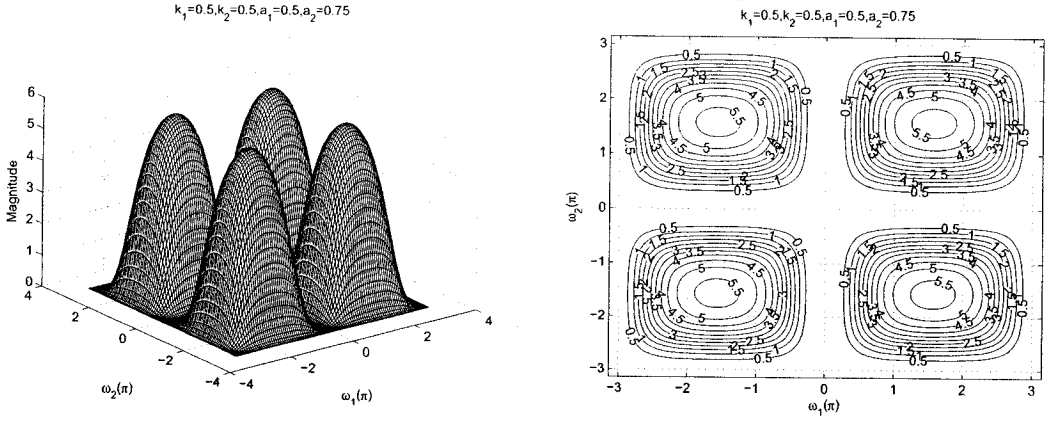

(c) $a_1 = 0.5$, $a_2 = 0.75$ and $k_1 = k_2 = 0.5$

Figure 4.39: 3-D amplitude frequency response and the contour response of the All-pole 2-D digital bandpass filter for $a_1 \neq a_2$ and $k_1 = k_2$

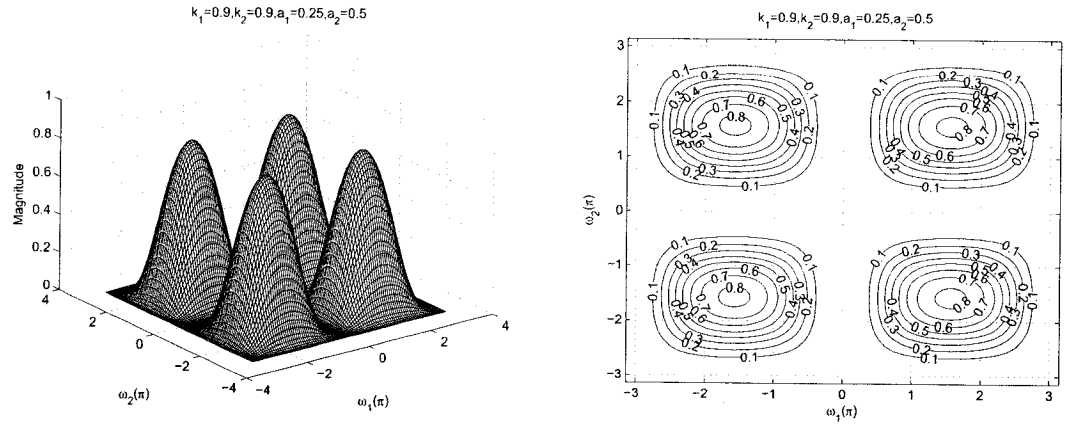

(a) $a_1 = 0.25$, $a_2 = 0.5$ and $k_1 = k_2 = 0.9$

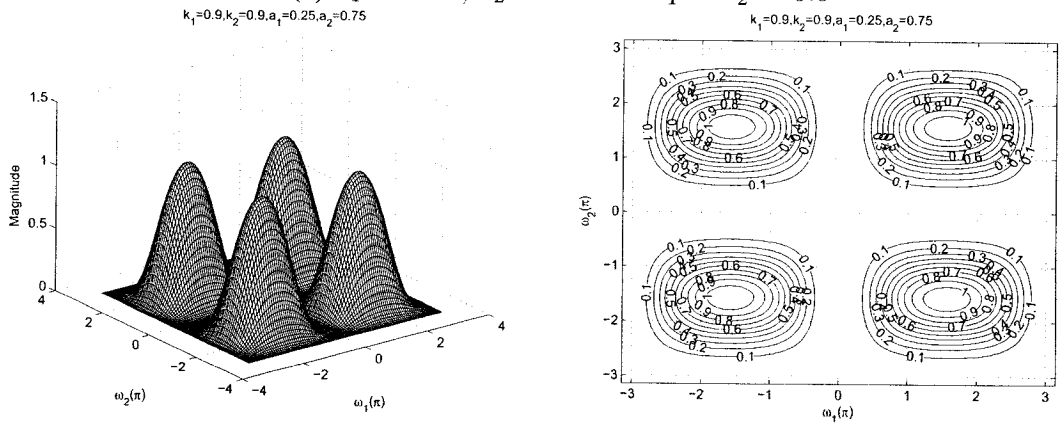

(b) $a_1 = 0.25$, $a_2 = 0.75$ and $k_1 = k_2 = 0.9$

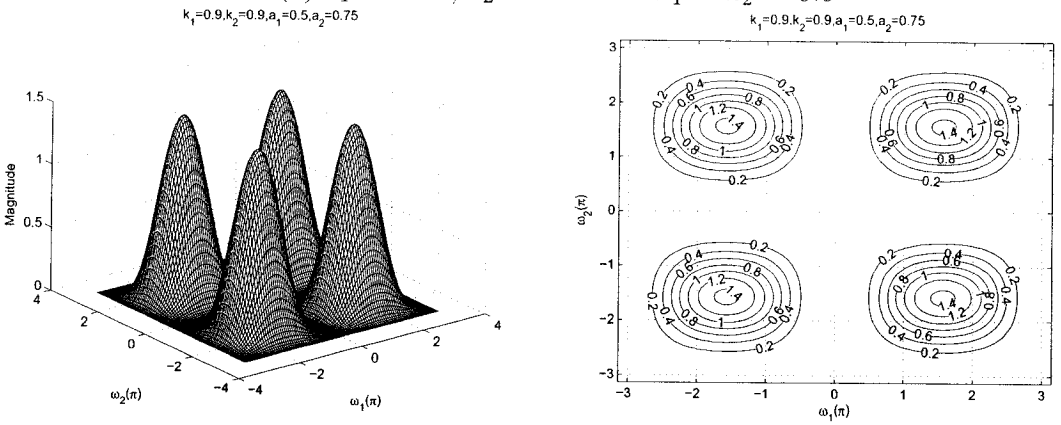

(c) $a_1 = 0.5$, $a_2 = 0.75$ and $k_1 = k_2 = 0.9$

Figure 4.40: 3-D amplitude frequency response and the contour response of the All-pole 2-D digital bandpass filter for $a_1 \neq a_2$ and $k_1 = k_2$

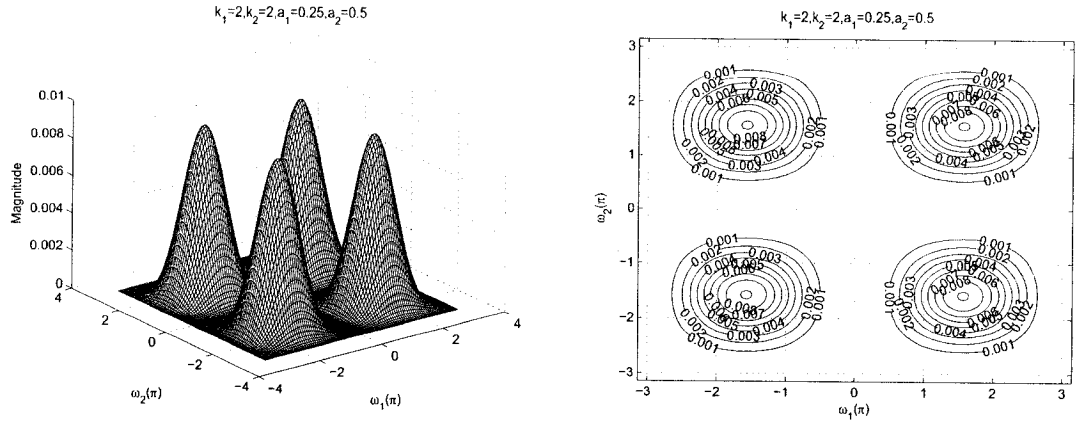

(a) $a_1 = 0.25$, $a_2 = 0.5$ and $k_1 = k_2 = 2$

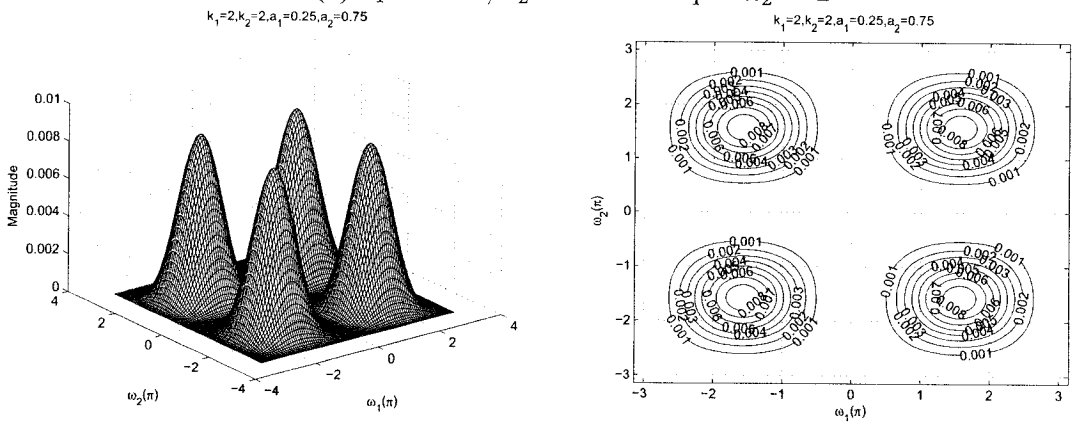

(b) $a_1 = 0.25$, $a_2 = 0.75$ and $k_1 = k_2 = 2$

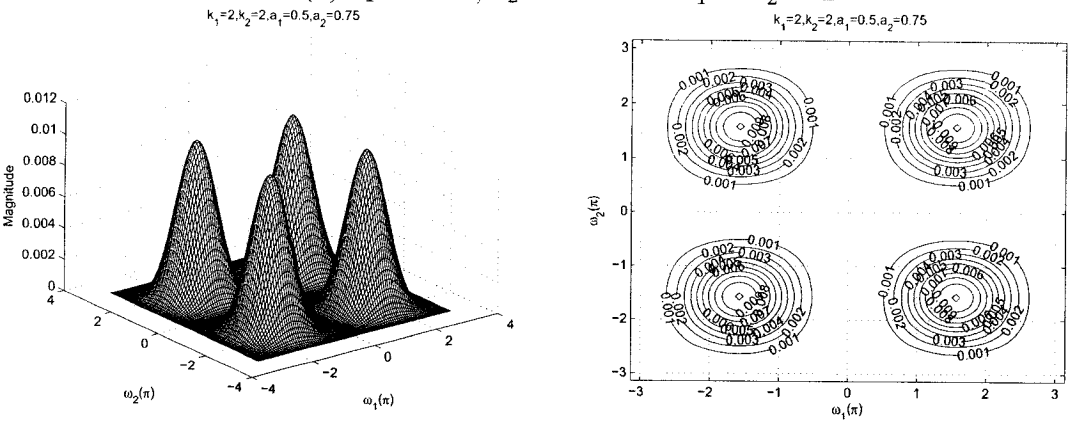

(c) $a_1 = 0.5$, $a_2 = 0.75$ and $k_1 = k_2 = 2$

Figure 4.41: 3-D amplitude frequency response and the contour response of the All-pole 2-D digital bandpass filter for $a_1 \neq a_2$ and $k_1 = k_2$

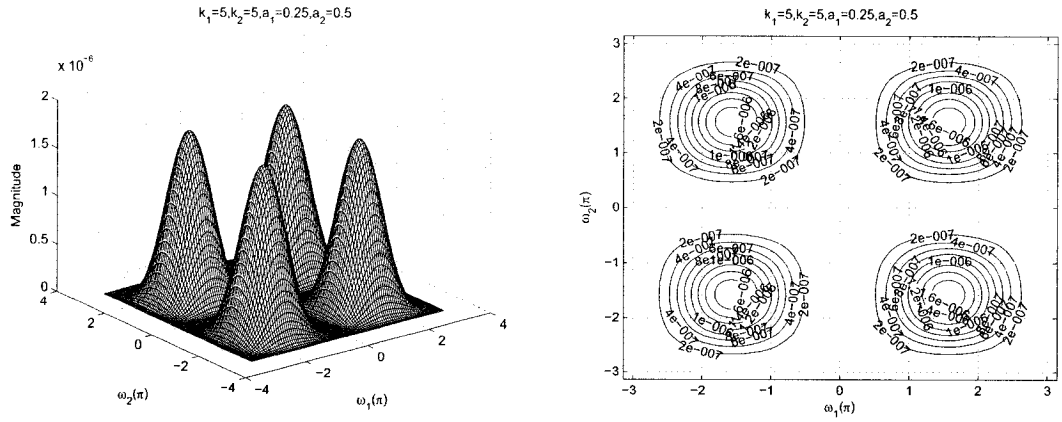

(a) $a_1 = 0.25$, $a_2 = 0.5$ and $k_1 = k_2 = 5$

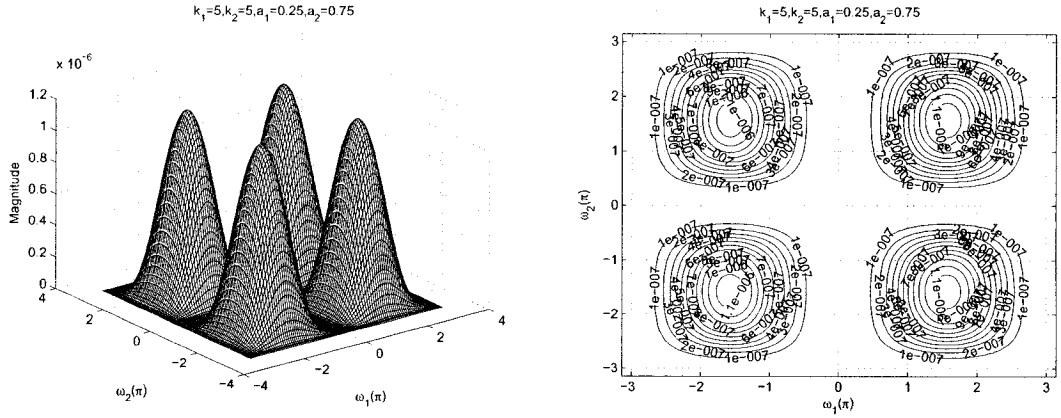

(b) $a_1 = 0.25$, $a_2 = 0.75$ and $k_1 = k_2 = 5$

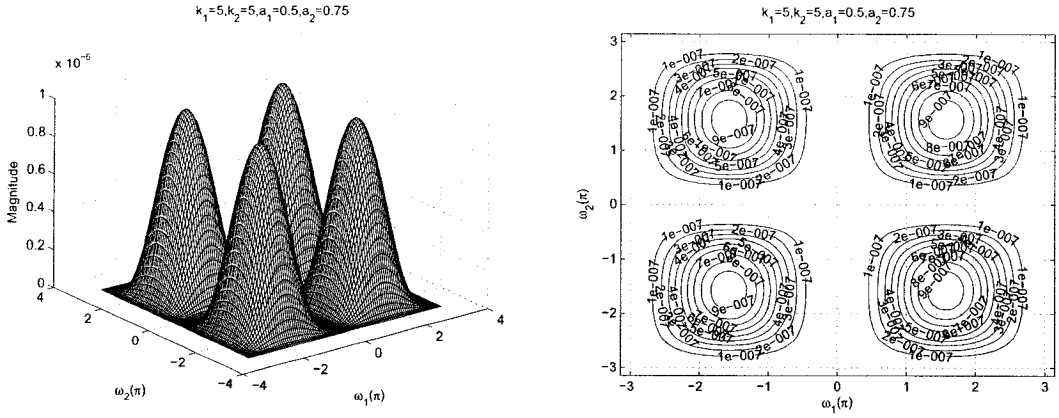

(c) $a_1 = 0.5$, $a_2 = 0.75$ and $k_1 = k_2 = 5$

Figure 4.42: 3-D amplitude frequency response and the contour response of the All-pole 2-D digital bandpass filter for $a_1 \neq a_2$ and $k_1 = k_2$

4.3.2.7 Frequency Response of the All-pole 2-D Digital Bandpass Filter with different values of a_1 and a_2 and different values of k_1 and k_2

In this section, we study the effect of coefficients when $a_1 \neq a_2$ and $k_1 \neq k_2$, and the remaining coefficients b_1 and b_2 are considered to be unity for the all-pole 2-D digital band-pass filter in Category B. The values of a_1 and a_2 vary from 0.25 to 0.5 and 0.5 to 0.5 respectively, and the values of k_1 and k_2 vary from 0.25 to 5 and 0.5 to 8 respectively.

As observed from the Figures 4.43 to 4.46, the coefficients k_1 and k_2 affect the passband width of the frequency response. In the Figures 4.43 (a), (b), (c) and 4.44 (a), there is a gradual decrease in the passband width of the contour response as the values of k_1 and k_2 are increased from 0.25 to 5 and from 0.5 to 8 respectively, for the different values of a_1 and a_2 as 0.25 and 0.5, respectively. At the same time there is also a gradual decrease in the amplitude of the contour response for the same values.

As observed from the Figures 4.43 to 4.46, the coefficients a_1 and a_2 affect the gain of the amplitude-frequency response. It can be clearly observed from the Figures 4.43 (a), 4.44 (b) and 4.45 (c), that the gain of the amplitude-frequency response increases from 5.5 to 10 when the values of a_1 and a_2 are increased from 0.25 to 0.75 and 0.5 to 0.9, respectively, keeping the same value of $k_1 = 0.25$ and $k_2 = 0.5$. In addition, the width of the passband increases and decreases periodically for the same.

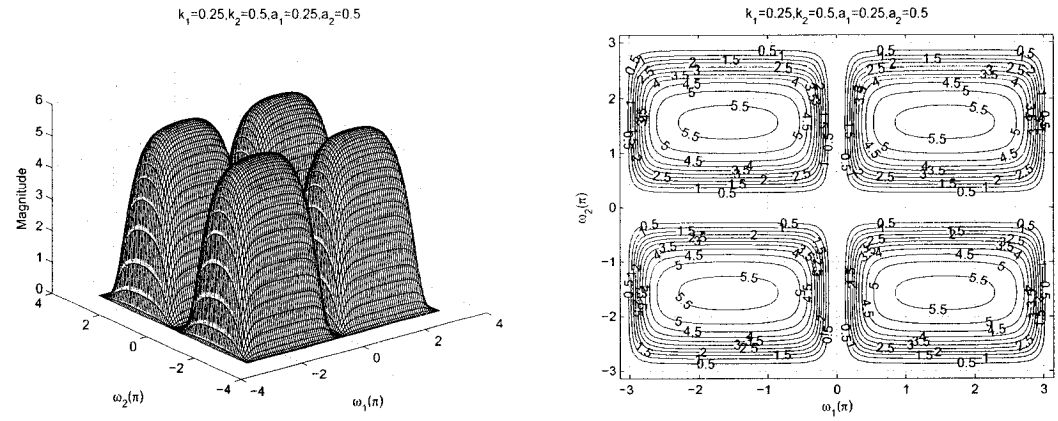

(a) $a_1 = 0.25$, $a_2 = 0.5$ and $k_1 = 0.25$, $k_2 = 0.5$

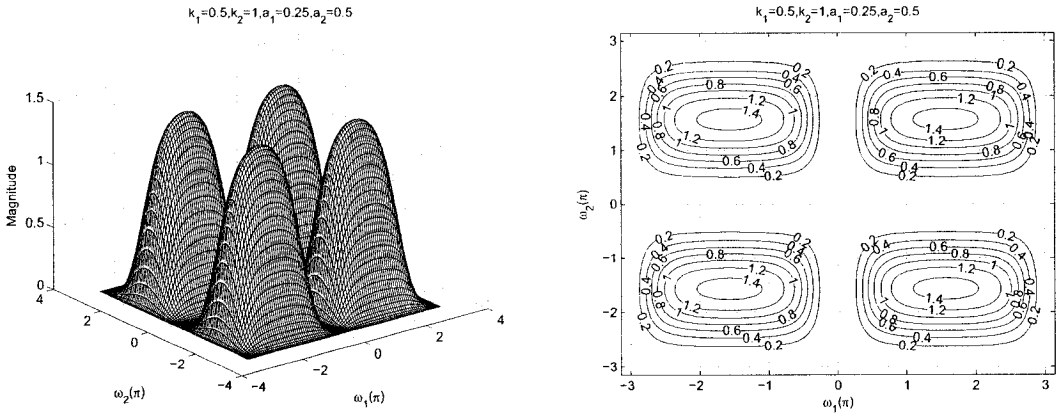

(b) $a_1 = 0.25$, $a_2 = 0.5$ and $k_1 = 0.5$, $k_2 = 1$

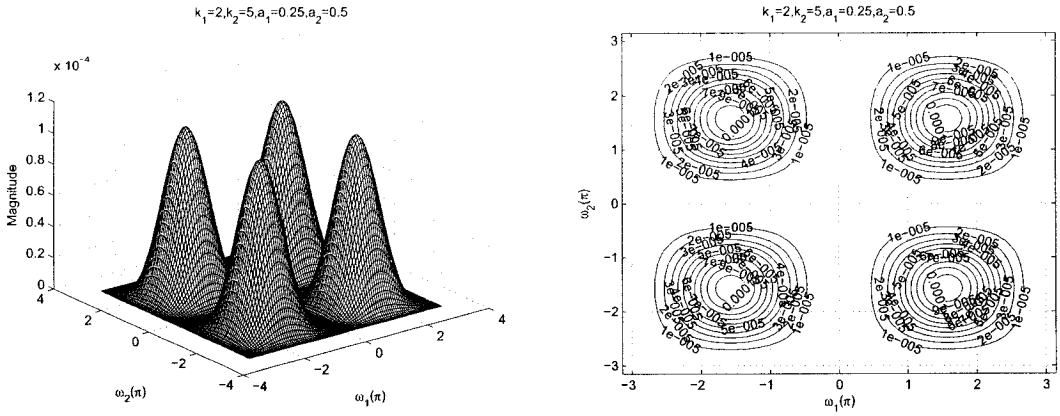

(c) $a_1 = 0.25$, $a_2 = 0.5$ and $k_1 = 2$, $k_2 = 5$

Figure 4.43: 3-D amplitude frequency response and the contour response of the All-pole 2-D digital bandpass filter for $a_1 \neq a_2$ and $k_1 \neq k_2$

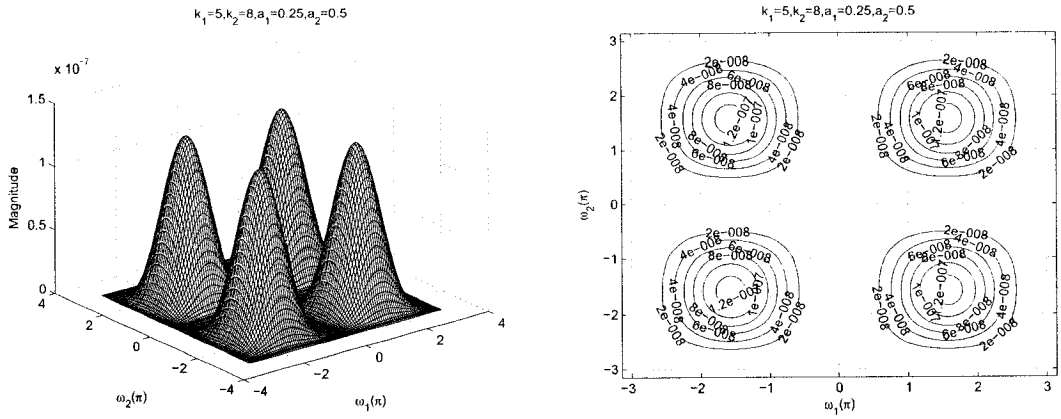

(a) $a_1 = 0.25$, $a_2 = 0.5$ and $k_1 = 5$, $k_2 = 8$

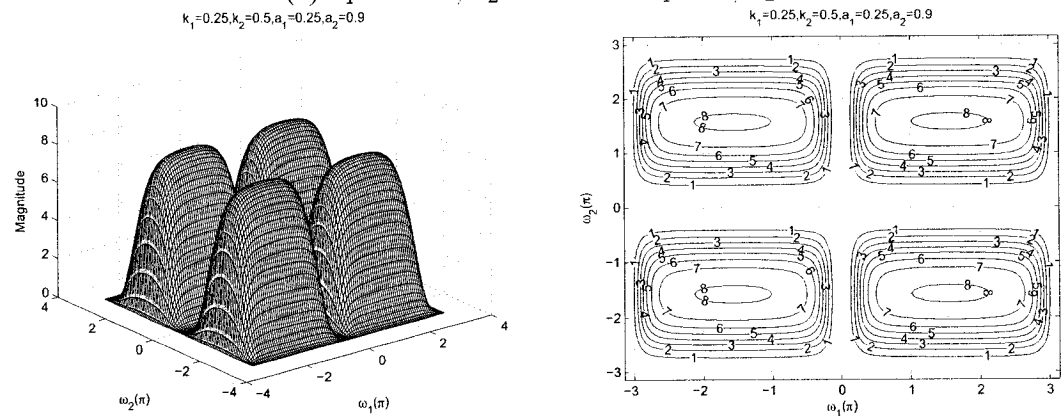

(b) $a_1 = 0.25$, $a_2 = 0.9$ and $k_1 = 0.25$, $k_2 = 0.5$

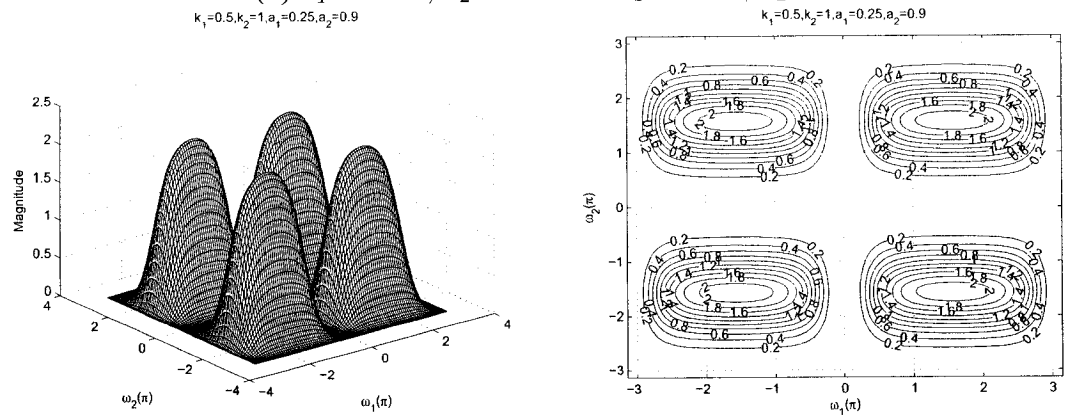

(c) $a_1 = 0.25$, $a_2 = 0.9$ and $k_1 = 0.5$, $k_2 = 1$

Figure 4.44: 3-D amplitude frequency response and the contour response of the All-pole 2-D digital bandpass filter for $a_1 \neq a_2$ and $k_1 \neq k_2$

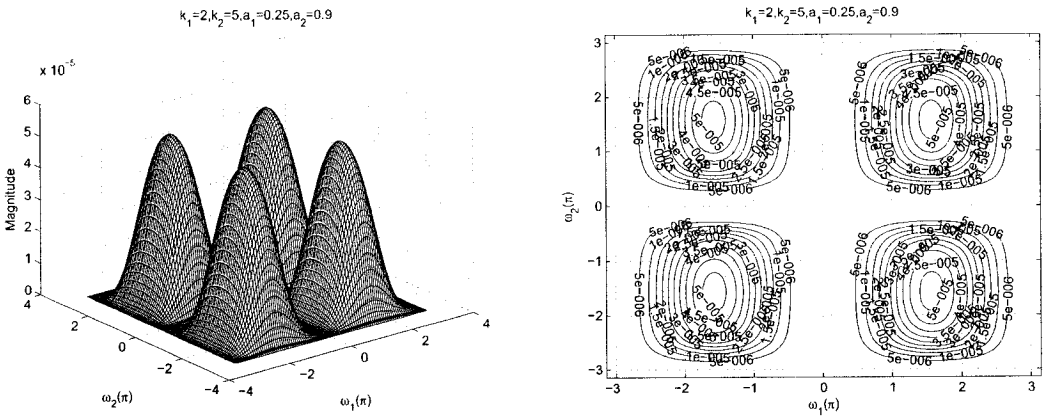

(a) $a_1 = 0.25$, $a_2 = 0.9$ and $k_1 = 2$, $k_2 = 5$

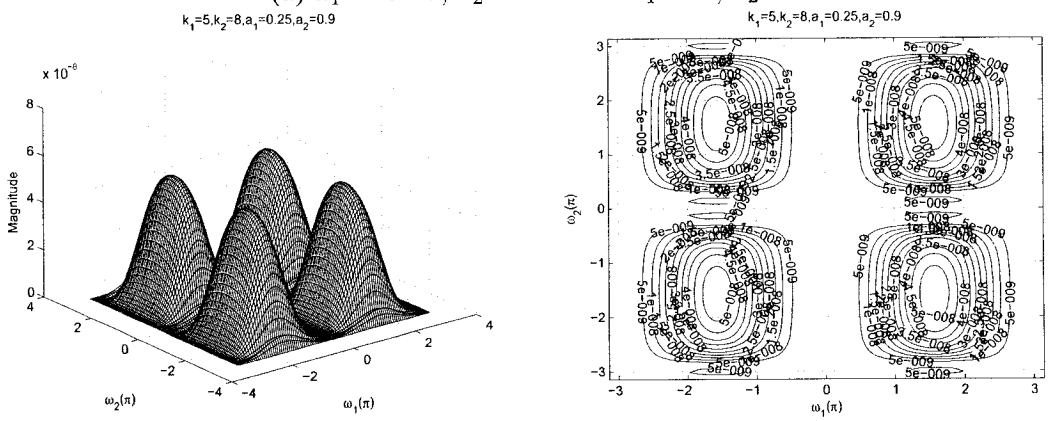

(b) $a_1 = 0.25$, $a_2 = 0.9$ and $k_1 = 5$, $k_2 = 8$

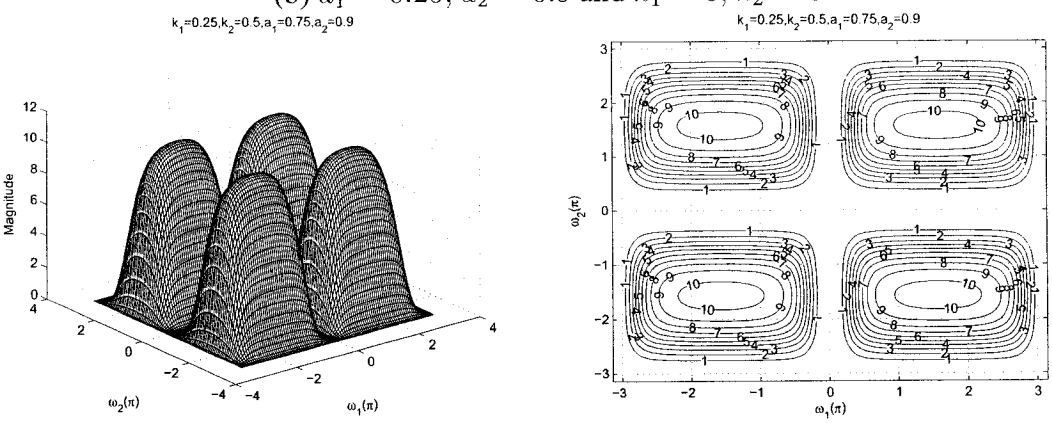

(c) $a_1 = 0.75$, $a_2 = 0.9$ and $k_1 = 0.25$, $k_2 = 0.5$

Figure 4.45: 3-D amplitude frequency response and the contour response of the All-pole 2-D digital bandpass filter for $a_1 \neq a_2$ and $k_1 \neq k_2$

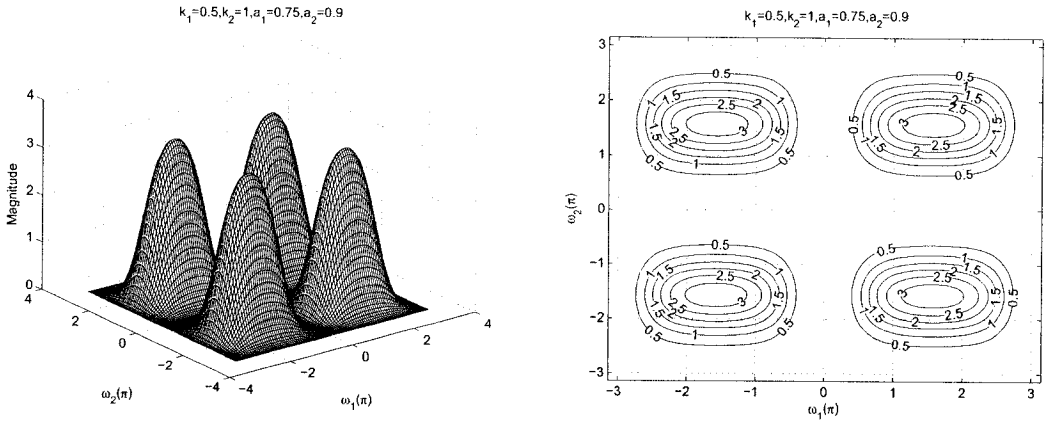

(a) $a_1 = 0.75$, $a_2 = 0.9$ and $k_1 = 0.5$, $k_2 = 1$

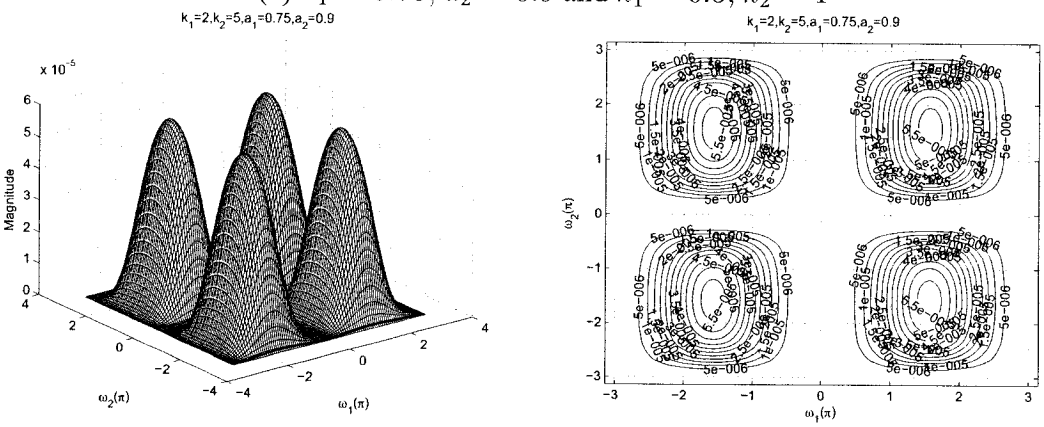

(b) $a_1 = 0.75$, $a_2 = 0.9$ and $k_1 = 2$, $k_2 = 5$

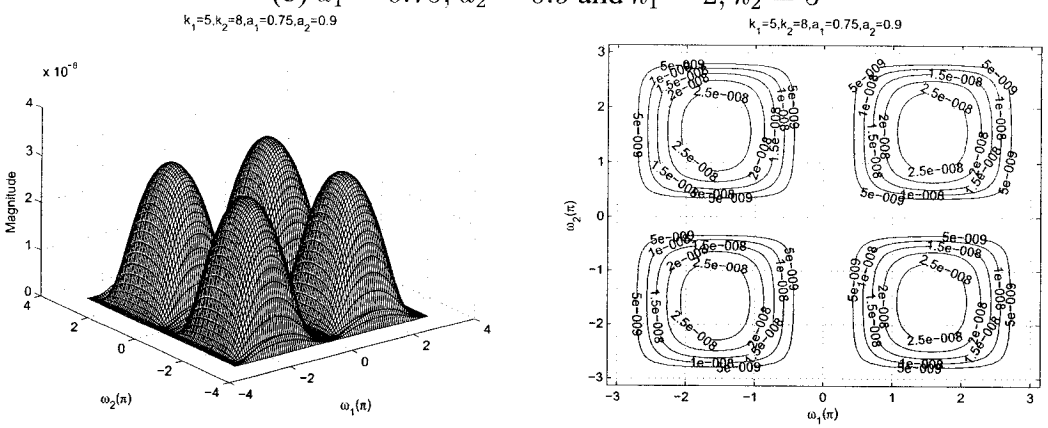

(c) $a_1 = 0.75$, $a_2 = 0.9$ and $k_1 = 5$, $k_2 = 8$

Figure 4.46: 3-D amplitude frequency response and the contour response of the All-pole 2-D digital bandpass filter for $a_1 \neq a_2$ and $k_1 \neq k_2$

4.3.2.8 Frequency Response of the All-pole 2-D Digital Bandpass Filter with same values of a_1 and a_2 and different values of k_1 and k_2

In this section, we study the effect of coefficients, where $a_1 = a_2$ and $k_1 \neq k_2$ and the remaining coefficients b_1 and b_2 are considered to be unity for the all-pole 2-D digital band-pass filter in Category B. The values of a_1 and a_2 vary from 0 to 1 and the values of k_1 and k_2 vary from 0.25 to 2 and 0.5 to 5 respectively.

As observed from the Figures 4.47 to 4.50, the coefficients k_1 and k_2 affect the passband width of the frequency response. In the Figures 4.47 (a), (b) and (c), there is a gradual decrease in the passband width of the contour response when the values of k_1 and k_2 are increased from 0.25 to 2 and 0.5 to 5 respectively, for the same values of $a_1 = a_2 = 0.25$. At the same time there is also a gradual decrease in the amplitude of the contour response.

As observed from the Figures 4.47 to 4.50, the coefficients a_1 and a_2 affect the gain of the amplitude-frequency response. It can be clearly observed from the Figures 4.47 (a), 4.48 (a), 4.49 (a) and 4.50 (a), that the amplitude of the contour response increases from 4.5 to 11 when the values of a_1 and a_2 are increased from 0.25 to 0.9 keeping the same value of $k_1 = 0.25$ and $k_2 = 0.5$. In addition, the width of the passband increases and decreases periodically for the same.

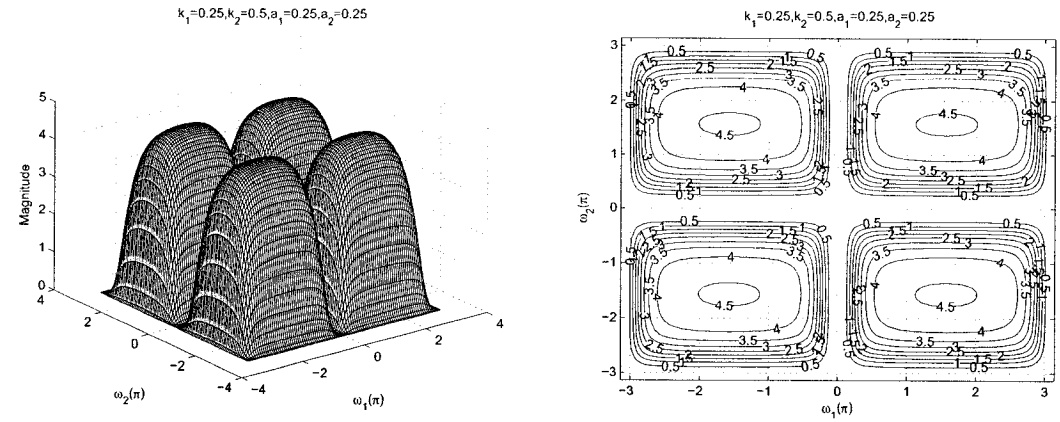

(a) $a_1 = a_2 = 0.25$ and $k_1 = 0.25$, $k_2 = 0.5$

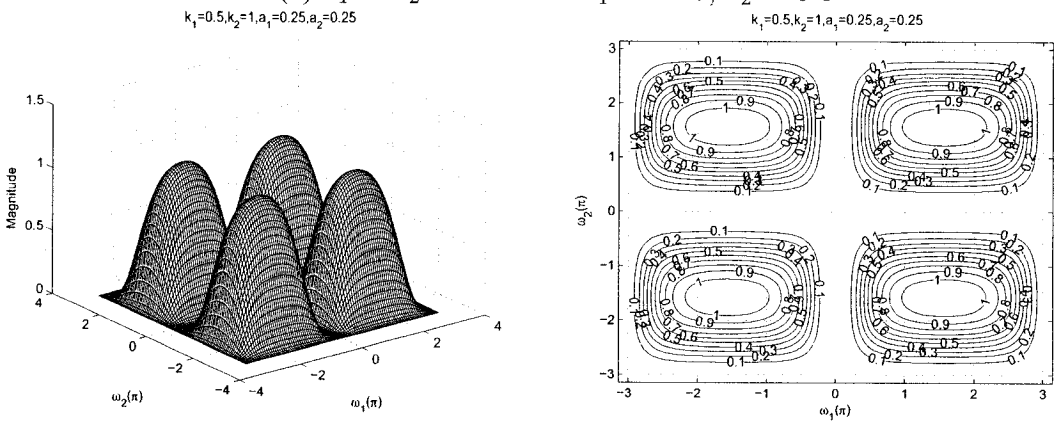

(b) $a_1 = a_2 = 0.25$ and $k_1 = 0.5$, $k_2 = 1$

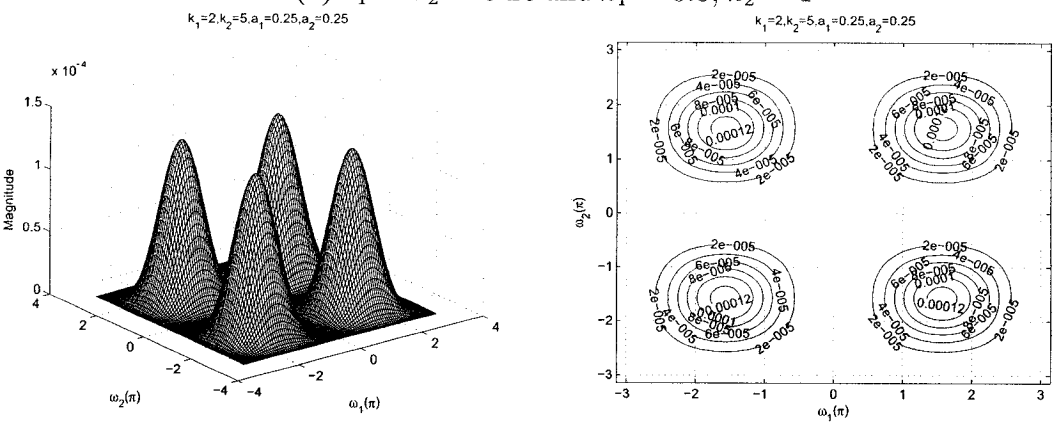

(c) $a_1 = a_2 = 0.25$ and $k_1 = 2$, $k_2 = 5$

Figure 4.47: 3-D amplitude frequency response and the contour response of the All-pole 2-D digital bandpass filter for $a_1 = a_2$ and $k_1 \neq k_2$

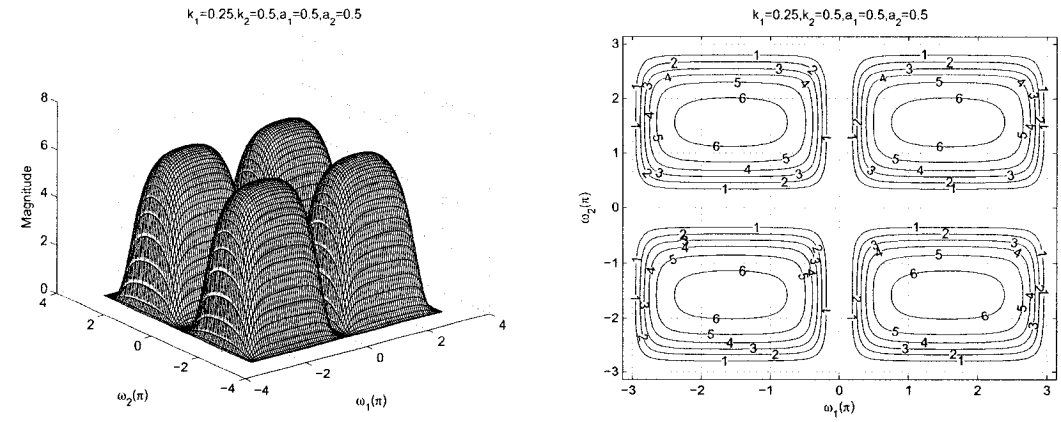

(a) $a_1 = a_2 = 0.5$ and $k_1 = 0.25$, $k_2 = 0.5$

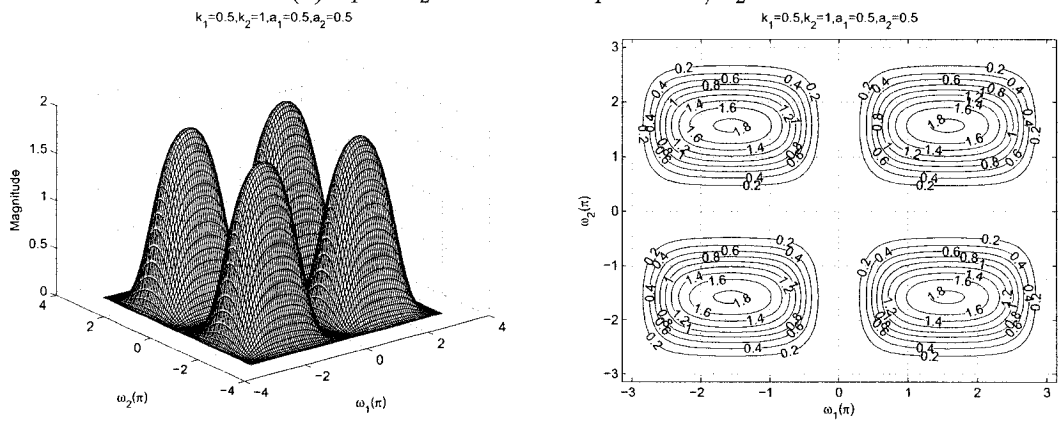

(b) $a_1 = a_2 = 0.5$ and $k_1 = 0.5$, $k_2 = 1$

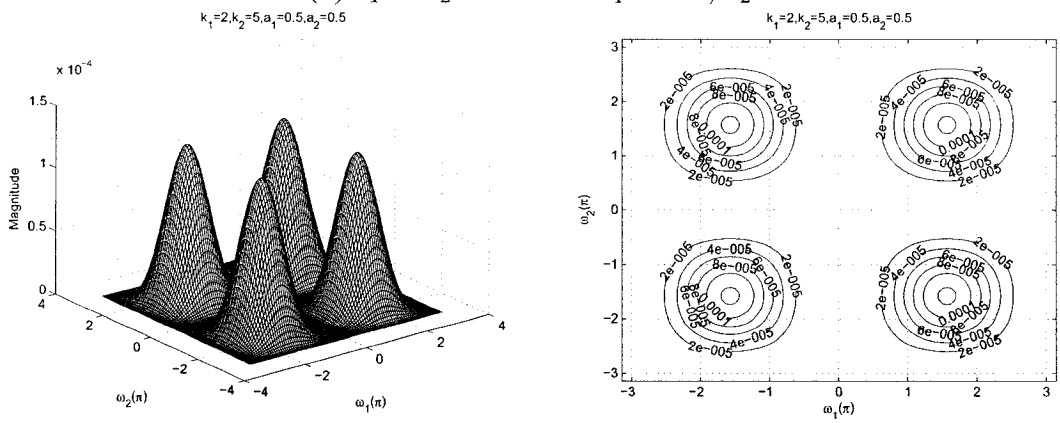

(c) $a_1 = a_2 = 0.5$ and $k_1 = 2$, $k_2 = 5$

Figure 4.48: 3-D amplitude frequency response and the contour response of the All-pole 2-D digital bandpass filter for $a_1 = a_2$ and $k_1 \neq k_2$

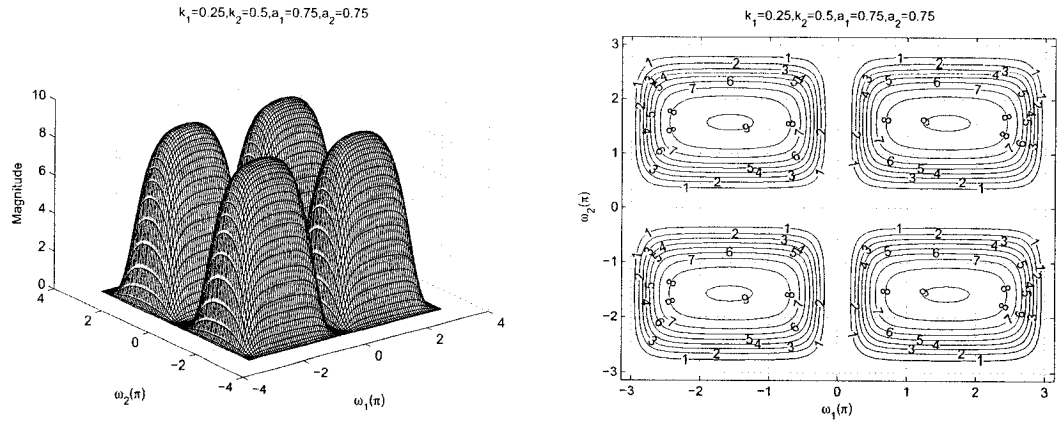

(a) $a_1 = a_2 = 0.75$ and $k_1 = 0.25$, $k_2 = 0.5$

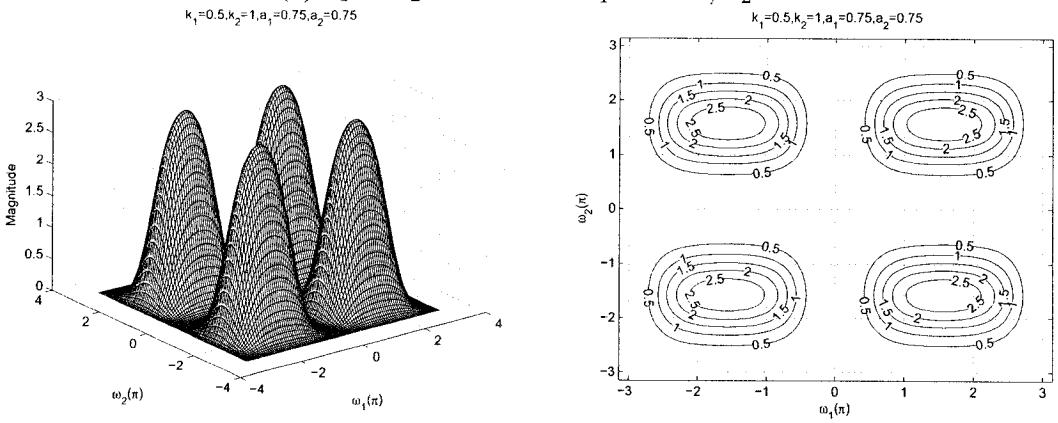

(b) $a_1 = a_2 = 0.75$ and $k_1 = 0.5$, $k_2 = 1$

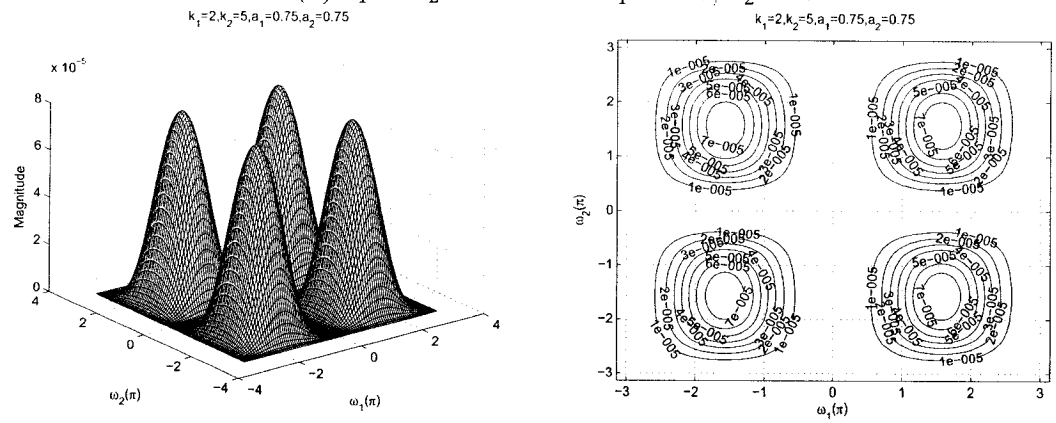

(c) $a_1 = a_2 = 0.75$ and $k_1 = 2$, $k_2 = 5$

Figure 4.49: 3-D amplitude frequency response and the contour response of the All-pole 2-D digital bandpass filter for $a_1 = a_2$ and $k_1 \neq k_2$

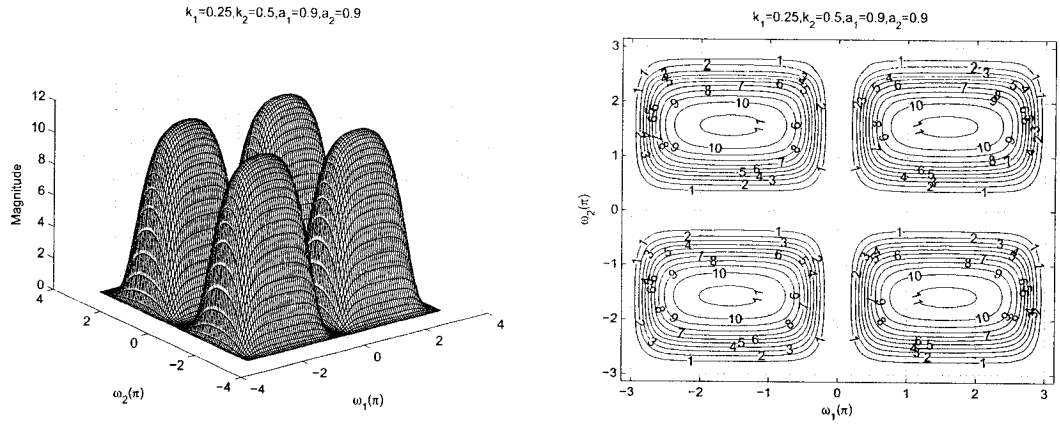

(a) $a_1 = a_2 = 0.9$ and $k_1 = 0.25$, $k_2 = 0.5$

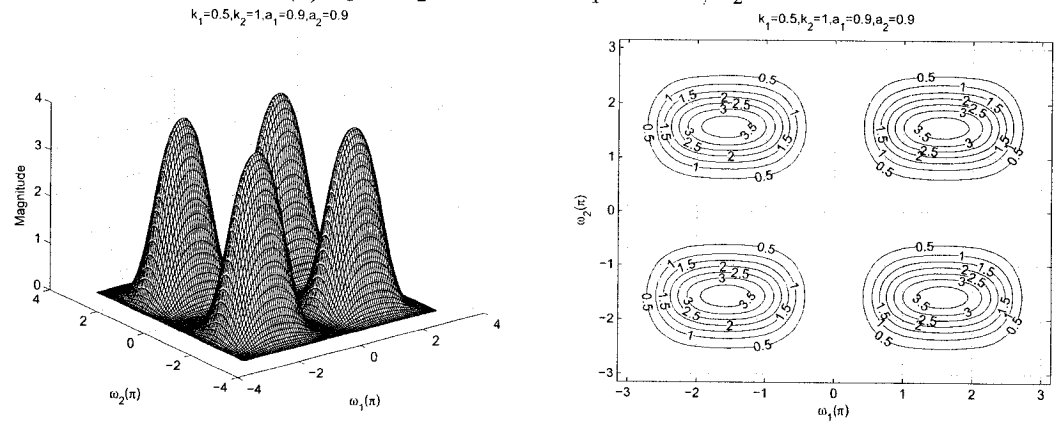

(b) $a_1 = a_2 = 0.9$ and $k_1 = 0.5$, $k_2 = 1$

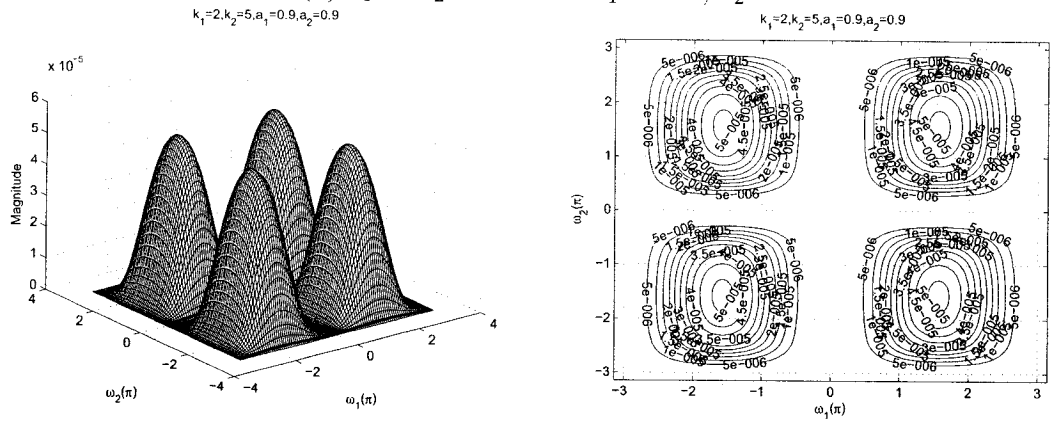

(c) $a_1 = a_2 = 0.9$ and $k_1 = 2$, $k_2 = 5$

Figure 4.50: 3-D amplitude frequency response and the contour response of the All-pole 2-D digital bandpass filter for $a_1 = a_2$ and $k_1 \neq k_2$

4.4 Summary

In this chapter, we have discussed the effect of the coefficients of the 2-D digital bandpass filter in Category A and Category B. The detailed analysis on each of the coefficient is discussed in Section 4.3.

The summary of the effect of the coefficients of the generalized bilinear transformation on 2-D digital bandpass filter in Category A are as follows.

On increasing the values of k_1 and k_2, as discussed in Sections 4.3.1.1 and 4.3.1.2 respectively, it is observed that when we increase the values of k_1 and k_2 from 0.1 to 5, the passband width along the $\omega_1 - axis$ and $\omega_2 - axis$, respectively, gradually decreases and at the same time there is a decrease in the amplitude of the contour response. Also, it is observed that there are ripples in the passband of the amplitude and contour response when the values of $1 < k_1,\ k_2 \leq 5$. On increasing the values of a_1 and a_2, as discussed in Sections 4.3.1.3 and 4.3.1.4, respectively, it is observed that when we increase the values of a_1 and a_2 from 0.1 to 0.9, the gain of the amplitude-response increases from 0.9 to 3.5 along the $\omega_1 - axis$ and $\omega_2 - axis$, respectively.

Sections 4.3.1.5 to 4.3.1.8 discuss the effect of the coefficients on the frequency response of the 2-D digital bandpass filter, viz. $a_1 = a_2$ and $k_1 = k_2$, $a_1 \neq a_2$ and $k_1 = k_2$, $a_1 \neq a_2$ and $k_1 \neq k_2$, and $a_1 = a_2$ and $k_1 \neq k_2$ respectively. It is observed in all the four cases that the coefficients k_1, k_2 affect the passband width and a_1, a_2 affect the gain of the amplitude-frequency response. As the values of the coefficients k_1 and k_2 are increased, the passband decreases and the magnitude of the contour response gradually decreases at the same time. As the values of the coefficients a_1 and a_2 are increased, the gain of the amplitude-frequency response of the 2-D digital bandpass filter increases. Also when the values $a_1 = a_2$ and $k_1 = k_2$, $a_1 = a_2$ and $k_1 \neq k_2$, the width of the passband increases and decreases periodically and when $a_1 \neq a_2$ and $k_1 = k_2$, $a_1 \neq a_2$ and $k_1 \neq k_2$, the width of the passband decreases. Also it can be seen that there are ripples in the passband of the amplitude and the contour response when the values of the coefficients of the generalized

bilinear transformation are in the range $1 \leq k_1,\ k_2 \leq 5$ and $a_1,\ a_2 \geq 0.75$.

The summary of the effect of the coefficients of the generalized bilinear transformation on the all-pole 2-D digital bandpass filter in Category B are as follows.

On increasing the values of k_1 and k_2, as discussed in Sections 4.3.2.1 and 4.3.2.2 respectively, it is observed that when we increase the values of k_1 and k_2 from 0.1 to 5, the passband width along the $\omega_1 - axis$ and $\omega_2 - axis$, respectively, gradually decreases and at the same time there is a decrease in the amplitude of the contour response. On increasing the values of a_1 and a_2, as discussed in Sections 4.3.1.3 and 4.3.1.4, respectively, it is observed that when we increase the values of a_1 and a_2 from 0.1 to 0.9, the gain of the amplitude-response increases from 0.7 to 1.6 along the $\omega_1 - axis$ and $\omega_2 - axis$, respectively.

Sections 4.3.2.5 to 4.3.2.8 discuss the effect of the coefficients on the frequency response of the all-pole 2-D digital bandpass filter, viz. $a_1 = a_2$ and $k_1 = k_2$, $a_1 \neq a_2$ and $k_1 = k_2$, $a_1 \neq a_2$ and $k_1 \neq k_2$, and $a_1 = a_2$ and $k_1 \neq k_2$ respectively. It is observed in all the four cases that the coefficients k_1, k_2 affect the passband width and a_1, a_2 affect the gain of the amplitude-frequency response. As the values of the coefficients k_1 and k_2 are increased, the passband decreases and the magnitude of the contour response gradually decreases at the same time. As the values of the coefficients a_1 and a_2 are increased, the gain increases and the width of the passband increases and decreases periodically of the amplitude-frequency response of the all-pole 2-D digital bandpass filter.

The comparison of the amplitude-frequency response of the 2-D bandpass filter in Category A and the all-pole 2-D bandpass filter in Category B is as follows:

It is observed in both the categories that the coefficients of the generalized bilinear transformation k_1, k_2 affect the passband width and a_1, a_2 affect the gain of the amplitude-frequency response. When we observe the effect of the coefficients on the frequency response of the 2-D digital bandpass filter in Sections 4.3.1.5 to 4.3.1.8 and all-pole 2-D bandpass filter in Sections 4.3.2.5 to 4.3.2.8, viz. $a_1 = a_2$ and $k_1 = k_2$, $a_1 \neq a_2$ and

$k_1 = k_2$, $a_1 \neq a_2$ and $k_1 \neq k_2$, and $a_1 = a_2$ and $k_1 \neq k_2$ in both the categories, it can be seen that for the values of $1 \leq k_1, k_2 \leq 5$, and $a_1, a_2 \geq 0.75$ in Category A, there are ripples present in the amplitude-frequency response 2-D digital bandpass filters in this range. Whereas for the same values of k_1, k_2 and a_1, a_2 in Category B there are no ripples present in the amplitude-frequency response of the all-pole 2-D digital bandpass filter. Also, it is observed that at high values of the coefficients of the generalized bilinear transformation, k_1, k_2, $a_1$and a_2, the cutoff frequencies of the all-pole 2-D digital lowpass filter and the all-pole 2-D digital highpass filter do not overlap and thus, we do not get the response of the all-pole 2-D digital bandpass filter in Category B.

Thus the effect of the various combinations of the coefficients of the generalized bilinear transformation on the proposed 2-D digital bandpass filters in Category A and Category B was analyzed and compared, and the selective 3-D magnitude and contour responses of the proposed 2-D digital bandpass filter and all-pole 2-D digital bandpass filter were plotted.

Chapter 5

All-pole 2-D Bandstop Filters using All-pass Filters

5.1 Introduction

In this chapter, the 2-D bandstop filters are analyzed. There are various methods to obtain 2-D bandstop filters. One method of obtaining 2-D bandstop filter is by using the 2-D lowpass filter. The 2-D analog lowpass filter is transformed to a bandstop filter, and the same is transformed to a digital filter by using the generalized bilinear transformation in Category A and Category B. Then, the coefficients of the 2-D digital bandstop filter are varied to analyze their effect in the design the 2-D digital band-stop filter.

In Section 5.2, we will proposed the transfer function for 2-D digital bandstop filters from the proposed 2-D lowpass filters in Category A and the transfer function for the all-pole 2-D digital bandstop filters from the proposed 2-D lowpass filter in discussed in Chapter 2. In Section 5.3, we will discuss and analyze the effects of the coefficients of the generalized transformation of the 2-D digital bandstop filter in Category A and Category B on the amplitude-frequency response. Section 5.4 gives the summary, discussions and comparisons of the analysis presented in this chapter.

5.2 Transfer Function of 2-D Digital Bandstop Filter

In this section, we will derive the transfer function of 2-D bandstop filter in analog and digital domain in Category A and Category B.

5.2.1 Transfer Function of the 2-D Digital Bandstop Filter in Category A

The transfer function of the 2-D digital bandstop filter is obtained by using the proposed 2-D analog lowpass filter. The analog 2-D lowpass filter is transformed to 2-D analog bandstop transformation which in turn is transformed to the 2-D digital bandstop filter by using the generalized bilinear transformation. The generation of the transfer function of the proposed 2-D lowpass filter is discussed in Sec 2.5.1 of Chapter 2. In the case of the bandstop filter the transformation $F(s)$ must map lowpass response to a bandstop response. The result is a bandstop filter with the center frequency ω_0 and the width B of the band rejected. The transformation used to transform 2-D analog lowpass filter to 2-D analog bandstop filter is [49],

$$s = \frac{Bs}{s^2 + \omega_0^2} \tag{5.1}$$

The transfer function of 2-D low pass filter in analog domain is given by eqn.(2.58). Applying lowpass to bandstop transformation to eqn. (2.58),

$$s_1 \rightarrow \frac{Bs_1}{s_1^2 + \omega_0^2} \tag{5.2}$$

$$s_2 \rightarrow \frac{Bs_2}{s_2^2 + \omega_0^2} \tag{5.3}$$

where $B = 1$ and $\omega_0 = 1$.

The resultant analog transfer function of 2-D bandstop filter is,

$$H(s_1,s_2)=\frac{\left[\begin{array}{c}4(s_1^2+1)^3(s_2^2+1)^3-1.656s_1^2(s_1^2+1)(s_2^2+1)^3-\\1.656s_2^2(s_1^2+1)^3(s_2^2+1)+0.685584s_1^2s_2^2(s_1^2+1)(s_2^2+1)\end{array}\right]}{\left[\begin{array}{c}s_1^3[s_2^3+2.41s_2^2(s_2^2+1)+2.41s_2(s_2^2+1)^2+(s_2^2+1)^3]+\\s_1^2(s_1^2+1)[2.41s_2^3+5.83s_2^2(s_2^2+1)+5.83s_2(s_2^2+1)^2+2.41(s_2^2+1)^3]+\\s_1(s_1^2+1)^2[2.41s_2^3+5.83s_2^2(s_2^2+1)+5.83s_2(s_2^2+1)^2+2.41(s_2^2+1)^3]+\\(s_1^2+1)^3[s_2^3+2_2^2(s_2^2+1)+2.41s_2(s_2^2+1)^2+1(s_2^2+1)^3]\end{array}\right]} \tag{5.4}$$

Applying generalized bilinear transformation, i.e., $s_1 \rightarrow k_1\frac{z_1-a_1}{z_1+b_1}$, $s_2 \rightarrow k_1\frac{z_2-a_2}{z_2+b_2}$, where $k_1>0, k_2>0, 0\leq a_1\leq 1, 0\leq a_2\leq 1$ and $b_1=b_2=1$ to the above eqn. (5.4), we get,

$$H(z_1,z_2)=\frac{P(z_1,z_2)}{Q(z_1,z_2)} \tag{5.5}$$

where

$$P(z_1,z_2)=\left[\begin{array}{c}4(k_1^2A^2+1)^3(k_2^2B^2+1)^3-1.656(k_1^2A^2)(k_1^2A^2+1)(k_2^2B^2+1)^3\\-1.656(k_2^2B^2)(k_1^2A^2+1)^3(k_2^2B^2+1)+\\0.685584(k_1^2A^2)(k_2^2B^2)(k_1^2A^2+1)(k_2^2B^2+1)\end{array}\right] \tag{5.6}$$

and

$$Q(z_1,z_2) = k_1^3A^3\left[\begin{array}{c}(k_2^3B^3)+\\2.41(k_2^2B^2)(k_2^2B^2+1)+\\2.41(k_2B)(k_2^2B^2+1)^2+\\(k_2^2B^2+1)^3\end{array}\right]$$

$$
\begin{aligned}
&+ \quad k_1^2A^2(k_1^2A^2+1)\left[\begin{array}{c} 2.41(k_2^3B^3)+ \\ 5.83(k_2^2B^2)(k_2^2B^2+1)+ \\ 5.83(k_2B)(k_2^2B^2+1)^2+ \\ 2.414(k_2^2B^2+1)^3 \end{array}\right] \\
&+ \quad k_1A(k_1^2A^2+1)^2\left[\begin{array}{c} 2.41(k_2^3B^3)+ \\ 5.83(k_2^2B^2)(k_2^2B^2+1)+ \\ 5.83(k_2B)(k_2^2B^2+1)^2+ \\ 2.41(k_2^2B^2+1)^3 \end{array}\right] \\
&+ \quad (k_1^2A^2+1)^3\left[\begin{array}{c} (k_2^3B^3)+ \\ 2.41(k_2^2B^2)(k_2^2B^2+1)+ \\ 2.41(k_2B)(k_2^2B^2+1)^2+ \\ 1(k_2^2B^2+1)^3 \end{array}\right]
\end{aligned} \tag{5.7}
$$

where $A = \frac{z_1-a_1}{z_1+b_1}$, and $B = \frac{z_2-a_2}{z_2+b_2}$. Eqn. (5.6) and Eqn. (5.7) gives the transfer function for 2-D digital bandstop filter in Category A.

5.2.2 Transfer Function of the All-pole 2-D Digital Bandstop Filter in Category B

The transfer function of the all-pole 2-D digital bandstop filter is obtained by using the proposed all-pole 2-D analog lowpass filter. The analog all-pole 2-D lowpass filter is transformed to the all-pole 2-D analog bandstop transformation which in turn is transformed to the all-pole 2-D digital bandstop filter by using the generalized bilinear transformation. The generation of the transfer function of the proposed all-pole 2-D lowpass filter is discussed in Sec 2.5.2 of Chapter 2. In the case of the all-pole bandstop filter the transformation $F(s)$ must map low-pass response to a bandstop response. The result is the bandstop filter with the center frequency ω_0 and the width B of the band rejected. The transformation used to

transform 2-D analog lowpass filter to 2-D analog bandstop filter is given by eqn. (5.1) [49].

The transfer function of the all-pole 2-D low pass filter in analog domain is given by eqn. (2.79). Applying lowpass to bandstop transformation to eqn. (2.79), .i.e. applying eqn. (5.2) and eqn. (5.3) to eqn. (2.79), where $B = 1$ and $\omega_0 = 1$.

The resultant analog transfer function of the all-pole 2-D bandstop filter is given by,

$$H(s_1, s_2) = \frac{\left[\; 4(s_1^2+1)^3(s_2^2+1)^3 \;\right]}{\left[\begin{array}{c} s_1^3[0.5s_2^3 + 1.414s_2^2(s_2^2+1) + 1.5s_2(s_2^2+1)^2 + 0.707(s_2^2+1)^3]+ \\ s_1^2(s_1^2+1)[1.414s_2^3 + 4s_2^2(s_2^2+1) + 4.24s_2(s_2^2+1)^2 + 2(s_2^2+1)^3]+ \\ s_1(s_1^2+1)^2[1.5s_2^3 + 4.24s_2^2(s_2^2+1) + 4.5s_2(s_2^2+1)^2 + 2.12(s_2^2+1)^3]+ \\ (s_1^2+1)^3[0.707s_2^3 + 2s_2^2(s_2^2+1) + 2.12s_2(s_2^2+1)^2 + 1(s_2^2+1)^3] \end{array}\right] \tag{5.8}$$

Applying generalized bilinear transformation, i.e., $s_1 \rightarrow k_1 \frac{z_1 - a_1}{z_1 + b_1}$, $s_2 \rightarrow k_1 \frac{z_2 - a_2}{z_2 + b_2}$, where $k_1 > 0$, $k_2 > 0$, $0 \leq a_1 \leq 1$, $0 \leq a_2 \leq 1$ and $b_1 = b_2 = 1$ to the above eqn. (5.8), we get,

$$H(z_1, z_2) = \frac{P(z_1, z_2)}{Q(z_1, z_2)} \tag{5.9}$$

where

$$P(z_1, z_2) = \left[\; 4(k_1^2A^2+1)^3(k_2^2B^2+1)^3 \;\right] \tag{5.10}$$

and

$$Q(z_1, z_2) \;=\; k_1^3A^3 \left[\begin{array}{c} 0.5(k_2^3B^3)+ \\ 1.414(k_2^2B^2)(k_2^2B^2+1)+ \\ 1.5(k_2B)(k_2^2B^2+1)^2+ \\ 0.707(k_2^2B^2+1)^3 \end{array}\right]$$

$$
\begin{aligned}
&+ \quad k_1^2A^2(k_1^2A^2+1)\begin{bmatrix} 1.414(k_2^3B^3)+ \\ 4(k_2^2B^2)(k_2^2B^2+1)+ \\ 4.24(k_2B)(k_2^2B^2+1)^2+ \\ 2(k_2^2B^2+1)^3 \end{bmatrix} \\
&+ \quad k_1A(k_1^2A^2+1)^2\begin{bmatrix} 1.5(k_2^3B^3)+ \\ 4.24(k_2^2B^2)(k_2^2B^2+1)+ \\ 4.5(k_2B)(k_2^2B^2+1)^2+ \\ 2.12(k_2^2B^2+1)^3 \end{bmatrix} \\
&+ \quad (k_1^2A^2+1)^3\begin{bmatrix} 0.707(k_2^3B^3)+ \\ 2(k_2^2B^2)(k_2^2B^2+1)+ \\ 2.12(k_2B)(k_2^2B^2+1)^2+ \\ 1(k_2^2B^2+1)^3 \end{bmatrix}
\end{aligned} \tag{5.11}
$$

where $A = \frac{z_1-a_1}{z_1+b_1}$, and $B = \frac{z_2-a_2}{z_2+b_2}$. Eqn. (5.10) and Eqn. (5.11) gives the transfer function for the all-pole 2-D digital bandstop filter in Category B.

5.3 Frequency Response of 2-D Digital Bandstop Filters

5.3.1 Frequency Response of 2-D Digital Bandstop Filter in Category A

The transfer function of the 2-D digital bandstop filter is obtained by using the proposed 2-D analog lowpass filter in Category A is discussed in Chapter 2. The analog 2-D lowpass filter is transformed to 2-D analog bandstop transformation which in turn is transformed to the 2-D digital bandstop filter by using the generalized bilinear transformation as explained in Section 5.2.1.

To investigate the manner in which each coefficient of the generalized bilinear trans-

formation effects the magnitude response of the resulting 2-D digital bandstop filter, we vary the values of the coefficients or fix some of the coefficients to specific values. It is possible to obtain a 2-D digital bandstop filter when the coefficients have the following limits: $k_i > 0$, $0 \leq |a_i| \leq 1$ and $b_i = 1$, where $i = 1, 2$. Let us consider the coefficients of the generalized bilinear transformation for the 2-D digital bandstop filter to be unity, i.e., $a_1 = 1$, $a_2 = 1$, $k_1 = 1$, $k_2 = 1$, $b_1 = 1$ and $b_2 = 1$ Under this condition, the 3-D amplitude-frequency response and the contour plots of the 2-D digital filter are shown in the Figure 5.1.

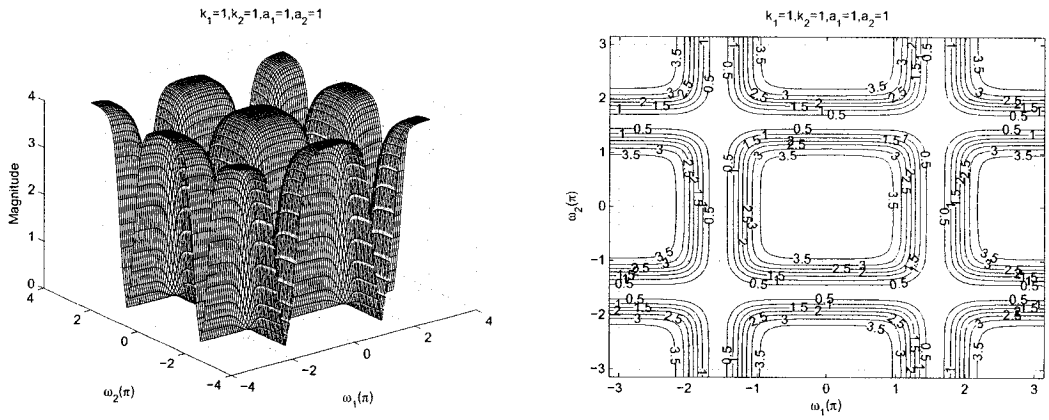

Figure 5.1: 3-D Amplitude-Frequency response and the contour response of the 2-D Digital Band-Stop Filter with all the coefficients values as unity

In the following, we will study the effects of these coefficients to the frequency responses of the 2-D digital bandstop filter [33, 48].

5.3.1.1 Frequency Response of 2-D Digital Bandstop Filter with different values of k_1

In this section, we study the manner in which k_1 affects the frequency response of the resulting 2-D digital bandstop filter and to separate the effect of the other coefficients, we vary the value of k_1, and fix all the other coefficients of the generalized bilinear transformation to unity, e.g. with $k_2 = 1$, $a_1 = 1$, $a_2 = 1$, $b_1 = 1$, and $b_2 = 1$. This was done so that no generality is lost and to make the situation simple. The values of k_1 are varied from

0.1 to 5 and the 3-D magnitude response and the contour plots for the 2-D digital bandstop filter with the values of $k_1 = 0.1$, $k_1 = 0.5$, $k_1 = 0.9$, $k_1 = 2$, and $k_1 = 5$ are shown in the Figures 5.2 and 5.3 .

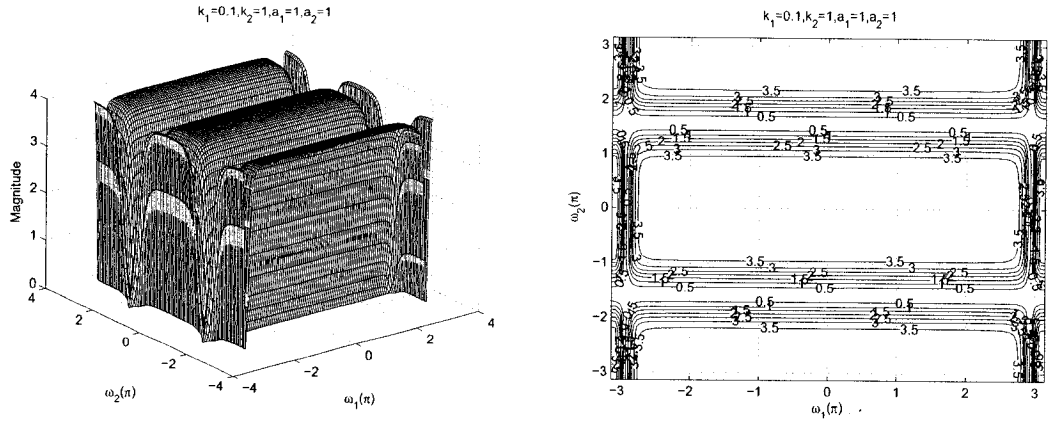

(a) $k_1 = 0.1$

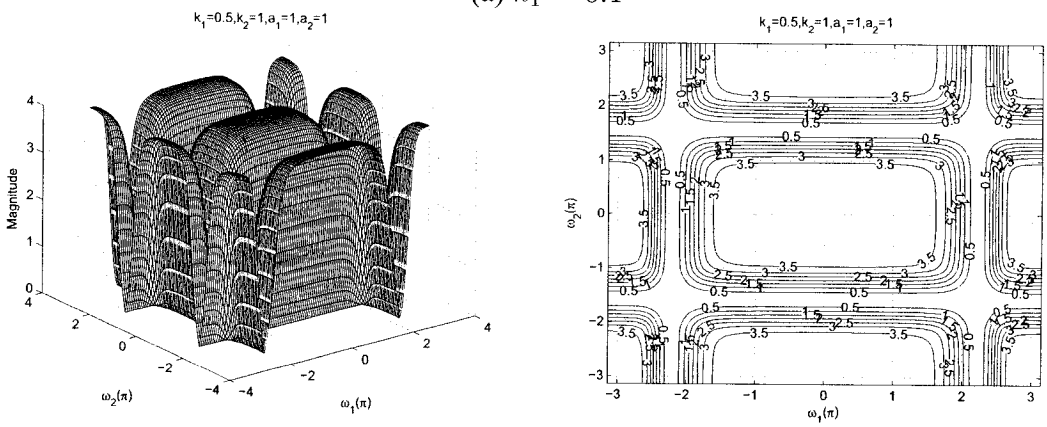

(b) $k_1 = 0.5$

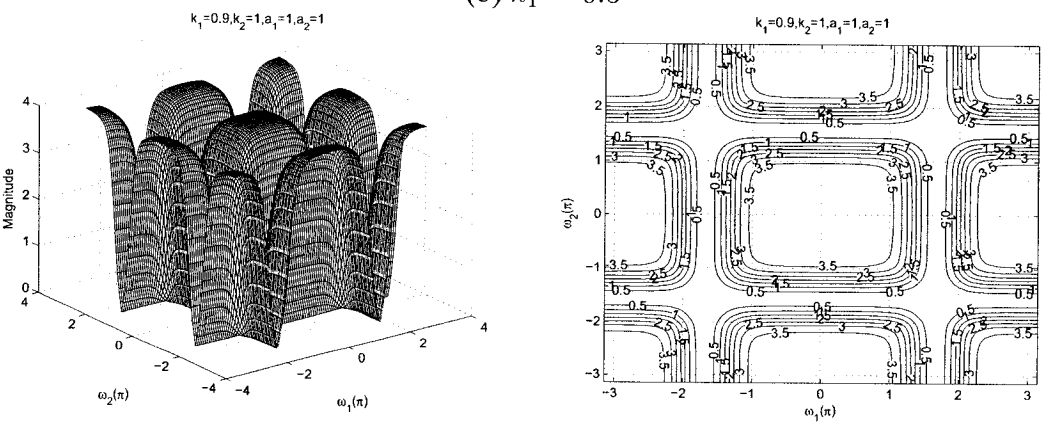

(c) $k_1 = 0.9$

Figure 5.2: 3-D amplitude frequency response and the contour of the 2-D digital bandstop filter for different values of k_1

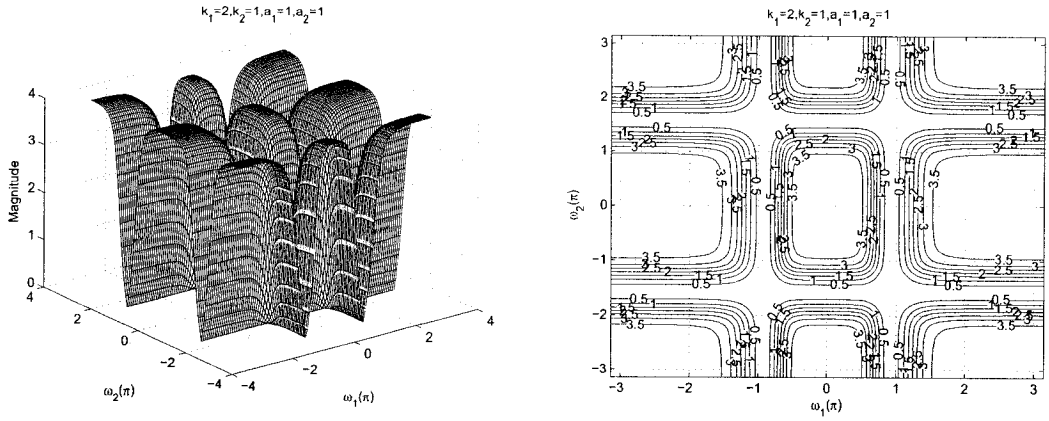

(a) $k_1 = 2$

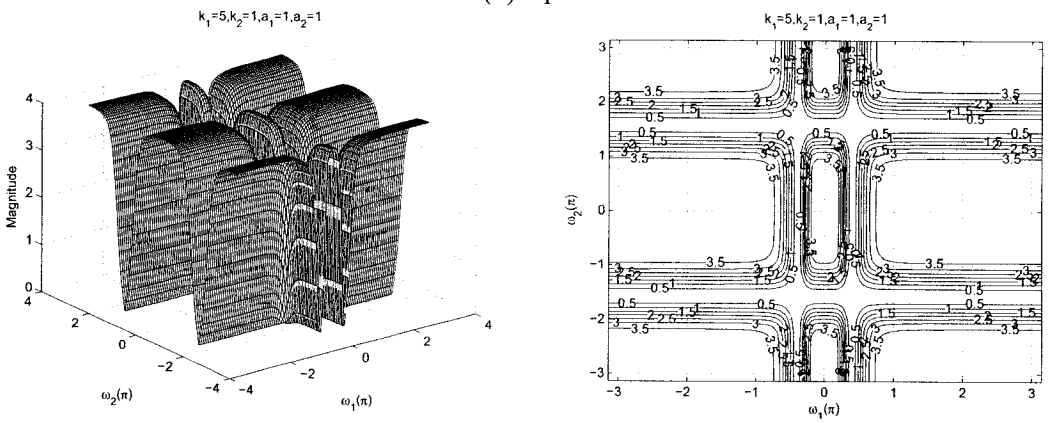

(b) $k_1 = 5$

Figure 5.3: 3-D amplitude frequency response and the contour of the 2-D digital bandstop filter for different values of k_1

It is observed from the diagrams that although the coefficient k_1 does not have any effect on the passband width along the $\omega_2 - axis$, it affects the center frequency of the filter response along the $\omega_1 - axis$. It also affects the width of the lower and the upper passbands, and the stopband width of the bandstop filter along the $\omega_1 - axis$. Initially, when the value of the coefficient $k_1 = 0.1$ (see Figure 5.2 (a)) the lower passband will have the maximum bandwidth in the available frequency range. As we increase the value of k_1 from 0.1 to 5, the cut-off frequency of the lower passband decreases and that of the upper passband increases. Also the width of the lower passband decreases and that of the upper passband increases along the $\omega_1 - axis$. The width of the stopband increases and decreases periodically for different values of k_1 as seen from the Figures 5.2 and 5.3 along

$\omega_1 - axis$. It is also observed that the amplitude of the contour response of the lower and upper passband remains constant.

5.3.1.2 Frequency Response of 2-D Digital Bandstop Filter with different values of k_2

In this section, we study the manner in which k_2 affects the frequency response behavior of the resulting 2-D digital bandstop filter and to separate the effect of the other coefficients, we vary the value of k_2, and fix all the other coefficients of the generalized bilinear transformation to unity, e.g. with $k_1 = 1$, $a_1 = 1$, $a_2 = 1$, $b_1 = 1$, and $b_2 = 1$. This was done so that no generality is lost and to make the situation simple. The values of k_2 are varied from 0.1 to 5 and the 3-D magnitude response and the contour plots for the 2-D digital bandstop filter with the values of $k_2 = 0.1$, $k_2 = 0.5$, $k_2 = 0.9$, $k_2 = 2$, and $k_2 = 5$ are shown in the Figures 5.4 and 5.5.

It is observed from the diagrams that although the coefficient k_2 does not have any effect on the passband width along the $\omega_1 - axis$, it affects the center frequency of the filter response along the $\omega_2 - axis$. It also affects the width of the lower and the upper passbands, and the stopband width of the bandstop filter along the $\omega_2 - axis$. Initially when the value of the coefficient $k_2 = 0.1$ (see Figure 5.4 (a)) the lower passband will have the maximum bandwidth in the available frequency range. As we increase the value of k_2 from 0.1 to 5, the cut-off frequency of the lower passband decreases and that of the upper passband increases. Also the width of the lower passband decreases and that of the upper passband increases along the $\omega_2 - axis$. The width of the stopband increases and decreases periodically for different values of k_2 as seen from the Figures 5.4 and 5.5 along $\omega_2 - axis$. It is also observed that the amplitude of the contour response of the lower and upper passband remains constant.

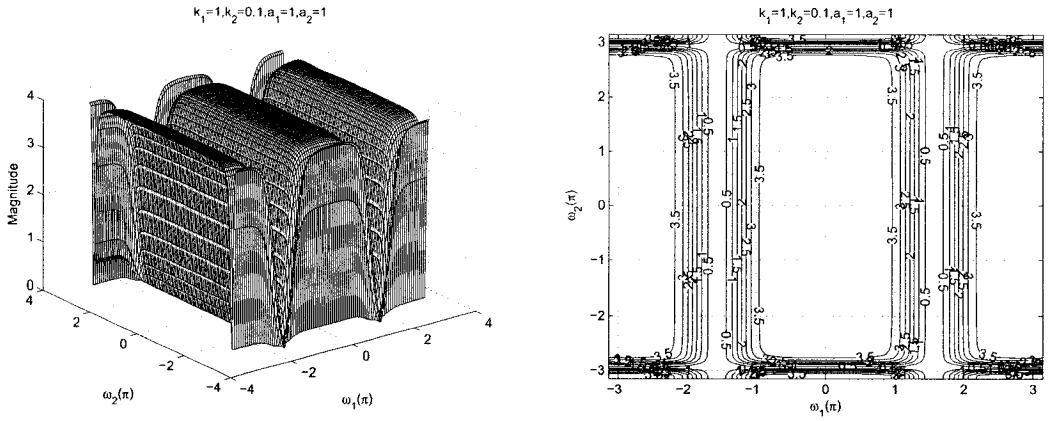

(a) $k_2 = 0.1$

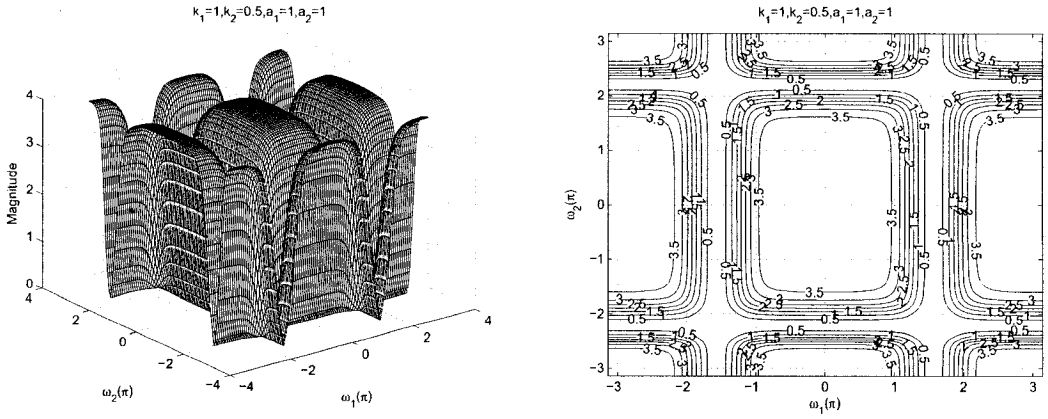

(b) $k_2 = 0.5$

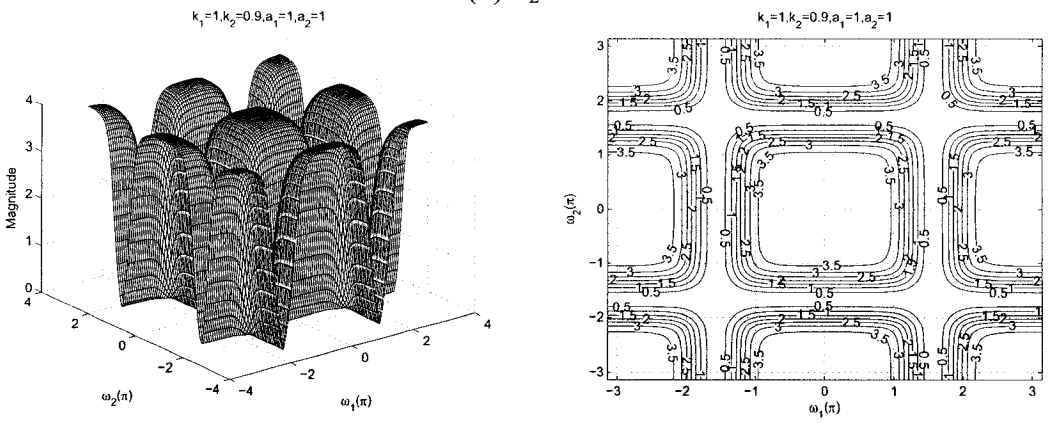

(c) $k_2 = 0.9$

Figure 5.4: 3-D amplitude frequency response and the contour of the 2-D digital bandstop filter for different values of k_2

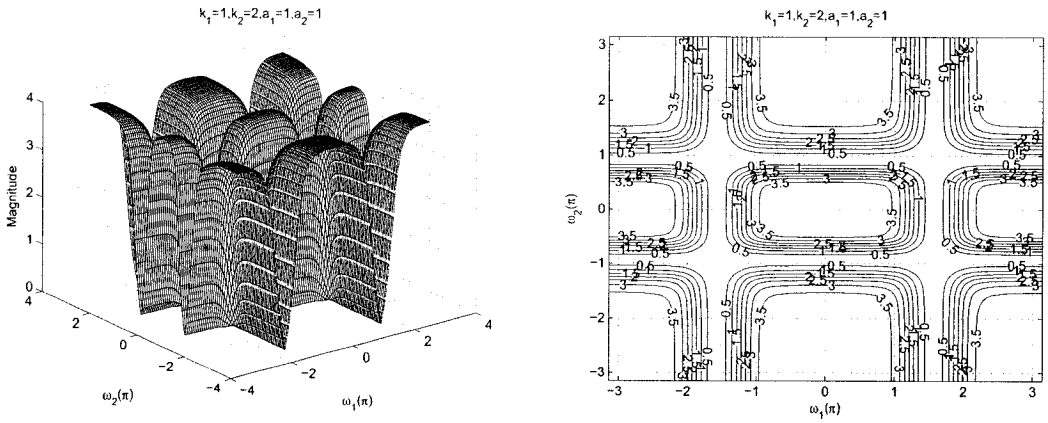

(a) $k_2 = 2$

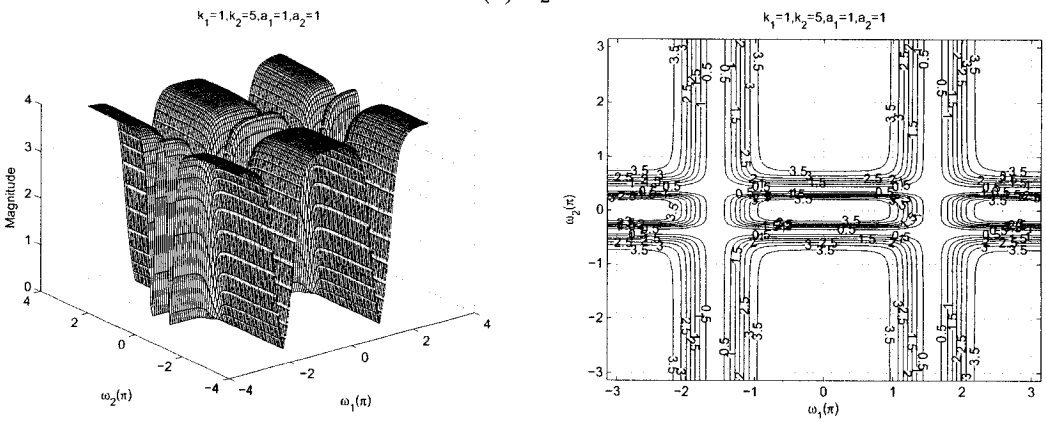

(b) $k_2 = 5$

Figure 5.5: 3-D amplitude frequency response and the contour of the 2-D digital bandstop filter for different values of k_2

5.3.1.3 Frequency Response of 2-D Digital Bandstop Filter with different values of a_1

In the Sections 5.3.1.1 and 5.3.1.2, the effect of the coefficient of k_1 and k_2 are studied. In this section, the effect of the coefficient a_1 is studied. The stable range of a_1 can be obtained with other specified coefficients of the generalized bilinear transformation. There are many combinations possible for the coefficients. To study the response with different values of a_1 properly, we fix other coefficients values to be equal to unity. The range of a_1 varies from 0.1 to 1 and the other coefficient values are specified as unity, i.e., $k_1 = 1$, $k_2 = 1$, $a_2 = 1$, $b_1 = 1$ and $b_2 = 1$.

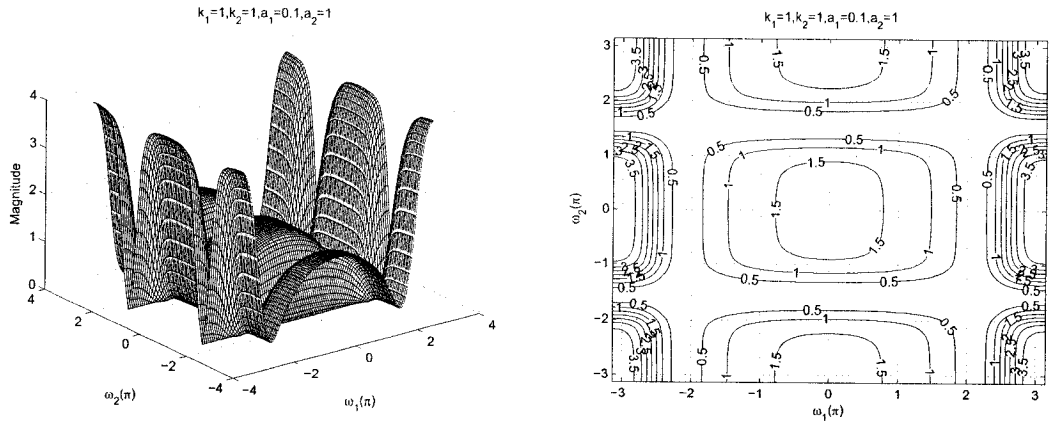

(a) $a_1 = 0.1$

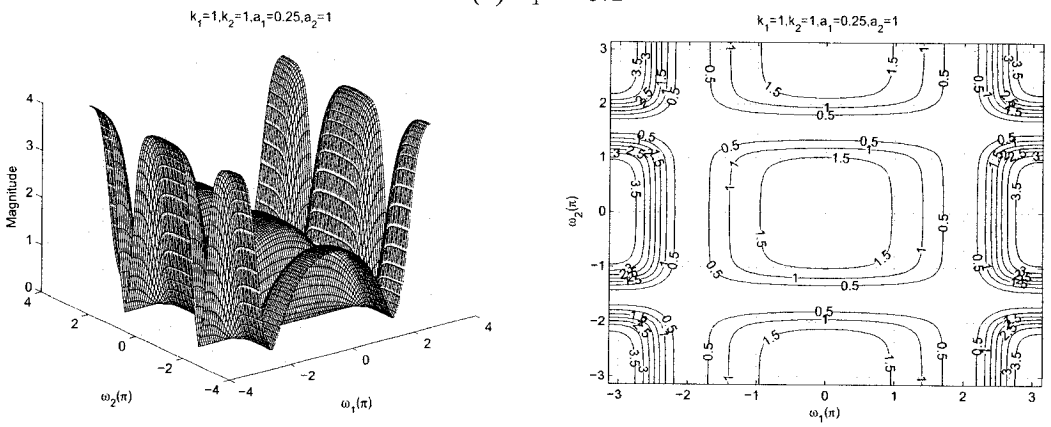

(b) $a_1 = 0.25$

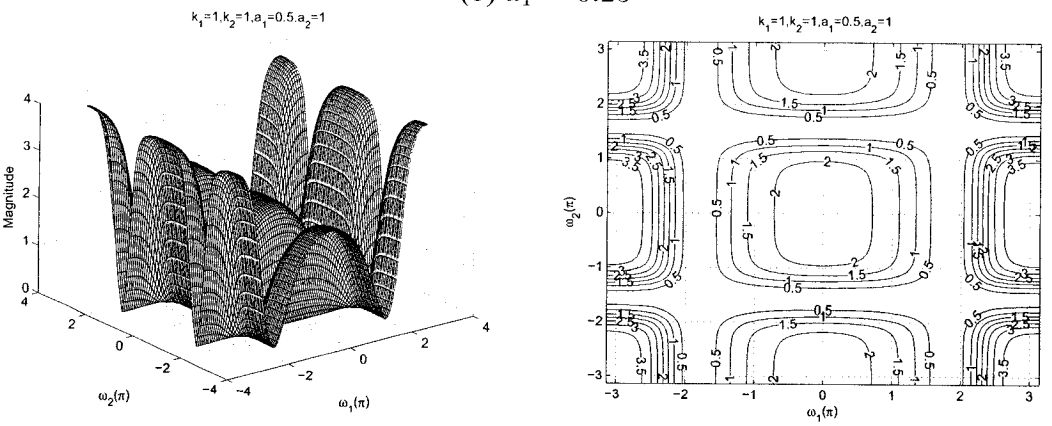

(c) $a_1 = 0.5$

Figure 5.6: 3-D amplitude frequency response and the contour of the 2-D digital bandstop filter for different values of a_1

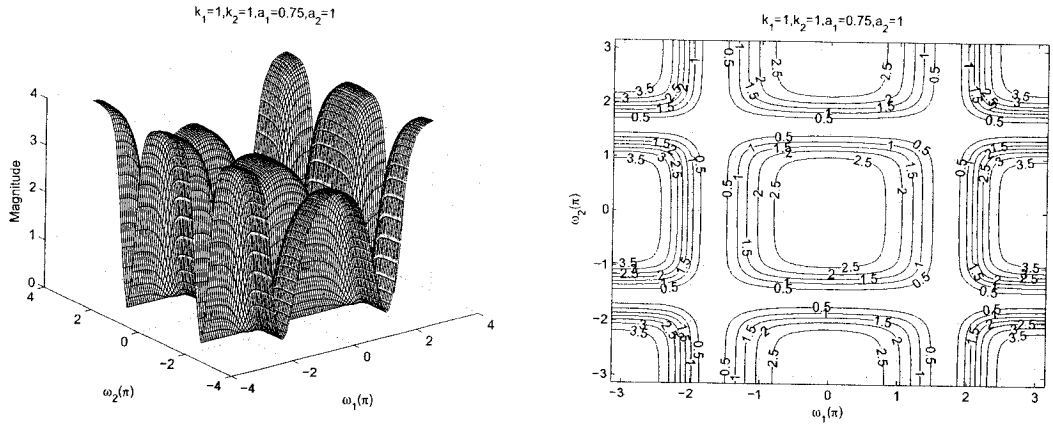

(a) $a_1 = 0.75$

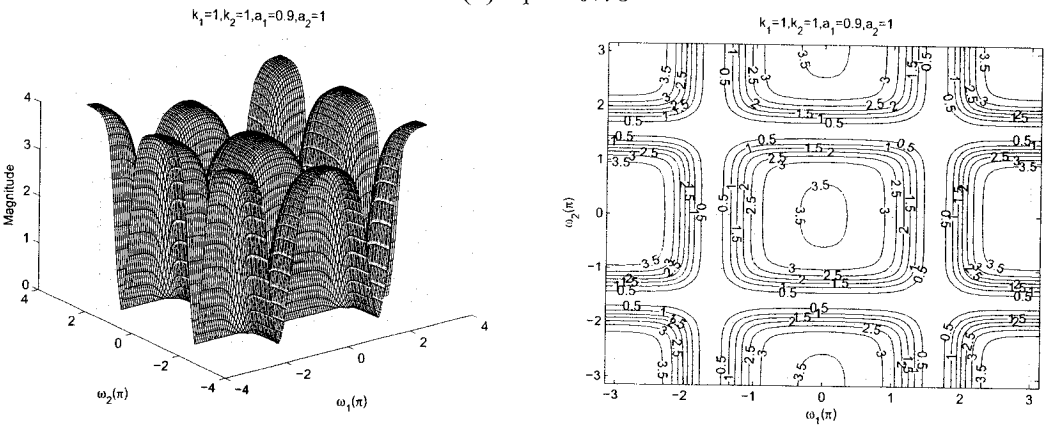

(b) $a_1 = 0.9$

Figure 5.7: 3-D amplitude frequency response and the contour of the 2-D digital bandstop filter for different values of a_1

By varying the value of a_1, the 3-D magnitude response and contour plots which represents different values of a_1, i.e. $a_1 = 0.1$, $a_1 = 0.25$, $a_1 = 0.5$, $a_1 = 0.75$, and $a_1 = 0.9$ are shown in the Figures 5.6 and 5.7. By making the value of $a_1 = 1$, it resembles the standard 2-D digital bandstop filter as shown in the Figure 5.1. It is observed from the diagrams that the coefficient a_1 affects the gain of the amplitude-frequency response. At the lowest value of $a_1 = 0.1$, the gain of the amplitude-frequency response of the lower passband is 1.5. As the value of a_1 increases, the gain increases and reach the maximum value at $a_1 = 1$. As seen from the Figure 5.6 and 5.7 that as we increase the value of a_1 from 0.1 to 0.9, the gain of the amplitude-frequency response of the lower passband increases from 1.5 to 3.5 along the $\omega_1 - axis$. At the same time the gain of the amplitude-frequency response of the upper

passband remains constant. It is also observed that the cut-off frequency of lower passband decreases and that of the upper passband increases along $\omega_1 - axis$. It is also evident from the diagrams that the coefficient a_1 does not have any effect along the $\omega_2 - axis$.

5.3.1.4 Frequency Response of 2-D Digital band-Stop Filter with different values of a_2

In the Section 5.3.1.3, the effect of the coefficient of a_1 was studied. In this section, the effect of the coefficient a_2 will be studied. The stable range of a_2 can be obtained with other specified coefficients of the generalized bilinear transformation. There are many combinations possible for the coefficients. To study the response with different values of a_2 properly, we fix other coefficients values to be equal to unity. The range of a_2 varies from 0.1 to 1 and the other coefficient values are specified as unity, i.e., $k_1 = 1$, $k_2 = 1$, $a_1 = 1$, $b_1 = 1$ and $b_2 = 1$.

By varying the value of a_2, the 3-D magnitude response and contour plots which represents different values of a_2, i.e., $a_2 = 0.1$, $a_2 = 0.25$, $a_2 = 0.5$, $a_2 = 0.75$, and $a_2 = 0.9$ are shown in the Figures 5.8 and 5.9. By making the value of $a_2 = 1$, it resembles the standard 2-D digital bandstop filter as shown in the Figure 5.1. It is observed from the diagrams that the coefficient a_2 affects the gain of the amplitude-frequency response. At the lowest value of $a_2 = 0.1$, the gain of the amplitude-frequency response of the lower passband is 1.5. As the value of a_2 increases, the gain increases and reach the maximum value at $a_2 = 1$. As seen from the Figure 5.8 and 5.9 that as we increase the value of a_2 from 0.1 to 0.9, the gain of the amplitude-frequency response of the lower passband increases from 1.5 to 3.5 along the $\omega_2 - axis$. At the same time the gain of the amplitude-frequency response of the upper passband remains constant. It is also observed that the cut-off frequency of lower passband decreases and that of the upper passband increases along $\omega_2 - axis$. It is also evident from the diagrams that the coefficient a_2 does not have any effect along the $\omega_1 - axis$.

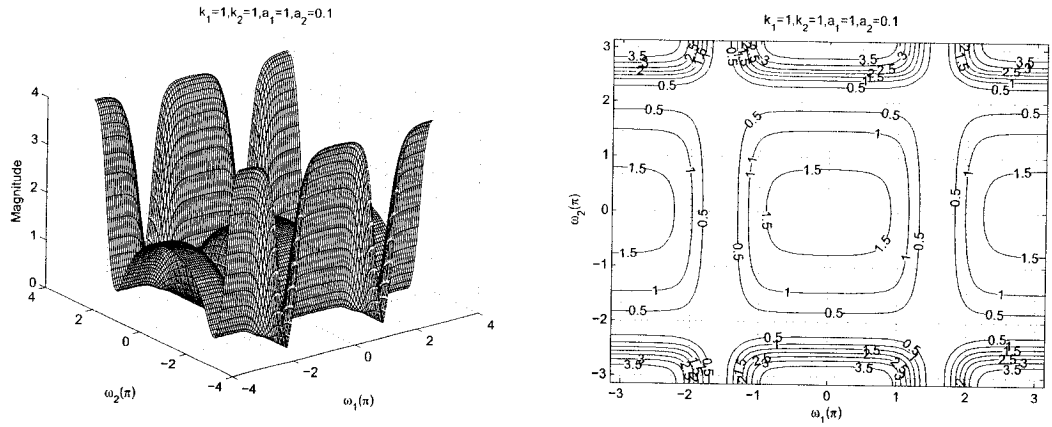

(a) $a_2 = 0.1$

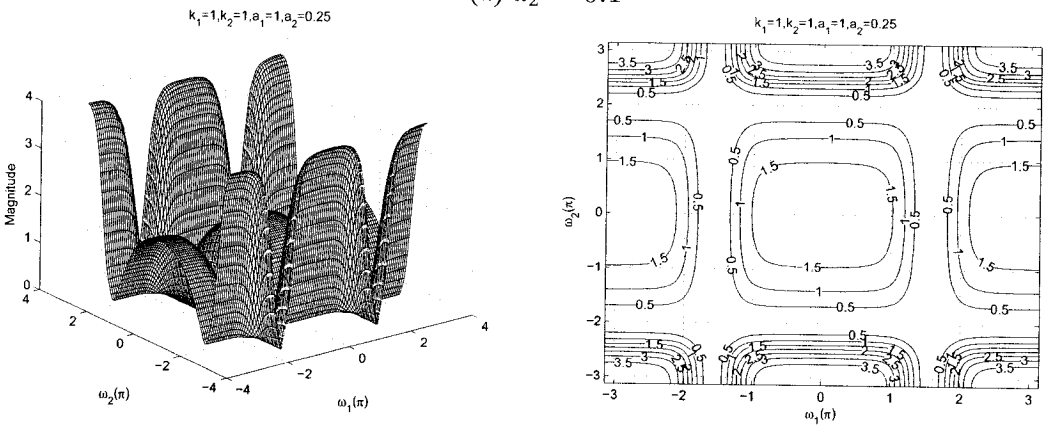

(b) $a_2 = 0.25$

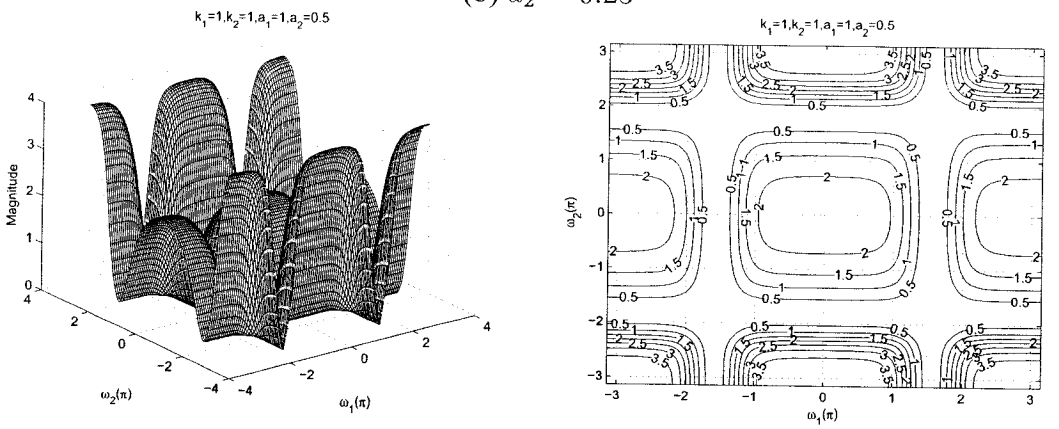

(c) $a_2 = 0.5$

Figure 5.8: 3-D amplitude frequency response and the contour of the 2-D digital bandstop filter for different values of a_2

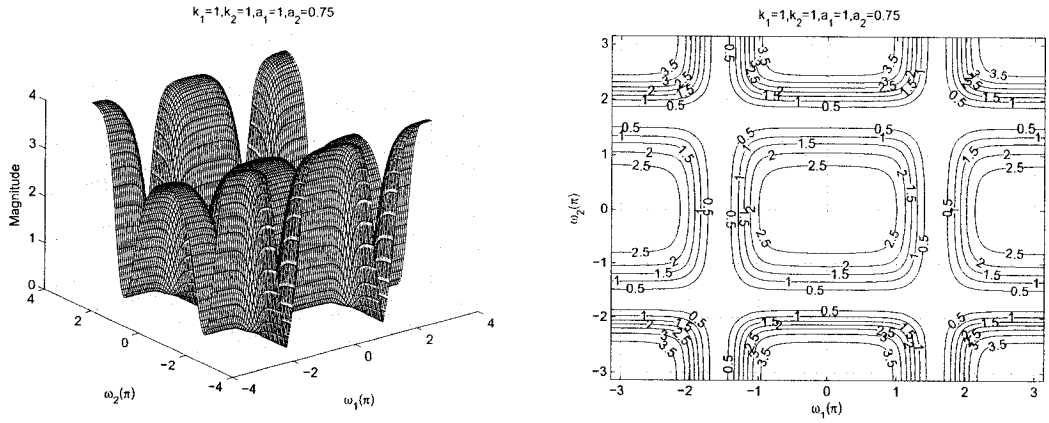

(a) $a_2 = 0.75$

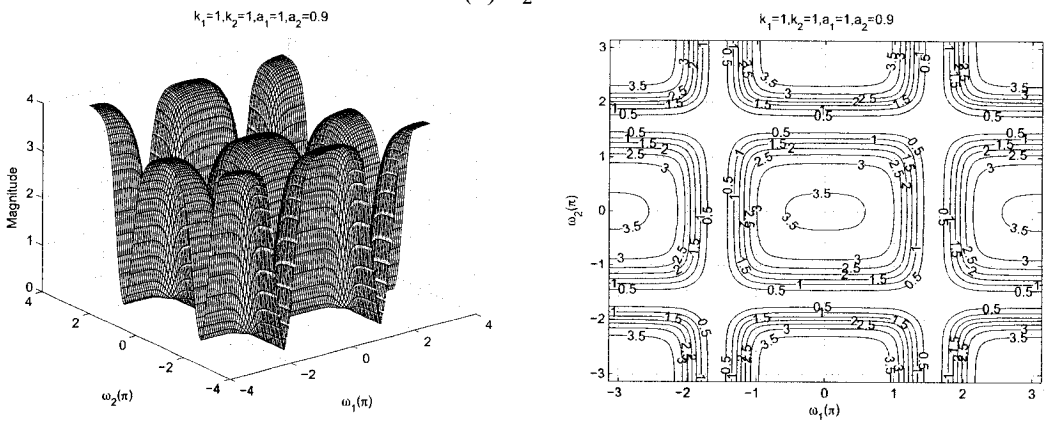

(b) $a_2 = 0.9$

Figure 5.9: 3-D amplitude frequency response and the contour of the 2-D digital bandstop filter for different values of a_2

5.3.1.5 Frequency Response of 2-D Digital Bandstop Filter with same values of a_1 and a_2 and same values of k_1 and k_2

In the Sections 5.3.1.1 to 5.3.1.4 the individual effect of the coefficients a_1, a_2, k_1 and k_2 were studied. In this section, we will study the effect of coefficients, where $a_1 = a_2$ and $k_1 = k_2$ and the remaining coefficients b_1 and b_2 are considered to be unity for the 2-D digital bandstop filter in Category A. The values of a_1 and a_2 ranges from 0 to 0.75 and the values of k_1 and k_2 ranges from 0 to 2.

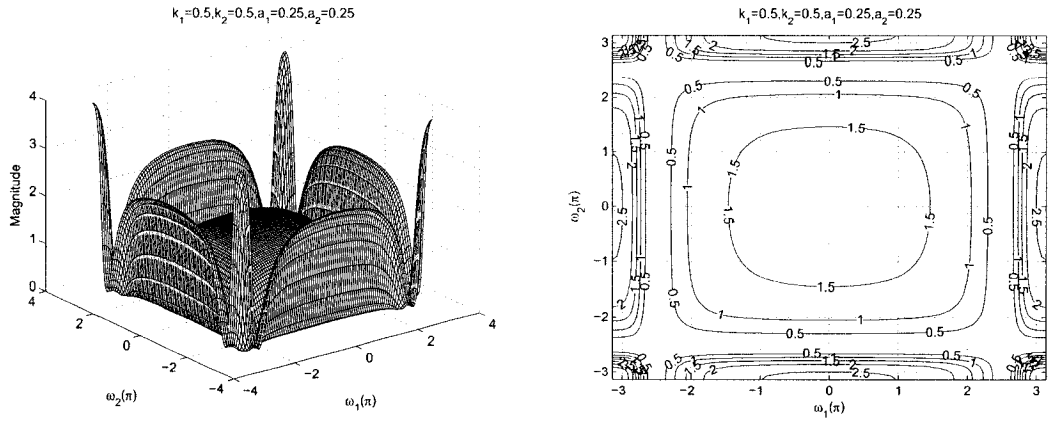

(a) $a_1 = a_2 = 0.25$ and $k_1 = k_2 = 0.5$

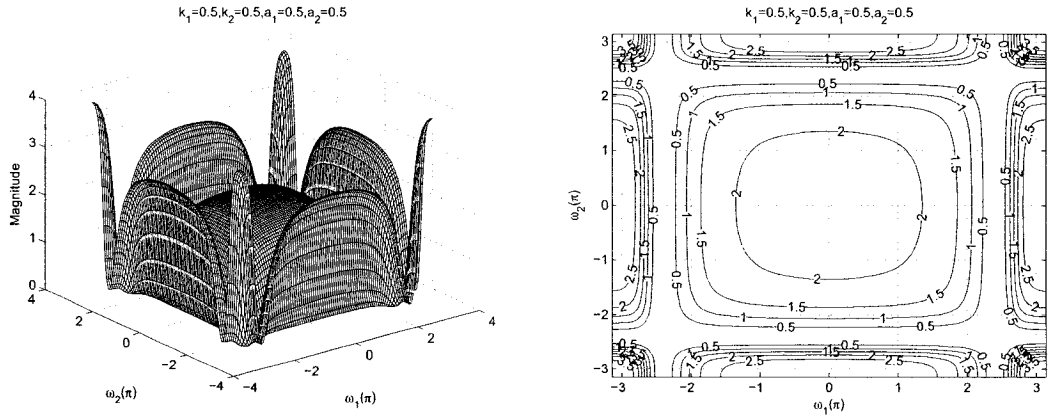

(b) $a_1 = a_2 = 0.5$ and $k_1 = k_2 = 0.5$

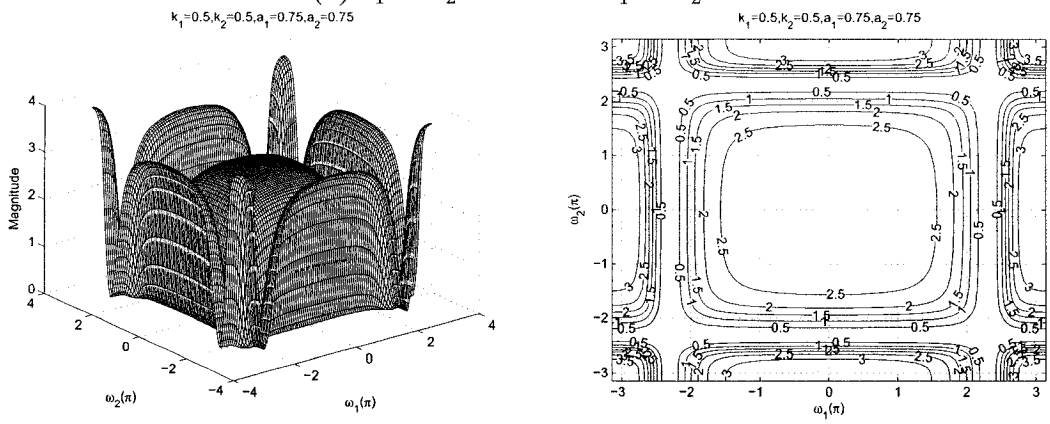

(c) $a_1 = a_2 = 0.75$ and $k_1 = k_2 = 0.5$

Figure 5.10: 3-D amplitude frequency response and the contour response of the 2-D digital bandstop filter for $a_1 = a_2$ and $k_1 = k_2$

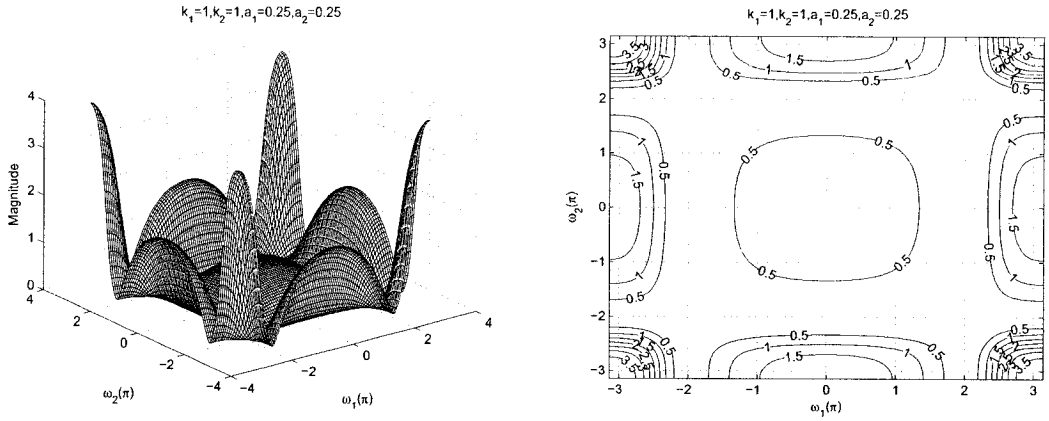

(a) $a_1 = a_2 = 0.25$ and $k_1 = k_2 = 1$

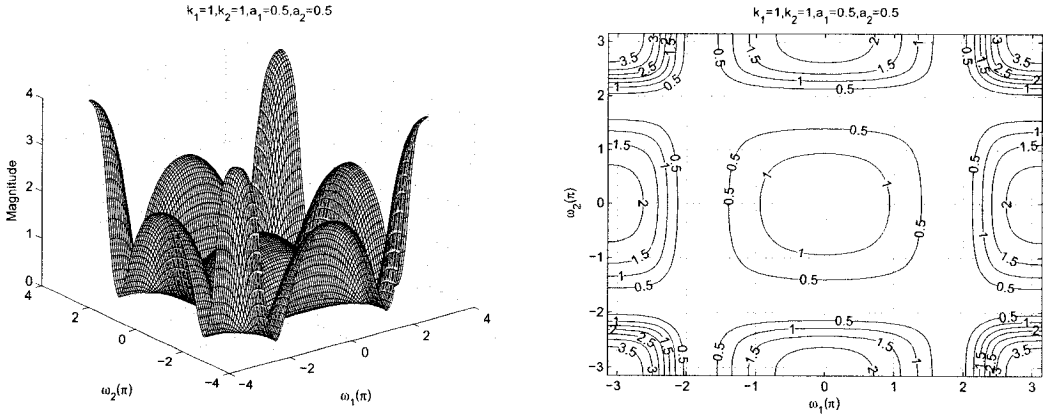

(b) $a_1 = a_2 = 0.5$ and $k_1 = k_2 = 1$

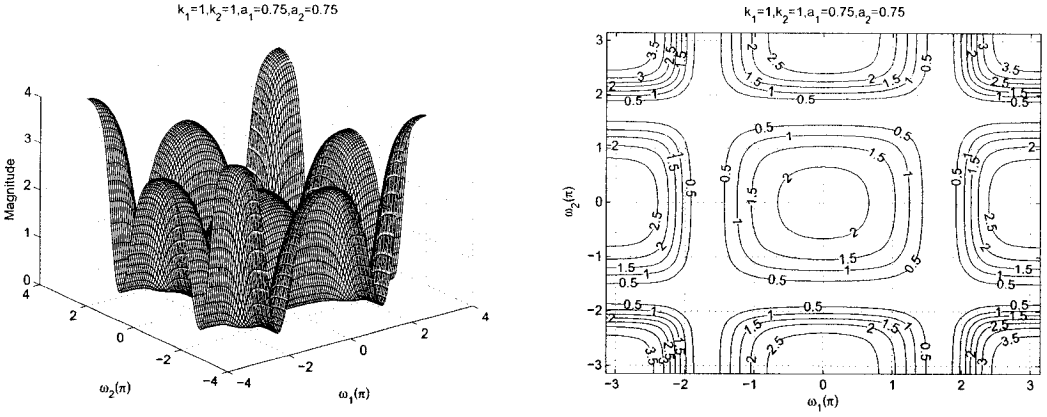

(c) $a_1 = a_2 = 0.75$ and $k_1 = k_2 = 1$

Figure 5.11: 3-D amplitude frequency response and the contour response of the 2-D digital bandstop filter for $a_1 = a_2$ and $k_1 = k_2$

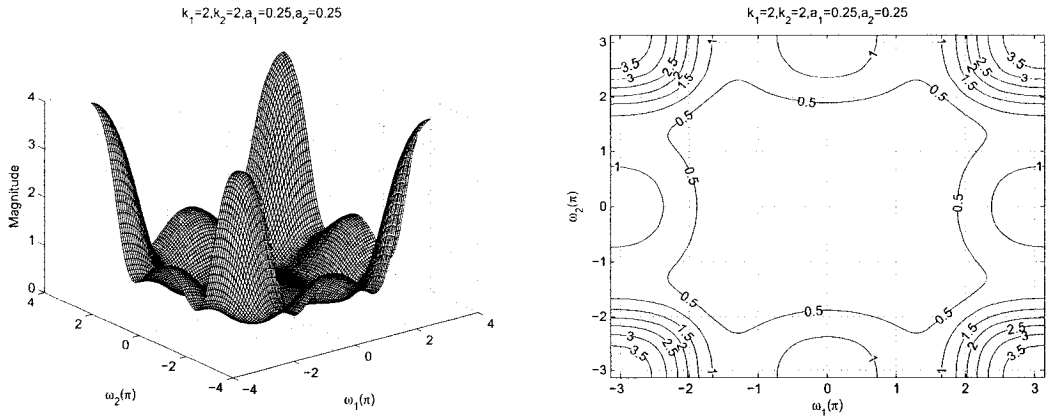

(a) $a_1 = a_2 = 0.25$ and $k_1 = k_2 = 2$

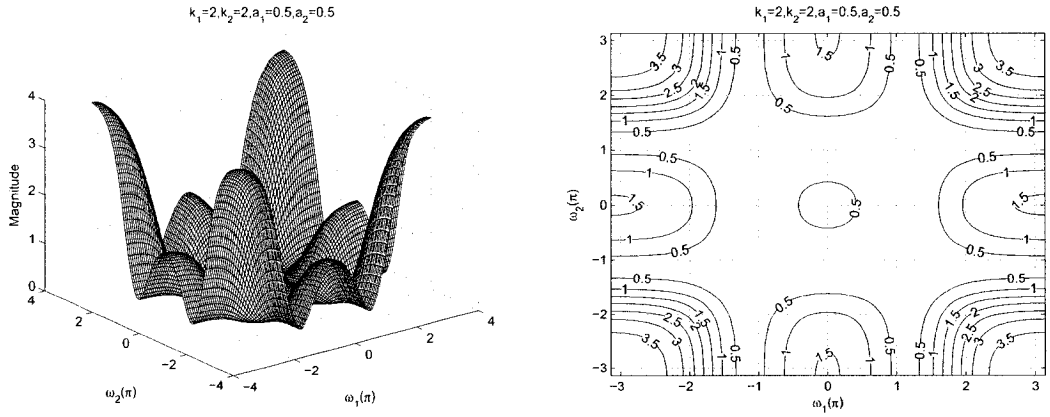

(b) $a_1 = a_2 = 0.5$ and $k_1 = k_2 = 2$

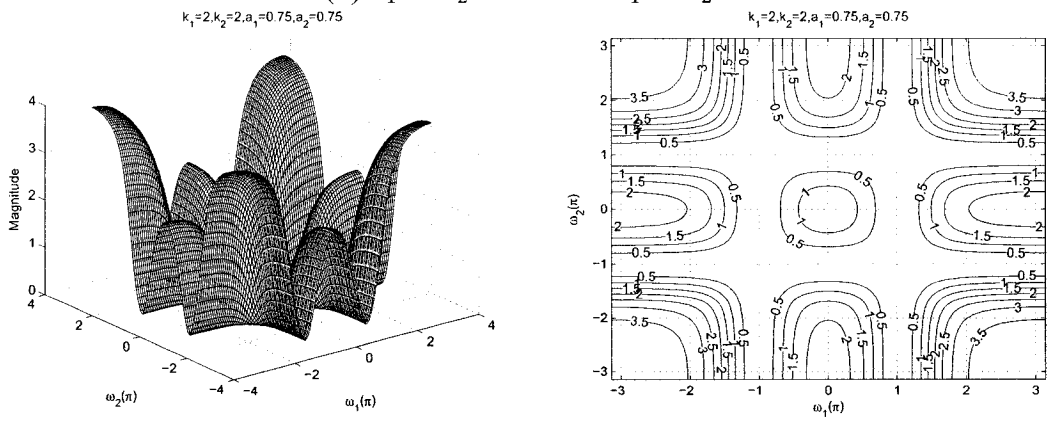

(c) $a_1 = a_2 = 0.75$ and $k_1 = k_2 = 2$

Figure 5.12: 3-D amplitude frequency response and the contour response of the 2-D digital bandstop filter for $a_1 = a_2$ and $k_1 = k_2$

As observed from the Figures 5.10 to 5.12, the coefficients k_1 and k_2 affect the passband width of the frequency response. In the Figures 5.10 (a) and 5.11 (a), there is an increase in the stopband width of the contour response, the cut-off frequency of the lower passband decreases and that of the upper passband increases as the values of k_1 and k_2 are increased from 0.5 to 1 for the same values of $a_1 = a_2 = 0.25$. In addition, the magnitude of the passband decreases for the same. It is observed from the Figure 5.12 (a), that when the values of $k_1 = k_2 > 1$ there is a rounding of the contour edges and the transition band of the 2-D digital bandstop filter cannot be clearly defined for the same values of $a_1 = a_2 = 0.25$. This is because the outer contour of the lower passband overlaps with the inner contour of the upper passband of the 2-D digital bandstop filter. Thus, the transition band is clearly visible for lower values of k_1 and k_2 as shown in Figures 5.10 (a) and 5.11 (a).

As observed from the Figures 5.10 to 5.12, the coefficients a_1 and a_2 affect the gain of the amplitude-frequency response. It can be clearly observed from the Figures 5.10 (a), (b) and (c), that the gain of the lower passband increases from 1.5 to 2.5 and that of the upper passband increases from 2.5 to 3.0 when the values of a_1 and a_2 are increased from 0.25 to 0.75 keeping the same values of $k_1 = k_2 = 0.5$. Also the width of the lower passband decreases and that of the upper passband increases for the same.

5.3.1.6 Frequency Response of 2-D Digital Bandstop Filter with different values of a_1 and a_2 and same values of k_1 and k_2

In this section, we will study the effect of coefficients, where $a_1 \neq a_2$ and $k_1 = k_2$ and the remaining coefficients b_1 and b_2 are considered to be unity for the 2-D digital bandstop filter in Category A. The values of a_1 and a_2 ranges from 0.25 to 0.5 and 0.5 to 0.75, respectively and the values of k_1 and k_2 ranges from 0.5 to 2.

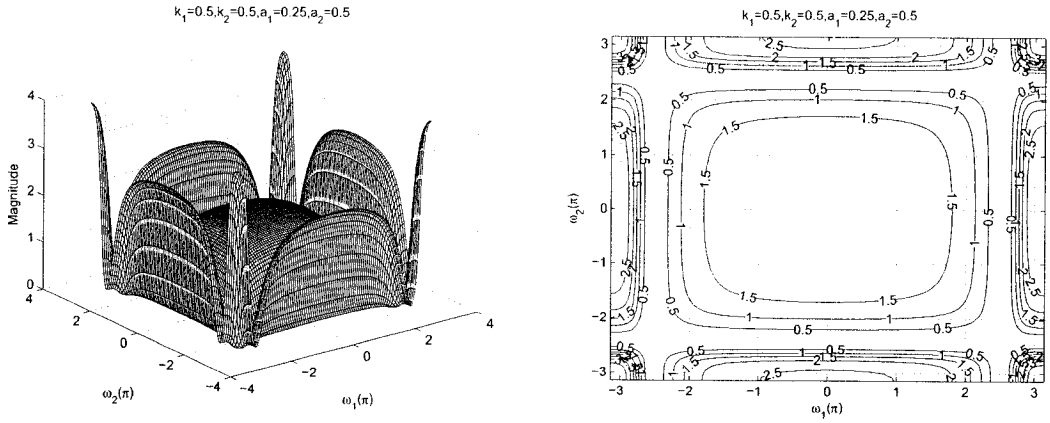

(a) $a_1 = 0.25,\ a_2 = 0.5$ and $k_1 = k_2 = 0.5$

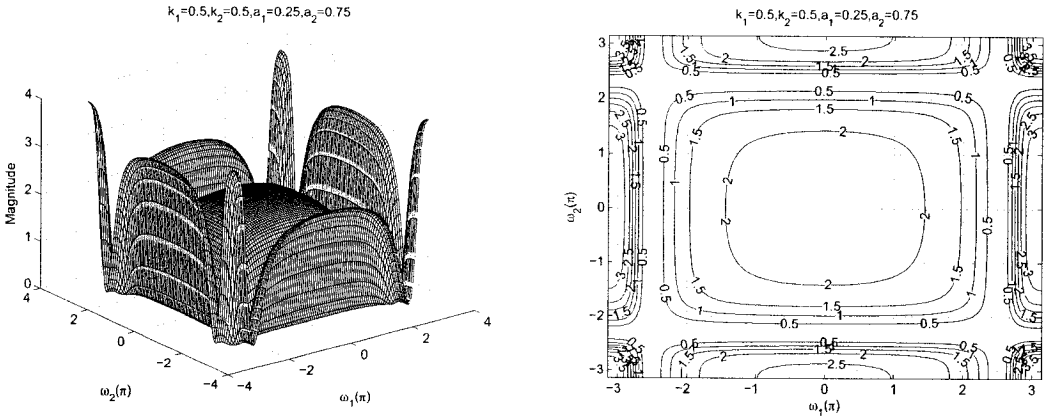

(b) $a_1 = 0.25,\ a_2 = 0.75$ and $k_1 = k_2 = 0.5$

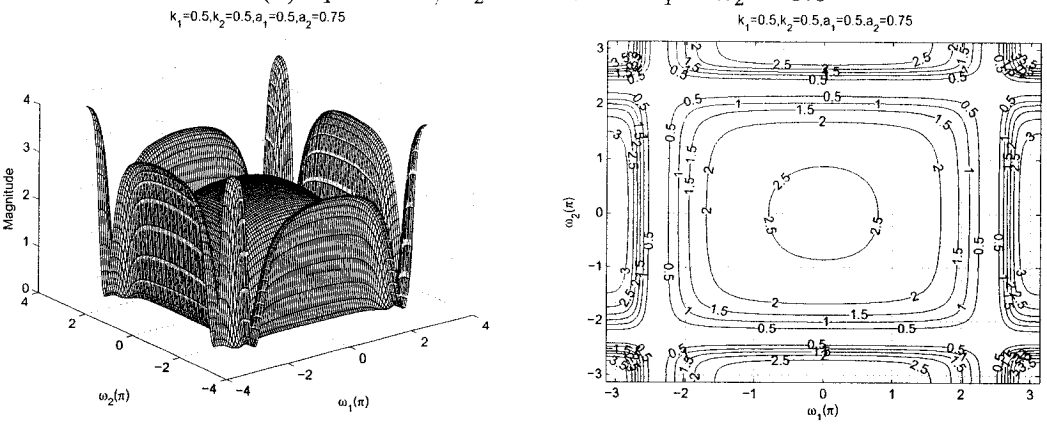

(c) $a_1 = 0.5\ a_2 = 0.75$ and $k_1 = k_2 = 0.5$

Figure 5.13: 3-D amplitude frequency response and the contour response of the 2-D digital bandstop filter for $a_1 \neq a_2$ and $k_1 = k_2$

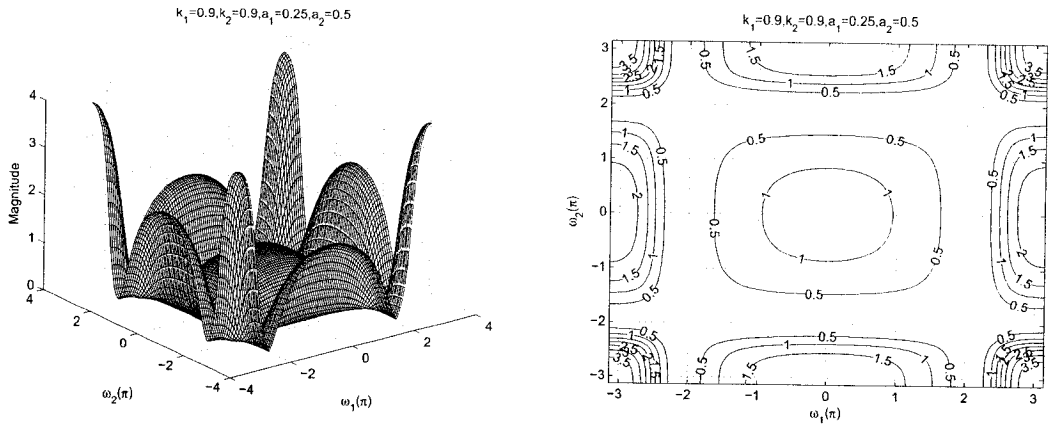

(a) $a_1 = 0.25,\ a_2 = 0.5$ and $k_1 = k_2 = 0.9$

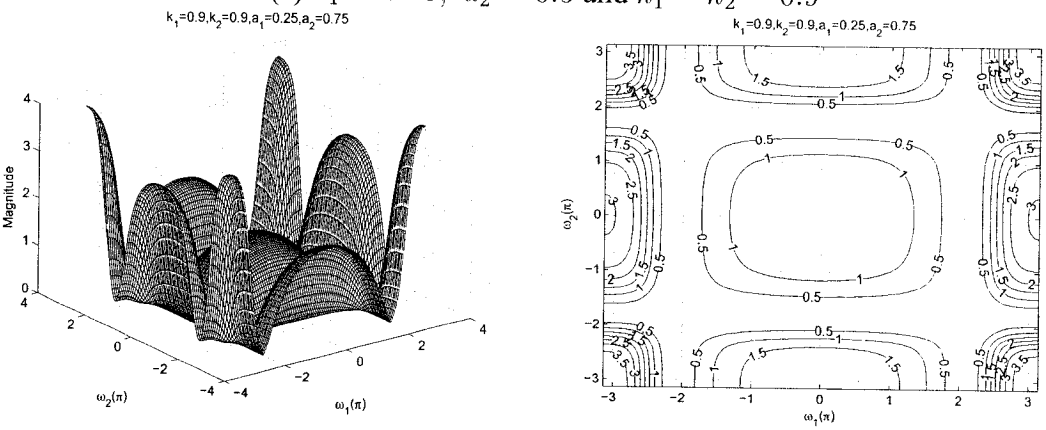

(b) $a_1 = 0.25,\ a_2 = 0.75$ and $k_1 = k_2 = 0.9$

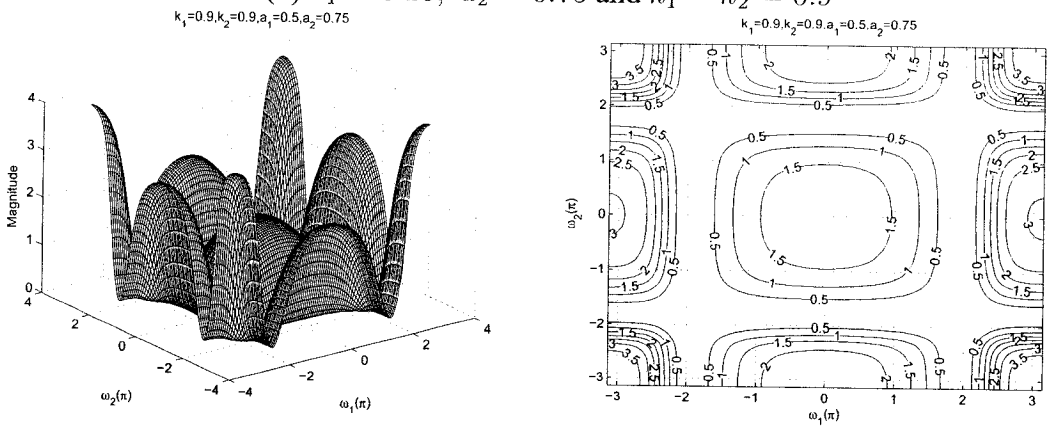

(c) $a_1 = 0.5,\ a_2 = 0.75$ and $k_1 = k_2 = 0.9$

Figure 5.14: 3-D amplitude frequency response and the contour response of the 2-D digital bandstop filter for $a_1 \neq a_2$ and $k_1 = k_2$

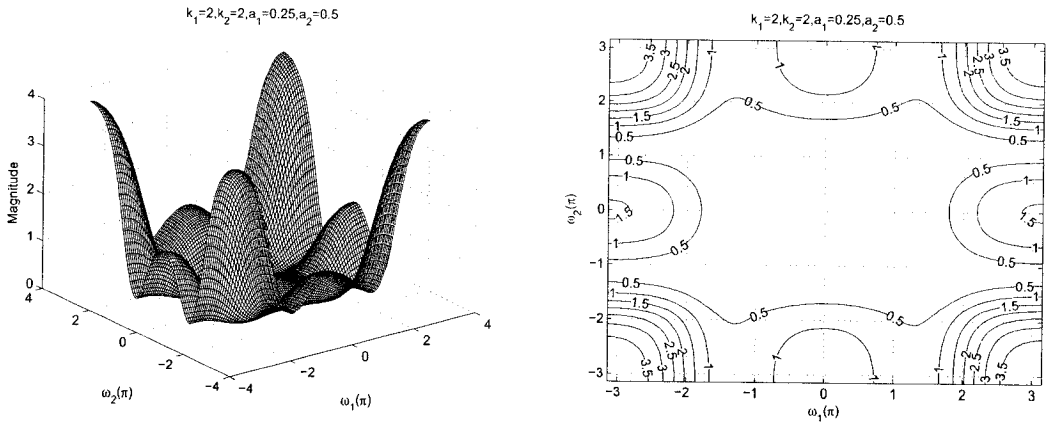

(a) $a_1 = 0.25,\ a_2 = 0.5$ and $k_1 = k_2 = 2$

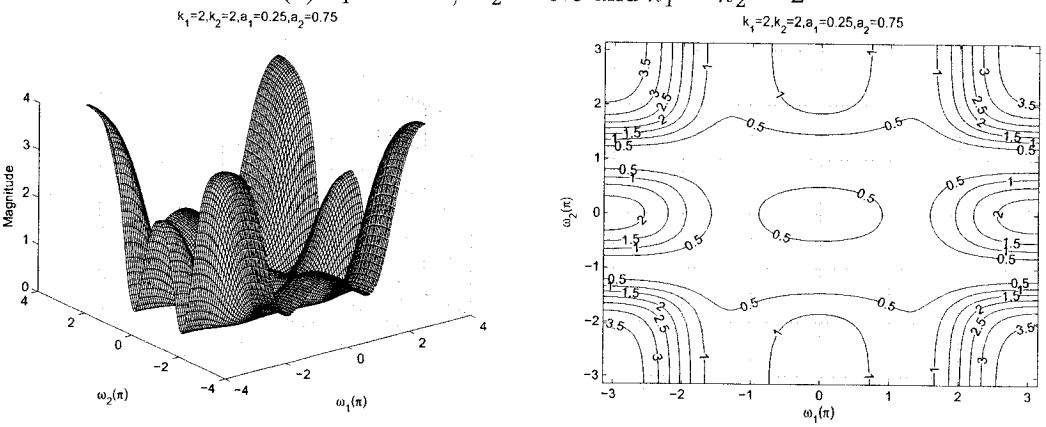

(b) $a_1 = 0.25\ a_2 = 0.75$ and $k_1 = k_2 = 2$

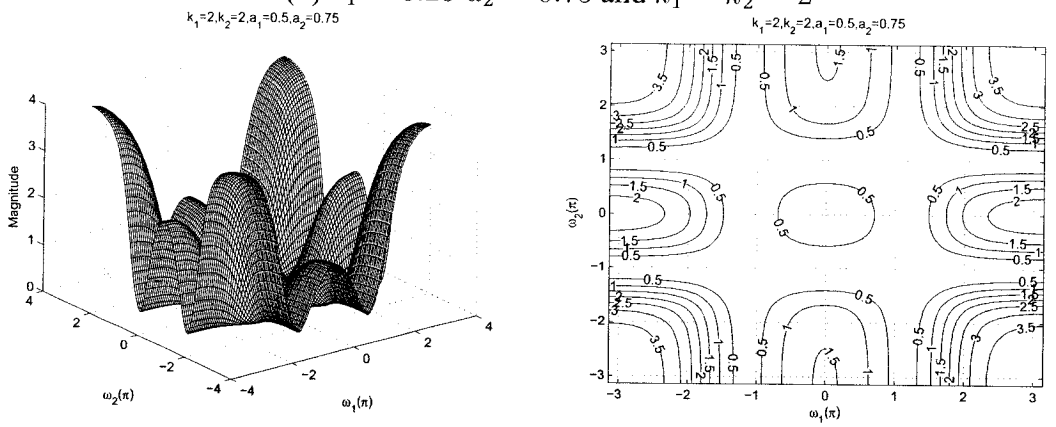

(c) $a_1 = 0.5,\ a_2 = 0.75$ and $k_1 = k_2 = 2$

Figure 5.15: 3-D amplitude frequency response and the contour response of the 2-D digital bandstop filter for $a_1 \neq a_2$ and $k_1 = k_2$

As observed from the Figures 5.13 to 5.15, the coefficients k_1 and k_2 affect the passband width of the frequency response. In the Figures 5.13 (a) and 5.14 (a), there is an increase in the stopband width of the contour response, the cut-off frequency of the lower passband decreases and that of the upper passband increases as the values of k_1 and k_2 are increased from 0.5 to 0.9 for the same values of $a_1 = 0.25$ and $a_2 = 0.5$. In addition, the magnitude of the passband decreases for the same. It is observed from the Figures 5.15 (a), that when the values of $k_1 = k_2 > 1$ there is a rounding of the contour edges and the transition band of the 2-D digital bandstop filter cannot be clearly defined for the same values $a_1 = 0.25$ and $a_2 = 0.5$. This is because the outer contour of the lower passband overlaps with the inner contour of the upper passband of the 2-D digital bandstop filter. The transition band of the 2-D digital bandstop filter is visible for lower values of k_1 and k_2 as shown in the Figures 5.13 and 5.14.

As observed from the Figures 5.13 to 5.15, the coefficients a_1 and a_2 affect the gain of the amplitude-frequency response. It can be clearly observed from the Figures 5.13 (a), (b) and (c), that the gain of the lower passband increases from 1.5 to 2.5 and that of the upper passband increases from 2.5 to 3 when the values of a_1 are increased from 0.25 to 0.5 and and a_2 is increased from 0.5 to 0.75, keeping the same value of $k_1 = k_2 = 0.5$. Also the width of the lower passband decreases and that of the upper passband increases for the same.

5.3.1.7 Frequency Response of 2-D Digital Bandstop Filter with different values of a_1 and a_2 and different values of k_1 and k_2

In this section, we study the effect of coefficients when $a_1 \neq a_2$ and $k_1 \neq k_2$, and the remaining coefficients b_1 and b_2 are considered to be unity for the 2-D digital bandstop filter in Category A. The values of a_1 and a_2 vary from 0.25 to 0.75 and 0.5 to 0.9, respectively and the values of k_1 and k_2 vary from 0.25 to 2 and 0.5 to 5, respectively.

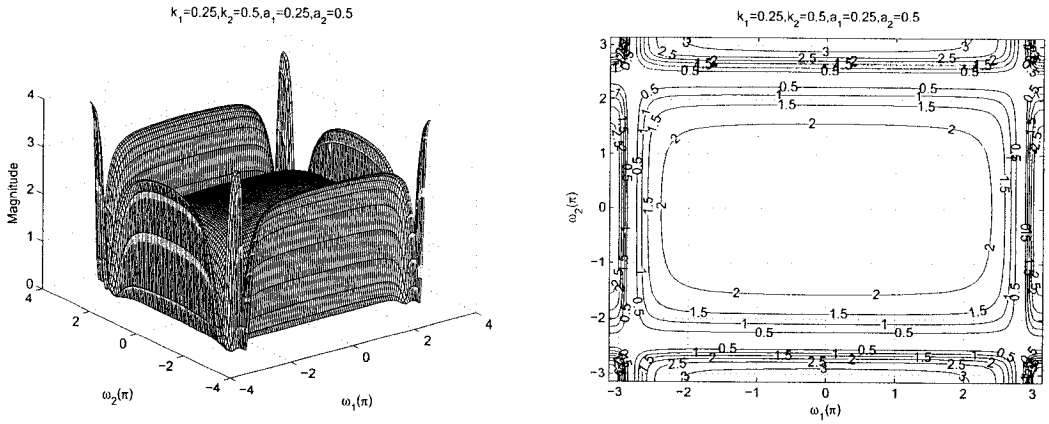

(a) $a_1 = 0.25$ $a_2 = 0.5$ and $k_1 = 0.25,\ k_2 = 0.5$

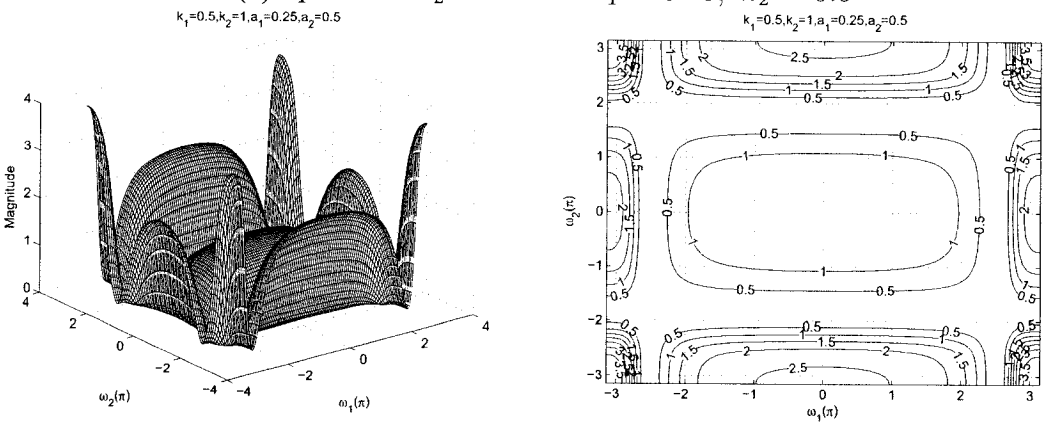

(b) $a_1 = 0.25,\ a_2 = 0.5$ and $k_1 = 0.5,\ k_2 = 1$

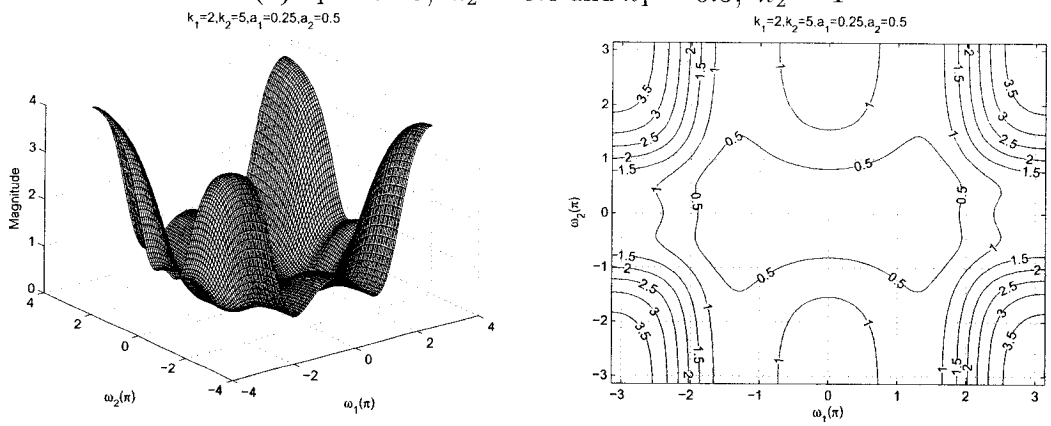

(c) $a_1 = 0.25,\ a_2 = 0.5$ and $k_1 = 2,\ k_2 = 5$

Figure 5.16: 3-D amplitude frequency response and the contour response of the 2-D digital bandstop filter for $a_1 \neq a_2$ and $k_1 \neq k_2$

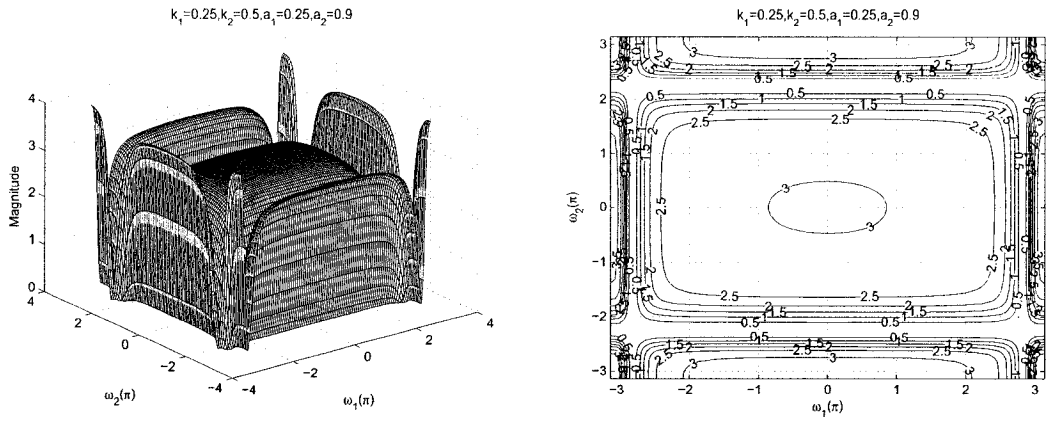

(a) $a_1 = 0.25,\ a_2 = 0.9$ and $k_1 = 0.25,\ k_2 = 0.5$

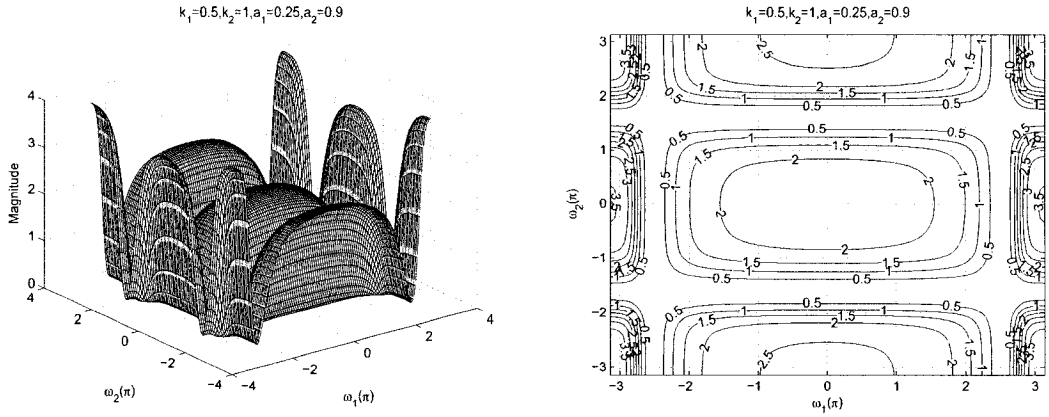

(b) $a_1 = 0.25,\ a_2 = 0.9$ and $k_1 = 0.5,\ k_2 = 1$

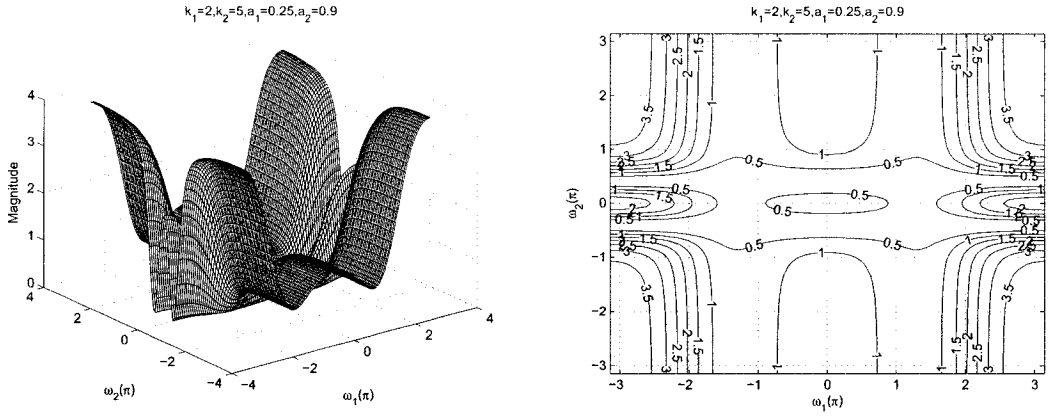

(c) $a_1 = 0.25,\ a_2 = 0.9$ and $k_1 = 2,\ k_2 = 5$

Figure 5.17: 3-D amplitude frequency response and the contour response of the 2-D digital bandstop filter for $a_1 \neq a_2$ and $k_1 \neq k_2$

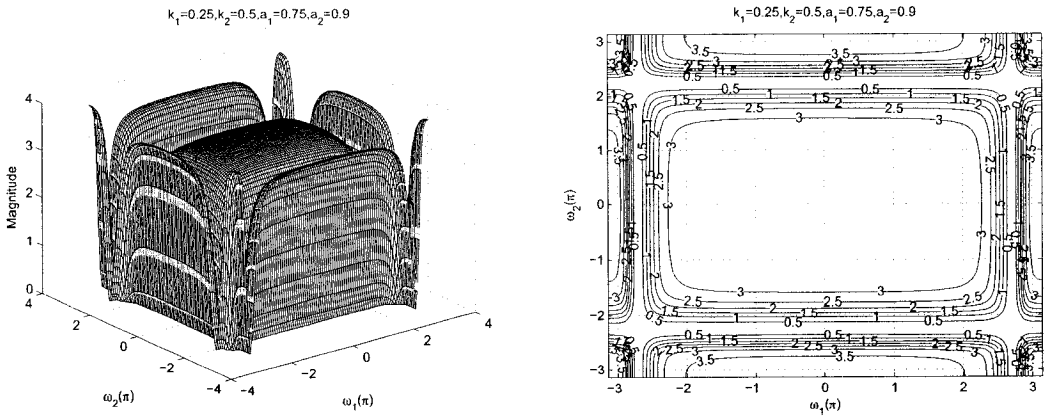

(a) $a_1 = 0.75,\ a_2 = 0.9$ and $k_1 = 0.25,\ k_2 = 0.5$

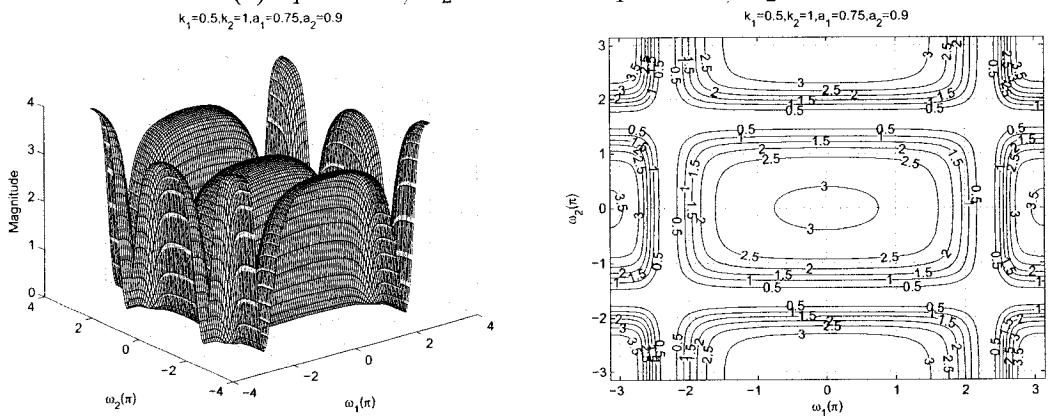

(b) $a_1 = 0.75,\ a_2 = 0.9$ and $k_1 = 0.5,\ k_2 = 1$

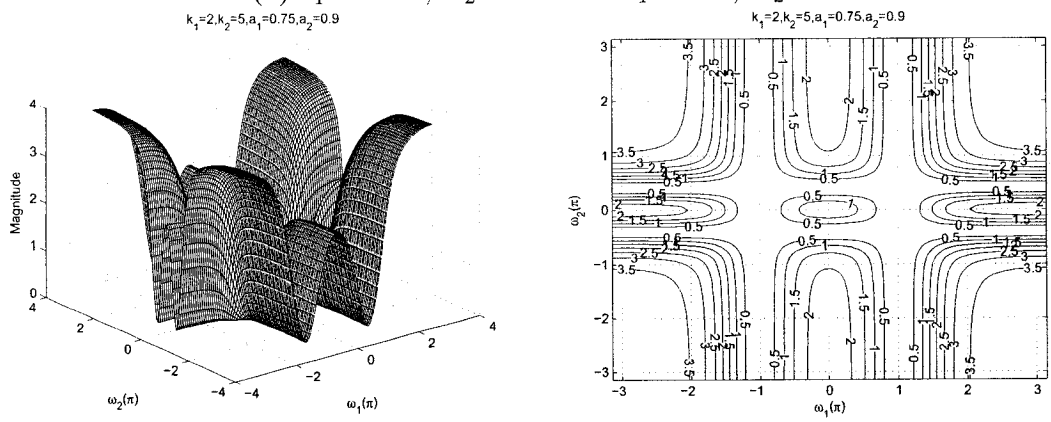

(c) $a_1 = 0.75,\ a_2 = 0.9$ and $k_1 = 2,\ k_2 = 5$

Figure 5.18: 3-D amplitude frequency response and the contour response of the 2-D digital bandstop filter for $a_1 \neq a_2$ and $k_1 \neq k_2$

As observed from the Figures 5.16 to 5.18, the coefficients k_1 and k_2 affect the passband width of the frequency response. In the Figures 5.16 (a) and (b), there is an increase in the stopband width of the contour response, the cut-off frequency of the lower passband decreases and that of the upper passband increases as the values of k_1 is increased from 0.25 to 0.5 and k_2 is increased from 0.5 to 1 for the same values of $a_1 = 0.25$ and $a_2 = 0.5$. In addition, the magnitude of the passband decreases for the same. It is observed from the Figures 5.16 (c), that when the values of $k_1 = k_2 > 1$ there is a rounding of the contour edges and the transition band of the 2-D digital bandstop filter cannot be clearly defined for the same values $a_1 = 0.25$ and $a_2 = 0.5$. This is because the outer contour of the lower passband overlaps with the inner contour of the upper passband of the 2-D digital bandstop filter. The transition band of the 2-D digital bandstop filter is visible for lower values of k_1 and k_2 as shown in the Figures 5.16 (a) and (b).

As observed from the Figures 5.16 to 5.18, the coefficients a_1 and a_2 affect the gain of the amplitude-frequency response. It can be clearly observed from the Figures 5.16 (a), 5.17 (a) and 5.18 (a), that the gain of the lower passband increases from 2 to 3 and that of the upper passband increases from 3 to 3.5 when the values of a_1 are increased from 0.25 to 0.75 and and a_2 is increased from 0.5 to 0.9, keeping the same value of $k_1 = 0.25$ and $k_2 = 0.5$. Also the width of the passband decreases and increases periodically for the same.

5.3.1.8 Frequency Response of 2-D Digital Bandstop Filter with same values of a_1 and a_2 and different values of k_1 and k_2

In this section, we study the effect of coefficients, where $a_1 = a_2$ and $k_1 \neq k_2$ and the remaining coefficients b_1 and b_2 are considered to be unity for the 2-D digital bandstop filter in Category A. The values of a_1 and a_2 vary from 0.25 to 0.75 and the values of k_1 and k_2 vary from 0.25 to 2 and 0.5 to 5, respectively.

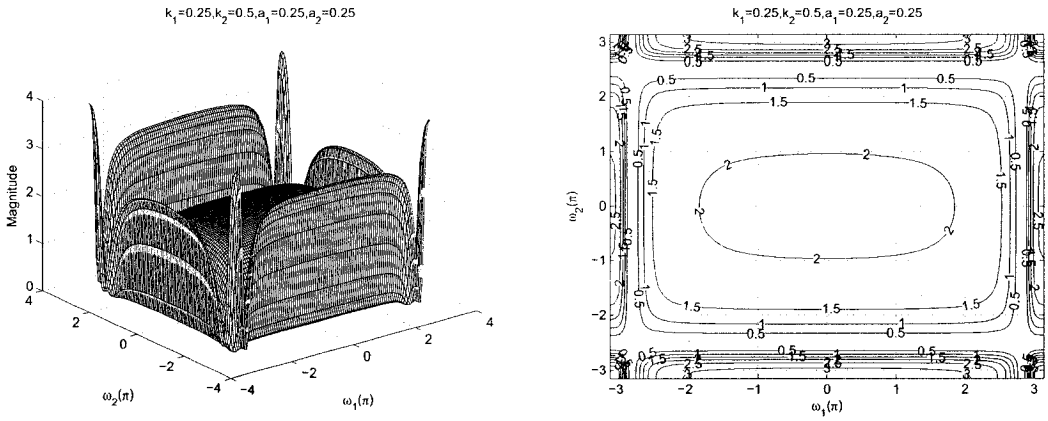

(a) $a_1 = a_2 = 0.25$ and $k_1 = 0.25$, $k_2 = 0.5$

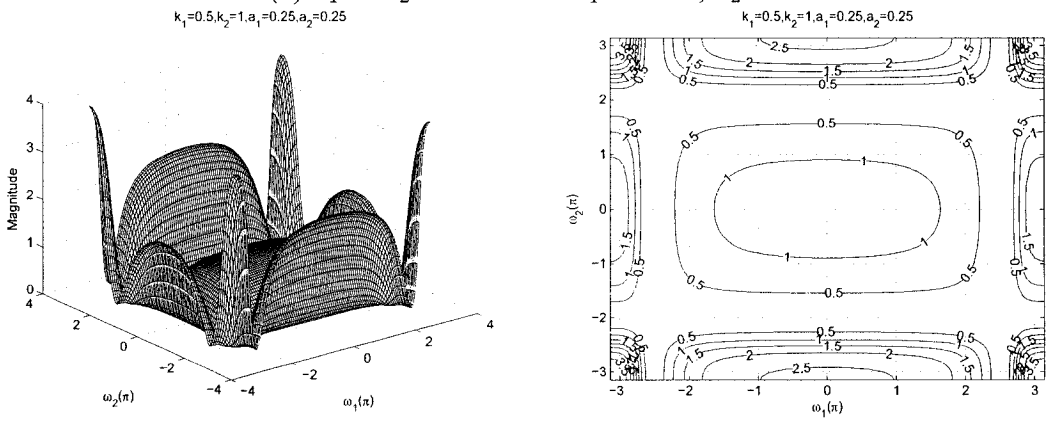

(b) $a_1 = a_2 = 0.25$ and $k_1 = 0.5$, $k_2 = 1$

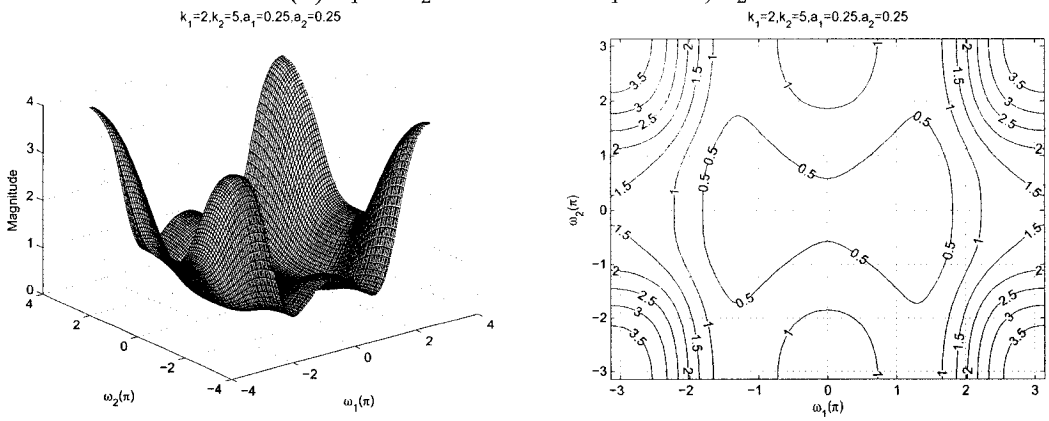

(c) $a_1 = a_2 = 0.25$ and $k_1 = 2$, $k_2 = 5$

Figure 5.19: 3-D amplitude frequency response and the contour response of the 2-D digital bandstop filter for $a_1 = a_2$ and $k_1 \neq k_2$

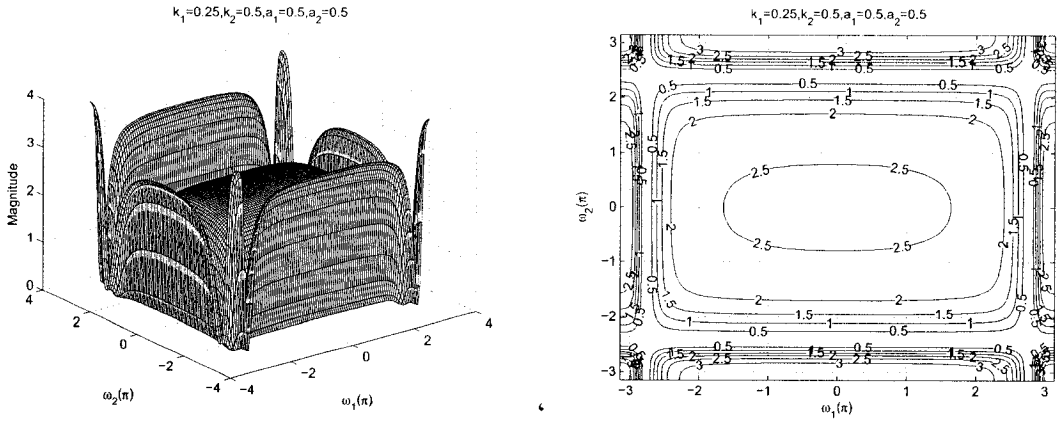

(a) $a_1 = a_2 = 0.5$ and $k_1 = 0.25$, $k_2 = 0.5$

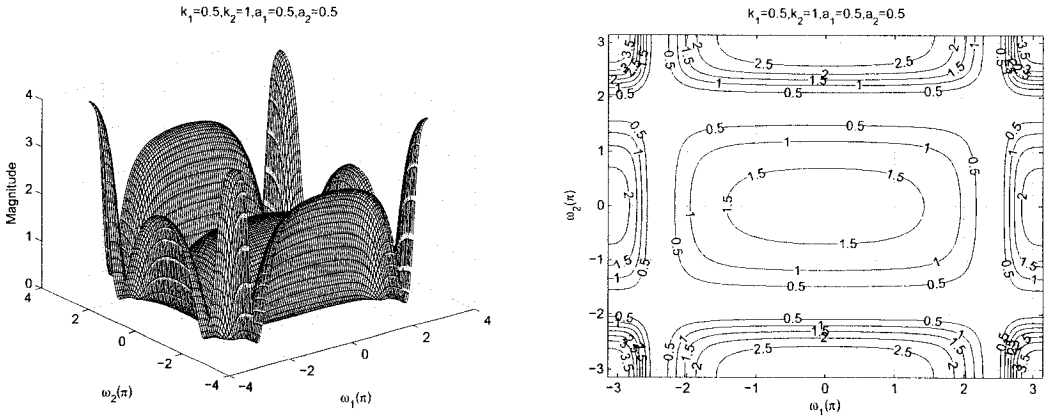

(b) $a_1 = a_2 = 0.5$ and $k_1 = 0.5$, $k_2 = 1$

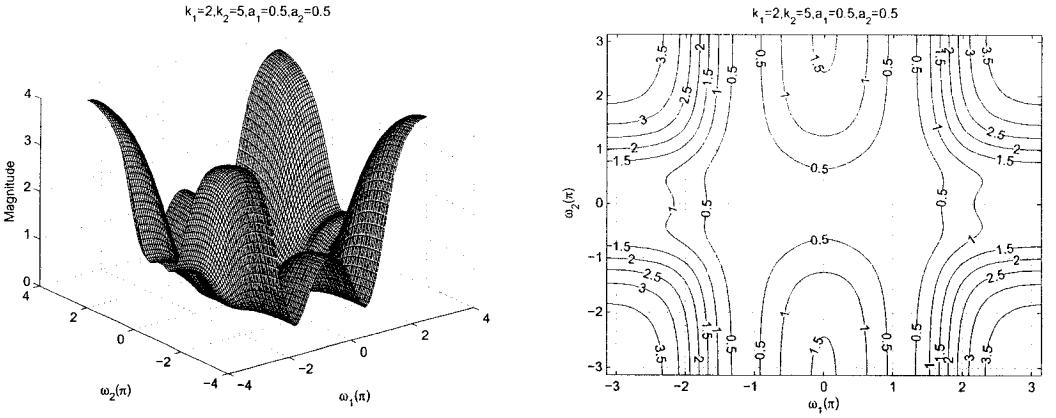

(c) $a_1 = a_2 = 0.5$ and $k_1 = 2$, $k_2 = 5$

Figure 5.20: 3-D amplitude frequency response and the contour response of the 2-D digital bandstop filter for $a_1 = a_2$ and $k_1 \neq k_2$

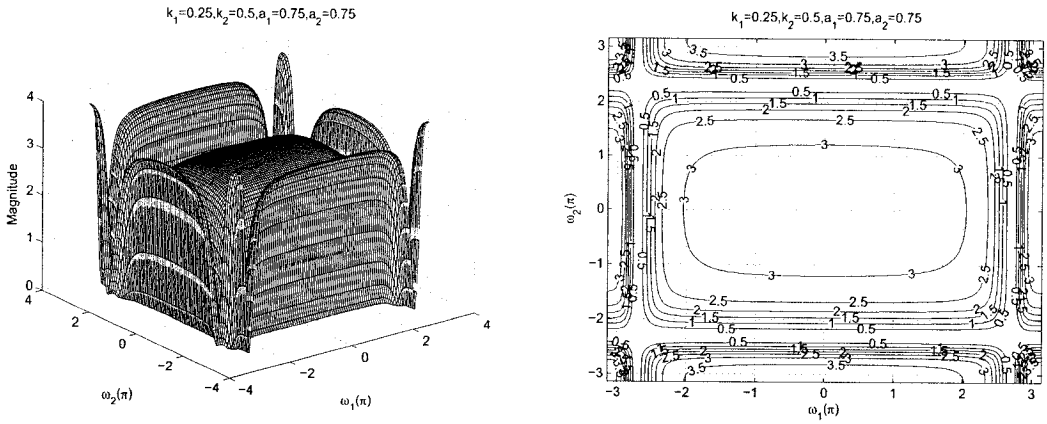

(a) $a_1 = a_2 = 0.75$ and $k_1 = 0.25$, $k_2 = 0.5$

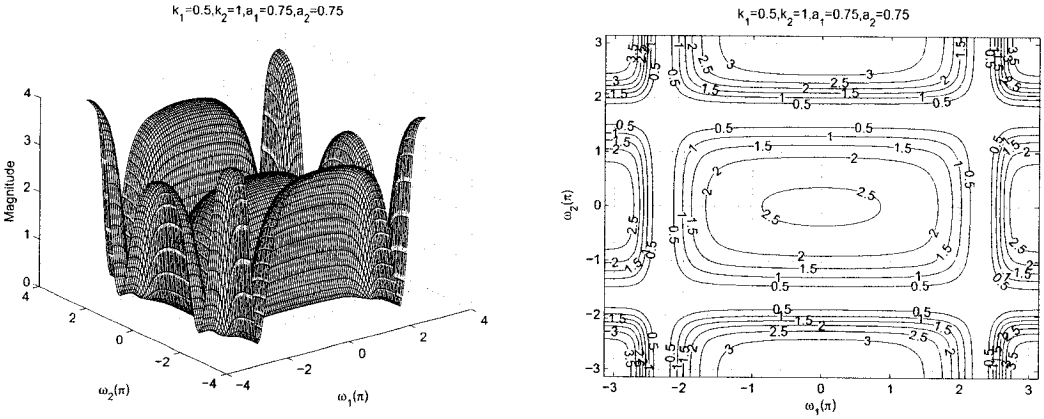

(b) $a_1 = a_2 = 0.75$ and $k_1 = 0.5$, $k_2 = 1$

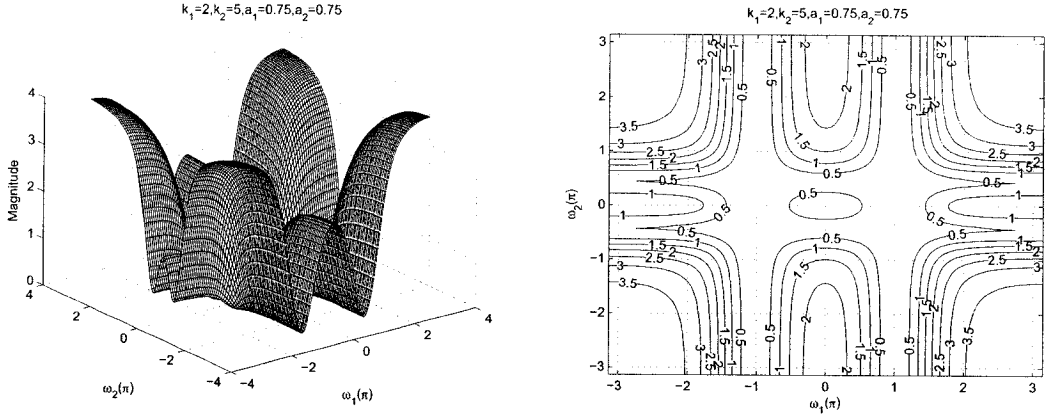

(c) $a_1 = a_2 = 0.75$ and $k_1 = 2$, $k_2 = 5$

Figure 5.21: 3-D amplitude frequency response and the contour response of the 2-D digital bandstop filter for $a_1 = a_2$ and $k_1 \neq k_2$

As observed from the Figures 5.19 to 5.21, the coefficients k_1 and k_2 affect the passband width of the frequency response. In the Figures 5.19 (a) and (b) there is an increase in the stopband width of the contour response, the cut-off frequency of the lower passband

decreases and that of the upper passband increases as the values of k_1 is increased from 0.5 to 2 and k_2 is increased from 0.5 to 1 for the same values of $a_1 = a_2 = 0.25$. In addition, the magnitude of the passband decreases for the same. It is observed from the Figure 5.19 (c), that when values of k_1 and k_2 are greater than 1, there is a rounding of the contour edges and the transition band of the 2-D digital bandstop filter cannot be clearly defined for the same values $a_1 = a_2 = 0.25$. This is because the outer contour of the lower passband overlaps with the inner contour of the upper passband of the 2-D digital bandstop filter. The transition band of the 2-D digital bandstop filter is visible for lower values of k_1 and k_2 as shown in the Figures 5.19 (a) and (b).

As observed from the Figures 5.19 to 5.21, the coefficients a_1 and a_2 affect the gain of the amplitude-frequency response. It can be clearly observed from the Figures 5.19 (a), 5.20 (a), and 5.21 (a), that the gain of the lower passband increases from 2 to 3 and that of the upper passband also increases from 3 to 3.5, when the values of a_1 and a_2 are increased from 0.25 to 0.75, keeping the same values of $k_1 = 0.25$ and $k_2 = 0.5$. Also the width of the passband increases and decreases periodically for for the same.

5.3.2 Frequency Response of the All-pole 2-D Digital Bandstop Filter in Category B

The transfer function of the all-pole 2-D digital bandstop filter is obtained by using the proposed all-pole 2-D analog lowpass filter in Category B is discussed in Chapter 2. The analog all-pole 2-D lowpass filter is transformed to the all-pole 2-D analog bandstop transformation which in turn is transformed to the all-pole 2-D digital bandstop filter by using the generalized bilinear transformation as explained in Section 5.2.2.

To investigate the manner in which each coefficient of the generalized bilinear transformation effects the magnitude response of the resulting all-pole 2-D digital bandstop filter, we vary the values of the coefficients or fix some of the coefficients to specific values. It is possible to obtain the all-pole 2-D digital bandstop filter when the coefficients have the

following limits: $k_i > 0$, $0 \leq |a_i| \leq 1$ and $b_i = 1$, where $i = 1, 2$. Let us consider the coefficients of the generalized bilinear transformation for the all-pole 2-D digital bandstop filter to be unity, i.e., $a_1 = 1$, $a_2 = 1$, $k_1 = 1$, $k_2 = 1$, $b_1 = 1$ and $b_2 = 1$ Under this condition, the 3-D amplitude-frequency response and the contour plots of the 2-D digital filter are shown in the Figure 5.22.

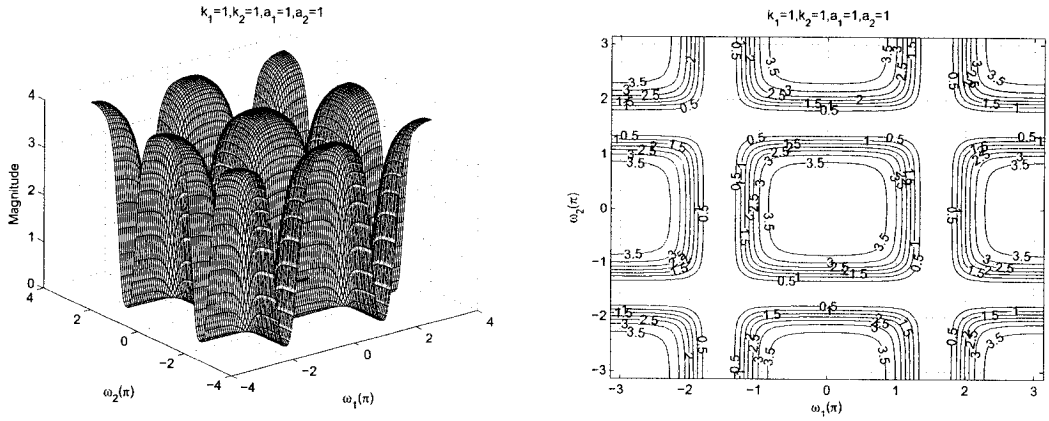

Figure 5.22: 3-D Amplitude-Frequency response and contour response of the All-pole 2-D Digital Bandstop Filter with all the coefficients values as unity

In the following, we will study the effects of these coefficients to the frequency responses of the all-pole 2-D digital bandstop filter [33, 48].

5.3.2.1 Frequency Response of the All-pole 2-D Digital Bandstop Filter with different values of k_1

In this section, we study the manner in which k_1 affects the frequency response of the resulting all-pole 2-D digital bandstop filter and to separate the effect of the other coefficients, we vary the value of k_1, and fix all the other coefficients of the generalized bilinear transformation to unity, e.g. with $k_2 = 1$, $a_1 = 1$, $a_2 = 1$, $b_1 = 1$, and $b_2 = 1$. This was done so that no generality is lost and to make the situation simple. The values of k_1 are varied from 0.1 to 5 and the 3-D magnitude response and the contour plots for the all-pole 2-D digital bandstop filter with the values of $k_1 = 0.1$, $k_1 = 0.5$, $k_1 = 0.9$, $k_1 = 2$, and $k_1 = 5$ are shown in the Figures 5.23 and 5.24.

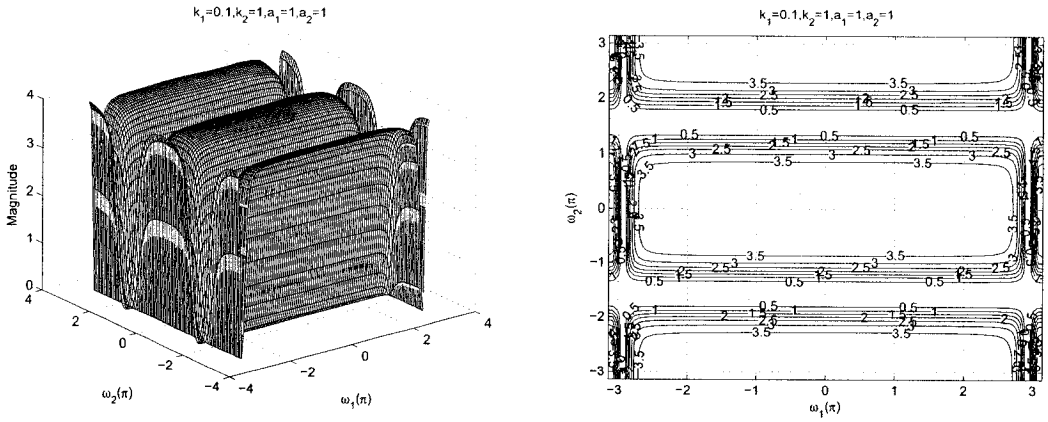

(a) $k_1 = 0.1$

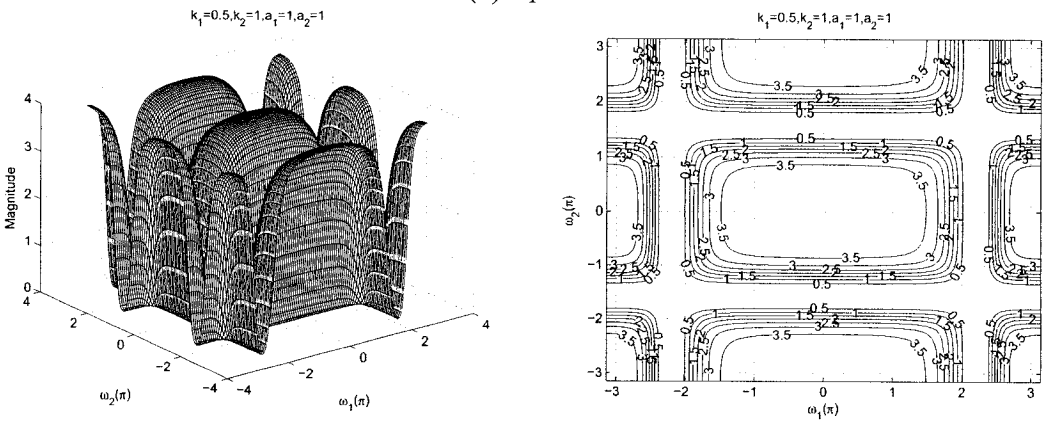

(b) $k_1 = 0.5$

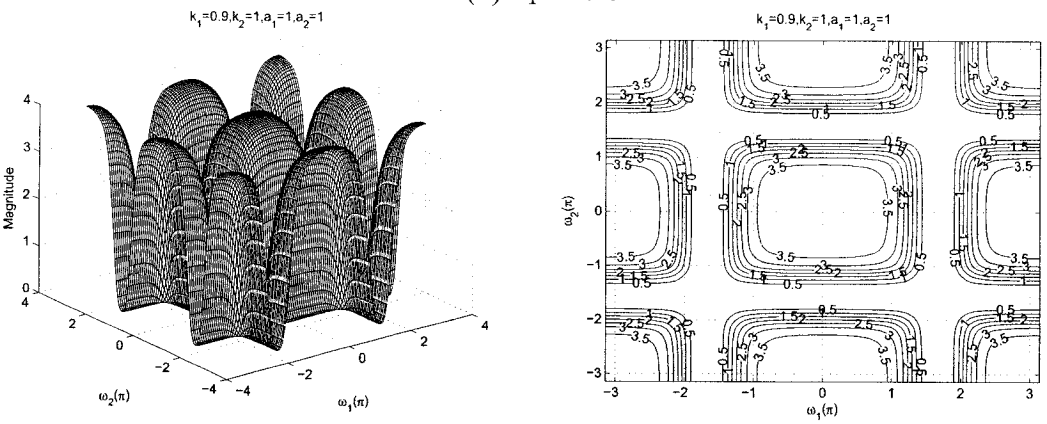

(c) $k_1 = 0.9$

Figure 5.23: 3-D amplitude frequency response and the contour of the All-pole 2-D digital bandstop filter for different values of k_1

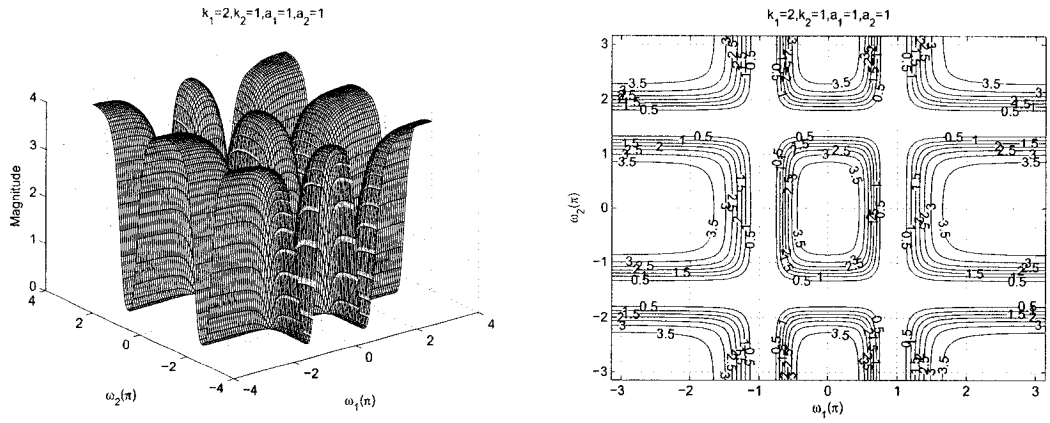

(a) $k_1 = 2$

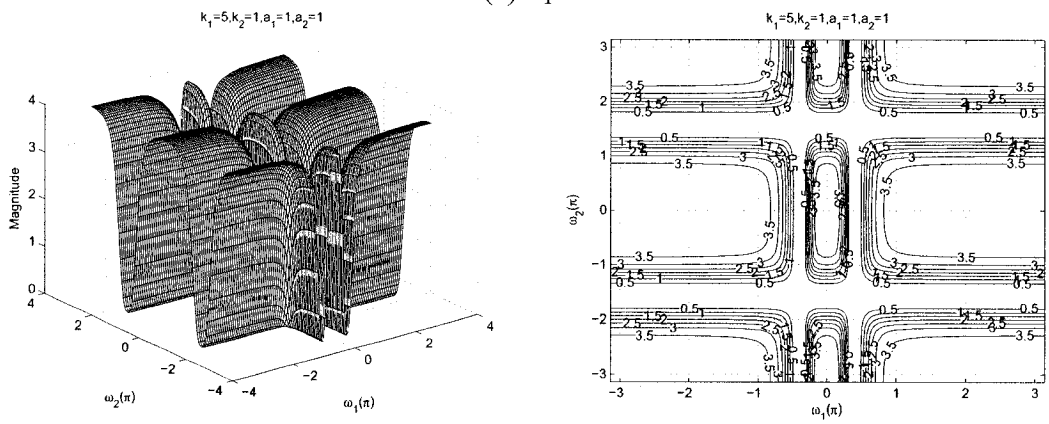

(b) $k_1 = 5$

Figure 5.24: 3-D amplitude frequency response and the contour of the All-pole 2-D digital bandstop filter for different values of k_1

It is observed from the diagrams that although the coefficient k_1 does not have any effect on the passband width along the $\omega_2 - axis$, it affects the center frequency of the filter response along the $\omega_1 - axis$. It also affects the width of the lower and the upper passbands, and the stopband width of the bandstop filter along the $\omega_1 - axis$. Initially, when the value of the coefficient $k_1 = 0.1$ (see Figure 5.23 (a)) the lower passband will have the maximum bandwidth in the available frequency range. As we increase the value of k_1 from 0.1 to 5, the cut-off frequency of the lower passband decreases and that of the upper passband increases. Also the width of the lower passband decreases and that of the upper passband increases along the $\omega_1 - axis$. The width of the stopband increases and decreases periodically for different values of k_1 as seen from the Figures 5.23 and 5.24

along $\omega_1 - axis$. It is also observed that the amplitude of the contour response of the lower and upper passband remains constant.

5.3.2.2 Frequency Response of the All-pole 2-D Digital Bandstop Filter with different values of k_2

In this section, we study the manner in which k_2 affects the frequency response behavior of the resulting all-pole 2-D digital bandstop filter and to separate the effect of the other coefficients, we vary the value of k_2, and fix all the other coefficients of the generalized bilinear transformation to unity, e.g. with $k_1 = 1$, $a_1 = 1$, $a_2 = 1$, $b_1 = 1$, and $b_2 = 1$. This was done so that no generality is lost and to make the situation simple. The values of k_2 are varied from 0.1 to 5 and the 3-D magnitude response and the contour plots for the all-pole 2-D digital bandstop filter with the values of $k_2 = 0.1$, $k_2 = 0.5$, $k_2 = 0.9$, $k_2 = 2$, and $k_2 = 5$ are shown in the Figures 5.25 and 5.26.

It is observed from the diagrams that although the coefficient k_2 does not have any effect on the passband width along the $\omega_1 - axis$, it affects the center frequency of the filter response along the $\omega_2 - axis$. It also affects the width of the lower and the upper passbands, and the stopband width of the bandstop filter along the $\omega_2 - axis$. Initially when the value of the coefficient $k_2 = 0.1$ (see Figure 5.25 (a)) the lower passband will have the maximum bandwidth in the available frequency range. As we increase the value of k_2 from 0.1 to 5, the cut-off frequency of the lower passband decreases and that of the upper passband increases. Also the width of the lower passband decreases and that of the upper passband increases along the $\omega_2 - axis$. The width of the stopband increases and decreases periodically for different values of k_2 as seen from the Figures 5.25 and 5.26 along $\omega_2 - axis$. It is also observed that the amplitude of the contour response of the lower and upper passband remains constant.

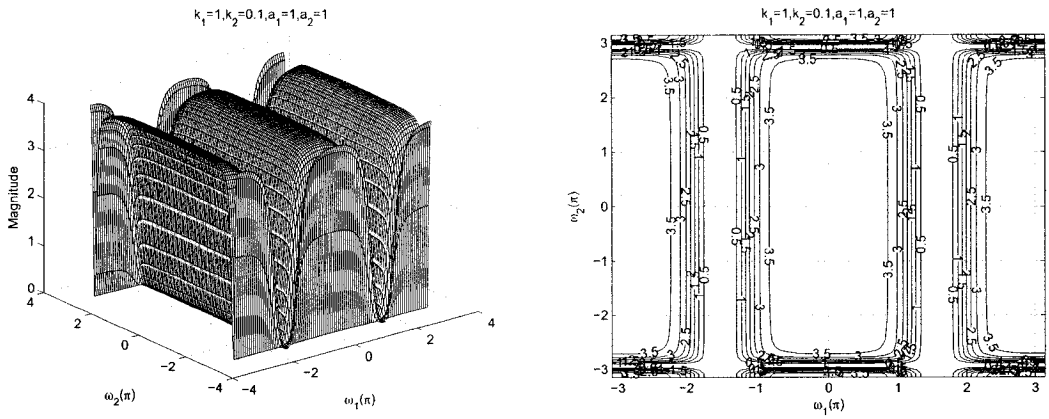

(a) $k_2 = 0.1$

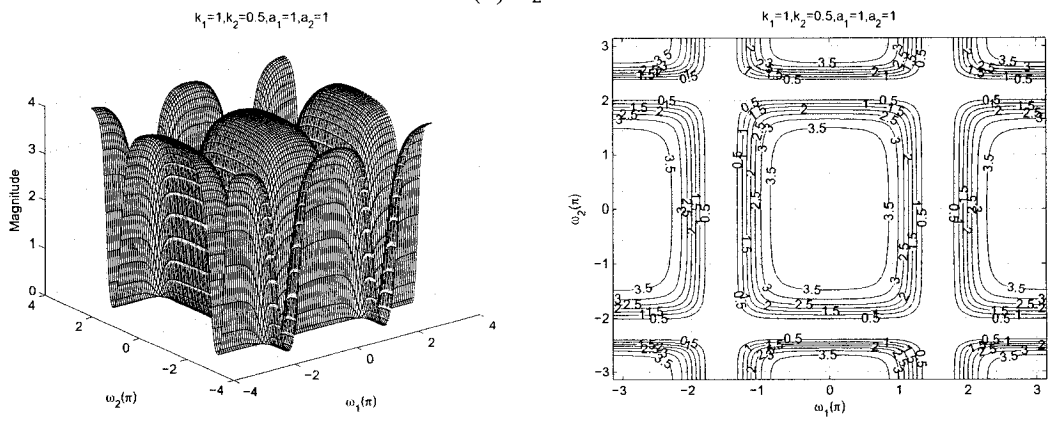

(b) $k_2 = 0.5$

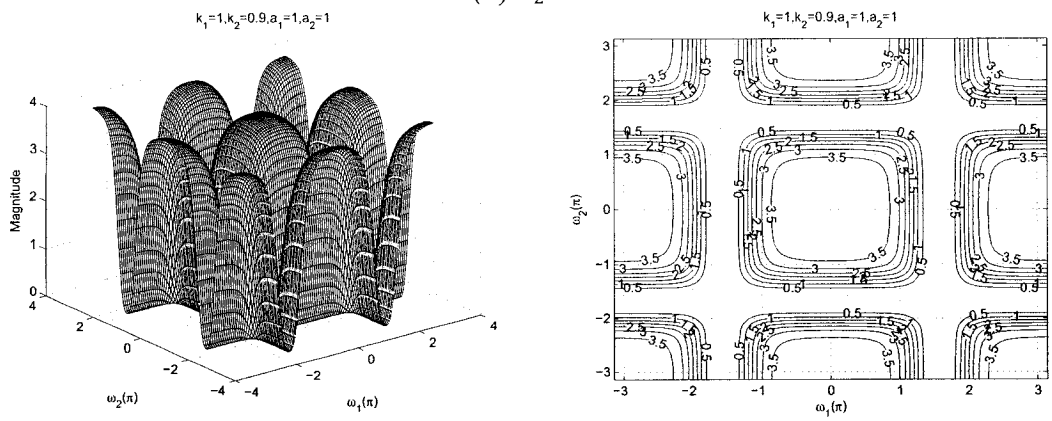

(c) $k_2 = 0.9$

Figure 5.25: 3-D amplitude frequency response and the contour of the All-pole 2-D digital bandstop filter for different values of k_2

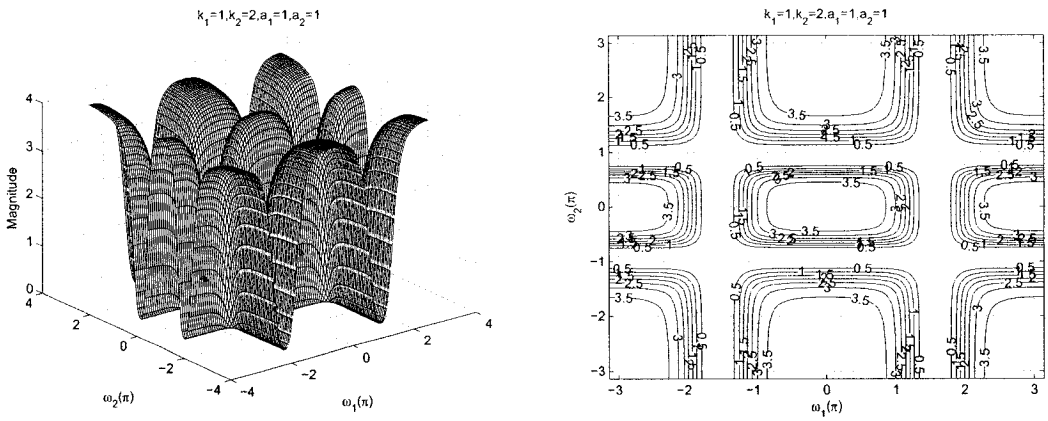

(a) $k_2 = 2$

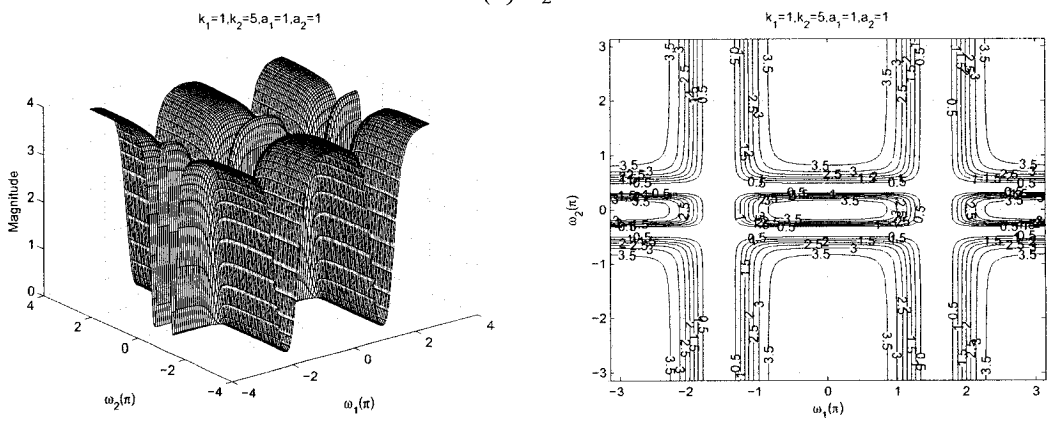

(b) $k_2 = 5$

Figure 5.26: 3-D amplitude frequency response and the contour of the All-pole 2-D digital bandstop filter for different values of k_2

5.3.2.3 Frequency Response of the All-pole 2-D Digital Bandstop Filter with different values of a_1

In the Sections 5.3.2.1 and 5.3.2.2, the effect of the coefficient of k_1 and k_2 are studied. In this section, the effect of the coefficient a_1 is studied. The stable range of a_1 can be obtained with other specified coefficients of the generalized bilinear transformation. There are many combinations possible for the coefficients. To study the response with different values of a_1 properly, we fix other coefficients values to be equal to unity. The range of a_1 varies from 0.1 to 1 and the other coefficient values are specified as unity, i.e., $k_1 = 1$, $k_2 = 1$, $a_2 = 1$, $b_1 = 1$ and $b_2 = 1$.

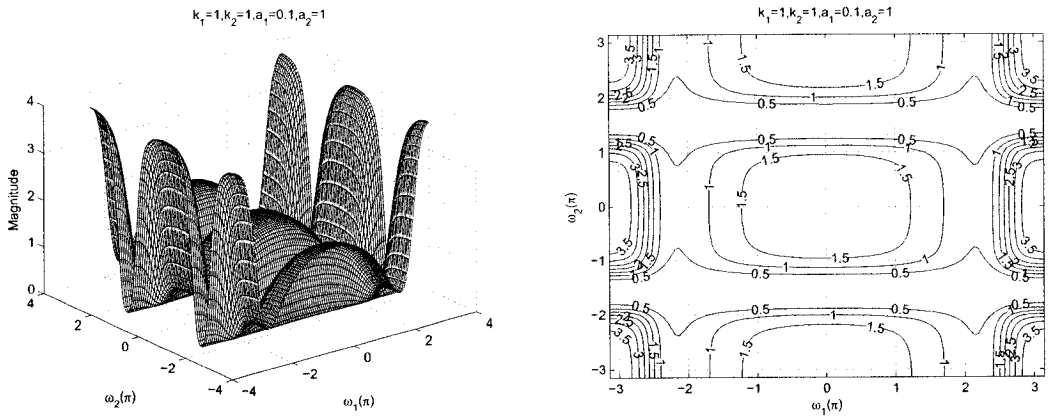

(a) $a_1 = 0.1$

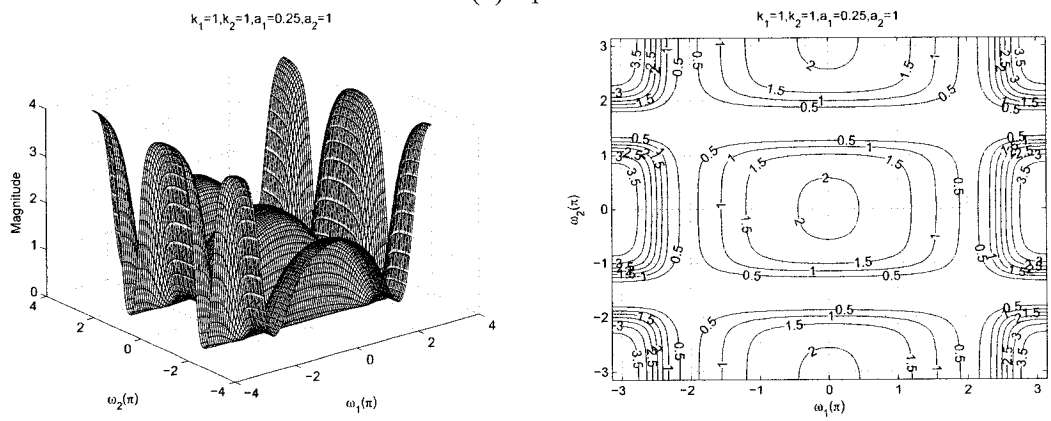

(b) $a_1 = 0.25$

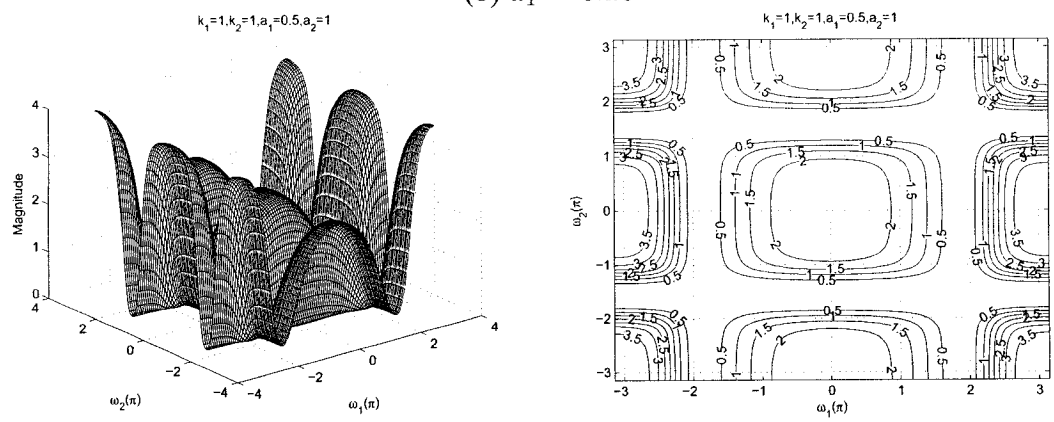

(c) $a_1 = 0.5$

Figure 5.27: 3-D amplitude frequency response and the contour of the All-pole 2-D digital bandstop filter for different values of a_1

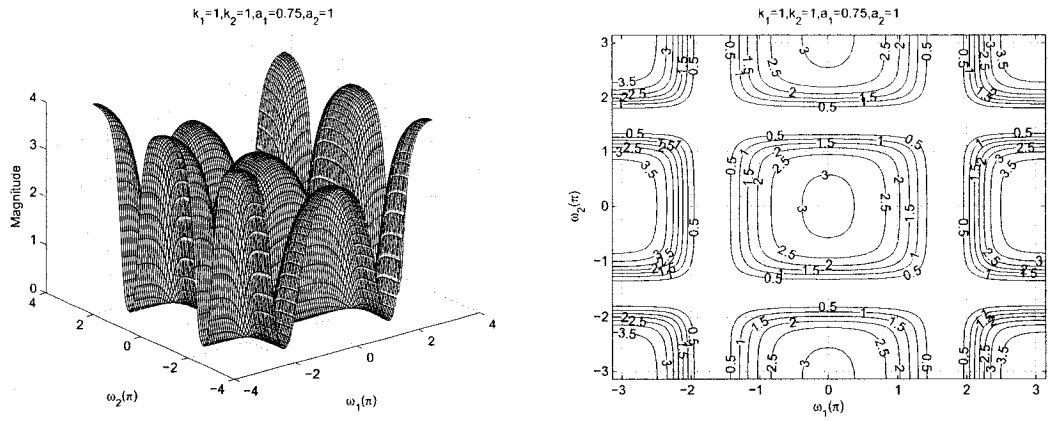

(a) $a_1 = 0.75$

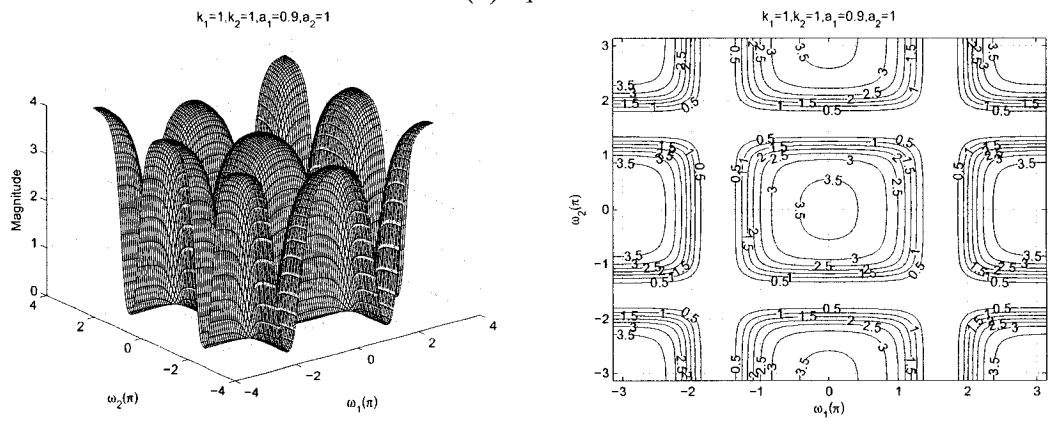

(b) $a_1 = 0.9$

Figure 5.28: 3-D amplitude frequency response and the contour of the All-pole 2-D digital bandstop filter for different values of a_1

By varying the value of a_1, the 3-D magnitude response and contour plots which represents different values of a_1, i.e. $a_1 = 0.1$, $a_1 = 0.25$, $a_1 = 0.5$, $a_1 = 0.75$, and $a_1 = 0.9$ are shown in the Figures 5.27 and 5.28. By making the value of $a_1 = 1$, it resembles the standard all-pole 2-D digital bandstop filter as shown in the Figure 5.22. It is observed from the diagrams that the coefficient a_1 affects the gain of the amplitude-frequency response. At the lowest value of $a_1 = 0.1$, the gain of the amplitude-frequency response of the lower passband is 1.5. As the value of a_1 increases, the gain increases and reach the maximum value at $a_1 = 1$. As seen from the diagrams, that as we increase the value of a_1 from 0.1 to 0.9, the gain of the amplitude-frequency response of the lower passband increases from 1.5 to 3.5 along the $\omega_1 - axis$. At the same time the gain of the amplitude-frequency response

of the upper passband remains constant. It is also observed that the cut-off frequency of lower passband decreases and that of upper passband increases along $\omega_1 - axis$. It is also evident from the Figures 5.27 and 5.28 that the coefficient a_1 does not have any effect along the $\omega_2 - axis$. When the value of $a_1 < 0.25$, there is rounding of the contour edges and the transition band of the all-pole 2-D digital bandstop filter cannot be clearly defined as shown in the Figure 5.27 (a). This is because the outer contour of the lower passband merges with the inner contour of the upper passband of the all-pole 2-D digital bandstop filter.

5.3.2.4 Frequency Response of 2-D Digital band-Stop Filter with different values of a_2

In the Section 5.3.2.3, the effect of the coefficient of a_1 was studied. In this section, the effect of the coefficient a_2 will be studied. The stable range of a_2 can be obtained with other specified coefficients of the generalized bilinear transformation. There are many combinations possible for the coefficients. To study the response with different values of a_2 properly, we fix other coefficients values to be equal to unity. The range of a_2 varies from 0.1 to 1 and the other coefficient values are specified as unity, i.e., $k_1 = 1$, $k_2 = 1$, $a_1 = 1$, $b_1 = 1$ and $b_2 = 1$.

By varying the value of a_2, the 3-D magnitude response and contour plots which represents different values of a_2, i.e., $a_2 = 0.1$, $a_2 = 0.25$, $a_2 = 0.5$, $a_2 = 0.75$, and $a_2 = 0.9$ are shown in the Figures 5.29 and 5.30. By making the value of $a_2 = 1$, it resembles the standard all-pole 2-D digital bandstop filter as shown in the Figure 5.22. It is observed from the diagrams that the coefficient a_2 affects the gain of the amplitude-frequency response. At the lowest value of $a_2 = 0.1$, the gain of the amplitude-frequency response of the lower passband is 1.5. As the value of a_2 increases, the gain increases and reach the maximum value at $a_2 = 1$. As seen from the diagrams, that as we increase the value of a_2 from 0.1 to 0.9, the gain of the amplitude-frequency response of the lower passband increases from 1.5

to 3.5 along the $\omega_2 - axis$. At the same time the gain of the amplitude-frequency response of the upper passband remains constant. It is also observed that the cut-off frequency of lower passband increases along $\omega_2 - axis$. It is also evident from the Figures 5.29 and 5.30 that the coefficient a_2 does not have any effect along the $\omega_1 - axis$. When the value of $a_2 < 0.25$, there is rounding of the contour edges and the transition band of the all-pole 2-D digital bandstop filter cannot be clearly defined as shown in the Figure 5.29 (a). This is because the outer contour of the lower passband merges with the inner contour of the upper passband of the all-pole 2-D digital bandstop filter.

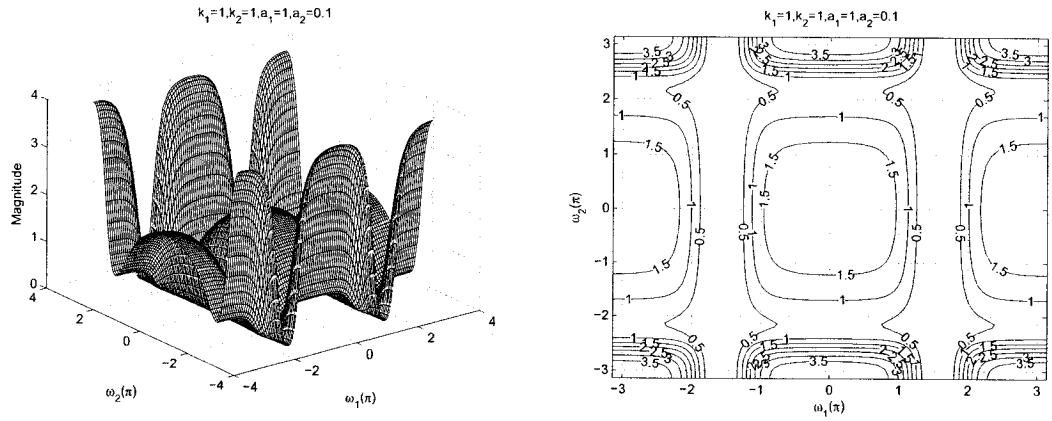

(a) $a_2 = 0.1$

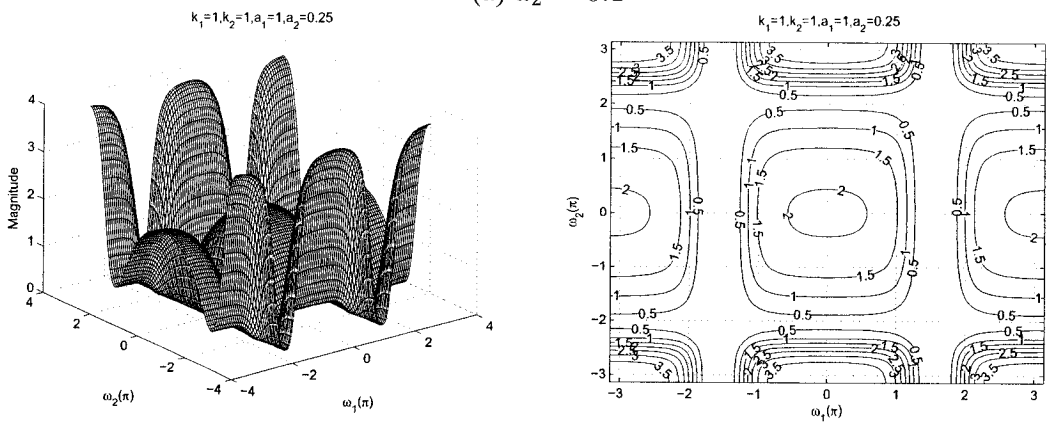

(b) $a_2 = 0.25$

Figure 5.29: 3-D amplitude frequency response and the contour of the All-pole 2-D digital bandstop filter for different values of a_2

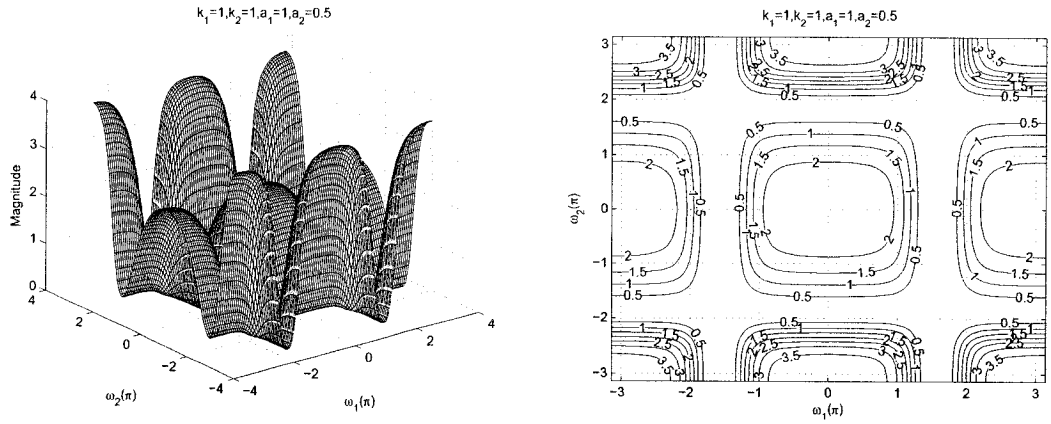

(a) $a_2 = 0.5$

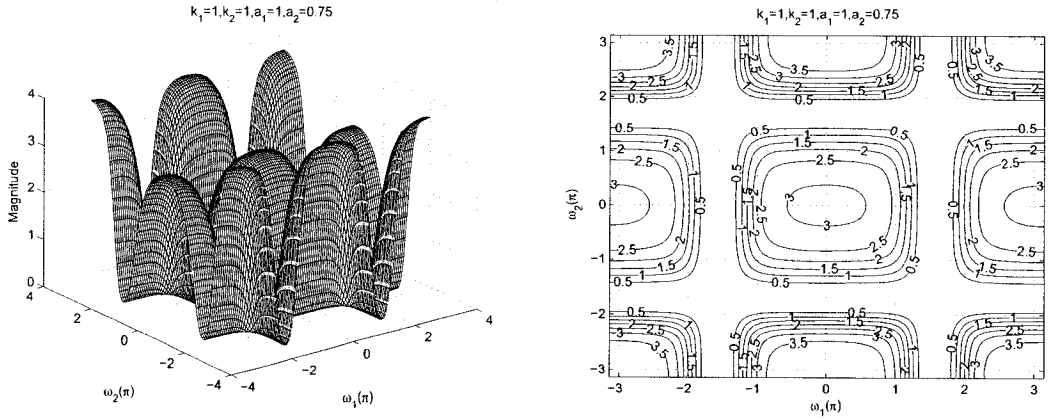

(b) $a_2 = 0.75$

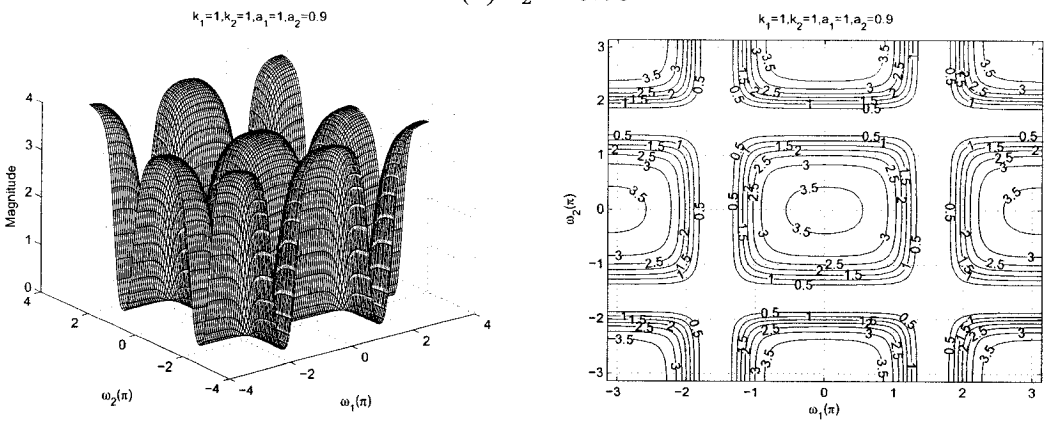

(c) $a_2 = 0.9$

Figure 5.30: 3-D amplitude frequency response and the contour of the All-pole 2-D digital bandstop filter for different values of a_2

5.3.2.5 Frequency Response of the All-pole 2-D Digital Bandstop Filter with same values of a_1 and a_2 and same values of k_1 and k_2

In the Sections 5.3.2.1 to 5.3.2.4 the individual effect of the coefficients a_1, a_2, k_1 and k_2 were studied. In this section, we will study the effect of coefficients, where $a_1 = a_2$ and $k_1 = k_2$ and the remaining coefficients b_1 and b_2 are considered to be unity for the all-pole 2-D digital bandstop filter in Category B. The values of a_1 and a_2 ranges from 0 to 0.75 and the values of k_1 and k_2 ranges from 0 to 2.

As observed from the Figures 5.31 to 5.33, the coefficients k_1 and k_2 affect the passband width of the frequency response. In the Figures 5.31 (a) and 5.32 (a), there is an increase in the stopband width of the contour response, the cut-off frequency of the lower passband decreases and that of the upper passband increases as the values of k_1 and k_2 are increased from 0.5 to 1 for the same values of $a_1 = a_2 = 0.25$. In addition, the magnitude of the lower passband decreases for the same. It is observed from the Figure 5.33 (a), that when the values of $k_1 = k_2 > 1$ there is a rounding of the contour edges and the transition band of the all-pole 2-D digital bandstop filter cannot be clearly defined for the same values of $a_1 = a_2 = 0.25$. This is because the outer contour of the lower passband overlaps with the inner contour of the upper passband of the all-pole 2-D digital bandstop filter. Thus, the transition band is clearly visible for lower values of k_1 and k_2 as shown in Figures 5.31 (a) and 5.32 (a).

As observed from the Figures 5.31 to 5.33, the coefficients a_1 and a_2 affect the gain of the amplitude-frequency response. It can be clearly observed from the Figures 5.31 (a), (b) and (c), that the gain of the lower passband increases from 1.5 to 3 and that of the upper passband increases from 3 to 3.5 when the values of a_1 and a_2 are increased from 0.25 to 0.75 keeping the same values of $k_1 = k_2 = 0.5$. Also the width of the lower passband decreases for the same.

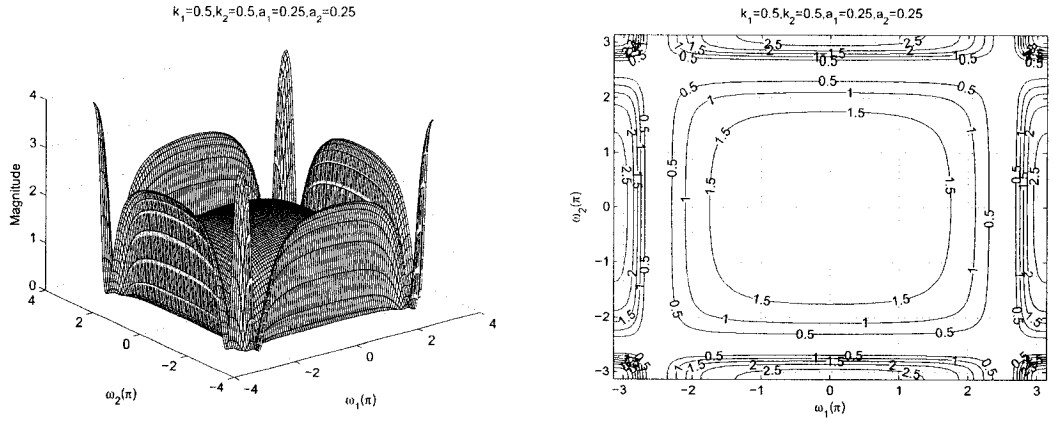

(a) $a_1 = a_2 = 0.25$ and $k_1 = k_2 = 0.5$

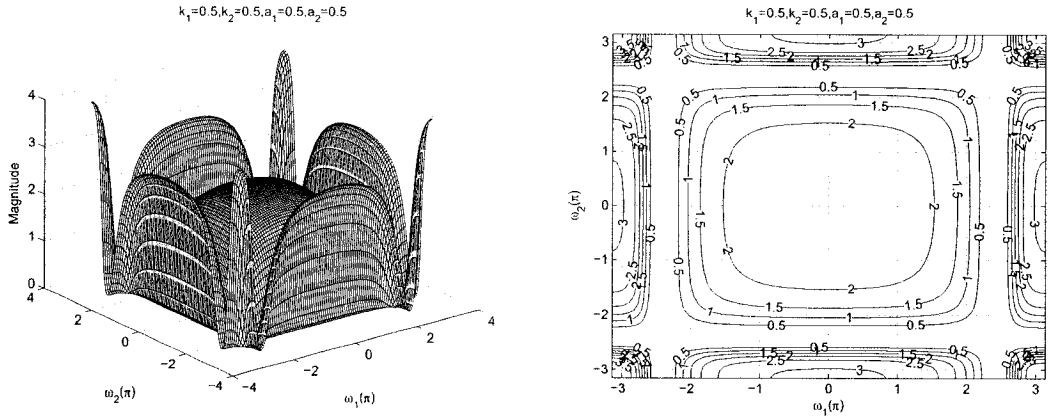

(b) $a_1 = a_2 = 0.5$ and $k_1 = k_2 = 0.5$

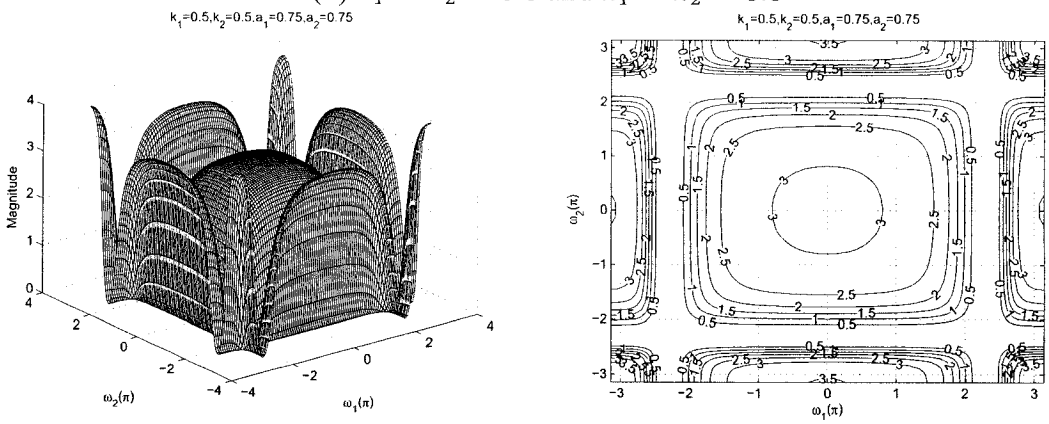

(c) $a_1 = a_2 = 0.75$ and $k_1 = k_2 = 0.5$

Figure 5.31: 3-D amplitude frequency response and the contour response of the All-pole 2-D digital bandstop filter for $a_1 = a_2$ and $k_1 = k_2$

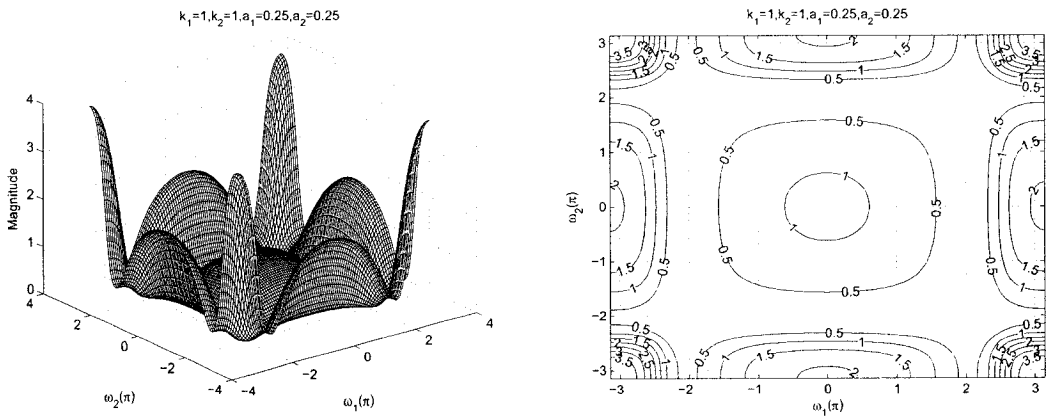

(a) $a_1 = a_2 = 0.25$ and $k_1 = k_2 = 1$

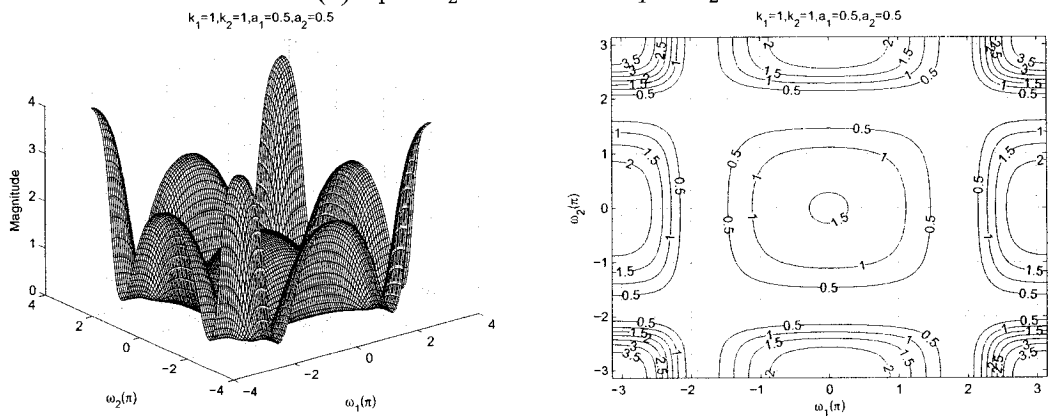

(b) $a_1 = a_2 = 0.5$ and $k_1 = k_2 = 1$

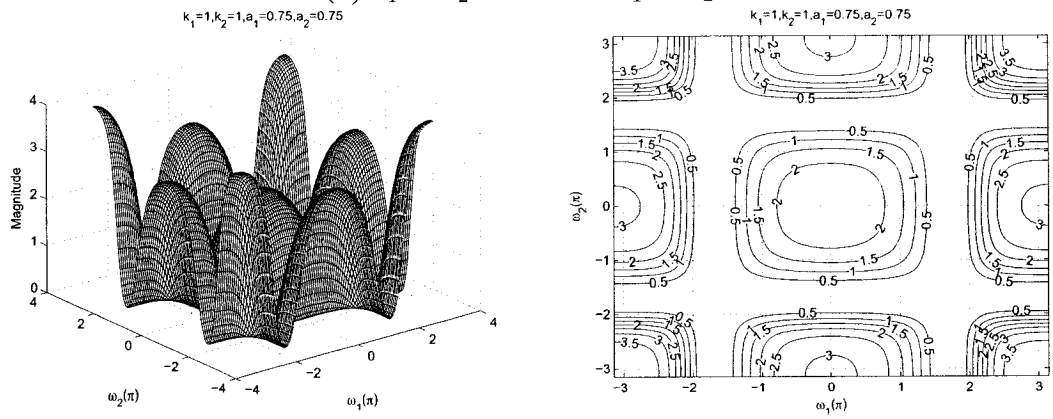

(c) $a_1 = a_2 = 0.75$ and $k_1 = k_2 = 1$

Figure 5.32: 3-D amplitude frequency response and the contour response of the All-pole 2-D digital bandstop filter for $a_1 = a_2$ and $k_1 = k_2$

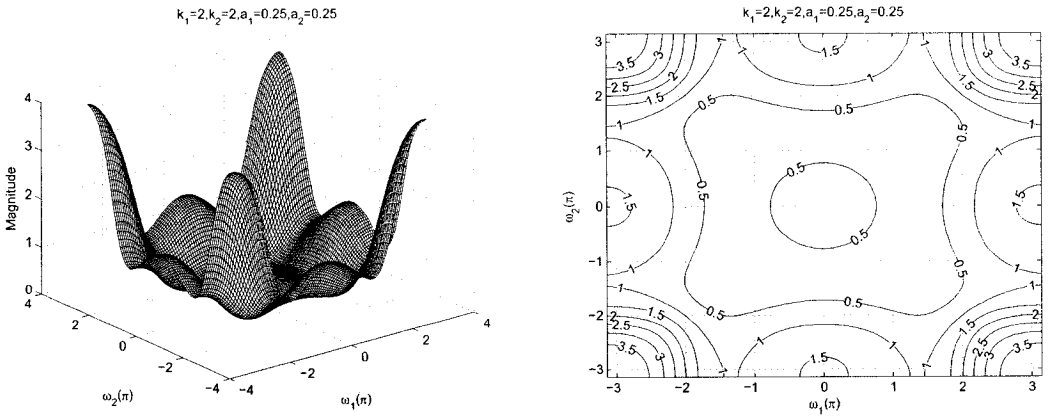

(a) $a_1 = a_2 = 0.25$ and $k_1 = k_2 = 2$

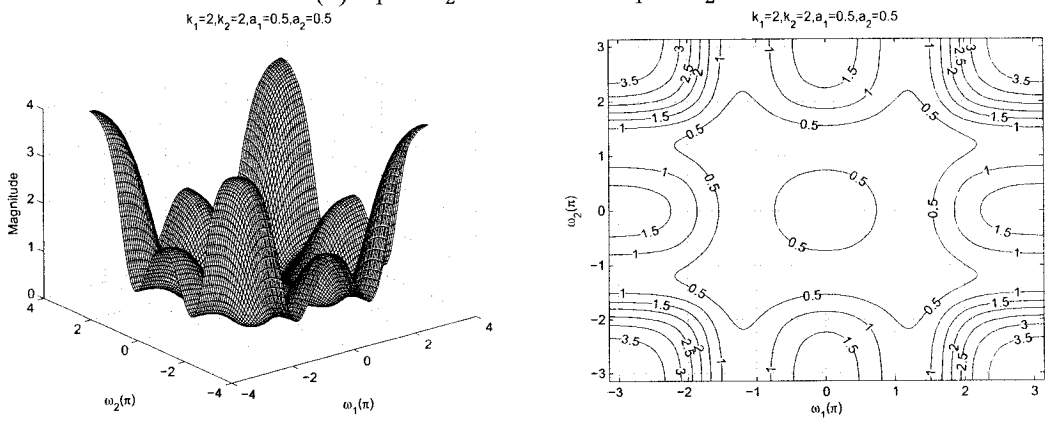

(b) $a_1 = a_2 = 0.5$ and $k_1 = k_2 = 2$

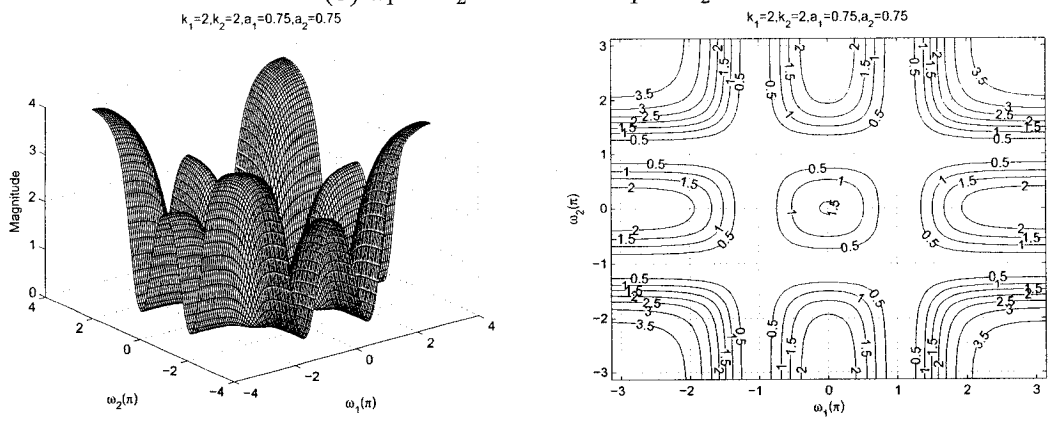

(c) $a_1 = a_2 = 0.75$ and $k_1 = k_2 = 2$

Figure 5.33: 3-D amplitude frequency response and the contour response of the All-pole 2-D digital bandstop filter for $a_1 = a_2$ and $k_1 = k_2$

5.3.2.6 Frequency Response of the All-pole 2-D Digital Bandstop Filter with different values of a_1 and a_2 and same values of k_1 and k_2

In this section, we will study the effect of coefficients, where $a_1 \neq a_2$ and $k_1 = k_2$ and the remaining coefficients b_1 and b_2 are considered to be unity for the all-pole 2-D digital bandstop filter in Category B. The values of a_1 and a_2 ranges from 0.25 to 0.5 and 0.5 to 0.75, respectively and the values of k_1 and k_2 ranges from 0.5 to 2.

As observed from the Figures 5.34 to 5.36, the coefficients k_1 and k_2 affect the passband width of the frequency response. In the Figures 5.34 (a) and 5.35 (a), there is an increase in the stopband width of the contour response, the cut-off frequency of the lower passband decreases and that of the upper passband increases as the values of k_1 and k_2 are increased from 0.5 to 0.9 for the same values of $a_1 = 0.25$ and $a_2 = 0.5$. In addition, the magnitude of the lower passband decreases for the same. It is observed from the Figures 5.36 (a), that when the values of $k_1 = k_2 > 1$ there is a rounding of the contour edges and the transition band of the all-pole 2-D digital bandstop filter cannot be clearly defined for the same values $a_1 = 0.25$ and $a_2 = 0.5$. This is because the outer contour of the lower passband overlaps with the inner contour of the upper passband of the all-pole 2-D digital bandstop filter. The transition band of the all-pole 2-D digital bandstop filter is visible for lower values of k_1 and k_2 as shown in the Figures 5.34 and 5.35.

As observed from the Figures 5.34 to 5.36, the coefficients a_1 and a_2 affect the gain of the amplitude-frequency response. It can be clearly observed from the Figures 5.34 (a), (b), and (c), that the gain of the lower passband increases from 2.0 to 2.5 and that of the upper passband increases from 2.5 to 3 when the values of a_1 are increased from 0.25 to 0.5 and and a_2 is increased from 0.5 to 0.75, keeping the same value of $k_1 = k_2 = 0.5$. Also the width of the passband increases and decreases periodically for different values of a_1 and a_2 for the same.

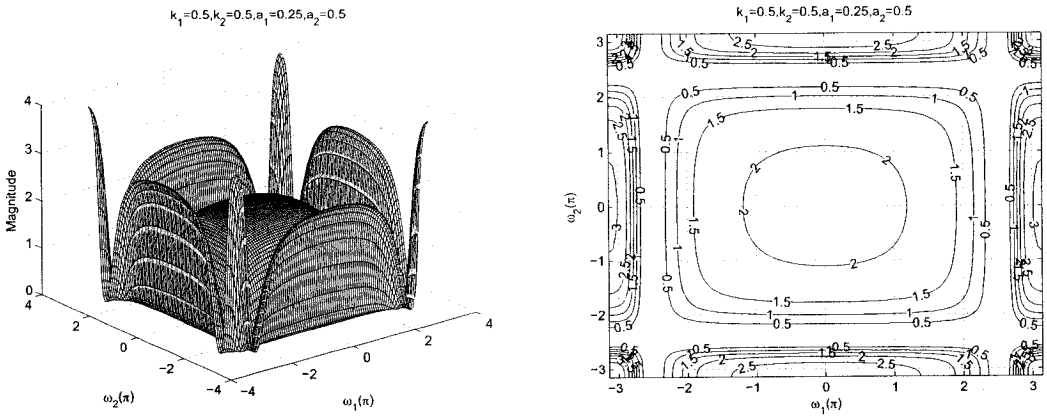

(a) $a_1 = 0.25,\ a_2 = 0.5$ and $k_1 = k_2 = 0.5$

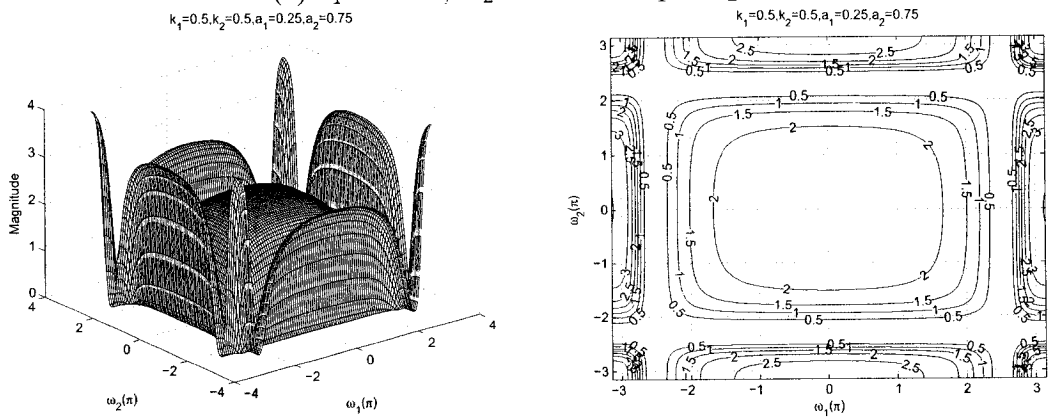

(b) $a_1 = 0.25,\ a_2 = 0.75$ and $k_1 = k_2 = 0.5$

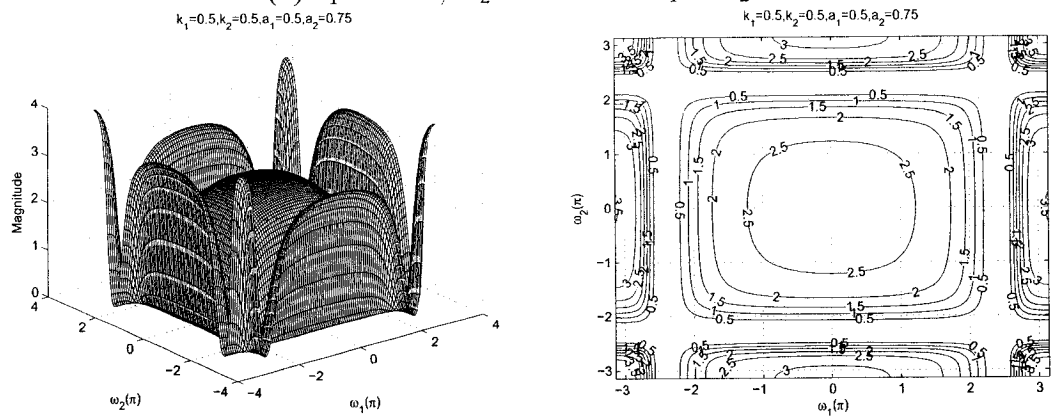

(c) $a_1 = 0.5,\ a_2 = 0.75$ and $k_1 = k_2 = 0.5$

Figure 5.34: 3-D amplitude frequency response and the contour response of the All-pole 2-D digital bandstop filter for $a_1 \neq a_2$ and $k_1 = k_2$

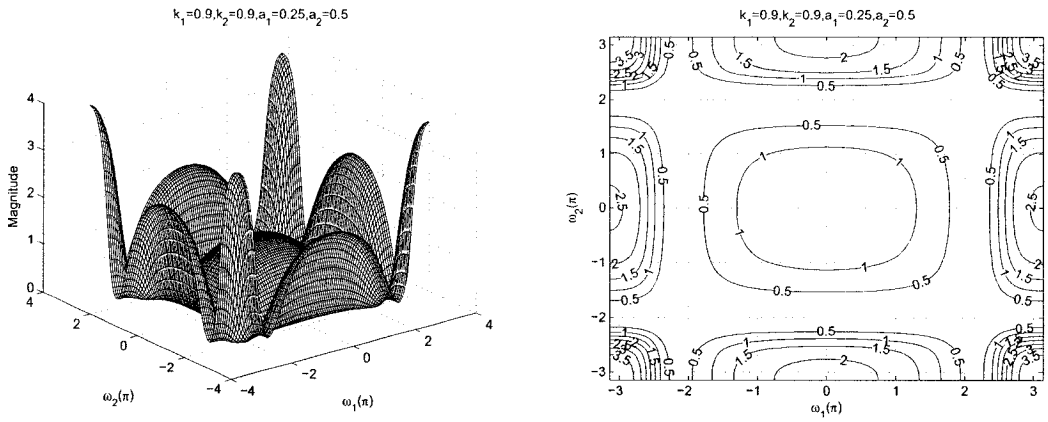

(a) $a_1 = 0.25,\ a_2 = 0.5$ and $k_1 = k_2 = 0.9$

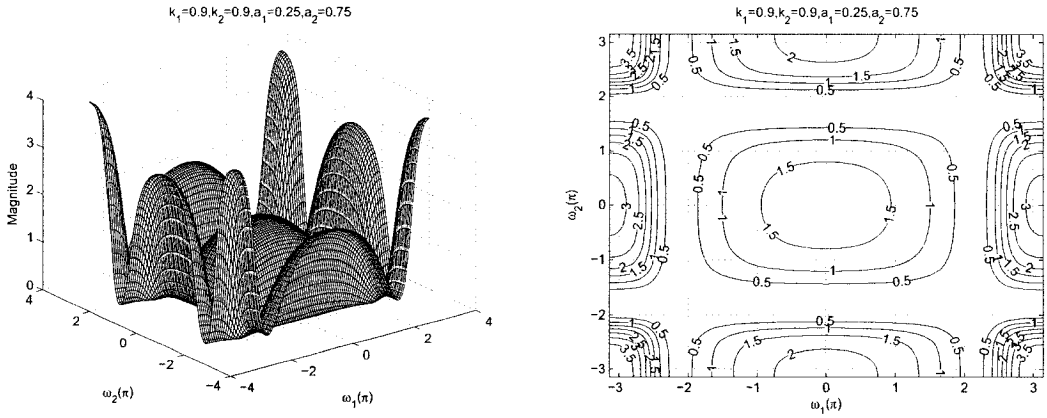

(b) $a_1 = 0.25,\ a_2 = 0.75$ and $k_1 = k_2 = 0.9$

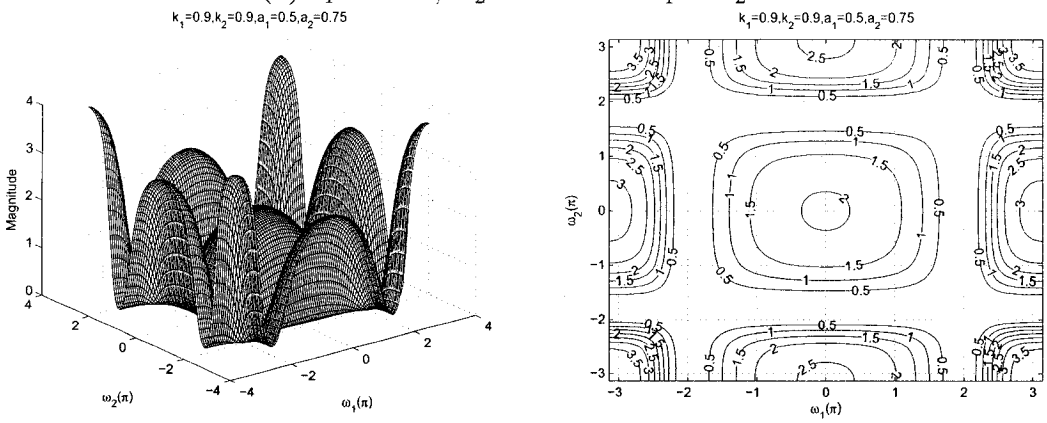

(c) $a_1 = 0.5,\ a_2 = 0.75$ and $k_1 = k_2 = 0.9$

Figure 5.35: 3-D amplitude frequency response and the contour response of the All-pole 2-D digital bandstop filter for $a_1 \neq a_2$ and $k_1 = k_2$

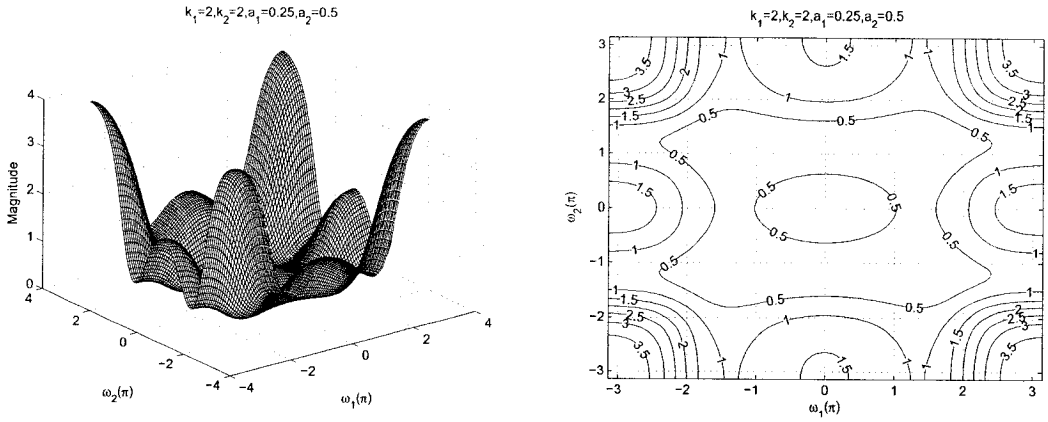

(a) $a_1 = 0.25,\ a_2 = 0.5$ and $k_1 = k_2 = 2$

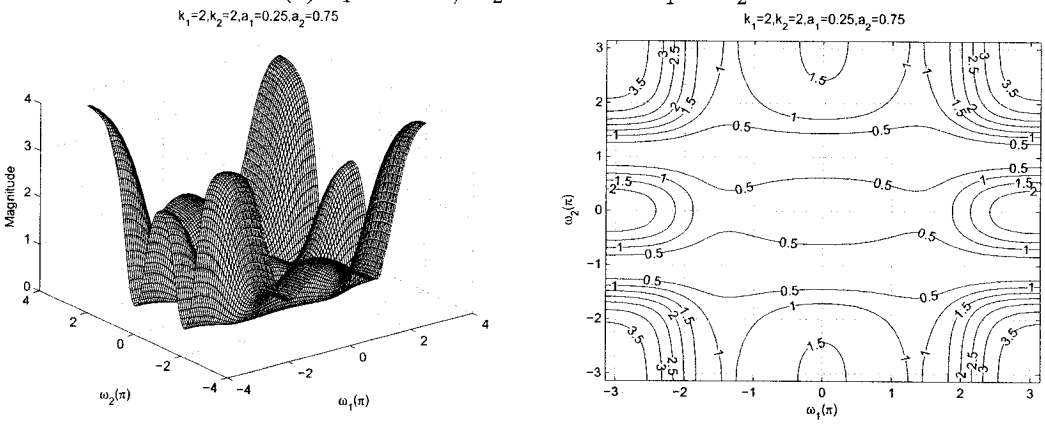

(b) $a_1 = 0.25,\ a_2 = 0.75$ and $k_1 = k_2 = 2$

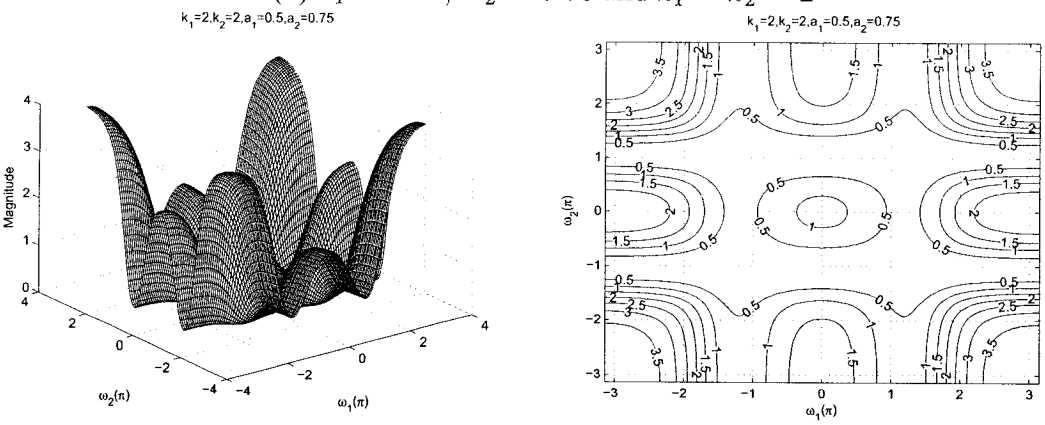

(c) $a_1 = 0.5,\ a_2 = 0.75$ and $k_1 = k_2 = 2$

Figure 5.36: 3-D amplitude frequency response and the contour response of the All-pole 2-D digital bandstop filter for $a_1 \neq a_2$ and $k_1 = k_2$

5.3.2.7 Frequency Response of the All-pole 2-D Digital Bandstop Filter with different values of a_1 and a_2 and different values of k_1 and k_2

In this section, we study the effect of coefficients when $a_1 \neq a_2$ and $k_1 \neq k_2$, and the remaining coefficients b_1 and b_2 are considered to be unity for the all-pole 2-D digital bandstop filter in Category B. The values of a_1 and a_2 vary from 0.25 to 0.75 and 0.5 to 0.9, respectively and the values of k_1 and k_2 vary from 0.25 to 2 and 0.5 to 5, respectively.

As observed from the Figures 5.37 to 5.39, the coefficients k_1 and k_2 affect the passband width of the frequency response. In the Figures 5.37 (a) and (b), there is an increase in the stopband width of the contour response, the cut-off frequency of the lower passband decreases and that of the upper passband increases as the values of k_1 is increased from 0.25 to 0.5 and k_2 is increased from 0.5 to 1 for the same values of $a_1 = 0.25$ and $a_2 = 0.5$. In addition, the magnitude of the passband decreases for the same. It is observed from the Figures 5.37 (c), that when the values of $k_1 = k_2 > 1$ there is a rounding of the contour edges and the transition band of the all-pole 2-D digital bandstop filter cannot be clearly defined for the same values $a_1 = 0.25$ and $a_2 = 0.5$. This is because the outer contour of the lower passband overlaps with the inner contour of the upper passband of the all-pole 2-D digital bandstop filter. The transition band of the all-pole 2-D digital bandstop filter is visible for lower values of k_1 and k_2 as shown in the Figures 5.37 (a) and (b).

As observed from the Figures 5.37 to 5.39, the coefficients a_1 and a_2 affect the gain of the amplitude-frequency response. It can be clearly observed from the Figures 5.37 (a), 5.38 (a) and 5.39 (a), that the gain of the lower passband increases from 2.5 to 3.5 and that of the upper passband increases from 3 to 3.5 when the values of a_1 are increased from 0.25 to 0.75 and and a_2 is increased from 0.5 to 0.9, keeping the same value of $k_1 = 0.25$ and $k_2 = 0.5$. Also the width of the passband increases and decreases periodically for the same.

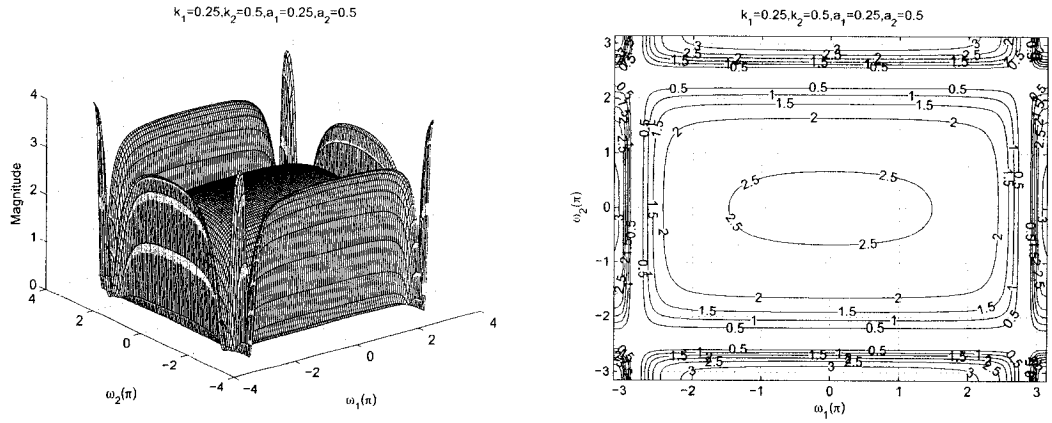

(a) $a_1 = 0.25,\ a_2 = 0.5$ and $k_1 = 0.25,\ k_2 = 0.5$

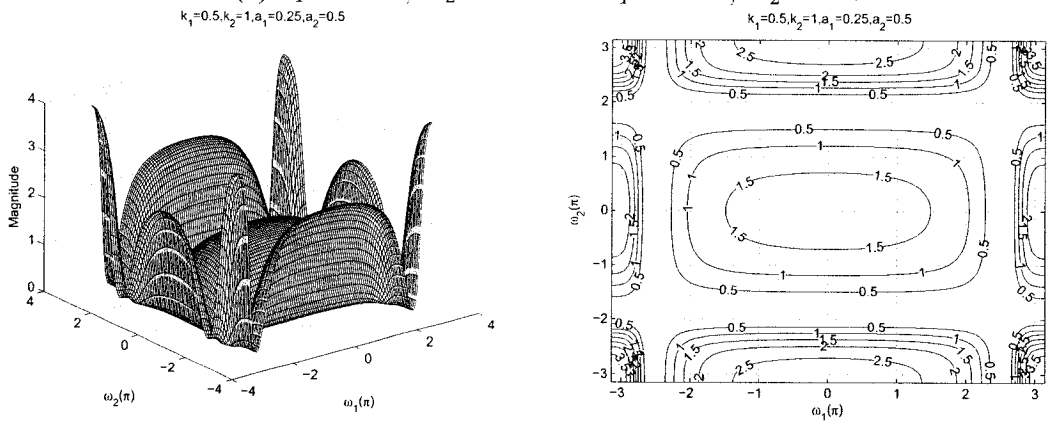

(b) $a_1 = 0.25,\ a_2 = 0.5$ and $k_1 = 0.5,\ k_2 = 1$

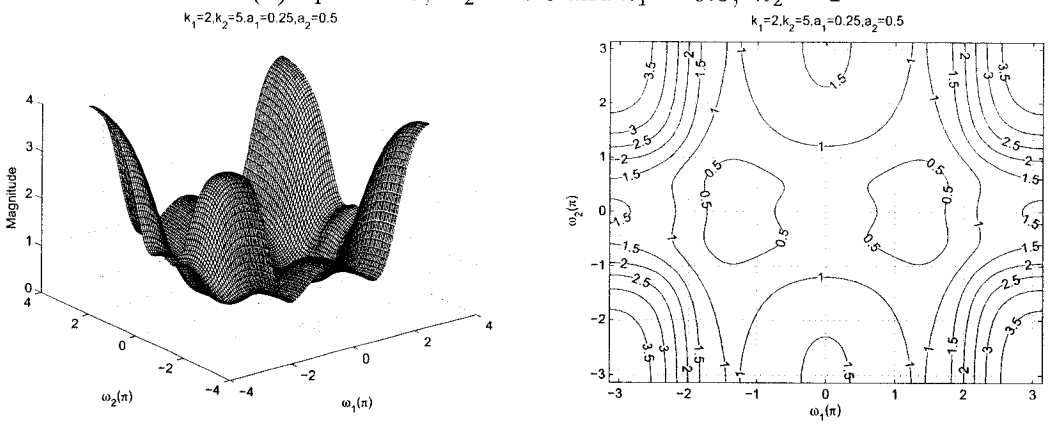

(c) $a_1 = 0.25,\ a_2 = 0.5$ and $k_1 = 2,\ k_2 = 5$

Figure 5.37: 3-D amplitude frequency response and the contour response of the All-pole 2-D digital bandstop filter for $a_1 \neq a_2$ and $k_1 \neq k_2$

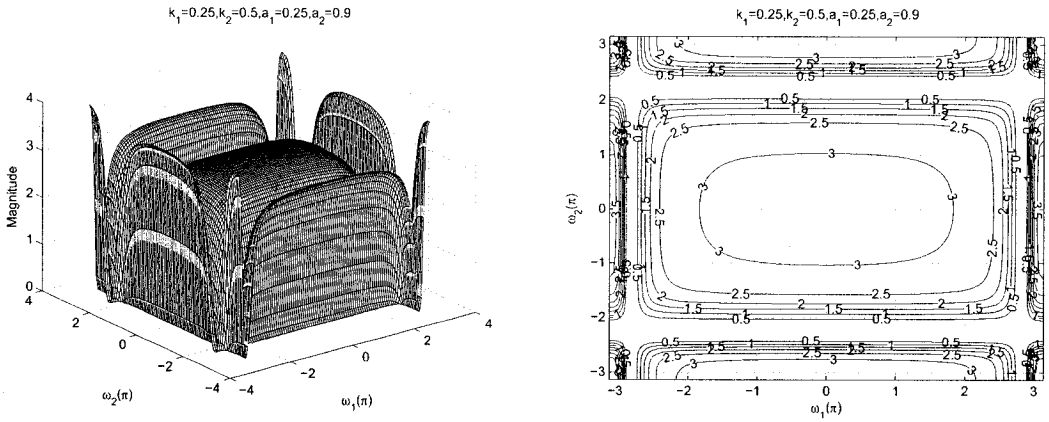

(a) $a_1 = 0.25,\ a_2 = 0.9$ and $k_1 = 0.25,\ k_2 = 0.5$

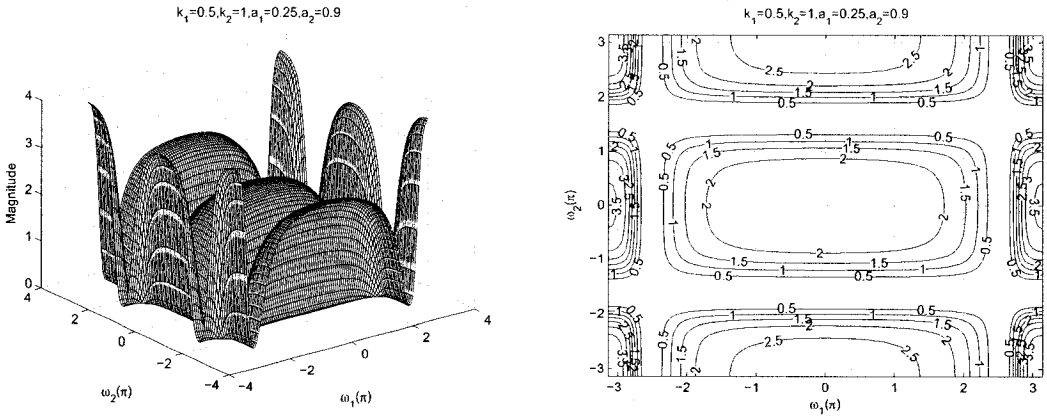

(b) $a_1 = 0.25,\ a_2 = 0.9$ and $k_1 = 0.5,\ k_2 = 1$

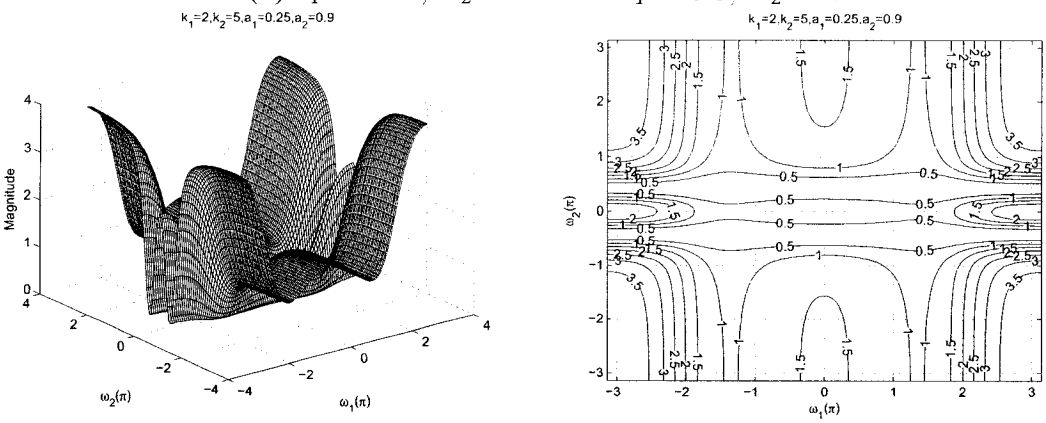

(c) $a_1 = 0.25,\ a_2 = 0.9$ and $k_1 = 2,\ k_2 = 5$

Figure 5.38: 3-D amplitude frequency response and the contour response of the All-pole 2-D digital bandstop filter for $a_1 \neq a_2$ and $k_1 \neq k_2$

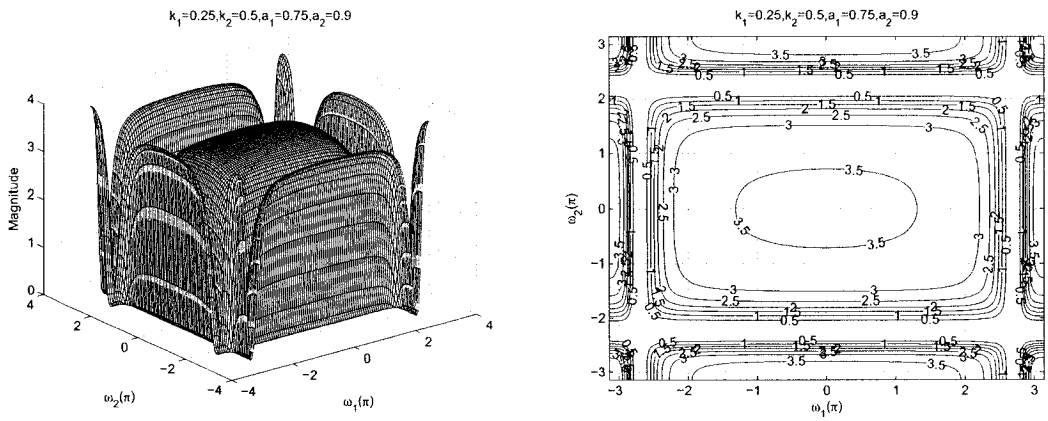

(a) $a_1 = 0.75,\ a_2 = 0.9$ and $k_1 = 0.25,\ k_2 = 0.5$

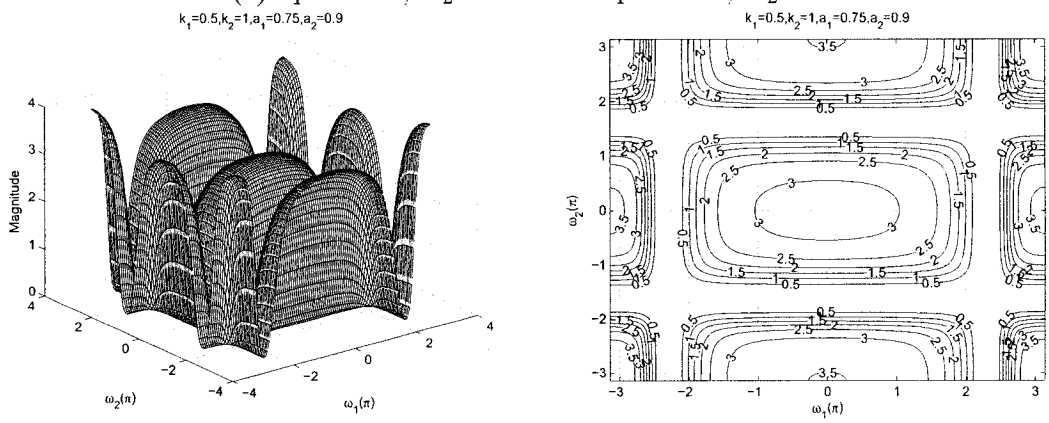

(b) $a_1 = 0.75,\ a_2 = 0.9$ and $k_1 = 0.5,\ k_2 = 1$

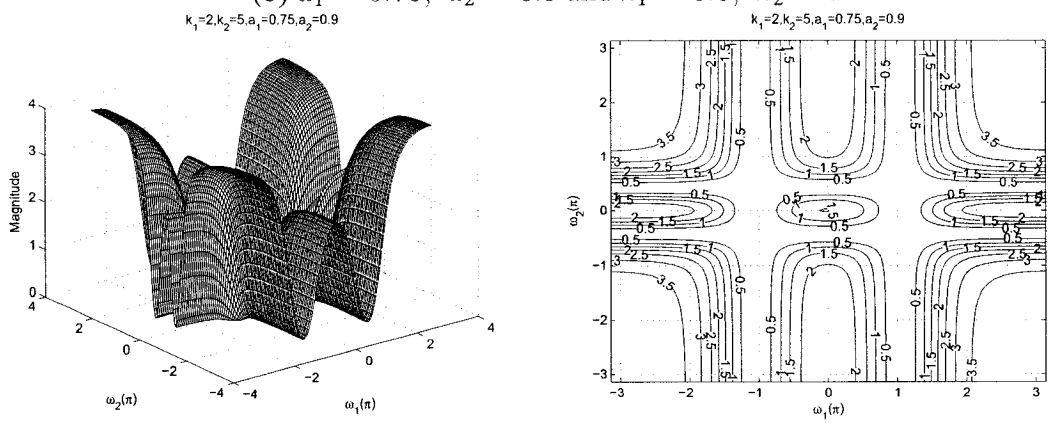

(c) $a_1 = 0.75,\ a_2 = 0.9$ and $k_1 = 2,\ k_2 = 5$

Figure 5.39: 3-D amplitude frequency response and the contour response of the All-pole 2-D digital bandstop filter for $a_1 \neq a_2$ and $k_1 \neq k_2$

5.3.2.8 Frequency Response of the All-pole 2-D Digital Bandstop Filter with same values of a_1 and a_2 and different values of k_1 and k_2

In this section, we study the effect of coefficients, where $a_1 = a_2$ and $k_1 \neq k_2$ and the remaining coefficients b_1 and b_2 are considered to be unity for the all-pole 2-D digital bandstop filter in Category B. The values of a_1 and a_2 vary from 0.25 to 0.75 and the values of k_1 and k_2 vary from 0.25 to 2 and 0.5 to 5, respectively.

As observed from the Figures 5.40 to 5.42, the coefficients k_1 and k_2 affect the passband width of the frequency response. In the Figures 5.40 (a) and (b), there is an increase in the stopband width of the contour response, the cut-off frequency of the lower passband decreases and that of the upper passband increases as the values of k_1 is increased from 0.5 to 2 and k_2 is increased from 0.5 to 1 for the same values of $a_1 = a_2 = 0.25$. In addition, the magnitude of the passband decreases for the same. It is observed from the Figure 5.40 (c), that when values of k_1 and k_2 are greater than 1, there is a rounding of the contour edges and the transition band of the all-pole 2-D digital band-stop filter cannot be clearly defined for the same values $a_1 = a_2 = 0.25$. This is because the outer contour of the lower passband overlaps with the inner contour of the upper passband of the all-pole 2-D digital band-stop filter. The transition band of the all-pole 2-D digital bandstop filter is visible for lower values of k_1 and k_2 as shown in the Figures 5.40 (a) and (b).

As observed from the Figures 5.40 to 5.42, the coefficients a_1 and a_2 affect the gain of the amplitude-frequency response. It can be clearly observed from the Figures 5.40 (a), 5.41 (a), and 5.42 (a), that the gain of the lower passband increases from 2 to 3 and that of the upper passband also increases from 3 to 3.5, when the values of a_1 and a_2 are increased from 0.25 to 0.75, keeping the same values of $k_1 = 0.25$ and $k_2 = 0.5$. Also the width of the passband decreases and increases periodically for for the same.

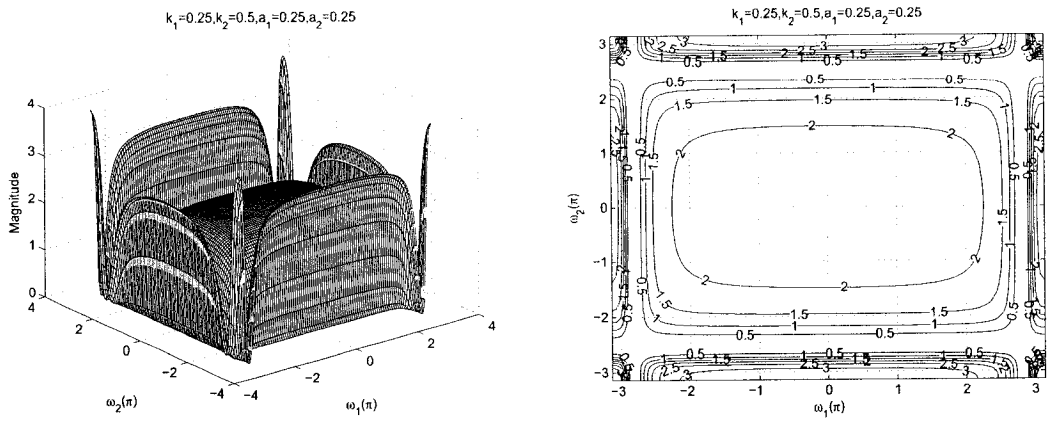

(a) $a_1 = a_2 = 0.25$ and $k_1 = 0.25,\ k_2 = 0.5$

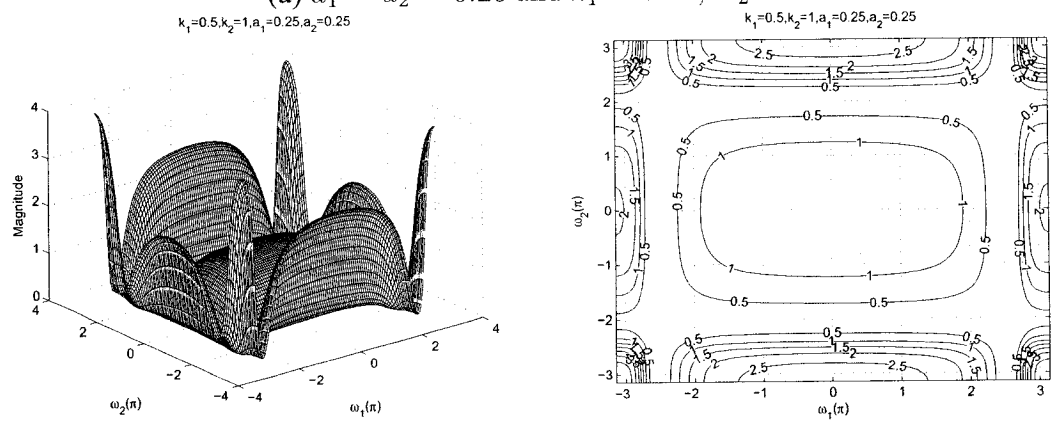

(b) $a_1 = a_2 = 0.25$ and $k_1 = 0.5,\ k_2 = 1$

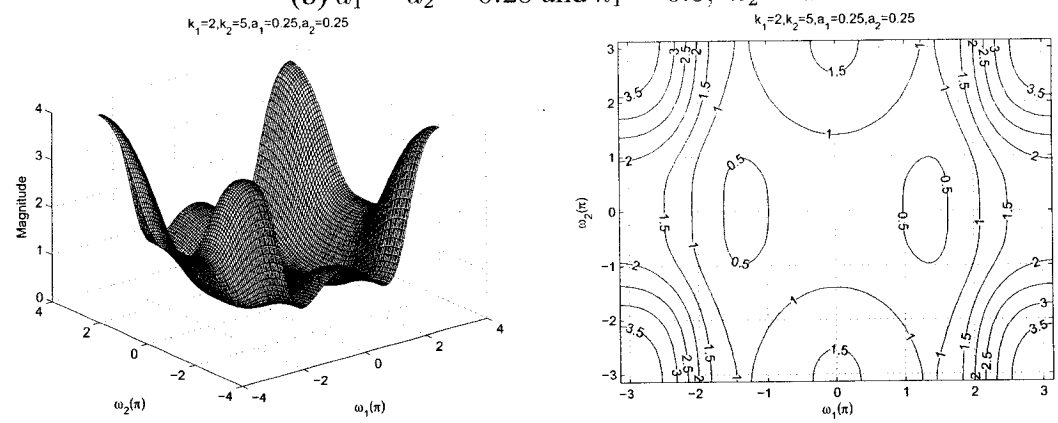

(c) $a_1 = a_2 = 0.25$ and $k_1 = 2,\ k_2 = 5$

Figure 5.40: 3-D amplitude frequency response and the contour response of the All-pole 2-D digital bandstop filter for $a_1 = a_2$ and $k_1 \neq k_2$

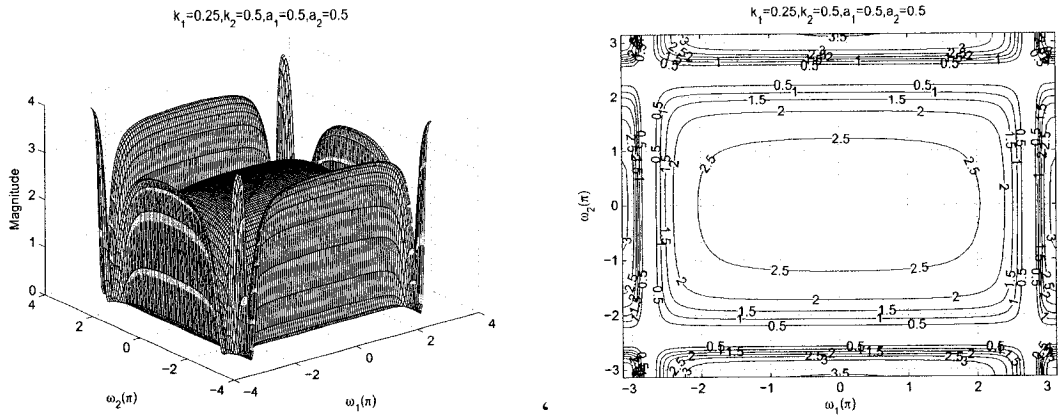

(a) $a_1 = a_2 = 0.5$ and $k_1 = 0.25,\ k_2 = 0.5$

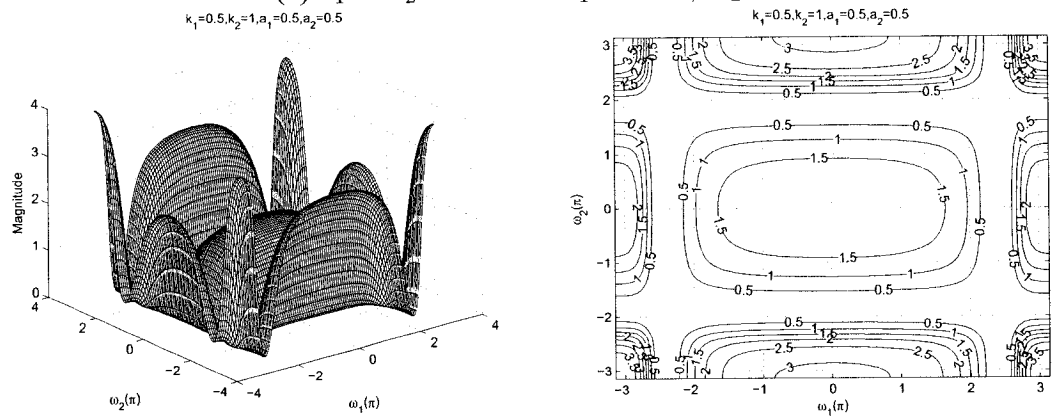

(b) $a_1 = a_2 = 0.5$ and $k_1 = 0.5,\ k_2 = 1$

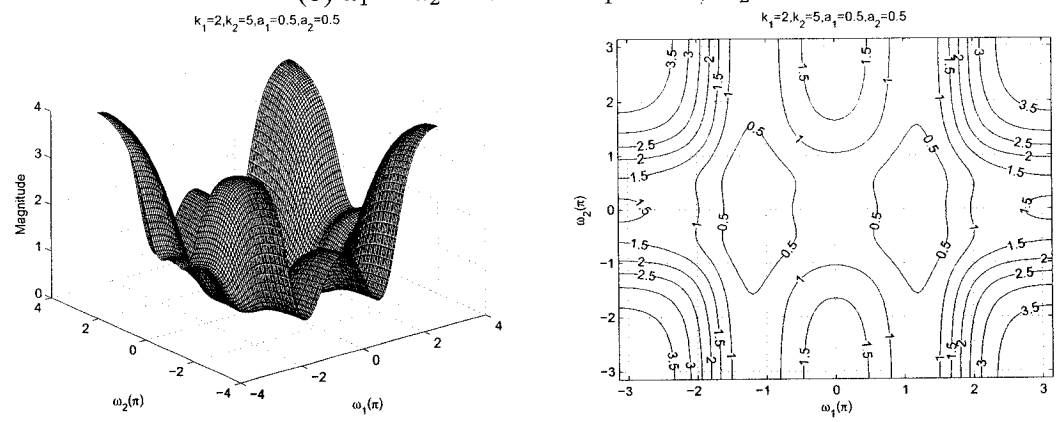

(c) $a_1 = a_2 = 0.5$ and $k_1 = 2,\ k_2 = 5$

Figure 5.41: 3-D amplitude frequency response and the contour response of the All-pole 2-D digital bandstop filter for $a_1 = a_2$ and $k_1 \neq k_2$

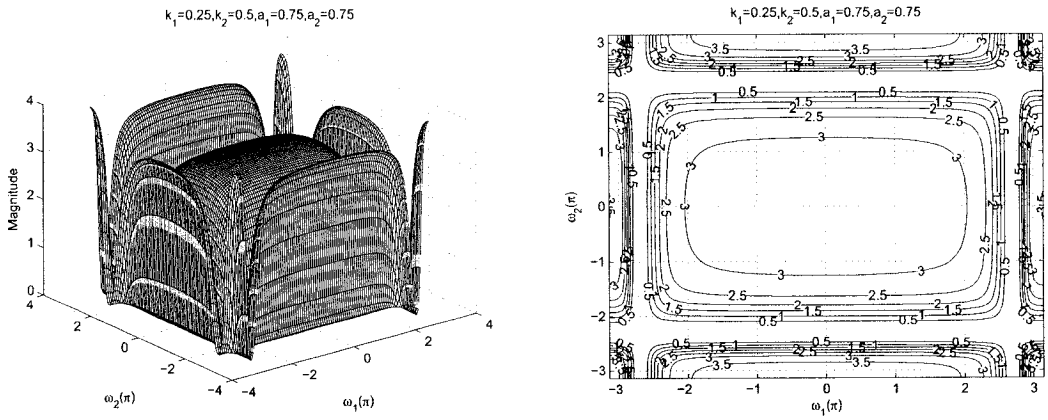

(a) $a_1 = a_2 = 0.75$ and $k_1 = 0.25,\ k_2 = 0.5$

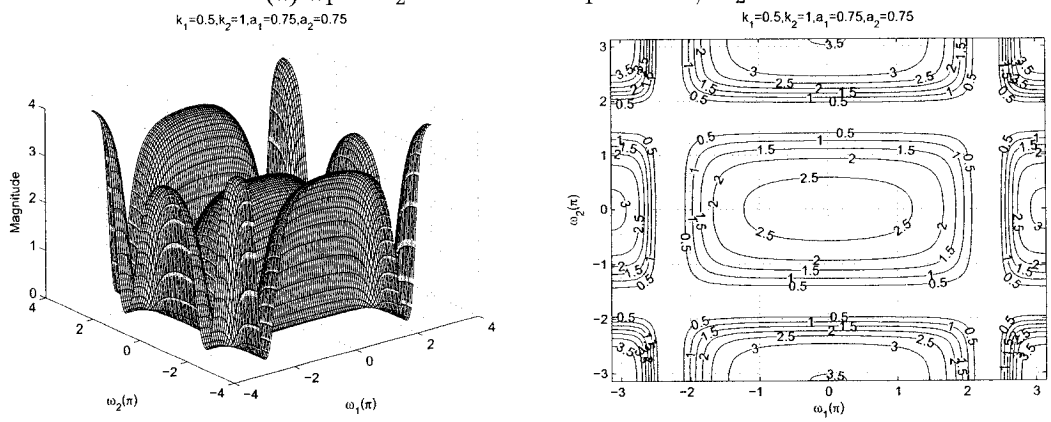

(b) $a_1 = a_2 = 0.75$ and $k_1 = 0.5,\ k_2 = 1$

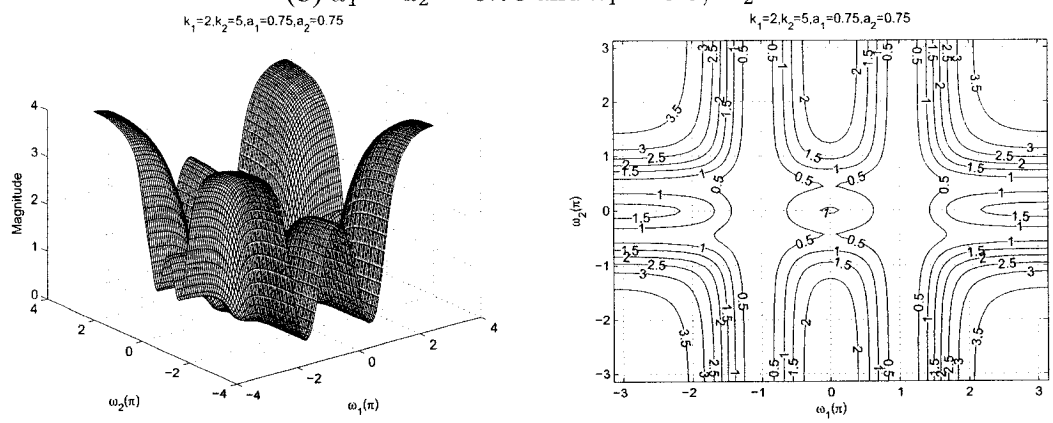

(c) $a_1 = a_2 = 0.75$ and $k_1 = 2,\ k_2 = 5$

Figure 5.42: 3-D amplitude frequency response and the contour response of the All-pole 2-D digital bandstop filter for $a_1 = a_2$ and $k_1 \neq k_2$

5.4 Summary

In this chapter, we have discussed the effect of the coefficients of the 2-D digital bandstop filter in Category A and Category B. The detailed analysis on each of the coefficient is discussed in Section 5.3.

The summary of the effect of the coefficients of the generalized bilinear transformation on 2-D digital bandstop filter in Category A are as follows.

On increasing the values of k_1 and k_2, as discussed in Sections 5.3.1.1 and 5.3.1.2 respectively, it is observed that when we increase the values of k_1 and k_2, it effects the passband width along the $\omega_1 - axis$ and $\omega_2 - axis$, respectively. When the values of $k_1$and k_2 are increased, the width of the stopband increases and decreases periodically, the width of the lower passband decreases and that of the upper passband increases. Also, the cut-off frequency of the lower passband decreases and that of the upper passband increases along the $\omega_1 - axis$ and $\omega_2 - axis$ and the amplitude of the contour response remains constant.

On increasing the values of a_1 and a_2, as discussed in Sections 5.3.1.3 and 5.3.1.4, respectively, it is observed that when we increase the values of a_1 and a_2 from 0.1 to 0.9, the magnitude of the lower passband increases from 1.5 to 3.5 along the $\omega_1 - axis$ and $\omega_2 - axis$, respectively. It is observed that cut-off frequency of the lower passband decreases and that of the upper passband increases as we increase the values of a_1 and a_2 respectively along the $\omega_1 - axis$ and $\omega_2 - axis$. Also the magnitude of the upper passband remains constant.

Sections 5.3.1.5 to 5.3.1.8 discuss the effect of the coefficients on the frequency response of the 2-D digital bandstop filter, viz. $a_1 = a_2$ and $k_1 = k_2$, $a_1 \neq a_2$ and $k_1 = k_2$, $a_1 \neq a_2$ and $k_1 \neq k_2$, and $a_1 = a_2$ and $k_1 \neq k_2$ respectively in Category A. It is observed in all the four cases that the coefficients k_1, k_2 affect the passband width and a_1, a_2 affect the gain of the amplitude-frequency response. As the values of k_1 and k_2 are increased, the cut-off frequency of the lower passband decreases and that of the upper passband increases and the width of the stopband increases. The magnitude of the passband decreases for the

the same. Also when the values of $k_1$and $k_2 > 1$, there is a rounding of the contours edges and the transition band of the 2-D digital bandstop filter cannot be clearly define. This is because the outer contour of the lower passband overlaps with the inner contour of the upper passband. The transition band is clearly visible for lower values of k_1 and k_2. As the values of a_1 and a_2 are increased, the gain of lower passband and the upper passband increases. Also, the width of the lower passband increases and decreases periodically for different combinations of a_1 and a_2.

The summary of the effect of the coefficients of the generalized bilinear transformation on the all-pole 2-D digital bandstop filter in Category B are as follows.

On increasing the values of k_1 and k_2, as discussed in Sections 5.3.2.1 and 5.3.2.2 respectively, it is observed that when we increase the values of k_1 and k_2, it effects the passband width along the $\omega_1 - axis$ and $\omega_2 - axis$, respectively. When the values of $k_1$and k_2 are increased, the width of the stopband increases and decreases periodically, the width of the lower passband decreases and that of the upper passband increases. Also, the cut-off frequency of the lower passband decreases and that of the upper passband increases along the $\omega_1 - axis$ and $\omega_2 - axis$ and the amplitude of the contour response remains constant.

On increasing the values of a_1 and a_2, as discussed in Sections 5.3.2.3 and 5.3.2.4, respectively, it is observed that when we increase the values of a_1 and a_2 from 0.25 to 0.9, the magnitude of the lower passband increases from 1.5 to 3.5 along the $\omega_1 - axis$ and $\omega_2 - axis$, respectively. It is observed that cut-off frequency of the lower passband decreases and that of the upper passband increases as we increase the values of a_1 and a_2 respectively along the $\omega_1 - axis$ and $\omega_2 - axis$. Also the magnitude of the upper passband remains constant. An important observation has been noted, when the values of a_1 and $a_2$are less than 0.25, there is rounding of the contour edges and the transition band of the all-pole 2-D digital bandstop filter cannot be clearly defined. This is because the outer contour of the lower passband overlaps with the inner contour of the upper passband.

Sections 5.3.2.5 to 5.3.2.8 discuss the effect of the coefficients on the frequency re-

sponse of the all-pole 2-D digital bandstop filter, viz. $a_1 = a_2$ and $k_1 = k_2$, $a_1 \neq a_2$ and $k_1 = k_2$, $a_1 \neq a_2$ and $k_1 \neq k_2$, and $a_1 = a_2$ and $k_1 \neq k_2$ respectively in Category B. It is observed in all the four cases that the coefficients k_1, k_2 affect the passband width and a_1, a_2 affect the gain of the amplitude-frequency response. As the values of k_1 and k_2 are increased, the cut-off frequency of the lower passband decreases and that of the upper passband increases and the width of the stopband increases. Also, the magnitude of the passband decreases. When the values of $k_1$and $k_2 > 1$, there is a rounding of the contours edges and the transition band of the all-pole 2-D digital bandstop filter cannot be clearly define. This is because the outer contour of the lower passband overlaps with the inner contour of the upper passband. The transition band is clearly visible for lower values of k_1 and k_2. As the values of a_1 and a_2 are increased, the gain of lower passband and the upper passband increases. Also, the width of the lower passband increases and decreases periodically for different combinations of a_1 and a_2.

The comparison of the amplitude-frequency response of the 2-D bandstop filter in Category A and the all-pole 2-D bandstop filter in Category B is as follows:

When the values of a_1 and a_2 is less than 0.25 in Category B, there is a rounding of the contour edges and hence the transition band of the all-pole 2-D digital bandstop filter is not visible where as in Category A the transition band of the 2-D digital band stop filter is visible. Also, the amplitude-frequency response for both the categories is almost same. This is because of the resulting transfer function for Category B is almost the same as the one used in Category A as the transfer function does not depend on the coefficients of the VSHP polynomial, it only depends on the coefficients of the generalized bilinear transformation.

Thus the effect of the various combinations of the coefficients of the generalized bilinear transformation on the proposed 2-D digital bandstop filters in Category A and Category B was analyzed and compared, and the selective 3-D magnitude and contour responses of the proposed 2-D digital bandstop filter and all-pole 2-D digital bandstop filter were plotted.

Chapter 6

An Application of 2-D Digital Filters in Image Processing

6.1 Introduction

The application of digital signal processing techniques in general, and that of digital filters in particular has expanded in many important areas such as speech signal processing, digital telephony and communications, facsimile and TV image processing, radar-sonar systems, biomedicine, space research and operative systems, geoscience, etc. Digital filters are widely applied to 1-D and multi-dimensional signals. The techniques used for 2-D systems can generally be extended to multi-dimensional systems. Examples of 2-D systems include image processing, seismic signal processing, meteorology, etc. This chapter discusses about the application of digital filters in digital images processing [50].

6.2 Digital Image Processing

The most common applications of the digital filters in image processing are in the areas of digital enhancement and restoration. To enhance images digitally, filters can be designed

to reduce noise by smoothing, emphasize some region of spectrum, sharpen edges, and implement other functions that produce improved images. Such improvement may be intended to provide a subjectively better image for humans to look at, or it may be intended as a preprocessor for higher level tasks, such as segmentation and pattern recognition or for machine vision. Digital restoration filters may be used to invert a degradation process. For example, the effect of known camera defocusing, or some other limitations, can be reduced or removed by developing a restoration model on it. Digital filters may also be applied in postprocessing after image coding, and in preprocessing before image segmentation [51].

An image may be defined as a 2-D function, $f(x, y)$, where x and y are spatial coordinates, and the amplitude of $f(x, y)$ at any pair of co-ordinates (x, y) is called the intensity or gray level of the image at that point [53]. When these values are all finite and discrete quantities, the image is called a digital image.

Fourier transforms are widely used in the field of image processing, where one commonly describes an image in terms of intensity values in a 2-D matrix. The 2-D digital filters can be applied in frequency domain for various standard applications, like image enhancement, image restoration, etc. [52, 53]. The 2-D Fourier transforms are effective tools for image processing. The 2-D Discrete Fourier Transform (DFT) of an image $f(x, y)$ of size M×N is given by,

$$F(\omega_1, \omega_2) = \frac{1}{MN} \sum_{x=0}^{M-1} \sum_{y=0}^{N-1} f(x, y) e^{-j2\pi((x\omega 1/M)+(y\omega_2/N))} \tag{6.1}$$

As in the 1-D case, this expression must be computed for values of $\omega_1 = 0, 1, 2, ..., M-1$ and also for $\omega_2 = 0, 1, 2, ..., N-1$. Similarly, for a given $F(\omega_1, \omega_2)$, we can obtain $f(x, y)$ with the 2-D Inverse Discrete Fourier Transform (IDFT), which is given by the expression

$$f(x, y) = \sum_{\omega_1=0}^{M-1} \sum_{\omega_2=0}^{N-1} F(\omega_1, \omega_2) e^{j2\pi((x\omega_1/M)+(y\omega_2/N))} \tag{6.2}$$

Also, one half of the convolution theorem for image, $f(x, y)$ and 2-D digital filter,

$h_d(x, y)$, with Fourier Transforms, $F(\omega_1, \omega_2)$ and $H_d(\omega_1, \omega_2)$, can be stated as

$$f(x, y) * h_d(x, y) \Leftrightarrow F(\omega_1, \omega_2) H_d(\omega_1, \omega_2) \tag{6.3}$$

In this chapter, we will show some examples in image processing by using standard images. In Sec. 6.3, we will study the effect of 2-D digital lowpass filtering for Category A and the all-pole 2-D lowpass filtering for Category B in image restoration, by applying it on images corrupted with known amount of noise. We will use white Gaussian noise and vary its variance to see the effect of filtering on images and discuss the results. In Sec. 6.4 summary, discussions and comparisons of the application presented in this chapter.

6.3 Application of 2-D Digital Lowpass Filters in Image Processing

Digital Filters are applied in image enhancement to try and improve the subjective appearance of images without attempting directly to invert the effect of any degradation. They may also be employed to enhance certain properties of the images and to suppress others [50]. The application of digital filters in image enhancement for three kind of applications such as a preprocessor to provide an improved image, as a noise reduction process and as a postprocessor to reduce the effects of noise introduced by some other form of processing.

The ultimate goal of noise reduction techniques is to improve an image in some predefined sense. The noise reduction techniques are oriented towards the modeling the degradation and applying the inverse process in order to recover the original image. The noise in digital images arises during image acquisition or image transmission. We degrade the image artificially by adding noise, which is assumed to be independent of spatial coordinates and uncorrelated with respect to the image itself, i.e., there is no correlation between the

pixel values of the image and the values of noise components [52, 53]. The lowpass filter in the spatial domain is equivalent to that of a smoothing filter as the lowpass filter blocks the high frequencies corresponding to sharp intensity changes, i.e., to the fine scale details and noise in the spatial domain image.

The original images are added with the Gaussian random noise with different noise levels, which are then input to the proposed 2-D digital lowpass filter in Category A with the transfer function given in eqn. (2.62) and all-pole 2-D digital lowpass filter in Category B with the transfer function given by eqn. (2.82). The probability density function (PDF) of a Gaussian random variable, z is given by

$$p(z) = \frac{1}{\sqrt{2\pi}\sigma} e^{-(z-\mu)^2/2\sigma^2} \tag{6.4}$$

where z represents gray level, μ is the mean of average values of z and σ is the standard deviation. σ^2 is called the variance of z. The Gaussian noise with zero mean, $n(x, y)$ is added to the image, $f(x, y)$ to get the noisy or degraded image, $f_d(x, y)$ which is given by,

$$f_d(x, y) = f(x, y) + n(x, y) \tag{6.5}$$

The 2-D low pass filter proposed in chapter 2 can be applied to reduce or remove the effect of the noise. Here we have used the 2-D lowpass filter obtained from the combination of all-pass filters, $H_d(\omega_1, \omega_2)$ with $z_1 = e^{j\omega_1}$ and $z_2 = e^{j\omega_2}$ which is proposed in chapter 2. There are two approaches to apply the proposed 2-D digital lowpass filter.

(a) By convolution of the 2-D lowpass filter, $h_d(x, y)$ with the noisy or degraded image $f_d(x, y)$ in the spatial domain, we expect to recover the image, $f_r(x, y)$.

$$f_r(x, y) = f_d(x, y) * h_d(x, y) \tag{6.6}$$

(b) By multiplication of the filter, $H_d(\omega_1, \omega_2)$ and the noisy and degraded image, $F_d(x, y) = DFT[f_d(x, y)]$ in the frequency domain, and then 2-D IDFT to get the filtered image.

$$f_r = IDFT[F_d(\omega_1, \omega_2).H_d(\omega_1, \omega_2)] \tag{6.7}$$

where the recovered image is close to the original image i.e. $f_r(x, y) \approx f(x, y)$.

There are various quality measures available in literature and those that correlate well with visual perception are quite complicated to compute. Most image processing systems are designed to minimize the mean square error (MSE), the quantitative measure between two images, $f_1(x, y)$ and $f_2(x, y)$, which is defined as

$$MSE = \frac{1}{MN} \sum_{x=0}^{M-1} \sum_{y=0}^{N-1} [f_1(x, y) - f_2(x, y)]^2 \tag{6.8}$$

where M×N is the image dimension and its product gives total number of pixels in the image. Instead of MSE, the peak signal-to-noise ratio (PSNR) in decibels (dB) is more often used as a quality measure. the PSNR is defined as

$$PSNR = 10 \log_{10} \frac{\Psi_{max}^2}{MSE} \tag{6.9}$$

where Ψ_{max} is the peak (maximum) intensity value of the image. For the most common eight bit gray image $\Psi_{max} = 255$.

We have considered images of 8-bit gray levels and corrupted them with additive white Gaussian noise with zero mean and standard deviation of σ. The corrupted image is then passed through the proposed 2-D digital lowpass filter in Category A and Category B based on the second approach.

We have considered images of 8-bit gray levels and corrupted them with additive white Gaussian noise with zero mean and standard deviation of σ. The corrupted image is then passed through the proposed 2-D digital lowpass filter in Category A and Category B based on the second approach.The original image, degraded image and the recovered images for different images and different noise levels are shown in the Figures 6.1 to 6.6 for Category A and Category B.

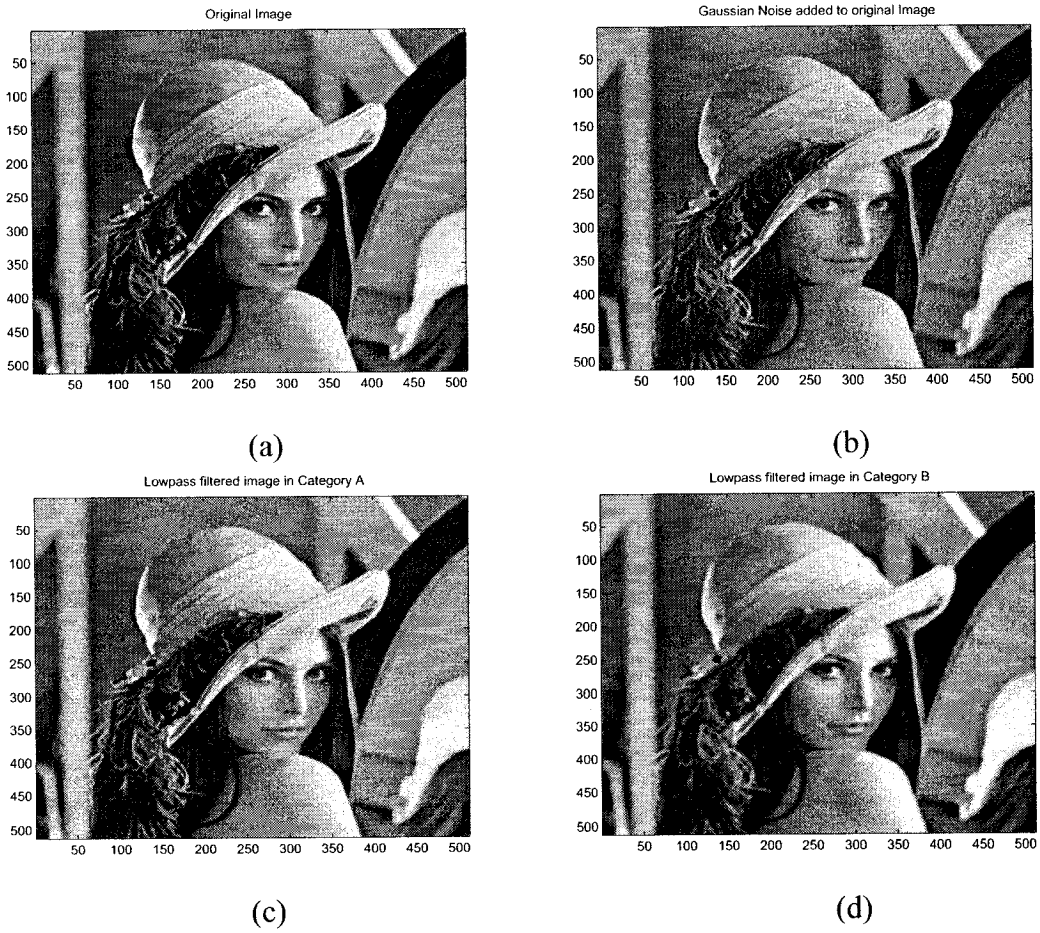

Figure 6.1: The Lena image (Size: 512 x 512) when degraded by additive Gaussian noise ($\sigma = 15$) and passed through 2-D digital Lowpass filter
(a) Original Image
(b) Noisy or degraded Image
(c) Filtered or output Image passed through 2-D digital lowpass filter in Category A
(d) Filtered or output Image passed through the all-pole 2-D digital lowpass filter in Category B

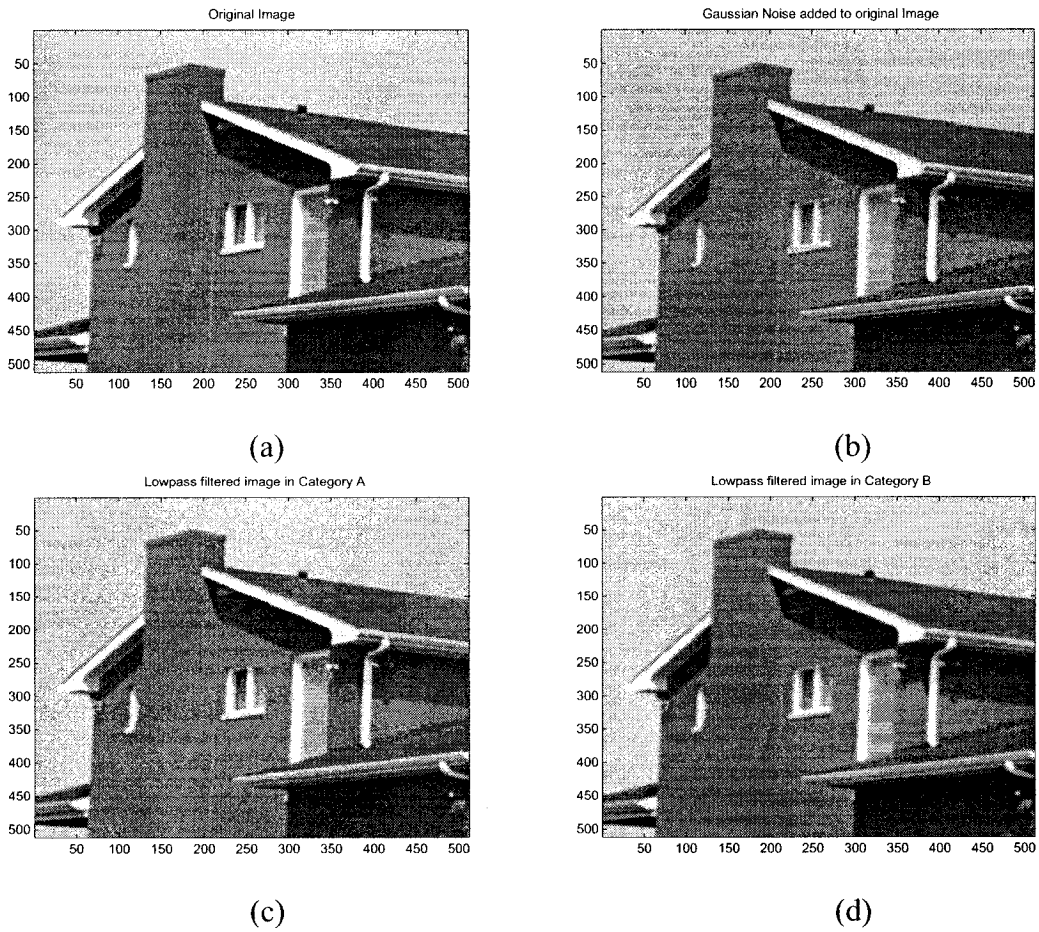

Figure 6.2: The House image (Size: 512 x 512) when degraded by additive Gaussian noise ($\sigma = 15$) and passed through 2-D digital Lowpass filter
(a) Original Image
(b) Noisy or degraded Image
(c) Filtered or output Image passed through 2-D digital lowpass filter in Category A
(d) Filtered or output Image passed through the all-pole 2-D digital lowpass filter in Category B

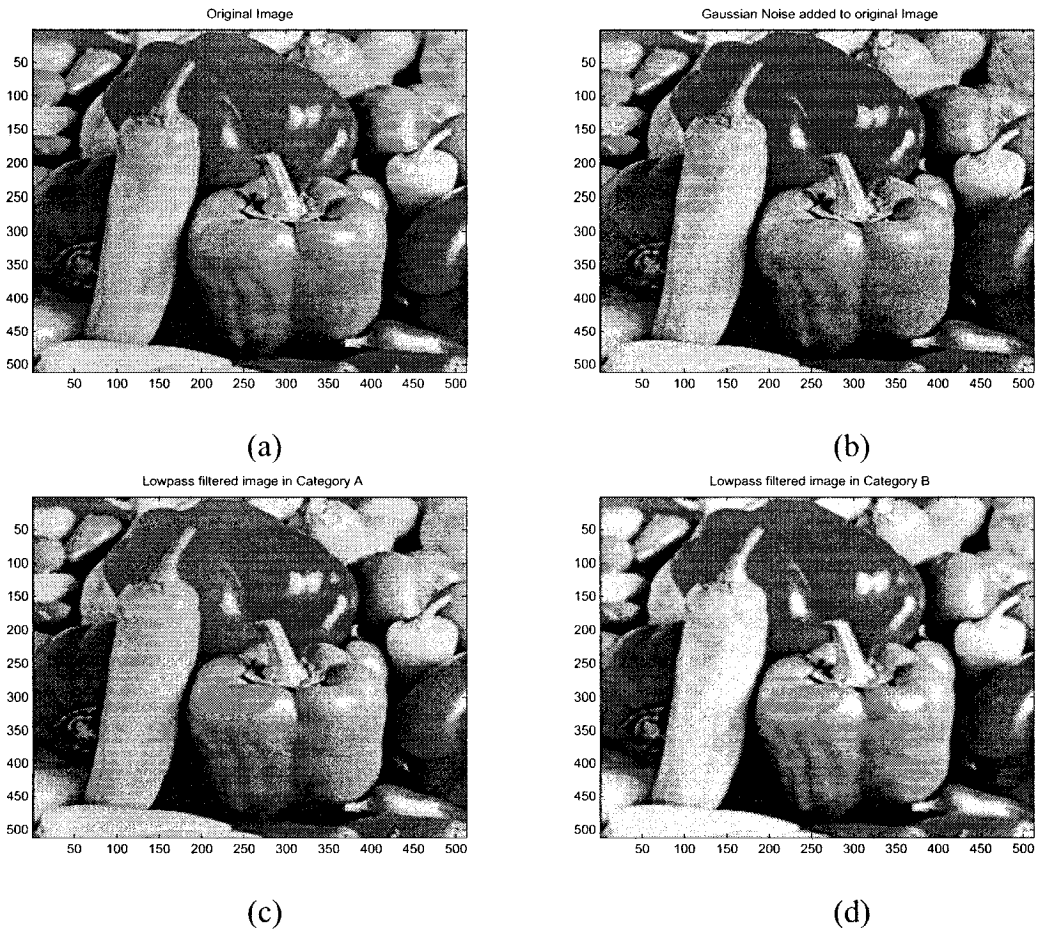

Figure 6.3: The Peppers image (Size: 512 x 512) when degraded by additive Gaussian noise ($\sigma = 15$) and passed through 2-D digital Lowpass filter
(a) Original Image
(b) Noisy or degraded Image
(c) Filtered or output Image passed through 2-D digital lowpass filter in Category A
(d) Filtered or output Image passed through the all-pole 2-D digital lowpass filter in Category B

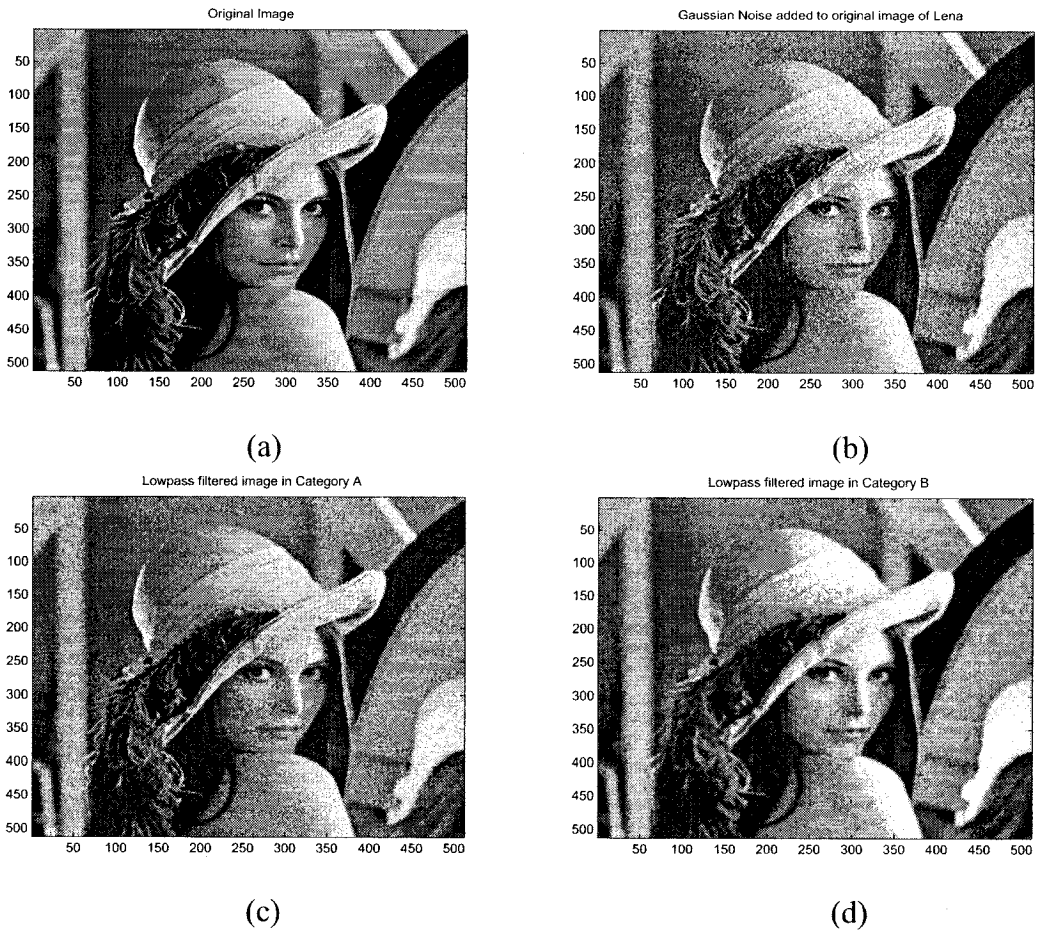

Figure 6.4: The Lena image (Size: 512 x 512) when degraded by additive Gaussian noise ($\sigma = 30$) and passed through 2-D digital Lowpass filter
(a) Original Image
(b) Noisy or degraded Image
(c) Filtered or output Image passed through 2-D digital lowpass filter in Category A
(d) Filtered or output Image passed through the all-pole 2-D digital lowpass filter in Category B

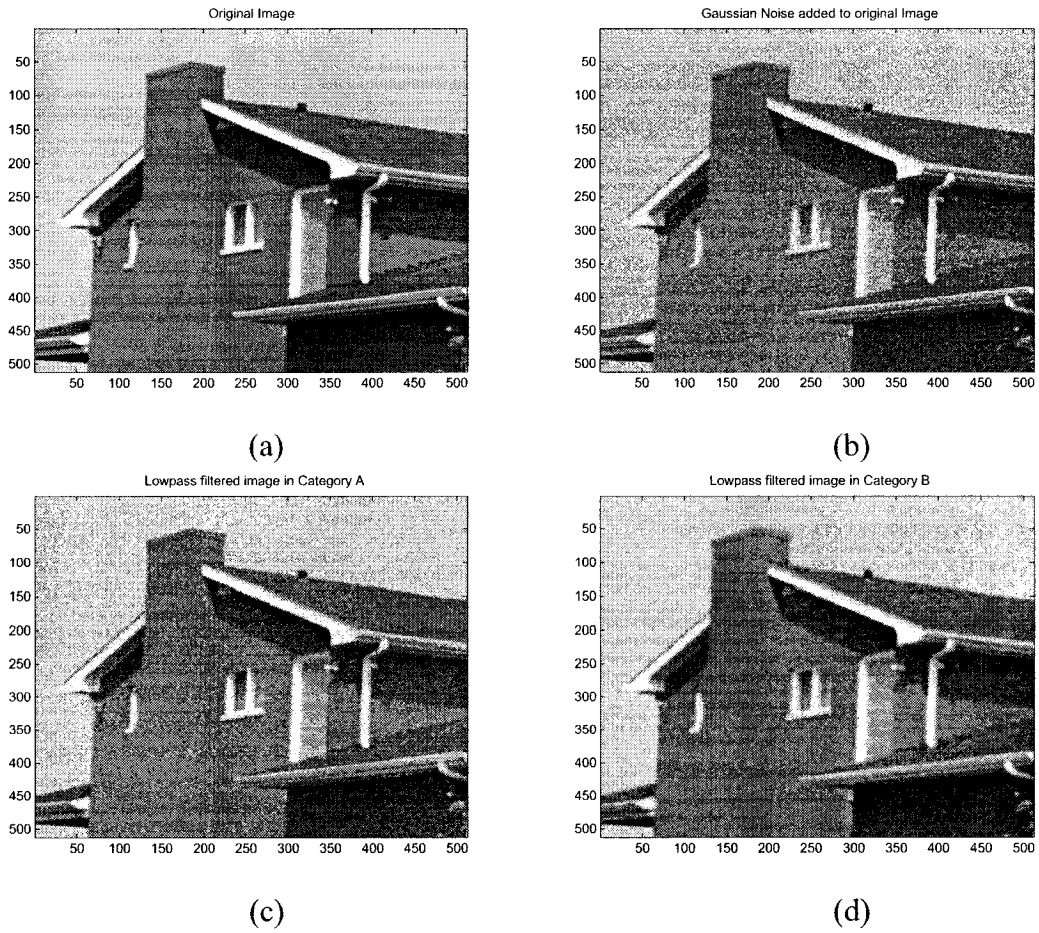

Figure 6.5: The House image (Size: 512 x 512) when degraded by additive Gaussian noise ($\sigma = 30$) and passed through 2-D digital Lowpass filter
(a) Original Image
(b) Noisy or degraded Image
(c) Filtered or output Image passed through 2-D digital lowpass filter in Category A
(d) Filtered or output Image passed through the all-pole 2-D digital lowpass filter in Category B

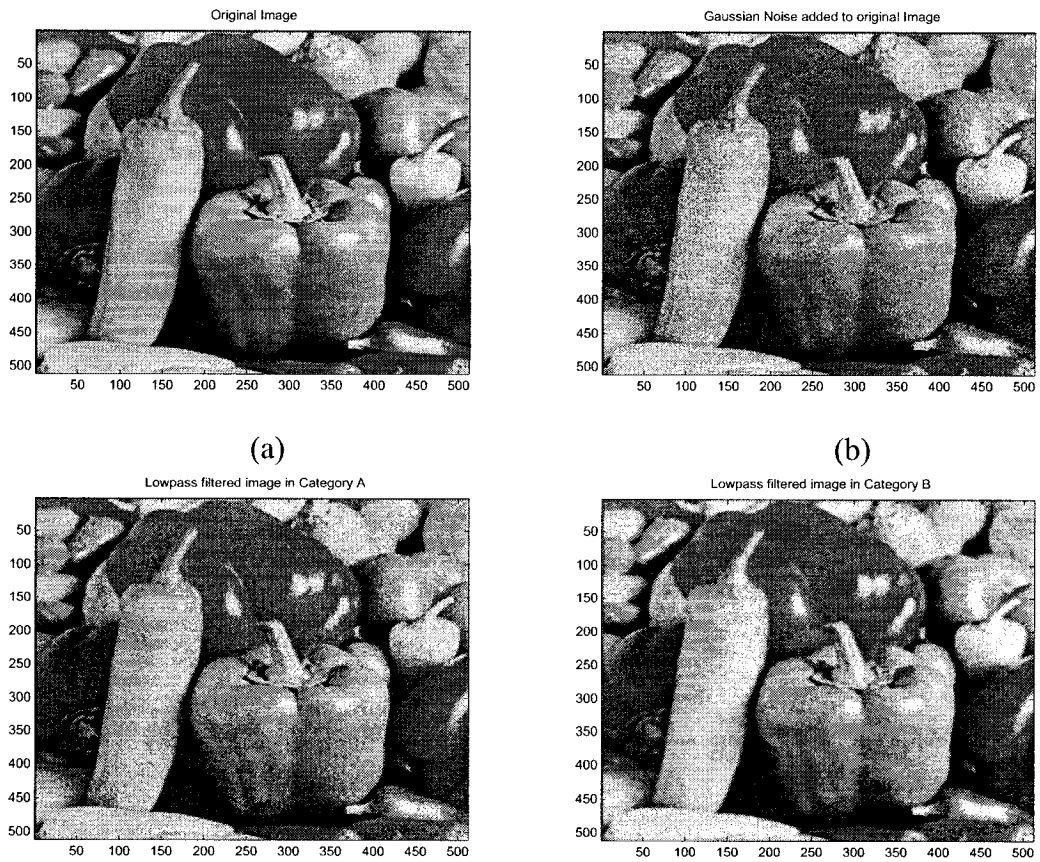

Figure 6.6: The Peppers image (Size: 512 x 512) when degraded by additive Gaussian noise ($\sigma = 30$) and passed through 2-D digital Lowpass filter
(a) Original Image
(b) Noisy or degraded Image
(c) Filtered or output Image passed through 2-D digital lowpass filter in Category A
(d) Filtered or output Image passed through the all-pole 2-D digital lowpass filter in Category B

Images (512X512)	σ = 15(PSNR=24.60 dB,MSE= 224.50)				σ = 30(PSNR=18.68 dB,MSE= 877.52)			
	Category A		Category B		Category A		Category B	
	PSNR (dB)	MSE	PSNR (dB)	MSE	PSNR(dB)	MSE	PSNR (dB)	MSE
Lena	30.72	55.68	31.47	52.74	25.68	178.81	28.68	95.38
Peppers	29.05	80.98	30.30	60.68	25.50	183.02	27.51	115.29
House	31.47	46.29	33.40	30.07	25.92	169.11	30.32	61.68

Table 6.1: PSNR and MSE for Noisy or Corrupted Image and Recovered Image at different Noise Level for Category A and Category B of 2-D Digital Lowpass Filter

The subjective test experiments are conducted with the three test model using the designed 2-D lowpass filter in Category A and the all-pole 2-D lowpass filter in Category B and the results are compared. The three test model, which are Lena, House and Peppers, of size 512 X 512 are taken and additive white Gaussian noise is added of different levels and then passed to the 2-D digital lowpass filter in Category A and the all-pole 2-D digital lowpass filter in Category B using same coefficients values $k_1 = 25$, $k_2 = 50$ and $a_1 = a_2 = 0.25$, the resultant will have noise reduced or recovered image. The MSE and PSNR of the output and the corrupted or noisy images are calculated with respect to the original image as reference for different levels of noise level and are shown in the Table 6.1

The PSNR and the MSE outputs for the designed 2-D digital lowpass filters in Category A and the all-pole 2-D digital lowpass filter in Category B are presented in Table 6.1. For the case where the input images have a PSNR of 24.6 dB, i.e., the power of the additive white Gaussian noise corrupting the image is not too high, the filter yields an improvement of 5-7 dB over the noisy image in Category A whereas in Category B, an improvement of 7-9 dB is achieved over the noisy images. A greater improvement of about 7-8 dB is achieved in Category A when the noise power is increased, i.e., when the the noisy input images have a PSNR of 18.68 dB, whereas in Category B, the filter yields an improvement of 10-12 dB over the noisy images. Thus, Category B yields better improvement over the noisy images when the images are passed through the all-pole 2-D digital filter as compared to that of 2-D digital lowpass filtering in Category A.

It is observed from the results that as we increase the noise level, i.e. standard deviation

σ, the PSNR value decreases and the MSE value increases. When we pass the images through the 2-D digital low pass filters in both categories, the recovered image loses its sharpness at the edges. This is because the high frequency content of the image constitutes the edges. It is noted that when the noise level, i.e. σ, is not high, the PSNR and the MSE of the noisy or corrupted image and the output recovered image are closer to each other with a small improvement in the recovered image. Figures 6.1, 6.2 and 6.3 show the visual output obtained by filtering the noisy images using the designed 2-D digital lowpass filter in Category A and all-pole 2-D digital lowpass filter in Category B. As is evident, the noise content has been reduced in all the images. However, the filter does cause some blurring around the edges because of the loss of the high frequency content during the course of lowpass filtering in both categories. The blurring caused by Category B filters is more than that caused by Category A filters. When σ is increased, there is a higher level of degradation in the image and the filtered results have considerable amount of improvement with the 2-D lowpass filtering and the all-pole 2-D lowpass filtering as shown in the Figures 6.4, 6.5 and 6.6. There is a significant amount of improvement in the recovered image and the effectiveness of the 2-D digital lowpass filtering can be easily observed in terms of quantitative measure as shown in Table 6.1 in both the categories. To get better filtered images from the noisy or corrupted images, such lower order lowpass filters can be further cascaded.

6.4 Summary

This chapter deals with the application of the 2-D digital lowpass filter in image processing for Category A and the all-pole 2-D lowpass filter in image processing in Category B. In image processing it is observed that most of the energy of a typical image is located at the low frequencies. On the other hand, energy of the noise is often spread across the frequency axes (e.g. white noise) or in the higher frequency range depending on its distribution func-

tion. The significant improvement of the degraded or noisy image can be achieved by using 2-D digital lowpass filters. The high frequency content of an image constitutes the edges and applying 2-D digital lowpass filtering technique will result in losing the sharpness of the images.

In Section 6.3, one simple application in image processing is provided using the proposed 2-D digital lowpass filter in Category A and All-pole 2-D digital lowpass filter in Category B. The standard images are corrupted by additive white Gaussian noise with zero mean and known variance. The 2-D digital lowpass filter with the given coefficient values is used to remove noise from each corrupted image in both the categories. The MSE and the PSNR of the corrupted and the recovered images are compared and shown in a tabular form for quantitative comparison of the image restoration for Category A and Category B. Thus, Category B yields better improvement over the noisy images when the images are passed through the all-pole 2-D digital filter as compared to that of 2-D digital lowpass filtering in Category A.

Apart from this application, the filter can also be used in the field of speech processing, digital communication such as digital telephony, digital telemetry and digital transmission and biomedicine. There are various applications possible using these types of filters. However, since the goal of this thesis is to study the variable characteristics of these filters, we did not give too much attention in implementing other types of applications.

Chapter 7

Conclusion and Future Work

7.1 Conclusions

In this thesis, a new technique for designing 2-D digital filters having variable magnitude characteristics has been proposed. The approach used to generate 2-D filters is to start with the second order Lowpass Butterworth filters connected in an all-pass manner. The analog transfer function of the 2-D lowpass filter is obtained and then transformed to 2-D digital lowpass filter through the generalized bilinear transformation in Category A and Category B. The stability conditions of the 2-D lowpass filter are defined and proven by verifying that the denominator of the transfer function polynomial is a very strict Hurwitz polynomial (VSHP). Also, the 2-D lowpass filters were further extended to 2-D digital highpass, digital bandpass and bandstop filters in Category A and Category B. In the end, we showed a few basic application of 2-D digital filter in image processing for Category A and Category B.

In Chapter 2, we generated the 2-D digital lowpass filter in Category A and Category B from the combination of all-pass filters and studied their characteristics. The stability conditions of the 2-D analog lowpass filter have been obtained and proven by verifying that the transfer function denominator polynomial is a very strict Hurwitz polynomial (VSHP)

in both the categories. The 2-D analog lowpass filters were transformed to the digital domain by applying the generalized bilinear transformation. The conditions for each of the generalized lowpass bilinear transformation was defined for the 2-D digital lowpass filter in Category A and Category B. The effect of each coefficient of the generalized bilinear transformations resulting in 2-D lowpass digital filter's magnitude response in Category A and the all-pole 2-D lowpass digital filter's magnitude response in Category B have been studied in detail.

In Chapter 3 and Chapter 4, we generated the 2-D digital highpass filter and bandpass filter, respectively, in Category A and Category B, by using the 2-D digital lowpass filter in Category A and the all-pole 2-D digital lowpass filter in Category B, proposed in Chapter 2. The effect of each coefficient of the generalized bilinear transformations resulting in 2-D highpass and bandpass digital filter's magnitude response in Category A and Category B have been studied in detail.

In Chapter 5, we generated the 2-D digital bandstop filter in Category A and Category B from the 2-D analog lowpass filter in Category A and Category B respectively proposed in Chapter 2. The 2-D analog lowpass filter is transformed to the 2-D analog bandstop filter using lowpass to bandstop transformation technique in both the categories. The 2-D digital bandstop filter was then generated by applying the generalized bilinear transformation to the 2-D analog bandstop filter in both the categories. The effects of each coefficient of the generalized bilinear transformations resulting in 2-D digital bandstop filter's magnitude response in Category A and the all-pole 2-D digital bandstop filter's magnitude response in Category B have been studied in detail.

In all the 2-D digital filters namely lowpass, highpass, bandpass and bandstop filters, in Category A and Category B, it is observed that in general, the coefficients k_1, k_2 mainly affected the passband width and a_1, a_2 mainly affected the gain of the amplitude-frequency response.

For the 2-D digital lowpass filter in Category A, as the values of the coefficients k_1 and

k_2 values were increased, the passband width and the magnitude of the amplitude-frequency response of the 2-D digital lowpass filter decreased. As the values of the coefficients a_1 and a_2 were increased, the magnitude of the amplitude-frequency response of the 2-D digital lowpass filter increased and the width of the passband increased and decreased periodically. For the all-pole 2-D digital lowpass filter in Category B, as the values of the coefficients k_1 and k_2 values were increased, the passband width and the magnitude of the amplitude-frequency response of the all-pole 2-D digital lowpass filter decreased. As the values of the coefficients a_1 and a_2 were increased, the magnitude of the amplitude-frequency response of the all-pole 2-D digital lowpass filter increased and the width of the passband increased and decreased periodically. Overall, the passband width decreased when the values of the coefficients of the generalized bilinear transformation k_1, k_2, a_1 and a_2 were increased.

For the 2-D digital highpass filter in Category A, as the values of the coefficients $k_1$and k_2 were increased, the stopband width of the 2-D digital highpass filter increased, i.e. the cut-off frequencies changed and also the magnitude of the amplitude-frequency response decreased. As the values of a_1 and a_2 were increased, the magnitude of the amplitude-response increased. For the all-pole 2-D digital highpass filter in Category B, as the values of the coefficients $k_1$and k_2 were increased, the stopband width of the all-pole 2-D digital highpass filter increased, i.e. the cut-off frequencies changed and also the magnitude of the amplitude-frequency response decreased. As the values of a_1 and a_2 were increased, the magnitude of the amplitude-response and the width of the stopband increased. Overall, the cut-off frequencies of the 2-D digital highpass filter changed when the values of the coefficients of the generalized bilinear transformation k_1, k_2, a_1 and a_2 were increased.

For the 2-D digital bandpass filter in Category A, as the values of the coefficients $k_1$and k_2 were increased, the passband width and the magnitude of the amplitude-frequency response decreased. As the values of the coefficients a_1 and a_2 were increased, the magnitude of the amplitude-response increased. Also, the width of the passband increased and decreased periodically for different combinations of a_1 and a_2. For the all-pole 2-D digital

bandpass filter in Category B, as the values of the coefficients k_1 and k_2 were increased, the passband width and the magnitude of the amplitude-frequency response decreased. As the values of the coefficients a_1 and a_2 were increased, the magnitude of the amplitude-response increased. Also, the width of the passband increased and decreased periodically for different combinations of a_1 and a_2.

For 2-D digital bandstop filter in Category A, as the values of the coefficients $k_1$and k_2 were increased, the cut-off frequency of the lower passband decreased and the cut-off frequency of the upper passband increased. Also, the width of the stopband increased and decreased periodically for different combinations of $k_1$and k_2. In addition, the magnitude of the amplitude-frequency response also decreased. For the values of k_1, $k_2 > 1$, it was observed that there were rounding of the contour edges and hence the transition band of the 2-D digital bandstop filter could not be clearly defined and was less visible. This is because the outer contour of the lower passband overlaps with the inner contour of the upper passband. Thus, the transition band is clearly visible for lower values of k_1 and k_2. As the values of the coefficients a_1 and a_2 were increased, the gain of the upper passband and that of the lower passband increased. Also, the width of the lower passband and upper passband increased and decreased for different combinations of a_1 and a_2. For the all-pole 2-D digital bandstop filter in Category B, as the values of the coefficients k_1 and k_2 were increased, the cut-off frequency of the lower passband decrease and the cut-off frequency of the upper passband increased. Also, the width of the stopband increased. In addition, the magnitude of the amplitude-frequency response also decreased. For the values of k_1, $k_2 > 1$, it was observed that there were rounding of the contour edges and hence the transition band of the 2-D digital bandstop filter could not be clearly defined and was less visible. This is because the outer contour of the lower passband overlaps with the inner contour of the upper passband. Thus, the transition band is clearly visible for lower values of k_1 and k_2. As the values of the coefficients a_1 and a_2 were increased, the width of the lower passband and upper passband increased and decreased periodically for different values of a_1 and a_2.

The gain of the upper passband and that of the lower passband increased.

An important conclusion which was found when forming the two categories of filter responses was that there were ripples in the amplitude-frequency response for the values in the range $1 < k_1,\ k_2 \leq 10$ and $a_1,\ a_2 \leq 0.5$ in Category A. This is because of the presence of the poles and zeros in the resulting transfer function of the 2-D filters in Category A. Whereas, there is no ripples present in the amplitude-frequency of the all-pole 2-D digital filters in Category B. Also, for the 2-D digital bandstop filters in Category A and Category B, an important observation conclusion was found is that amplitude-frequency response for Category B is almost the same as that of Category A. This is because of the resulting transfer function for Category B is almost the same as the one used in Category A as the transfer function does not depend on the coefficients of the VSHP polynomial, it only depends on the coefficients of the generalized bilinear transformation.

Chapter 6 discusses the application of the 2-D digital filters in Category A and the all-pole 2-D digital filters in Category B in image processing. An important conlusion was found that Category B yields better improvement over the noisy images when the images are passed through the all-pole 2-D digital filter as compared to that of 2-D digital lowpass filtering in Category A. Since our thesis is mainly concerned with studying the variable magnitude characteristics of the 2-D digital filters, proper attention has not been given to the implementation of the applications of these filters. Although we have shown some examples of the application of the 2-D digital lowpass filter in image processing for both the categories and has been compared. The 2-D lowpass filters in both the categories were used to recover standard images degraded by the additive white Gaussian noise.

7.2 Directions for Future work

In this thesis, we have limited our study to the positive values of the coefficients of the generalized bilinear transformation. Different combinations of the coefficients of the gen-

eralized bilinear transformation can be studied for the negative values and the effect of these coefficients on the amplitude-frequency response can be evaluated. We have used second-order Butterworth polynomial as the starting point for our design. In this thesis, we have proposed the transfer function of 2-D lowpass filters in both the categories up to the fourth order. Using this transfer function, different types of filters, such as highpass, band-pass, and bandstop filters, can be obtained for higher orders and their amplitude-frequency response can be explore in future.

Different types of second-order polynomials such as Papoulis, Filanovsky or Thomson-Bessel can be used as the design starting point and different types of transfer functions of the 2-D filters can be designed and the effect of the coefficients of the generalized bilinear transformation can be studied. We can also study the effect of the coefficients of the 2-D digital filters in both the categories obtained from other types of transformations, e.g. impulse invariance method etc. The phase response of the filters proposed in this thesis has not been studied and that can also be explore in future. Depending on the combination of properties like symmetry, amplitude characteristics (monotonic responses, responses with ripples) and the response in the stop band, suitable values have to be determined for the coefficients of the generalized bilinear transformation. This can be obtained by adopting suitable techniques. It is envisaged that these types of 2-D digital filters have potential applications in other areas like speech processing, biomedical image processing, video processing, digital telephony and communication systems, etc.

Appendix

1. MATLAB code to plot the 3-D amplitude-frequency response and the contour response of the 2-D Digital Lowpass Filter using All-pass Filter in Category A.

```
clear; k1 = input('Enter the k1 coeeficient value =');
if(k1<0 | k1>100)
error('k1 range is between 1 to 100'); end
k2 = input('Enter the k2 coeeficient value =');
if(k2<0 | k2>100)
error('k2 range is between 1 to 100'); end
a1 = input('Enter the a1 coeeficient value =');
if(a1<-1 | a1>1)
error('a1 range is between -1 to 1'); end
a2 = input('Enter the a2 coeeficient value =');
if(a2<-1 | a2>1)
error('a2 range is between -1 to 1'); end
w1=-pi:pi/50:pi; w2=-pi:pi/50:pi;
z1=exp(-j*w1); z2=exp(-j*w2); [Z1, Z2] = meshgrid(z1,z2);
b1=1; b2=1; s1= (k1*(Z1-a1)) ./ (Z1+b1); s2= (k2*(Z2-a2)) ./ (Z2+b2);
h1=(((s1).^2) - (1.414*s1)+1) ./ ((s1).^2 + (1.414*s1)+1);
h2=((-s1) + 1) ./ (s1+1); h12= h1 + h2;
h3=(((s2).^2) - (1.414*s2)+1) ./ ((s2).^2 + (1.414*s2)+1);
h4=(-(s2) + 1) ./ ((s2)+1); h34= h3 + h4;
h= h12 .* h34; mesh(w1,w2,abs(h));
title(['k_1=',num2str(k1),',','k_2=',num2str(k2),',','a_1=',num2str(a1),',',...
'a_2=',num2str(a2)]); xlabel('\omega_1(\pi)'); ylabel('\omega_2(\pi)');
```

```
zlabel('Magnitude'); figure [c1,c2]= contour(w1,w2,abs(h)); clabel(c1,c2); grid on;
title(['k_1=',num2str(k1),',','k_2=',num2str(k2),',','a_1=',num2str(a1),',',...
'a_2=',num2str(a2)]); xlabel('\omega_1(\pi)'); ylabel('\omega_2(\pi)');
% End of the code
```

2. MATLAB code to plot the 3-D amplitude-frequency response and the contour response of the All-pole 2-D Digital Lowpass Filter using All-pass Filter in Category B.

```
clear; k1 = input('Enter the k1 coeeficient value =');
if(k1<0 | k1>100)
error('k1 range is between 1 to 100'); end
k2 = input('Enter the k2 coeeficient value =');
if(k2<0 | k2>100)
error('k2 range is between 1 to 100'); end
a1 = input('Enter the a1 coeeficient value =');
if(a1<-1 | a1>1)
error('a1 range is between -1 to 1'); end
a2 = input('Enter the a2 coeeficient value =');
if(a2<-1 | a2>1)
error('a2 range is between -1 to 1'); end
w1=-pi:pi/50:pi; w2=-pi:pi/50:pi;
z1=exp(-j*w1); z2=exp(-j*w2); [Z1, Z2] = meshgrid(z1,z2);
b1=1; b2=1; s1= (k1*(Z1-a1)) ./ (Z1+b1); s2= (k2*(Z2-a2)) ./ (Z2+b2);
h1=(((s1).^2) - (1.414*s1)+1) ./ ((s1).^2 + (1.414*s1)+1);
h2=((-0.707*s1) + 1) ./ ((0.707*s1)+1); h12= h1 + h2;
h3=(((s2).^2) - (1.414*s2)+1) ./ ((s2).^2 + (1.414*s2)+1);
h4=((-0.707*s2) + 1) ./ ((0.707*s2)+1); h34= h3 + h4;
```

```
h= h12 .* h34; mesh(w1,w2,abs(h));
title(['k_1=',num2str(k1),',','k_2=',num2str(k2),',','a_1=',num2str(a1),',',...
'a_2=',num2str(a2)]); xlabel('\omega_1(\pi)'); ylabel('\omega_2(\pi)');
zlabel('Magnitude'); figure [c1,c2]= contour(w1,w2,abs(h)); clabel(c1,c2); grid on;
title(['k_1=',num2str(k1),',','k_2=',num2str(k2),',','a_1=',num2str(a1),',',...
'a_2=',num2str(a2)]); xlabel('\omega_1(\pi)'); ylabel('\omega_2(\pi)');
% End of the code.
```

3. MATLAB code to plot the 3-D amplitude-frequency response and the contour response of the 2-D Digital Highpass Filter using All-pass Filter in Category A

```
clear; k1 = input('Enter the k1 coeeficient value =');
if(k1<0 | k1>100) error('k1 range is between 1 to 100'); end
k2 = input('Enter the k2 coeeficient value =');
if(k2<0 | k2>100) error('k2 range is between 1 to 100'); end
a1 = input('Enter the a1 coeeficient value =');
if(a1<-1 | a1>1) error('a1 range is between -1 to 1'); end
a2 = input('Enter the a2 coeeficient value =');
if(a2<-1 | a2>1) error('a2 range is between -1 to 1'); end
w1=-pi:pi/50:pi; w2=-pi:pi/50:pi;
z1=exp(-j*w1); z2=exp(-j*w2); [Z1, Z2] = meshgrid(z1,z2);
b1=-1; b2=-1; s1= (k1*(Z1+a1)) ./ (Z1+b1+eps); s2= (k2*(Z2+a2)) ./ (Z2+b2+eps);
h1=(((s1).^2) - (1.414*s1)+1) ./ ((s1).^2 + (1.414*s1)+1);
h2=((-s1) + 1) ./ (s1+1); h12= h1 + h2;
h3=(((s2).^2) - (1.414*s2)+1) ./ ((s2).^2 + (1.414*s2)+1);
h4=(-(s2) + 1) ./ ((s2)+1); h34= h3 + h4;
h= h12 .* h34; mesh(w1,w2,abs(h));
```

```
title(['k_1=',num2str(k1),',','k_2=',num2str(k2),',','a_1=',num2str(a1),',',...
'a_2=',num2str(a2)]); xlabel('\omega_1(\pi)'); ylabel('\omega_2(\pi)');
zlabel('Magnitude'); figure [c1,c2]= contour(w1,w2,abs(h)); clabel(c1,c2); grid on;
title(['k_1=',num2str(k1),',','k_2=',num2str(k2),',','a_1=',num2str(a1),',',...
'a_2=',num2str(a2)]); xlabel('\omega_1(\pi)'); ylabel('\omega_2(\pi)');
% End of the code.
```

4. MATLAB code to plot the 3-D amplitude-frequency response and the contour response of the All-pole 2-D Digital Highpass Filter using All-pass Filter in Category B

```
clear; k1 = input('Enter the k1 coeeficient value =');
if(k1<0 | k1>100) error('k1 range is between 1 to 100'); end
k2 = input('Enter the k2 coeeficient value =');
if(k2<0 | k2>100) error('k2 range is between 1 to 100'); end
a1 = input('Enter the a1 coeeficient value =');
if(a1<-1 | a1>1) error('a1 range is between -1 to 1'); end
a2 = input('Enter the a2 coeeficient value =');
if(a2<-1 | a2>1) error('a2 range is between -1 to 1'); end
w1=-pi:pi/50:pi; w2=-pi:pi/50:pi;
z1=exp(-j*w1); z2=exp(-j*w2); [Z1, Z2] = meshgrid(z1,z2);
b1=-1; b2= -1; s1= (k1*(Z1+a1)) ./ (Z1+b1+eps); s2= (k2*(Z2+a2)) ./ (Z2+b2+eps);
h1=(((s1).^2) - (1.414*s1)+1) ./ ((s1).^2 + (1.414*s1)+1);
h2=((-0.707*s1) + 1) ./ (0.707*s1+1); h12= h1 + h2;
h3=(((s2).^2) - (1.414*s2)+1) ./ ((s2).^2 + (1.414*s2)+1);
h4=((-0.707*s2) + 1) ./ ((0.707*s2)+1); h34= h3 + h4;
hp= h12 .* h34; mesh(w1,w2,abs(hp));
title(['k_1=',num2str(k1),',','k_2=',num2str(k2),',','a_1=',num2str(a1),',',...
```

```
'a_2=',num2str(a2)]); xlabel('\omega_1(\pi)'); ylabel('\omega_2(\pi)');
zlabel('Magnitude'); figure [c1,c2]= contour(w1,w2,abs(hp)); clabel(c1,c2); grid on;
title(['k_1=',num2str(k1),',','k_2=',num2str(k2),',','a_1=',num2str(a1),',',...
'a_2=',num2str(a2)]); xlabel('\omega_1(\pi)'); ylabel('\omega_2(\pi)');
% End of the code.
```

5. MATLAB code to plot the 3-D amplitude-frequency response and the contour response of the 2-D Digital Bandpass Filter using All-pass Filter in Category A

```
clear; k1 = input('Enter the k1 coeeficient value =');
if(k1<0 | k1>100) error('k1 range is between 1 to 100'); end
k2 = input('Enter the k2 coeeficient value =');
if(k2<0 | k2>100) error('k2 range is between 1 to 100'); end
a1 = input('Enter the a1 coeeficient value =');
if(a1<-1 | a1>1) error('a1 range is between -1 to 1'); end
a2 = input('Enter the a2 coeeficient value =');
if(a2<-1 | a2>1) error('a2 range is between -1 to 1'); end
w1=-pi:pi/50:pi; w2=-pi:pi/50:pi;
z1=exp(-j*w1); z2=exp(-j*w2); [Z1, Z2] = meshgrid(z1,z2);
% 2-D Low Pass Filter
s1= (k1*(Z1-a1)) ./ (Z1+1); s2= (k2*(Z2-a2)) ./ (Z2+1);
h1=(((s1).^2) - (1.414*s1)+1) ./ ((s1).^2 + (1.414*s1)+1);
h2=((-s1) + 1) ./ (s1+1); h12= h1 + h2;
h3=(((s2).^2) - (1.414*s2)+1) ./ ((s2).^2 + (1.414*s2)+1);
h4=(-(s2) + 1) ./ ((s2)+1); h34= h3 + h4; hlp= h12 .* h34;
% 2-D High Pass Filter
s1= (k1*(Z1+a1)) ./ (Z1-1+eps) ; s2= (k2*(Z2+a2)) ./ (Z2-1+eps);
```

```
h5=(((s1).^2) - (1.414*s1)+1) ./ ((s1).^2 + (1.414*s1)+1);
h6=((-s1) + 1) ./ (s1+1); h56= h5 + h6;
h7=(((s2).^2) - (1.414*s2)+1) ./ ((s2).^2 + (1.414*s2)+1);
h8=(-(s2) + 1) ./ ((s2)+1); h78= h7 + h8; hhp= h56 .* h78;
% 2-D Digital Band-pass filter by cascading 2-D low pass and high filters.
hbp =hlp .* hhp; mesh(w1,w2,abs(hbp));
title(['k_1=',num2str(k1),',','k_2=',num2str(k2),',','a_1=',num2str(a1),',',...
'a_2=',num2str(a2)]); xlabel('\omega_1(\pi)'); ylabel('\omega_2(\pi)');
zlabel('Magnitude'); figure [c1,c2]= contour(w1,w2,abs(hbp)); clabel(c1,c2); grid on;
title(['k_1=',num2str(k1),',','k_2=',num2str(k2),',','a_1=',num2str(a1),',',...
'a_2=',num2str(a2)]); xlabel('\omega_1(\pi)'); ylabel('\omega_2(\pi)');
% End of the code.
```

6. MATLAB code to plot the 3-D amplitude-frequency response and the contour response of the All-pole 2-D Digital Bandpass Filter using All-pass Filter in Category B

```
clear; k1 = input('Enter the k1 coeeficient value =');
if(k1<0 | k1>100) error('k1 range is between 1 to 100'); end
k2 = input('Enter the k2 coeeficient value =');
if(k2<0 | k2>100) error('k2 range is between 1 to 100'); end
a1 = input('Enter the a1 coeeficient value =');
if(a1<-1 | a1>1) error('a1 range is between -1 to 1'); end
a2 = input('Enter the a2 coeeficient value =');
if(a2<-1 | a2>1) error('a2 range is between -1 to 1'); end
w1=-pi:pi/50:pi; w2=-pi:pi/50:pi;
z1=exp(-j*w1); z2=exp(-j*w2); [Z1, Z2] = meshgrid(z1,z2);
% All-pole 2-D Low Pass Filter
```

```
s1= (k1*(Z1-a1)) ./ (Z1+1); s2= (k2*(Z2-a2)) ./ (Z2+1);
h1=(((s1).^2) - (1.414*s1)+1) ./ ((s1).^2 + (1.414*s1)+1);
h2=((-0.707*s1) + 1) ./ (0.707*s1+1); h12= h1 + h2;
h3=(((s2).^2) - (1.414*s2)+1) ./ ((s2).^2 + (1.414*s2)+1);
h4=((-0.707*s2) + 1) ./ ((0.707*s2)+1); h34= h3 + h4; hlp= h12 .* h34;
% All-pole 2-D High Pass Filter
s1= (k1*(Z1+a1)) ./ (Z1-1+eps) ; s2= (k2*(Z2+a2)) ./ (Z2-1+eps);
h5=(((s1).^2) - (1.414*s1)+1) ./ ((s1).^2 + (1.414*s1)+1);
h6=((-0.707*s1) + 1) ./ (0.707*s1+1); h56= h5 + h6;
h7=(((s2).^2) - (1.414*s2)+1) ./ ((s2).^2 + (1.414*s2)+1);
h8=((-0.707*s2) + 1) ./ ((0.707*s2)+1); h78= h7 + h8; hhp= h56 .* h78;
% All-pole 2-D Digital Band-pass filter by cascading All-pole 2-D Digital
%lowpass and highpass filters.
hbp =hlp .* hhp; mesh(w1,w2,abs(hbp));
title(['k_1=',num2str(k1),',','k_2=',num2str(k2),',','a_1=',num2str(a1),',',...
'a_2=',num2str(a2)]); xlabel('\omega_1(\pi)'); ylabel('\omega_2(\pi)');
zlabel('Magnitude'); figure [c1,c2]= contour(w1,w2,abs(hbp)); clabel(c1,c2); grid on;
title(['k_1=',num2str(k1),',','k_2=',num2str(k2),',','a_1=',num2str(a1),',',...
'a_2=',num2str(a2)]); xlabel('\omega_1(\pi)'); ylabel('\omega_2(\pi)');
% End of the code.
```

7. MATLAB code to plot the 3-D amplitude-frequency response and the contour response of the 2-D Digital Bandstop Filter using All-pass Filter in Category A

```
clear; k1 = input('Enter the k1 coeeficient value =');
if(k1<0 | k1>100) error('k1 range is between 1 to 100'); end
k2 = input('Enter the k2 coeeficient value =');
```

```
if(k2<0 | k2>100) error('k2 range is between 1 to 100'); end
a1 = input('Enter the a1 coeeficient value =');
if(a1<-1 | a1>1) error('a1 range is between -1 to 1'); end
a2 = input('Enter the a2 coeeficient value =');
if(a2<-1 | a2>1) error('a2 range is between -1 to 1'); end
w1=-pi:pi/50:pi; w2=-pi:pi/50:pi;
z1=exp(-j*w1); z2=exp(-j*w2); [Z1, Z2] = meshgrid(z1,z2);
B=1; w0=1; b1=1; b2=1;
% Low pass to bandstop transformation & the GBT of the bandstop filter
S1= (k1*(Z1-a1)) ./ (Z1+b1); S2= (k2*(Z2-a2)) ./ (Z2+b2);
s1 = B*S1 ./ ((S1).^2+(w0)^2); s2 = B*S2 ./ ((S2).^2+(w0)^2);
h1=(((s1).^2) - (1.414*s1)+1) ./ ((s1).^2 + (1.414*s1)+1);
h2=((-s1) + 1) ./ (s1+1); h12= h1 + h2;
h3=(((s2).^2) - (1.414*s2)+1) ./ ((s2).^2 + (1.414*s2)+1);
h4=(-(s2) + 1) ./ ((s2)+1); h34= h3 + h4; hbs= h12 .* h34;
mesh(w1,w2,abs(hbs));
title(['k_1=',num2str(k1),',','k_2=',num2str(k2),',','a_1=',num2str(a1),',',...
'a_2=',num2str(a2)]); xlabel('\omega_1(\pi)'); ylabel('\omega_2(\pi)');
zlabel('Magnitude'); figure [c1,c2]= contour(w1,w2,abs(hbs)); clabel(c1,c2); grid on;
title(['k_1=',num2str(k1),',','k_2=',num2str(k2),',','a_1=',num2str(a1),',',...
'a_2=',num2str(a2)]); xlabel('\omega_1(\pi)'); ylabel('\omega_2(\pi)');
% End of the code.
```

8. MATLAB code to plot the 3-D amplitude-frequency response and the contour response of the All-pole 2-D Digital Bandstop Filter using All-pass Filter in Category B

```
clear; k1 = input('Enter the k1 coeeficient value =');
```

```
if(k1<0 | k1>100) error('k1 range is between 1 to 100'); end
k2 = input('Enter the k2 coeeficient value =');
if(k2<0 | k2>100) error('k2 range is between 1 to 100'); end
a1 = input('Enter the a1 coeeficient value =');
if(a1<-1 | a1>1) error('a1 range is between -1 to 1'); end
a2 = input('Enter the a2 coeeficient value =');
if(a2<-1 | a2>1) error('a2 range is between -1 to 1'); end
w1=-pi:pi/50:pi; w2=-pi:pi/50:pi;
z1=exp(-j*w1); z2=exp(-j*w2); [Z1, Z2] = meshgrid(z1,z2);
B=1; w0=1; b1=1; b2=1;
% Low pass to bandstop transformation & the GBT of the bandstop filter
S1= (k1*(Z1-a1)) ./ (Z1+b1); S2= (k2*(Z2-a2)) ./ (Z2+b2);
s1 = B*S1 ./ ((S1).^2+(w0)^2); s2 = B*S2 ./ ((S2).^2+(w0)^2);
h1=(((s1).^2) - (1.414*s1)+1) ./ ((s1).^2 + (1.414*s1)+1);
h2=(((-0.707*s1)) + 1) ./ ((0.707*s1)+1); h12= h1 + h2;
h3=(((s2).^2) - (1.414*s2)+1) ./ ((s2).^2 + (1.414*s2)+1);
h4=((-0.707*s2) + 1) ./ ((0.707*s2)+1); h34= h3 + h4; hbs= h12 .* h34;
mesh(w1,w2,abs(hbs));
title(['k_1=',num2str(k1),',','k_2=',num2str(k2),',','a_1=',num2str(a1),',',...
'a_2=',num2str(a2)]); xlabel('\omega_1(\pi)'); ylabel('\omega_2(\pi)');
zlabel('Magnitude'); figure [c1,c2]= contour(w1,w2,abs(hbs)); clabel(c1,c2); grid on;
title(['k_1=',num2str(k1),',','k_2=',num2str(k2),',','a_1=',num2str(a1),',',...
'a_2=',num2str(a2)]); xlabel('\omega_1(\pi)'); ylabel('\omega_2(\pi)');
% End of the code.
```

9. MATLAB code to corrupt the image by additive Gaussian Noise & recover the image using 2-D Digital Lowpass Filter in Category A

```
clear; k1 = input('Enter the k1 coeeficient value =');
```

```
if(k1<0 | k1>100)
error('k1 range is between 1 to 100'); end
k2 = input('Enter the k2 coeeficient value =');
if(k2<0 | k2>100)
error('k2 range is between 1 to 100'); end
a1 = input('Enter the a1 coeeficient value =');
if(a1<-1 | a1>1)
error('a1 range is between -1 to 1'); end
a2 = input('Enter the a2 coeeficient value =');
if(a2<-1 | a2>1)
error('a2 range is between -1 to 1'); end
w1=-pi:pi/256:pi-pi/256; w2=-pi:pi/256:pi-pi/256;
z1=exp(-j*w1); z2=exp(-j*w2); [Z1, Z2] = meshgrid(z1,z2);
s1= (k1*(Z1-a1)) ./ (Z1+1); s2= (k2*(Z2-a2)) ./ (Z2+1);
% Adding Noise to the Image
noise=15; % Other noise level=30 has been used.
x=double(imread('lena.png')); % Other images used are Peppers and House
x=x(:,:,1); x_rand=noise*randn(size(x));
y=double(uint8(x+x_rand)); fy=(fftshift(fft2(y)));
% Transfer Function of all-pole 2-D digital lowpass filter
h1=(((s1).^2) - (1.414*s1)+1) ./ ((s1).^2 + (1.414*s1)+1);
h2=((-s1) + 1) ./ (s1+1); h12= h1 + h2;
h3=(((s2).^2) - (1.414*s2)+1) ./ ((s2).^2 + (1.414*s2)+1);
h4=(-(s2) + 1) ./ ((s2)+1); h34= h3 + h4; h= h12 .* h34; h=h./max(max(h));
% Multiplying degraded inage and lowpass filter in frequency domain
fily=fy.*abs(h); est_x=abs((ifft2(fily)));
% Calculating PSNR and MSE values
```

```
psnr_noisy= 10*log10(255^2.*prod(size(x))./sumsqr(x-y));
est_psnr_filtered=10*log10(255^2.*prod(size(x))./sumsqr(x-est_x));
mse_noisy=(sumsqr(x-y)/prod(size(x)));
est_mse_filtered=(sumsqr(x-est_x)/prod(size(x)));
% Outputing Orignal, Noisy and filtered images
figure; imagesc(x);title('Original Image'); colormap(gray);
figure; imagesc(y);title(' Gaussian Noise added to original Image'); colormap(gray);
figure; imagesc(est_x);title(' Lowpass filtered image in Category A'); colormap(gray);
% End of the code.
```

10. MATLAB code to corrupt the image by additive Gaussian Noise & recover the image using the All-pole 2-D Digital Lowpass Filter in Category B

```
clear; k1 = input('Enter the k1 coeeficient value =');
if(k1<0 | k1>100)
error('k1 range is between 1 to 100'); end
k2 = input('Enter the k2 coeeficient value =');
if(k2<0 | k2>100)
error('k2 range is between 1 to 100'); end
a1 = input('Enter the a1 coeeficient value =');
if(a1<-1 | a1>1)
error('a1 range is between -1 to 1'); end
a2 = input('Enter the a2 coeeficient value =');
if(a2<-1 | a2>1)
error('a2 range is between -1 to 1'); end
w1=-pi:pi/256:pi-pi/256; w2=-pi:pi/256:pi-pi/256;
z1=exp(-j*w1); z2=exp(-j*w2); [Z1, Z2] = meshgrid(z1,z2);
```

```
s1= (k1*(Z1-a1)) ./ (Z1+1); s2= (k2*(Z2-a2)) ./ (Z2+1);
% Adding Noise to the Image
noise=15; % Other noise level =30
x=double(imread('lena.png')); % Other images used are Peppers and House
x=x(:,:,1); x_rand=noise*randn(size(x));
y=double(uint8(x+x_rand)); fy=(fftshift(fft2(y)));
% Transfer Function of all-pole 2-D digital lowpass filter
h1=(((s1).^2) - (1.414*s1)+1) ./ ((s1).^2 + (1.414*s1)+1);
h2=((-0.707*s1) + 1) ./ (0.707*s1+1); h12= h1 + h2;
h3=(((s2).^2) - (1.414*s2)+1) ./ ((s2).^2 + (1.414*s2)+1);
h4=((-0.707*s2) + 1) ./ ((0.707*s2)+1); h34= h3 + h4; h= h12 .* h34; h=h./max(max(h));
% Multiplying degraded inage and lowpass filter in frequency domain
fily=fy.*abs(h); est_x=abs((ifft2(fily)));
% Calculating PSNR and MSE values
psnr_noisy= 10*log10(255^2.*prod(size(x))./sumsqr(x-y));
est_psnr_filtered=10*log10(255^2.*prod(size(x))./sumsqr(x-est_x));
mse_noisy=(sumsqr(x-y)/prod(size(x)));
est_mse_filtered=(sumsqr(x-est_x)/prod(size(x)));
% Outputing Orignal, Noisy and filtered images
figure; imagesc(x);title('Original Image'); colormap(gray);
figure; imagesc(y); title(' Gaussian Noise added to original Image'); colormap(gray);
figure; imagesc(est_x); title(' Lowpass filtered image in Category B'); colormap(gray);
% End of the code.
```

References

[1] A. Antonious, "Digital Filters: Analysis and Design", Mcgraw-Hill Series, 1990.

[2] D. E. Johnson, "Introduction to Filter Theory", Prentice-Hall, Inc., 1976.

[3] A. V. Oppenheim, R. W. Schafer and J. R. Buck, "Discrete Signal Processing", Prentice-Hall Inc., Second Edition, 1998

[4] M.E. Valkenburg, "Analog Filter Design", Holt, Rinehart and Winston, 1982.

[5] T.B. Deng, " Design of Linear Phase Variable 2-D Filters Using Real-Complex Decompositon", *IEEE Transcation on Circuits and Systems,* vol.45, pp. 330-339, March 1998.

[6] S.K. Mitra, Y. Neuvo, and H. Roivanien, " Design of Recursive Digital Filters with Variable Characteristics", *Journal of Circuit Theory Applications,* vol.18, pp. 107-119, 1990.

[7] D. Childers and A. Durling, "Digital Filtering and Signal Processing", West Publishing Company, 1975

[8] C.S. Gargour, V. Ramachandran, R. P. Ramachandran & F. Awad, "Variable Magnitude Characteristics of 1-D IIR Discrete Filters by a Generalized Bilinear Transformation", *IEEE Symp. on Circuits & Systems,* Lansing MI, Aug 8-11, 2000.

[9] S.S. Abuja and S.C. Dutta Roy, "Variable -cutoff two-dimensional lowpass FIR digital filters," *Electron Letter*, vol. 14, no. 14, pp. 422-423, July 1978.

[10] P.A. Regalia, S. K. Mitra, P.P. Vaidyanathan, "The digital All-pass Filter: a versatile processing building block", *Proceedings of the IEEE,* vol 76, no. 1, pp. 19-37, January 1988

[11] A. Fettweis, "Pseudopassivity, sensitivity, and stability of wave digital filters," *IEEE transactions on Circuits and Systems*, vol. CT-19, pp. 668-673, Nov. 1972.

[12] P. P. Vaidyanathan and S.K. Mitra, "Low passband sensitivity digital filters: A generalized viewpoint and synthesis procedures," *Proceedings of the IEEE*, vol. 72, pp. 404-423, April 1984.

[13] S.K. Mitra, P.A. Regalia, and P.P. Vaidyanathan, "Bounded compled transfer function, and its application to low sensitivity filter design, " *Proceedings of the International Symposium on Circuits and Systems"*, pp. 452-455, San Jose, CA, May 1986.

[14] V. Ramachandran, C.S. Gargour, M. Ahmadi, "Generation of transfer functions realizable by sum or difference of two multivariable all-pass structures, *Computers and Electrical Engineering,* vol. 26, pp. 387-400, 2000.

[15] T. Saramaki, "On the design of filters as a sum of two all-pass filters", *IEEE Transactions on Circuits and Systems* vol 32, no.11, pp. 1191-1193, 1985.

[16] S. K. Mitra, K. Hirano, "Digital all-pass networks", *IEEE Transactions on Circuits and Systems* 1974; vol. 21, np. 5, pp. 688-700, 1974.

[17] P. S. Reddy, P. Sathyanarayana, M. N. S. Swamy, "Realization of first and second-order 2-D all-pass digital filters", *IEEE Transactions on Circuits and Systems*, vol. 36, no. 8, pp. 1146-1147, 1989.

[18] K. Manivannan, C. Eswaran, "Minimal multiplier realization of 2-D all-pass digital filters", *IEEE Transactions on Circuits and Systems*, vol. 35, no. 4, pp. 480-482, 1988.

[19] E. I. Jury, " Inners and Stability of Dynamic Systems", John Wiley and Sons, 1974.

[20] V. Ramachandran, M. Ahmadi, "Some properties of multivariable mirror-image and anti-mirror image polynomials obtained by bilinear transformations of Hurwitz polynomials", *IEEE Transactions on Circuits and Systems*, vol. 37, no. 6, pp. 828-831, 1990.

[21] V. Ramachandran, M. Ahmadi, "Some properties of multivariable mirror-image and anti-mirror image polynomials obtained by bilinear transformations of Hurwitz polynomials", *IEEE Transactions on Circuits and Systems,* vol. 34, no. 9, pp. 1088-1090, 1987.

[22] V. Ramachandran, "Determination of discrete transfer function from its real (or imaginary) part on the unit circle", *IEEE Transactions on Acoustics, Speech and Signal Processing,* vol. 37, no. 3, pp. 440-442, 1989.

[23] V. Ramachandran, A. S. Rao, "The real part of a multivariable positive real function and some applications", *IEEE Transactions on Circuits and Systems*, vol. 21, no. 5, pp. 598-605, 1974.

[24] M. N. S. Swamy and H. C. Reddy, " Two-variable Analog Ladders with Appilcations", *Multidimensional Systems: Techniques and Applications* (Edited by S.G. Tzafestas), Chapter 6, New York: Marcel Dekkar, 1986,

[25] D. E. Dudgeon and R. M. Mersereau, "Multidimensional Digital Signal Processing", Prentice-Hall signal processing series.

[26] J. S. Lim, "Two-dimensional Signal and Image Processing", Prentice Hall Inc., 1990.

[27] T. S. Huang, "Two-Dimensional Windows", *IEEE Transactions on Audio and Electroacoustices*, vol 20, no. 1, pp. 260-269, May 1978.

[28] R.L. Rabiner and B. Gold, "Theory and application of Digital Signal Processing", Prentice Hall, 1975.

[29] V. Ramachandran and C.S. Gargour, "Generation of Very Strict Hurwitz Polynomial and Applications to 2-D Filter Design", *Control and Dynamics Systems, Multidimensional Systems: Signal Processing and Modeling Techniques*, Academic Press Inc., vol 69, pg 211-254, 1995.

[30] D. Goodman, "Some stability properties of two-dimensional linear shift-invariant digital filters", *IEEE Transactions on Circuits and Systems*, vol. 24, no. 4, pp. 201-208, April 1977.

[31] D. Goodman, "Some diffuculties with double bilinear transformation in 2-D digital filter design", *Proceedings of the IEEE*, vol.66, no.7, pp.796-797, July 1978.

[32] M.N.S. Swamy, L.M. Roytman and N. Marinovic, "A necessary condition for the BIBO stability of 2-D filters", *IEEE Transactions on Circuits and Systems II: Analog and Digital Signal Processing*, vol.39, no. 7, pp. 475-476, July 1992.

[33] C.S. Gargour, V. Ramachandran, R. P. Ramachandran, "Generation of a class of 2-D Transfer Function Yielding Variable Magnitude and Contour Characteristics", *ISCAS 2001*, pp.797-800 Sydney, Australia, May 2001

[34] E. Dubois and M.L. Blostein, "A circuit analog method for the design of recursive two-dimensional digital filters", *Proceedings IEEE Internet. Symp. Circuits Syst.*, pp. 451-454, 1975.

[35] P. A. Ramamoorthy and L. T. Bruton, "Frequency Domain Approximation of stable multi-dimensional discrete filters", Proc. IEEE Internet. Symp. Circuits Syst., pp. 654-657, 1977.

[36] R. E. Twogood and S. K. Mitra, "Computer-aided design of separable two dimensional digital filters", *Proceedings IEEE Transactions on Acoustic,Speech and Signal Processing*, vol. 25, no. 2, pp. 165-169, 1977.

[37] S. Basu and A. Fettweis, "Test for two dimensional scattering Hurtwitz Polynomials", *Circuits, Syst., Signal Processing*, vol. 3, no. 2, pp. 225-242, 1984.

[38] V. Ramachandran, "Some similarities and dissimilarities between single-variable and two-variable reactance functions", *IEEE, Circuits and Systems Newsletter*, vol. 10, no.1, pp. 11-14, Feb. 1976.

[39] M. Marden, " Geometry of Polynomials", *American Mathematical Society*, pp. 22, 1966

[40] V. Ramachandran and C.S. Gargour, "Generation of stable 2-D transfer function having variable magnitude characteristics", *Control and Dynamics Systems, Multidimensional Systems: Signal Processing and Modeling Techniques*, Academic Press Inc., vol 69, pp 255-297, 1995.

[41] V. Ramachandran and M. Ahmadi, "Design of 2-D stable recursive filters by generation of VSHP using Terminated n-port Gyrator Networks", *Journal of the Franklin Institute*, vol. 316, no. 5, pp. 373-380, November 1983.

[42] M.A. Abiri, V. Ramachandran and M. Ahmadi, " An alternative approach in generating 2-Variable Very Strict Hurwitz Polynomial (VSHP) and its appilcations", *Journal of the Franklin Institute*, vol. 324, no. 2, pp. 187-203, 1987.

[43] V. Ramachandran and M. Ahmedi, "Design of 2-D stable analog and recursive filters using properties of the derivatives of even or odd parts of Hurwitz Polynomials", *Journal of the Franklin Institute*, vol. 315, no. 4, pp. 259-267, April 1983.

[44] M. Ahmedi, S. Golikeri and V. Ramachandran, "A new method for the design of 2-D stable recursive digital filters satisfying prescribed magnitude and group delay response", *IEEE International Conference on Acoustics, Speech and Signal Processing*, ICASSP' 83, vol. 8, pp. 399-402, April 1983.

[45] H. Ruston and J. Bordogna, "Electric Networks: Functions, Filter, Analysis", New york, McGraw-Hill, 1966.

[46] A. V. Oppenheim, W. F. G. Mechklenbrauker and R. M. Mersereau, " Variable cutoff linear phase digital filters", *IEEE Transactions on Circuits System*, vol. 23, pp. 199-203, April 1976.

[47] D. Goodman, "Some Difficulties with Double Bilinear Transformation in 2-D Digital Filter Desing", *Proceeding of IEEE*, vol. 65, pp. 905-914, June 1978.

[48] C.S. Gargour, V. Ramachandran and P. Ramachandran, "Modification of filter responses by the generalized bilinear transformation and the inverse bilinear transformation", *Canadian Conference on Electrical and Computer Engineering, IEEE CCECE' 2003*, vol. 3, pp. 2043-2046, May 4-7, 2003.

[49] James H. McClellan, "The Design of Two-Dimensional Filters by Transformations", *Proceedings of 7th Annual Princeton Conference on Information Sciences and Systems*, pp. 247-251, 1973.

[50] V. Cappellini, A.G. Constantinides and P. Emilliani, "Digital Filters and their applications", Academic Press, 1978.

[51] R. King, M. Ahmadi, R. G. Naquib, A. Kwabwe and M. A. Sadjadi, "Digital Filtering in One and Two Dimensions", Plenum Press, New York, 1989.

[52] R. C. Gonzalez and R. E. Woods, "Digital Image Processing", Pearson Education, Inc., Second Edition, 2002.

[53] T. Bose, "Digital Signal and Image Processing", John Wiley and Sons, Inc., 2004.